C-1

GEOLOGY AND ORE DEPOSITS OF THE STEWART MINING CAMP, BRITISH COLUMBIA

By

DANI JAMES ALLDRICK

B.Sc.(Hons.), The University of Western Ontario, 1974
M.Sc., Imperial College, University of London, 1978

A THESIS SUBMITTED IN PARTIAL FULFILLMENT OF

THE REQUIREMENTS FOR THE DEGREE OF

DOCTOR OF PHILOSOPHY

in

THE FACULTY OF GRADUATE STUDIES

Department of Geological Sciences

We accept this thesis as conforming

to the required standard

THE UNIVERSITY OF BRITISH COLUMBIA

April, 1991

© Dani James Alldrick, 1991

In presenting this thesis in partial fulfilment of the requirements for an advanced degree at the University of British Columbia, I agree that the Library shall make it freely available for reference and study. I further agree that permission for extensive copying of this thesis for scholarly purposes may be granted by the head of my department or by his or her representatives. It is understood that copying or publication of this thesis for financial gain shall not be allowed without my written permission.

Department of Geological Sciences

The University of British Columbia
Vancouver, Canada

Date April 4, 1991

DE-6 (2/88)

ABSTRACT

The Stewart mining camp in northwestern British Columbia is abundantly mineralized with widely distributed, texturally and mineralogically varied, precious and base metal deposits. This report documents the geologic setting of the mining camp and the geologic features of the major mineral deposit types.

The Stewart camp is underlain by a 5-kilometre-thick Upper Triassic to Lower Jurassic (Norian? to Toarcian) island arc complex of calc-alkaline basalts, andesites and dacites with interbedded sedimentary rocks. Coeval (211-189 Ma) hornblende granodiorite plutons intruded the arc at two to five kilometres depth. Rocks were deformed during mid-Cretaceous (110 ± 5 Ma) tectonism that produced north-northwest-trending folds, penetrative fabric and lower greenschist facies regional metamorphism (290° ± 20°C, 4.5 ± 1.5 kb). Mid-Eocene (54.8-44.8 Ma) biotite granodiorite of the Coast Plutonic Complex intruded the deformed Mesozoic arc complex.

Two mineralizing events formed over 200 mineral occurrences in the district. These two metallogenic epochs were brief (<5 million years), regional-scale phenomena characterized by different base and precious metal suites. The Early Jurassic ore-forming episode produced Au and Au-Ag-Zn-Pb-Cu deposits. The mid-Eocene episode produced Ag-Pb-Zn ± W ± Mo deposits.

Early Jurassic deposits have a characteristic lead isotope signature ($^{206}Pb/^{204}Pb$ = 18.816; $^{207}Pb/^{204}Pb$ = 15.617) and include gold-pyrrhotite veins, gold-silver-base metal veins, and stratabound pyritic dacites. All Early Jurassic mineral occurrences are late- to post-intrusive deposits that were emplaced in andesitic to dacitic host rocks at the close of volcanic activity, about 190-185 million years ago.

Transitional gold-pyrrhotite veins (Scottie Gold mine) formed in *en echelon* tension gashes developed in country rock around Early Jurassic plutons during late magma movement. Epithermal gold-silver-base metal veins and breccia veins (Big Missouri and Silbak Premier mines) were deposited along shallower sub-volcanic faults and in hydrothermal breccia zones formed along dyke contacts. Stratabound pyritic dacite tuffs (Mount Dilworth and Iron Cap prospects) formed where venting fumarolic fluids and hotspring pools deposited abundant fine pyrite in local areas on a cooling ignimbrite sheet.

Eocene deposits also have a characteristic lead isotope signature ($^{206}Pb/^{204}Pb$ = 19.147; $^{207}Pb/^{204}Pb$ = 15.627) and include silver-rich galena-sphalerite veins, gold-silver skarns and, beyond the study area, porphyry molybdenum deposits. These mineral occurrences are related to Middle Eocene plutons of the Coast Plutonic Complex. All are late- to post-intrusive deposits emplaced about 50-45 million years ago.

Mesothermal silver-lead-zinc veins (Prosperity/Porter Idaho and Riverside mines) were deposited in brittle zones along major fault structures. Skarns (Oral M and Red Reef prospects) developed where plutons cut limestone or limy siltstone units within minor turbidite sequences. Major porphyry molybdenum deposits (Kitsault mine and Ajax) developed where mid-Eocene stocks were emplaced in thick turbidite sequences.

Diagnostic features such as lead isotope ratios, stratigraphic and plutonic associations, alteration assemblages, sulphide mineralogy and textures, and precious metal ratios allow discrimination amoung these different deposit types. Using these criteria, the most prospective areas for each deposit type have been targetted for exploration.

TABLE OF CONTENTS

Page

ABSTRACT ii

Table of Contents iv
List of Figures vi
List of Tables xiii
List of Plates ix

ACKNOWLEDGEMENTS xi

CHAPTER 1: INTRODUCTION 1

1.1. Field Area 1
1.2. Stewart Mining Camp 3
1.3. Previous Geological Work 3
1.4. Present Study 6

CHAPTER 2: REGIONAL GEOLOGIC SETTING 8

2.1. Stratigraphy of Stikinia 8
2.2. Intrusive Events in Stikinia 18
2.3. Tectonic History of Stikinia 20
2.4. Geologic History of Stikinia 24

CHAPTER 3: GEOLOGY OF THE STEWART MINING CAMP 29

3.1. Lithostratigraphy and Nomenclature 29
3.1.1. STUHINI GROUP 29
3.1.2. HAZELTON GROUP 33
3.1.3. BOWSER LAKE GROUP 73
3.2. Intrusive Rocks 74
3.2.1. TEXAS CREEK PLUTONIC SUITE 75
3.2.2. HYDER PLUTONIC SUITE 85
3.2.3. STIKINE VOLCANIC BELT 98
3.3. Petrochemistry 98
3.3.1. VOLCANIC ROCKS 98
3.3.2. PLUTONIC ROCKS 108
3.4. Structure 111
3.5. Metamorphism and Alteration 117
3.6. Geochronometry 133
3.7. Summary Geologic History 146

CHAPTER 4: MINERAL DEPOSITS 149

4.1 Distribution 149
4.2 Classification 152
4.2.1 PRELIMINARY CLASSIFICATION 152
4.2.2 LEAD ISOTOPE STUDIES 152
4.2.3 DEPOSIT CLASSIFICATION 162
4.3 Characteristics 164
4.3.1 EARLY JURASSIC DEPOSITS 164
4.3.1.1 Scottie Gold Mine 164
4.3.1.2 Deposits of the Big Missouri Area 179
4.3.1.3 Silbak Premier Mine 201
4.3.1.4 Stratabound Pyritic Dacite 228
4.3.2. EOCENE DEPOSITS 229
4.3.2.1.Prosperity/Porter Idaho Mine 229
4.4. Local Exploration Guidelines 244

CHAPTER 5: ORE GENESIS AND METALLOGENY 253

5.1. Ore Deposit Models 253
5.1.1. EARLY JURASSIC DEPOSITS 253
5.1.2. EOCENE DEPOSITS 264
5.2. Regional Models 266
5.2.1. GENETIC MODELS 266
5.2.2. METALLOGENIC MODELS 272
5.3. Regional Exploration Strategies 276
5.3.1. EARLY JURASSIC 276
5.3.2. EOCENE 278

CHAPTER 6. CONCLUSIONS 280

BIBLIOGRAPHY 282

APPENDICES

I. PETROCHEMICAL DATA 306
II. URANIUM-LEAD DATA AND ANALYTICAL TECHNIQUES 310
III. LEAD ISOTOPE DATA AND ANALYTICAL PROCEDURES 317
IV. DEPOSIT SAMPLING AND ANALYTICAL RESULTS 325
V. HISTORIC GENETIC MODELS 345

Maps in Sp. Collection Div.

LIST OF FIGURES

		Page
Figure 1.1	Location of study area	2
Figure 2.1	Physiographic and tectonic belts of the Canadian Cordillera	9
Figure 2.2	Tectonic elements of northern British Columbia	11
Figure 2.3	Stratigraphy of Stikinia	12
Figure 2.4	Distribution of the Hazelton Group an the Stewart Complex	13
Figure 2.5	Evolution of stratigraphic nomenclature for the Hazelton group	14
Figure 2.6	Intrusive events in Stikinia and the Canadian Cordillera	19
Figure 2.7	Subduction zone geometry of the Canadian Cordillera	22
Figure 2.8	Terranes and composite terranes of the Canadian Cordillera	23
Figure 2.9	Geological history of Stikinia	25
Figure 3.1	Geologic setting of the study area	30
Figure 3.2	Geology of the Stewart mining camp (2 maps)	~~in pocket~~
Figure 3.3	Schematic stratigraphy of the Stewart mining camp	31
Figure 3.4	Evolution of stratigraphic nomenclature for the Stewart mining camp	32
Figure 3.5	Phenocryst and fragment variations in Stewart stratigraphy	34
Figure 3.6	Stratigraphic correlation for pyroxene porphyry units	37
Figure 3.7	Stratigraphy within the Mount Dilworth Formation	57
Figure 3.8	Alteration screening plots	101
Figure 3.9	Silica histograms	103
Figure 3.10	Harker silica variation diagrams	104
Figure 3.11	Total alkali *versus* silica discriminant diagrams	105
Figure 3.12	Tectonic environment discriminant plot	106
Figure 3.13	Modal compositions of plutonic rocks	109
Figure 3.14	Plutonic rock discriminant diagrams	110
Figure 3.15	Metamorphic grade in the Stewart mining camp	119
Figure 3.16	Distribution of alteration within an andesitic stratovolcano	127
Figure 3.17	General relationships of temperature, deformation and argon loss	138
Figure 3.18	Thermal and igneous history of the Stewart district	140

Figure 4.1 Mineral occurrences, gossans and topographic features ~~in pocket~~
Figure 4.3 Growth curve for lead isotope evolution 157
Figure 4.4 Stewart camp galena lead isotope data 158
Figure 4.4 Geological setting of the Scottie Gold mine 167
Figure 4.5 Surface veins at the Scottie Gold mine 168
Figure 4.6 Cross section through the Big Missouri orebody 181
Figure 4.7 Fault offsets along the Big Missouri ridge 183
Figure 4.8 Geological cross section through the Silbak Premier mine area 204
Figure 4.9 Geological cross section through Main Zone, Silbak Premier mine 205
Figure 4.10 Distribution of ore zones at the Silbak Premier mine ~~in pocket~~
Figure 4.11 Distribution of alteration zones in the Silbak Premier mine 216
Figure 4.12 Paragenetic sequence of opaque minerals at the Silbak Premier mine 224
Figure 4.13 Distribution of veins on Mount Rainey 230
Figure 4.14 Geological map of the Mount Rainey summit 232
Figure 4.15 Vein geometry at Prosperity/Porter Idaho mine 234
Figure 4.16 Prospective areas for Early Jurassic and Eocene ore deposit types 246

Figure 5.1 Fracturing mechanisms for Scottie Gold mine 254
Figure 5.2 Genetic model for the Scottie Gold mine 255
Figure 5.3 Ore deposit model for Big Missouri mine 257
Figure 5.4 Genetic model for Big Missouri deposits 258
Figure 5.5 Ore deposit model for Silbak Premier mine 260
Figure 5.6 Genetic model for the Silbak Premier mine 261
Figure 5.7 Genetic model for stratabound pyritic dacite 265
Figure 5.8 Sequence of development of epithermal settings 267
Figure 5.9 Genetic model for the Early Jurassic 268
Figure 5.10 Ore potential in an andesitic stratovolcano 269
Figure 5.11 Ore deposit model for the Middle Eocene 270
Figure 5.12 Genetic model for the Middle Eocene 271
Figure 5.13 Metallogenic models for the Stewart camp 273
Figure 5.14 Volcanic centres within the Stewart Complex 277

LIST OF TABLES

Page

Table 1.1 Past Production in the Stewart Mining Camp 4
Table 1.2 Present reserves in the Stewart Mining Camp 5

Table 3.1 Textural distinctions between Premier Porphyry flow and Premier Porphyry tuff 45
Table 3.2 Evidence for subaerial *versus* subaqueous deposition of the Unuk River formation 49
Table 3.3 Hyder Plutonic Suite sequence of intrusion 97
Table 3.4 Structural history of the Stewart district 116
Table 3.5 Metamorphic minerals and phase transitions 118
Table 3.6 Classification of alteration types 121
Table 3.7 Classification of alteration types by age and genetic process 122
Table 3.8 Dates from the Stewart mining camp in chronological order 134
Table 3.9 Potassium-argon dates from the Stewart camp 135
Table 3.10 Uranium-lead zircon data from the Stewart camp 136
Table 3.11 Closure temperatures for argon loss in minerals 137
Table 3.12 Geologic history of the Stewart mining camp 144
Table 3.13 Comparison of geologic histories for southeast Alaska and the Canadian Cordillera 145

Table 4.1 Distribution of mineral occurrences in strata, intrusive rocks and structures 151
Table 4.2 Preliminary deposit classification 153
Table 4.3 Galena lead isotope sample sites 155
Table 4.4 Galena lead isotope data 156
Table 4.5 Summary of diagnostic features ..... ~~in pocket~~
Table 4.6 Metallogenic epochs and ore deposit types 163
Table 4.7 Mineral deposit classification table ..... ~~in pocket~~
Table 4.8 Table of ore zone names (Scottie Gold mine) 169
Table 4.9 Past production and present reserves from deposits in the Big Missouri area 184
Table 4.10 Past production and present reserves for deposits in the Silbak Premier mine area 208
Table 4.11 Stages of veining at the Silbak Premier mine 211
Table 4.12 Sequence of ore deposition at the Prosperity/Porter Idaho mine 243

LIST OF PLATES

Page

Plate 3.1A: Bedded plagioclase-hornblende ash flow, Premier Porphyry Member, Unuk River Formation 44
Plate 3.1B: Regolith layer between massive beds of K-feldspar porphyritic flow, Premier Porphyry Member, Unuk River Formation 44
Plate 3.2A: Vent facies, Premier Porphyry Member, Unuk River Formation 47
Plate 3.2B: Megabreccia. Vent facies, Premier Porphyry Member, Unuk River Formation 47
Plate 3.2C: Fall-back breccia. Vent facies, Premier Porphyry Member, Unuk River Formation 47
Plate 3.3A: Rhythmic graded beds. Betty Creek Formation 53
Plate 3.3B: Bedded coarse wacke with scour channel. Betty Creek formation. 53
Plate 3.3C: Hematitic wackes. Betty Creek formation 53
Plate 3.4A: Stratigraphy of Mount Dilworth Formation 59
Plate 3.4B: Mount Dilworth Formation, spectacular gossans of the Pyritic Tuff 59
Plate 3.5A: Upper Lapilli Tuff Member of Mount Dilworth Formation 61
Plate 3.5B: Middle Welded Tuff Member of Mount Dilworth Formation 61
Plate 3.5C: Lower Dust Tuff Member of Mount Dilworth Formation 61
Plate 3.6A: Intraformational conglomerate. Upper Wacke Member of Salmon River Formation 70
Plate 3.6B: Rhythmically interbedded siltstones. Lower Siltstone Member of the Salmon River Formation 70
Plate 3.6C: Basal Fossiliferous Limestone Member of the Salmon River Formation 70
Plate 3.7A: Premier Porphyry dyke, Silbak Premier Mine 82
Plate 3.7B: Chilled margin of Premier Porphyry dyke 82
Plate 3.7C: Three aspects of Premier Porphyry dyke: type rock; strongly altered rock; mylonite 82
Plate 3.7D: Multiply rimmed K-feldspar crystal in Premier Porphyry dyke 82
Plate 3.8A: The Portland Canal dyke swarm 90
Plate 3.8B: Photomicrograph of lamprophyre dyke 90
Plate 3.9A: Photomicrograph of pressure shadow around pyrite crystal 125
Plate 3.9B: Photomicrograph of strong chlorite-carbonate alteration in Premier Porphyry dyke rock 125
Plate 3.9C: Strong epidote alteration in lapilli tuff 125
Plate 3.10A: Progressive sericite-carbonate-pyrite alteration of andesitic lapilli tuff 131
Plates 3.10B and C: Photomicrographs of sericitic alteration front at microscopic scale 131

Plate 4.1A: Main Vein. Scottie Gold mine 172
Plates 4.1B and C: Strongly sheared and altered wallrock. Scottie Gold mine 172
Plate 4.1D: Marginal zone of Main Vein. Scottie Gold mine 172
Plate 4.2A: Photomicrograph of gold grain within pyrrhotite veinlet. Scottie Gold mine 177
Plate 4.2B: Photomicrograph of disseminated gold within massive pyrrhotite. Scottie Gold mine 177
Plate 4.2C: Photomicrograph of gold grains within a chalcopyrite veinlet. Scottie Gold mine 177
Plate 4.3A: Ore from Province deposit shows clasts of early-formed vein in sulphide-rich quartz-carbonate vein 188
Plate 4.3B: Symmetric vein growth. Dago Hill deposit 188
Plate 4.3C: Wallrock clasts show classic cockade texture. Big Missouri mine 188
Plate 4.3D: Chalcedonic veinlets. Dago Hill Deposit 188
Plate 4.4A: Photomicrograph of pyrite hosting chalcopyrite, galena and electrum. Dago Hill deposit 194
Plate 4.4B: Characteristic features of delafossite. S-1 deposit 194
Plate 4.5A: Photomicrograph of colloform pyrite growth. S-1 deposit 196
Plate 4.5B: Photomicrograph of pyrite encrustations around quartz crystals. S-1 deposit 196
Plate 4.5C: Carbon-rich matrix to breccia vein. Dago Hill deposit 196
Plate 4.6A: Progressive alteration front obscures original lapilli tuff texture. Dago Hill deposit 200
Plate 4.6B: A white quartz veinlet truncated by a chalcedony-pyrite veinlet. Dago Hill deposit 200
Plate 4.6C: The Silbak Premier minesite 200
Plate 4.7A: Shattered wallrock with vein network, Silbak Premier mine 214
Plate 4.7B: Photomicrograph of intersecting veinlets of different ages. Silbak Premier mine 214
Plate 4.7C: Sulphide cemented breccia. Silbak Premier mine 214
Plate 4.7D: Low sulphide breccia clast of chalcedony. Silbak Premier mine 214
Plates 4.8A and B: Photomicrograph of zoned pyrite. Silbak Premier mine 221
Plate 4.8C: Intersecting vein networks resemble mosaic breccia. Silbak Premier mine 221
Plate 4.8D: Rebrecciated vein. Silbak Premier mine 221
Plate 4.9A: Mineralized fault breccia. Prosperity/Porter Idaho mine 237
Plates 4.9B and C: Mineralized breccia. Prosperity/Porter Idaho mine 237
Plate 4.10A: Photomicrograph of shatter zone in wallrock. Prosperity/Porter Idaho mine 241
Plate 4.10B: Photomicrograph of lacy pyritic network. Prosperity/Porter Idaho mine 241
Plates 4.10C and D: Photomicrographs of native silver. Prosperity/Porter Idaho mine 241

ACKNOWLEDGEMENTS

This study was proposed by A. Panteleyev in 1981. It was initiated in 1983 with the support and encouragement of A. Sutherland Brown, Director, and W. McMillan, Manager, of the Geological Survey Branch, BCMEMPR.

Thesis advisors A.J. Sinclair, R.L. Armstrong and C.I. Godwin provided advice about general procedures, guidance about specific research techniques, and improved the manuscript with thorough editing. Sections of this report received careful reviews by W.J. McMillan and J.K. Mortensen.

Major and minor element analyses and assays were completed by P. Ralph, V. Vilkos, B. Bhagwanani and M. Chaudhry of the BCMEMPR laboratory. R.L. Player prepared all thin sections, polished sections and polished thin sections. E.M. Alldrick entered analytical data into computer files and checked them. Computer programs for data plotting were developed by D.G. MacIntyre. The manuscript was typed by D. Bulinckx. The task of drafting figures was shared with B. Fletcher, J. Armitage, P. Chicorelli, M. Taylor and K. Hancock.

I acknowledge the interest, hospitality and logistical support provided by four mining companies who arranged tours and sampling trips: Westmin Resources Limited, Scottie Gold Mines Limited, Pacific Cassiar Limited and Esso Minerals Canada Limited. The writer has benefitted from discussions with many geologists during this study; my thanks to R. Anderson, D. Brown, G. Dawson, S. Dykes, P. Folk, J. Greig, P. McGuigan, M. Kenyon, H. Meade, W. Melnyk, D. Novak, A. Randall, N. Tribe, D. Williams and P. Wodjak for sharing their data and ideas.

Financial support for fieldwork, study leave and much of the analytical work was provided by the British Columbia Ministry of Energy, Mines and Petroleum Resources and is gratefully acknowledged. Additional funding was provided by a Natural Sciences and Engineering Research Council operating grant to R.L. Armstrong and a Canada/British Columbia Mineral Development Agreement grant to C.I. Godwin.

My wife, Eileen, has encouraged and supported me throughout this long adventure...asking only that I finish school before our son, David, starts.

CHAPTER 1
INTRODUCTION

The Stewart mining camp has a long history of underground gold-silver production and is entering a new era of major open-pit precious metal mining. The district is abundantly mineralized with over 200 widely distributed, varied mineral occurrences. This report documents the geologic setting of the mining camp and geologic features of the major mineral deposit types. Objectives of this study are: to classify all mineral occurrences into groups of similar deposit type, to determine characteristic features of each group as an aid in exploration, and to deduce processes of formation and controls on emplacement of these deposits. New ideas about the tectonic setting and metallogenic history of this district are also presented.

1.1 THE FIELD AREA

LOCATION AND ACCESS

The area lies near the eastern margin of the Coast Mountains at the head of the Portland Canal, a 115-kilometre-long fjord which marks the southeastern boundary between the Alaskan Panhandle and northwestern British Columbia. The field area covers 750 square kilometres centred near the Silbak Premier mine; it includes the town of Stewart, British Columbia and the village of Hyder, Alaska (Figure 1.1). Stewart can be reached by road from Vancouver and has air service to Terrace and Smithers. The main access route within the area is the Granduc mine road, a gravel haul road running north from Hyder and terminating at the Tide Lake Airstrip.

TOPOGRAPHY

The study area is near the southern end of the Boundary Ranges of the Coast Mountains. Elevations range from sea level to 2544 metres on Mitre Mountain. Topography is rugged; the area is characterized by precipitous glaciated valley walls and rounded ridge crests. The dominant topographic pattern is north-trending ridges and intervening glaciated valleys (Figure 1.1).

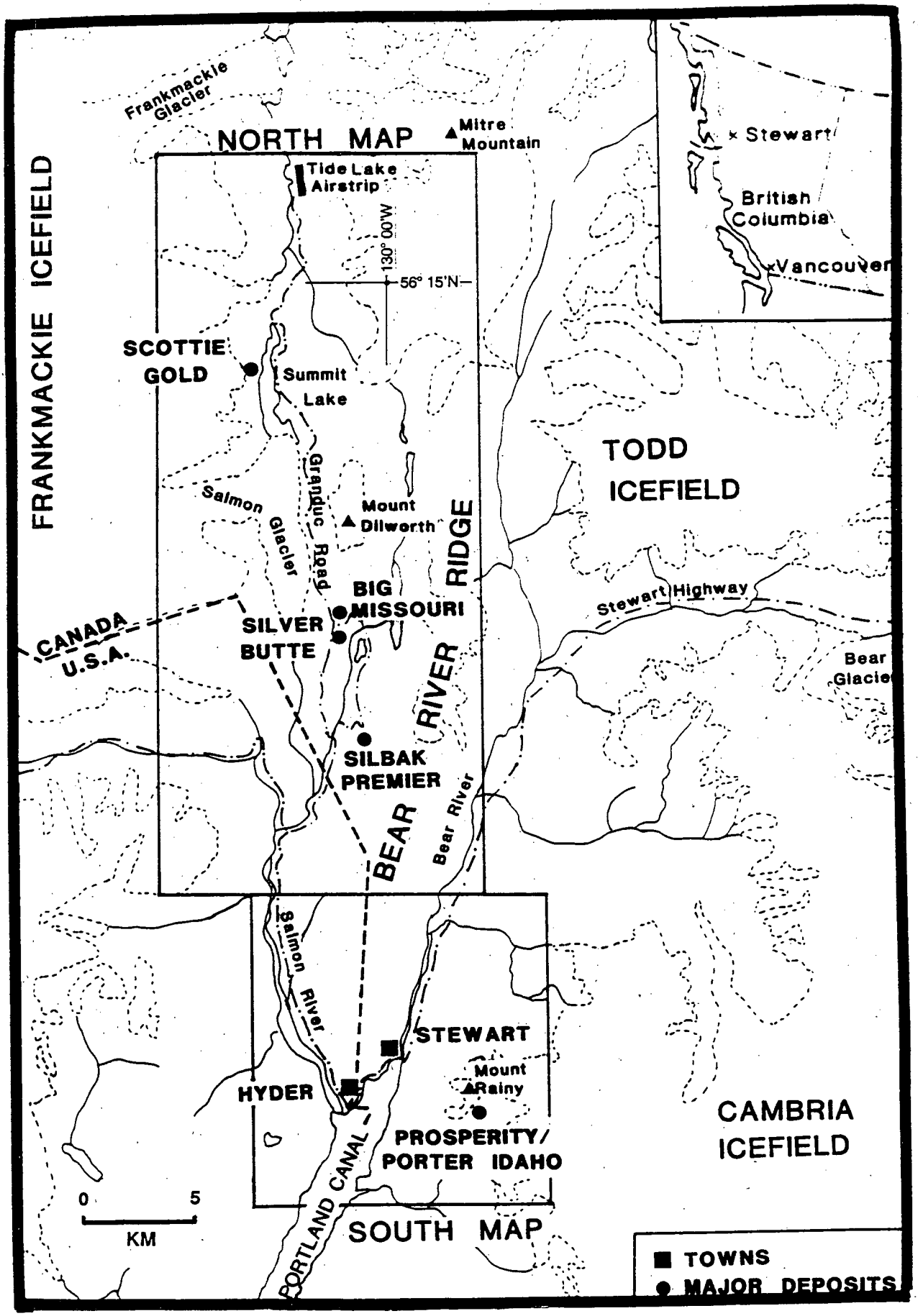

FIGURE 1.1: Location of study area

1.2 THE STEWART MINING CAMP

MINING HISTORY

A large party of placer gold prospectors reached the head of the Portland Canal in 1898. After stream gravel panning failed to locate significant placer deposits the group turned to lode gold prospecting and met with intermittent success marked by discovery of many small gold and silver properties. In 1910, exploration of some gossanous bluffs led to the discovery of the Silbak Premier orebodies. In 1929, before the stock market crash, there were over 40 mining companies active in the district.

Readers particularly interested in the early mining history of the district are referred to Grove (1971, p.17-19), to the archives of the Stewart museum, and to extensive records in the Legislative Library, Victoria.

PRODUCTION HISTORY AND PRESENT RESERVES

Past production for all deposits in the area are listed in Table 1.1. Present ore reserves for all deposits are listed in Table 1.2.

1.3 PREVIOUS GEOLOGIC WORK

Geologic work began in the Stewart area in 1906. Studies up to 1965 were reviewed in Grove (1971, p.19). His summary is complemented by detailed tables listing all geological reports and maps for the Premier mine (Brown, 1987, p.7) and for the whole of north-central British Columbia (Brown, 1987, p.9). Previous thesis studies in the Stewart area have been completed by White (1938), Seraphim (1947), Grove (1973), Galley (1981), Brown (1987) and MacDonald (1990). Comprehensive reference lists for every mineral property are included in recently revised MINFILE listings.

Ongoing geological work includes regional-scale mapping by R.G. Anderson of the Geological Survey of Canada and mapping of the Silbak Premier and Big Missouri areas by Westmin Resources Limited.

TABLE 1.1: Past Production in the Stewart Mining Camp (to January, 1988)

PROPERTY	MAP NO.	MINFILE NO.	DATE	PAST PRODUCTION (TONNES)	Au gm/T	Ag gm/T	Cu %	Pb %	Zn %	WO_3 %
EAST GOLD	N3	104B-033	1939-1954	43.5	1207.	3313.	0.07	4.8	1.3	
SCOTTIE GOLD	N12	104B-034	1981-1985	197 522.		16.5	16.			
SPIDER	N28	104A-010	1925, 1933-1936	22.2	14.2	8238.		3.5	3.9	
SILVER TIP	N36	104B-043	1915,1950, 1951,1957	26.3	11.8	2610.		14.	19.	
BIG MISSOURI	N50	104B-046	1938-1942	768 943.	2.37	2.13		*	*	
DAGO HILL	N55	104B-045	1934,1950	13.6	48.	3952.	0.12	0.46		
INDIAN	N76	104B-031	1925,1952	12 870.	3.04	119.7		4.4	5.5	
SILBAK PREMIER	N82,87, 88,89	104B-054	1919-1953, 1959-1968	4 276 714.	13.	274.	*	0.66	0.2	
RIVERSIDE	N121	104B-073	1925,1927, 1941-1950	26 437.	2.89	102.1	0.13	3.9	*	0.12
DUNWELL	S6	103P-054	1926-1941	45 710.	6.72	224.4	.03	1.83	2.43	
UNITED EMPIRE	S29,34	103P-050	1925 1934,1936	163.	2.10	1136.7		7.4		
MOLLY B	S46	103P-085	1940,1941	290.	2.36	12.01	0.72			
SILVERADO	S51	103P-088	1927	13.		3662.4				
PROSPERITY/ PORTER IDAHO	S57,58	103P-089	1922, 1924-1932, 1938,1939, 1947,1950, 1981	27 268.	1.00	2692.97	0.10	5.1	0.03	

TABLE 1.2: Present Reserves in the Stewart Mining Camp (to January, 1988)

PROPERTY	MAP NO.	MINFILE NO.	RESERVES (category)	Au g/T	Ag g/T	Pb %	Zn %
SCOTTIE GOLD	N12	104B-034	28 992(m)	18.51			
SILVER TIP	N36	104B-043	816(g)	4.8	970.3	4.2	6.2
BIG MISSOURI GROUP	N50	104B-046	1 528 788(m)	3.12	22.97		
			3 684 984(g)	2.50	21.26		
SILVER BUTTE	N58	104B-150	105 590(m)	10.6	39.7		
			339 512(g)	17.31	36.69		
SILBAK PREMIER	N82,87, 88,89	104B-054	6 500 000(m)	2.16	80.23		
PROSPERITY/ PORTER IDAHO	S57,58	103P-089	826 400(g)		668.5	5.0	5.0

(m)= Mineable Reserves
(g)= Geological Reserves

1.4 THE PRESENT STUDY

CONCEPT

Definition of the problem and development of the objectives of this thesis evolved after the 1982 field season. Visits to several properties, and literature review of many more, emphasized the complexities in sulphide and gangue mineralogy, metal contents, alteration, and structural settings of the mineral occurrences. This work also revealed the variety of deposit-scale genetic models that had been invoked for each major deposit (Table 5.1). Although no solution to deposit classification/ore genesis problems was obvious in 1982, this study grew from the conviction that a change in perspective to a district-scale view might reveal important similarities and differences among deposits. The original thesis proposal (May, 1984) outlined problems and listed aspects to be investigated, without predicting the outcome, as follows:

> The many ore deposits and mineral prospects of the area show wide variations in ore mineralogy, gangue mineralogy, alteration mineralogy and structural setting, but all are hosted in andesite tuffs and flows of the Jurassic Hazelton Group along the eastern margin of the Coast Plutonic Complex. In addition to intense alteration localized around mineral deposits, andesites have been overprinted by a complex pattern of regional alteration plus regional metamorphism.
>
> Planned research will investigate:
> - Characteristics of the major types of mineral deposits and relationships between deposits
> - Stratigraphic and structural settings of the deposits
> - Characteristics and distribution of local and regional alteration patterns
> - Timing of mineralization with respect to host volcanics, intrusions, regional alteration and regional metamorphism.

FIELDWORK

Fieldwork was carried out during 1982, 1983 and 1984. Mapping traverses were recorded on 1:10,000-scale air photographs and compiled on 1:25,000-scale field maps.

Four major deposits, representing significantly different deposit types, were selected for detailed examination. In addition to surface mapping and underground visits each deposit was sampled in three separate underground locations by chip sample lines. At Big Missouri drill core was sampled instead of underground faces.

RESEARCH METHODS

Rock samples were collected on regional traverses and from deposit-scale sampling. Polished sections, polished thin sections and thin sections were prepared and studied. Sawn rock slabs were polished for textural studies.

Samples of ore and altered rocks from 34 deposits were assayed and samples from 22 occurrences had additional trace metal determinations carried out. Four U-Pb, eight K-Ar and sixty Pb-Pb analyses were completed.

The route to the present report was neither obvious nor straight. What started out as an exercise in mineral deposit classification ultimately required modification of accepted ages of major plutons, inversion of stratigraphic columns, and rotation of the dips of whole mountains of strata through as much as 90 degrees from orientations established for decades.

CHAPTER 2
REGIONAL GEOLOGIC SETTING

The study area lies in the Coast Mountains along the western margin of the Intermontane tectonic belt, adjacent to the Coast Plutonic Complex (Figure 2.1). According to terrane concepts the present study area lies entirely within Stikinia (Figure 2.8). The Intermontane Belt roughly coincides with the Intermontane Composite Terrane (Intermontane Superterrane or Superterrane I) of Monger (1984).

2.1 STRATIGRAPHY OF STIKINIA

STIKINE ASSEMBLAGE: The oldest rocks within Stikinia, termed Stikine assemblage by Monger (1977a) and Asitka assemblage by Wheeler and McFeely (1987), consists of Devonian to Permian sedimentary successions with interbedded volcanic packages. This regionally extensive assemblage is exposed around the northern periphery of the Bowser Basin.

STUHINI/TAKLA GROUP: The Stuhini/Takla Group is a Late Triassic volcanic and sedimentary rock sequence of Carnian to Norian age that encircles the Bowser Basin. The Stuhini Group comprises pyroxene porphyritic basalts to basaltic andesites, bladed feldspar porphyry volcaniclastic rocks and derived sedimentary rocks. The Takla Group consists of pyroxene and pyroxene-feldspar porphyritic flows grading laterally to distal sedimentary facies, overlain by feldspar porphyritic volcanic rocks with proximal volcaniclastic sedimentary facies.

HAZELTON GROUP: The Lower to Middle Jurassic Hazelton Group consists of calcalkaline basalt to rhyolite and derived volcaniclastic sedimentary rocks that are well exposed around the perimeter of the Bowser Basin (Figure 2.4). Historic subdivisions are compared to stratigraphic divisions defined in this study in Figure 2.5.

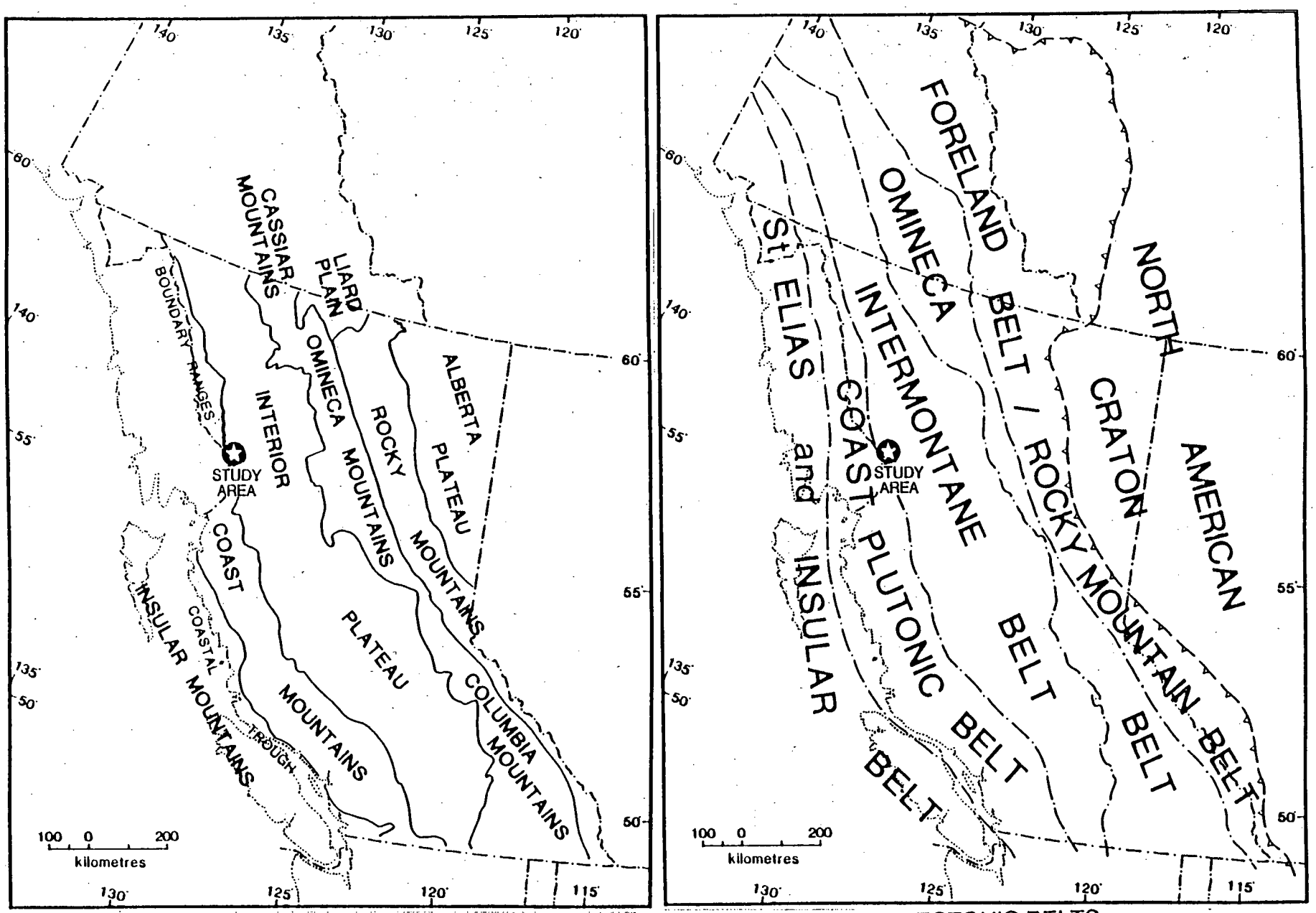

A. PHYSIOGRAPHIC BELTS

B. TECTONIC BELTS

FIGURE 2.1: Physiographic and tectonic belts of the Canadian Cordillera (modified from CIMM Special Volume 15)

LEGEND

ACCRETED TERRANES

Paleo-Arc

ST = Stikine Terrane

Q = Quesnel Terrane

Paleo-Ocean Floor

CC = Cache Creek Terrane

SM = Slide Mountain Terrane

POST-ACCRETION SEDIMENTS

Overlap Assemblages

BL = Bowser Lake Group

SK = Skeena Group

SU = Sustut Group

Bowser Basin Perimeter

PLUTONIC ROCKS

CPC = Coast Plutonic Complex

OCB = Omineca Crystalline Belt

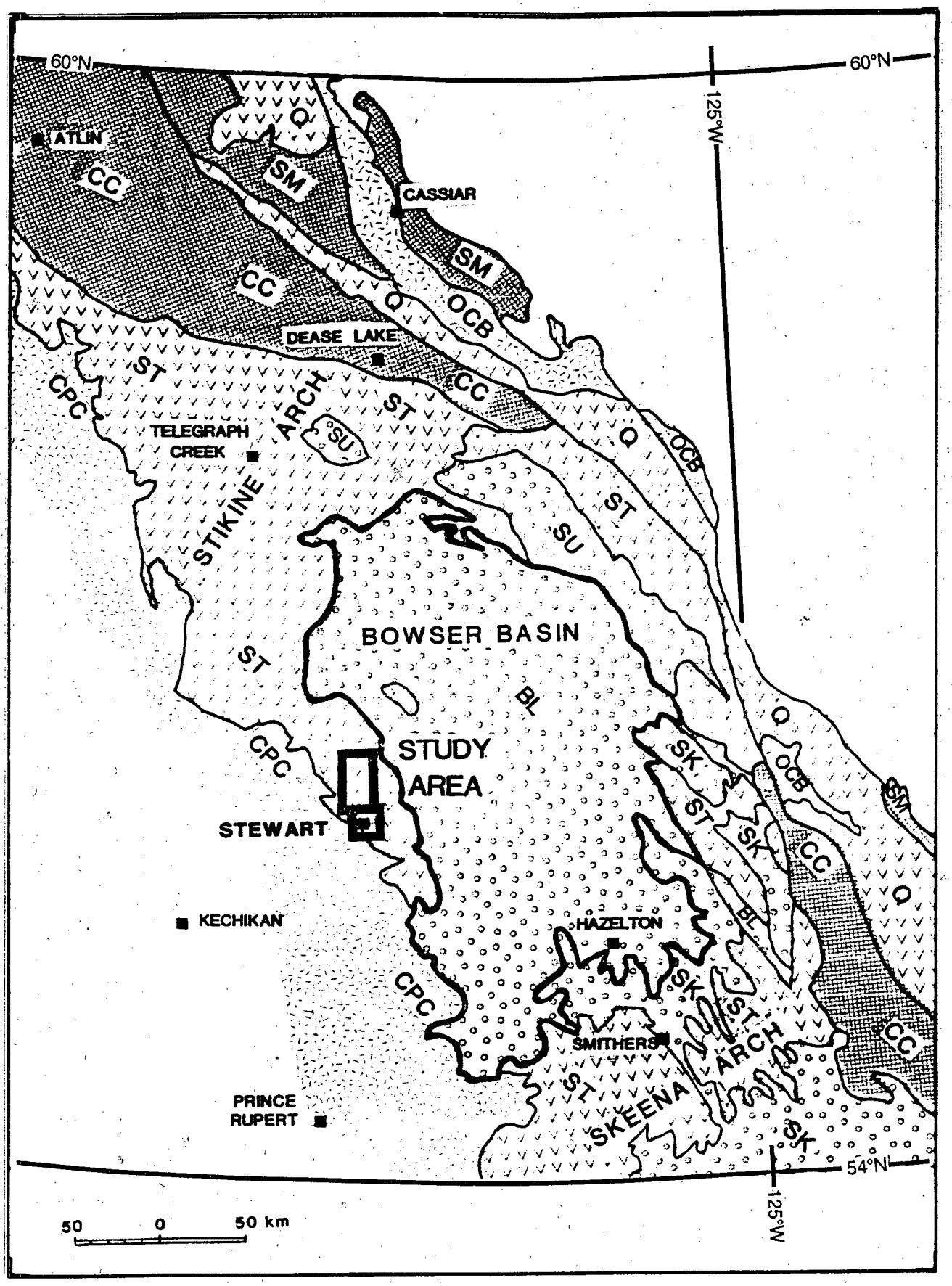

FIGURE 2.2: Tectonic elements of northern British Columbia (Modified from DNAG map, Brookfield, in press)

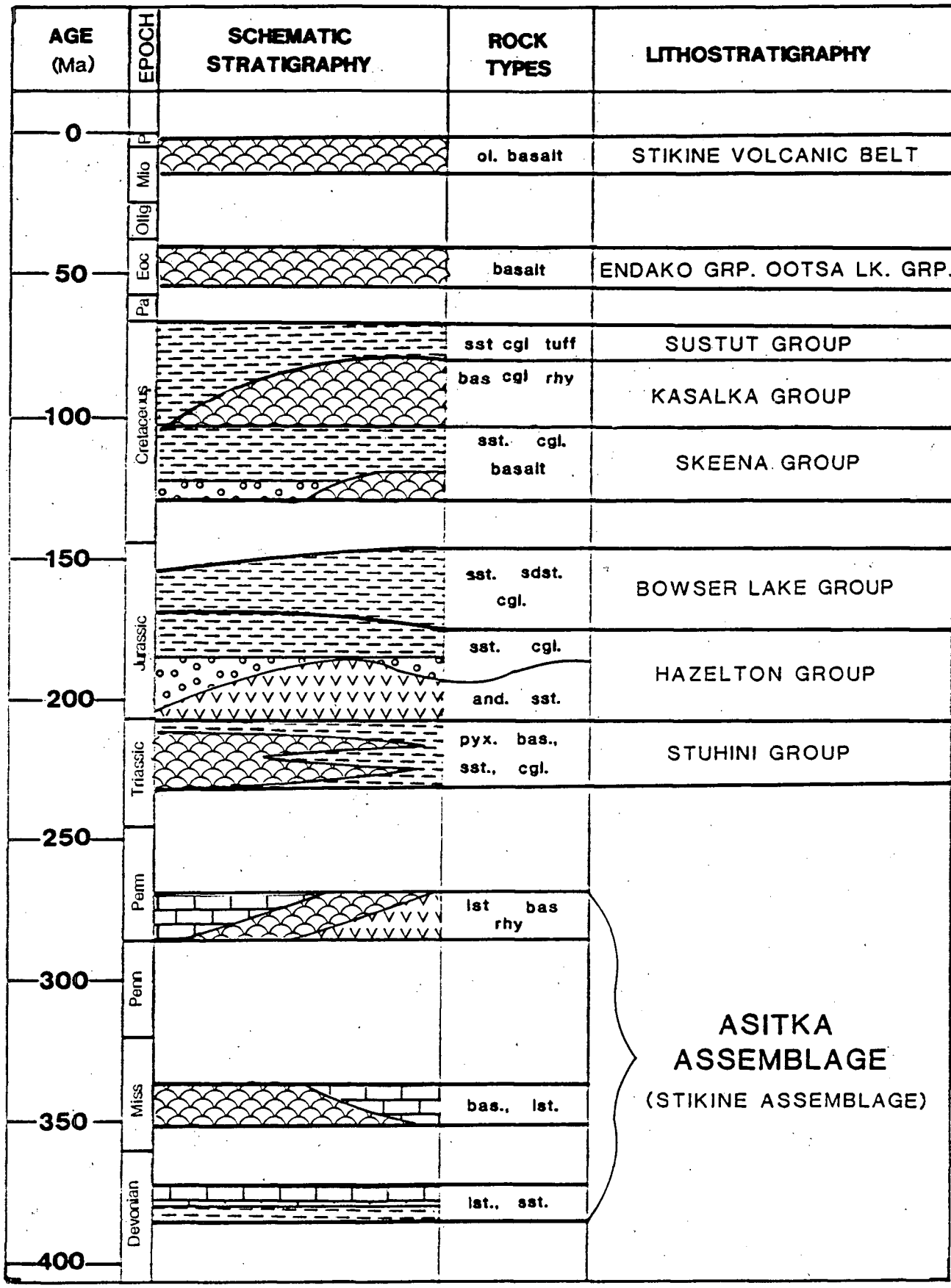

FIGURE 2.3: Stratigraphy of Stikinia

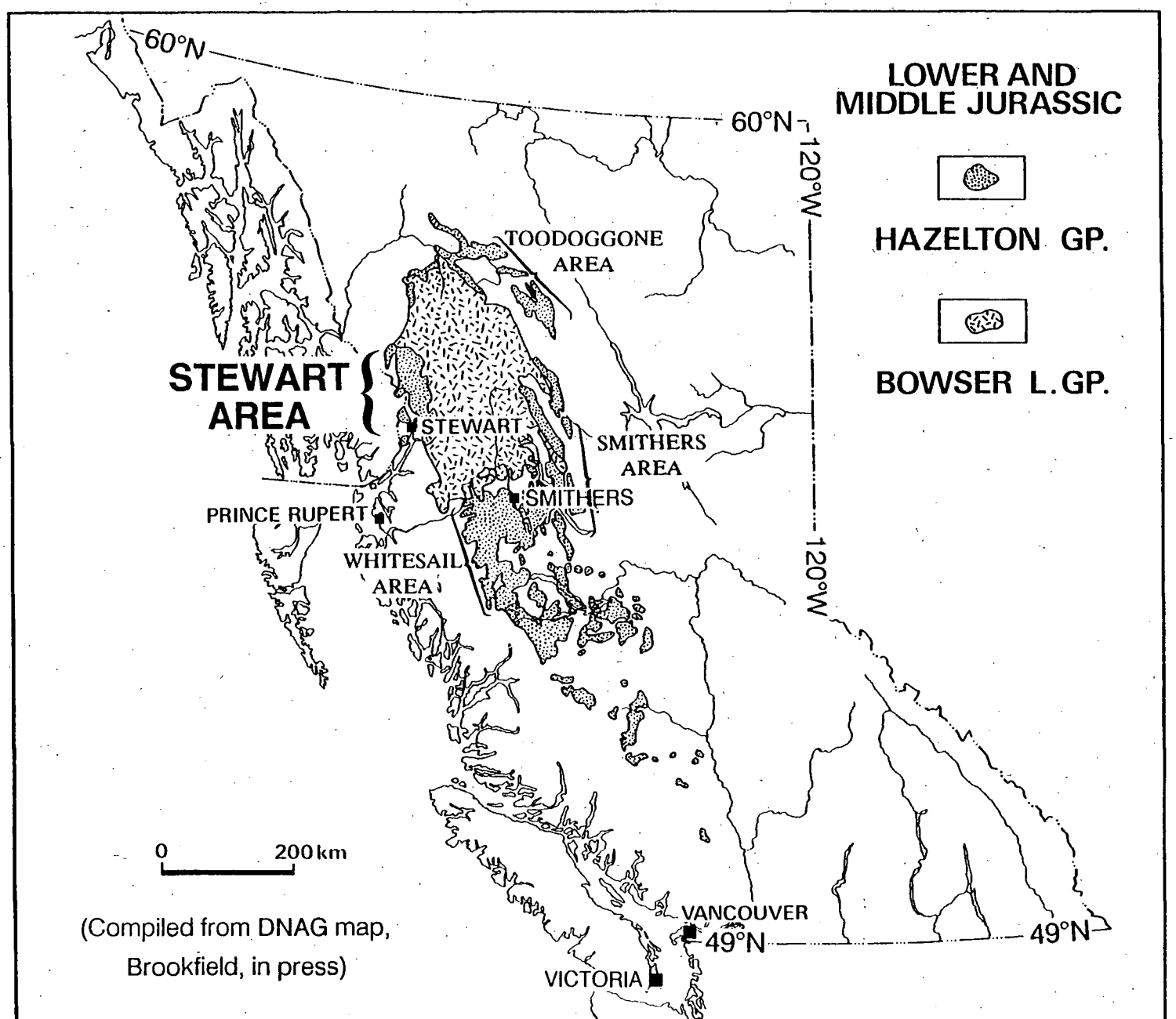

FIGURE 2.4: Distribution of the Hazelton Group and Bowser Lake Group rocks in central British Columbia

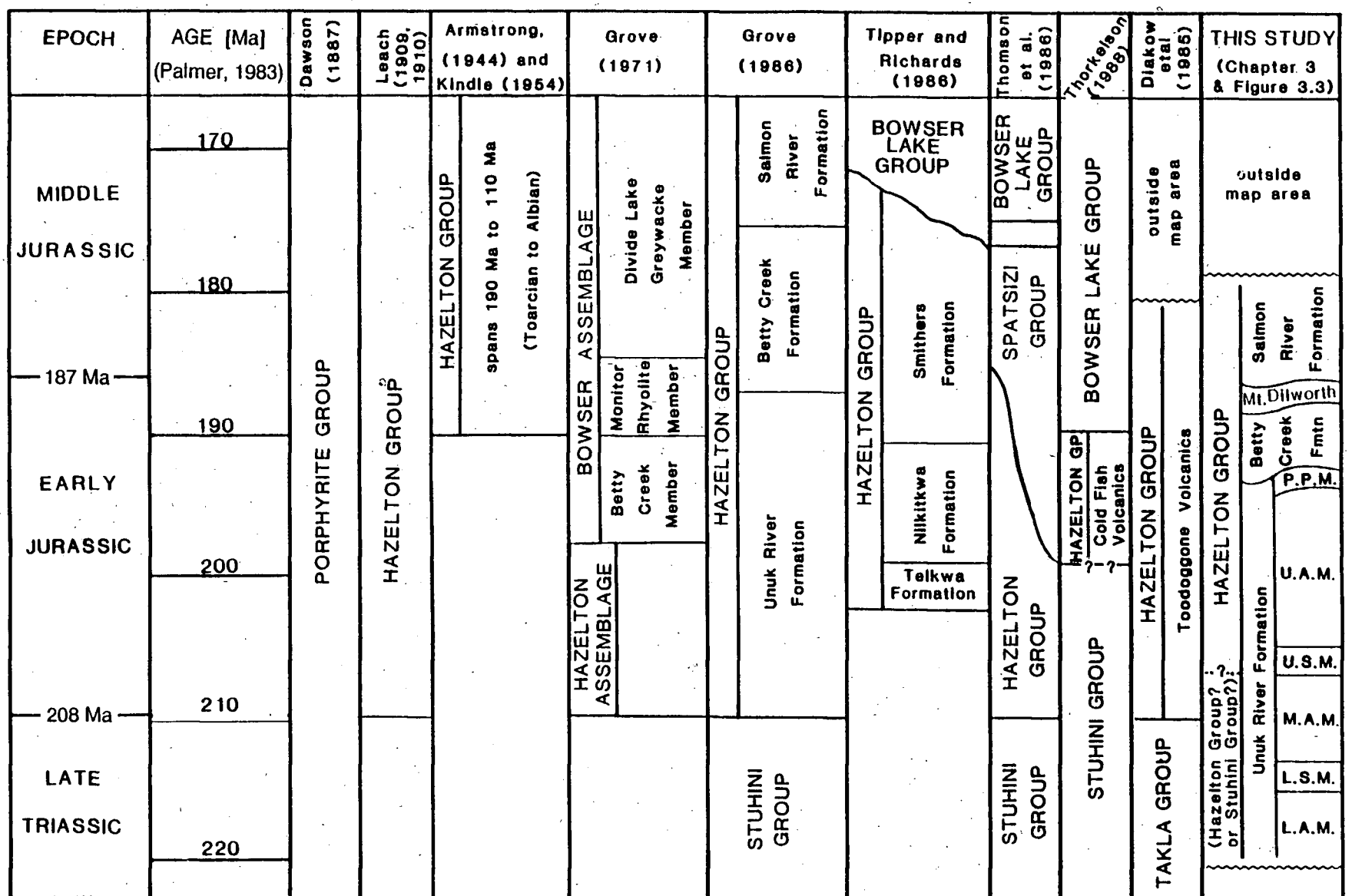

FIGURE 2.5: Evolution of stratigraphic nomenclature for the Hazelton Group (see also Figure 3.4)

P.P.M. = Premier Porphyry Member, U.A.M. = Upper Andesite Member, U.S.M. = Upper Siltstone Member,

M.A.M = Middle Andesite Member, L.S.M. = Lower Siltstone Member, L.A.M. = Lower Andesite Member

SMITHERS AREA (Southeast)

Tipper and Richards (1976) divided the Hazelton Group of the Smithers area into lower Telkwa Formation, middle Nilkitkwa Formation and upper Smithers Formation. Within the Sinemurian Telkwa Formation they recognized five distinct facies dominated by basaltic to rhyolitic volcanic rocks with laterally equivalent sedimentary rocks. Lower Pleinsbachian to Middle Toarcian Nilkitkwa Formation comprises interbedded shale, greywacke, andesitic to rhyolitic tuffs and breccias, and minor limestone. Middle Toarcian to Lower Callovian Smithers Formation consists of an assemblage of poorly sorted, fossiliferous, fine to medium grained clastic sedimentary rocks with minor intercalated tuffaceous shale, tuff and volcanic breccia.

STEWART AREA (West)

The large exposure of Hazelton Group rocks on the western rim of the Bowser Basin has been termed the Stewart complex (Figure 2.4, Grove, 1986). In the Stewart area, Grove divided the Hazelton Group into the lower Unuk River Formation, middle Betty Creek Formation and upper Salmon River Formation. Type areas for both the Betty Creek and Salmon River Formations are in the northern part of the present study area. Grove defined the Lower Jurassic, Hettangian to Lower Toarcian, Unuk River Formation as a predominantly andesitic sequence of lava flows, pyroclastic rocks and epiclastic and clastic sedimentary units. Lower to Middle Jurassic, Middle Toarcian to Middle Bajocian, Betty Creek Formation is characterized by bright red and green volcaniclastic sedimentary rocks with intercalated andesitic volcanic flows, pillow lavas, chert and carbonate lenses. Middle to Upper Jurassic, Upper Bajocian to Upper Oxfordian, Salmon River Formation is a thick sequence of complexly folded, colour-banded tuffaceous siltstones and lithic wackes. The base of the Salmon River Formation is marked by rhyolite, chert and carbonate lenses.

TOODOGGONE AREA (Northeast)

Hazelton age sequences on the northeast rim of the Bowser Basin include the Toodoggone volcanics, the Cold Fish volcanics and the Spatsizi "Group".

Carter (1972) named the informal Toodoggone volcanic belt that outcrops northeast of the Bowser and Sustut basins. The sequence is a thick pile of flat-lying subaerial dacitic tuffs and minor sediments that is coeval with Lower Jurassic Telkwa and Nilkitkwa Formations in the Smithers area (L. Diakow, personal communication, 1988).

Thomson *et al.* (1986) proposed the informal name, Cold Fish volcanics, for a volcanic package exposed along an 85-kilometre by 10-kilometre erosional window through overlying sedimentary rocks of the Bowser Lake Group. Thorkelson is presently examining these rocks in detail (1988) and has described them as a Lower Pleinsbachian to Lower Toarcian sequence of subaerial to submarine felsic to mafic lava flows and tuffs with minor shale and limestone. Cold Fish volcanics are therefore coeval with the Nilkitkwa Formation to the south and the upper Toodoggone volcanics to the east.

Thomson (1985) and Thomson *et al.* (1986) defined the Lower to Middle Jurassic Spatsizi Group at the northern end of the Bowser Basin. This varied sequence of sedimentary formations and tuffs are interpreted as the basinward sedimentary facies equivalents of the nearby Cold Fish volcanics. The sedimentary Spatsizi Group ranges in age from early Pliensbachian to early Bajocian, and is therefore contemporaneous with the sedimentary Nilkitkwa and Smithers Formations of the Hazelton Group defined by Tipper and Richards (1976).

WHITESAIL AREA (South)

The Whitesail Formation was defined by Woodsworth (1980), described in the Tahtsa Lake area by MacIntyre (1985), and dated at 184±4 Ma (van der Heyden, 1989, p.58-59). The unit has a gradational upper contact with thin bedded argillites, siltstones and cherts similar to the Smithers and Salmon River Formations. There are striking similarities between the Whitesail Formation (MacIntyre, 1985) and the Mount Dilworth Formation of

the Stewart area, which is described in this report. MacIntyre's (1985) description of the Whitesail Formation follows:

> FELSIC VOLCANIC -- CHERT UNIT (WHITESAIL FORMATION (?); LMjC) Siliceous light grey, greenish grey, and dark grey volcanic rocks conformably overlie, and are, in part, interbedded with red and green volcanic units of the Telkwa Formation. These rocks are typically thin bedded, and in places are finely laminated. The predominant rock types are welded lapilli tuff, mottled cherty tuff, and banded or massive dacite and rhyodacite. Eutaxitic textures are common in the more siliceous fragmental rocks. These felsic volcanic rocks grade upward into alternating beds of mottled and banded grey chert, siliceous argillite, and siltstone which may be part of the Smithers Formation. Stratabound lenses of pyrite and pyrrhotite, up to several centimetres thick, are common in this part of the section.

BOWSER LAKE GROUP: The Bowser Lake Group comprises a thick sequence of Middle Jurassic to Late Jurassic sedimentary and rare volcanic rocks. The type area lies northeast of the study area. Chert pebble conglomerates are diagnostic of the base of the Bowser Lake Group and these are overlain by shale, siltstone and intraformational conglomerates.

SKEENA GROUP: The Lower to Middle Cretaceous (Hautervian to Albian) Skeena Group consists of a sedimentary sequence of basal conglomerates overlain by a thick succession of distal turbidites. Minor amygdaloidal basalt flows are interbedded near the base of the sequence (MacIntyre, 1985).

KASALKA GROUP: MacIntyre (1985) defined the Middle to Late Cretaceous (105 to 80 Ma) Kasalka Group. The sequence consists of a predominantly volcanic package of basalts to rhyolites overlying a distinctive maroon basal conglomerate. Tuffaceous members

interbedded with Sustut Group sedimentary rocks are probably products of contemporaneous "Kasalka" explosive volcanism.

SUSTUT GROUP: The Sustut Group consists of a thick sequence of Middle Albian to Maastrichtian continental sediments with minor conglomerates and airfall ash tuffs.

EOCENE VOLCANICS: Volcanic rocks of the Ootsa Lake Group were first defined by Duffell (1959). Volcanics of the Endako Group were defined by Armstrong (1949). The Ootsa Lake Group is a succession of continental calcalkaline basalt to rhyodacite volcanic rocks. The Endako Group is preserved as scattered plagioclase porphyritic basalt flows.

MIOCENE TO HOLOCENE VOLCANICS: Souther (1977) labelled this region of more than 100 recent volcanic centres the Stikine volcanic belt. Lavas are mainly olivine basalt and range from 17 Ma to Recent, with the youngest age 130 years B.P. (Grove, 1986).

2.2 INTRUSIVE EVENTS IN STIKINIA

The magmatic evolution of the Canadian Cordillera was episodic, with distinct lulls between magmatic pulses. Episodes vary in location, intensity, duration, extent and character and appear to be linked to changes in plate motion. Armstrong (1988) and Woodsworth *et al.* (in press) define eight magmatic periods in northern British Columbia (Figure 2.6). Magmatic events which affected the Stewart area are reviewed here.

EARLY JURASSIC (210 to 185 Ma): Several plutons of economic significance were emplaced in the Canadian Cordillera in this period: the Guichon batholith, Copper Mountain intrusions, Iron Mask batholith and Island intrusive suite in southern British Columbia, and the Texas Creek plutonic suite in the Stewart area. All have been interpreted as the coeval subvolcanic magma chambers to early Jurassic island arc volcanic complexes.

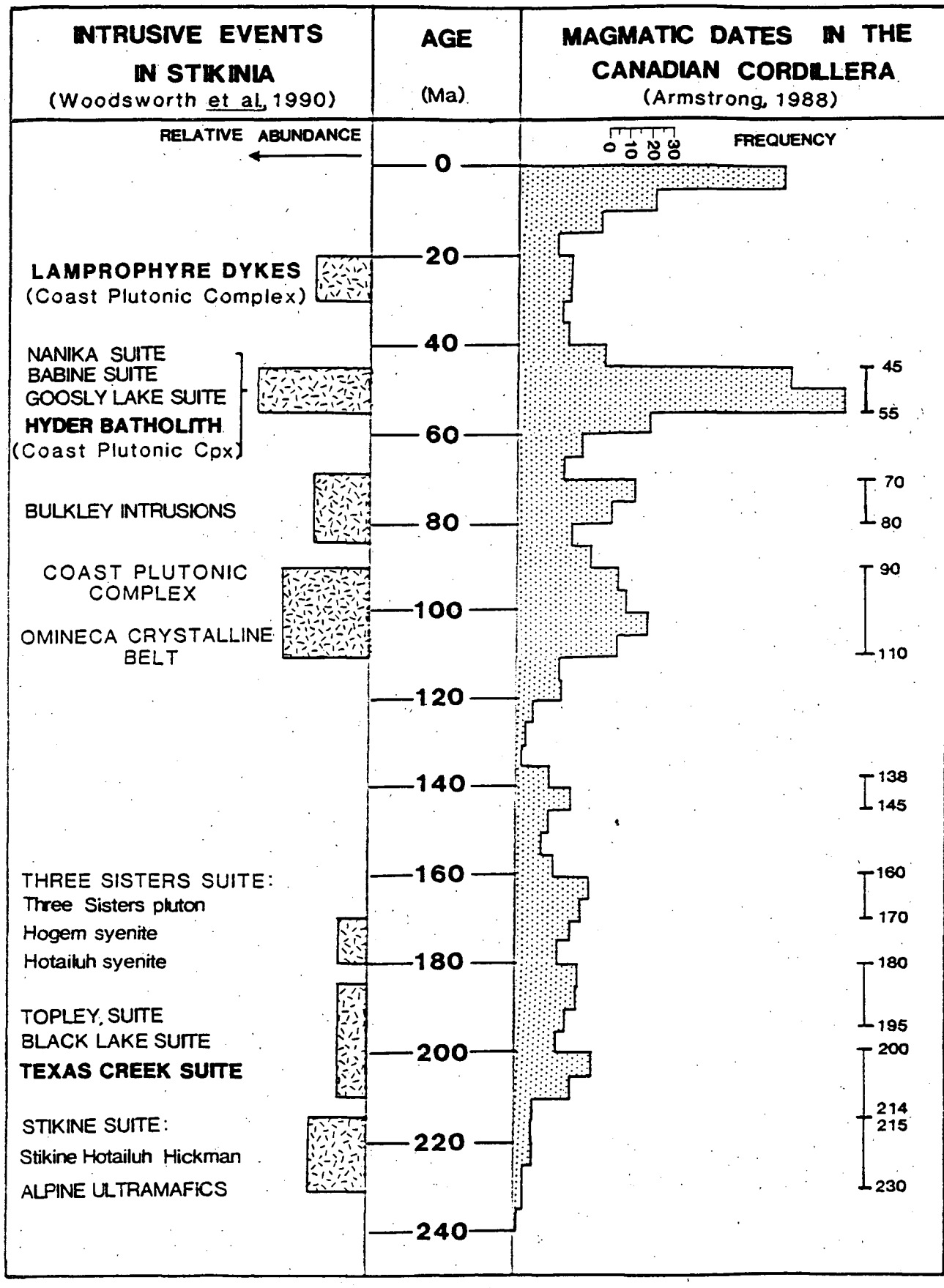

FIGURE 2.6: Intrusive events in Stikinia and the Canadian Cordillera

Within Stikinia Early Jurassic plutons are relatively small. All are interpreted to be the source of Hazelton Group volcanic rocks. The calcalkaline Texas Creek suite, within this study area, is represented by batholiths and stocks of distinctive coarse grained hornblende granodiorite that contain potassium feldspar megacrysts.

MIDDLE CRETACEOUS (110 to 90 Ma): Mid-Cretaceous granitic rocks are concentrated in two broad geographic belts that coincide with two zones of metamorphic rocks in the Canadian Cordillera: the Omineca Crystalline Belt and the Coast Plutonic Complex (Figure 2.1B). Mid-Cretaceous intrusive rocks are particularly abundant in the western portion of the Coast Plutonic Complex. Within this small time span these I-type plutons are interpreted to be pre-, syn- and post-tectonic with respect to the regional deformation and metamorphism (Woodsworth *et al.*, in press).

EARLY TERTIARY (55 to 45 Ma): Armstrong (1988) characterizes this final major magmatic episode as "a spectacular, short-lived event with rapid onset and equally rapid decline. The actual duration could not have been much more than 5 million years".

Within Stikinia small high-level Eocene plutons and dykes mark a period of widespread intrusive activity. Woodsworth *et al.* (in press) have defined three suites: the granitic Nanika suite, granodioritic Babine suite and gabbroic Goosly Lake suite (Figure 2.6). Several stocks are related to major molybdenum and copper-molybdenum orebodies: Berg, Kitsault, Ajax, Granisle and Bell. Intrusions are coeval with intermediate to felsic pyroclastic rocks of the Ootsa Lake and Buck Creek Groups and mafic volcanic rocks of the Endako Group.

2.3 TECTONIC HISTORY OF STIKINIA

2.3.1 SUBDUCTION ZONES

Prevailing tectonic models suggest there were two active subduction zones in the Triassic and early Jurassic, providing magmas to the separate Insular and Intermontane

terranes (Figure 2.7a; Griffiths, 1977; Griffiths and Godwin, 1983; Armstrong, 1988). Polarity of Triassic-Jurassic subduction zones is uncertain (Marsden and Thorkelson, in press) but from Cretaceous time onward there is strong evidence for eastward-dipping subduction (Armstrong, 1988).

Polarity of the Eocene volcanic arc is well documented (Ewing, 1981; Armstrong, 1988): subalkaline quartz diorite bodies occur in the Coast Plutonic Belt; Intermontane rocks grade eastward from calcalkaline to alkaline; easternmost occurrences are invariably alkaline, which is the normal pattern in wide subduction-related magmatic arcs (Gill, 1981).

2.3.2 TERRANE ACCRETION (from Armstrong, 1988)

Relationships between terranes are illustrated in Figures 2.2, 2.7, 2.8 and 2.9.

Earliest terrane linkage was between the Cache Creek and Quesnel terranes where Cache Creek rocks were caught up in an active accretion wedge (Monger, 1984; Patterson and Harakal, 1984). The timing of the connection between Stikinia and the Cache Creek is uncertain, but Upper Triassic rocks of both Stikinia and Quesnel terranes (Stuhini and Takla Groups) are very similar and Early Jurassic (212-204 Ma) plutonic rocks are common to both terranes. Therefore these three terranes were probably linked when Early Jurassic arc magmatism began in northern Stikinia (Monger, 1984).

Until Toarcian time contrasting environments existed on the partially assembled Stikinia, Cache Creek and Quesnel Terranes, and on the oceanic Slide Mountain Terrane to the east. But all four terranes, which were independent of each other in the Permian (Monger, 1977a), had been at least loosely assembled by the end of the Early Jurassic to form Superterrane I (Figures 2.2 and 2.8b).

As Superterrane I was thrust onto North America in early to mid-Jurassic time, these four loosely assembled terranes collided sequentially with each other. All deformation within Superterrane I terminated before emplacement of late Middle to early Late Jurassic plutons. This large part of the Canadian Cordillera was therefore in place against North America by the mid-Jurassic, but perhaps not at its present latitude.

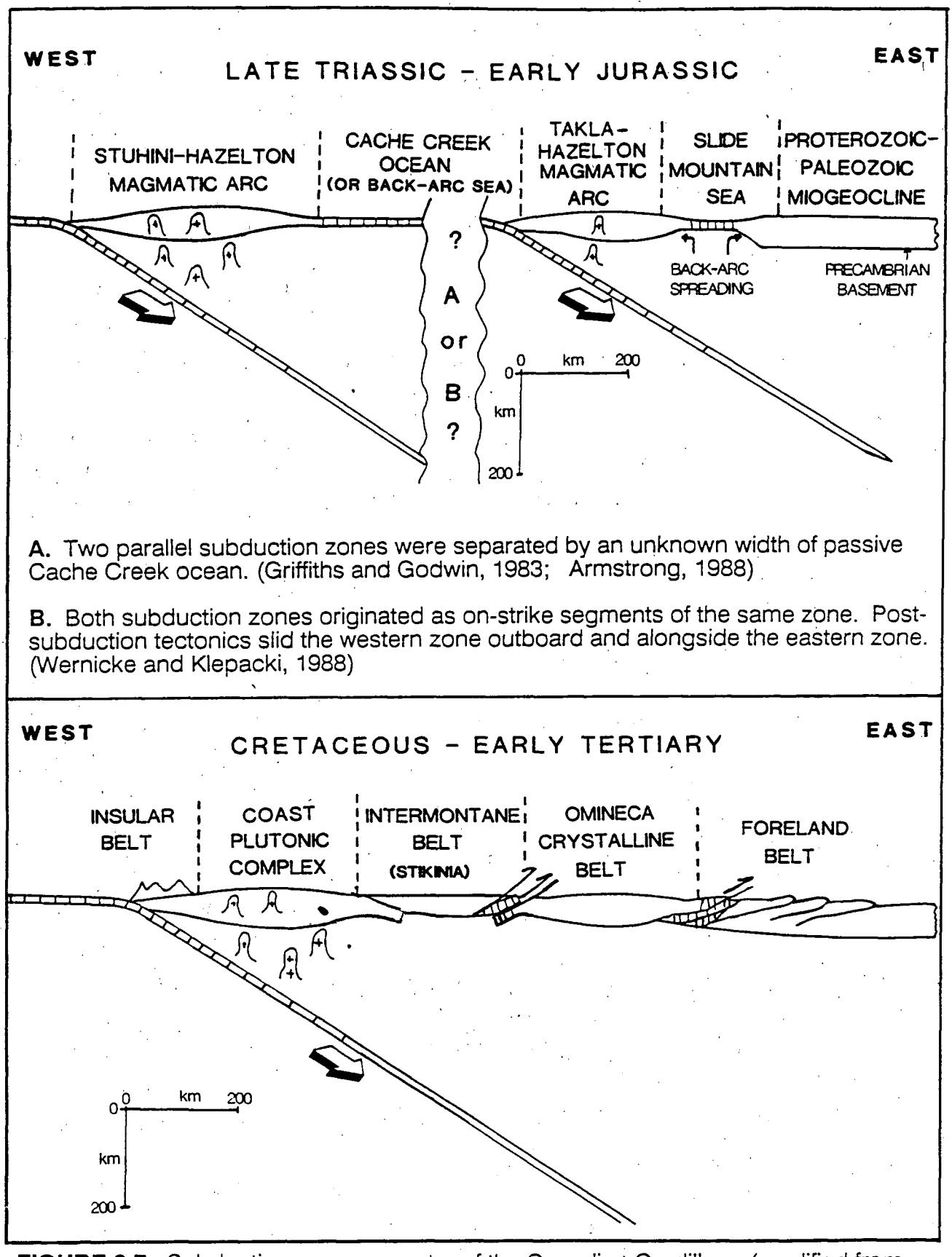

A. Two parallel subduction zones were separated by an unknown width of passive Cache Creek ocean. (Griffiths and Godwin, 1983; Armstrong, 1988)

B. Both subduction zones originated as on-strike segments of the same zone. Post-subduction tectonics slid the western zone outboard and alongside the eastern zone. (Wernicke and Klepacki, 1988)

FIGURE 2.7: Subduction zone geometry of the Canadian Cordillera (modified from Griffiths and Godwin, 1983)

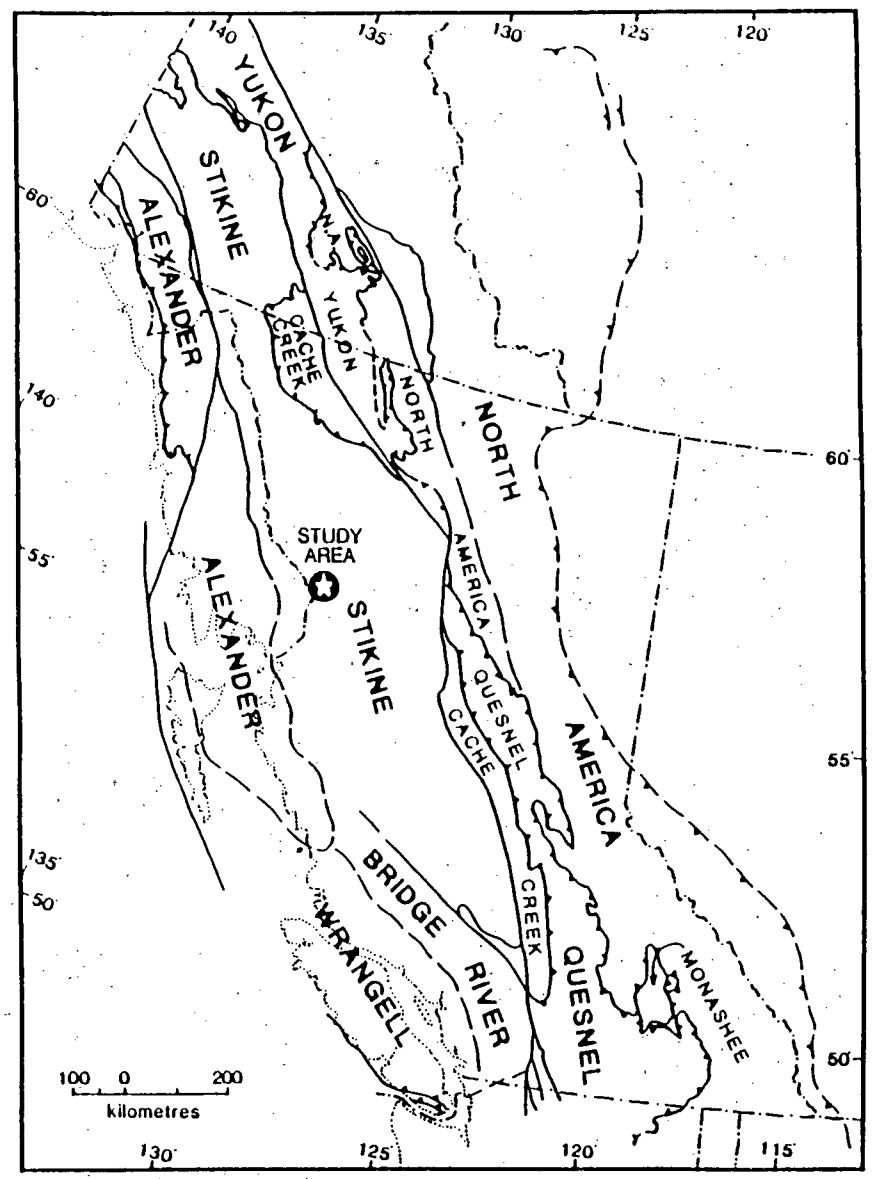

A. TERRANES (Armstrong, 1988)

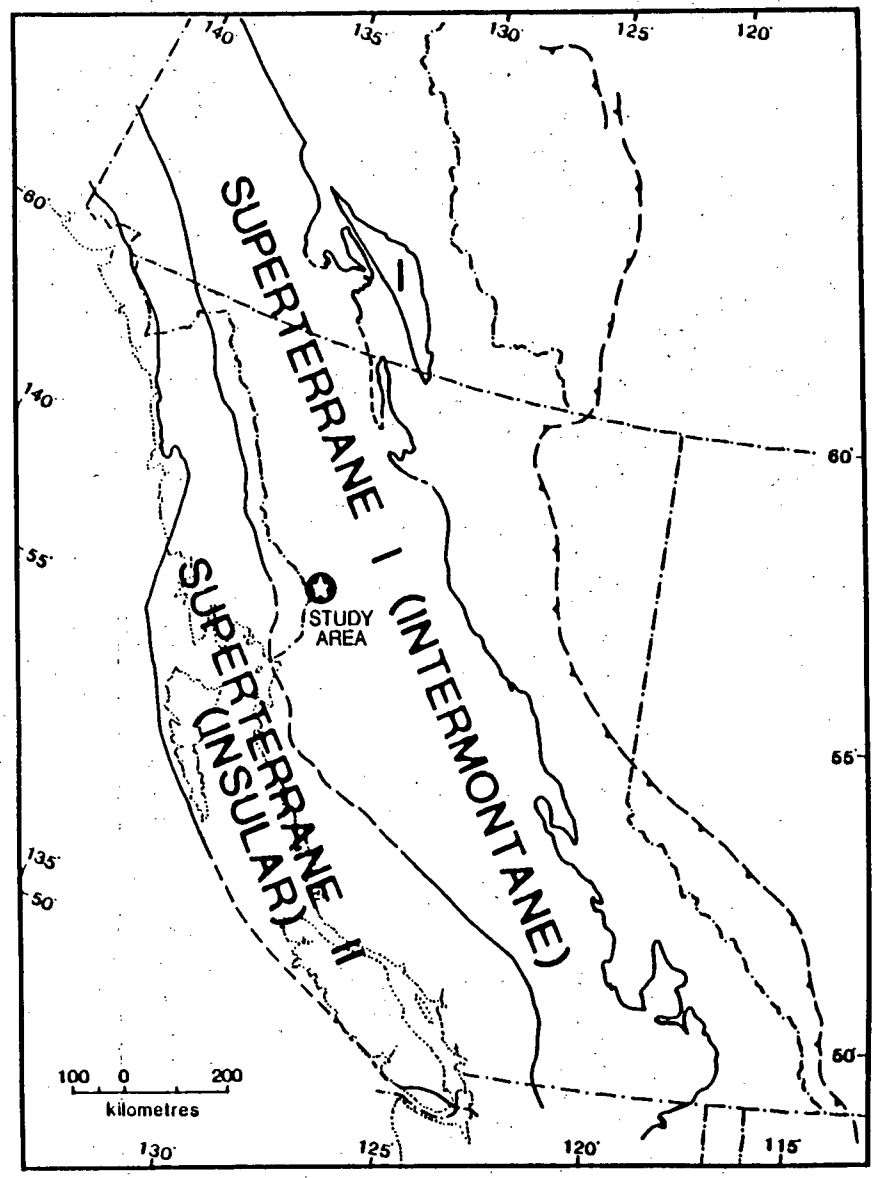

B. COMPOSITE TERRANES (SUPERTERRANES) (Monger, 1984)

FIGURE 2.8: Terranes and composite terranes of the Canadian Cordillera

The overlap assemblage of the Gravina-Nutzotin belt (Berg *et al.*, 1972) links the Alexander and Wrangell terranes in Alaska by Late Jurassic time to form Superterrane II (Coney *et al.*, 1980). Ongoing work suggests links between these terranes in the Paleozoic. The Jurassic Bridge River-Hozameen-Tyaughton-Taku ocean separating Superterranes I and II closed between early to mid-Jurassic.

Thus, assembly of the Canadian Cordillera was largely complete by the Late Jurassic, and by mid-Cretaceous an Andean-type magmatic arc was established on the Cordilleran margin of North America.

2.4 GEOLOGIC HISTORY OF STIKINIA

A synthesis of the preceeding stratigraphic, plutonic and tectonic relationships is summarized in this section and illustrated schematically in Figure 2.9.

380 TO 330 Ma: The lower and middle Stikine assemblages, may represent remnants of two mid-Paleozoic volcanic arcs.

280 TO 250 Ma: The unconformable upper Stikine assemblage of may record a third magmatic arc complex.

250 TO 230 Ma: The Tahltanian orogeny deformed the Stikine assemblage prior to deposition of Upper Triassic volcanics.

230 TO 210 Ma: The volcanic arc assemblages of the Stuhini/Takla Group were produced by two subduction zones. Cache Creek and Quesnel terranes linked in the Late Triassic, but Stikinia was not yet linked to other terranes.

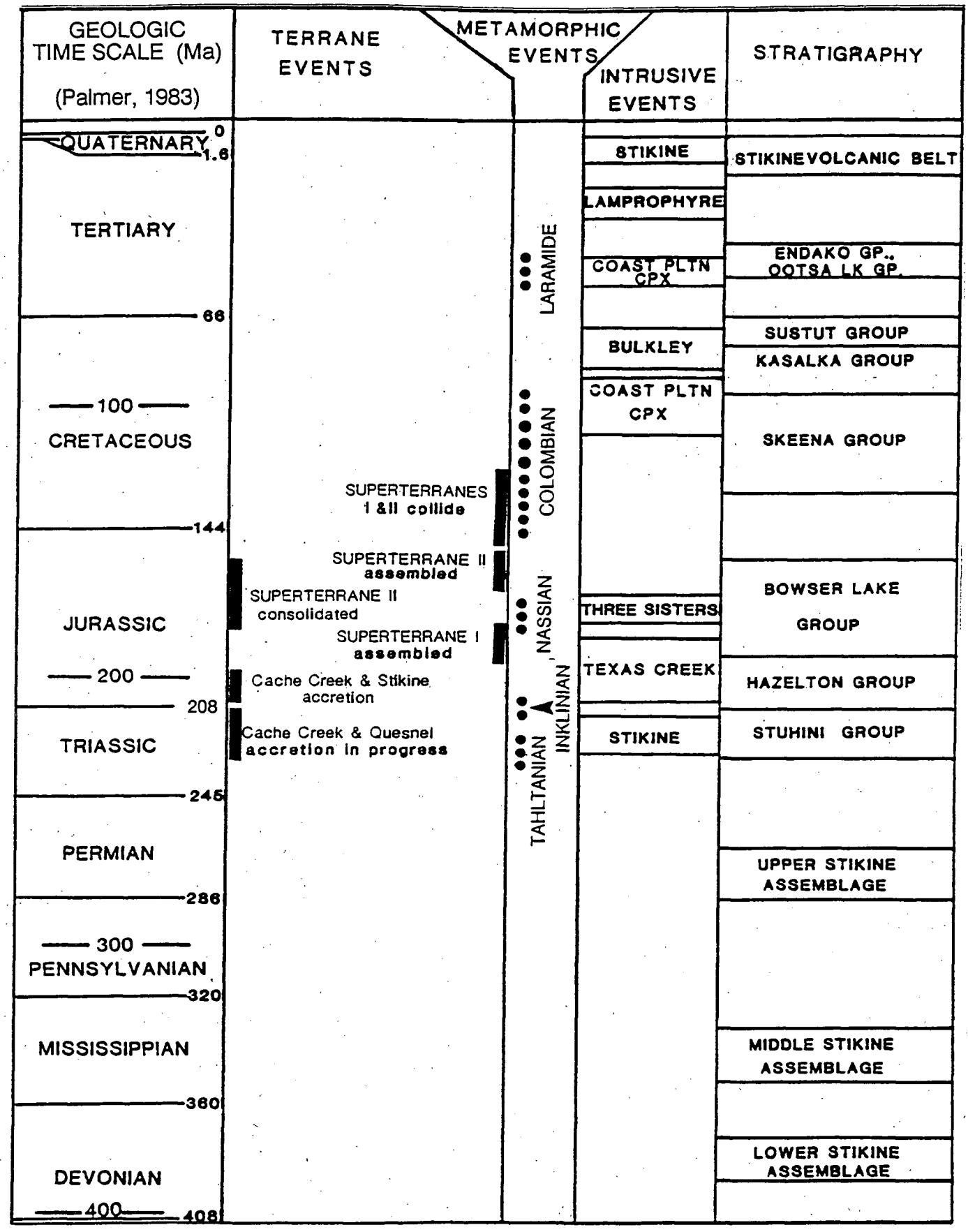

FIGURE 2.9: Geological history of Stikinia

210 TO 190 Ma: In earliest Jurassic, plutons intruded and pinned the collision zone of the Cache Creek and Quesnel terranes. The partially assembled Superterrane I (Stikinia-Cache Creek-Quesnel) linked with the Slide Mountain terrane in Toarcian time (190 Ma).

On Stikinia, Upper Triassic Stuhini/Takla mafic volcanic strata were gradational into Early Jurassic intermediate to felsic Hazelton Group units. Early Jurassic batholiths throughout the Intermontane Belt were coeval subvolcanic magma chambers within the "Hazelton" island arc complex, analogous to modern arcs of the southwest Pacific.

190 TO 155 Ma: One east-dipping subduction zone operated through the Late Jurassic. In the period 190 to 180 Ma the linked terranes of Superterrane I collided with North America. Starting in Toarcian time, Slide Mountain rocks were thrust eastward onto the North American continental margin. Between Early to Middle Jurassic, Toarcian to Bajocian, time, Stikinia was overridden by the Cache Creek terrane. Mid-Jurassic plutons pinned these consolidated terranes and then a prolonged magmatic lull began throughout the Canadian Cordillera.

The Smithers/Whitesail/Mount Dilworth/Salmon River/Spatsizi Formations of the upper Hazelton Group accumulated between 190 to 180 Ma. The Bowser Lake Group was deposited in the Bowser Basin between 180 and 150 Ma (Cookenboo and Bustin, 1989). The Bowser Basin was a slowly sinking depression that accumulated clastic sediment from surrounding elevated areas. It has been devoid of magmatism since the Middle Jurassic, earning it the label "cold spot" (Armstrong, 1988).

155 TO 125 Ma: From Early Cretaceous onward a single eastward-dipping subduction zone developed on the Cordilleran margin. The major magmatic lull continued throughout much of the Early Cretaceous. Sediments of the Bowser Lake Group accumulated until 150 Ma. From 150 to 125 Ma the absence of both plutonic and volcanic rocks coincides with regional gaps in the stratigraphic record, indicating a time of emergence, erosion and external drainage (Armstrong, 1988; Cookenboo and Bustin, 1989). Renewed plutonism began about 130 Ma within the Coast Plutonic Complex.

125 TO 110 Ma: The magmatic lull continued in the Intermontane Belt, but magmatic activity in the Coast plutonic complex increased. Deposition of Skeena Group sediments and Kasalka Group volcanics progressed throughout this period.

110 TO 90 Ma: An Andean-type, continental margin magmatic arc was fully established by the mid-Cretaceous. Renewed magmatism along the western Coast Plutonic Complex and the Omineca Belt peaked during this period. Accompanying tectonism, deformation and regional metamorphism within the western Intermontane Belt peaked from 110 to 100 Ma.

90 TO 70 Ma: Transpression related to oblique subduction produced right-lateral transcurrent faulting, carrying displaced terranes northward (Monger, 1984). Right-lateral displacement along the Tintina Fault on the west side of the Omineca Belt moved the Bowser Basin hundreds of kilometres northward (Eisbacher, 1981).

Plutonism, with extrusive phases, was abundant in Stikinia and in the western and central parts of the Coast plutonic complex. Sedimentary rocks and intercalated tuffs of the Sustut Group were deposited during uplift of the Omineca Belt to the east and the Coast Plutonic Complex to the west (Eisbacher, 1981).

70 TO 60 Ma: No evidence of volcanism or sedimentation was preserved on Stikinia during this short magmatic lull.

60 TO 40 Ma: This period spans the final major magmatic episode in the Canadian Cordillera. Within Stikinia, plutons were small, high-level stocks and dykes with contemporaneous volcanic packages.

40 to 20 Ma: This period was characterized by localized plutonism in the Coast Plutonic Complex. High-level granite and granite porphyry intrusions include the Quartz Hill molybdenum deposit. The Oligocene was marked by widespread, but volumetrically small, lamprophyre dyke emplacement.

Cooling, uplift and unroofing of the Coast Plutonic Complex accompanied east-west extension represented by north-trending faults. North- to northeast-trending faults and joints controlled distribution of Oligocene to Recent intrusive and volcanic rocks.

20 TO 0 Ma: East-dipping subduction has continued along our west coast until the present. Throughout the Miocene a flood of alkali-olivine basalt issued from a multitude of vents and fissures to form plateau lavas. Intermittent eruption has continued throughout Pliocene, Pleistocene and into Recent time.

CHAPTER 3
GEOLOGY OF THE STEWART MINING CAMP

3.1 LITHOSTRATIGRAPHY AND NOMENCLATURE

A simplified geological map of the study area is presented in Figure 3.1; more detailed geology is presented at 1:50,000 scale on Figure 3.2. Regional stratigraphy presented in this report (Figure 3.3) is the latest step in the evolution of stratigraphic subdivisions started by McConnell (1913) and revised by Schofield and Hanson (1922), Hanson (1929, 1935) and Grove (1971, 1973, 1986) (Figure 3.4). Grove (1973, 1986) established the current stratigraphic nomenclature. Only one modification is made, the felsic volcanic sequence, Monitor Rhyolite, which Grove included within the Salmon River Formation, has been raised to formational status in this study and has been renamed the Mount Dilworth Formation or Mount Dilworth Dacite.

Fossil samples from the map area have been collected and reported by workers such as Schofield and Hanson (1922), Hanson (1935), Grove (1971), Grove (1986), Anderson (written communication, 1986), and Brown (1987). All previously reported and newly located fossil occurrences are shown on Figure 3.2.

3.1.1 Stuhini Group

Some features suggest that the lower three members of the Unuk River Formation of the Lower Jurassic Hazelton Group might be more appropriately included in the Upper Triassic Stuhini Group. The Lower Andesite Member includes fine grained pyroxene crystal tuffs. The Middle Andesite Member includes similar fine grained crystal tuffs and many local exposures of coarse grained pyroxene porphyritic flows. Brown (1987) reported an imprecise zircon date of 210(+24,-14) Ma for welded andesitic tuff within the overlying Upper Andesite Member.

There are no fossils and no dates to indicate the absolute age of these lower members. Furthermore there is no consensus on criteria (lithostratigraphy, petrochemistry,

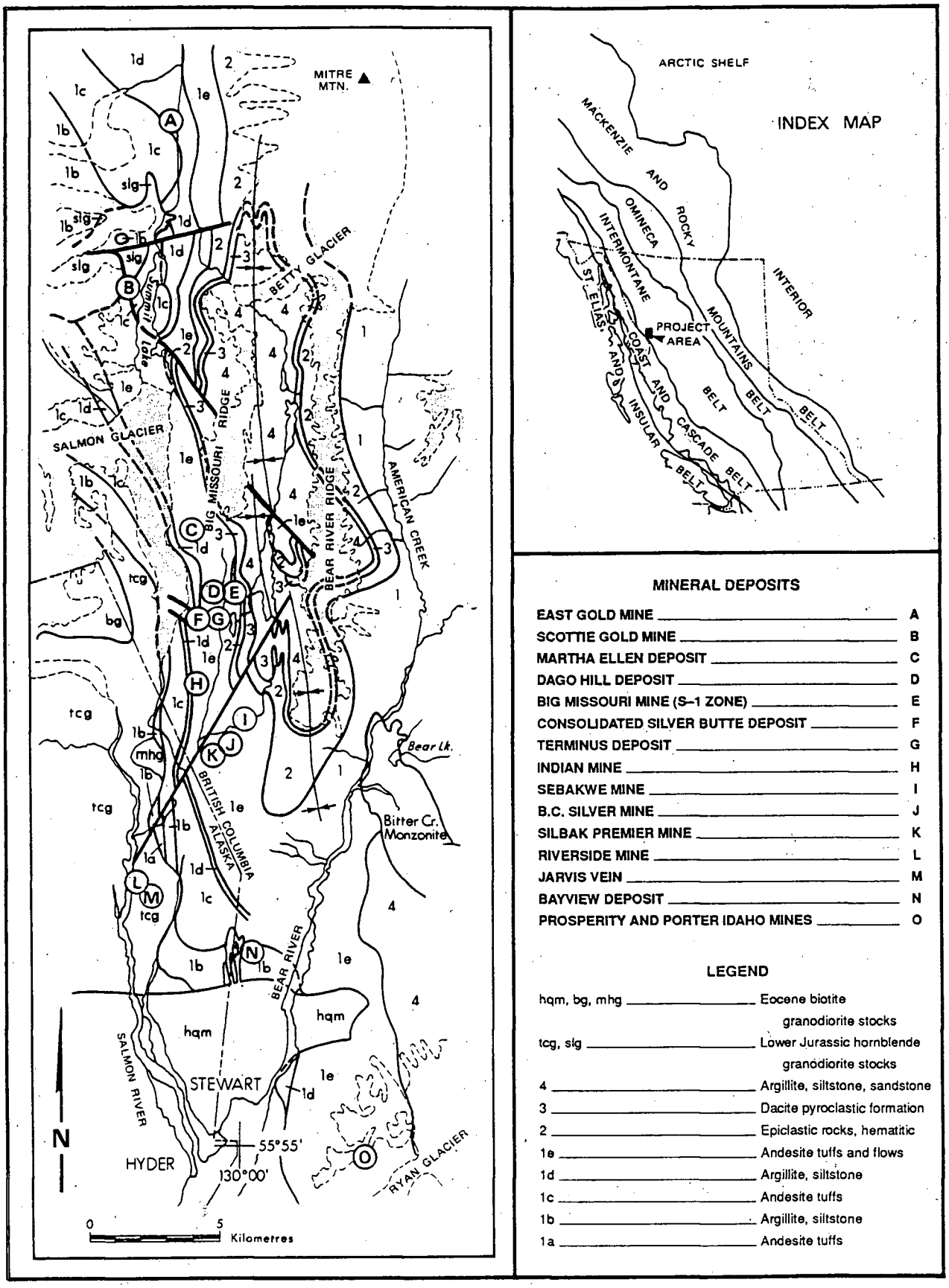

FIGURE 3.1: Geologic setting of the study area

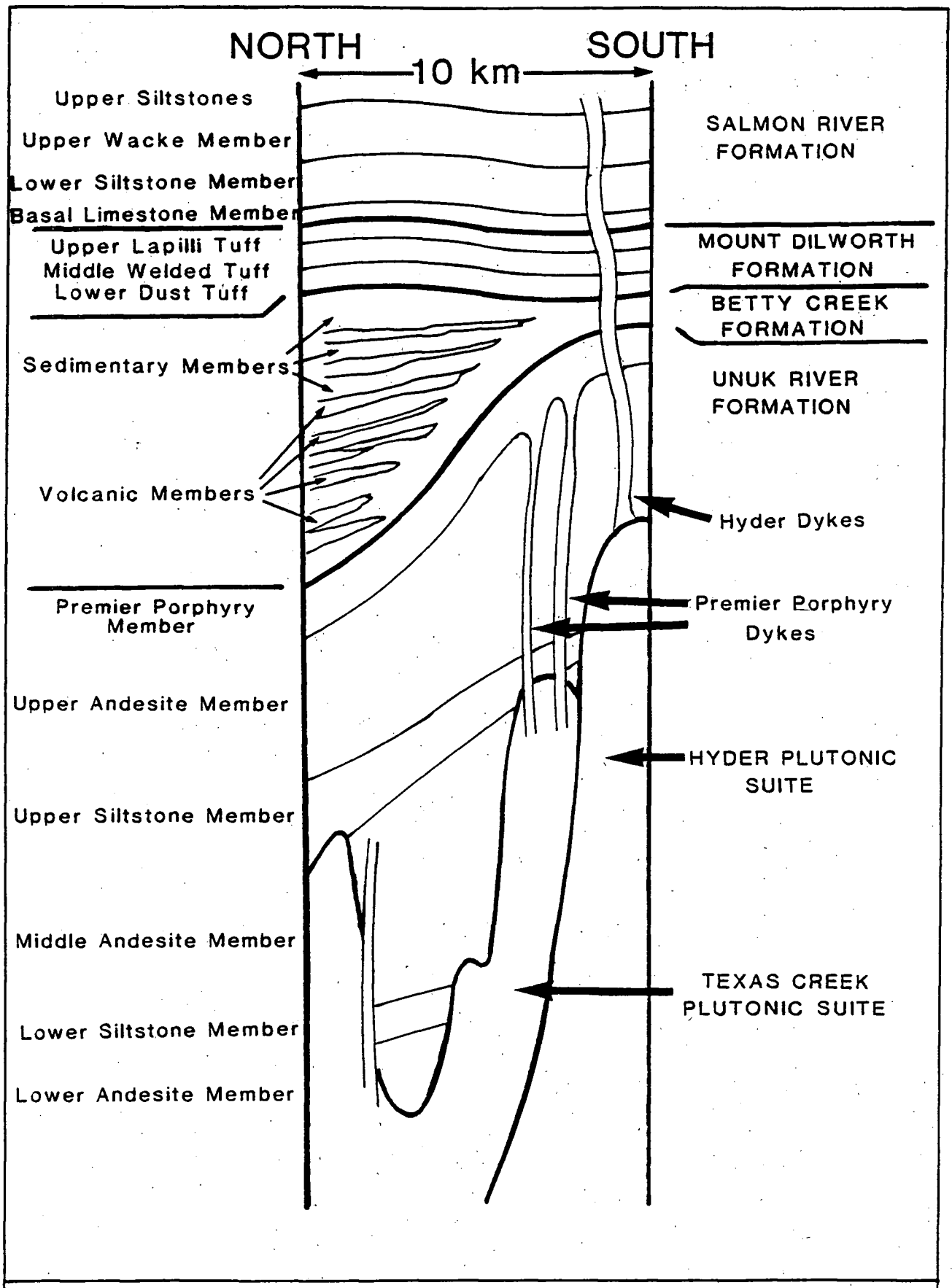

FIGURE 3.3: Schematic stratigraphy of the Stewart mining camp

EPOCH	AGE	McConnell 1913	Schofield and Hanson 1922	Hanson 1929	Grove 1986		Read 1979	Galley 1981	Brown 1987	THIS STUDY
Upper Jurassic		Nass Formation	Nass Formation	Nass Formation	BOWSER LAKE GP	Nass Fm	BOWSER LAKE GROUP	BOWSER LAKE GROUP	BOWSER LAKE GROUP	outside map area
Middle Jurassic	Cll	Bear River Formation	Salmon River Formation	Bear River Formation	HAZELTON GROUP	Salmon River Fm				
	Bth									
	Bjc		Bear River Formation			Betty Creek Fm	1	1a to 1d	SPATSIZI GP	Salmon River Fm
	A								gap	
Lower Jurassic	Toarcian	Bitter Creek Formation		Bitter Creek Formation		Unuk River Fm	2		HAZELTON GROUP: Hr Hw	Mount Dilworth Fm
	Pliensb.						3	1e and 2a	H, Hg, Hm	Betty Creek Fm
	Sinemur.						4	2b	Hv	Unuk River Fm
	Hettang.								Hs, Hv	
Upper Triassic	Norian				STUHINI GROUP		?	?	?	STUHINI GP? / outside map area

FIGURE 3.4: Evolution of stratigraphic nomenclature and age assignments for the Stewart mining camp

geochronology, biostratigraphy) for definition of the Stuhini/Hazelton Group boundary so it seems simplest to include these members in the Hazelton Group pending further studies.

3.1.2 Hazelton Group

The Hazelton Group is a mixed volcanic and sedimentary rock sequence of that spans the Lower Jurassic epoch. Volcanic units progressively change in composition from basalt through andesite to dacite over a total thickness of five kilometres (Figure 3.9). This compositional change is paralleled by a change in colour from dark olive green to light grey, and by progressive changes in associated phenocrysts (Figure 3.5).

3.1.2.1 UNUK RIVER FORMATION

The Unuk River Formation is a thick sequence of massive green to greenish grey andesitic tuffs and lava flows with minor interbeds of sedimentary rocks. The thick andesitic package was termed the Unuk River Formation based on Grove's (1973, 1986) regional studies north of the present map area. This unit hosts all major mineral deposits in the map area.

Distribution and Thickness

The Unuk River Formation is exposed along a north-south belt through the centre of the map area. The base of this sequence lies to the west engulfed in the Coastal batholith, but the formation is at least 4500 metres thick within the map area.

Contact Relationships

The upper contact is typically a sharp, ragged to smoothly undulating erosional boundary with significant paleorelief. Porphyritic andesite flows or tuffs are overlain by grits to conglomerates of the Betty Creek Formation.

Stratigraphy

Significant revisions have been made to Grove's (1973, 1986) internal stratigraphic divisions. These follow from recognition of regionally distributed feldspar porphyritic

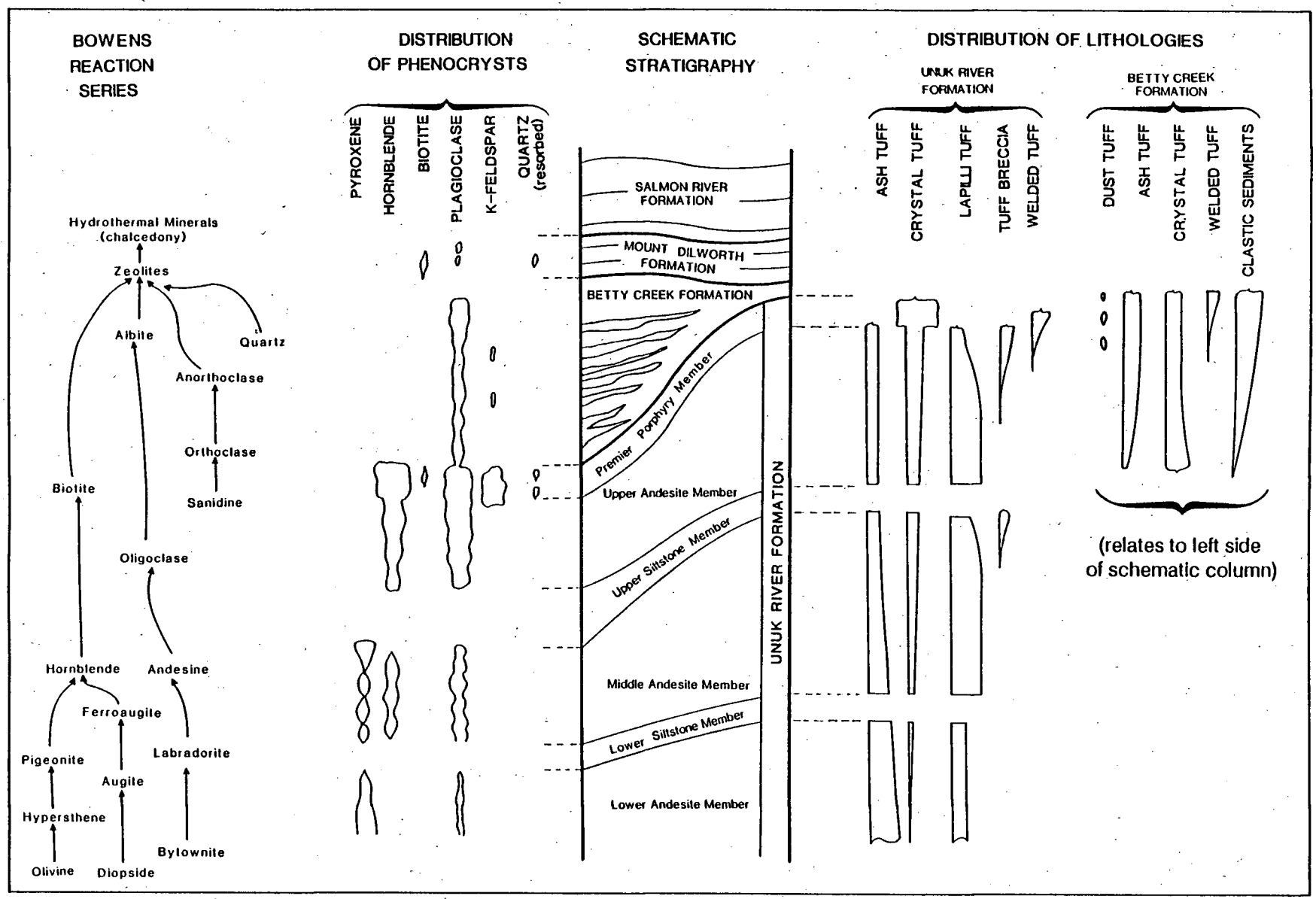

FIGURE 3.5: Phenocryst and fragment variations in schematic Stewart stratigraphy

andesite flows and tuffs at the top of the formation and two continuous siltstone members within the succession. The dark grey to black, thin bedded siltstone units mark periods of volcanic quiescence and provide important stratigraphic and structural markers within the predominantly andesitic succession. They facilitate determination of bedding attitudes, stratigraphic tops and fault offsets throughout the map area.

Overall, the Unuk River Formation is a thick, monotonous sequence of medium green andesitic rocks that are preserved as weakly to moderately foliated greenschists. In more detail, the volcanic rocks range from dust to ash tuff, crystal tuff, lapilli tuff, monolithic pyroclastic breccia and lava flows. Plagioclase and less commonly hornblende or augite phenocrysts or crystal fragments characterize the volcanics. Phenocryst distribution is illustrated in Figure 3.5. Individual tuff beds show little evidence of sorting, or preferred orientation of crystals or lithic fragments except in zones of ductile deformation.

Intermittent exposures and rapid lateral facies changes in the tuffs hinder tracing and correlation of individual strata along strike, but a general zoning pattern of clast size and crystal abundances within the sequence has been recognized (Figure 3.5). Lapilli tuffs are uniformly distributed but medium to coarse ash tuffs are most abundant in the lower part of the sequence and crystal tuffs and crystal-lithic tuffs are somewhat more abundant in the upper part of the sequence. Tuff breccias occur near the top of both the middle and upper members of the sequence. Very coarse tuff breccias are known only at the top of the succession near the Mount Dilworth vent area.

Lower Andesite Member

The Lower Andesite Member has been examined along the Granduc road near the wreckage of Nine-mile bridge, along the southern spine of Mineral Hill, and along the east bank of the Salmon River in the vicinity of Flower Pot Rock. The unit is at least 500 metres thick, but the lower contact has not been defined. This member is composed of massive to well bedded ash tuffs (Plate 3.7B). No lapilli were noted in outcrop and no phenocrysts

were noted in hand samples, but a thin section of ash tuff collected near Flower Pot Rock has abundant fine grained (~0.5 mm) pyroxene grains and crystals.

Lower Siltstone Member

The Lower Siltstone Member lies west of the map area along most of the Salmon River valley. In the north, it forms a roof pendant in the Summit Lake granodiorite, and reappears at the Outland Silver Bar prospect (Figure 3.2A and Klepaki, 1980). The Lower Siltstone Member crops out again in the bed of the Salmon River at the north and south ends of Mineral Hill and is exposed along the southern spine of Mineral Hill. Thickness ranges from 50 to greater than 200 metres.

Middle Andesite Member

The Middle Andesite Member is best exposed on the hill south of Indian Lake and in the area around the Scottie Gold mine. The unit is at least 1500 metres thick and comprises dust tuff, ash tuff, lapilli tuff and minor tuff breccia with interbedded medium to coarse volcaniclastic sedimentary rocks.

Massive pyroxene porphyritic flows crop out near the top of the Middle Andesite Member around the Granduc millsite and along the road network to the Roanan vein and other deposits south of the Alaskan border. An isolated exposure of massive augite porphyritic basalt in the Long Lake area (Dupas, 1985) may be the stratigraphic equivalent of the pyroxene porphyries of the Middle Andesite Member (Figure 3.6).

Upper Siltstone Member

The Upper Siltstone Member can be traced through the map area from the Haida claim (Portland prospect) at the north edge of the map to the Bear River Ridge between Mount Dolly and Mount Welker. Offsets of this unit provide evidence for major movement along the Millsite, Morris Summit and Slate Mountain faults.

The unit varies in thickness from as little as 50 metres near the Indian mine to more than a kilometre thick in the northern map area. The upper contact can be a sharp change

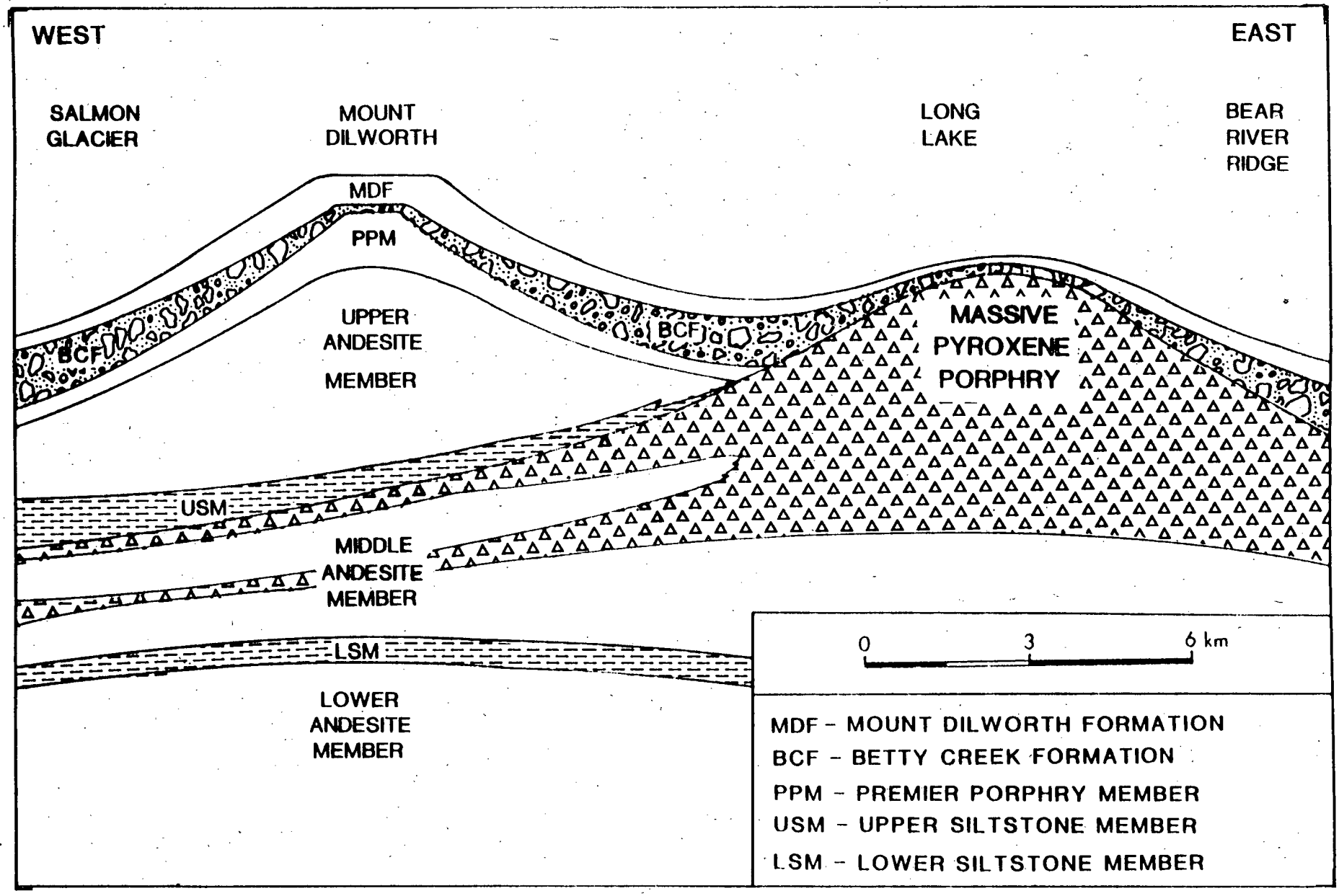

FIGURE 3.6: Schematic stratigraphic correlation for pyroxene porphyry units of the Middle Andesite Member. Vertical exaggeration 2:1.

from dark grey thin bedded siltstone to massive green andesitic tuff, as along the western slope of Troy Ridge; but typically the thin bedded strata is overlain with a sharp upper contact by the basal black tuff facies of the Upper Andesite Member.

On the west side of the Tide Lake flats the Upper Siltstone Member hosts precious metal veins at the East Gold mine. Pyritic areas in the siltstones produce brightly coloured, gossanous exposures that crop out from north of the East Gold mine southward to the Millsite fault (Figure 4.1a). Purple-brown hornfelsed calc-silicate-veined siltstone that hosts minor sulphide mineralization in the Molly B and Red Reef adits on Mount Rainey are also Upper Siltstone Member rocks (Figure 4.1b).

Upper Andesite Member

The Upper Andesite Member is a thick sequence of massive tuffs with minor flows and local lenses of sedimentary rock. It is about 2000 metres thick and capped by regionally extensive crystal tuffs of the Premier Porphyry Member.

Black Tuff Facies

The base of the Upper Andesite is marked by a 0 to 250 metre thick, massive black fine grained to locally fragmental rock that has been called basalt flow and basaltic andesite tuff (Galley, 1981, p.79), dacite (McGuigan and Dawson, 1985) and black andesite tuff (Alldrick, 1982, 1987). The upper contact of this unit grades over 10 to 50 centimetres into green chloritic tuffs. This gradational colour boundary undulates across large, texturally uniform outcrops. These relationships suggest that the black rocks are andesitic airfall tuffs that were deposited on top of the thin bedded silts in a very shallow anoxic basin. The tuff apparently accumulated until it built up to and above sea level where it was preserved without carbon.

Thin sections show that the massive black rocks include not only layers of carbon-impregnated ash tuff, feldspar crystal tuff, and lapilli tuff, but also massive siltstone, feldspathic wacke, and granule to pebble conglomerates of roughly-rounded volcanic debris. Therefore the unit consists of intimately mixed massive sediments and tuffs,

transitional between underlying thin bedded black siltstones and overlying massive green andesite tuff. Whole rock analyses plot as andesite (Appendix I).

Main Sequence

A monotonous succession of greenstones and minor sedimentary lenses comprises the main sequence of the Upper Andesite Member. These rocks have previously been studied in detail by Grove (1971, 1973, 1986), Read (1979), Galley (1981) and Brown (1987). It is difficult to distinguish individual units because of the uniform green colour and pervasive foliation of the rocks. Lithologies range from dust and ash tuffs to lapilli tuffs and tuff breccias; crystal tuffs display varying abundances of plagioclase and hornblende. Overall variations in clast size and in phenocryst composition and abundance are illustrated in Figure 3.5.

Generally massive fine grained aphanitic ash tuffs have local fine plagioclase and hornblende phenocrysts set in an altered ash matrix. These rocks are pervasively chloritized and contain up to five percent disseminated fine grained pyrite. Chlorite defines the penetrative foliation of the rocks and gives a phyllitic sheen to some broken surfaces.

Fragmental rocks are open framework volcanic breccias and may represent airfall lapilli tuff, flow breccias, ungraded pyroclastic flow breccias, or less likely, lava flow breccias. Exposures are typically massive with no preferred orientation but local zones of ductile deformation result in plate-like flattened fragments. Correlation of these fragmental units, even over short distances between outcrops and drill holes, is difficult. The apparent lack of continuity could be due to rapid facies variations, slumping, post-depositional erosion and small scale, post-lithification faulting.

The top of the Upper Andesite Member is andesitic lapilli tuff to coarse tuff breccia. Regionally, the largest angular fragments range up to 40 centimetres long. In one small area on Mount Dilworth a single bed contains blocks that are up to 1.5 metres across including an intact hexagonal fragment of columnar-jointed andesite, 1.2 metres across.

Deep green to greyish green fragmental rocks are typically monolithologic; fragments are generally matrix-supported and textures are displayed best on recently glaciated surfaces or on deeply weathered surfaces. Fragments are typically angular, but some exposures show subrounded and well-rounded clasts. Fragmental rocks contain lithic, pumice and crystal fragments. Lithic fragments consist of varieties of ash tuffs, variable plagioclase and hornblende porphyritic rocks, and lithified fragmental rocks. The matrix is composed of fine lithic chips and glass shards in a groundmass of quartz, feldspar and sericite-, chlorite- and carbonate-altered ash and dust. Some weathered exposures show resistant fragments in recessive matrix, others resistant matrix with recessive fragments. Possibly the former represent airfall lapilli tuffs and the latter either hot pyroclastic flows or flow top breccias.

Pyrite is disseminated in both fragments and groundmass as angular subhedral grains to euhedral cubes. Typically pyrite makes up about 2 percent of these rocks, but local exposures of intense chlorite-pyrite alteration contain up to 5 percent disseminated medium grained pyrite; these zones are within 2 kilometres of the Silbak Premier mine.

Within the Upper Andesite Member, local lenses of maroon to purple to grey siltstone, sandstone and conglomerate are preserved. Epiclastic rocks record periods of erosion and volcanic quiescence during the overall development of the andesitic volcano. These hematitic sedimentary units are distinctive and may be useful markers on a property scale.

A thin lens ($\leq$30 metres) of black to dark grey sedimentary rock crops out high on the northwest slope of Troy Ridge (Figure 3.2a). The unit is exposed around the shore of a long, narrow lake and consists of thin bedded siltstone and gritty limestone. The unit wedges out to the south but its northern extent is unknown. These rocks mark local subaqueous conditions on what is interpreted to be a subaerial volcanic edifice; conditions of formation might be analogous to sediments in Spirit Lake at Mount Saint Helens, Washington.

Premier Porphyry Member

This distinctive member contains plagioclase, potassium feldspar and hornblende phenocrysts and marks the top of the Unuk River Formation throughout the map area. Regionally the member can be divided into three units; on more local scales a variety of additional facies are preserved.

The rocks are texturally similar to dykes of Premier Porphyry which cut both the underlying strata (Plate 3.7B) and the Texas Creek batholith. Brown (1987, pages 113-118) renamed these units to avoid confusion between stratabound and intrusive phases. Here, the writer prefers to stress the genetic link between the intrusive and extrusive phases of these economically and stratigraphically important rocks. All gold deposits in and around the Silbak Premier and Big Missouri mines occur stratigraphically below this member.

Massive to Layered Plagioclase Porphyry

The lowest unit of the Premier Porphyry Member is the thickest and most continuous. The plagioclase-hornblende phyric rock is massive to crudely laminated. Plagioclase crystals (<6 millimetres) stand out clearly (Plate 3.1A) but the hornblende crystals are smaller and only evident with careful hand sample study. Layering reflecting variable grainsize sorting is typically 1 to 2 centimetres thick and the rock appears more indurated and less foliated than andesitic tuffs lower in the sequence; it is interpreted to be welded or partially welded airfall crystal tuff. The definition of the layering is variable, some exposures are essentially massive. This unit does not normally carry K-feldspar crystals; a few small and/or broken orthoclase rhombs were noted in widespread outcrops (Plate 3.1A). Good examples of this rock type are found eastward and uphill of the Silbak Premier mine, on the west slope of Troy Ridge, and in a continuous exposure over several hundred square metres on the southeast of Brucejack Lake (Alldrick and Britton, 1988).

Premier Porphyry Flow

The Premier Porphyry flow unit is a dark green to medium greyish green or grey to black, massive, indurated, crystal-rich rock with megacrystic potassium feldspar and smaller plagioclase and hornblende crystals. An interlocking, felted groundmass of microlites indicates the rock is a flow. Good exposures crop out on the western slopes of Mitre Mountain and Troy Ridge, along the bottom of Daisy Lake (which drains annually), along the west side of Mount Dilworth, on the ridge crest south of the peak of Slate Mountain, and uphill from the Silbak Premier minesite. This unit forms in exposures up to 100 metres thick on the northern part of the west face of 49 Ridge.

Crystals include small (3 to 5 millimetre) white, subhedral to euhedral plagioclase and larger (1 to 5 centimetre) buff-coloured, euhedral orthoclase. Locally 5 to 10 millimetre long hornblende crystals are visible, but they are generally obscured by strong chlorite alteration. The matrix is fine grained and usually chloritized.

In thin section the rock shows embayed, partially resorbed quartz grains. The large feldspar crystals are euhedral with little rounding or fracturing. Plagioclase may occur as glomeroporphyritic clusters and all feldspars show a thin, clear, inclusion-free rim. Both Read (1979) and Galley (1981) report minor amounts of biotite in thin section examination of samples collected near the Big Missouri deposit. No biotite was noted in samples examined in this study.

Premier Porphyry Tuff

This rock is characterized by its maroon colour and by potassium feldspar megacrysts and plagioclase and hornblende crystals. It crops out in several areas between the High Ore prospect and Windy Point and is distinguished from the underlying green Premier Porphyry flow by its hematite content, which produces a purple to greyish purple colour, and by its non-crystalline aphanitic matrix. This unit was first defined by Plumb (1957) as "purple tuff" and was termed "dacite maroon porphyry flow" by Brown (1987).

Plate 3.1A: Bedded plagioclase-hornblende ash flow, uphill from Premier Glory Hole. Note rare, coarse K-feldspar crystals (arrow). Massive to layered plagioclase porphyry member, Unuk River formation. Lens cap for scale.

Plate 3.1B: Mappable hematitic regolith layer between massive beds of K-feldspar porphyritic flow, north end of 49 Ridge. Premier Porphyry flow (green), Premier Porphyry member, Unuk River formation. Hammer for scale.

Plate 3.1A

Plate 3.1B

Based on microscopic textural features summarized in Table 3.1 this rock is interpreted as a massive, subaerially deposited airfall crystal tuff.

TABLE 3.1
TEXTURAL DISTINCTIONS BETWEEN PREMIER PORPHYRY FLOW AND PREMIER PORPHYRY TUFF

Flow	Tuff
■ rimmed feldspars	■ no feldspar rims
■ few or no lithic chips	■ lithic clasts common
■ euhedral phenocrysts	■ broken and/or rounded phenocrysts
■ interlocking crystalline matrix	■ fine ash matrix
■ glomeroporphyritic feldspars	

Continuity of this unit south of High Ore or north of Windy Point has not been demonstrated, but it may continue as a green, chloritized tuff. Distinction between tuff and flow facies are best made by thin section study, although Read (1979) felt slabbed samples were adequate.

Other Facies

In the Mount Dilworth area, the 100 metre thick exposure of Premier Porphyry flows is separated midway by a thin hematitic sandstone layer (Plate 3.1B) parallel to the borders of the flow. The sandstone regolith was traced along the cliff face on the west side of 49 Ridge for 150 metres. This sedimentary layer records a brief period of subaerial weathering, followed by continued extrusion of similar flows.

A vent area has been documented at the south end of 49 Ridge. The facies indicators are: (i) a wedge-shaped bed of angular to well rounded (milled) clasts of Premier Porphyry rock that is interpreted as a fall-back breccia in a vent area (Plate 3.2C), and (ii) very coarse tuff breccia at the top of the Upper Andesite Member (Plates 3.2A and 2B). The fissure itself is exposed in the vertical cliff at the south end of 49 Ridge where blocks of black Premier Porphyry up to 3 metres in diameter are suspended in a matrix of massive to

Plate 3.2A: Large angular block of black K-feldspar megacrystic flow in similar groundmass, south cliff of 49 Ridge. Close-up of rock face shown in **Plate 3.2B**. Vent facies, Premier Porphyry member, Unuk River formation.

Plate 3.2B: Megabreccia of black K-feldspar megacrystic blocks, south cliff of 49 Ridge. Close-up shown in **Plate 3.2A**. Vent facies, Premier Porphyry member, Unuk River formation.

Plate 3.2C: Milled fall-back breccia of dark green K-feldspar megacrystic boulders, east cliff of 49 Ridge. Vent facies, Premier Porphyry member, Unuk River formation.

Plate 3.2A

Plate 3.2B

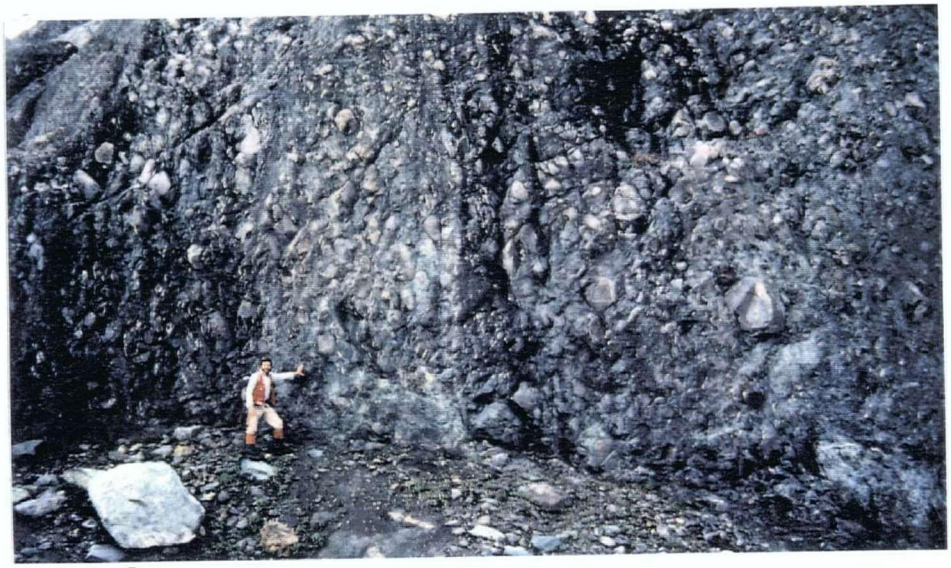

Plate 3.2C

foliated ash and crystals of similar material (Plate 3.2A). This vent area was probably a parasitic cone on the flanks of a large composite stratovolcano.

Petrochemistry

The volcanic rocks are sub-alkaline, calc-alkaline, potassium- and iron-rich andesites with minor basalts to basaltic andesites (Section 3.3).

Provenance

The rocks of the Unuk River Formation represent an andesitic volcanic pile and intraformational epiclastic rocks. The formation is regarded as a well preserved lower Jurassic composite stratovolcano, with paleotopographic peaks at or near Mount Dilworth (Upper Andesite Member) and at the north end of Long Lake (Middle Andesite Member).

Depositional Environment

Most workers have interpreted strata of the Unuk River Formation as a subaqueous volcanic pile. In this study the composite stratovolcano is regarded as a predominantly subaerial structure with two brief periods of marine transgression recorded by the thin bedded siltstone members. Evidence and arguments for and against this interpretation are summarized in Table 3.2.

Age

Rocks of the Unuk River Formation have not yielded diagnostic fossils within the map area. A more aggressive search is recommended in the Lower and Upper Siltstone Members, where precise ages would be particularly helpful.

The base of the Unuk River Formation has not been defined in the map area and rocks low in the sequence have not been dated. Rocks of the uppermost Premier Porphyry Member are interpreted to be 195 Ma old based on correlation with U/Pb zircon ages from nearby Premier Porphyry dykes. The entire Unuk River Formation is regarded as an Early Jurassic, Sinemurian(?) to mid-Pleinsbachian, volcanic pile composed of onlapping to

TABLE 3.2: EVIDENCE FOR SUBAERIAL VERSUS SUBAQUEOUS DEPOSITION OF THE UNUK RIVER FORMATION

- Conspicuous absence of pillowed flows in seven decades of mapping
- Meteoric water component in fluid inclusions (McDonald, 1990a)

Key to Symbols in Following Lists

P = present; **A** = conspicuously absent;
? = insufficient data or not applicable

3.2a: Characteristics of Subaerial Fallout Deposits (simplified from Fisher and Schmincke, 1984)

? - Minor lenticularity close to source
? - Ash layers wedge out against steep surface irregularities
? - Grading may be normal and reverse
P - Fabric in beds is commonly isotropic
P - Elongate fragments are uncommon
P - Bedding planes are generally gradational; bedding planes are distinct only where deposition is on weathered or erosional surfaces or different rock types
A - Sorting is moderate to good
? - Size and sorting vary with distance within single layers
P - Silicic and intermediate compositions more common than mafic
P - Intermediate composition commonly associated with large composite volcanoes
P - Proximal facies include: lava flows, pyroclastic flows, domes,pyroclastic tuff breccias, avalanche deposits and debris flows
P - Intermediate facies include: coarser-grained tephra, some lava flows, pyroclastic flows, ash falls and reworked fluvial deposits
? - Distal facies include: fine fallout tephra with no co-eval coarse-grained pyroclastic rocks or lava flows
P - Coarser-grained pyroclastic deposits gradually decrease, reworked pyroclastic deposits gradually increase away from source

3.2b: Characteristics of Submarine Fallout Tephra (simplified from Fisher and Schmincke, 1984)

A - Plane parallel beds extend for hundreds of km^2
? - Normal grading; crystal and lithic-rich bases to shard-rich tops
? - Inverse grading only if pumice is present
A - Basal contacts sharp, upper contacts diffuse
? - Sorting: good to poor depending on bioturbation
P - Sizes and sorting varies irregularly, but there is an overall size decrease with increasing distance from source
A - Ancient layers in terrestrial geologic settings are altered to clays and zeolites; known as bentonites
A - Tephra commonly interbedded with pelagic calcareous or siliceous oozes, or with muds and silts, depending on proximity to land. Commonly interbedded with nonvolcanic or tuffaceous shale or siltstone
A - Terrigenous materials accumulate as interbedded turbidites

overlapping volcanic and derived sedimentary members from a series of nearby, actively erupting volcanic vents.

3.1.2.2 BETTY CREEK FORMATION

This formation is a complex succession of distinctively coloured red and green epiclastic sedimentary rocks interbedded with andesitic to dacitic tuffs and flows. The formation was first defined by Grove (1971) as a member of the "Bowser assemblage". He redefined it (1973, 1986) as a formation within the Hazelton Group with its type area along the canyon of Betty Creek in the northern part of the map area.

Thickness and Distribution

The formation varies in thickness from 4 to 1200 metres. It is exposed continuously throughout the map area except for the 2 kilometre interval between Union Lake and Fetter Lake where it may be absent or overprinted and obscured by intense alteration.

Sections through the Betty Creek Formation from Daisy Lake to Slate Mountain have no interbedded volcanic rocks. In contrast, on Mount Rainey the andesites of the Unuk River Formation are capped by a thick sequence of dacitic volcanic rocks and there are few interbedded sedimentary rocks. The varying abundance of sedimentary and volcanic rocks is likely controlled by paleotopography and distribution of volcanic vents. The volcanic flows and tuffs may have been extruded from other nearby volcanic centres to form onlapping units in the Salmon River area that interfinger with a thick sedimentary wedge shed from the Mount Dilworth paleovolcano.

Contact Relationships

The basal contact is typically marked by a sharp colour change from greenish chloritic andesitic tuffs of the Unuk River Formation to maroon clastic sedimentary rocks. The basal sediments are commonly conglomerates developed on lithologically similar underlying andesites. The contact varies from irregular to smoothly undulating. The upper contact is a

sharp smooth boundary between purple, hematitic grits or wackes and overlying aphanitic massive dust tuffs of the Mount Dilworth Formation.

Stratigraphy

Sedimentary Facies

Brightly coloured sedimentary rocks range from mudstones, siltstones, sandstones, wackes and grits up to coarse boulder conglomerates. The bedding, textures and colouring of these beds are distinctive. The matrix is typically hematitic, brick red to maroon to purple, but local greenish and mottled purple and green units occur near the base of the sequence. The iron oxide that gives the sandstones their strong reddish shades lies within the intergranular clay fraction (Plate 3.3).

Striking exposures of multicoloured, heterolithic boulder conglomerates are widespread. Rounded cobbles and boulders of volcanic rock within these beds range in colour from red to purple, green and grey. Most of the clasts are andesitic volcanics similar in texture and composition to rocks in the underlying Unuk River Formation. Conglomerates are predominantly matrix supported (Plate 3.3C), but clast-supported "boulder beds" with boulders up to 40 centimetres diameter crop out along Bear River Ridge. Individual conglomeratic beds are massive to crudely sorted. Crudely sorted layers may show either reversely graded or symmetrically graded beds, a characteristic feature of lahars (Fisher and Schmincke, 1984).

Monolithic cobble and boulder conglomerate beds are common near the base of the sequence, particularly where the formation thins on Mount Dilworth and at the northeast end of Long Lake. The textures and mineralogy of the angular to subrounded clasts are identical to those of the immediately underlying andesitic rocks.

The general depositional environment is subaerial although some sedimentary units exhibit waterlain textures. Scattered exposures of grit to mudstone beds show normal grading (Plate 3.3A), crossbedding (Plate 3.3C), scour marks (Plate 3.3B) and rhythmic

Plate 3.3A: Rhythmic graded beds of coarse wacke (grey) to hematitic mudstone (maroon), east shore of Daisy Lake. Strike north, tops to east towards Troy Ridge. Betty Creek formation (see **Plate 3.4A** for location).

Plate 3.3B: Bedded coarse wacke (grey) with finer sandstone (white) and siltstone (purple), east and uphill from Premier Gloryhole. Scour channel indicates strata are upright. Betty Creek formation. Lens cap for scale.

Plate 3.3C: Medium-bedded hematitic wackes and pebble conglomerates, west side of Troy Ridge. Grading and crossbeds (in layer below boulders and hammer); both beds are upright. Betty Creek formation.

Plate 3.3A

Plate 3.3B

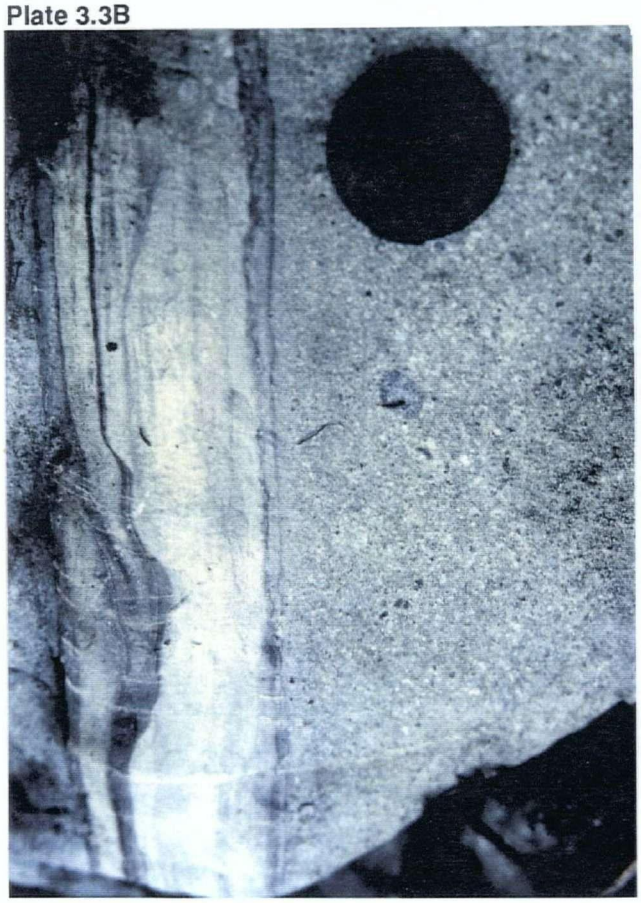

Plate 3.3C

bedding (Plate 3.3A); they represent stream channel deposits where debris flow fans have been reworked on the lower flanks of a stratavolcano. On both limbs of the Dilworth syncline these sedimentary structures show consistent stratigraphic tops toward the synclinal axis on Mount Dilworth (Figure 3.2A).

Volcanic Facies

Volcanic facies interbedded with the sedimentary rocks include dust tuff, ash tuff, feldspar crystal tuff, lapilli tuff and porphyritic lava flows. Units on the slopes of Mitre Mountain and along the northern Bear River Ridge are predominantly dacitic. Those exposed on the southern Bear River Ridge, uphill from the Silbak Premier mine, are a deeper green colour and seem more andesitic in character. As a generalization, within a single stratigraphic section, volcanic units grade upward from andesitic to dacitic composition.

The dacitic tuffs range from pale waxy yellow or yellow-green crystal tuffs and welded tuffs to pale green coarse ash tuffs and dust tuffs. Crystal tuffs host medium grained (0.5 to 1.0 centimetre), white, subhedral to euhedral feldspar phenocrysts. No hornblende phenocrysts have been noted, but there are rare fine grained ($\leq$5 millimetre) quartz crystals in some samples. Rare dacitic welded tuffs exhibit eutaxitic textures with flattened fiammé up to 12 centimetres long.

Petrochemistry

Two whole rock analyses from tuffs within the Betty Creek Formation plot within the overlapping areas of the dacite and andesite fields (Alldrick, 1985 and Appendix I).

Provenance and Depositional Environment

The clastic sediments have likely been derived by weathering and erosion of Unuk River Formation tuffs and flows. The Betty Creek Formation is interpreted as a subaerial clastic apron of poorly sorted lahars and reworked debris flows interbedded with andesitic to dacitic volcanic rocks on the flanks of an emergent andesitic stratovolcano constructed

of Unuk River Formation rocks. Areas where the Betty Creek Formation thins or wedges out represent paleotopographic highs.

Age

No fossils or isotopic dates have been obtained from the Betty Creek Formation, but constraints include the Early Jurassic, Toarcian, fossil assemblage at the base of the overlying Salmon River Formation, and Early Jurassic U-Pb dates from underlying andesitic dykes and flows (194.8$\pm$2.0 Ma). Thus the most likely age range for accumulation of the sediments, tuffs and flows of the Betty Creek Formation is Early Jurassic, mid-Pliensbachian to mid-Toarcian (195 to 190 Ma).

3.1.2.3 MOUNT DILWORTH FORMATION

The felsic volcanic sequence in the map area is composed of dense, resistant, variably welded dacite tuffs. Individual members display distinct lateral facies variations and textural changes that can be related to volcanic centres, paleotopography and depositional environment.

In this study the unit has been named the Mount Dilworth Formation or Mount Dilworth dacite. This felsic volcanic package is thin but continuous throughout the region. It is a resistant cliff-former and an important regional stratigraphic marker and thus warrants formational status. Mount Dilworth is the preferred type area because it offers several sections that are continuously exposed in outcrop and that are free from the complications of minor faults and folds. In contrast exposures near Monitor Lake are a series of discontinous outcrop knobs in an area of complex small scale folding and faulting. Additional attractions of the Mount Dilworth area are relative ease of access and a wider variety of discrete, mappable facies and members within this formation.

Distribution and Thickness

The formation is exposed in a continuous, north-south elongated oval outcrop pattern within the map area. This distribution reflects the regional doubly-plunging

"synclinorium" in the center of the map area. Thickness ranges from 20 to 120 meters, but appears even greater near Union Lake and Monitor Lake where outcrop patterns are complicated by faulting.

Contact Relations

The basal contact is a sharp, gently undulating surface. Massive, aphanitic grey to green to maroon dust tuffs overlie purple to maroon clastic sediments of the Betty Creek Formation. In some exposures the contact is marked by a one to three meter interval of interbedded hematitic sediments and dust tuffs. The upper contact is typically a sharp but ragged surface between coarsely fragmental felsic lapilli tuffs and overlying calcareous grits of the Salmon River Formation. Where the uppermost member of the Mount Dilworth Formation is the Black Tuff, the upper contact of the formation is smooth with a sharp break between massive black tuffaceous mudstones and the overlying calcareous grits.

Stratigraphy

Stratigraphic relations within the Mount Dilworth Formation are shown on Figure 3.7 and on Plate 3.4A. Despite local heterogeneities and facies variations, the three major members of the formation--the Lower Dust Tuff, Middle Welded Tuff, and Upper Lapilli Tuff--can be distinguished in sections throughout the map area.

Lower Dust Tuff Member

The lowest member of the Mount Dilworth Formation is a massive aphanitic dust tuff (fine ash tuff) composed of volcanic dust and fine lithic particles. This unit is regionally distributed throughout the map area and beyond. The dust tuff blankets underlying Betty Creek sedimentary rocks and ranges in thickness from 3 to 15 meters. The unit has sharp conformable contacts with adjacent units.

This rock is typically olive grey to grey, but bright turquoise coloured zones occur near Summit and Divide Lakes and local purple and bright maroon hematitic alteration zones give the rock a swirled or marbled pattern (Plate 3.4B). At the southeast corner of

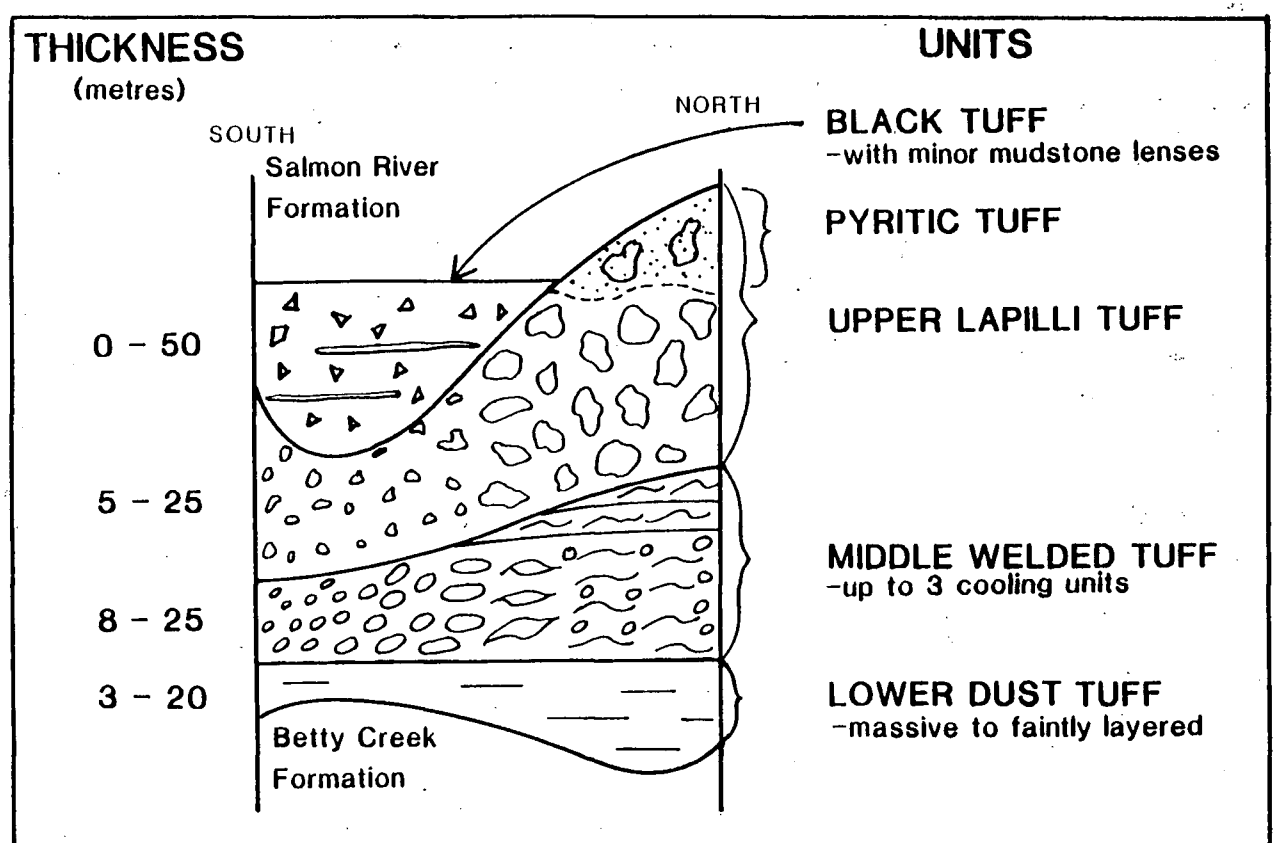

FIGURE 3.7: Stratigraphy within the Mount Dilworth formation

Plate 3.4A: Complete stratigraphy of Mount Dilworth formation exposed in cliff along east side of Daisy Lake. Overlying Salmon River formation includes well-bedded shales, siltstones and wackes and basal fossiliferous limestone. Looking north from Windy Point to Scottie Gold minesite in background.

Plate 3.4B: Stratigraphy in Mount Dilworth formation, north end of 49 Ridge. Note colour-mottling of Lower Dust Tuff and spectacular gossans of the Pyritic Tuff. Height from base of photo to top of pyritic knob: 30 metres.

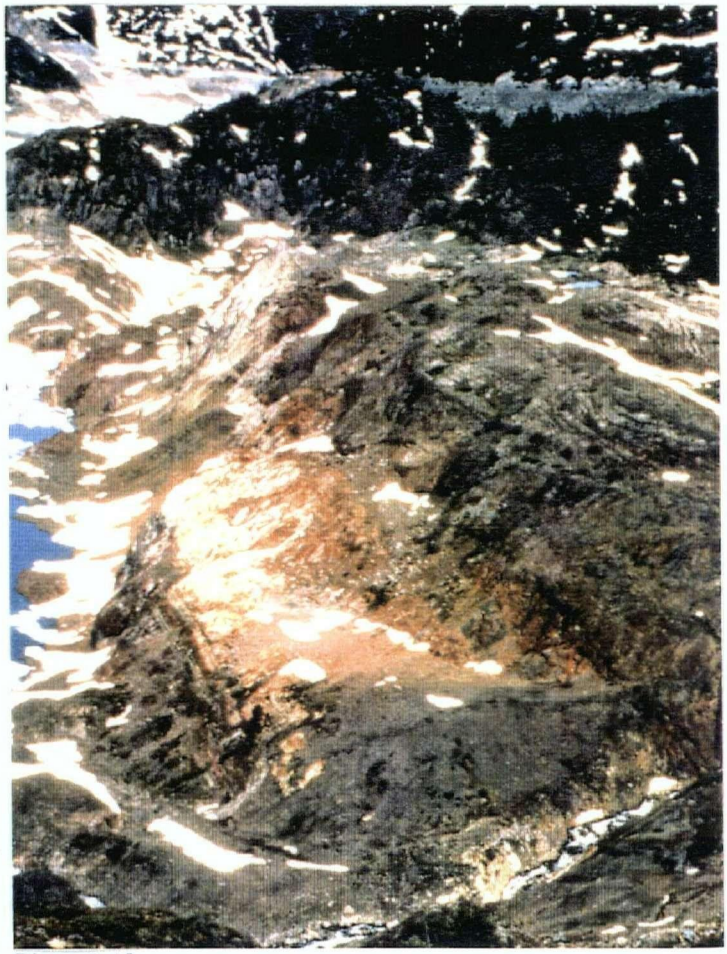

Plate 3.4A

Plate 3.4B

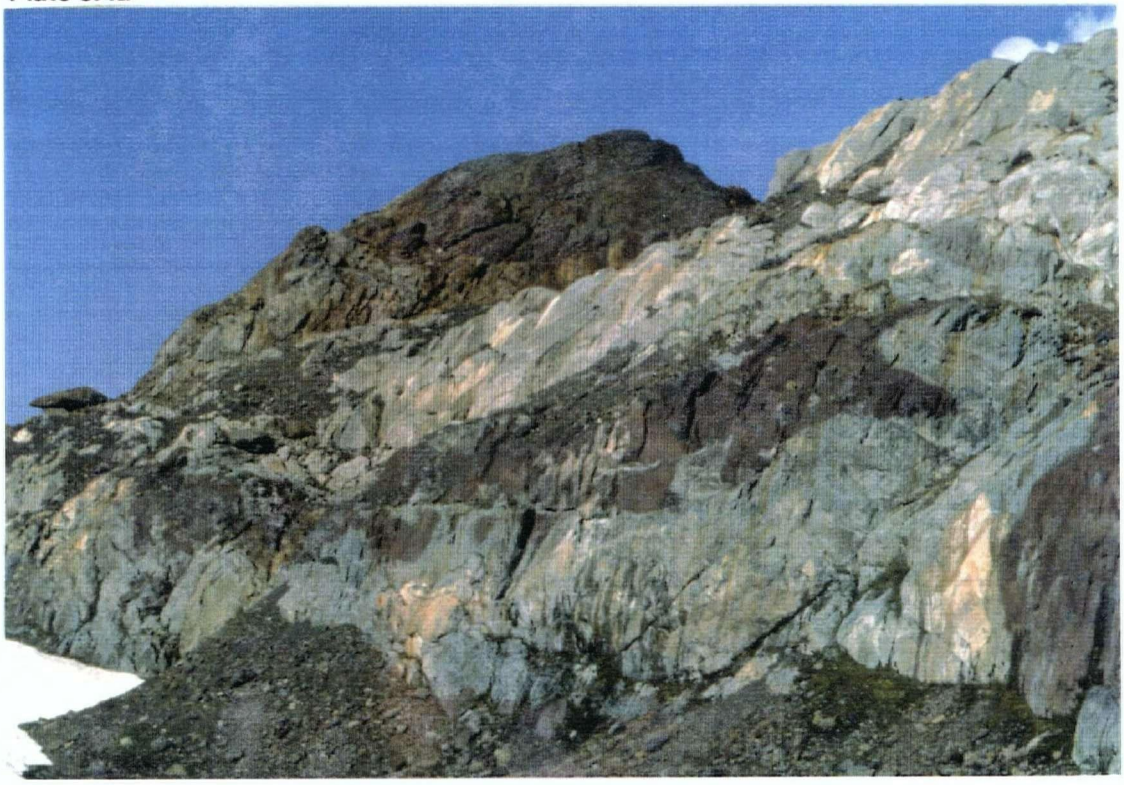

Plate 3.5A: Upper Lapilli Tuff member of Mount Dilworth formation, south end of Mount Dilworth. Note swirled bombs of flow-banded dacite. Hammer for scale.

Plate 3.5B: Middle Welded Tuff member of Mount Dilworth formation, north end of 49 Ridge. Large fiammé in welded tuff. Hammer for scale.

Plate 3.5C: Lower Dust Tuff member of Mount Dilworth formation, Windy Point roadcut. Turquiose-grey colour is typical; fine lithic chips and large euhedral pyritic crystal are unusual variations. Hammer for scale.

Plate 3.5A

Plate 3.5B

Plate 3.5C

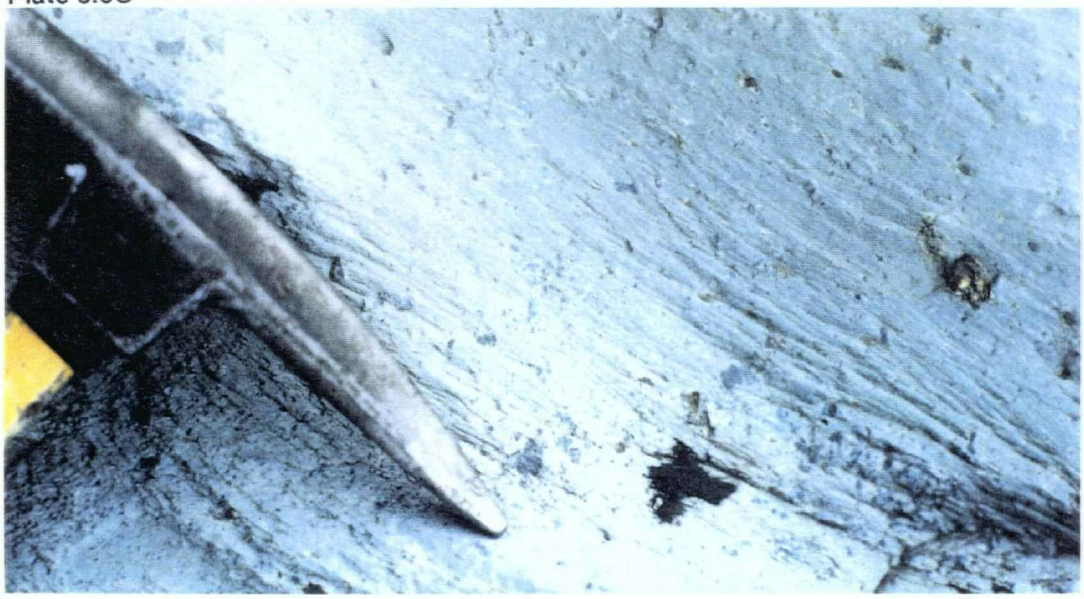

Summit Lake along the Upper Granduc Road, the dust tuff contains fine silica filled vesicles and large euhedral pyrite crystals up to 1 centimeter across (Plate 3.5C).

At microscopic scale the rock is predominantly (>70%) fine ash, with fine (<1 mm) lithic and crystal fragments of quartz, feldspar and hornblende. The groundmass may be massive to moderately foliated and is commonly extensively altered to carbonate and sericite. Samples collected along the east side of Monitor Lake contain glass shards and fragments of chalcedony.

Middle Welded Tuff Member

The middle welded ash flow tuff is the most variable of the three regionally extensive members of the Mount Dilworth Formation. It forms a series of laterally varying dacitic facies sandwiched between the other two members that are texturally more consistent. The lower contact of this member is sharp and planar, the upper contact is sharp but irregular.

In the Mount Dilworth to Monitor Lake area, sections through this member show that mixed fiammé and angular felsic lapilli at the base are overlain by pumice lapilli tuff. Well exposed sections show progressively more intense welding and compaction down-section (Plate 3.5B); equidimensional pumice clasts grade downward into black glassy fiammé. Outside the Mount Dilworth area subrounded pumice lapilli are mixed with varied siliceous lithic clasts, but the rocks are not obviously welded.

Midway between the south edge of the Mount Dilworth snowfield and Union Lake one outcrop shows bedding and small dune forms (10 cm amplitude) in fine creamy ash tuff at the base of this member. These dune forms are interpreted as base surge features; no internal truncation of layers was noted but asymmetry suggests the blast was from the north of the exposure. Along the northwest slope of Mount Dilworth a similar bed of white to cream-weathering massive fine siliceous ash tuff forms a thin (30 cm) resistant layer at the base of the Welded Tuff Member. At this location this bed is overlain by three ash flow cooling units, each containing progressively less compressed pumice clasts up-section, all

included within the middle member. Elsewhere along the Mount Dilworth ridge, only a single cooling unit has been noted within this member.

In thin section, rocks of this member host fiammé-like wisps on all scales. Veinlets and fragments of microcrystalline quartz (chalcedony) are common, as are broken crystals of both plagioclase and potassium feldspar. In some samples, partially collapsed fiammé are wholly altered to aggregates of chlorite, quartz, calcite and epidote.

Upper Lapilli Tuff

The regionally extensive upper member of the Mount Dilworth Formation is a siliceous lapilli tuff to tuff breccia. The lower contact of this unit is generally sharp, irregular to undulating, but may be locally indistinct. The upper contact is gradational to sharp against the pyritic tuff facies, gradational into the black tuff facies, and irregular but sharp against the basal fossiliferous wackes and calcareous grits of the Salmon River Formation.

Fragments are predominantly swirled flow banded dacite bombs or spatter (Plate 3.5A), but clasts of other siliceous volcanic rocks are also common. Regionally, the fragment size ranges up to a maximum of 10 to 15 centimeters, and the overall size range is that of a lapilli tuff. However along the southwest edge of the Mount Dilworth snowfield, large swirled flow banded bombs up to 50 centimetres long are preserved. This local increase in fragment size suggests that the southern part of Mount Dilworth was a vent area for this member. The unit may be partially welded but contains neither pumice fragments nor fiammé. Along much of its strike length the groundmass is medium to dark grey (Alldrick, 1985, figure 117).

In thin section the groundmass has a massive to subtly layered glassy or welded texture. Clasts are lithic chips, cryptocrystalline quartz and scattered feldspar crystals. Disseminated pyrite is often present in the matrix and in some lithic chips. Minor (1%) biotite occurs in exposures of this member along the southeast side of Summit Lake. North of Goat Creek many of the finer lithic chips are well rounded.

Pyritic Tuff

A prominently gossanous, pyritic, fragment-rich unit is exposed along the west side of Mount Dilworth (Plate 3.4B) and the east side of Summit Lake (Plate 3.4A). This member ends abruptly in a gossanous cliff at the south end of Mount Dilworth, but progressively thins northward, finally wedging out high on the western slope of Troy Ridge. Another area of exposure has been documented at the northeast end of Long Lake by Dupas (1985, p.313) where it was appropriately termed the "Iron Cap" by early workers (Plumb, 1956). The upper and lower contacts of this unit are typically sharp but irregular. Locally the lower contact may be gradational over less than a meter; the upper contact may be an interbedded sequence of sedimentary rocks and dacitic tuffs.

Along the southwest edge of the Mount Dilworth snowfield the unit carries clasts of flow banded siliceous volcanic rock, clasts of massive felsic tuffs or flows, and large rounded boulders (up to 0.5 meter diameter) of coarse crystalline calcite aggregates. As in the underlying member, fragment size decreases progressively northward from rounded boulders to cobbles, then to lapilli.

In thin section, the unit contains lithic fragments, broken feldspar crystals and chips of microcrystalline quartz (chalcedony). Lithic fragments may show microscopic scale flow-banding. Disseminated pyrite comprises up to 50% of the matrix, but is more typically 10% to 15%. Pyrite occurs in some lithic clasts but not in others. In samples from exposures north of Goat Creek, charcoal to black varieties of this unit are impregnated with up to 30% fine pyrite, not carbon. Some samples are cut by fine veinlets of chalcedonic quartz and some of these veinlets show internal growth layering in thin section.

The pyritic unit is not continuous along strike but occurs as a series of discontinuous lenses of strong pyritic impregnation. Despite, or perhaps because of, careful mapping and extensive sampling along its entire strike length, this unit seems complex and may represent penecontemporaneous but post-depositional impregnation of pyrite into a variety of lithologies. Although the predominant rock type is lapilli tuff identical to the underlying

Upper Lapilli Tuff Member, in some exposures the pyrite-rich unit is a carbonate-mudstone-cemented debris flow with heterolithic volcanic and carbonate clasts. For these reasons the pyritic facies is interpreted to represent pyrite impregnation around fumarolic centers, possibly with related calcareous mud-filled brine pools (Figure 3.7). The host lithology is therefore the upper layer of the Upper Lapilli Tuff Member.

Black Tuff

The Black Tuff Member is a thick unit of carbonaceous crystal and lithic lapilli tuffs with local mudstone and siltstone lenses. Lapilli consist of crowded feldspar porphyry lava or crystal tuff, limestone, pumice and rare massive pyrite. The rock is well displayed in the waste dumps at the south end of the penstock tunnel near the Long Lake dam and in abandoned drill core near the Lakeshore workings south of Monitor Lake.

This member has been traced in outcrop from the south end of Mount Dilworth southward to the crest of Slate Mountain and is also exposed in a few discontinuous outcrops south and southeast of Monitor Lake. The Black Tuff Member overlies the Upper Lapilli Tuff Member and either overlies or is the stratigraphic equivalent of the Pyritic Tuff facies to the north. The contact between the Black Tuff and the underlying Upper Lapilli Tuff is gradational. Both units host disseminated sulphides and pyritic lithic clasts, but the Black Tuff also hosts angular clasts of massive, medium grained pyrite aggregates. East of Silver Lakes, bluish grey chalcedony veins cut this unit in exposures within the Start adit and in outcrops north of the adit.

In thin section the crystal-rich tuffs are seen to contain up to 50 percent feldspar crystals and up to 5 percent ragged chlorite flakes after biotite, plus a few well-rounded quartz grains. Galley (1981) and Brown (1987) also identified biotite in thin section studies, but the mineral cannot normally be seen in hand sample. The rock matrix is composed of volcanic ash, dust and fine carbon. Some samples show crude bedding as a slight change in overall matrix grain size. Fine chalcedony veinlets cut through some samples.

Compositions for plagioclase in samples throughout the Mount Dilworth Formation range from An_{32} to An_{40} with most samples falling into the andesine range, An_{36} to An_{38}.

Two alternate interpretations might account for the limited strike extent of the thick, distinctive Black Tuff unit; (i) it may represent an erosional remnant of an originally extensive unit or, (ii) deposition was restricted to the area now occupied by the unit. The latter interpretation requires that the Black Tuff was deposited in a topographic low such as a volcanic crater or a caldera. If this depression was an anoxic water-filled basin it would account for local sediment lenses and the intense carbon impregnation throughout the unit.

Petrochemistry

All lithologies of the Mount Dilworth Formation look highly siliceous and have been identified as rhyolites during field examination by all workers[1]. Grove identified the rock as rhyolite based on field observation and thin section study. Galley (1981, p.166-168) obtained the first whole rock analyses from this lithology. His results plot entirely within the dacite field, yet he used the term Dilworth Rhyolite for this rock type. Brown (1987, p.213) obtained whole rock data for a single sample from the east side of Monitor Lake. Although this data also plots within the dacite field, Brown continued to use the established name "rhyolite" for these rocks (p.45-46). Alldrick (1985, p.328) presented whole rock data for three samples; two plot as dacites and one as andesite near the andesite-dacite border. On the basis of all the analytical data (Figure 3.11) this rock unit is dacite.

Provenance and Depositional Environment

The formation represents fallout and pyroclastic flow deposits from a series of subaerial explosive felsic volcanic eruptions that proceeded in quick sucession, apparently becoming progressively more violent. Based on clast size, one vent area was near the south end of Mount Dilworth. The formation was deposited subaerially on the flanks of an exposed volcanic cone. The general absence of sedimentary deposits between units

[1] Most geologists misidentify hand samples of dacite as "rhyolite" (Sabine *et al.*, 1985).

confirms there was little or no time between eruptions. The uppermost Black Tuff Member was deposited under sub-aqueous conditions, perhaps in a fault-bounded caldera or crater lake (Figure 5.9). Interbedded sedimentary rocks within the pyritic facies suggests subsidence followed the final major eruption.

Age

There are no fossils associated with the felsic volcanic rocks of the Mount Dilworth Formation. Brown (1987) has reported an imprecise Early Jurassic U-Pb date (197$\pm$14) Ma from the Mount Dilworth Formation in the Monitor Lake area. The formation is immediately overlain by Toarcian limestones and is underlain by the mid-Pliensbachian to Toarcian Betty Creek Formation. Therefore the Mount Dilworth Formation records a voluminous but short-lived volcanic event in Toarcian time (about 185 Ma ago).

3.1.2.4 SALMON RIVER FORMATION

The Salmon River Formation is a thick assemblage of complexly folded, thin to medium bedded siltstones and wackes with minor interbedded intraformational conglomerates, limestones and siliceous tuffaceous siltstones (Plate 3.6). Grove (1973, 1986) selected the summit, northern slopes and eastern cliffs of Mount Dilworth and Troy Ridge as the type area for the formation.

Distribution and Thickness

Salmon River strata are preserved as a large trough-like erosional remnant in the northeast part of the map area. The formation is at least 1000 metres thick in the map area, although its top has not been identified.

Contact Relationships

This thick sedimentary sequence has a rough to undulating, sharp contact with underlying felsic fragmental tuffs. The writer regards this as a paraconformable contact, formed during foundering and rapid subsidence of a subaerial volcanic edifice immediately

after its last violent and voluminous eruptive event. The depositional break between formations would be of the duration of a diastem. Lithologic evidence that supports this interpretation includes: minor interbedded wackes with ripple marks in the upper metre of the pyritic tuffs at the northeast end of Long Lake, interbedded tuffaceous and pyritic limestones, siltstones and cherty units in the lower part of the Salmon River strata.

Stratigraphy

Basal Limestone Member

Thin, pyritic, fossiliferous limestone crops out at the base of the formation throughout the area. The unit was first noted by Schofield and Hanson (1922) at Divide Lake. The best exposures are seen at the cliff top near the southeast corner of Summit Lake, just north of the 49 Ridge, on the crest of Slate Mountain, and at the northeast end of Long Lake.

The unit comprises dark grey to black carbonate cemented grit with interbedded lenses, pods and nodules of fossiliferous gritty limestone. Both the calcareous grits and fossiliferous limestones host sparsely disseminated pyrite, which is more abundant where the unit is underlain by the pyritic volcanic facies.

The calcareous grits contain local, scattered granules and pebbles of volcanic lithologies. Thin conglomeratic layers at Summit Lake and on Slate Mountain contain rounded pebbles of pumice. These local pumice conglomerate beds may represent rafted pumice, suggesting minor felsic volcanism continued during marine transgression. The grits also have up to 10 percent fine grained angular altered feldspar grains, indicating rapid erosion and deposition with little weathering and reworking of the sands.

The limestone is buff to grey, sandy to gritty with some black siltstone chips or rip-up clasts. The thin member is fossiliferous throughout the map area and locally contains up to 50 percent fossil debris. The most precise fossil age comes from recent sampling of the Basal Limestone Member on Troy Ridge by Anderson (written communication, 1986). Fossils include abundant belemnites and lesser pelecypods, including Weyla; many fossils

Plate 3.6A: Intraformational conglomerate. Zone of rounded black slabs and blocks of siltstone within a thicker bed of coarse wacke. Upper Medium-Bedded Wacke member of Salmon River formation. Northwest edge of the Mount Dilworth Snowfield.

Plate 3.6B: Rhythmically interbedded black limy siltstones and white siliceous tuffaceous siltstones, Lower Thin-Bedded Siltstone member of the Salmon River formation. Scale bar in centimetres. (Brown photo.)

Plate 3.6C: Fossil and mudchip-rich gritty limestone. Basal Fossiliferous Limestone member of the Salmon River formation. Southwest edge of Mount Dilworth Snowfield.

Plate 3.6A

Plate 3.6B

Plate 3.6C

are preserved as fragments. The key fossils form an overlap assemblage characteristic of Toarcian time.

The upper contact of this basal member is typically marked by a bedding plane fault that separates this unit from overlying thin bedded siltstones. The fault is marked by a massive quartz vein in some areas. Where the fault is absent, the upper contact is conformable.

Lower Siltstone Member

The lower 50 to 100 metres of the main sedimentary succession consists of black to grey, thin to medium bedded calcareous siltstones and shales with minor intercalated limestones and siliceous tuffaceous beds. The sequence has been described by Grove (1971), Alldrick (1985) and Brown (1987) and is well exposed on the northern slope of Mount Dilworth, east of Mineral Gulch.

The rhythmically interbedded siltstones to fine grained sandstones occur as beds 5 to 10 centimetres thick (Plate 3.6B). Shale partings between these layers are a few millimetres thick. The siltstone is well bedded and finely laminated; shale is massive, intensely cleaved or weakly phyllitic.

The slates and siltstones locally contain minor amounts of disseminated pyrite, and pyrite seams outline some bedding planes producing characteristic banded, iron-stained weathered surfaces. The buff weathering limestone lenses, pods and concretions are regionally distributed but thin, and occur near the base of the siltstone sequence. The limestones locally contain a few fossils. Both Grove (1986) and Anderson (written communication, 1986) have recovered Middle Jurassic fossil suites from this strata. Siliceous beds, first reported by Grove (1973, 1986), were studied in detail by Brown (1987) who describes the beds as planar to undulating layers of siliceous, radiolaria-bearing shale less than 5 centimetres thick.

In thin section siltstones are composed of silt sized quartz, feldspar and lithic chips in a carbonaceous, calcareous clay matrix. Brown (1987) noted detrital muscovite flakes in

one sample. Read (1979) describes strongly foliated phyllitic zones within the siltstone composed of muscovite, chlorite, quartz and feldspar. Grove (1973, 1986) reports thin lenses of calcarenite and quartz sandstone interspersed within the siltstone sequence. Tuffaceous beds contain glass shard outlines, bubble wall fragments, plagioclase microlites and quartz fragments, indicating that minor or distant pyroclastic volcanism was contemporaneous with marine deposition (Brown, 1987).

The siltstone sequence is characterized by abundant scour-and-fill structures, graded bedding and crossbedding; tops are toward the axis of the Mount Dilworth syncline. Ripple marks recorded at the northeast corner of Long Lake by Dupas (1985), display amplitudes of about 2 centimetres and wavelengths of about 8 centimetres.

This member is interpreted to be a sequence of rhythmically bedded marine clastic sediments derived from the erosion of predominantly volcanic terrane. The lower contact of this member is usually marked by a 5 metre to 30 metre thick zone of intense deformation and quartz veining adjacent to a bedding plane fault.

Upper Wacke Member

Conformably overlying the Lower Siltstone Member are medium to light grey wackes and intraformational conglomerates (Plate 3.6A). Quartz greywackes, greywackes and arkosic wackes are included in this sequence. Most of these rocks form fairly massive beds a few metres to several metres thick with minor interbeds of thin bedded siltstone. The conglomerates consist of subparallel black siltstone slabs and cobbles in a grey sandstone matrix. The beds within this member may represent stacked turbidite fans.

Still higher in the sedimentary succession the strata are rhythmically bedded dark grey siltstones. They were not examined in this study.

Provenance

The clastic rocks of this formation were derived mainly from weathering and erosion of a volcanic complex. Some beds may have formed by mixing of varying proportions of

water-transported volcanic detritus and airfall ash and crystals from distant felsic pyroclastic activity.

Depositional Environment

Sediment was deposited on the flanks of an extinct volcano in a shallow to moderately deep marine basin, relatively near subaerial source rocks. The thin rhythmic bedding suggests transport was predominantly by mass-flow processes such as turbidity flows. The high carbon content and general absence of fossils and bioturbation through most of the sequence indicate the beds were rapidly deposited in muddy water.

Age

The Basal Fossiliferous Limestone is Early Jurassic, Toarcian. Although an upper age cannot be demonstrated, the absence of the distinctive basal chert pebble conglomerate units of the Bowser Lake Group in the study area, despite their presence to the east (Meziadin Junction) and to the west (Tom Mackay Lake), suggests that the youngest rocks in the succession pre-date Bowser time and are therefore Middle Jurassic, but older than Upper Bajocian.

3.1.3 BOWSER LAKE GROUP

The term "Bowser Lake Group" was first applied in the map area by Duffell and Souther (1964) and has since been applied by Grove (1971), Read (1979), Galley (1981), Dykes *et al.* (1984) and Brown (1987) to the thick sedimentary package at the top of the stratigraphic succession. Grove (1973, 1986) later renamed these strata the Salmon River Formation of the Hazelton Group.

Tipper and Richards (1976) and Eisbacher (1981) concluded that the base of the Bowser Lake Group is a time-transgressive contact ranging from Upper Bajocian to Upper Bathonian in age. There are no fossils in the map area that are diagnostic of this period. All fossils collected within the sequence have been described as Mesozoic, middle Mesozoic and Middle Jurassic (*e.g.* Brown, 1987), not sufficiently precise to indicate Bowser-age

strata. Thus the upper sedimentary package in the map area has a Toarcian fossil assemblage at its base and its upper age is undetermined.

None of the strata within the map area can be correlated with Bowser Lake Group on the basis of existing paleontological and lithological evidence. Therefore the uppermost sedimentary strata mapped are called the Salmon River Formation of the Hazelton Group and are correlative with the Smithers Formation of Tipper and Richards (1976).

3.2 INTRUSIVE ROCKS

Plutonic rocks underlie about 100 square kilometres or 15 percent of the map area. In the southwestern corner they form a continuous mass of superimposed plutons; to the northeast, discrete stocks and a variety of dykes are scattered throughout the stratified rocks. Definitive studies on these rocks include pioneering fieldwork by Buddington (1929) and comprehensive petrographic work by Smith (1977). The 60 thin sections and 15 polished slabs that were examined in this study supplement these two major studies by the United States Geological Survey. Terminology conforms to the classification scheme of Streckeisen (1975).

Based on field relationships, modal and chemical compositions, textures and extensive dating, intrusive rocks of the region have been grouped into two plutonic suites in agreement with guidelines established by the North American Commission on Stratigraphic Nomenclature (1983). Both suites are represented by batholiths, stocks and a variety of dykes; the older suite also has sills and volcanic extrusive phases.

The Early Jurassic Texas Creek granodiorite suite is characterized by an overall coarse grain size, abundant coarse hornblende and locally by very coarse potassium feldspar phenocrysts or megacrysts. The Eocene Hyder granodiorite suite is characterized by overall medium grain size, biotite, equigranular plagioclase and orthoclase, and trace amounts of fine grained golden sphene. The marked difference in hornblende *versus* biotite contents and the presence of alteration and foliation in the older Texas Creek granodiorite suite rocks are the most reliable field distinctions between the two suites.

3.2.1 TEXAS CREEK PLUTONIC SUITE

The Texas Creek plutonic suite or Texas Creek granodiorite suite includes the Texas Creek batholith, the Summit Lake stock, Premier Porphyry dykes and related dykes and sills within the area. Extrusive equivalents of these plutonic rocks have been described in this report and there are additional intrusive and extrusive phases of this suite beyond the map area (Grove, 1986; Britton and Alldrick, 1988; and Britton *et al.*, 1989, 1990).

3.2.1.1. TEXAS CREEK BATHOLITH

Buddington (1929, p.22) defined the Texas Creek batholith. The pluton crops out in the southwestern part of the map area and extends far to the west. The batholith is roughly 15 kilometres in diameter with a total area of about 205 square kilometres.

The Texas Creek batholith is composed of hornblende granodiorite to monzodiorite to quartz diorite. Two phases have been recognized: in the central and western areas within Alaska the batholith is very coarse grained equigranular rock; along the eastern margin it is porphyritic with a medium to coarse grained groundmass. The porphyritic phase hosts hornblende phenocrysts up to 2 centimetres long and potassium feldspar phenocrysts from 3 to 5 centimetres long.

Based on isotopic dates and field relationships, the equigranular phase was emplaced first, followed by the porphyritic phase. Similar phase relationships have been recognized in the Early Jurassic Lehto batholith on the Iskut River (Britton *et al.*, 1990).

Along the eastern contact, the Texas Creek batholith usually displays a narrow zone, up to a few tens of metres wide, of medium to dark greenish grey chloritic alteration that is sometimes accompanied by a crude foliation. Shearing and broken grains suggest that this narrow zone results from crushing along the granodiorite contact.

Buddington (1929, p.27) commented on the absence of contact metamorphism in the adjacent country rocks:

> One of the most amazing features of the geology of this district is the almost complete failure of the Texas Creek intrusives to produce any observable contact metamorphism in the country rock.

The general lack of contact metamorphic effects suggests that there was not a major thermal or chemical contrast between the intrusions and country rocks, and that pressures from rising magma and late-stage fluid accumulations were relieved by faulting, dyke injections or by regular venting of volatiles to surface.

MAIN PHASE

The core of the batholith was examined along the West Fork of Texas Creek. Core rocks are massive, equigranular, medium to coarse grained hornblende granodiorite, with up to 15 percent coarse euhedral hornblende. This hornblende-rich, coarse grained texture is a characteristic feature of the Texas Creek batholith that can be recognized through all alteration and deformation.

In thin section, feldspar crystals show a myriad of fine crystal inclusions of apatite and lesser zircon. Near the margins of the batholith, coarse inclusion-rich plagioclase grains show a thin inclusion-free overgrowth rim. Similar textures occur in Premier Porphyry dykes and in extrusive rocks of the Premier Porphyry Member. In many samples of the equigranular phase, anhedral quartz displays interdigitating, sutured boundaries.

Hornblende crystals are typically large, euhedral to subhedral, and are commonly twinned. Some hornblende hosts small zircon crystals. Many hornblende crystals have minor interlamellar biotite but no free biotite was noted. Chlorite alteration of the amphiboles varies in intensity, but is a characteristic feature. The granodiorite also contains accessory apatite, sphene and zircon.

Toward the eastern margin of the batholith much (60 to 100 percent) of the hornblende is altered to chlorite, the rock has subparallel microfractures filled by chlorite, and coarse inclusion-rich plagioclase grains are strongly altered to sericite. Even where plagioclase is intensely sericitized, potassium feldspar is fresh and unaltered. Quartz grains in these margin areas show moderately strained extinction.

PORPHYRY PHASE

The eastern margin of the Texas Creek batholith is generally feldspar porphyritic, coarse grained hornblende granodiorite. This porphyritic margin or border phase is up to several hundred metres wide, but may be locally absent as near the wrecked bridge on the Texas Creek Road at the south end of Mineral Hill. The rock is dull greenish grey to light grey and the large phenocrysts give outcrops a mottled appearance.

Phenocrysts comprise up to several percent of the rock volume, and are 1 to 4 centimetres long, white to faintly pink to buff euhedral orthoclase crystals similar to those in Premier Porphyry dykes and extrusive rocks. Phenocrysts enclose small euhedral crystals of hornblende and plagioclase. Potassium feldspar in the groundmass is generally interstitial to hornblende and plagioclase. Buddington (1929, p.26) reports microperthite and notes that it usually shows only a very slight amount of the plagioclase phase. Plagioclase is oligoclase-andesine and occurs in euhedral to subhedral lath-shaped crystals.

Quartz has bimodal grain size. It is both coarse grained and contemporaneous with other coarse mineral phases, and fine grained and interstitial to earlier-formed minerals.

Abundant hornblende occurs as euhedral, columnar black prisms up to 2.0 centimetres long. Many crystals show perfectly euhedral cross sections and they are commonly twinned. Buddington (1929, p.26) reported a minor amount of biotite in the porphyry phase.

Accessory minerals, including sphene, zircon, apatite and magnetite, form about 1 percent of the rock volume. Pyrite is rarely present.

Prismatic hornblende and orthoclase crystals display a subtle preferred orientation in some outcrops and hand samples, producing a "gneissic" grain to the rock. This texture is attributed to original flow lamination during emplacement or final crystallization of the batholith. It is not related to mylonitization.

The porphyry phase shows varying degrees of alteration. Sharply euhedral hornblende and interlamellar biotite are partly to completely altered to chlorite, but quartz

shows only slightly strained extinction. Plagioclase is extensively altered to fine sericite aggregates, but some crystals show thin, clear, unaltered rims. Buddington (1929, p.27) notes that plagioclase can also host minor epidote and chlorite alteration near Tertiary plutons. Potassium feldspar is fresh and unaltered.

3.2.1.2. SUMMIT LAKE STOCK

The Summit Lake stock is a remarkably fresh, medium to coarse grained hornblende granodiorite. The rock is generally equigranular, with only rare potassium feldspar phenocrysts. Thin sections show there is a finer grained interstitial groundmass among the coarse grained hornblende, biotite, plagioclase, potassium feldspar and quartz.

Potassium feldspar crystals are essentially unaltered. Some display a ring of fine blebs of quartz near the rim. Plagioclase (oligoclase) is 25 to 40 percent sericitized. Plagioclase in the Summit Lake stock display subtle, thin clear rims but the texture is not as obvious as examples from the Texas Creek batholith to the south. Most quartz occurs as in the fine grained interstitial groundmass. The few large quartz grains are sutured.

Total mafic mineral content is 18 to 20 percent. Coarse, sharply euhedral green hornblende is commonly twinned. Inclusion-rich red-brown biotite composes 2 to 5 percent of the rock. The biotite is more readily chloritized than the typically fresh hornblende. The rock also contains rare tiny zircons and interstitial rosettes of chlorite.

Textures at the intrusive contact suggest passive emplacement, but the granodiorite is somewhat altered. The hornblende is wholly altered to very pale green chlorite, quartz is only slightly strained, and plagioclase shows minor (15 percent) sericitization.

3.2.1.3 TEXAS CREEK DYKES AND SILLS

The Texas Creek plutonic suite includes a variety of dyke phases. Schofield and Hanson (1972) referred to these dykes as "Premier Sills". Brown (1987) proposed the term "potassium feldspar porphyry" as a descriptive alternative to "Premier Porphyry". The writer has used the term "two feldspar porphyry" in past articles, but Premier Porphyry is

preferred because of its current widespread use and the close relationship between these dykes and all the major ore zones at the Silbak Premier mine. The rock hosts potassium feldspar megacrysts and plagioclase phenocrysts in a fine grained to aphanitic groundmass.

Premier Porphyry dykes cut all the lower members of the Unuk River Formation and the margin of the Texas Creek batholith. They do not cut the Premier Porphyry Member or any of the overlying strata. They are regarded as subvolcanic dykes coeval with the extrusive Premier Porphyry Member at the top of the Unuk River Formation.

In outcrop, Premier Porphyry dykes weather green to greyish green and are massive to weakly foliated. Outcrops are characteristically blocky weathering and less foliated than the country rock andesitic tuffs (Plate 3.7A). In some exposures potassium feldspar megacrysts weather out leaving large rectangular pits. Intrusive contacts are rarely found in outcrop, but good examples of chilled dyke margins have been noted during underground mapping, drill core examination, and mapping along the Salmon River (Plate 3.7B).

Three varieties of Premier Porphyry dykes are recognized based on detailed mapping and drill core logging at the Silbak Premier mine[1] (Brown, 1987):

- Potassium feldspar megacrystic, plagioclase-hornblende porphyry is the "typical" Premier Porphyry dyke. (The extrusive equivalents of this dyke rock are Premier Porphyry tuff and Premier Porphyry flow of the Premier Porphyry Member.)
- Plagioclase-hornblende porphyry is texturally similar to the potassium feldspar megacrystic porphyry, but contains few or no quartz and potassium feldspar phenocrysts. The extrusive equivalent of this dyke rock is the massive to layered Plagioclase Porphyry of the Premier Porphyry Member.
- Plagioclase porphyry is hornblende poor, least abundant, and may be a gradational phase of plagioclase-hornblende porphyry.

[1]Geologists at the minesite emphasized the difficulties of distinguishing between these rocks by respectively naming these same three dyke types:
- Premier Porphyry Proper.
- Premier Porphyry Probable.
- Premier Porphyry Problematic.

On both property and regional scales the megacrystic variety is the most abundant and will be described here as the type rock.

Typical Premier Porphyry dykes (Plate 3.7) are medium to dark green rocks with large (up to 5.0 centimetres) potassium feldspar megacrysts, plagioclase phenocrysts (up to 8 millimetres) and hornblende phenocrysts (up to 1.0 centimetre) in a fine grained to aphanitic altered groundmass. The fine-grained groundmass, lower hornblende content, and presence of pervasive chloritic alteration distinguish hand samples of Premier Porphyry dyke from the coarse grained, hornblende-rich, generally less altered rocks of the Texas Creek batholith and Summit Lake stock.

In thin section, typical Premier Porphyry consists of phenocrysts of orthoclase, plagioclase, hornblende and rounded quartz in a groundmass of quartz and potassium feldspar crystals. Potassium feldspar usually constitutes up to 4 percent of the rock; crystals average about 1.0 centimetre long. Rocks hosting up to 50 percent phenocrysts are called "crowded porphyry". Rare phenocrysts up to 5 centimetres long have been noted. Cores and rings of fine hornblende and plagioclase inclusions are common. Some megacrysts display simple twinning. Two X-ray diffractometer analyses of potassium feldspar megacrysts indicated compositions of 88 percent and 96 percent potassium feldspar which were classified as "low sanidine" based on degree of Al/Si disorder (Brown, 1987).

Grove (1971) suggested the potassium feldspar phenocrysts have a metasomatic origin. However, Vernon (1986) demonstrated primary igneous origins for potassium feldspar megacrysts and the potassium feldspar megacrysts in rocks throughout the map area are regarded as primary igneous phenocrysts.

Plagioclase phenocrysts, mainly oligoclase, constitute 25 to 35 percent of the rock and range from 2.0 to 8.0 millimetres long. Like equivalent extrusive and plutonic rocks, samples of Premier Porphyry dykes often host plagioclase phenocrysts that have thin clear rims around sericitized cores.

Plate 3.7A: Premier Porphyry dyke in trench wall near 2 Level adit, Silbak Premier Mine. Hammer for scale.

Plate 3.7B: Chilled margin along irregular contact of Premier Porphyry dyke cutting bedded tuffs of Lower Andesite Member, Unuk River formation. Exposed in bank of Salmon River near Flower Pot Rock. Hammer for scale.

Plate 3.7C: Three aspects of Premier Porphyry dyke:

I) Type rock with moderate chloritic alteration;
II) Strongly sericite-carbonate-pyrite altered dyke rock from south rim of Premier Glory Hole;
III) Strongly chloritized mylonite cuts Premier Porphyry dyke adjacent to Lindeborg vein in underground workings of Riverside mine.
Scale bar in centimetres.

Plate 3.7D: Multiply rimmed K-feldspar crystal in Premier Porphyry dyke. Plane polarized light; length of photo 2.2 mm.

Plate 3.7A

Plate 3.7B

Plate 3.7C

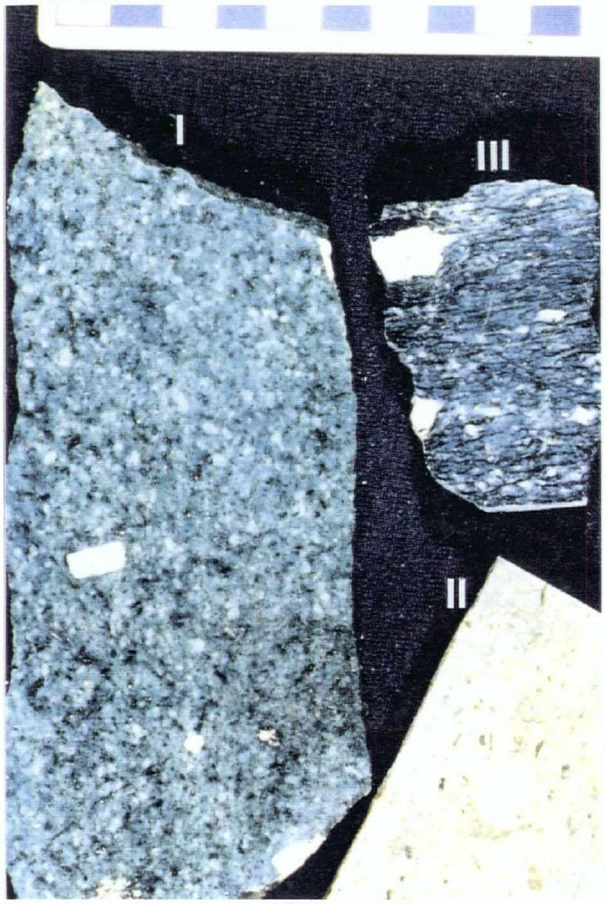

Plate 3.7D

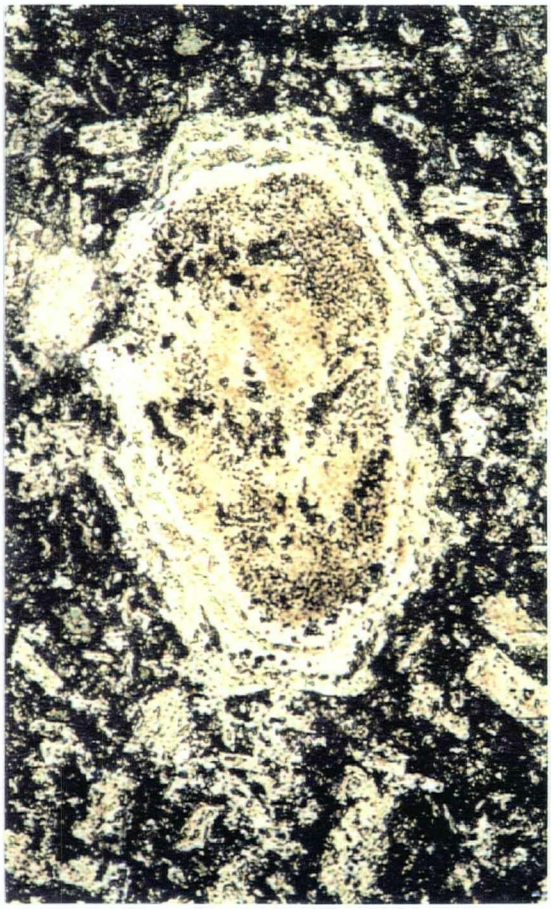

Scattered, small (<4 millimetres) quartz eyes are present in accessory amounts (up to 4 percent) in some dyke exposures. They are typically nodular to lobate and strongly embayed, indicating substantial resorption.

Euhedral hornblende phenocrysts make up 2 to 8 percent of the rock and average 3 millimetres long, with local examples up to 1.0 centimetre long. Hornblende is pervasively altered to chlorite ± pyrite and may only be preserved as chloritized remnants.

Apatite, sphene, zircon, pyrite and magnetite are accessory minerals. The rock typically contains about 2 percent very fine grained euhedral pyrite. Pyrite grains typically show pronounced quartz-chlorite-sericite pressure shadows, indicating a post-sulphide deformation event at elevated temperatures (Plate 3.9A).

The groundmass is fine grained to aphanitic and is generally strongly altered. Rare fresh samples show fine grained, interlocking to micrographic quartz and potassium feldspar.

Alteration generally consists of abundant very fine grained sericite, lesser fine grained carbonate, and minor chlorite and pyrite. In some dyke samples carbonate flooding is the dominant alteration; in other samples chlorite alteration is dominant. Plagioclase is altered to sericite aggregates with some carbonate, and the hornblende is primarily altered to chlorite. Alteration is not pervasive or ubiquitous even within a single outcrop; some samples are fairly fresh with little alteration of the groundmass and with unaltered hornblende crystals.

Mill Porphyry dykes crop out just uphill from the 3000 Level portal at the Scottie Gold mine and were intersected in the underground workings. They are generally similar to Premier Porphyry dykes but the potassium feldspar phenocrysts are stubby, somewhat rounded in outline and are buff to dull pink in colour. The matrix is very dark green and the dykes host abundant small, dark, dioritic xenoliths. These dykes have not been dated.

Salmon River dykes are potassium feldspar and hornblende porphyritic dykes with a coarse grained groundmass. The rock appears to be fresh in hand sample, but hornblende is partially chloritized and plagioclase is strongly sericitized.

Salmon River dykes cut the eastern contact of the Texas Creek batholith and country rock andesite tuffs of the Middle Andesite Member near the toe of the Salmon Glacier. Although these dykes might be deeper, coarse grained 'roots' to Premier Porphyry dykes, there is a difference of nearly 6 million years in zircon dates from these two dyke types (Table 3.10). Also, Premier Porphyry dykes have been noted at still deeper stratigraphic levels near Flower Pot Rock in the Salmon River.

Premier Porphyry sills were first reported by McGuigan and Dawson (1985) who identified two sill-like feldspar-porphyritic lenses at the Indian mine. These north trending sills dip 70 degrees east, parallel to bedding in nearby outcrops of the Upper Siltstone Member. Sills consist of large orthoclase phenocrysts in a fine grained hornblende granodiorite groundmass. Lane (1986) also reports stratabound, sill-like bodies of Premier porphyry rock south of the Premier gloryhole at the Simcoe and Pictou prospects. These sills could be stratabound injections of Premier Porphyry dyke material, but Branch (1976) suggests that subvolcanic sills may represent evacuated and collapsed magma chambers from early eruptive cycles.

3.2.1.4 PETROCHEMISTRY

Major element analyses of five plutonic and dyke rock samples from the Texas Creek suite were completed in this study. These results are presented in Section 3.3 and show that rocks of the Texas Creek granodiorite suite are subalkaline, calcalkaline intrusions with elevated potassium contents. Whole rock analyses from sub-volcanic Premier Porphyry dykes fall within the andesite field on a total alkali *versus* silica plot (Figure 3.11). This confirms the petrographic evidence of the strongly resorbed quartz crystals; free quartz was metastable in this magma, therefore the dykes are not dacites.

3.2.1.5 AGE

Isotopic dates from a variety of plutonic rocks of the Texas Creek plutonic suite range from 211 to 186 Ma, spanning the Early Jurassic. The oldest dates come from the core of the main batholith, the youngest dates from dyke phases.

3.2.1.6 GEOLOGIC SETTING

Rocks of the Texas Creek granodiorite suite were emplaced in a shallow subvolcanic setting below and within a Lower Jurassic andesitic stratovolcano. Some dykes were volcanic feeders that produced extrusive units on the paleosurface. Intrusion and crystallization proceeded over a 25 million year period from the deepest, earliest batholithic rocks to the shallower, youngest dyke phases.

Following emplacement, rocks of the Texas Creek plutonic suite were subjected to superimposed hydrothermal alteration and associated sulphide mineralization, episodes of both brittle and ductile faulting, and lower greenschist facies metamorphism. These rocks were deformed in the same regional deformation that affected stratified country rocks, and were later cut by intrusions of the Tertiary Hyder plutonic suite.

3.2.2 HYDER PLUTONIC SUITE

In the Stewart region the continental scale Coast Plutonic Complex trends northwest. Part of the main body lies along the southwest edge of the study area (Figure 3.1). Its eastern boundary is defined as the eastern limit of continuous Eocene plutonic rocks (Anderson, 1989). Buddington (1929) included the main Coast Range batholith and all the satellitic plutonic rocks to the east in the "Hyder Quartz Monzonite suite" or Hyder plutonic suite. Major studies of these rocks have been completed by Buddington (1929), Smith (1977), Grove (1986) and Woodsworth *et al.* (1990).

The Hyder Plutonic Suite includes a batholith, a large stock, several minor plugs and widespread dykes. The batholith lies within the eastern margin of the Coast Plutonic Complex. Smaller stocks in the map area are outlying satellites of the Coast Plutonic

Complex that are mineralogically and texturally similar to the main batholith. The varied dykes, collectively termed Hyder dykes, occur as prominent swarms of regional extent and as randomly distributed, isolated dykes in the intervening country rock. Although the plutons have associated dyke phases, they lack preserved extrusive equivalents.

Major plutons range in composition from granite to tonalite to quartz monzonite (Figure 3.13). These rocks are characterized by overall medium grain size, biotite, equigranular white plagioclase and orthoclase, and trace amounts of fine grained golden sphene. In comparison with Early Jurassic plutons, these Tertiary plutons are biotite rich, more siliceous and less altered. Associated dyke phases range from aplite to lamprophyre. Emplacement of the Hyder Plutonic Suite has produced variable contact metamorphism, including mechanical, thermal and metasomatic effects. This regionally extensive suite hosts major molybdenum deposits and many minor silver, lead, zinc, gold and tungsten occurrences throughout the district.

3.2.2.1 HYDER BATHOLITH

The Hyder batholith extends along the eastern side of the Coast Plutonic Complex from the Unuk River area southeastward along the Alaska border through the head of the Portland Canal at Stewart to Observatory Inlet and Alice Arm (Grove, 1986, p.69). This overall length is 175 kilometres and the width averages 16 kilometres. It is bordered on the west by the Central Gneiss Complex and on the east by stratified country rocks.

The Hyder batholith is well exposed along tidal zones of the Portland Canal and at roadcuts and quarries at Stewart, Hyder, and northward along the Granduc mine road to the Fish Creek bridge. The batholith ranges in composition from biotite granodiorite to quartz monzodiorite. The rock is fresh, light grey to pinkish grey, massive, medium grained, biotite-rich with minor hornblende, and locally slightly porphyritic. Fine grained golden sphene crystals are characteristic. Large outcrops show blocky joint patterns. Intrusive contacts are marked by biotite hornfels of argillaceous country rocks, epidote

disseminations and veins in tuffaceous and plutonic country rocks and local skarn development in calcareous sediments.

Based on biotite K-Ar dates, the Hyder batholith is Eocene, 48.8 Ma (Smith, 1977). Since none of the major Tertiary dyke swarms in the region cuts the batholith, this date places an upper limit on the age of the dyke swarms.

Locally, the Hyder batholith is spatially related to silver-rich galena-sphalerite-freibergite veins at the Porter Idaho, Silverado and Bayview mines near the town of Stewart. Regionally, discovery of the huge Quartz Hill molybdenum deposit in Alaska and the Molly May/Molly Mack molybdenite occurrences south of Anyox spurred interest in the main batholith of the Coast Plutonic Complex as a setting for molybdenum deposits.

3.3.2.2. BOUNDARY STOCK

The Boundary granodiorite stock, which straddles the international border southwest of Salmon Glacier, was not examined in this study. The stock was defined by Buddington (1929, p.32) from exposures of granodiorite around the Boundary Glacier (Munro Glacier on Canadian maps). It has been described in detail by Buddington (1929) and Smith (1977) and is briefly described by Kretschmar and Kretschmar (1980a) in an assessment report. It was not examined by Grove.

The Boundary granodiorite is an inequigranular, hypidiomorphic, medium grained, biotite-hornblende granodiorite (Smith, 1977, p.40). Hand samples are fresh, dull white, with scattered grains of pale pink orthoclase and grey glassy quartz; they are speckled with mafic crystals and tiny crystals of honey-coloured sphene are common. In contrast to the older Texas Creek batholith, which it intrudes, the Boundary stock is more massive, lighter coloured with a pinkish hue and contains conspicuous biotite. The Boundary granodiorite also resembles the Hyder batholith. However, the Boundary stock is generally finer grained; its hornblende needles are more euhedral, more abundant and more distinct; and all its minerals are slightly inequigranular.

3.2.2.3 OTHER STOCKS

Stocks much smaller than the Boundary granodiorite are defined where grandiorite porphyry dyke swarms have coalesced into small elongate plutons more than 400 metres wide. They are important features in property scale mapping and are ideal locations to study the inter-relationships between dykes and plutons.

The Mineral Hill stock crops out on the broad, flat top of Mineral Hill, five kilometres west of the Silbak Premier mine. Only its southern contact with argillites has been located but the stock is at least 800 metres wide; its eastern edge is assumed to grade into a myriad of southeast-trending dykes that line the Salmon River canyon along the southeast side of Mineral Hill.

The International stock is a wide exposure of coalesced plagioclase porphyritic, biotite granodiorite dykes exposed along the cut line of the international border at the Granduc mine road. The stock is mappable for more than a kilometre to the southeast, but to the northwest it ends abruptly in the canyon of Cascade Creek where it is truncated by the Cascade Creek/Slate Mountain Fault.

The Bunting stock crops out north-northwest of Mount Bunting at the snowline (Plumb, 1956). It lies southeast of the adits at the Spider prospect. This small, southeasterly elongate stock was also formed by coalescing felsic dykes.

The Oxedental stock is the best exposed of these small thickened dyke zones and is readily accessible along the lower Granduc mine road (Plate 3.8A). This porphyry contains coarse quartz and feldspar phenocrysts and displays distinctive flow-banding.

3.2.2.4 HYDER DYKES

The Stewart Complex hosts an extensive array of Tertiary dykes and dyke swarms, collectively termed the Hyder dykes. Textures and compositions are highly variable, ranging from aplite to lamprophyre, but plagioclase porphyritic granodiorite with biotite-rich, fine grained to aphanitic light grey groundmass is common. Some workers have restricted the name "Hyder dykes" to refer only to the granodiorite porphyry dykes, but

Plate 3.8A: Looking east from Mount Bayard across the Salmon Glacier to Mount Dilworth, the Granduc mine road and the Portland Canal dyke swarm. (Hembling photo.)

Plates 3.8B: Hornblende lamprophyre dyke (spessartine) cutting Summit Lake stock near toe of Berendon Glacier. Plane polarized light; length of photo 3.3 mm.

Plate 3.8A

Plate 3.8B

Late Tertiary aplite, microdiorite and lamprophyre dykes are considered to be late phases of the Hyder Plutonic episode in this study.

DYKE SWARMS

Rocks in the Salmon River valley are cut by two major southeast-trending swarms of felsic to mafic dykes and by a third less dense belt of intermediate to mafic dykes. Both major swarms are composed of four main dyke lithologies, the third swarm is composed only of the two youngest, more mafic dyke lithologies.

In the two major swarms intrusive rock comprises more than 40 percent of the bedrock; locally, only narrow lenses and slices of country rock separate the anastamosing dykes. The cumulative thickness of intrusive rock in these two southeast-trending swarms represents a northeasterly crustal extension of at least 1.5 kilometres.

The Portland Canal dyke swarm is the longest of the three swarms. McConnell (1913); Schofield and Hanson (1922) and Hanson (1929, 1935) all reported this swarm, but its location and regional extent have been best described by Grove (1971, 1986).

The Portland Canal swarm has been traced continuously southeastward from Mount Bayard to Mount Dickie and finally to Mount Trevor, located in the centre of the Cambria Icefield. The known length is 42 kilometres and the inferred length to Mount Trevor is 56 kilometres. Its northwestern limit has not been determined. However, the writer has identified major felsic dykes along the north wall of the Salmon Glacier northwest of Mount Bayard and further northwest in the cliffs of the Scottie Dog Mountain near the Granduc mine. This indicates a possible total length of 67 kilometres. The swarm has an indicated width of 2 kilometres on the accompanying map (Figure 3.2A), but the boundaries of the swarm are somewhat arbitrarily drawn where dykes make up 40 percent or more of the bedrock. Outside these drawn boundaries dykes crop out for up to 500 metres.

Dykes in the swarm generally trend east-southeast to southeast and dip steeply southwest, but dips flatten to about 45 degrees where dykes cross thin bedded argillites of

the Salmon River Formation south of Mount Dilworth. Individual dykes are up to 150 metres thick and can be traced to depths of hundreds of metres and lengths of thousands of metres. Myriad smaller dykes in the swarm, from a few to 60 metres wide, form a complex, anastamosing network. Dykes locally merge into plutonic bodies greater than 400 metres wide. Toward these minor Tertiary plutons, dykes are progressively closer together, thicker and more numerous, ultimately coalescing into the stocks.

Hanson (1929) suggested that the dykes of this swarm may be the top of an elongated stock. He envisaged a southeast-trending zone of weakness developed roughly parallel with the border of the Coast Range batholith during its intrusion, and predicted the dykes would coalesce at depth into the batholith or outlying stocks.

Variations in texture and composition have been noted within individual dykes as well as between dykes. The most abundant felsic dykes are equigranular or fine to coarse porphyries, and may be flow-brecciated. Modal compositions for these felsic dykes range between granite, quartz monzonite, granodiorite and quartz diorite (Grove, 1986). Other dykes in the swarm include aplites, microdiorites and lamprophyres.

No absolute age determinations have been made on any of the dykes in this swarm, but Brown (1987) reported that the Portland Canal swarm was more differentiated than the Boundary biotite-hornblende quartz monzonite dyke swarm and suggested that the Portland Canal swarm was slightly younger.

Several mineral occurences and a few deposits are located within this dyke swarm (Figure 4.16b). At some deposits like the Martha Ellen orebody, post-ore dykes cut across the mineral zones but are not themselves affected by the mineralization. At other showings the Portland Canal dykes were the locus for sulphide mineralization. Many dykes have been fractured and faulted, the spaces in the dykes and in adjacent country rocks are filled with coarse grained quartz and silver-rich galena and sphalerite, for example: Outland Silver Bar, Silver Basin, Lion, Unicorn, Silver Hill, Silver Tip, Spider, Lois, M.J. and Silver

Crown. None of these occurrences have been major producers, although Silver Tip does have significant reserves (Plumb, 1957a).

The Boundary dyke swarm is the second major southeast-trending dyke swarm and lies along the international border between Cantu Mountain and Mount Welker, passing through the Silbak Premier mine area. It extends beyond the map area in both directions.

The Boundary dyke swarm has a length of at least 22 kilometres, from Mount Jefferson Coolidge to the Bear River, and a width of 3 kilometres. The Boundary swarm has the same general southeast strike and steep southwest dip (135°/70°SW) as the Portland Canal swarm and includes a similar variety of dykes ranging from quartz monzonite and monzodiorite to aplite, microdiorite and lamprophyre. Granodiorite porphyry dykes are especially abundant within this belt. The most spectacular, continuous exposures are at the summit of Mount Welker. More accessible outcrops are along the Silbak Premier mine road, the Granduc mine road (Plate 3.8A) and at the confluence of Cascade Creek and the Salmon River.

The Berendon dyke swarm is the third, narrower, less crowded belt of dykes. This swarm trends south along the west side of Tide Lake Flats, and across the upper portal (3600 Level) area at Scottie Gold mine to August Mountain (Wares and Gewargis, 1982). From August Mountain the swarm swings southeast and continues over the crest of Mount Dilworth. Southeast of Mount Dilworth, toward Mount Bunting, this swarm merges with the wider Portland Canal dyke swarm.

This belt of dykes is significant because it is dominantly composed of microdiorite (andesite) dykes with many subparallel thin lamprophyre dykes. Older, more felsic, dykes are absent. These younger dykes clearly trend north to north-northwest where felsic dykes are absent. Therefore the northwesterly trend of younger, more mafic, dykes within the two major swarms is due to deflection or 'capture' of these dykes by the resistant, thicker, felsic dykes of the two main swarms.

DYKE PHASES

Hyder dykes have been grouped into four categories based on similar compositions, textures and relative ages. The oldest are massive, equigranular to porphyritic, fine grained to medium grained, light grey biotite or biotite-hornblende granodiorites that are up to 60 metres wide, and rarely, much wider. These are cut by buff to pinkish to white, massive to flow-banded, saccharoidal aplite or "rhyolite" dykes up to 5 metres wide. Aphanitic to fine grained, greyish green microdiorite or "andesite" dykes range up to 10 metres in width. These in turn are cut by thin, dark brownish grey, variably porphyritic lamprophyre dykes that are generally less than 50 centimetres wide.

Pale granodiorite porphyry dykes show significant variations in both composition and texture. Modal compositions range from granite to diorite, but massive plagioclase porphyritic biotite granodiorite is most common. Dykes are generally light grey in outcrop, but some exposures have been described as light bluish grey (Brown, 1987). In hand specimen the rock is characterized by pink to buff to white plagioclase phenocrysts, up to 5 millimetres long, that form up to 45 percent of the rock. Equigranular dykes are fine to medium grained; plagioclase, biotite, and occasionally hornblende, orthoclase or quartz can be recognized. The groundmass of the porphyritic dykes is aphanitic to fine grained.

A single U-Pb zircon date of 54.8 ± 1.3 Ma (Alldrick *et al.*, 1987) agrees with field relationships that show these dykes cutting all rocks except the younger plutons and dykes of the Hyder Plutonic suite.

Aplite dykes are sparsely distributed throughout the region. They seem to be more numerous within the two major southeast-trending dyke swarms and within the Tertiary plutons, and are probably genetically related to them.

Dykes generally range up to 5 metres wide and tend to weave or meander through the country rock, rather than have a rectilinear form. Consequently the dykes trend in many directions and have variable dips. However, within the major dyke swarms their trend is generally parallel to the resistant, bounding plagioclase porphyry dykes.

Aplite forms fine grained to saccharoidal, white to cream to buff to pale pink dykes with distinctive flow-banding and aphanitic chill margins. Flow-banding ranges from a few millimetres to a few centimetres thick, but is not present in all dykes. Some samples have distinct quartz eyes. Aplite is extensively sericitized and generally lacks mafic minerals.

Aplite dykes cut the Hyder batholith and the granodiorite porphyry dykes, but they are cut by younger younger lamprophyre dykes. Rb-Sr dates from aplite indicate a middle Eocene age of 44 ± 4 Ma (Brown, 1987). The relative ages of the aplite and microdiorite dykes are unknown.

Greenish grey or medium to dark grey sparsely porphyritic microdiorite dykes are distributed throughout the region and are the dominant lithology of the Berendon dyke swarm. Many outcrops show unequivocally that these dykes crosscut Tertiary Hyder plutons, while being cut by younger lamprophyre dykes.

Microdiorite dykes range up to 6 metres wide and typically display chilled margins and blocky fractures. Hand samples have an aphanitic to fine grained texture that may be porphyritic. Dykes are composed of small phenocrysts of plagioclase ± hornblende in a felted groundmass of interlocking plagioclase laths, lesser hornblende laths, and minor interlocking interstitial quartz and potassium feldspar (Buddington, 1929).

"Lamprophyre dyke", as used in this report, conforms to the definition by Rock (1977):

> an alkali-rich porphyritic dyke-rock with intermediate to very low SiO_2 content and moderate to high colour index, carrying essential primary amphibole and/or mica, and typified by panidiomorphic texture and by lack of felsic phenocrysts and lack of groundmass olivine.

It is clear that some workers have included varieties of older microdiorite dykes in a lamprophyre classification and that other workers have included younger pyroxene and olivine-bearing basaltic dykes as lamprophyres. True lamprophyres are sparsely distributed throughout the region. Most of the dykes are less than 50 centimetres wide. Thicker lamprophyre dykes rarely change attitude or thickness, but thinner dykes (<20 centimetres) change attitude or pinch out abruptly. Although dykes are rectilinear at large

scales, at outcrop scale they undulate slightly. Dyke contacts are sharp, parallel surfaces. Chilled margins are common but quite thin. Closely spaced joints make them easily eroded, so that many dykes are marked by deeply incised clefts.

Lamprophyre dykes vary in mineralogy, texture and hand specimen appearance. In outcrop, dykes are dark green, dark grey or dark brownish grey; fresh samples are charcoal to jet black. All these dykes are shoshonitic (Rock, 1977), but both biotite-rich minettes (Brown, 1987) and hornblende-rich spessartites (Buddington, 1929) have been reported. The three dykes studied by the writer were fresh, porphyritic to equigranular spessartites.

Buddington's (1929) study of these dykes is the most comprehensive. Porphyritic minettes are characterized by prominent biotite phenocrysts up to 3 millimetres long hosted in a massive, dark grey, aphanitic groundmass (Brown, 1987). Spessartite dykes are composed of 40 percent euhedral, deep green hornblende, 56 percent subhedral plagioclase, minor magnetite and trace hypersthene (Plate 3.8B).

Brown (1987) reported an Oligocene K-Ar date (25.2 ± 1 Ma) for a biotite lamprophyre. Carter (1981, p.88) also reports Oligocene K-Ar dates (36.5 ± 1.2; 34.4 ± 1.5) from two lamprophyre samples in the Alice Arm area.

3.2.2.5 PETROCHEMISTRY

There are no chemical analyses for any of the many different rocks of the Hyder plutonic suite in the Stewart area. However, Carter (1981, p.91) presents major element analyses for five similar plutonic rocks of identical age in the Alice Arm area south of Stewart. These plot as calc-alkaline granites to granodiorites on a Total Alkali *versus* Silica diagram (Figure 3.14a)

3.2.2.6 AGE

Granodiorite porphyry dykes cut all stratified rocks and all Early Jurassic plutonic rocks, but do not cut Tertiary plutons and dykes. Based on these field relationships and on age determinations, the emplacement of these dykes slightly preceded intrusion of the main

Tertiary plutons. Thus the plutons obliterated these precursor dykes. Dykes of aplite, microdiorite and lamprophyre cut all other rocks, and likely originated as late phases of the batholith. Tertiary plutons and dykes of the Hyder plutonic suite crosscut all regional folds, but are offset by most major and minor faults. In a few locations dykes are deflected along pre-existing fault zones.

Isotopic dates are available for most of the intrusive rocks of the Hyder suite and range from 55 to 25 Ma, a 30 million year period similar to the 25 million year span of dates from the Texas Creek suite. Dating is discussed in detail in Section 3.6, but based on field relationships and isotopic dates the general sequence of Tertiary intrusion is summarized in Table 3.3.

TABLE 3.3: Hyder Plutonic Suite--Sequence Of Intrusion
(Ages derived from isotopic dates and/or field relationships)

Epoch	Age (Ma)	Lithodemes/Phases
late Oligocene	35-25	Lamprophyre dykes.
early Oligocene	45-35?	Microdiorite dykes.
mid-Eocene	44	Aplite dykes.
mid-Eocene	48-49	Hyder batholith/Bitter Creek stock.
mid-Eocene	52?	Precursor Portland Canal dyke swarm
mid-Eocene	51-52	Boundary stock/Davis River stock.
early Eocene	55?	Precursor Boundary dyke swarm.
early Eocene	55	Granodiorite porphyry dykes.

Since the Boundary stock is slightly older than the Hyder and Bitter Creek plutons, their spatially associated precursor dyke swarms (Boundary and Portland Canal respectively) are probably also slightly different in age. It is impressive that these small age differences were correctly deduced for the plutons (Buddington, 1929, p.33) and for the dyke swarms (Brown, 1987, p.52) based on petrographic studies alone!

3.2.2.7. GEOLOGIC SETTING

The main batholith of the Coast Plutonic Complex and outlying satellitic stocks and dykes are interpreted as subduction-related plutonic rocks emplaced above the eastward subducting Pacific Plate in early Tertiary time. Emplacement of major intrusions ended

when relative plate motions changed from co-linear (high-angle) convergence to transcurrent (oblique) geometry about 42 Ma (Armstrong, 1988). The plutonic episode was followed by faulting, uplift and rapid erosion.

3.2.3 STIKINE VOLCANIC BELT

In Miocene time, alkali-olivine flood basalts formed plateau lavas. The lava issued from regional networks of vents and fissures (Souther, 1972; Smith, 1973). This volcanic activity culminated in the late Miocene to early Pliocene and continued intermittently through to the present day.

3.2.3.1 BASALTIC DYKES

Basaltic dykes have been reported by Buddington (1929) and, under the classification of lamprophyres, by Smith (1973, 1977; see Rock, 1977, p.140). The dark porphyritic rock has augite, plagioclase and rare olivine phenocrysts in a sub-ophitic groundmass of plagioclase and pyroxene. These widespread dykes may have been the feeders to Miocene volcanic flows that were eroded in this area, but are preserved elsewhere (Souther 1972, 1988, and 1990).

3.3 PETROCHEMISTRY

> The limited correlation between mineralogy and chemical composition is a common problem in igneous petrology and there is no agreement whether modal mineralogy, normative mineralogy, bulk chemical composition, historical precedent, oxide activities, or democratic plebiscite should form the basis for classification.
>
> **J.B. Gill, 1981**

3.3.1 VOLCANIC ROCKS

The petrochemistry of the Upper Andesite Member of the Unuk River Formation was previously discussed by Galley (1981), Alldrick (1985) and Brown (1987). In this report, chemistry is compared and contrasted at formational scale. The patterns show a systematic chemical evolution that is parallelled by the colour index and phenocryst assemblage of the rocks (Figures 3.5 and 3.9).

3.3.1.1 PHENOCRYST DISTRIBUTION

The stratigraphic distribution of phenocrysts shows an evolution that closely resembles Bowen's reaction series (Figure 3.5). The significance of different phenocrysts in andesites is reviewed by Gill (1981, Chapter 6). Plagioclase phenocrysts may range in composition from An_{15} to An_{99}; plagioclase phenocrysts in the Unuk River Formation fall in the range An_{25} to An_{45}. Characteristic features of plagioclase phenocrysts in orogenic andesites are present in Stewart rocks, for example, inclusion-rich zones, regions of oscillatory zoning, and clear normally-zoned mantles. Gill concludes that hornblende phenocrysts, which are conspicuously abundant in Stewart, are relatively uncommon in andesites and are largely restricted to medium and high-potassium andesites, to topographically and stratigraphically high levels of stratovolcanoes, and to formation in magma chambers at high crustal levels. Finally, he notes that quartz phenocrysts in andesites are almost always embayed. The presence of *metastable* quartz may reflect assimilaton of sialic rock, mixing of mafic and acid magmas, or high-pressure crystallization.

3.3.1.2 CHEMISTRY

Chemical analyses have helped classify volcanic rock types, determine their type and degree of alteration, and establish their tectonic affinities.

MAJOR ELEMENT CHEMISTRY

Alteration Screening

Alteration is the principal cause of lack of concordance between classification by petrographic description and by the Total Alkali *versus* Silica plot (Sabine *et al.*, 1985). Petrography is an essential step for classification of every volcanic rock and can readily identify all significantly altered rocks. Not only can altered rocks be screened and eliminated from the chemical data set by microscopic examination, but it is usually possible to reliably identify the original rock type despite its alteration overprint.

Altered samples must be eliminated from the data set before chemistry-based classification schemes can be applied to the remaining "unaltered" samples. To complement microscopic study, de Rosen-Spence (1976) developed three discriminant plots for separating chemically altered volcanic rocks from data sets. These plots identify alteration effects involving the most mobile elements: Na, Mg, Ca and Si. The plots separate unaltered subalkaline rocks from strongly altered samples and also separate unaltered subalkaline rocks from unaltered alkaline rocks. Screening plots were applied to all the available data sets (Figure 3.8); the results were alarming. Only 22 percent of the writer's data, 19 percent of Galley's data and 33 percent of Brown's data were retained as "unaltered" samples. Three additional samples, not picked up by the screening plots, were deleted from the data sets based on thin section study. A large proportion of the rejected samples fall in the "sodium depleted" field on the Na_2O *versus* SiO_2 plot. Petrographic work suggests these samples may have been affected by replacement of sodium by potassium in plagioclase. Sericitization in the Stewart area is common in most rocks and particularly intense in plagioclase phenocrysts. A plot of Na_2O *versus* K_2O (Figure 3.8d) shows a strong linear correlation between the two components, also implying selective replacement of sodium by potassium.

Four recommendations are proposed for dealing with variably altered volcanic rocks in Hazelton Group strata of the Stewart complex:

- Do not assume rocks are unaltered based on hand sample examination alone. Even careful sampling will not avoid significantly altered samples.
- Thorough petrographic description is an essential step that will identify all strongly altered samples and indicate alteration mineral assemblages.
- Application of discriminant plots as alteration screens will help identify moderately altered samples that may have been overlooked, and will give important insight into the bulk chemistry of the alteration process.

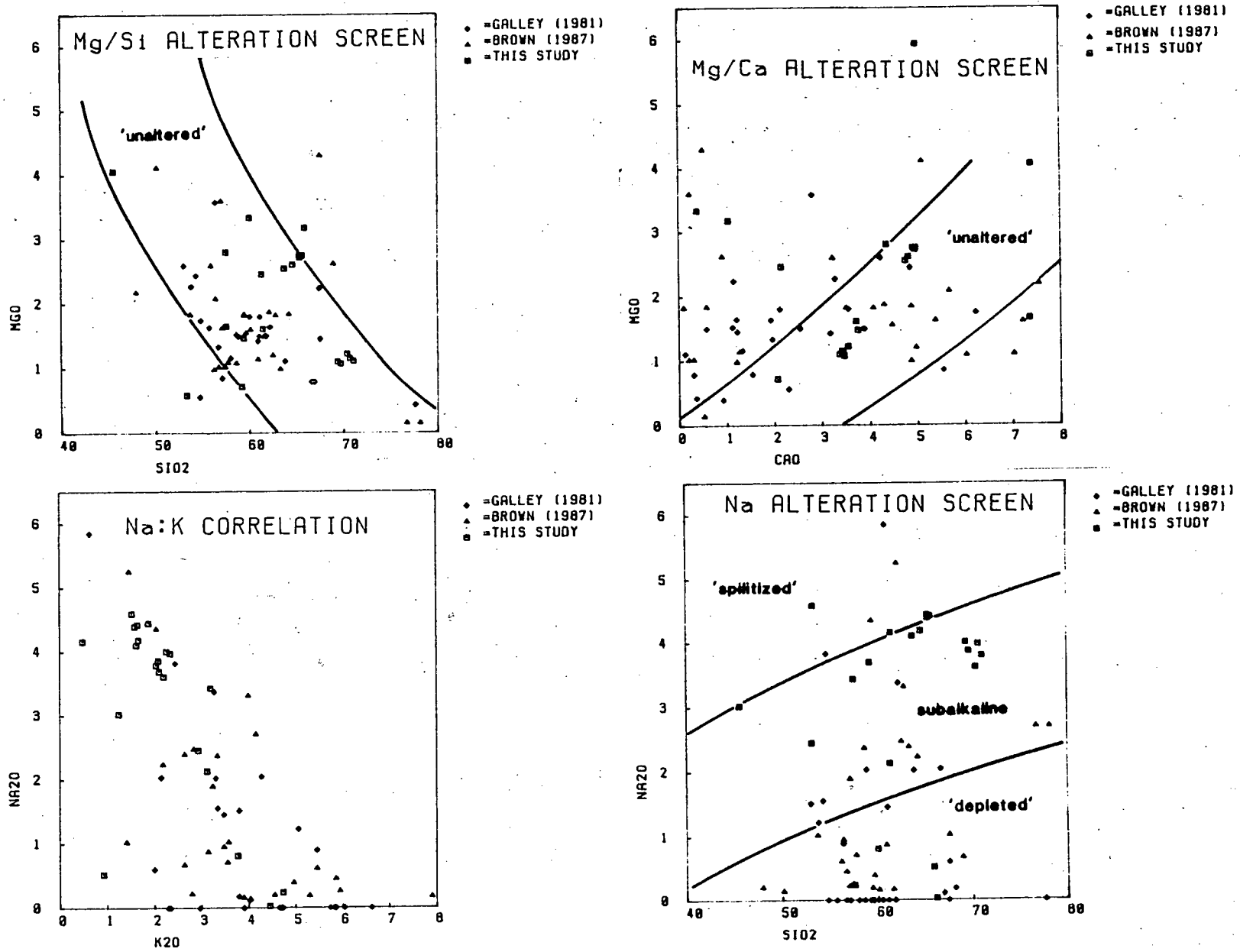

FIGURE 3.8: Alteration screening plots (from De Rosen-Spence, 1975)

- All iron-based discriminant plots must be interpreted with caution because most rock samples from the region contain some pyrite and many have hydrothermal chlorite alteration.

> Silica contents...are the best single discriminants for distinguishing andesites from basalts or dacites, they increase regularly relative to various differentiation indices and they have more immediacy to most people than do combinational parameters.
> **James B. Gill, 1981**

Histograms of total weight percent silica (Figure 3.9) are simple but effective diagrams that clearly separate the different lithological groups and show the progressive, more felsic evolution up-section.

> Concentrations of Fe, Ti, P, V and possibly Nb, Cu and Zn all remain constant or go through a maximum in tholeiitic orogenic andesites but consistently correlate negatively with silica in calcalkaline ones.
> **James B. Gill, 1981**

Composite Harker silica variation diagrams have been plotted for four main stratigraphic divisions and correlate well with calcalkaline orogenic andesites (Figure 3.10). Na_2O and CaO show strong negative correlation; Al_2O_3, MgO, FeO^* and TiO_2 show weak negative correlations; P_2O_5 is slightly negative relative to SiO_2 and K_2O shows a broad cloud of scatter reflecting the variable sericitization of these rocks. The strong scatter in the iron plot is from the dacites. The Na_2O distribution is not similar to that predicted by Gill (1981) and reflects selective potassium replacement. The TiO_2 analyses are almost all less than 1.2 percent, indicating a convergent margin, island arc environment (Gill, 1981).

The new I.U.G.S. classification scheme (Figure 3.11) shows that the "basalt" and "andesite" field terms are appropriate. Stewart andesites are dominantly high-silica andesites. Both the TAS plot (Figure 3.11) and the silica histogram (Figure 3.9) show that Premier Porphyry subvolcanic intrusive rocks are high-silica andesites. Strongly sericitized Premier Porphyry samples plot as trachyandesites (Figure 3.11). Finally, samples from the Mount Dilworth Formation plot as low-silica dacite, rather than rhyolite as suggested by Grove (1971), Galley (1981), and Brown (1987).

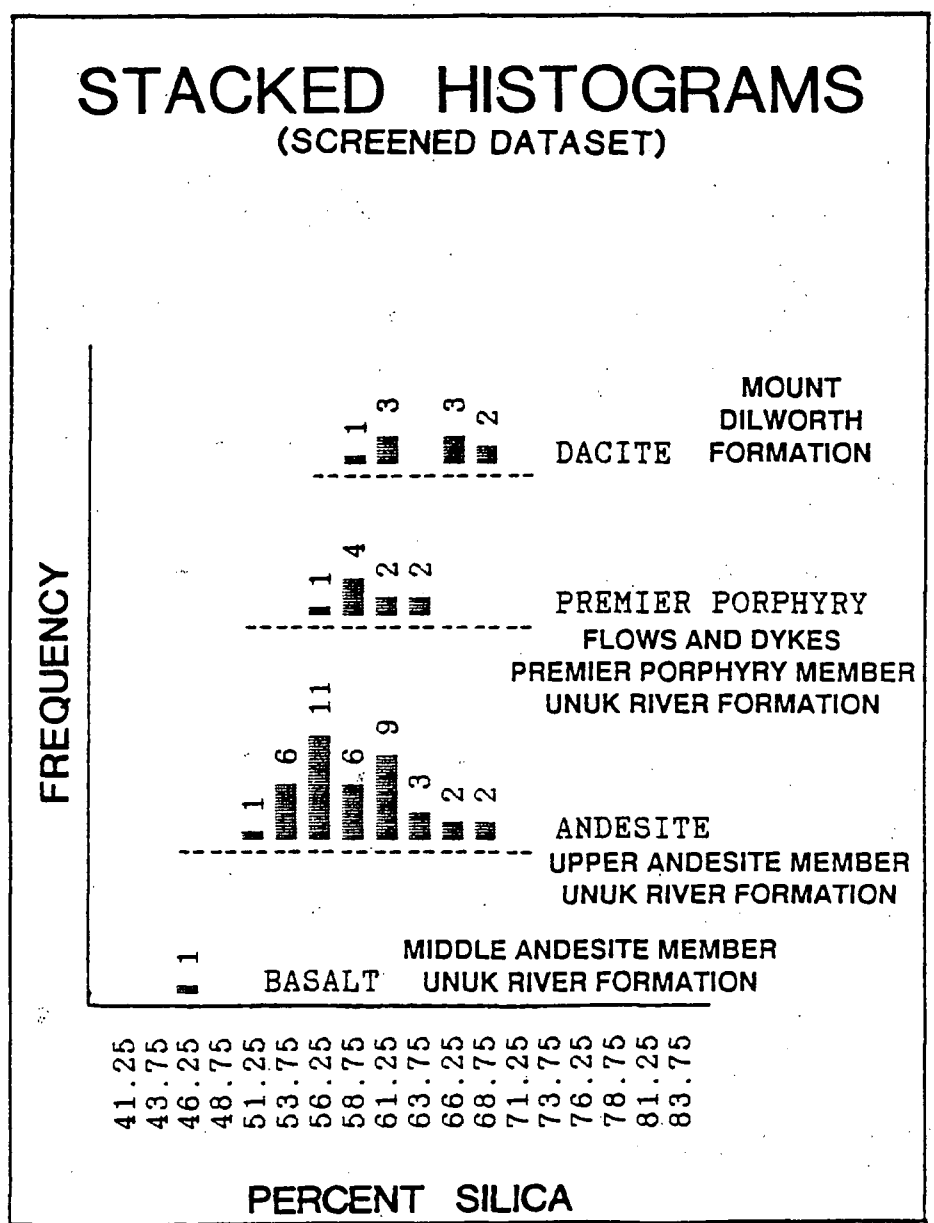

FIGURE 3.9: Silica histograms

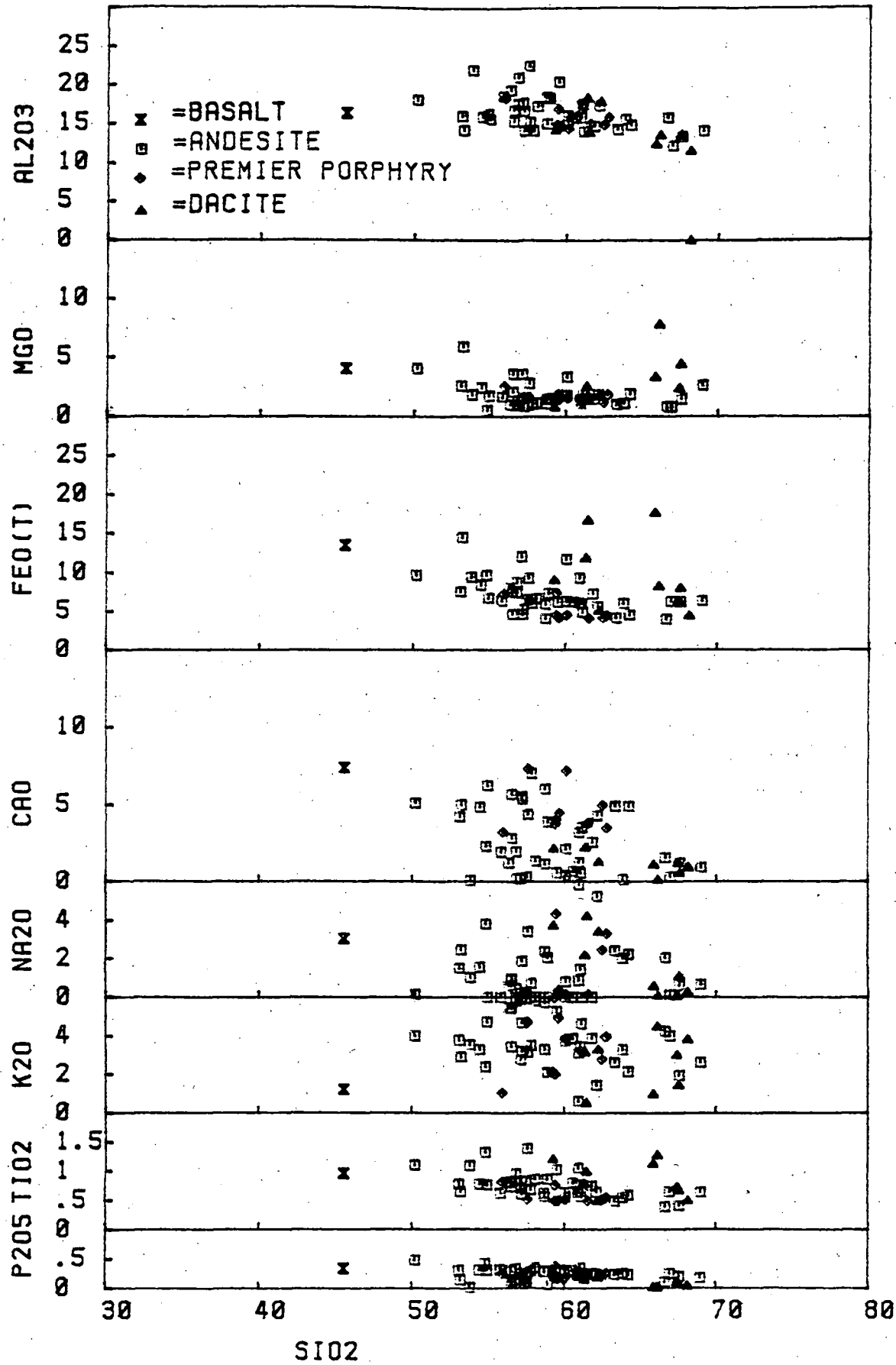

FIGURE 3.10: Harker silica variation diagrams

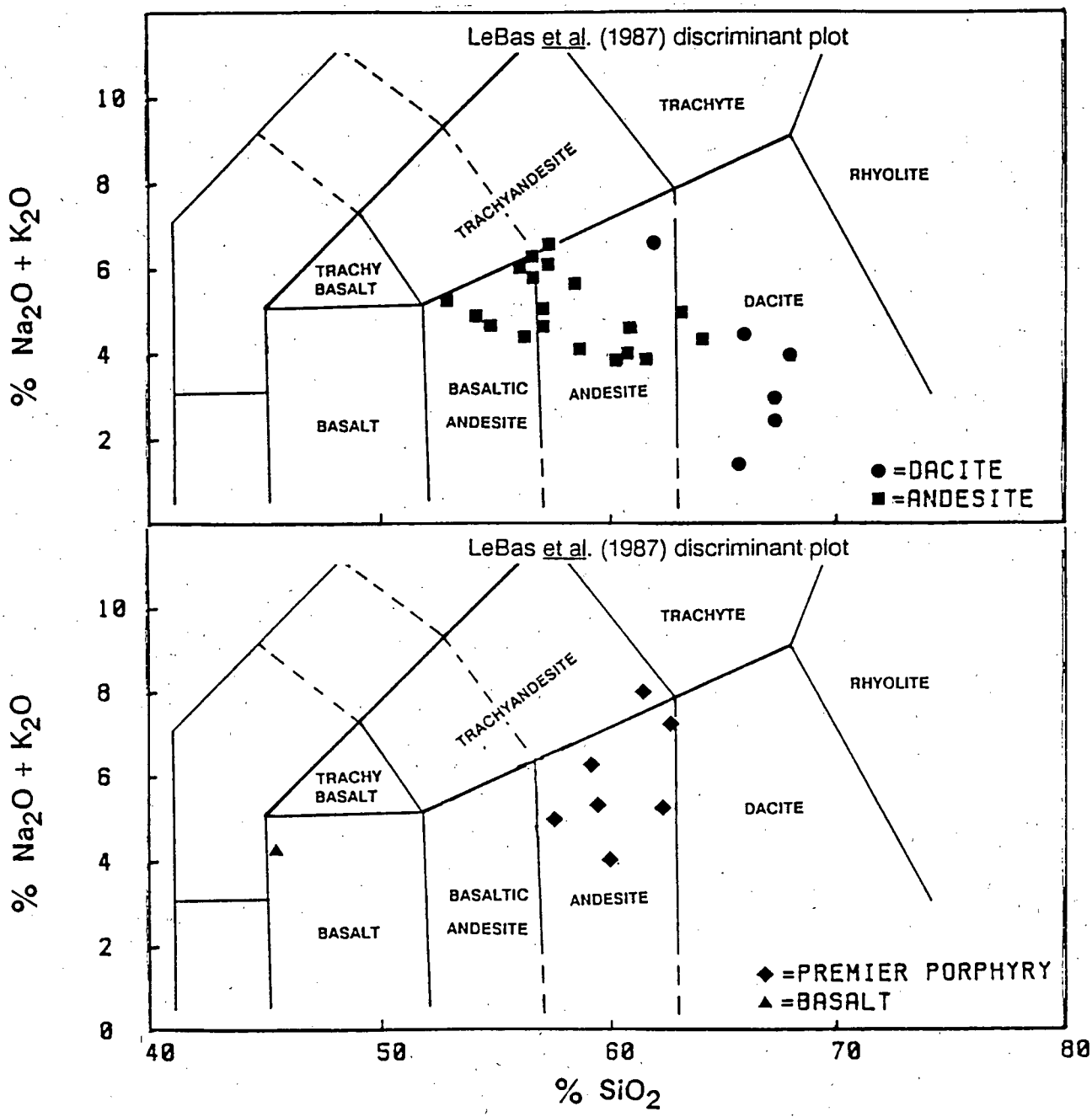

FIGURE 3.11: Total alkali versus silica discriminant diagrams

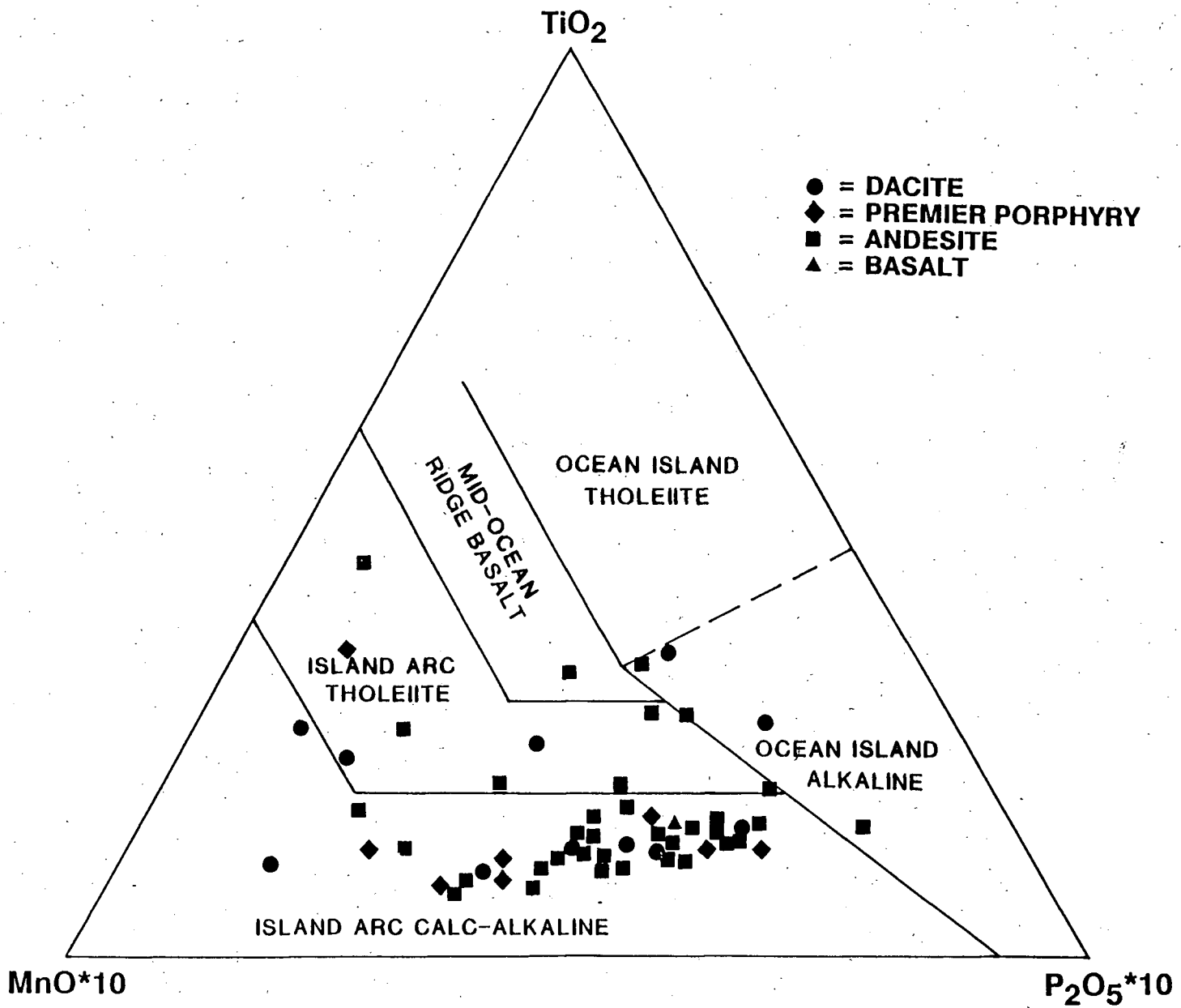

FIGURE 3.12: Tectonic environment discriminant plot (Mullen, 1983)

Application of the tectonic environment discriminant plot of Mullen (1983) in Figure 3.12 classifies most of the Stewart samples as calcalkaline rocks from a convergent-margin, island-arc environment.

MINOR AND TRACE ELEMENT CHEMISTRY

Trace element studies conducted by Brown (1987) suggest the rocks are calcalkaline, high-potassium, high-silica, orogenic andesites as defined by Gill (1981). Chondrite normalization diagrams plotted by Brown (1987) show patterns consistent with those of the convergent plate margin suites of Erdman (1985).

3.3.1.3 CONCLUSIONS

Monger (1977) identified the Hazelton Group as a volcanic arc assemblage well before detailed chemical analyses of these rocks began in the Stewart area. Three studies and several dozen analyses later, we have marginally improved this picture. Diagnostic plots of major element chemical data are of limited value, largely due to widespread hydrothermal alteration in the mineralized area. Iron-based discriminant plots are particularly misleading. Na_2O and K_2O-based discriminant plots are similarly suspect due to sericitic alteration.

Hazelton Group volcanic rocks are a subalkaline, potassium-rich, iron-rich(?), calcalkaline suite that ranges in composition from basalt through andesite to dacite over a stratigraphic thickness of 5 kilometres. This compositional change is paralleled by a progressive change in colour from dark olive green to light grey and by progressive evolution of associated phenocrysts. Augite porphyritic basalts are subalkaline. Intermediate volcanic rocks are medium- to high-potassium, high-silica andesites, and are chemically similar to modern andesites of the Chilean Andes. Premier Porphyry rocks are high-potassium, high-silica andesites. Felsic volcanic rocks of the Mount Dilworth Formation are low-silica dacites.

The subaerial volcanoes of the Stewart camp formed along the central axis of a volcanic arc and were established on crust approximately 30 kilometres thick Gill, 1981, p.46-49). The topographic setting envisioned is an arc-island chain of major islands and isolated subaerial volcano-islands (similar to Indonesian examples or the eastern Aleutians), resting on thickened or "continental" crust.

3.3.2 PLUTONIC ROCKS

There are scores of modal composition determinations for medium to coarse grained plutonic rocks of the Stewart camp, but major element chemical analyses are limited to 13 samples. Five samples of plutonic rock from this study and eight samples from Brown's (1987) work are the only petrochemical analyses completed on plutonic rocks.

No modal composition determinations were undertaken in this study. Earlier data from Buddington (1929), Smith (1977) and Grove (1986) are replotted here (Figure 3.13) using Strekeisen's (1979) nomenclature. The diagram shows that Texas Creek rocks range from granodiorite to monzodiorite and quartz diorite while Hyder suite rocks range from granite (syenogranite) to tonalite and are slighly more quartz and alkali feldspar rich. Due to the large area of overlap in modal compositions, a Streckeisen diagram alone would not be a reliable discriminant plot for plutonic rocks in this area.

Major element analyses from the Texas Creek plutonic suite and from the Hyder plutonic suite in the Alice Arm area are plotted on discriminant diagrams from Cox *et al.* (1979) and Brown (1982) in Figure 3.14. All plots clearly show that the Texas Creek batholith, Summit Lake stock and Premier Porphyry dykes are chemically similar and likely comagmatic; the wider scatter of the dyke analyses is attributed to alteration. The more siliceous rocks of the Hyder plutonic suite are chemically distinct.

Rocks of the Texas Creek suite are subalkaline, calcalkaline, high potash monzonites to diorites that are chemically identical and probably comagmatic with Hazelton Group volcanic rocks. Rocks of the Hyder suite are subalkaline, calcalkaline granites to granodiorites and have no preserved extrusive equivalents.

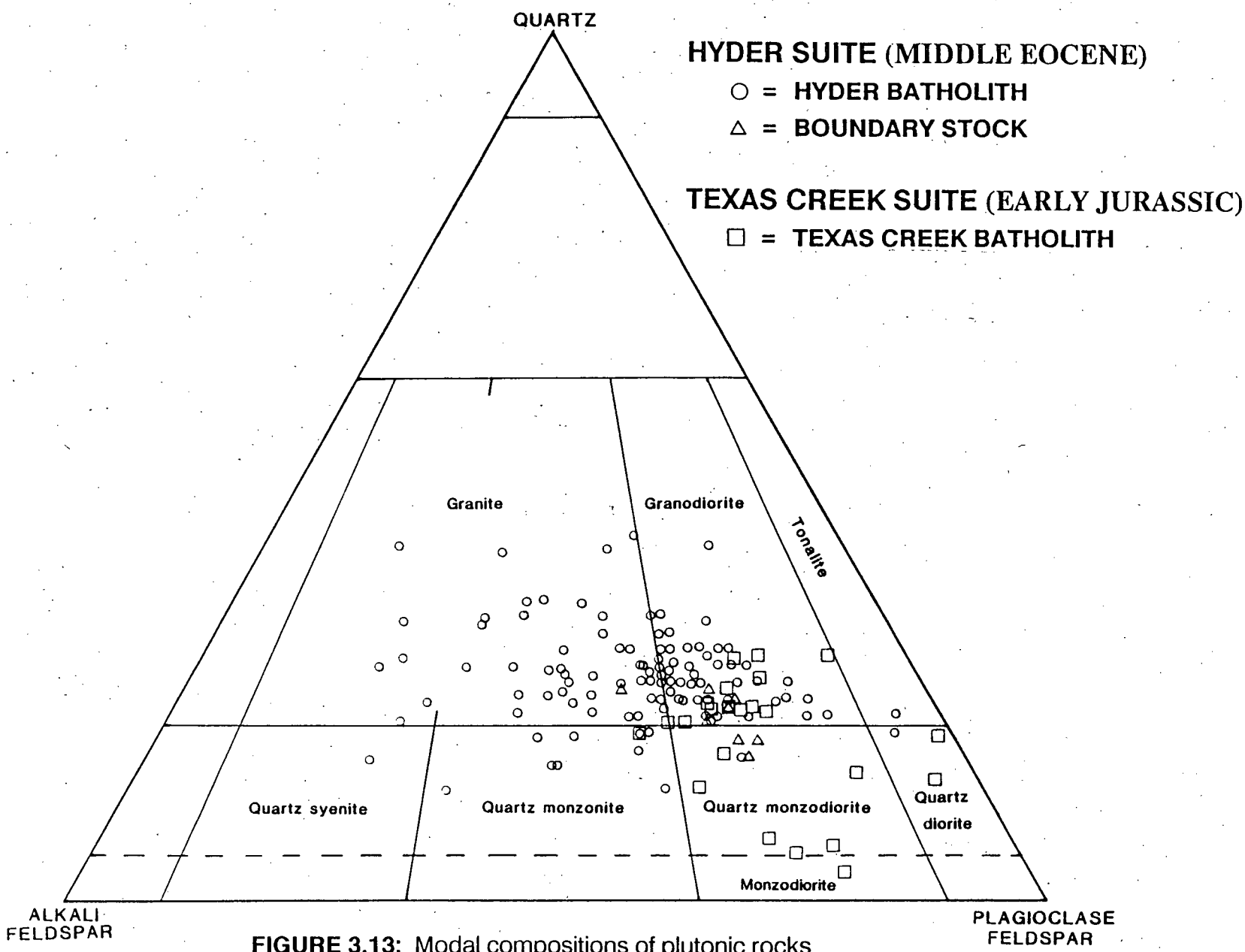

FIGURE 3.13: Modal compositions of plutonic rocks (after Streckeisen, 1975)

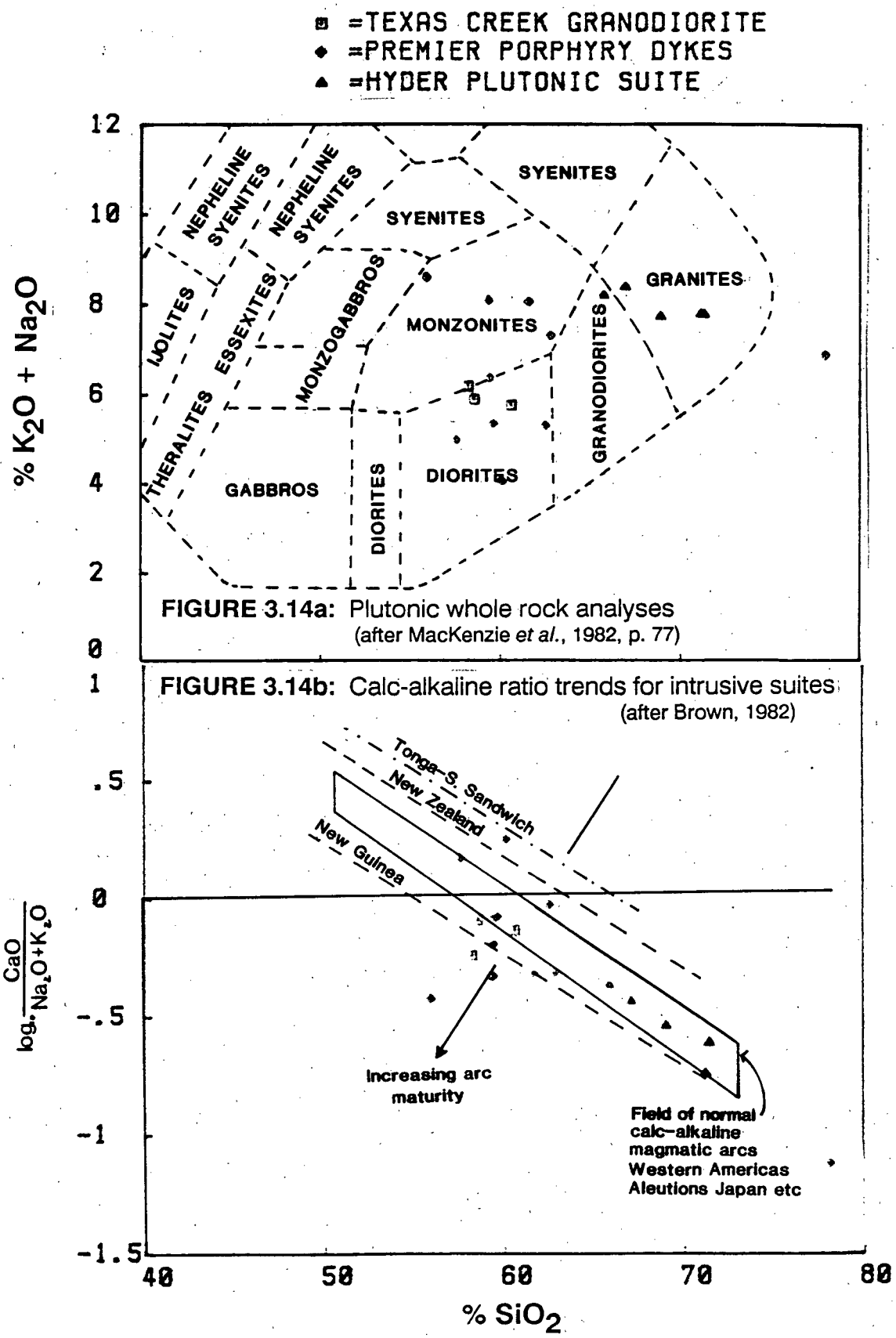

FIGURE 3.14: Plutonic rock discriminant diagrams

3.4. STRUCTURE

The map area lies in a single structural domain or sub-area. All rocks have been subjected to the same series of stress regimes, although different lithologies have deformed differently. Brown's (1987) study includes the most comprehensive structural analysis to date. Shorter studies by Grove (1971), Read (1979) and Galley (1981) emphasize the complexity and the wide variety of interpretations that are possible.

Rocks in the study area display a variety of fabrics and structures on all scales. Structural elements include:

- primary bedding (S_0) measured in sediments, felsic volcanics and rare sedimentary intervals in massive andesitic sequences,
- northwest-trending folds (F_1) that vary from open in volcanics, to tight to isoclinal in turbidites,
- minor axial-planar cleavage (S_1) related to small, tight folds formed during regional-scale folding,
- west-dipping foliation (F_2) of brittle to ductile origin
- west-plunging lineations (L_3) and geometrically related extensional quartz veins and joints (S_3) (Brown, 1987),
- southeastward-trending, subvertical ductile shear zones (F_4),
- brittle faults of many scales, orientations and ages.

3.4.1 FOLDS

Folding is the dominant structural feature of area. The main fold structure is a northerly trending **regional scale fold system** of *en echelon* synclines. Individual synclines trend north-northwest with steeply dipping to vertical axial planes. Each syncline is an open to tightly folded doubly plunging canoe-shaped structure. Volcanic and sedimentary rocks of the Hazelton Group are deformed into open cylindrical folds. Sedimentary rocks of the overlying Salmon River Formation occupy the synclinal cores and display disharmonic tight to isoclinal folds on many scales. Bedding-plane faults or décollement surfaces formed

where ductility contrasts between the siltstones and underlying felsic volcanics caused failure.

Intermediate-scale minor folds, tens of metres wide, have been noted in several areas and are related to the formation of the major fold system. **Outcrop-scale minor folds** have only been noted in siltstone units, and are grouped into two classes:

- Strongly contorted minor folds are varieties of drag folds, and can be found wherever siltstone packages are cut by faults or intruded by major dikes.
- Some outcrop-scale minor folds within the Salmon River Formation are disharmonic space accommodations of plastically deformed siltstones that maintain axial planar continuity with the regional fold pattern.

3.4.2 FAULTS, MYLONITES AND CATACLASITES

Faulting is abundant on both local and regional scales, but there are unresolved questions about absolute and relative ages of fault displacement.

Small-scale faults are ubiquitous and create difficulties in locating and correlating offset mineralized zones and in estimating dilution factors for ore reserve calculations. These brittle faults are preserved as narrow fault breccias or pinching and swelling bands of fault gouge up to 30 centimetres thick.

Major faults are separated into five groups:

- regional-scale north-trending, subvertical shears
- northerly trending, west-dipping shears
- southeast to northeast-trending "cross faults" that cut the northerly structural grain
- décollement surfaces or bedding plane slips that occur near the base of the Salmon River Formation
- mylonite zones.

Regional scale faults form major topographic lineaments that control drainage. These northerly to north-northeasterly trending, subvertical to steeply west-dipping, ductile to brittle faults include the Long Lake, Fish Creek, Skookum Creek, Salmon River and

Cascade Creek faults.

Examples of map scale, **northerly trending moderately west-dipping normal and reverse faults** are the Harris Creek fault, the Union Creek fault and its northern extension, the Mineral Gulch fault, and the series of parallel faults around and south of the Silver Butte property. The faults probably originated as ductile, compressional reverse faults, and were reactivated as brittle faults during later extensional episodes.

Easterly "crossfaults" are brittle, subvertical faults that have strong, but narrow, foliation envelopes. These faults trend from northeast to southeast and show lateral offsets up to 1 kilometre. Examples are: the East Gold fault, Millsite fault, Morris Summit fault, Dumas Creek fault, Windy Point fault and Hercules fault.

Décollement surfaces or bedding plane slips are common around the perimeter of the Salmon River Formation outcrop area. These slips indicate detachment during folding near the contact with underlying dacitic strata of lower ductility.

Intrusion of the **northwesterly trending dike swarms** was accompanied by at least 1.5 kilometres of northeastward extension. Many dikes have sharp, planar, brittle wallrock contacts.

Buddington (1929, page 16) first reported east-trending "gneissic structures" or **mylonites** in granodiorites and noted that they are parallel to strong foliation zones in the greenstone country rock. Discrete mylonite bands, a few metres wide at most, have been identified from the southernmost exposures of the Texas Creek batholith to as far north as Cooper Creek. At the Silbak Premier mine, mylonite zones are exposed in the disrupted, clast-rich, banded sulphide zone at the 2 Level portal and in bedrock trenches near the glory hole.

There are at least three orientations to mylonite zones in the map area:

- North-trending subvertical faults like the Long Lake fault (Brown, 1987) and the Fish Creek fault (Smith, 1977).

- North-trending, west-dipping fault zones commonly contain ductily deformed, flattened clasts.
- Southeast-trending, steeply northeast-dipping mylonites deform and offset Jurassic ore at the Silbak Premier mine and provide the locus for the Tertiary ore veins at the Riverside mine.

Moderately west-dipping, flattened angular clasts and rounded cobbles are common in outcrops and underground exposures throughout the southern half of the map area; these exposures are all examples of ductile deformation. In the past, the orientation of flattened clasts has been recorded as bedding, but where continuous exposures are available, it is possible to walk out of the deformed zone into similar rock with equant angular or rounded clasts.

The extensive zones of **cataclasite** illustrated by Grove (1971, 1986) and the single zone indicated by Smith (1977) could not be located in the field or recognized in dozens of thin sections from these areas. Grove's photomicrographs are typical of foliated, sericitically altered, fine lapilli tuffs within the Unuk River Formation. The writer concludes that all the "cataclasites" of the Salmon River valley are actually moderately to strongly foliated, moderately altered andesitic lapilli tuffs and crystal-lithic tuffs.

3.4.3 FOLIATION

Foliation is a fundamental characteristic of regionally metamorphosed rock. In the Stewart area, primary foliation is present as bedding and as rare flow banding in some dikes, plutons and extrusive flows. Secondary foliation is present as rare axial-planar slaty cleavage, as schistosity, as flattened clasts in conglomerates or fragmental tuffs, and as gneissic or mylonitic fluxion structures described in the preceding section.

The dominant foliation in andesitic rocks of the Unuk River Formation is a north-trending penetrative foliation dipping moderately westward (30° to 70°W). This west-dipping foliation remains one of the most readily observed yet difficult to explain phenomena of the Stewart mining camp. In this report the foliation is regarded as

coalesced or superimposed foliation envelopes that surround most fault zones in the district. These foliation envelopes extend into wallrocks adjacent to both brittle and ductile faults. Envelopes associated with minor brittle faults are narrower, a few tens of metres at most; envelopes associated with major, ductile faults may be well over 100 metres wide with foliation intensity becoming progressively stronger toward the core of the shear. Faults are so widespread that most outcrops in the region show some degree of foliation; but this mechanism for foliation development also explains the seemingly random, local areas of unfoliated, unstrained, massive tuffs that have been encountered during mapping programs--there is no fault zone nearby. In any single outcrop, the most prominent foliation likely represents the largest or youngest faulting in the area as foliation envelopes from younger faults overprint and obscure pre-existing foliation envelopes.

The foliation envelope of a fault may be obvious while the recessively weathered fault itself is hidden. Intensely foliated outcrops of andesite tuff near the junction of the Silbak Premier and Big Missouri mine roads are coplanar with a broad, multiple fault zone mapped in the 6 Level adit at the Silbak Premier mine (P. Wodjak, personal communication, 1985), which is probably the Slate Mountain fault.

West-dipping foliation is emphasized by flattened angular volcanic fragments in the andesitic tuffs and similar flattened cobbles in the conglomerates. These flattened clasts show that many of the faults were ductile in nature. West-dipping foliation and flattened fragments record east-west compression at the relatively elevated temperatures needed to produce semiductile to ductile deformation. Compression was probably accompanied by a series of ductile reverse faults. Subsequent Tertiary doming due to batholith emplacement produced an extensional regime that reactivated many of these faults, producing west-dipping, extensional, normal faults with ductile fabrics in their wallrocks.

TABLE 3.4: STRUCTURAL HISTORY OF THE STEWART DISTRICT

AGE (Ma)	STRUCTURAL AND TECTONIC EVENTS	OTHER GEOLOGIC EVENTS
0		
	Minor fault adjustments	flood basalts
	Reactivation of older faults	lamprophyre dykes
35	Minor E-W extension	microdiorite dykes
48		
	Regional doming and extension Normal, west-dipping faults	Hyder batholith and satellite stocks
52		
	NE-SW extension	Granodiorite Dyke Swarms
56		
	Tectonic and magmatic lull	
100		
	Regional Metamorphism (Greenschist facies) Folding, with decollements developed along base of Salmon River formation (early) Reverse faults and west-dipping foliation Mylonites Pencil lineation (late)	No strata preserved (Probably none deposited) No intrusive rocks
120		
150	Tectonic and magmatic lull	
		Turbidites
185		Subsidence
190	Subduction terminates	Subaerial arc volcanism
210		
	Convergent margin subduction	Subaqueous arc volcanism
230		

3.4.1 STRUCTURAL HISTORY

The structural history of the area is summarized in Table 3.4. The undulating fold axes of the regional-scale folds can be attributed to inhomogeneous contraction along nearly horizontal, east-northeast stress/strain axes. The similar geometry of west-dipping ductile shear zones and foliation suggests a common origin with the folds during east-west compression. However, upright folds probably formed early, followed by sequential development of west-dipping foliation.

Eocene dike emplacement was accompanied by significant northeast-southwest crustal extension. The north-trending pattern of microdiorite and lamprophyre dikes suggests minor east-west extension in Late Tertiary time.

3.5. METAMORPHISM AND ALTERATION

3.5.1. METAMORPHISM

Regional metamorphic grade throughout the area is lower greenschist facies. Two independent lines of evidence indicate that temperatures reached 290°C at pressures of 4.5 kilobars about 110 million years ago.

Most previous studies have defined the regional metamorphic grade as sub-greenschist to greenschist, or even sub-amphibolite facies (Read, 1979, Galley, 1981, and Brown, 1987), although Grove (1971) felt that metamorphic grades reached lower amphibolite facies. Comparison of mineral assemblages documented in this study and in earlier work with experimental phase transitions (Heitanen, 1967, Winkler, 1979 and Liou *et al.*, 1985) narrows the possible range of P,T conditions considerably.

The key mineral assemblages preserved in the rocks and other diagnostic minerals that are conspicuous by their absence are listed in Tables 3.5a and 3.5b. Relevant mineral phase transitions are listed in Table 3.5c. The P,T boundaries defined by these equations are plotted on Figure 3.15 and indicate that the rocks in the region have been metamorphosed to lower greenschist facies. Pressure was 4500 bars ± 1500 bars; temperature was 300°C ± 25°C.

TABLE 3-5: Metamorphic minerals and phase transitions

TABLE 3-5 A: Metamorphic minerals identified.

Albite	Leucoxene (?)
Carbonate/Calcite	Prehnite (Brown, 1987)
Chlorite	Pyrite
Epidote	Sericite

TABLE 3-5 B: Metamorphic minerals conspicuous by their absence in petrographic studies.

Biotite (minor primary biotite altered to chlorite)
Hornblende (abundant primary hornblende altered to chlorite)

Ca-plagioclase	Glaucophane
Chloritoid	Magnetite
Cordierite	Pumpellyite

Garnet (locally present in small skarn zones)

TABLE 3-5 C: Bounding univariant equilibria for equations in FIGURE 3.15.

1. chlorite + white mica + quartz = cordierite + phlogopite + fluid
2. chlorite + white mica + quartz = cordierite + biotite + Al_2SiO_5 + fluid
3. Fe-chlorite + quartz ± magnetite = almandine garnet
4. chlorite + albite + tremolite = glaucophane + clinozoisite + quartz + fluid
5. chlorite + zoisite + quartz + fluid = lawsonite + pumpellyite

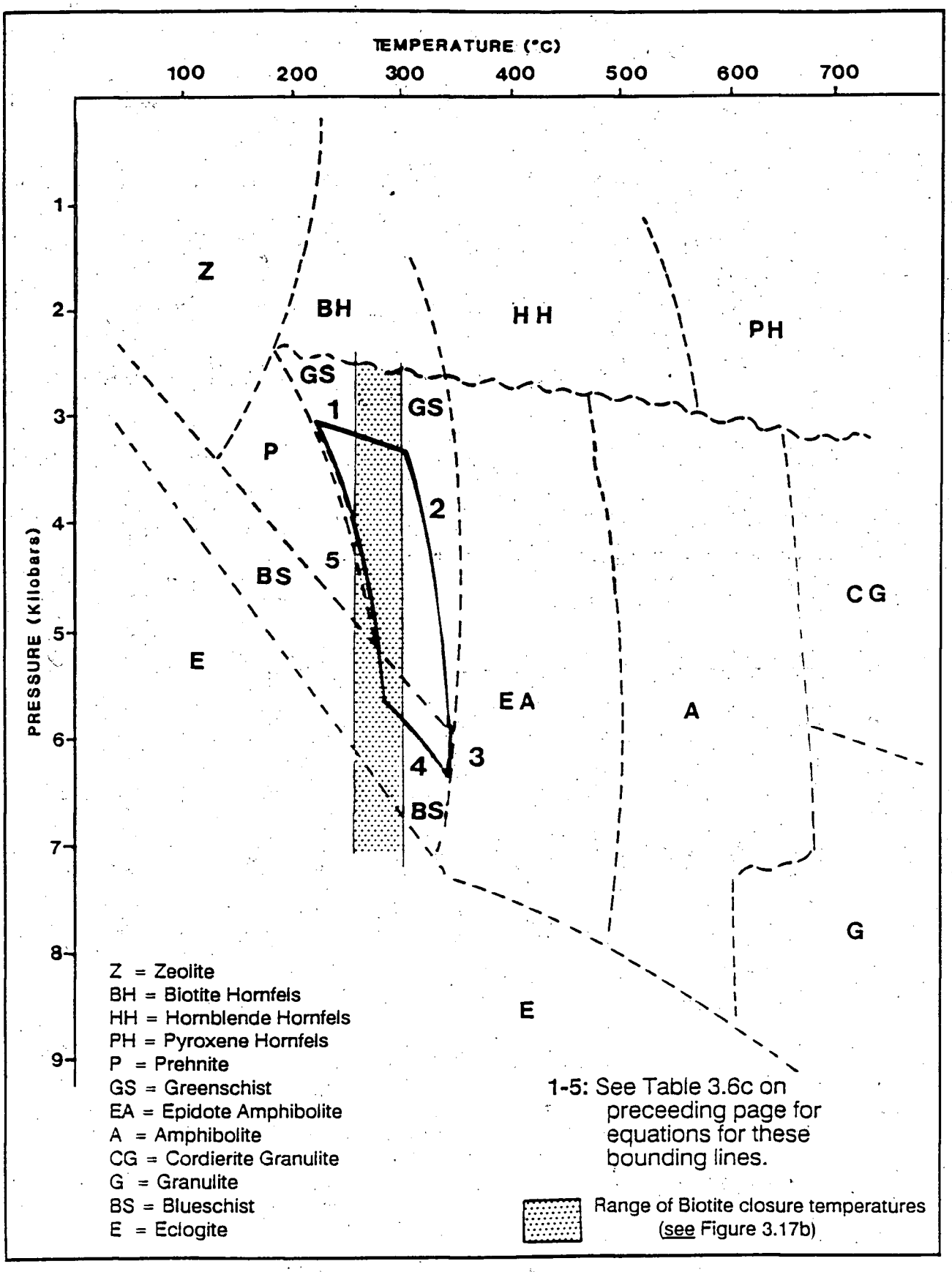

FIGURE 3.15: Regional metamorphic grade in the Stewart mining camp

(Modified from Hietanen, 1967, Winkler, 1979, and Chou et al., 1985)

From field relationships, the timing of metamorphism and deformation must lie between deposition of the youngest sediments (Bajocian, 175 Ma) and the onset of intrusion of the unmetamorphosed Hyder Plutonic Suite (Early Eocene, 55 Ma).

Microscopic textures show syndeformational mineral growth suggesting the physical deformation and thermal metamorphism that affected the region were contemporaneous. Pressure shadows around euhedral pyrite are filled by chlorite or by quartz with minor sericite (Plate 3.9A). Chlorite and quartz crystals are commonly curved, indicating rotation of the stress field or rotation of the rock within a stress field during mineral growth.

One unexpected result from geochronometry work in this study was determination of the age and maximum temperature of the regional metamorphic event (Section 3.6). Resetting of potassium-argon dates from biotite, sericite and feldspar indicate a thermal peak of 280°C ± 20°C was reached 110 ± 10 million years ago.

Contact metamorphism around intrusive bodies is minor and discontinuous. Where Tertiary plutons cut calcareous sedimentary rocks, zones of brownish to purplish biotite hornfels are developed. Bedding in the rock is usually preserved; one outstanding example of biotite hornfels is exposed along the main drift of the Skookum (Mountainview) adit, located southeast of the Riverside mine (West and Benson, 1954).

3.5.2 ALTERATION

Alteration is a conspicuous feature in hand samples of all andesitic rocks and some intrusive rocks in the area. At microscopic scale all rocks show alteration effects except some samples of the Hyder Plutonic suite. This section summarizes the types of alteration assemblages so that they can be readily compared, and indicates the extent, interpreted age, and process of formation of these assemblages.

"Alteration" is used in its broadest sense to include metamorphic and surface weathering products, since some of these features were mapped as hydrothermal alteration in the past. This arrangement also allows comparison and contrast of assemblages formed by regional metamorphism and geothermal processes.

TABLE 3.6: CLASSIFICATION OF ALTERATION TYPES BY MINERALOGY, INTENSITY AND EXTENT
(Numbers in parentheses refer to discussion in text)

KEY: **W** = Weak; **M** = Moderate; **S** = Strong; **I** = Intense

DIAGNOSTIC MINERALS(S)	REGIONAL (>15 km)	MINING CAMP (5-15 km)	PROPERTY (0.1-5 km)	LOCAL (<100 m)
Chlorite (+ Pyrite)	W (1)	M (4)	S (6)	I (9)
Hematite	S (2)		S (16)	
Carbonate	W-M (3)			I (8)
Sericite (+ Carbonate) (+ Pyrite)			M-S (5)	S-I (10)
Pyrite			M-S (14)	M (12)
Epidote			M-S (7)	W-M (15)
Biotite			S-I (11)	
Hornblende				W-M (17)
Skarn (calc-silicates)				S-I (13)

TABLE 3.7: CLASSIFICATION OF ALTERATION TYPES BY AGE AND GENETIC PROCESS
(Numbers in parentheses refer to discussion in text)

LOWER JURASSIC:

I. BROAD GEOTHERMAL PROCESSES

Deep, strong chlorite + pyrite **(4)**
Shallow, moderate carbonate **(3)**
Local strong carbonate flooding **(8)**

II. FOCUSSED HYDROTHERMAL PROCESSES

Strong, sheared chloritic margin of Texas Creek batholith **(6)**
Strong, sericite + carbonate + pyrite bleaching of turbidites **(5)**
Intense chlorite **(9)**
Intense sericite + carbonate + pyrite **(10)**
Moderate coarse pyrite **(12)**
Stratabound pyrite in dacites **(14)**
Hornblende metasomatism around Summit Lake stock **(17)**

III. SURFACE WEATHERING

Strong hematitic alteration of some tuffs and most coarse clastic sediments **(2 and 16)**

MID-CRETACEOUS:

IV. REGIONAL METAMORPHISM

Lower greenschist facies mineralogy **(1)**

EOCENE:

V. CONTACT METAMORPHIC, METASOMATIC AND HYDROTHERMAL PROCESSES

Biotite hornfels **(11)**
Skarn **(13)**
Epidote **(7 and 15)**

Alteration types are listed according to their extent in Table 3.6, ranging from regional scale phenomena affecting hundreds of square kilometres down to small alteration patches affecting areas less than 100 square metres. Alteration assemblages are then separated into groups according to interpreted age and process of formation in Table 3.7.

Alteration extent, intensity and mineralogy is often lithology-dependent, reflecting the permeability, chemistry or paleotopographic position of the host. In the case of focussed or channelled hydrothermal fluids, alteration assemblages are primarily structurally controlled but may still show irregular distributions reflecting lithological changes in the wallrock of the structural conduit.

1. Lower greenschist facies regional metamorphism is indicated by a chlorite-carbonate-sericite-pyrite-epidote mineral assemblage (Plate 3.9A). Macroscopic examination of slabbed rocks shows that metamorphic grade is roughly the same throughout the Salmon River area. Alteration is weak to moderate; the fresh rock colour is medium greenish grey. Although it is a subjective distinction,
regionally metemorphosed tuffs can be readily separated from the more intensely altered hydrothermal propylite zones. Propylitized rock is greener, hosts coarser pyrite porphyroblasts and has more calcite and thus a stronger reaction to HCl. Two areas of extensive exposures of typical greenschist facies rocks, well away from hydrothermally altered zones, are on the western slope of Troy Ridge and along the south side of the Morris Summit Glacier, southwest of the Morris Summit fault.

2. Strong hematitic alteration characterizes the sedimentary rocks of the Betty Creek Formation, part of the Premier Porphyry Member of the Unuk River Formation, and minor coarse clastic sedimentary lenses within the Upper Andesite Member of the Unuk River Formation. Hematitic alteration in these distinctive brick red to purple rocks is attributed to subaerial oxidation by meteoric water on the exposed paleosurface.

3. The Lower Dust Tuff Member of the Mount Dilworth Formation displays weak carbonate alteration consisting of 10 to 15 percent, evenly distributed, fine grained

Plate 3.9A: Pressure shadow around pyrite crystal shows sequntial (but penecontemporaneous?) growth of sericite, quartz and chlorite. Silbak Premier mine. Crossed nicols; length of photo 1.2 mm.

Plate 3.9B: Photomicrograph showing strong chlorite-carbonate alteration in groundmass of Premier Porphyry dyke rock. Silbak Premier mine. Plane polarized light; length of photo 3.0 mm.

Plate 3.9C: Andesite lapilli tuff. Strongly altered with clasts wholly replaced by yellowish green epidote. Exposure in Silverado Creek, 400 metres below Silverado millsite, Mount Rainey. Hammer for scale.

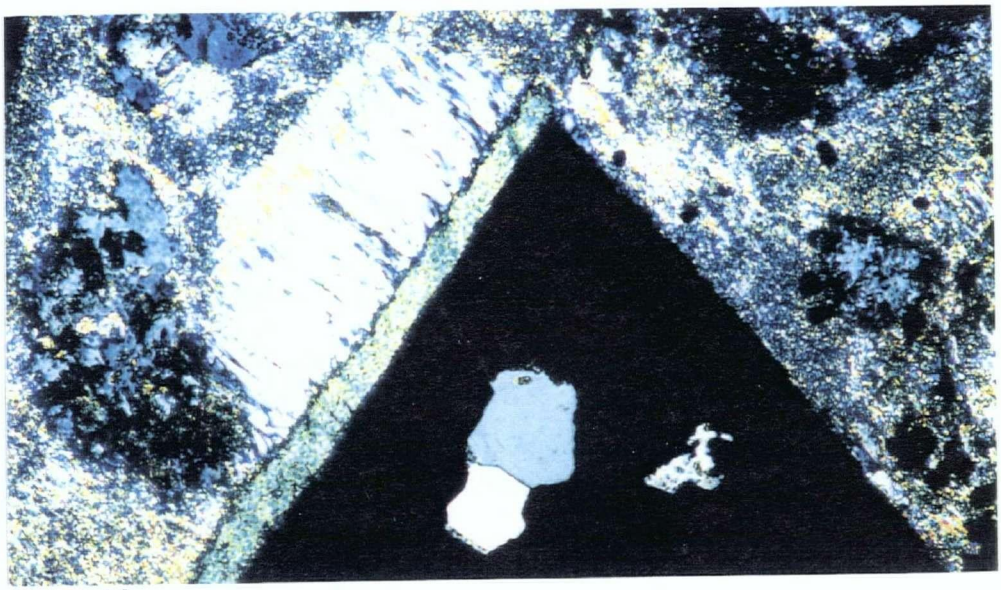

Plate 3.9A

Plate 3.9B

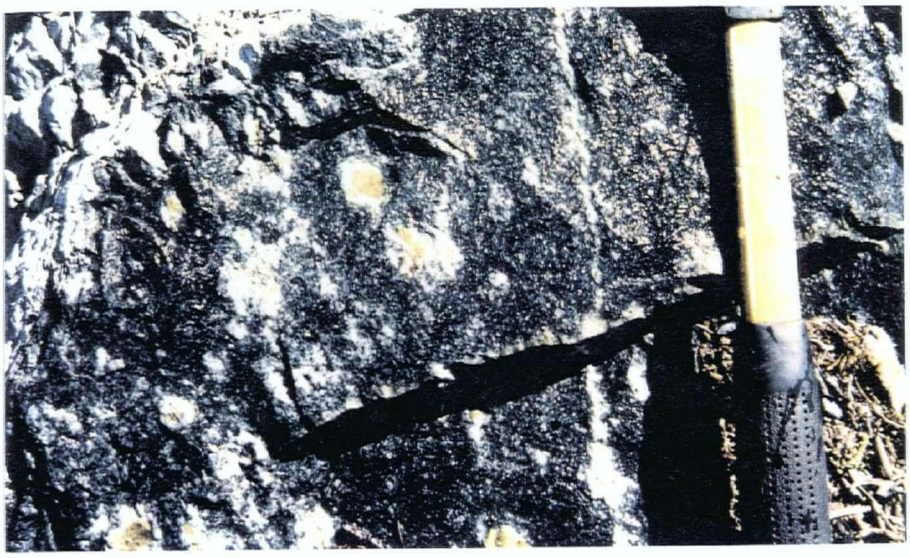

Plate 3.9C

carbonate. Overlying units are partially to strongly welded and served as an impermeable cap to circulating groundwaters. This carbonate flooding is interpreted as an extensive, shallow carbonate alteration that is developed from circulating sulphate bicarbonate groundwaters that characteristically overlie geothermal systems in andesitic stratovolcanoes (Henley and Ellis, 1983, and Figure 3.16).

4. Broad areas of strong propylitic alteration are common throughout the mineralized areas of the Unuk River Formation. Strong chloritic alteration and associated euhedral pyrite affect a large area of the Upper Andesite Member from well south of the Silbak Premier mine northwards to the 49, Lila and Harry prospects just south of Summit Lake. Clasts in fragmental volcanic rocks may be selectively epidotized. These large propylitic zones are attributed to deep circulation of chloride-rich brines characteristic of hydrothermal convection cells within recent island arc andesitic stratovolcanos (Henley and Ellis, 1983, and Figure 3.16).

5. Strong sericite-carbonate-pyrite alteration forms a distinctive gossanous horizon that extends northwards along Tide Lake Flats from the Millsite fault to the East Gold mine, gradually decreasing in intensity further northwestward and fading out at Thomas Creek (Figure 4.1a). The brightly coloured band is composed of thin bedded black siltstones of the Upper Siltstone Member. It represents a relatively permeable unit that selectively channelled hot fluids northward and southward away from the Summit Lake stock, which intrudes the unit just downstream from the toe of Berendon Glacier.

The pyritic rock has been aggressively sampled for assay and is generally barren, but hosts the high grade veins of the East Gold mine near its northern end, just before the alteration intensity begins to diminish. The alteration process is likely similar to structurally controlled sericite-carbonate-pyrite zones to the south, but this zone deserves special attention because of its stratigraphic control and its demonstration of a direct connection between the Lower Jurassic stock, sericitic alteration, and a high grade gold deposit.

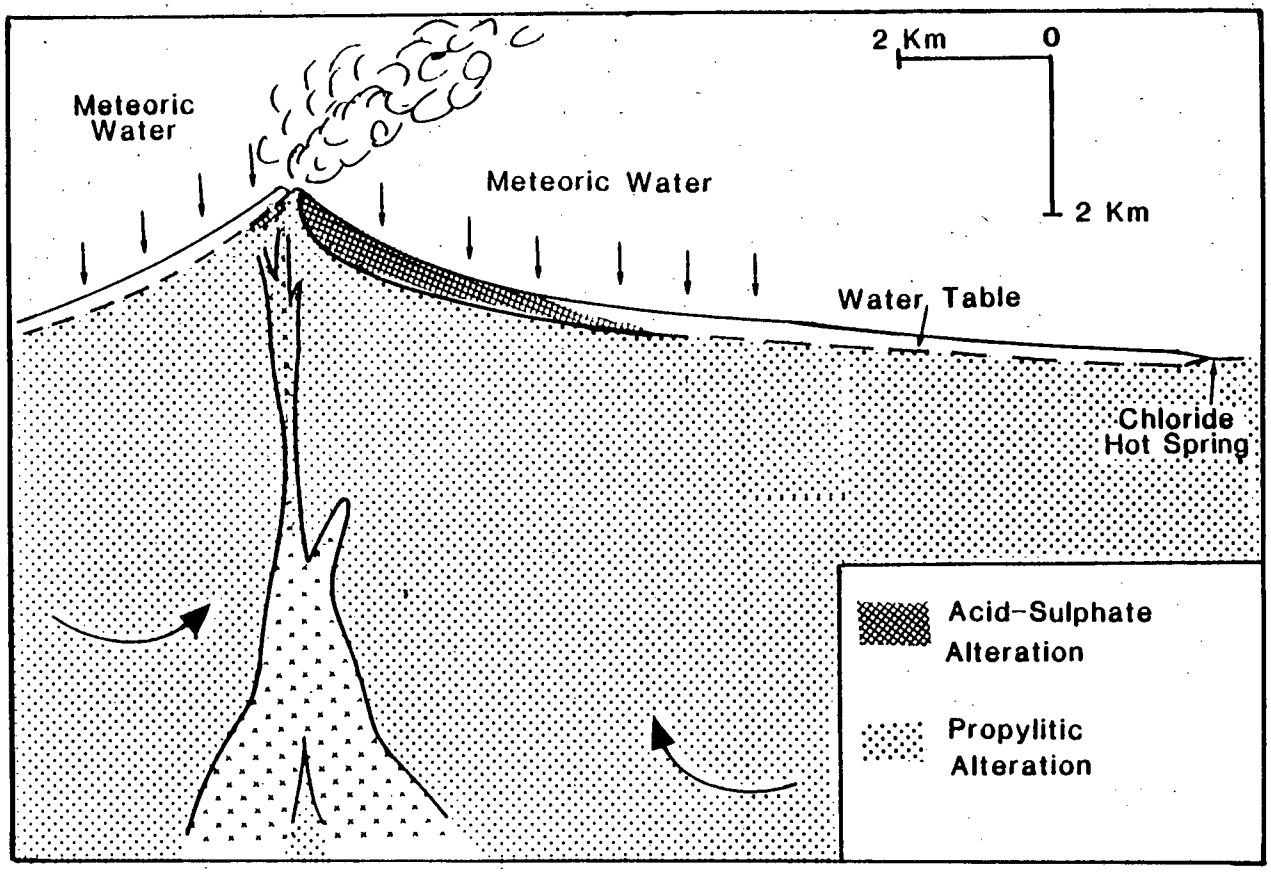

FIGURE 3.16: Distribution of alteration within an andesitic stratovolcano (modified from Henley and Ellis, 1983)

6. Strong chloritic alteration is locallized along much of the eastern contact of the Texas Creek batholith where the margin is crushed and crudely foliated. The alteration is interpreted as syn-volcanic geothermal propylitic alteration concentrated in a highly permeable zone along the margins of the pluton. The crushing and foliation are due to late stage intrusion and to volume changes in the core of the large pluton after the outer margin had crystallized.

7. Strong epidote alteration is disseminated in andesitic to dacitic country rocks around the perimeter of Tertiary plutons. Significant, but less extensive zones of epidote alteration are also common around Tertiary dykes, and are distributed along and around permeable faults or shear zones that have been cut by Tertiary plutons or dykes. Alteration along shears can extend more than one kilometre from the intrusion. Alteration typically occurs as fine to medium grained disseminated epidote that is preferentially weathered from outcrop surfaces, and is only evident in fresh rock and drill core. Close to plutons, lithic fragments may be wholly replaced by epidote (Plate 3.9C). In both intrusive and country rocks, within a few metres of the contact, crosscutting narrow veinlets of epidote and minor specular hematite are common.

8. Strong carbonate flooding is preserved as local zones within the broad propylitic alteration zones in the massive andesite tuffs. Hand samples are very pale green to off-white and have a bleached or 'silicified' appearance. The rock is quite soft however, and gives a strong reaction to HCl. Thin sections show groundmass, phenocrysts and fragments are flooded by up to 35 percent fine grained carbonate. This alteration is interpreted as remnant islands of early (shallow) hydrothermal carbonate flooding have escaped subsequent overprinting by later (deeper) chloride-rich brines as the volcanic edifice grew. Several zones of carbonate-flooded rock crop out in the bush between Cascade Creek and the switchback on the Big Missouri road.

9. Intense chlorite alteration is common in wallrocks adjacent to many ore shoots. It is most evident in the deeper levels of the Silbak Premier mine (Plate 3.9B). At shallower levels

this alteration is absent, representing either non-deposition or overprinting by subsequent sericite-carbonate-pyrite alteration. This classic propylitic alteration is accompanied by up to five percent medium to coarse grained disseminated euhedral pyrite.

This alteration type is attributed to intense propylitzation alongside long-lived fluid channelways. The transition to the broader propylitic envelope of regional greenschist metamorphism is gradational, but the two differing intensities are readily distinguished in hand sample. An easily accessible example is the roadcut through the Hope prospect on the Granduc mine road; wallrocks on the south side of the sub-vertical sulphide zone show intense propylitic alteration.

10. Strong sericite-carbonate-pyrite alteration is a characteristic feature of the wallrock at all the deposits in the Big Missouri area, and at ore shoots in the shallower levels of the Silbak Premier mine. The rocks are strongly bleached to an off-white color and have a silicified look--although they are not generally silicified. Altered wallrocks in the Big Missouri area show progressive alteration of andesitic tuffs (Plate 3.10A). Original rock textures are commonly obscured (Plate 4.6A). The carbonate component is often more abundant than the white mica, but broken rock tends to fail along the micaceous foliation, creating the appearance of a strongly sericitized rock, sometimes termed sericite schist. Alteration may extend up to 50 metres outward from ore zones and grades abruptly into broad propylitic alteration over distances of only a few metres (Plates 3.10A and 4.6A). This alteration preceeded, accompanied and followed sulphide deposition along long-lived or reactivated channelways within the stratovolcano.

Sericite-carbonate-pyrite alteration is regarded as typical hydrothermal sericitic alteration introduced by hydrothermal brines at moderate to shallow depths. This assemblage is a common feature in the wallrocks of epithermal ore deposits (Silberman and Berger, 1985).

11. Dense mats of fine grained biotite hornfels are a common feature of siltstone units cut by plutons of the Hyder plutonic suite. Hornfels has a characteristic red-brown to purplish

Plate 3.10A: Progressive sericite-carbonate-pyrite alteration (bleaching) of chloritic andesitic lapilli tuff in Dago Hill drill hole at depths of 34, 36 and 37.5 metres respectively. Note variation in lapilli textures. Alteration has virtually obscured lapilli in the most altered sample which is cut by a blue-grey chalcedony and sulphide veinlet. Note abrupt transition from chloritic to sericite-carbonate bleaching in central core piece. BQ drill core, scale bar in centimetres. Samples 81-58-21 and 81-58-22. Dago Hill deposit

Plate 3.10B and C: Two photomicrographs of sericitic alteration front at microscopic scale, superimposed on dacitic tuff in wallrock at Prosperity/Porter Idaho mine. Plane polarized light; length of photos 3.0 mm.

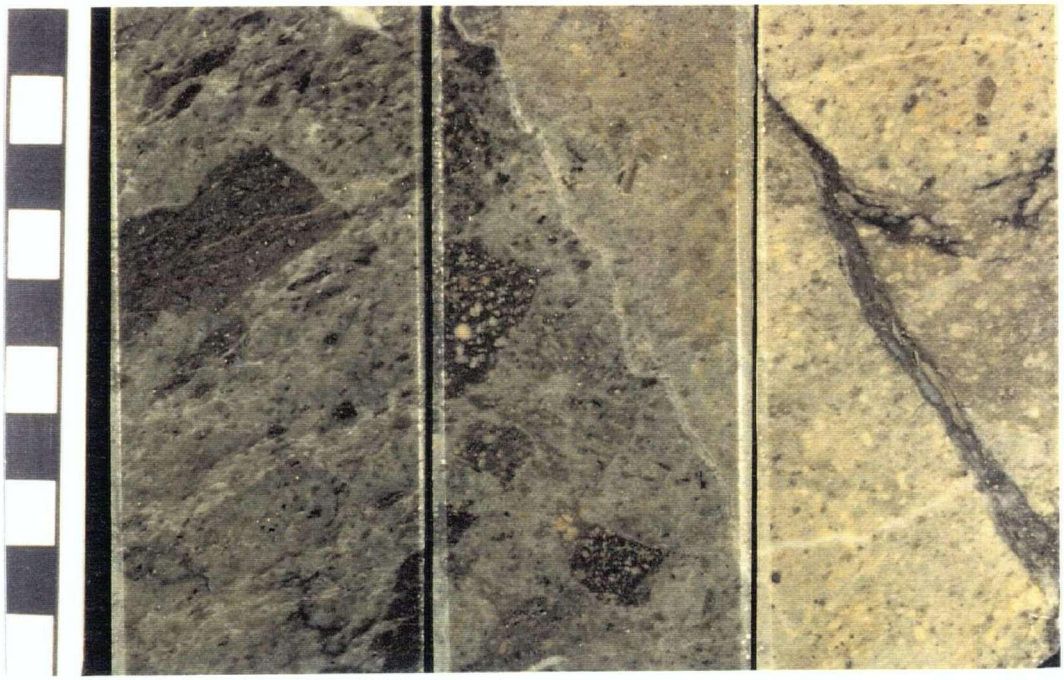

Plate 3.10A

Plate 3.10B

Plate 3.10C

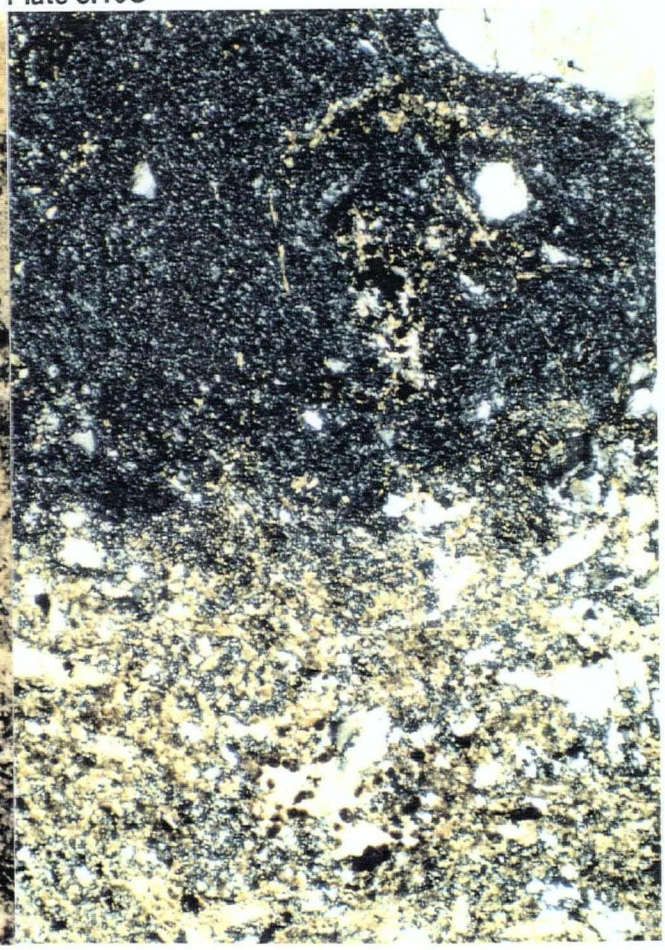

colour and is so fine grained that original bedding is well preserved in most exposures. Biotite hornfels rarely extends more than 100 to 200 metres from the intrusive contact. Hornfels is well exposed in the Molly B and Red Reef adits near Stewart, and in the Skookum (Mountainview) adit southeast of the Riverside mine.

12. Very coarse grained disseminated pyrite is distributed over a narrow zone in the wallrocks of ore shoots and subeconomic sulphide zones at the Silbak Premier mine, at many deposits along the Big Missouri Ridge, and at many other prospects and showings. Euhedral crystals range up to 1 centimetre across and show strongly striated surfaces. Quartz inclusions indicate porphyroblastic growth. This pyrite may be an integral part of the associated propyllitic and sericitic alteration in the wallrock, but has a more restricted distribution and may be a useful guide to ore proximity within a broader propylitic or sericitic zone. The pyrite is interpreted to have formed by hydrothermal circulation around structural conduits in the stratovolcano.

13. Small skarn zones have formed where limy beds are cut by Tertiary plutons and dykes. These skarns have limited extent, a few tens of metres long and a few metres thick at most, reflecting the thickness of the original limestone or limy siltstone that has been metasomatized. Zoning includes symmetrically layered coarse grained garnet-quartz-diopside-tremolite. Good exposures are in the Molly B adit, in the Red Reef adit and elsewhere in scattered outcrops on the lower northwest slope of Mount Rainey.

In summary, complex, scattered and locally overprinted alteration records four processes of formation that affected the rocks at different times, at different intensities and in different volumes:

- Oxidation due to subaerial weathering
- Hydrothermal alteration and related mineralization due to a subvolcanic, syn-volcanic geothermal convection system in an andesitic stratovolcano
- Lower greenschist facies regional metamorphism
- Contact metamorphism and metasomatism peripheral to plutons.

3.6 GEOCHRONOMETRY

This report presents a revised interpretation of the geologic history of the Stewart area based on new potassium-argon dates and all previously published geochronological data from the district. Isotopic dates from the Stewart mining camp are erratically distributed over a 186 million year range from Triassic to Oligocene (Table 3.8). Dates from samples of the same rock unit vary significantly. However, when this array of dates is combined with field observations, closure temperatures for argon loss in minerals, and the concept of the "metamorphic veil" (Armstrong, 1966), a simple explanation emerges.

Isotopic dating near Stewart has been reported by Smith (1977), Alldrick *et al.* (1986, 1987) and Brown (1987). Additional dates from the Stewart complex are published in Carter (1981), Devlin (1987), Britton *et al.* (1989) and Anderson (1990).

Analytical methods are summarized in Appendix II. All the dates in this report have been recalculated with the decay constants and atomic ratios recommended by the International Union of Geological Sciences Subcommission on Geochronology (Steiger and Jäger, 1977).

3.6.1. RESULTS

New potassium-argon dates are listed in Table 3.9. Dates from Smith (1977) have been recalculated and are listed in Table 3.8. Uranium-lead dates are presented with analytical data in Table 3.10.

3.6.2. DISCUSSION

It was hoped that the new potassium-argon analyses would reveal the age of mineralization at the Silbak Premier mine, the Dago Hill deposit near the Big Missouri mine, and the Indian mine. However, significantly different dates were obtained from two samples of altered wallrock from a single diamond-drill hole at the Dago Hill deposit. These results indicate that a simple interpretation of the dates, as direct measurements of the age of alteration and mineralization, is not valid. In addition, contrasting dates

TABLE 3.8: Dates from the Stewart mining camp in chronological order

Apparent Age (Ma)	Rock Unit	Rock Type	Mineral	Analytical Method
†211 ± 6	tcg	Hornblende granodiorite stock	Hornblende	K/Ar
†202 ± 6	tcg	Hornblende granodiorite stock	Hornblende	K/Ar
195.0 ± 2.0	tcg	Hornblende granodiorite stock	Zircon	U/Pb
194.8 ± 2.0	tcg	Premier Porphyry dyke	Zircon	U/Pb
192.8 ± 2.0	tcg	Hornblende granodiorite stock	Zircon	U/Pb
189.2 ± 2.2	tcg	Hornblende granodiorite dyke	Zircon	U/Pb
186 ± 6	tcg	Hornblende lamprophyre dyke	Hornblende	K/Ar
†130 ± 3	tcg	Hornblende granodiorite stock	Biotite	K/Ar
†108 ± 3	tcg	Hornblende granodiorite stock	Biotite	K/Ar
101 ± 3	le	Sericite-flooded andesite tuff	Whole Rock	K/Ar
89.0 ± 3.0	tcg	Sericite-flooded Premier Porphyry	Whole Rock	K/Ar
87.2 ± 3.0	tcg	Sericite-flooded Premier Porphyry	Whole Rock	K/Ar
81.9 ± 2.8	vein	K-feldspar in quartz vein	K-feldspar	K/Ar
78.5 ± 2.8	le	Sericite-flooded andesite tuff	Whole Rock	K/Ar
62.9 ± 2.3	tcg	K-feldspar-flooded Premier Porphyry	Whole Rock	K/Ar
54.8 ± 1.3	hqm	Biotite granodiorite dyke	Zircon	U/Pb
†53.8 ± 2.0	hqm	Biotite granodiorite stock	Hornblende	K/Ar
†52.2 ± 4.0	hqm	Biotite granodiorite stock	Biotite	K/Ar
†51.6 ± 2.0	hqm	Biotite granodiorite stock	Hornblende	K/Ar
†50.5 ± 2.0	hqm	Biotite granodiorite stock	Biotite	K/Ar
†50.4 ± 2.0	hqm	Biotite granodiorite stock	Biotite	K/Ar
†49.9 ± 2.0	hqm	Biotite granodiorite stock	Hornblende	K/Ar
48.4 ± 1.7	hqm	Biotite granodiorite stock	Biotite	K/Ar
†47.3 ± 1.0	hqm	Biotite granodiorite stock	Biotite	K/Ar
45.2 ± 1.6	tcg	Hornblende granodiorite stock	Biotite	K/Ar
†44.8 ± 1.5	hqm	Biotite granodiorite stock	Biotite	K/Ar
42.7 ± 1.5	le	Sericite-flooded andesite tuff	Whole Rock	K/Ar
25.2 ± 1.0	dyke	biotite lamprophyre dyke	Biotite	K/Ar

† Dates from Smith (1977), recalculated with IUGS decay constants.

TABLE 3.9: Potassium-Argon dates from the Stewart camp.

Sample No.	Location (Minfile No.)	Mineral or Concentrate	%K	^{40}Ar rad. 10^{-6} cc/gm	% ^{40}Ar rad. / ^{40}Ar total	^{40}Ar. rad. / ^{40}K $\times 10^{-3}$	Apparent Age (Ma) ($\pm 1\sigma$)
Premier G.H.[1] Lat. 56°03.1′ Long. 130°00.7′	Southeast rim of Silbak Premier gloryhole (MI 104B-54)	Whole rock, sericite flooded	6.38 ± 0.09 n = 3	22.624	93.1	5.301	89.0 ± 3.0
PM84-29-232′[1] Lat. 56°03.1′ Long. 130°00.7′	Core sample from Premier gloryhole area (MI 104B-54)	Whole rock, sericite flooded	4.92 ± 0.02 n = 3	17.079	95.2	5.189	87.2 ± 3.0
PM84-25-369′[1] Lat. 56°03.1′ Long. 130°00.7′	Core sample from Premier gloryhole area (MI 104B-54)	K-feldspar, from quartz vein	11.44 ± 0.03 n = 3	37.268	94.3	4.870	81.9 ± 2.8
81-58-25′[1] Lat. 56°06.4′ Long. 130°00.7′	Dago Hill zone, Big Missouri camp (MI 104B-45)	Whole rock, sericite flooded	4.13 ± 0.07 n = 3	16.681	89.8	6.038	101 ± 3
81-58-68′[1] Lat. 56°06.4′ Long. 130°00.7′	Dago Hill zone, Big Missouri camp (MI 104B-45)	Whole rock, sericite flooded	4.52 ± 0.03 n = 3	14.087	86.0	4.659	78.5 ± 2.8
IM-10[1] Lat. 56°04.6′ Long. 130°01.9′	Galena Cuts zone, Indian mine (MI 104B-31)	Whole rock, sericite flooded	5.68 ± 0.05 n = 5	9.542	87.4	2.511	42.7 ± 1.5
L-2[1] Lat. 56°14.8′ Long. 130°04.3′	Blueberry vein (MI 104B-133)	Hornblende, from lamprophyre dyke	0.847 ± 0.017 n = 5	6.433	90.9	11.359	186 ± 6
A84-1-8[1] Lat. 56°02.0′ Long. 129°55.0′	Roadside quarry on Stewart Hwy.	Biotite, Bitter Creek granodiorite	6.75 ± 0.06 n = 5	12.878	79.7	2.852	48.4 ± 1.7
DB-84-25[2] Lat. 56°03.3′ Long. 130°00.5′	Trench 2190 at Premier gloryhole	Whole rock K-feldspar flooded	5.92 ± 0.05 n = 2	14.721	82.2	3.717	62.9 ± 2.3
B-383[2] Lat. 55°59.3′ Long. 130°03.8′	Roadcut 2.0 km south of Riverside mine	Biotite, Texas Creek granodiorite	4.17 ± 0.02 n = 2	7.416	84.4	2.659	45.2 ± 1.6
AT84-27-5[2] Lat. 56°04.4′ Long. 130°02.4′	Roadcut on east side of Indian Lake	Biotite, lamprophyre dyke	7.22 ± 0.01 n = 2	7.133	68.0	1.477	25.2 ± 1.0

[1] K analyses by P.F. Ralph and B. Bhagwanani, Ministry of Energy, Mines and Petroleum Resources; D. Alldrick samples.
[2] K analyses by K. Scott, The University of British Columbia; D. Brown (1987) samples.
All Ar analyses by J.E. Harakal, The University of British Columbia.

TABLE 3.10: Uranium-lead zircon dates from the Stewart mining camp

Sample No.	Location [UTM]	Sample Properties	Weight (mg)	Concentration (ppm) U	Concentration (ppm) Pb	Observed $^{206}Pb/^{204}Pb$	Atomic Ratios[3,4] $^{206}Pb/^{238}U$	Atomic Ratios[3,4] $^{207}Pb/^{235}U$	Atomic Ratios[3,4] $^{207}Pb/^{206}Pb$	Model Ages (Ma)[4] $^{206}Pb/^{238}U$	Model Ages (Ma)[4] $^{207}Pb/^{235}U$	Model Ages (Ma)[4] $^{207}Pb/^{206}Pb$	Concordia Age (Ma)[4]
A84-1	(130°05'55"W 56°14'00"N)	nm, 150-215μm	16.3	459	13.6	8841	0.03035±16	0.2092±11	0.04998± 07	192.8±1.0	192.9±0.9	194.2± 3.3	192.8±2.0
	[09-432250E 6232320N]	m, <45μm	1.3	1908	55.6	8473	0.02952±16	0.2041±11	0.05014± 09	187.5±1.0	188.6±0.9	201.4± 4.0	
		m, <45μm	1.5	887	26.2	6499	0.02962±16	0.2048±11	0.05015± 13	188.2±1.0	189.2±0.9	202.0± 5.8	
A84-2	(130°03'13"W 56°05'28"N)	nm, >150μm	14.2	349	10.2	8110	0.02979±17	0.2049±11	0.04990± 06	189.2±1.1	189.3±0.9	190.3± 2.8	189.2±2.2
	[09-434400E 6216475N]	m, <75μm	0.3	898	27.8	1278	0.03056±17	0.2101±73	0.04987±162	194.1±1.1	193.7±6.1	189.1±76.	
A84-3	(130°03'13"W 56°05'28"N)	nm, >150μm	10.5	596	18.6	1839	0.03062±17	0.2113±15	0.05006± 25	194.4±1.0	194.7±1.3	197.7±11.7	195.0±2.0
	[09-434400E 6216475N]	nm, >150μm, abd	4.3	510	15.6	6189	0.03072±16	0.2117±11	0.04999± 09	195.0±1.0	195.0±0.9	194.4± 4.1	
		m, <45μ	1.3	1272	38.3	6639	0.03004±16	0.2078±11	0.05016± 09	190.8±1.0	191.7±0.9	202.6± 4.1	
A84-5	(130°00'50"W 56°03'06"N)	nm, >150μm	5.3	343	10.84	1081	0.03020±16	0.2090±12	0.05018± 17	191.8±1.0	192.7±1.0	203.5± 7.6	194.8±2.0
	[09-436760E 6212240N]	nm, >150μm, abd	2.9	378	11.7	1864	0.03067±16	0.2120±13	0.05013± 19	194.8±1.0	195.2±1.1	201.2± 8.9	
AT-34-3[2]	(130°01'22"W 56°03'02"N)	nm, >150μm	5.0	362.2	4.14	629	0.01064±06	0.0702±05	0.04789± 02	68.2±0.4	68.9±0.5	93.7±10.1	54.8±1.3
	[09-436300E 6212130N]	m, <75μm	1.0	431.2	4.34	226	0.00853±12	0.0554±14	0.04713± 93	54.8±0.8	54.8±1.3	55.6±46.	

[1] All analyses by J.K. Mortensen, Geological Survey of Canada, Ottawa.
[2] Data provided by R.G. Anderson, Geological Survey of Canada, Vancouver.
[3] The errors apply to the last digits of the atomic ratios.
[4] All errors shown are 1σ errors, except for 2σ errors in final column.
Isotopic composition of blank: 6/4:17.75, 7/4:15.5, 8/4:37.3
Isotopic composition of common lead is based on the Stacey and Kramer (1975) model: 6/4=11.152, 7/4=12.998, 8/4=31.23 at 3.7 Ga with $^{238}U/^{204}Pb=9.74$, $^{232}Th/^{204}Pb=37.19$.
Decay constants: 6/4= 0.155125, 7/4=0.98485, 8/4=137.88.

NOTE: $^{206}Pb/^{238}U$ analyses on the coarse, non-magnetic zircon fractions of samples A84-1-,2,-3 and -5 are concordant*, and thus represent very precise ages for these rocks. Nevertheless, uranium-lead analyses from zircon are always susceptible to errors caused by lead loss or zircon inheritance. Although the concordia ages listed in this table are not significantly affected, examination of the total data set of model ages suggests that both phemomena may be present in the zircon populations to a small degree. The effects of these phenomena and their geological significance are discussed in Appendix II.

* A concordant U-Pb analysis can be defined as any data point having a 2σ error ellipse that significantly overlaps concordia (J.K. Mortensen, personal communication, 1991).

obtained by Smith (1977) for hornblende and biotite separates from samples of Texas Creek granodiorite suggest that there has been argon loss from at least some mineral phases in these rocks. A brief review of the vulnerability of minerals to argon loss follows.

Minerals will lose argon gas from their crystal lattices when heated to moderate temperatures over geologically short periods of time (Armstrong, 1966; Dodson, 1973; York, 1984). The lowest temperature at which minerals rapidly lose argon has been termed the "threshold temperature" (Armstrong, 1966), "closure temperature" (Dodson, 1973), and "blocking temperature" (York, 1984). Closure temperature is largely dependent on mineral type and grain size. Parrish and Roddick (1984) have compiled closure temperatures for mineral phases and mineral groups (Table 3.11).

TABLE 3.11: CLOSURE TEMPERATURES FOR ARGON LOSS IN MINERALS (from Parrish and Roddick, 1984)

MINERAL	CLOSURE TEMPERATURE
Hornblende	530° ± 40°C
Muscovite	~350°C
Biotite	280° ± 40°C
K-feldspar	130° ± 15°C
Microcline	~110°C

Armstrong (1966) argued that temperature increases during regional metamorphism would drive off argon from many minerals whose potassium-argon dates would then be reset to record only the time of the final cooling of the orogen. If the temperatures were high enough all potassium-argon dates relating to the pre- and syn-metamorphic history of the rocks would be lost or degraded to younger values. This concept of a "metamorphic veil" is illustrated schematically for a high grade region in Figure 3.17a. In the case of high grade regional metamorphism, all mineral groups would have their potassium-argon "clocks" reset because the temperature during metamorphism far exceeds the closure temperatures of all minerals.

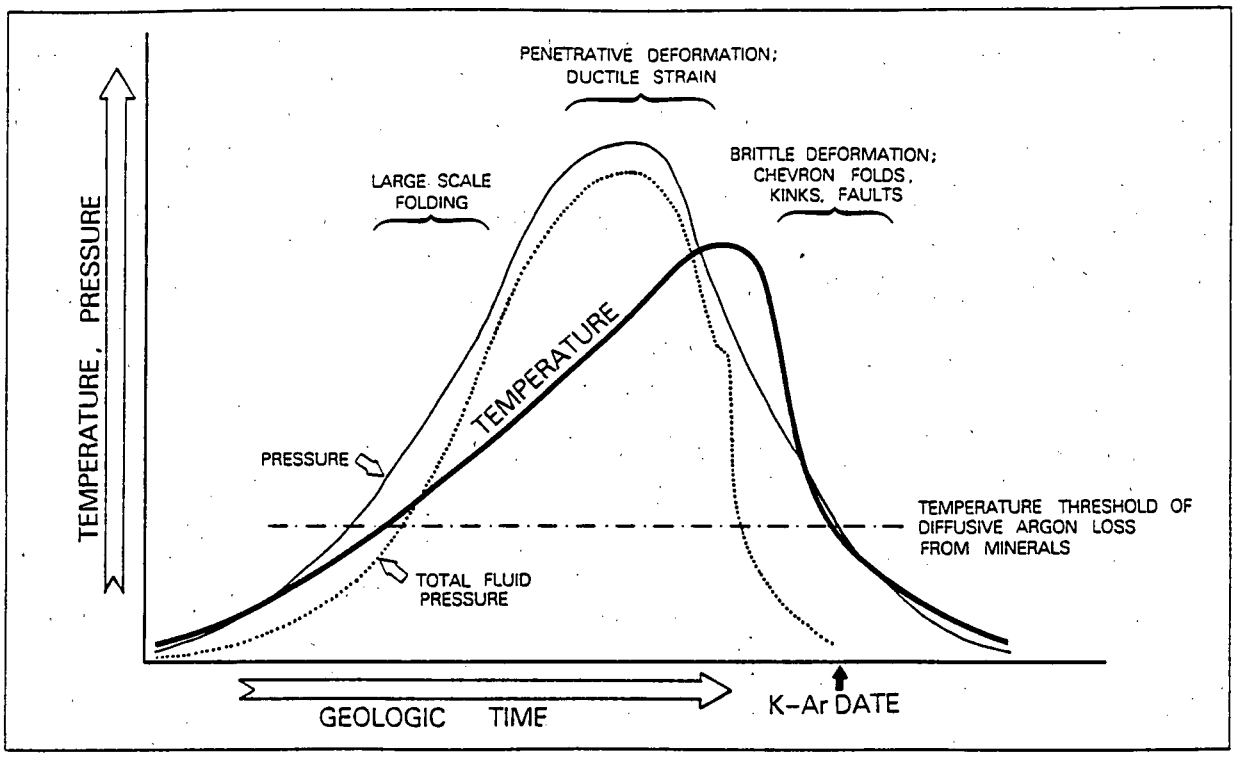

3.17a: General relationships of temperature, pressure, deformation and argon loss from minerals in the metamorphic interior of an orogenic belt (from Armstrong, 1966).

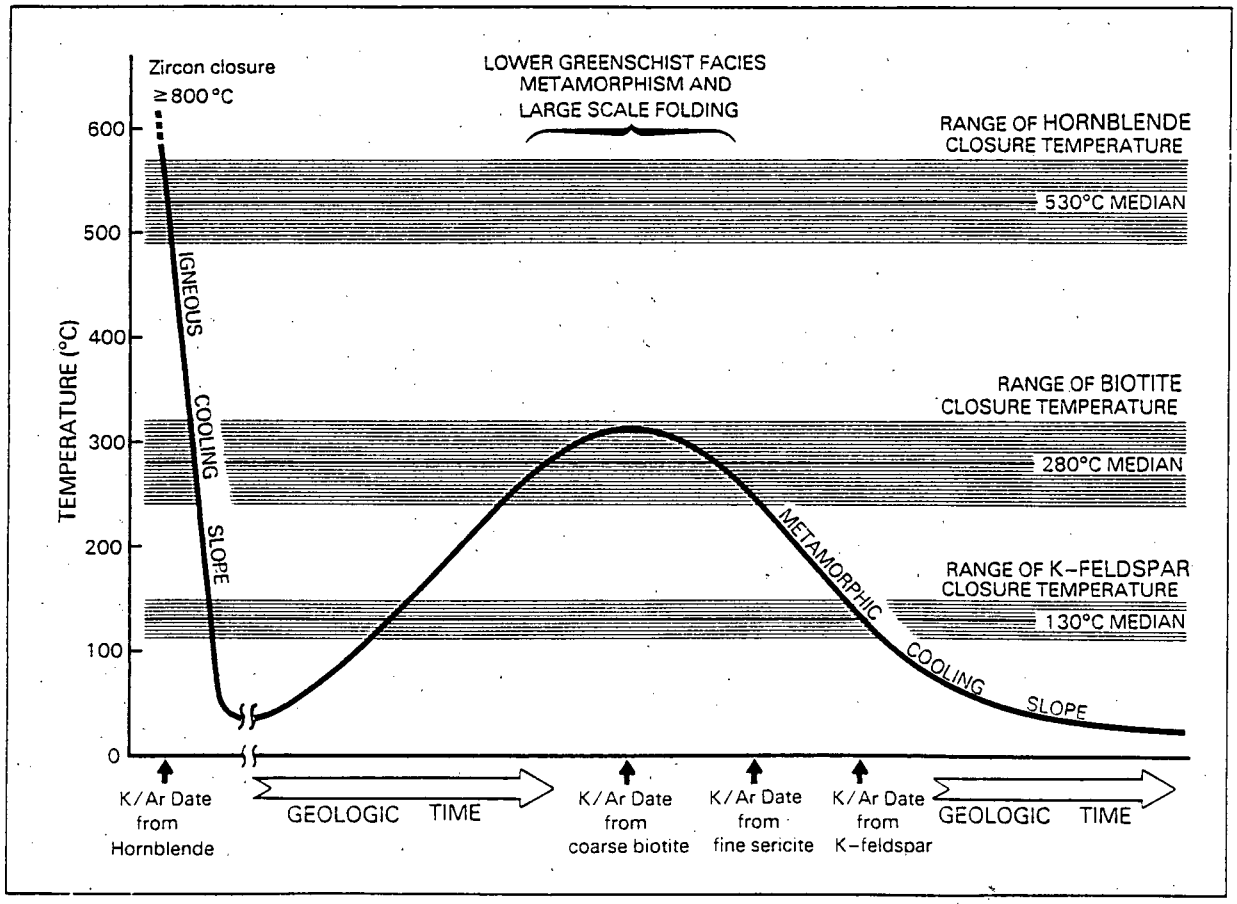

3.17b: General relationships of temperature, deformation and argon loss for minerals dated in the Stewart mining camp.

FIGURE 3.17: General relationships of temperature, deformation and argon loss for potassium-argon samples

Regional metamorphic grade in the Stewart area was low to mid greenschist facies indicating a thermal peak of 240°C to 320°C (Figure 3.15). From the closure temperatures listed in Table 3.11 only certain mineral groups should show argon loss during lower greenschist facies metamorphism. Figure 3.17b shows a schematic diagram which predicts the effects of lower greenschist facies temperatures on potassium-argon dates for a variety of minerals.

Note that although the closure temperature for coarse grained igneous muscovite is estimated at 350°C, fine grained hydrothermal "sericite" that is present in the Stewart samples will be some variety of muscovite, paragonite, hydromuscovite, illite or phengite, and may even be a mixed, layered aggregate of a few of these minerals (Deer *et al.*, 1963, p.215-216). The closure temperature for sericite is not known, but the fine grained, hydrous mineral aggregate would be particularly susceptible to water loss and argon diffusion during heating. Therefore the closure temperature for hydrothermal sericite is probably below 300°C and thus similar to biotite.

3.6.3. INTERPRETATION

All dates from Table 3.9 are displayed on Figure 3.18. Note that this figure includes uranium-lead dates from zircons which are estimated to have closure temperatures of >500°C and thus are not susceptible to thermal resetting at greenschist facies temperatures. As illustrated in Figures 3.17a and b, the "date" of a mineral represents the last time the mineral cooled down through its closure temperature, whether that temperature drop resulted from original cooling of an igneous magma or from cooling after a metamorphic event.

The broad band on Figure 3.18 represents the interpreted thermal history for the Stewart mining camp. The fine black lines represent the interpreted thermal history of discrete igneous bodies such as dykes and stocks. The cooling curve after each thermal peak is drawn through the data points but the thermal peak itself represents the probable age of emplacement. The temperature rise to each thermal peak and details of any prior

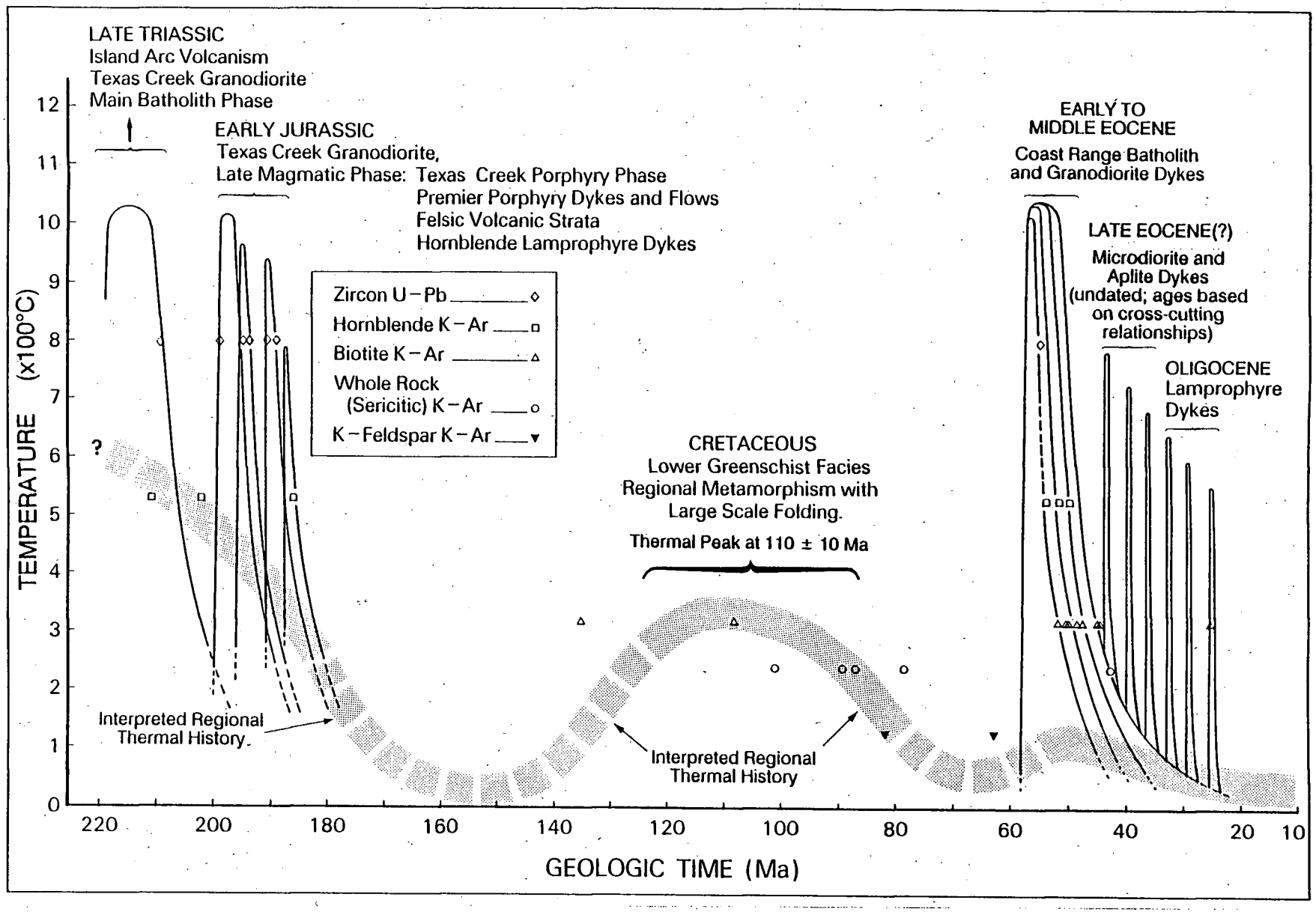

FIGURE 3.18: Igneous, metamorphic and thermal history of the Stewart district (Isotopic dates versus closure temperatures. All data are listed in **Tables 3.8, 3.9** and **3.10**.)

cooler interval cannot be exactly reconstructed. For igneous bodies the temperature rise can be considered virtually instantaneous--a vertical line, but for the regional metamorphic event the temperature rise is hidden behind the metamorphic veil and must be hypothetical--a dashed grey band.

The dates for two mineral groups, biotites from the Texas Creek granodiorite and sericite-rich rocks from to the Silbak Premier, Dago Hill (Big Missouri) and Indian deposits, require further comment.

Biotite separates from the Texas Creek granodiorite are clearly reset since their potassium-argon dates do not match those for hornblende separates from the same samples (Table 3.8). Also, the potassium-argon dates for the reset biotites differ by 22 million years even though the dates for the two hornblende separates lie within analytical error of each other. This is interpreted to be the result of only partial argon loss from the older biotite (sample 3S-008 of Smith, 1977). Partial argon loss occurs either when the thermal peak is short lived, such as country rock intruded by a narrow dyke, or when the thermal peak barely reaches a temperature equal to the closure temperature for the mineral. Coarse grained igneous biotites are estimated in general to have closure temperatures of 240°C to 320°C and, since the thermal peak of regional metamorphism was probably not a short lived event, the temperatures during regional metamorphism are inferred to have reached but not exceeded 300°C. It is also possible that the two biotites had slightly different closure temperatures, or that the maximum temperature during regional metamorphism varied between the sample locations, which were 3 kilometres apart (Smith, 1977). A third biotite separate from the Texas Creek granodiorite, sample B-383 in Table 3.9, has been dated at 45.2 Ma. This sample was collected near the northern contact of the Hyder stock and the potassium-argon ratio of the biotite has been thermally reset by the Tertiary intrusion.

Two dates for sericite-rich altered dyke rock from the Silbak Premier mine, 87.2 and 89.0 Ma, fall within analytical error of each other and are considered the most representative values for thermally reset sericite dates. The potassium feldspar date from

the Silbak Premier mine, 82 Ma, gives a reasonable additional control for the cooling curve after regional metamorphism.

The dates for two sericite-rich altered andesite samples from a single drill hole at Dago Hill are different, 78.5 Ma and 101 Ma. Thin section study of these two samples shows that the deeper core sample, which yields the younger date, is composed of sericite and carbonate-altered andesitic ash tuff. The shallower core sample is similarly altered andesitic crystal tuff containing large laths of hornblende that have been extensively altered to coarse sericite (Alldrick *et al.*, 1987) The closure temperature for hornblende is well above the thermal peak reached during regional metamorphism (Figure 3.17) so the remnant hornblende would probably retain some of the radiogenic argon generated since its original magmatic crystallization prior to metamorphism. The older date is thus attributed to a mixture of argon from older (Jurassic) hornblende and younger (reset to Cretaceous) sericite.

The whole rock sample of sericite and carbonate-altered andesite from the Indian mine has a potassium-argon date of 42.7 million years. From Figure 3.18, two interpretations might explain this date:

(1) The alteration and the associated ore deposit formed in Eocene time, about 43 Ma.

(2) The alteration and the associated ore deposit formed prior to Eocene time but the potassium-argon "clock" has been reset by Eocene igneous or hydrothermal activity.

The geology of the Indian mine is well described by McGuigan (1985) and Grove (1971). Lead isotope data show that galena from the Galena Cuts open stope has an isotopic composition identical to other ore deposits of Middle Eocene age (Section 4.2), indicating that sulphides at the Indian mine were precipitated in Eocene time. Thus the 43 Ma potassium-argon date for the altered wallrock at the Indian mine probably represents the age of emplacement of the sulphides along the controlling fault structure. Three varieties of Tertiary dykes have been identified on the Indian mine property (McGuigan,

1985) but the nearest major body of Eocene intrusive rock crops out on the summit and the northern slope of Mineral Hill, 3 kilometres south-southwest of the Indian mine.

The formation of the Dago Hill and Silbak Premier deposits must predate the 110 ± 10 Ma regional metamorphic event, since the isotopic ratios of the alteration envelopes surrounding these deposits are thermally reset by the metamorphism. Black stylolites of insoluble residue are common within the coarse crystalline carbonate gangue at several mineral deposits in the Big Missouri camp. These stylolites are pressure-solution features that also suggest the deposits predated regional deformation. Fine to medium grained euhedral pyrite crystals associated with the alteration envelopes at the Big Missouri deposits exhibit well developed pressure shadows in thin section (Plate 3.9A), also indicating that the mineralization and alteration predate metamorphism. The age of ore deposition at the Big Missouri, Silbak Premier, Silver Butte, Scottie Gold and similar deposits is estimated at 185 million years based on field relationships (Chapters 4 and 5).

Late lamprophyre dykes crosscut all other rock types, alteration, and mineralization in the Stewart area. These dykes are part of a Tertiary lamprophyre dyke province defined by Smith (1973) who interpreted a Miocene age of emplacement based on field relationships. Carter (1981), Brown (1987) and Devlin (1987) have obtained Oligocene dates on biotite lamprophyre dykes in the Stewart and Alice Arm districts. The age range for these dykes is illustrated on Figure 3.18. The data suggest that Smith's (1973) Tertiary lamprophyre dyke province is dominantly Oligocene in age.

The new data and interpretations presented in this report allow significant revisions to the geologic history of the district (Table 3.12). Recent compilations of isotopic dates for southeast Alaska (Smith *et al.*, 1979 and Brew and Morrell, 1983) and for the whole of the Canadian Cordillera (Armstrong, 1988) provide a regional and continent scale context for the geologic history of the Stewart area (Table 3.13).

TABLE 3.12: Geologic history of the Stewart mining camp

Age (Ma)	Event
35-25	Emplacement of biotite lamprophyre dykes.
45-35	Emplacement of microdiorite or "andesite" dykes along NNW trend, locally deflected by biotite granodiorite dykes.
48-43	Formation of argentiferous galena-sphalerite-freibergite vein deposits and spatially associated MoS_2 and WO_3 deposits.
55-45	Intrusion of Hyder, Boundary, Davis River, Bitter Creek and Mineral Hill stocks of the Coast Range batholith. Biotite granodiorite to biotite quartz monzonite. Continuing dyke intrusion.
55	Crustal extension and intrusion of major WNW-trending biotite granodiorite dyke swarms marked onset of emplacement of stocks at depth.
110-90	Lower greenschist facies regional metamorphism reaches a thermal peak. Moderate deformation along north-trending fold axes. Major folds and slaty cleavage formed.
190-160	Marine transgression, flysch sedimentation with minor intraformational conglomerates (Unit 4). Relative quiescence.
190-185	Waning magmatic activity marked by emplacement of hornblende lamprophyre dykes at depth.
~190	Subaerial felsic volcanism (Unit 3). Emplacement of dykes at depth. Formation of gold-silver vein and breccia deposits. Deposition of barren pyrite around fumarolic centres at surface.
195-190	Deposition of subaerial epiclastic sediments and interbedded andesitic to dacitic tuffs and flows (Unit 2). (Emplacement of minor dykes at depth?)
195	Intrusion of porphyry phase of Texas Creek granodiorite, Premier Porphyry dykes, and extrusion of Premier Porphyry flows and tuff breccias.
215-195	Andesitic volcanic activity (Unit 1), predominantly subaerial with two periods of marine transgression; coeval intrusion of main phase of Texas Creek granodiorite.

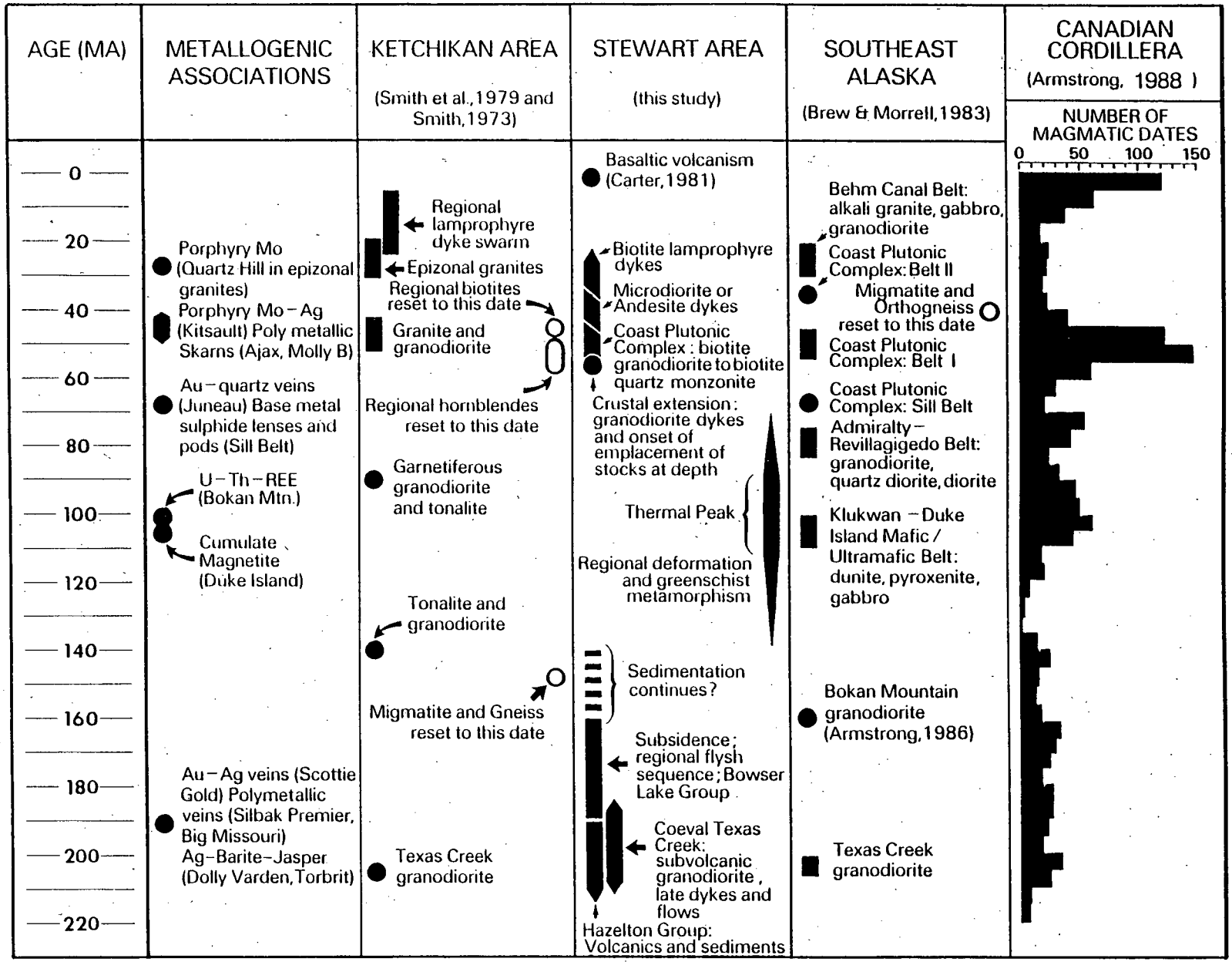

TABLE 3.13: Comparison of geologic histories for Stewart, southeast Alaska and the Canadian Cordillera. Bar = significant timespan, solid circle = short timespan or limited dating, open circle = minimum date only.

3.6.5. CONCLUSIONS

When isotopic dates are plotted against mineral closure temperatures, a simple thermal history can be deduced:

1. Late Triassic to Early Jurassic volcanism and coeval subvolcanic intrusion (211 to 190 Ma) was followed by dyke emplacement (190 to 185 Ma) and by quiescent flysch sedimentation (Toarcian to Callovian, 185 to 160 Ma).

2. Moderate deformation associated with lower greenschist facies regional metamorphism reached its thermal peak about 110 ± 10 Ma.

3. Stocks and dykes of the Coast Plutonic Complex intruded the deformed rocks in early to middle Eocene time, 55 to 45 Ma, followed by a 20 million year period of aplite, microdiorite and biotite lamprophyre dyke emplacement.

3.7. SUMMARY GEOLOGIC HISTORY

This section highlights the tectonic processes that have affected the Stewart camp by combining elements of the geologic history of the study area, established in this chapter, with the tectonic evolution of Stikinia, reviewed in Chapter 2.

Basaltic volcanic and sedimentary rocks of the Stuhini Group were laid down on a metamorphosed platform of Stikine assemblage rocks. This was the first phase in the evolution of a single Late Triassic to Early Jurassic arc that evolved from basaltic flows (Stuhini Group) through andesitic volcanism (Unuk River Formation) to dacitic pyroclastics (Betty Creek and Mount Dilworth Formations). Each volcanic phase was accompanied by emplacement of subvolcanic intrusions that are preserved as suites of progressively shallower, progressively more siliceous plutons. Compositional evolution over this 40 million year period is attributed to progressive thickening of the crust.

Early Jurassic volcanism was predominantly subaerial. Intervolcanic periods were marked by subsidence, submergence, and deposition of turbidites. Re-emergence of each new volcanic edifice was due to swelling over recharged magma chambers and to aggradation of the volcano above sea level. Topographically, the volcano was part of a

semi-continuous chain of large and small volcanic islands, similar to the central and eastern Aleutians and to many examples in the southwest Pacific such as the New Ireland/Solomon Islands chain.

Bulk chemistry and prominent hornblende phenocrysts of the Unuk River Formation andesites suggest these lavas erupted along the main axis of an arc. A general northwest trend to Hazelton volcanic centres is suspected (Alldrick, 1989). The arc was established over a Mesozoic subduction zone that is poorly constrained, but probably dipped northeasterly.

Volcanism terminated abruptly in Toarcian time (~187-185 Ma) with the thin, widespread, dacite pyroclastic blanket of the Mount Dilworth Formation. The end of volcanism was followed by subsidence of the subaerial volcanic arc. Sedimentation was initially gritty, shallow-water fossiliferous limestones at the base of the Salmon River Formation, followed by a thick accumulation of carbonaceous turbidites and wackes.

As sediments accumulated in the Bowser Basin through the Upper Jurassic, final amalgamation of the two superterranes was completed to the west of Stikinia. From 150 to 125 Ma there is a lull in plutonism and volcanism and region-wide gaps in the stratigraphic record that indicate a period of tectonic and magmatic quiescence and widespread emergence and erosion.

In the Early Cretaceous an eastward-descending subduction zone was established well west of Stikinia. The arc was fully developed by the mid-Cretaceous (110 to 90 Ma) when magmatism peaked. Accompanying tectonism was characterized by: greenschist faces regional metamorphism, east-northeast compression, and deformation that produced a north-northwest-trending undulating fold system. Folds were overprinted by east-verging ductile reverse faults and foliation that began in the Stewart area and propagated eastward across the Bowser Basin.

Transpression related to oblique subduction during the Late Cretaceous (90 to 70 Ma) may have initiated large, north-trending fault structures such as the Long Lake fault. These faults remained intermittently active into late Tertiary time.

No significant magmatic activity or sedimentation was recorded in Stikinia over the period 70 to 55 Ma, but the following 10 million years, 55 to 45 Ma, spans the final major magmatic episode in the Canadian Cordillera. Plutons emplaced in the Stewart area include the batholith, satellitic stocks, and extensive dyke swarms of the Hyder suite. Intrusion was preceded and accompanied by northeast extension. Waning magmatism between 45 and 25 Ma was marked by a succession of aplite, microdiorite and lamprophyre dykes, and by reactivation of old faults.

CHAPTER 4
MINERAL DEPOSITS

The Stewart mining camp is a richly and complexly mineralized district. The first impression when looking at a mineral deposits distribution map is of the unusually large number of mineral occurrences in the 750 square kilometer study area (Figures 4.1a and b) and the broad areal distribution of these showings. The geological maps (Figures 3.2a and b) show an apparent lack of clear stratigraphic and/or plutonic controls to distribution. In the first two sections of this chapter, empirical geologic criteria are used to sort, group and classify these numerous occurrences. The final classification scheme is presented in Section 4.2.3. Specific examples from each deposit group are described in detail in Section 4.3. The characteristic features of each group are used to design deposit specific exploration guidelines in Section 4.4.

4.1. DISTRIBUTION

Areas with higher densities of occurrences are evident on Figure 4.1. The following two sub-sections consider whether there is a simple topographic or geological factor controlling the distribution of these more intensely mineralized zones.

4.1.1. GEOGRAPHIC DISTRIBUTION

Mineral deposits range topographically from the Molly B adit collared at the high tide line along the Portland Canal to the surface trace of the Prosperity-Porter Idaho "D Vein" shear structure at 1875 metres elevation near the summit of Mount Rainey (Figure 4.13). Other high altitude mineral occurrences include M.C. (1600 metres), Hicks (1590 metres), M.J. (1585 metres), Silver Cliff (1535 metres) and A.E.I. (1500 metres) (Figure 4.1a). The deepest production is recorded from Riverside mine that produced ore from an underhand stope and two inclined winzes below the main Mill Level at 320 metres elevation. The highest workings in the Prosperity-Porter Idaho mine reach 1750 metres elevation. The uppermost workings in the Scottie Gold mine stopped at 1160 metres due to

the overlying Morris Summit Glacier. Clearly altitude, terrain and snow or ice cover are not limiting factors for production decisions in this district.

Access has been a factor affecting discovery and therefore distribution of mineral zones. Most deposits are within an easy hike of the historic horse trail route along the east side of the Salmon River valley. Later roadworks have even revealed some deposits (for example, Sixmile, Riverside, Lower Daly-Alaska, Hope, and 96 Group.

The prospectors adage, 'the best place to look for ore is next to a mine', is in part a self-fulfilling prophecy. The higher density of mineral occurrences near the Scottie Gold mine, along the Big Missouri Ridge, on the hillside around the Silbak Premier mine, and uphill from the Riverside mine reflect more intense prospecting efforts in these areas over several decades.

In summary, although geographic features have not deterred exploration or production in remote or precipitous areas, ease of access and the 'philosophy' of prospecting have contributed to higher densities of mineral occurrences along access routes and around major deposits.

4.1.1. GEOLOGIC DISTRIBUTION

Mineral occurrences were categorized in table form according to their distribution in various strata, intrusive rocks, and structures. There was duplication of some entries, since deposits like the Silbak Premier and Silver Tip mines are locallized in tuffs, along the contacts of dykes, and the best grades and/or tonnage is concentrated near cross-faults.

The stratigraphic distribution of mineral occurrences (Table 4.1a) and the association of mineral occurrences with plutonic rocks (Table 4.1b) are fairly straightforward, but the distribution of mineral occurrences by structure (Table 4.1c) was difficult to quantify. There are no stratiform deposits and, apart from the barren pyritic dacites of the Mount Dilworth Formation, there are no stratabound deposits *sensu strictu.* Many smaller showings were not visited and early descriptions do not identify key

TABLE 4.1: Quantitative distribution of 205 mineral occurrences in specific strata, intrusive rocks and structures

(From Table 4.7)

4.1a: STRATIGRAPHIC DISTRIBUTION OF 166 MINERAL OCCURRENCES

STRATIGRAPHIC UNIT	TOTAL NUMBER OF MINERAL OCCURRENCES	
Salmon River Fm	24	
Mount Dilworth Fm	11	
Betty Creek Fm	7	
Unuk River Fm	124	
Premier Porphyry Mbr		3
Upper Andesite Mbr		62
Upper Siltstone Mbr		26
Middle Andesite Mbr		38
Lower Siltstone Mbr		11
Lower Andesite Mbr		1

4.1b: DISTRIBUTION OF 108 MINERAL OCCURRENCES WITHIN OR PROXIMAL TO INTRUSIVE ROCKS

LITHODEME	TOTAL NUMBER OF MINERAL OCCURRENCES	
HYDER PLUTONIC SUITE:	44	
HYDER BATHOLITH		18
BOUNDARY STOCK		0
HYDER DYKES		22
Granodiorite Porphyry		29
Aplite Dykes		2
Microdiorite Dykes		5
Lamprophyre Dykes		7
TEXAS CREEK PLUTONIC SUITE	64	
TEXAS CREEK BATHOLITH		40
SUMMIT LAKE STOCK		8
PREMIER PORPHYRY DYKES		22

4.1c: STRUCTURAL DISTRIBUTION OF 205 MINERAL OCCURRENCES

STRUCTURE	TOTAL NUMBER OF MINERAL OCCURRENCES	
STRATABOUND	7	
DISSEMINATED	23	
CROSS-CUTTING		
BRITTLE FRACTURES		98
BRITTLE FAULTS		74
BROAD SHEAR ZONES AND DUCTILE FAULTS		29
BRECCIAS VEINS		44
MASSIVE VEINS		95
STOCKWORKS		57
DYKE MARGINS		31

structures, so the variety of reported structural settings are listed on Table 4.1c, but the total number of occurrences in each structural setting may not be reliable.

Experience in other mining camps suggested that stratigraphy and structure may hold the key to distinguishing different deposit types among the many prospects in the area. As the three tables show, each of these criteria can indeed be used to sort and separate out groups of deposits in the Stewart camp. Unfortunately, deposits of different ages occur within each group (Table 4.7, in pocket). Deposit classifications based solely on stratigraphic position or plutonic association or structural setting do not work in the Stewart mining camp and are probably not reliable anywhere in the Stewart region.

4.2 CLASSIFICATION

4.2.1. PRELIMINARY CLASSIFICATION SCHEMES

There are three "fixed points" in the evolution of ideas about the classification and genesis of the 200-plus mineral occurrences in the district:

- Consideration of structural settings separated deposits into 3 categories (Alldrick, 1983);
- Consideration of structural setting, sulphide mineralogy, gangue textures and gold:silver ratios allowed separation into six different deposit categories of only two different ages (Table 4.2 and Alldrick, 1985a, 1985b); finally,
- The combination of galena lead isotope data and the same parameters applied in the 1985 analysis separated mineral occurrences into one stratabound deposit type and three vein deposit types, representing only two different ages of mineralization (Alldrick, *et al.*, 1987, and Alldrick, Gabites and Godwin, 1987). Each vein deposit type includes mineralogically and texturally variable veins in a variety of stratigraphic and structural settings.

4.2.2. LEAD ISOTOPE STUDIES

In 1986, a suite of galena samples, representing ten deposits on eight properties, was submitted for lead isotope analysis. The results of this work, reported in Alldrick, Gabites

TABLE 4.2: Preliminary deposit classification
(modified from Alldrick, 1985, p.336-339)

DEPTH OF EMPLACEMENT	EARLY JURASSIC (~180? Ma)	MIDDLE EOCENE (~50 Ma)
SURFACE	Stratabound pyritic dacites (Mount Dilworth, Iron Cap)	
SHALLOW (Xenothermal)	Ag-Pb-Zn veins with vuggy quartz (Start)	
MODERATE (Epithermal)	Ag-Au-base metal veins (Big Missouri, Silbak Premier)	
INTERMEDIATE (Mesothermal)	Au-pyrrhotite veins (Scottie Gold, Camp)	Ag-Pb-Zn veins massive, quartz-poor (Prosperity/Porter Idaho)
DEEP (Hypothermal)		WO_3/MoS_2 veins (Riverside, Molly B)

and Godwin (1987), were so unexpected and definitive that additional samples were immediately processed. This section presents galena lead isotope data from 21 mineral occurrences on 18 properties in the Stewart area. Occurrences are listed in Table 4.3, shown on Figure 4.1, and detailed property descriptions are provided in MINFILE.

PRINCIPLES OF LEAD ISOTOPE INTERPRETATION

The "lead-lead" or "common lead" method of isotopic dating is based on accurate measurement of lead isotope abundances fixed in the ore minerals of a deposit against a background of changing ratios of radiogenic lead isotopes in source rocks over geologic time (Figure 4.2). Galena is used because once it has crystallized, its lead isotopic composition remains absolutely constant due to absence of any radioactive elements in its crystal lattice structure. The reference isotope, ^{204}Pb, is not produced by radioactive decay and so has always been constant in amount. Faure (1986) and Godwin *et al.* (1988, p.7-21) review the chemical, mathematical and theoretical basis for this technique.

ANALYTICAL METHODS

All lead analysed was extracted from medium to coarse grained hand-picked galena. Sample preparation and lead isotope analyses were completed by J.E. Gabites in the Geochronology Laboratory, Department of Geological Sciences, The University of British Columbia. Details of the analytical procedure are outlined in Godwin *et al.* (1990), Godwin *et al.* (1988, p.22-24) and Gulson (1986, p.191-203). The complete data set together with comprehensive data plots and discussion of analytical errors are presented in Appendix III.

RESULTS

Table 4.3 lists deposit name, location, host lithology, deposit type and MINFILE number. Table 4.4 presents galena lead isotope data from 21 deposits that plot as two discrete clusters on Figure 4.3. To simplify plots and improve clarity, only the 21 values indicated on Table 4.4 have been plotted on Figure 4.3, with a dotted line circling the total

TABLE 4.3: Galena lead isotope sample sites in the Stewart mining camp

B.C. LEADFILE Number	Deposit Name	Mineral Occurrence	Map Number* [this study]	MINFILE Number
30415	BIG MISSOURI GROUP	Creek	N49	104B-086
		Calcite Cuts	N54	104B-148
		Terminus	N59	104B-002
		Martha Ellen	N33	104B-092
		Hercules, Dumas	N33	104B-092
		Province	N53	104B-147
		Province West	N52	104B-136
30492	PROSPERITY/PORTER IDAHO		S57,S58	103P-089
30493	SCOTTIE GOLD		N12	104B-034
30494	SILBAK PREMIER GROUP	Glory Hole	N89	104B-054
		Northern Lights	N87	104B-053
		2 Level Portal	N89	104B-054
		Lesley Creek Bridge	N135	
30495	CONSOLIDATED SILVER BUTTE	Silver Butte	N58	104B-095
30616	SPIDER		N28	104A-010
30720	CONSOLIDATED SILVER BUTTE	Packer Fraction	N134	104B-095
30765	BAYVIEW		S36	103P-051
30766	SILVERADO		S51	103P-088
30923	START		N61	
30939	INDIAN		N76	104B-031
50055	JARVIS (HOWARD)		S5	103O-001
50058	RIVERSIDE		N121	104B-073

*** N = Figure 4.1a; S = Figure 4.1b**

TABLE 4.4: Galena lead isotope data for the Stewart mining camp

(These are the data points plotted on FIGURE 4.4.
See Appendix III for complete data set and related data plots)

TABLE 4.4a: DATA FOR 'JURASSIC' DEPOSIT CLUSTER

B.C. LEADFILE Number	Deposit Name	$^{206}Pb/^{204}Pb$	$^{207}Pb/^{204}/Pb$
30415-006	Creek	18.820	15.615
30415-002	Calcite Cuts	18.858	15.646
30415-007	Terminus	18.823	15.609
30415-AVG	Martha Ellen	18.826	15.615
30415-013	Hercules	18.734	15.612
30415-AVG	Province	18.824	15.604
30415-005	Province West	18.781	15.643
30493-001	Scottie Gold	18.804	15.608
30494-006	Premier: Glory Hole	18.836	15.617
30494-AVG	Northern Lights	18.828	15.607
30494-AVG	Premier: 2 Level	18.837	15.619
30495-AVG	Silver Butte	18.820	15.612
CLUSTER AVERAGE		**18.816**	**15.617**

TABLE 4.4b: DATA FOR 'EOCENE' DEPOSIT CLUSTER

B.C. LEADFILE Number	Deposit Name	$^{206}Pb/^{204}Pb$	$^{207}Pb/^{204}/Pb$
30492-AVG	Prosperity/Porter Idaho	19.121	15.622
30494-005	Lesley Creek*	19.220*	15.748*
30616-001	Spider	19.085	15.609
30720-001	Packer Fraction	19.177	15.629
30765-AVG	Bayview	19.152	15.620
30766-AVG	Silverado	19.159	15.640
30923-AVG	Start	19.134	15.638
30939-AVG	Indian	19.155	15.623
50055-AVG	Jarvis	19.168	15.625
50058-AVG	Riverside	19.176	15.639
CLUSTER AVERAGE (excluding Lesley Creek)		**19.147**	**15.627**

*Pb contamination suspected, see text.

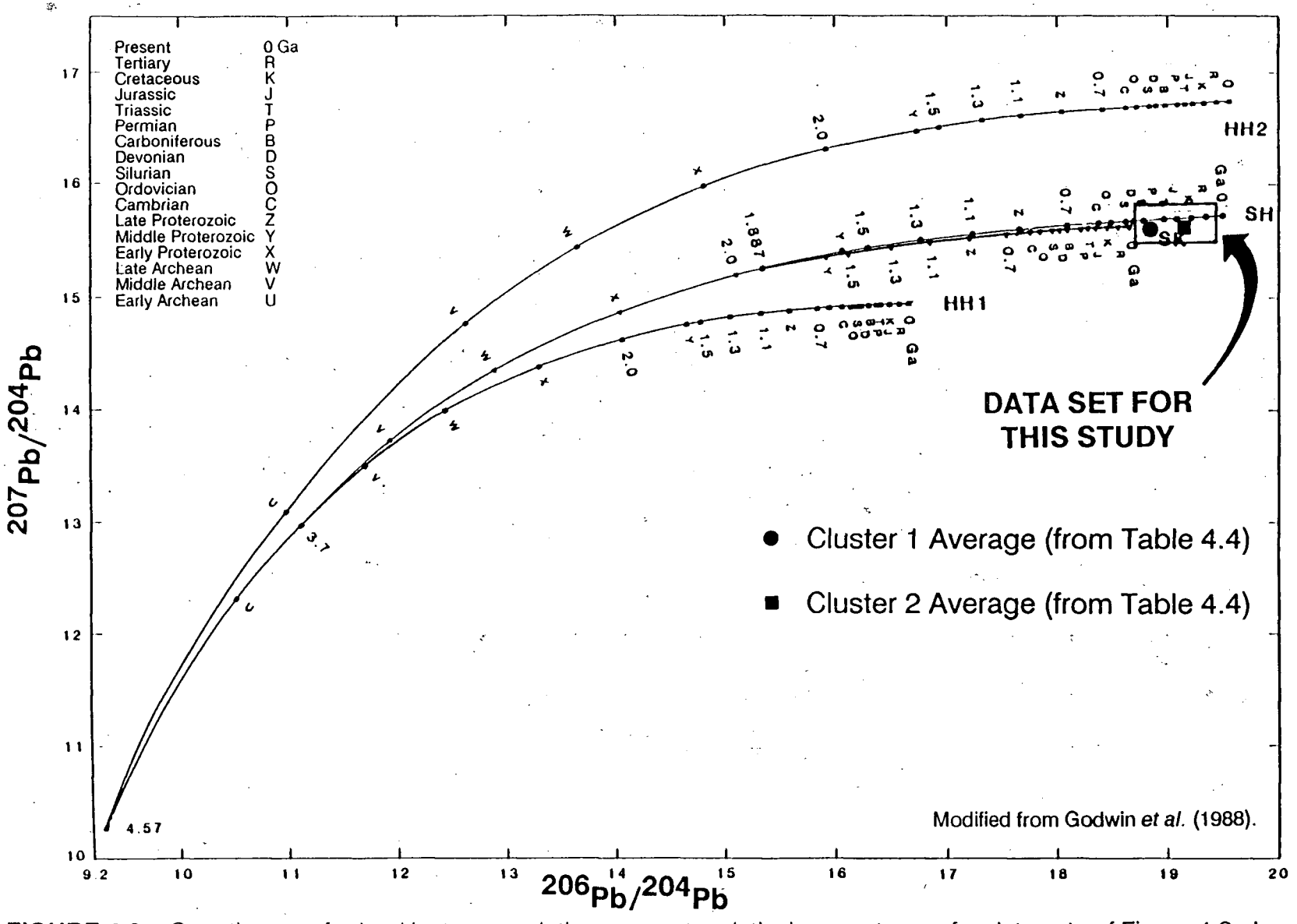

FIGURE 4.2: Growth curve for lead isotope evolution suggests relatively recent ages for data sets of Figure 4.3. Lead evolution curves are for the models of Holmes and Houtermans (HH1 and HH2), Stacey and Kramers (SK), and Godwin and Sinclair (SH). Ages are in billions of years. Note that curve SK evolves from 3.7 billion years on curve HH1, and that curve SH departs from SK at 1.887 billion years.

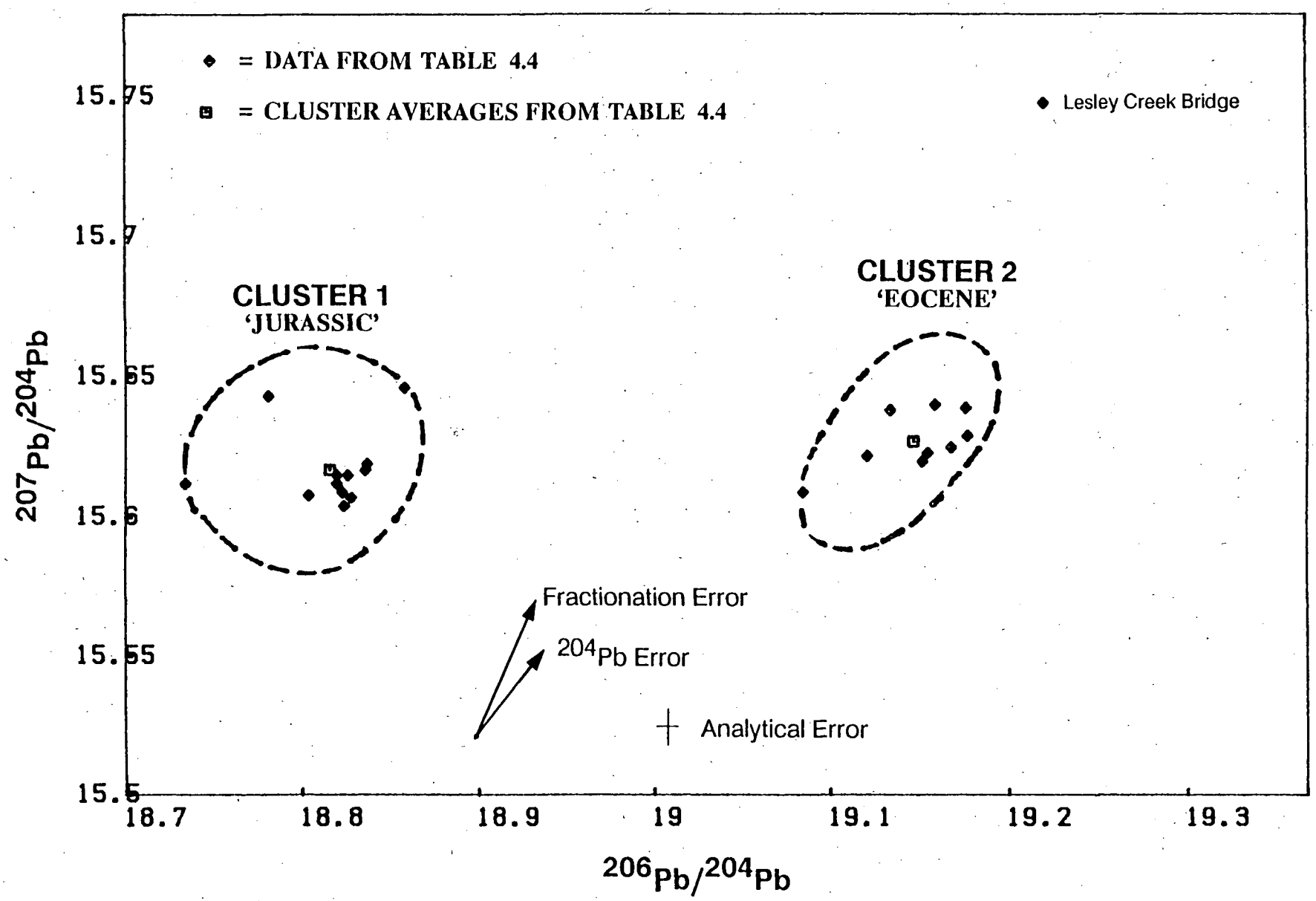

FIGURE 4.3: Stewart camp galena lead isotope data. Analytical error is 2σ.

field of all data points[1]. The complete data set is tabulated and plotted in Appendix III.

INTERPRETATION

"Common lead" isotope data can yield crude absolute age determinations if a suitable model is available for interpretation[2]. A model may also provide indications about the source of elemental lead in an ore deposit. Model development usually requires a large database from rocks and sulphides which must be assembled before meaningful absolute age determinations can be attempted. However, even small lead isotope data sets are useful for indicating relative age relationships among deposits, and between deposits and host rocks. Such 'fingerprint' interpretation of lead isotope data is a simple but powerful tool when combined with other geological data. The following interpretations are derived from the data in Figure 4.3:

- The position of the data clusters in Figures 4.2 and 4.3 suggests that all deposits sampled in this study are Phanerozoic, and likely post-Paleozoic.
- Comparing relative positions of the two data clusters of Figures 4.2 and 4.3 with the progressive evolution of lead isotope ratios suggests that galena of deposits in Cluster 2 could be significantly younger than galena of Cluster 1 deposits. This relative age relationship is consistent with interpretations based on geological evidence.
- Two tight clusters of data shown in Figure 4.3 clearly define two separate metallogenic events in the Stewart area.

[1]Data from the Lesley Creek bridge area, along the road to Big Missouri, are interpreted as strongly fractionated lead isotopes and probably result from analysis of tetrahedrite or impure galena.

[2]The reader is referred to papers by Holmes (1946), Houtermans (1946), Stanton and Russell (1959), Armstrong (1968), Stacey and Kramers (1975), Cumming and Richards (1975), Doe and Zartman (1979), Godwin and Sinclair (1982), Andrew, Godwin and Sinclair (1984), Gulson (1986) and Godwin, Gabites and Andrew (1988) for the development and applications of "model curves" to lead isotope data.

- Tightness of the two data clusters indicates that each ore-forming event was a short-lived episode in geologic time, drawing homogeneous lead from a uniform or well-mixed or well-sampled source rock(s).
- Both data clusters represent deposits that are distributed over a 30 kilometre strike length, thus the two metallogenic events that formed these deposits were both regional phenomena.
- Although the Indian and Silbak Premier mines are less than 2 kilometres apart, the data indicate these deposits formed at significantly different times, with the Indian mine being the younger of the two.

Data clusters of Figure 4.3 support the interpretation of Jurassic and Tertiary metallogenic epochs based on field studies and geochronology reported in Chapter 3. The two ore-forming episodes were not closely related genetic processes. Specifically, Cluster 1 deposits formed cogenetically with calc-alkaline Hazelton Group volcanic rocks of the Stikinia terrane about 190 million years ago. Cluster 2 deposits are epigenetic veins related to Eocene intrusion of dominantly granodioritic plutons.

When these interpretations are combined with other studies, they provide corroborative support for many established interpretations, raise questions about some earlier theories, and suggest an application for systematic lead isotope analysis in exploration programs in the Stewart area.

Data listed in Table 4.4 indicate that ore at the Indian mine is cogenetic with mineralization at the Porter Idaho and Riverside mines, Bayview, Spider and Silverado prospects, and the Start and Jarvis veins. Porter Idaho and Bayview were interpreted as Eocene deposits based on field relationships (Alldrick, 1985 and Alldrick and Kenyon, 1984) and on potassium-argon dates from associated intrusive rocks (Smith, 1977). This age interpretation is also supported by a new potassium-argon date of 42.7 Ma from the altered host rocks at the Indian mine (Section 3.6).

Alldrick (1985, p.337) concluded that Indian mine ores formed at the same time as nearby oreshoots at the Silbak Premier mine, on the basis of textural and mineralogical similarities between coarse grained galena-sphalerite ores found at Indian mine and in the deepest levels of the Silbak Premier mine (termed the Northern Lights or Premier Border zone). However, galena lead isotopes from Northern Lights fall within Jurassic Cluster 1 and are therefore genetically related to other overlying Premier oreshoots (Cluster 1), but not to the nearby Indian mine mineralization (Cluster 2).

The deposits of Cluster 1 include both gold-silver-pyrrhotite veins, such as Scottie Gold mine, and silver-gold-lead-zinc-copper deposits such as Silbak Premier mine. In contrast, deposits of Cluster 2 are silver-lead-zinc veins characterized by high silver grades and by spatially associated molybdenum (Mountainview) and/or tungsten (Riverside). For prospect classification, lead isotope analysis from galena in a small exposure or in a weakly mineralized vein would indicate whether the mineral occurrence was related to the earlier gold-silver(-base metal) event or to the later silver-lead-zinc(-molybdenum-tungsten) mineralizing episode.

CONCLUSIONS

Lead isotope data from the Stewart mining camp do not provide absolute age dates for the formation of mineral deposits, but are consistent with dates determined by other methods. The formation of 21 varied mineral deposits can be attributed to just two mineralizing events: one in Early Jurassic time and one in Eocene time. Both metallogenic epochs were brief, regional-scale phenomena. Deposits from the younger mineralizing episode may be emplaced adjacent to or superimposed on older deposits.

In the Stewart area, routine lead isotope analysis would be a practical aid for exploration programs focused on specific metals. The method is an effective technique for evaluating the commodity potential of a mineral showing or for setting exploration priorities on large claim groups that host several varied mineral occurrences.

4.2.3 FINAL DEPOSIT CLASSIFICATION

Nicolini (1970) developed the concept of comprehensive ore deposit data collection and analysis into a structured system called Gitology. Ridge (1983) presented a strongly-argued case for the importance and effectiveness of objective data *versus* genetic models in mineral exploration. Major texts by Laznicka (1985), and Cox and Singer (1986) were based on a similar approach and the same general concept was followed here.

A variety of deposit-specific geological parameters were applied as classification criteria during the evolution of this study. The criteria were of necessity empirical--it was essential to first separate out similar groups of deposits before any attempt was made to analyse the overall characteristics of each group and to deduce the process of formation for each deposit type. The preliminary classification was based on only three citeria (Table 4.2) but the final classification scheme was considerably more rigorous (Table 4.7, in pocket).

Lead isotope data reliably separate 21 mineral occurrences into two distinct deposit groups with specific ages, but there are 184 other mineral occurrences in the study area without lead isotope data. The lead isotope signature is just one distinctive geological feature of the two deposit groups. Once all the other characteristic features are determined, all showings in the area can be compared to these diagnostic features and categorized as Early Jurassic or Eocene deposits without resorting to additional lead isotope work.

A classification table was developed for the mineral occurrences of the Stewart camp using the features listed across the top of Table 4.7 (in pocket). Analysis of this table allowed separation of 205 mineral occurrences into groups with similar characteristics. Twenty-one occurrences were first sorted into two groups using lead isotope data as a "primary" diagnostic characteristic. For these same 21 deposits additional "secondary" diagnostic or characteristic features of the Jurassic and Tertiary deposit groups were identified (Table 4.5, in pocket), then all other mineral occurrences lacking lead isotope data were sorted according to these secondary diagnostic features. Three distinctive deposit

TABLE 4.6: Metallogenic Epochs and Ore Deposit Types
(from Table 4.7, in pocket)

EARLY JURASSIC (195-185 Ma)	MIDDLE EOCENE (55-45 Ma)
STRATABOUND PYRITIC DACITES	
Ag-Au-BASE METAL VEINS	
Au-PYRRHOTITE VEINS	
	Ag-Pb-Zn VEINS
	SKARNS

TABLE 4.6: Summary of diagnostic features for Stewart mineral deposits.

(From Table 4.7 and Section 4.3)

DIAGNOSTIC FEATURE CATEGORIES	DEPOSIT TYPES				
	EOCENE DEPOSITS		JURASSIC DEPOSITS		
	Skarns	Ag-Pb-Zn Veins	Au-Pyrrhotite Veins	Au-Ag-Base Metal Veins	Stratabound Pyritic Dacites
Pb:Pb Ratio		'Eocene' cluster	'Jurassic' cluster	'Jurassic' cluster	
Au:Ag Ratio		>1:200, <1:10,000	>1:1, <1:5	>1:5, <1:200	
Ore Minerals		scheelite dominant galena-sphalerite minor pyrite	massive pyrrhotite-pyrite arsenopyrite trace chalcopyrite electrum	dominant pyrite minor chalcopyrite electrum gold polybasite	
Gangue Minerals		ankerite	calcite chlorite	calcite chlorite k-feldspar chalcedony carbon	
Ore Textures		medium to coarse grained massive aggregates		cryptocrystalline to fine grained zones laminated comb quartz book structure colloform vuggy growth zones (cockade) metamorphic overprint	
Vein Textures		massive veins rare vugs		coarse quartz-calcite intergrowths chalcedony clasts ore clasts vein clasts vuggy abundant primary fluid inclusions chalcedony veinlets metamorphic overprint	
Alteration	skarn hornfels epidote	hornfels epidote rare minor pyrite	pyrite envelope chlorite envelope silica	pyrite envelope broad chlorite envelope silica sericite k-feldspar carbonate	
Structures	stratabound	massive, tabular veins (southeast strike, subvertical) dyke margin (granodiorite)	en echelon veins metamorphic overprint	vein stockworks, breccia veins dyke margin (Premier Porphyry) disseminated metamorphic overprint	stratabound disseminated metamorphic overprint
Host Rock	? Lower Slst. Mbr Hyder batholith ? Boundary stock	Salmon River Fm Mount Dilworth Fm Betty Creek Fm Premier Porphyry Mbr Middle And. Mbr Lower Slst. Mbr Hyder batholith ? Boundary stock Portland Canal dyke swarm Boundary dyke swarm granodiorite dykes	Middle And. Mbr Premier Porphyry dyke Blueberry dyke Summit Lake stock	Premier Porphyry dyke Blueberry dyke	Mount Dilworth Fm

TABLE 4-7b: Discussion of Mineral Deposit Classification Chart (Table 4-7a)

SUMMARY

Although ore chemistry (assays and trace metal analyses) and ore mineralogy are of most interest to exploration geologists, these features seem to be the least reliable indicators of age and deposit type. Virtually any other feature about a deposit will give more insight into deposit type, including gangue mineralogy, ore textures, vein texture or 'structure', alteration minerals, and stratigraphic and plutonic associations.

SYMBOLS

x = present (no amounts or textures known or implied). Future work on this chart demands careful research to replace these minimally informative 'ticks' with more detailed descriptions.

x? = presence reported but unlikely (based on subsequent reports or on field examination)

? = presence not reported, but probable.

M = major amount (>50%)

c = common (>5%; <50%)

a = accessory amount (>2%; <5%)

m = minor amount (>1%; <2%)

t = trace amount (<1%)

DISCUSSION OF COLUMNS

Every column shows exceptions to the general patterns, with the notable exception of the lead isotope data. Therefore, for most deposits, several diagnostic criteria must be satisfied before classification can be completed with confidence.

Au-Ag Ratios
Vintage assay data is always suspect. On a property with dozens of available assays, those with the highest gold values were preferentially reported, regardless of silver grades. Reported gold-silver ratios are therefore sometimes biased towards gold.

Ore Chemistry
There are too few data available from most showings to determine any diagnostic patterns.

Ore Minerals
Only iron and base metal sulphide minerals are regularly reported. Relative abundances of these minerals are a potential diagnostic feature but most reports fail to indicate amounts.

Gangue Minerals
A surprising number of gangue minerals are diagnostic, which demonstrates the value of careful tabulation of all deposit data in a chart form. For calcite, abundances less than 5% can be found in both Jurassic and Eocene deposits, but amounts over 5% are characteristic of Jurassic deposits.

Ore Textures
Ore textures are rarely discussed or illustrated in reports, yet these features can be highly diagnostic and are visually distinctive. Sawn or slabbed samples are usually necessary.

Vein Textures
Vein textures or small-scale structures are described frequently, but the literature suffers from poorly defined terms. Consequently some reported textures are 'suspect'.

Alteration
Altered wallrock usually has greater volume than the ore zone it surrounds, but it is rarely described in preliminary property examinations. Easily recognized alteration minerals are highly diagnostic and deserve careful attention and documentation.

Structural Setting
Some structural features suffer from being interpretive, and terminology is poorly defined. Some similarities between Jurassic and Eocene structural sites for ore deposition should be expected since both groups of deposit types were likely generated by hydrothermal convection around plutons and their related dykes.

Host Rock
Early versions of this chart included host rock lithology (Table 4.5) but this is redundant because most stratigraphic members are dominated by single lithologies or limited lithological ranges.
Diagnostic stratigraphic associations had not been suspected and could not be deduced until documentation and resolution of the regional stratigraphy was completed (Chapter 3). Similarly, misinterpretation of the ages of some plutons in previous studies prevented earlier recognition of diagnostic plutonic associations.

CONSTRUCTION

These charts can be prepared by hand on a large roll of grid (graph) paper. This method has the advantage of being readily transported, updated and studied in field camp or office. Application of a spreadsheet program is a real help, especially when sorting deposits into categories. A second advantage is their capability to 'store' or 'hide' substantial additional information alongside each symbol; thus the complete quote and reference from the original information source can be hidden at its appropriate pigeonhole, even though the chart printout shows only a single-character symbol. Table 4.7a was prepared with a Lotus program. The stored data file occupies 93K bytes on a diskette, but data entry and file manipulation require 1.0M bytes of RAM memory.

SOURCES

Information for preparation of this table was compiled from MINFILE, provincial and federal government reports, public and private company reports, and field examination of several dozen showings.

types had already been recognized among the deposits that fell into the Jurassic age group, using diagnostic features previously selected to develop Table 4.2. Therefore Jurassic occurrences were sorted again and the resulting final sorted chart is presented as Table 4.7 (in pocket) and summarized in Table 4.6. Features of deposits from each of the four main deposit groups are described in Section 4.3. Genesis of each deposit group is considered in the next chapter.

Empirical classification criteria do not indicate genetic processes but they do divide the seemingly endless variety of mineral deposits in the Stewart mining camp into only a few groups, each with readily recognizable diagnostic features. Lead isotope data can indicate both common ages and common origins among deposits and deposit groups where such relations are not clear from other interpretive methods. And equally significant, the lead isotopes can distinguish different ages and origins among deposits that may have some common features (*e.g.*, Indian mine and the 6 Level ores at the Silbak Premier mine).

Once deposits had been sorted into groups with common characteristics, other more complex, poorly documented features proved to be diagnostic as well. For example, the style, intensity and mineralogy of associated alteration envelopes seemed too variable, too erratic and too poorly documented to be useful diagnostic criteria during this study, but there are characteristic alteration minerals or assemblages associated with each of these deposit groups.

4.3. DEPOSIT CHARACTERISTICS

This section describes features of four ore deposits and the pyritic dacite that were examined during this study.

4.3.1 EARLY JURASSIC DEPOSITS

4.3.1.1 SCOTTIE GOLD MINE

Scottie Gold mine (Figure 4.1a) lies on the east side of Morris Summit Mountain at 1100 metres elevation. The showings were initially staked in 1928. Trenching, diamond

drilling and several phases of underground development were carried out between 1931 and 1948. There was no further work until the Northair Group optioned the ground in 1978. Production started on October 1, 1981 and continued until February 18, 1985.

GEOLOGIC SETTING

Geological reports on the property include Minister of Mines Annual Reports for 1946, 1947 and 1948, Seraphim (1947), Wares and Gewargis (1982), and Dick (1988); an extensive bibliography is included in MINFILE (104B-34).

Ore zones are hosted in andesitic volcanic rocks near the eastern edge of a large hornblende granodiorite stock. Host rocks are matrix supported andesitic tuff breccias and lapilli tuffs with intercalated ash tuffs, volcanic sandstones and volcanic conglomerates of the Middle Andesite Member of the Unuk River Formation. Massive tuffs vary from coarse ash tuffs to fine grained crystal-rich tuffs composed of plagioclase and plagioclase-pyroxene-hornblende phenocrysts. Coarse pyroxene porphyritic basalt was excavated in the railway tunnel. Mafic minerals are partially to wholly replaced by chlorite.

Two kilometres northeast of the mine, thin bedded siltstones trend north, dip vertically and show tops to the east; two kilometres west of the mine, around the topographic station on the ridge crest, several outcrops of thin bedded wacke strike southeast, and dip steeply northeast with tops to the northeast. No bedding has been recognized within the mine workings.

The mine sequence is intruded on the northwest by the Summit Lake stock. This coarse grained equigranular to subtly potassium feldspar porphyritic hornblende granodiorite is part of the Early Jurassic Texas Creek plutonic suite with a U/Pb date of 192.8 Ma. The nearest surface exposure to the mine workings is 500 metres uphill to the west. The pluton has not been intersected in drill holes or underground workings so the closest approach to the ore zones is unknown, but is probably less than 500 metres. Contact relationships suggest relatively passive emplacement, but the pluton has produced a distinctive metasomatic alteration assemblage. Near the contact with the stock, andesites

are bleached and impregnated with fine to very coarse grained accessory hornblende (up to 3 centimetres long) and minor fine pyrite. Bleaching is due to carbonate ± sericite flooding.

Country rock and ore zones are cut by green microdiorite dykes and dark brown lamprophyre dykes of the Berendon dyke swarm. Lamprophyre dykes are spessartite with fresh fine hornblende phenocrysts and calcite-filled amygdules.

The Morris Summit fault is a regional scale structure (Figure 3.2a) that trends north-northwest through the mine area between the 3000 Level and 3600 Level portals, dipping southwest at 30 to 45 degrees. In the 3000 Level drift the fault zone is 0.5 metre wide, dipping 32 degrees southwest with slickensides sub-parallel to the dip with an azimuth of 258 degrees. The Morris Summit fault lies east of the ore zones. There is no consensus about the absolute displacement across this major fault. Individual lines of evidence support arguments for normal, reverse and dextral strike-slip movement. In plan, the relative sense of offset is dextral. Resolution of this problem is an important key to exploration along its eastern side. There are indications from two 1987 drill holes that mineral zones west of the fault may be 'rolled' or drag-folded into the immediate hangingwall of the fault, parallel to the dip. Therefore vein extensions may have been offset in the footwall block east of the fault.

MINERAL DEPOSITS

Mineralization on the Scottie Gold property occurs as a series of separate veins hosted in complex, subparallel shear or fracture zones (Figures 4.4 and 4.5). Names for these individual veins are summarized in Table 4.8

The four southern veins alongside the Morris Summit Glacier are major structures trending about 130 degrees and dipping 75 to 80 degrees northeast. The L, N and M Zones have a horizontal separation of about 50 metres; the O Zone is roughly 110 metres further to the northeast. There are many cross-structures or splays that also carry ore. Local

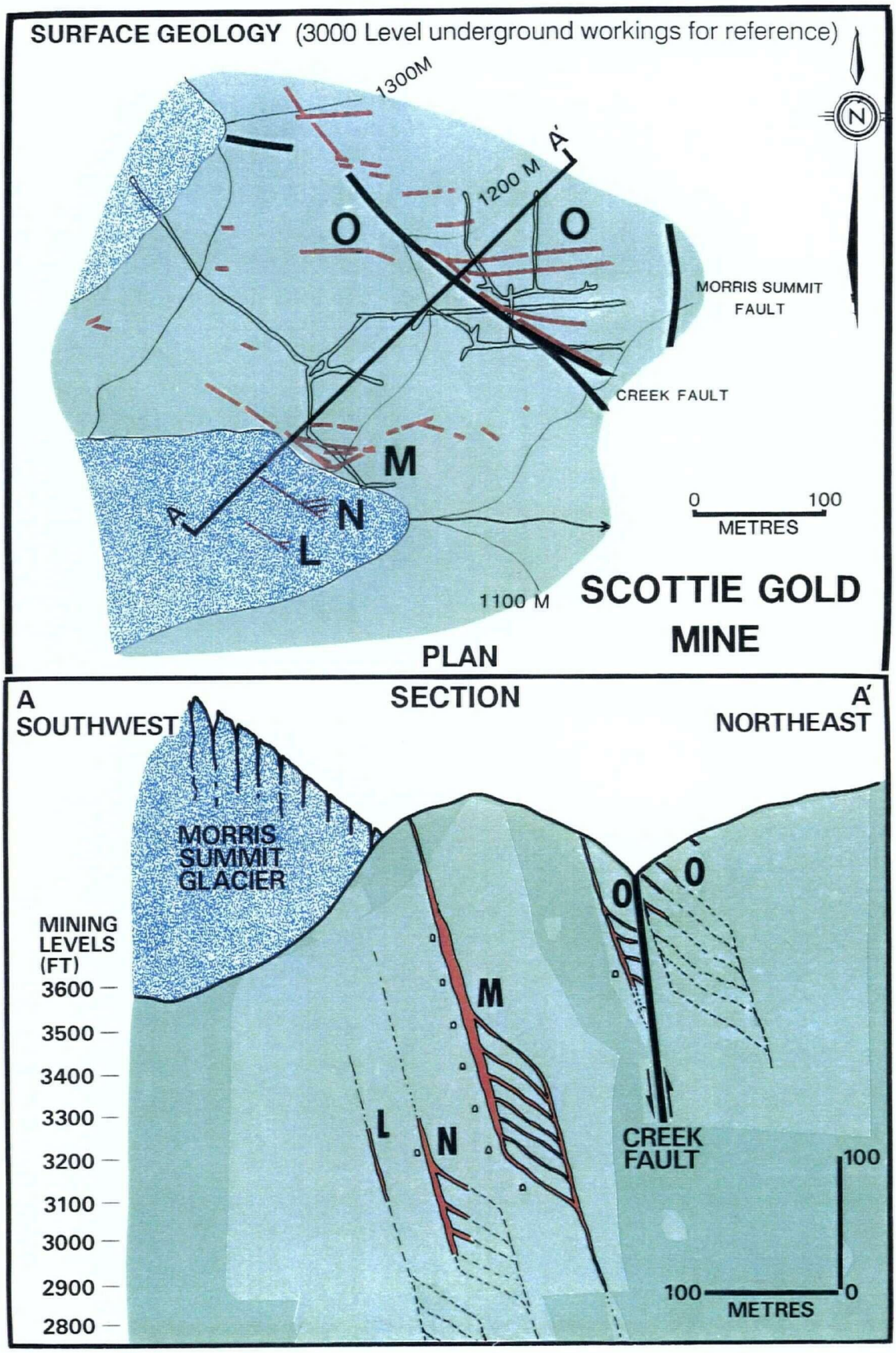

FIGURE 4.4: Geological map and cross-section through the Scottie Gold mine (Simplified from company plans. See Figure 4.5 for detailed geology.)

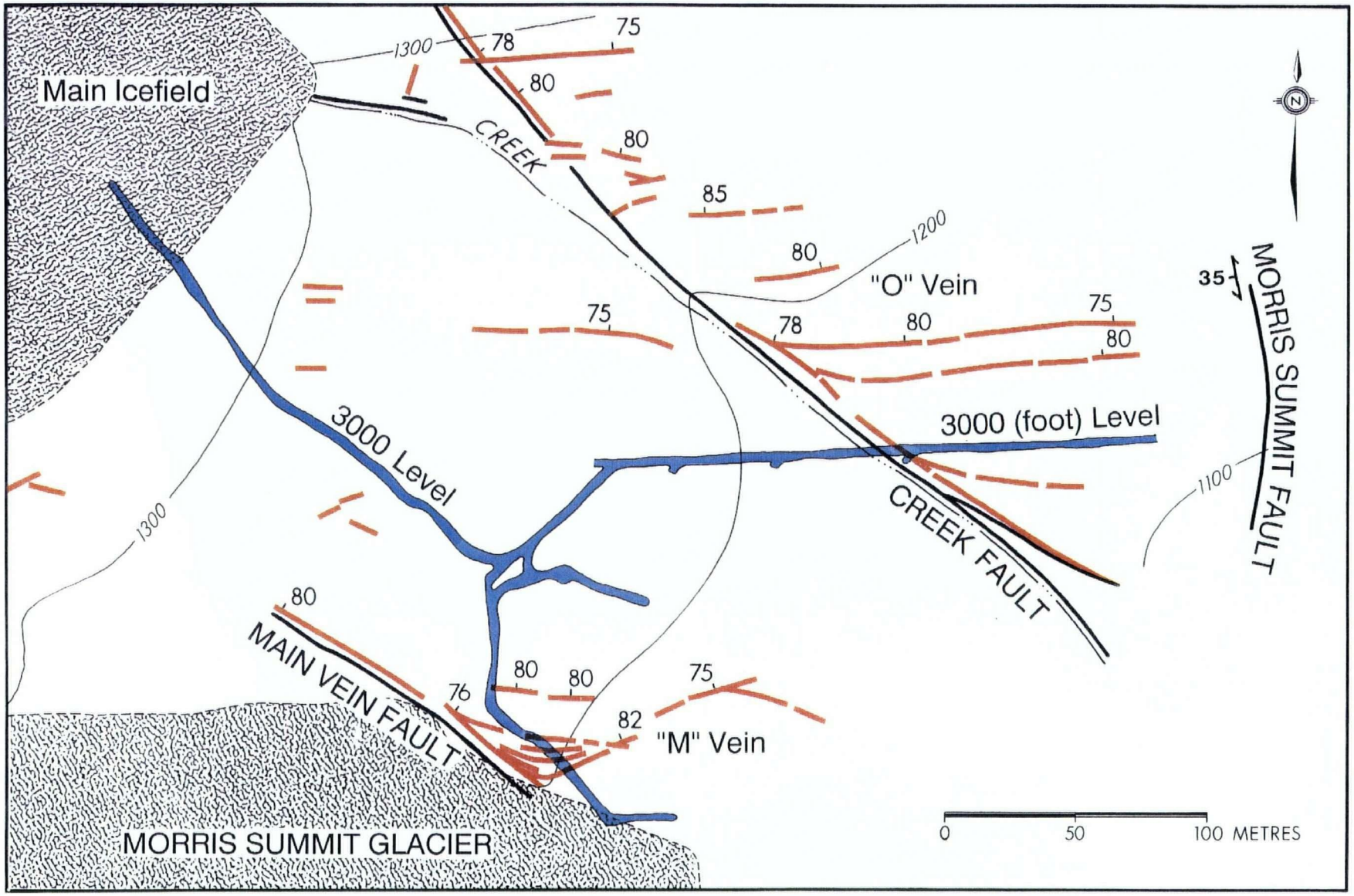

FIGURE 4.5: Distribution of veins on surface at the Scottie Gold mine. Country rock is massive andesite tuffs. (Outcropping veins in red. 3000 Level underground workings in blue for reference. From company plans.)

TABLE 4.8: Evolution of ore zone names at Scottie Gold mine

	SOUTH						NORTH
1947			Morris Summit		Scottie		
			Main Zone	North Zone			
1980-1983	L	B,N	A Vein; Mine Vein; Main Vein [East Main (Doublet); West Main (McLeod Zone)]	Creek	Scottie North		Scottie Point
					South Showing	North Showing	
Current	L	N	M	O	C	D	E
Underground Development?	No	Yes	Yes	Yes	No	No	No
Past Production?	No	Yes	Yes	No	No	No	No

flexures or rolls are common in all the veins; the West Vein averages 130°/75°NE overall, but orientation in the 36-95 stope is 145°/63°NE.

The greatest ore production has come from M Zone which is described here. Other zones had similar sulphide and gangue mineralogy and ore grades, but were generally narrower with less complex structure. M Zone occurs as two major, parallel vein structures, the West Vein (Main Vein West, West Mine Vein, McLeod West Zone) and the East Vein (Main Vein East, East Mine Vein, McLeod East Zone). These two major veins are connected by 'rungs' of many narrower veins, called the Sixties Veins (Figure 5.1). Overall trend and dip of the M Zone is 130°/75°NE, Sixties Veins trend and dip 060°/80°NW or about 70 degrees to the main veins. M Zone extends vertically at least 450 metres from surface at 1280 metres to the deepest drill hole intersections at 830 metres. M Zone is at least 150 metres long, but for 100 metres of this, the northwest end of the Main veins is 10 centimetres to 1 metre wide with erratic gold values. On every mine level the productive section of the M Zone is roughly 40 metres long.

West Vein is a simple massive vein deposit with a moderate alteration envelope, whereas the East Vein is more complex, showing small scale structural control and a more intense alteration envelope (Figure 5.1, Plates 4.1B and C). The minor but mineralized Sixties Veins, connecting the two major veins, commonly constitute ore. There are enough differences among the West Vein, East Vein and the interconnecting Sixties Veins that they are described separately.

The West Vein is the most massive, regular vein in the mine (Plate 4.1A), averaging 5 metres in width and locally reaching 7 metres. The southwest wall of the vein is marked by spectacular sulphide slickensides along a narrow brittle fault called the Main Vein fault or Southern Boundary fault. On every mine level, the West Vein trends southeastward (130°/75°NE) parallel to this fault until the vein detaches or rolls away from the fault to a trend of 110 degrees at the southeast end of the mine where gold values abruptly decrease

Plate 4.1A: The M Vein (Main Vein West) in the 'roof' of a drift along 3600 Level. Note perfect symmetry of the massive pyrrhotite core and quartz-sulphide marginal zones. Pods, blebs and lenses of pyrrhotite are also present in foliated wallrock. Strapping is 15 centimetres wide.

Plates 4.1B and C: Strongly sheared wallrock shows rich pink to coral carbonate alteration (rhodochrosite). Second view shows distribution of sulphide trains, mainly pyrite, within this sheared, altered wallrock. Scale bar in centimetres.

Plate 4.1D: Sphalerite-rich quartz vein from marginal zone of Main Vein. Scale bar in centimetres.

Plate 4.1A

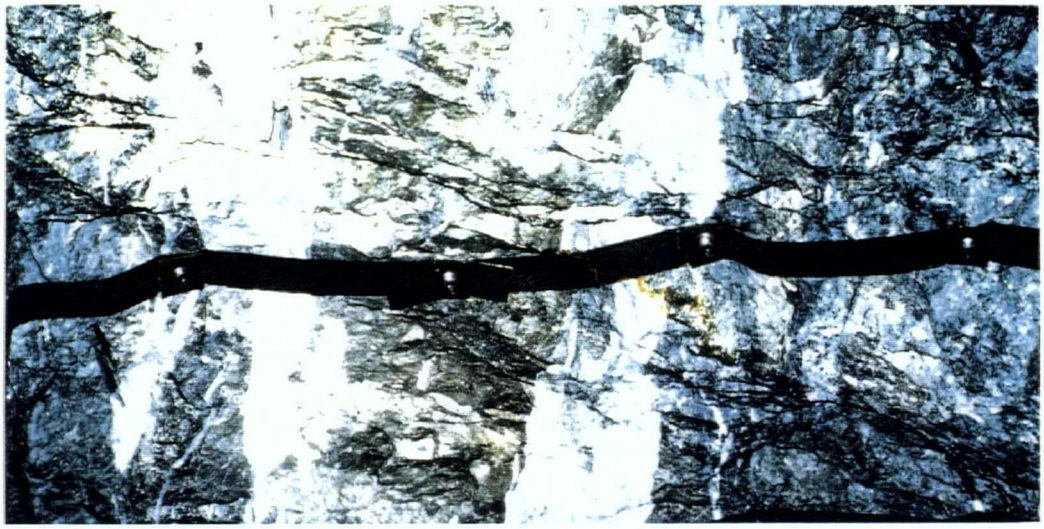

Plate 4.1B

Plate 4.1C

Plate 4.1D

and the vein itself horsetails out and disappears. The northwest limit of the West Vein has not been determined, but the vein is at least 150 metres long.

The core of the vein is massive, fine grained, distinctly pinkish to bronze-coloured, non-magnetic pyrrhotite with little or no associated pyrite (Plate 4.1A). The only other component is minor scattered knots or blebs of quartz, calcite and chlorite. This core zone ranges from 4 to 6 metres wide along the productive part of the vein. The immediate margins of this pyrrhotite core consist of overprinted swarms of quartz-carbonate veins and veinlets hosting accessory to minor pyrrhotite, pyrite, sphalerite and galena (Plates 4.1A and D) with intervening wallrock fragments or inclusions that are intensely altered by sericite, carbonate and chlorite. These marginal vein swarms are typically 0.5 to 1 metre wide on both sides of the massive pyrrhotite core (Plate 4.1A). Gold values within this marginal rock are erratic and only locally constitute ore.

The East Vein is narrower and more erratic than the West Vein and can be seen to pinch-and-swell and bifurcate along its overall 130 degree trend, parallel to the West Vein. D. Williams documented the East Vein as two adjacent, parallel vein structures with screens of strongly altered wallrock sandwiched between them. Both veins constitute ore. Each vein consists of a massive sulphide core that is narrower but similar to the West Vein. The sulphide core is composed of roughly equal amounts of fine grained pyrrhotite and pyrite, in contrast to the West Vein which is dominantly pyrrhotite. Quartz-carbonate margins at the East Vein are similar to the West Vein, but wider, and have veins and veinlets penetrating randomly into the country rock. These quartz-carbonate vein swarms host galena, sphalerite, pyrrhotite and pyrite with fragments of altered country rock. They are erratically gold bearing, locally constituting ore. The East Vein trends southeastward to outcrop.

The intervening Sixties Veins connect the West and East Veins. The Sixties Veins trend 060 degrees and dip 80 degrees to the northwest. They are individually much thinner than either of the main veins, locally pinching down to 2 to 3 centimetres. However, they

commonly constitute ore due to consistently high grades of better than 70 grams per tonne gold. Sixties Veins occur either as miniature copies of the larger veins (massive pyrrhotite cores with quartz-carbonate-sulphide margins) or they consist only of quartz-carbonate vein-hosted sulphide mineralization with substantial disseminations, blebs and seams of fine grained pyrrhotite. All country rock between the Sixties Veins is variably altered as a result of overlapping alteration envelopes from adjacent veins.

The abrupt mineralogical change between the pyrrhotite core zone and the symmetrical quartz-carbonate margins suggests these ore zones originated as composite veins (Durney and Ramsay, 1973, p.72-76). Subsequent shearing and recrystallization has obscured evidence of a median suture and original fibrous growth.

Prior to this study it had not been determined in what form or where gold occurred within ore zones; rare free gold required a hand lens for detection and was noted only within the marginal quartz-carbonate vein zones. Gold values are distributed erratically across and along all veins, even though veins are continuous and the pyrrhotite cores appear to be homogeneous. Whole stopes on the West Vein grade up to 50 grams gold per tonne, locally exceeding 70 grams per tonne, but sections of the East Vein and Sixties Veins can be either very high grade or virtually barren in exposures that appear to be identical. Distribution of silver values in the veins also appears to be random, but silver was not routinely assayed.

SAMPLING

Three chip sample sections totalling 25 samples were collected at Scottie Gold mine. Each sample exceeded 10 kilograms. Two were collected from M Zone (32-93 and 36-95 stopes) and one across N Zone (32-92 stope) (Appendix IV). M Zone samples were collected across the current stope face, the N Zone sample was collected along the walls of the cross-cut. In addition, seven selective grab samples were collected for trace element analysis. Analytical results are listed in Appendix IV and summarized in Table 4.7 (in pocket).

MINERALOGY

Ore petrography has been completed by Seraphim (1947) and the writer. For this study ore and gangue mineralogy and textures were examined in 5 polished thin sections, 15 polished sections, 44 thin sections and 48 polished rock slabs.

In order of abundance opaque minerals include pyrrhotite, pyrite, sphalerite, chalcopyrite, galena, arsenopyrite, native gold, tennantite and rare chalcocite.

Pyrite commonly shows evidence of cracking, crushing and shearing. Pyrrhotite however has totally annealed with roughly 120 degree triple junctions (Plate 4.2B). Cracks within pyrite are filled by trace copper minerals (Plate 4.2C) or by pyrrhotite (Plate 4.2A). The minerals along these cracks represent plastic flow, or crystalline growth along the fracture, or recrystallization along the walls of the crack that has turned a thin selvage of the host pyrite grain into pyrrhotite. The latter process seems to fit the textural evidence best. Pyrite and pyrrhotite also occur as blebs and patches and as sheared streaks or strings of crushed grains in the quartz-carbonate marginal zones and in adjacent, intensely altered wallrock.

Chalcopyrite occurs in trace to minor amounts in both the pyrrhotite core zone and marginal quartz-carbonate zone, but is more abundant in the core zone where it is distributed along fractures in pyrite (Plate 4.2C), commonly with associated gold, and along grain boundaries in massive, recrystallized and annealed pyrrhotite (Plate 4.2B). Tennantite and tetrahedrite, distinguished by their respective greenish and bluish tints, have only been noted in the core zone as late fracture fillings in pyrite, with associated chalcopyrite and gold.

Sphalerite and galena are common in the quartz-carbonate envelope (Plate 4.1D), but are virtually absent in the pyrrhotite core. Arsenopyrite occurs locally within the pyrrhotite core as fine to coarse grained euhedral, commonly cracked crystals. Broken crystals are enveloped by pyrrhotite. Zones of arsenopyrite are not associated with highest gold grades, but generally assay in the 17 grams gold per tonne range.

Plate 4.2A: Gold grain within pyrrhotite 'veinlet' cutting large, rounded, brittly fractured pyrite grain. Sample SG 3695-2. Length of photo 0.32 mm.

Plates 4.2B: Typical form and size for disseminated gold within massive pyrrhotite. Crossed polars show that gold blebs are locallized along pyrrhotite grain boundaries. Sample of M Zone ore from a working face that averaged 69 grams per tonne gold. Length of photo 0.6 mm.

Plate 4.2C: Two gold grains within a chalcopyrite veinlet filling a fracture through a pyrite grain. Sample SG-7. Length of photo 0.16 mm.

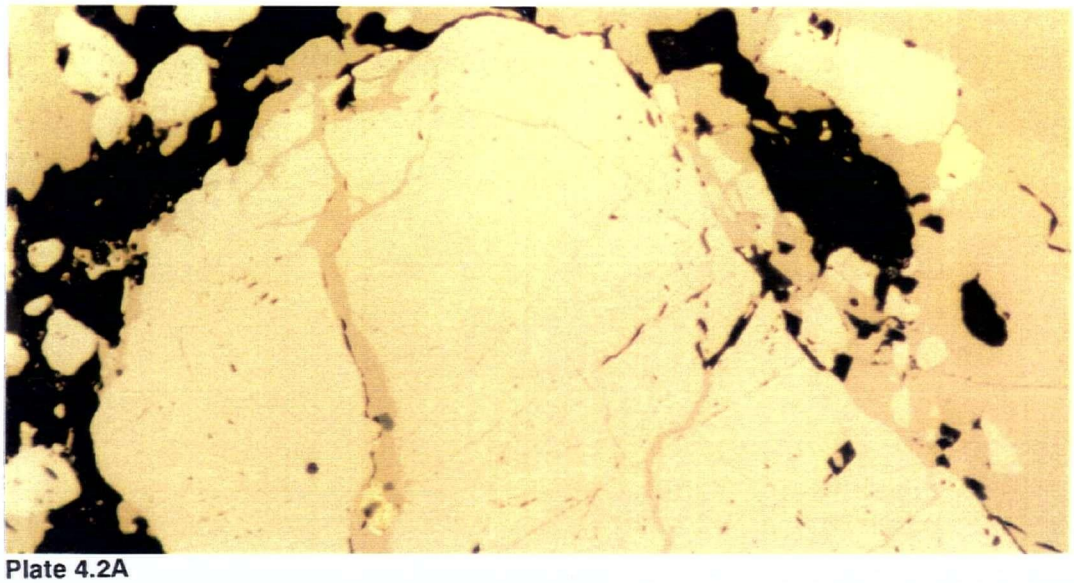

Plate 4.2A

Plate 4.2B

Plate 4.2C

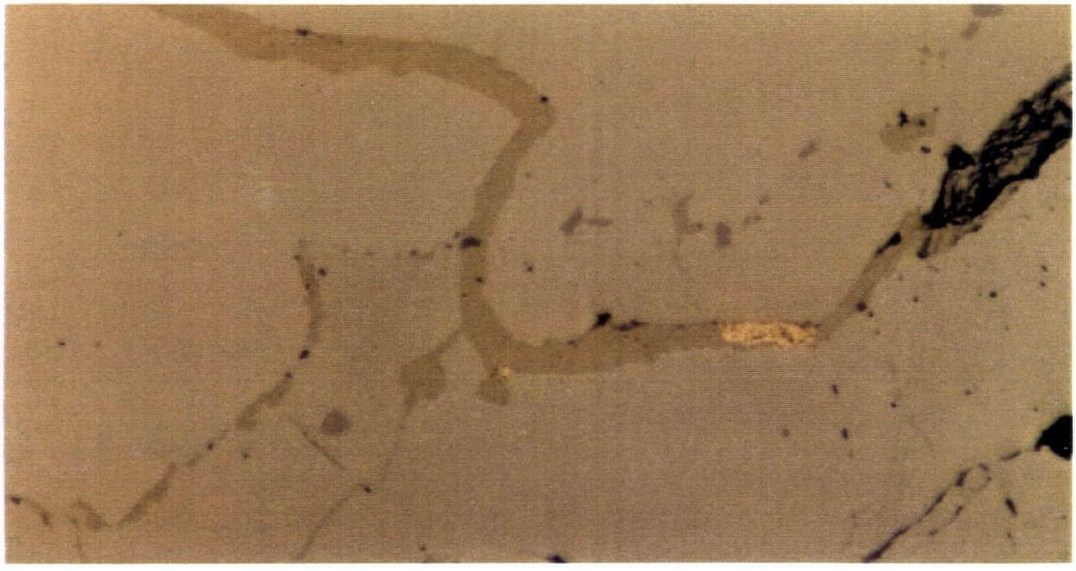

Native gold occurs as ubiquitous fine blebs and grains in the pyrrhotite core zone. Gold grains are typically 10-40 microns in diameter, the largest grain observed measured 120 microns across. Gold is most commonly associated with chalcopyrite (Plate 4.2C). Free gold also occurs floating in massive pyrrhotite (Plate 4.2B). It is much less abundant and more erratically distributed in quartz-carbonate envelopes where it may be associated with pyrrhotite-pyrite blebs or quartz-carbonate gangue.

Gangue minerals include quartz, carbonate, sericite, chlorite, minor epidote and trace clinozoisite. The four most abundant gangue minerals display both massive and sheared forms. Major shear structures in the quartz-carbonate margin zone and the immediately adjacent wallrock are dominantly replaced by sericite and carbonate with lesser amounts of chlorite and quartz. Some large quartz chips floating in massive pyrrhotite are aggregates of long fibrous crystals suggesting growth prior to brecciation and shearing. Some thin sections show elongate strings of quartz granules resembling mylonitic ribbon grains.

ALTERATION

Andesitic volcanic rocks on the property show strong propylitic alteration with pervasive chlorite, minor epidote and trace disseminated pyrite. Alteration intensity increases progressively within 10 metres of the ore zones. Pyrrhotite, pyrite and chalcopyrite occur as fine disseminations and hairline fracture coatings adjacent to the main mineral deposits and seem to be associated with the most abundant chloritization.

Within the underground workings wallrock alteration immediately adjacent to the quartz-carbonate vein margin is abundant chlorite alternating with two lighter coloured alteration types that have been described from hand samples as silicification and as hematization producing a pink chert. Thin sections show that the light, colourless alteration is dominantly sericite and calcite with grains of crushed quartz. The pinkish alteration type (Plates 4.1B and C) is entirely composed of fine to coarse grained carbonate aggregate that is free of hematite even under high magnification, and is therefore probably rhodochrosite,

or its iron- or calcium-rich solid solutions: ponite, manganosiderite, kutnohorite or manganocalcite.

Wallrock alteration ranges from massive, unfoliated, alternating patches of chlorite, sericite-carbonate, and pink carbonate with scattered knots or blebs of sulphide aggregate, to strongly foliated, banded segregations of alternating green, white and pink alteration types with intermittent streaks of sulphides.

(Discussion of Ore Genesis begins on page 253.)

4.3.1.2 DEPOSITS OF THE BIG MISSOURI AREA

The Big Missouri mine and several other nearby orebodies and prospects lie on or adjacent to Big Missouri Ridge at an average elevation of 900 metres (Figure 4.1a). The ridge lies midway between Salmon Glacier on the west and Long Lake on the east, and trends southward from the south end of Mount Dilworth to the Indian mine, a distance of 8 kilometres.

GEOLOGIC SETTING

All gold-silver occurrences in the Big Missouri area are hosted within the Upper Andesite Member of the Unuk River Formation. The Upper Andesite Member is similar to descriptions in Section 3.1 and includes the basal Black Tuff facies that is well exposed on the hillside along and above the Granduc mine road. The Main Sequence includes typical medium green andesitic ash tuffs and lapilli tuffs, abundant plagioclase-hornblende-phyric crystal tuffs, and minor tuff breccias.

The Upper Andesite Member is underlain on the west by the Upper Siltstone Member. The contact is commonly sheared, but locally is exposed as an unsheared, undisrupted, "welded" contact of thin bedded siltstones overlain by massive tuffs. Rhythmically bedded, thin bedded turbidites display graded beds showing tops to the east. Dips along the Granduc mine road and in nearby outcrops above and below the road range

from 27 to 72 degrees eastward and average about 55 degrees east, an attitude originally recognized by Schofield and Hanson (1922, p.34).

The Upper Andesite Member is overlain on the east by maroon and green facies of the Premier Porphyry Member, first described in this area by Read (1979). This member has been traced along the eastern side of Dago Hill (Figure 4.6) and seems to mark the eastern limit and stratigraphic cap to all the mineral zones on Dago Hill.

The superjacent Betty Creek Formation thins down to only a few metres near Tunnel Lake. Southward, near the northeast end of Silver Lakes, the Betty Creek Formation shows bedding dipping from 82 degrees west to vertical with tops to the east. To the north, between Tunnel Lake and Union Lake, the formation is either absent, recessively weathered, or obscured by intense hydrothermal alteration.

The Mount Dilworth Formation near Dago Hill was the focus of Galley's (1981) study and the reader is referred to his detailed lithological descriptions. All members and facies of the formation have been identified in the Dago Hill area except the Pyritic Tuff facies which ends abruptly at the south end of Mount Dilworth. Orientation of distinctive fiammé in the Middle Welded Tuff Member and subtle bedding in the Lower Dust Tuff Member range from shallow to moderately eastward dips. Fiammé at the north end of Dago Hill strike south-southeastward and dip 42 degrees east-northeast. The fiammé are at the base of a 10-metre-thick single cooling unit of welded tuff that displays progressively more compressed pumice clasts down-section. Base surge dune forms exposed in this member north of Union Lake also show tops to the east.

Based on all bedding attitudes noted in adjacent units, massive andesitic tuffs of the Upper Andesite Member are interpreted to dip eastward in the Big Missouri area. No bedding has been reported in this unit in the immediate area, despite several phases of detailed, property-scale mapping. A thin lens of well bedded hematitic wackes, exposed along Big Missouri road, lies within the Upper Andesite Member and dips steeply eastward.

E–W CROSS-SECTION THROUGH THE BIG MISSOURI MINE

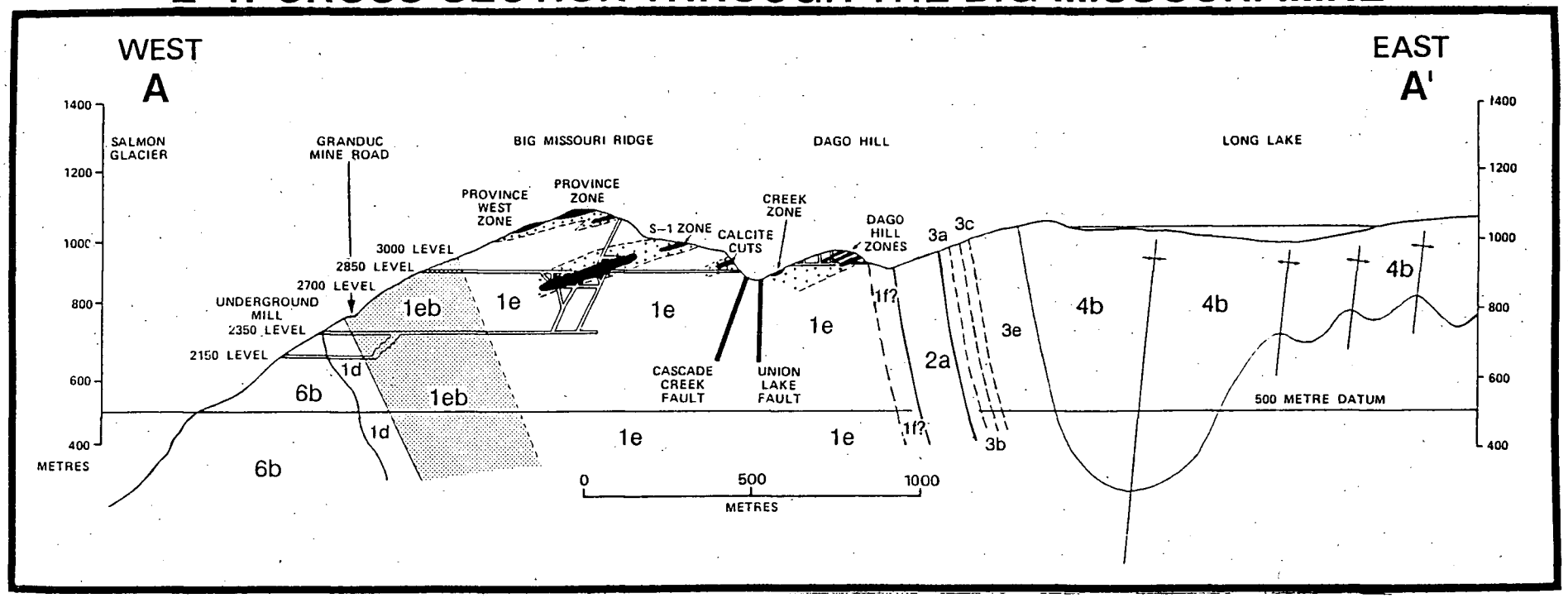

FAULT

FOLD AXIS; ANTICLINE, SYNCLINE

GEOLOGICAL CONTACT; FORMATIONS

GEOLOGICAL CONTACT; FACIES, MEMBERS

MINE WORKINGS

MINERAL DEPOSIT, QUARTZ–CARBONATE BRECCIA VEIN WITH DISSEMINATED TO SEMI–MASSIVE SULFIDES

ALTERATION HALO, SERICITE, SILICA, QUARTZ VEINING

FIGURE 4.6: Cross section through the Big Missouri mine area.
(See **Figure 3.2a** for section location and Legend)

Intrusive rocks along Big Missouri Ridge range from batholiths to dykes. The floor of the portal into the Silver Butte workings shows the eastern contact of coarsely K-feldspar porphyritic Texas Creek batholith intruding andesitic tuff; this is the highest stratigraphic level of intrusion known for these rocks. Recent road excavations north of Silver Butte have exposed an irregular dyke of Premier Porphyry. It cuts thin bedded turbidites of the Upper Siltstone Member. The Martha Ellen deposit lies inside the Portland Canal dyke swarm and the southern end of the orebody is cut by a Tertiary granodiorite porphyry dyke.

Faulting is abundant on a range of scales. The Silver Butte deposit lies within a fault-bounded, stratigraphically down-dropped block. Bounding faults have steep westerly dips. Two other major north-trending faults on the east side of the ridge, the Union Creek and Cascade Creek faults, dip moderately to steeply westward (Figure 4.7a and b). History of movement along these latter two faults may be complex (Section 3.4), but distribution of outcrop patterns across the faults suggests relative normal offset of up to several tens of metres. Determination of direction and amount of offset on these two faults are a key to resolving the number of ore zones and the exploration potential on the property (Figures 4.7a and b).

In summary, the stratigraphic succession on Big Missouri Ridge is a steeply to moderately eastward-dipping stratigraphic package lying on the western limb of a major north-trending syncline (Figure 4.6). There is no evidence for existence of minor folds within the Upper Andesite Member; the mineral deposits are tabular features that are well delineated by drilling and underground workings and clearly show no evidence of small scale folding (Figure 4.6).

MINERAL DEPOSITS

Within a 2.5 kilometre radius of the Big Missouri mine there are 25 deposits and prospects (Figure 4.1a and Table 4.9). Five of these have been classified as Tertiary-age silver-lead-zinc deposits in this study, the remainder are classified as Early Jurassic gold-

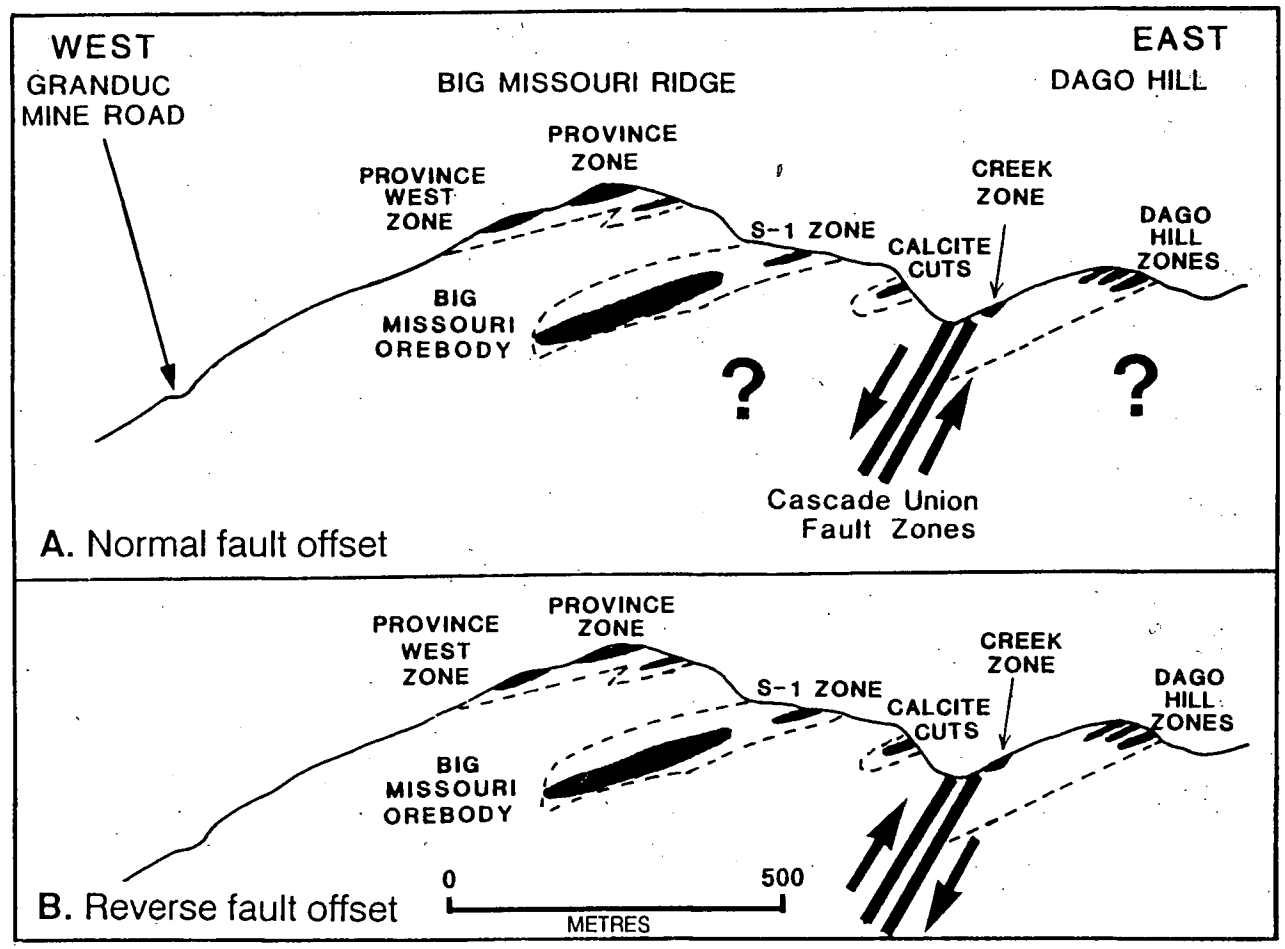

FIGURE 4.7: Net fault offset across the combined Cascade Creek and Union Creek fault zones may be "normal" or "reverse".
A. If normal, zones on the west and east sides of the fault are unrelated and additional zones **(?)** may exist at depth.
B. If reverse, then the largest zones on the west and east sides of the fault may have originally been one continuous shoot.
(See **Figure 4.6** for geology and **Figure 3.2a** for location.)

TABLE 4.9a: PAST PRODUCTION IN THE BIG MISSOURI AREA

PROPERTY	MAP NO.	MINFILE NO.	DATE	PAST PRODUCTION (tonnes)	Au g/T	Ag g/T	Cu %	Pb %	Zn %
SPIDER	N28	104A-010	1925, 1933-1936	22.2	14.2	8238.		3.5	3.9
SILVER TIP	N36	104B-043	1915,1950, 1951,1957	26.3	11.8	2610.		14.	19.
BIG MISSOURI	N50	104B-046	1938-1942	768 943.	2.37	2.13		*	*
DAGO HILL	N55	104B-045	1934,1950	13.6	48.	3952.	0.12	0.46	

* Shipments reported; no grades known

TABLE 4.9b: PRESENT RESERVES IN THE BIG MISSOURI AREA

PROPERTY	MAP NO.	MINFILE NO.	RESERVES* (tonnes)	Au gm/T	Ag gm/T	Pb %	Zn %
SILVER TIP	N36	104B-043	816(g)	4.8	970.3	4.2	6.2
BIG MISSOURI GROUP	N50	104B-046	1 685 200(m) 3 684 984(g)	3.12 2.50	22.97 21.26		
Martha Ellen	N33	104B-092	647 900(m)	2.78	23.05		
Northstar	N46	104B-146	47 100(m)	4.28	20.57		
Creek	N49	104B-086	7 500(m)	2.40	116.23		
Dago Hill	N55	104B-045	297 000(m)	2.85	49.71		
S-1	N48	104B-084	422 700(m)	3.84	8.23		
Province	N53	104B-147	263 000(m)	2.50	13.37		
SILVER BUTTE	N58	104B-150	105 590(m) 339 512(g)	10.6 17.31	39.7 36.69		

* Reserve Categories: (m) = mineable; (g) = geological

silver (± base metal) deposits (Table 4.7, in pocket). This section reviews the local structural and textural features of these Early Jurassic deposits.

All but one of these 20 deposits have a north-south strike and a gentle westward dip (20 degrees), and thus are oriented virtually perpendicular to stratigraphy (Figure 4.6). Based on their crosscutting attitude, and many distinctive textures and structural features to be described in this section, these Early Jurassic mineral deposits are all interpreted as epigenetic veins.

Deposit dimensions range from impressively large to surprisingly small. The S-1 vein system and its down-dip continuation (the original Big Missouri orebody) have an east-west dip length of 700 metres and a north-south strike length of 120 metres. The Creek deposit, composed of semi-massive to massive sulphide, is at the opposite end of the size scale. This zone is 2 metres thick with a strike length of only 35 metres and an up-dip length of only 15 metres (thought to terminate against a fault). Reserves total 7500 tonnes.

Average thicknesses and drill intersections on all showings are in the 1 to 3 metre range. Maximum thicknesses are more difficult to determine because many existing cross-sections include the peripheral alteration envelope as part of the mineral zone, the actual quartz-carbonate vein is significantly thinner. The thickest drill intersections on Dago Hill are given as 2 metres (Galley, 1981, p.122), 5 metres (Dykes *et al.*, 1988, p.6) and 9 metres (Dykes *et al.*, 1988, figure 9). Sections of the original underground Big Missouri ore zone were at least 6 metres thick and could have been greater.

In general, the strike length of economic sections of these veins is significantly less than dip length, so that their longest dimension is consistently east-west, or in terms of the original (pre-folding) depositional setting, vertical. Certainly this is the case for S-1 Zone and Dago Hill. Drill information suggests a small but real southward rake to these zones, so that the trend of their long dimension is close to west-southwest (see figure 10b in Dykes *et al.*, 1988).

Different veins have slightly different dips (Figure 5.2). The Dago Hill deposits dip 25°W, Calcite Cuts dips 21°W, S-1 dips 18°W and Province and Province West dip 15°W. These differences are real and measurable, but are perhaps too small to be significant. Nevertheless it seems more than a coincidence that the variation is systematic. This radial or fan pattern is exactly what would be expected from a series of originally vertical and parallel veins after the host stratigraphy had been deformed in the manner that this region has been folded (Figures 4.6, 4.7 and 5.2).

Wallrock contacts are sharp, but complicated by extensive fracturing and peripheral quartz-carbonate and chalcedony vein networks that criss-cross shattered, altered wallrocks (Plates 4.3B and C, and 4.6B). Some ore zones show distinctive changes in lithology between structural footwall and hangingwall rocks. However, some vein intersections, such as the interval from 10.7 to 12.5 metres in DDH 82-42 on the S-1 zone, have exactly the same lithology in hanging wall and foot wall country rocks.

Mineral deposits range from quartz-carbonate veins containing trace to minor amounts of sulphides, to zones of semi-massive sulphide veins with accessory quartz-carbonate gangue. The dominant vein type is a complex quartz-carbonate ± sulphide-hosted breccia vein. Clasts are typically present (Plates 4.3A and C), locally absent, and vary from sharply angular to subrounded but are not spherical. Clasts are wallrock andesite, quartz-carbonate vein material (indicating a re-brecciated vein), blue-grey microcrystalline to cryptocrystalline quartz (chalcedony) and sulphide chips.

<u>Wallrock clasts</u> may be strongly bleached and sericite-, carbonate- and silica-altered. Some fragments are medium to dark green and moderately chloritized. Clasts are massive ash tuff, lapilli tuff and crystal tuff and are interpreted to have formed by plucking or 'spallation' of fractured wallrock. Lack of significant rounding and abrasion in most clasts and lack of superimposed bleaching in some clasts suggest they have not been remobilized great distances within the vein.

Plate 4.3A: Slabbed ore sample from the Province deposit shows clasts of early, banded, sulphide-poor vein rock preserved in more sulphide-rich quartz-carbonate vein material. Scale bar in centimetres.

Plate 4.3B: Crudely symmetric vein growth of coarse-grained quartz and calcite with late infilling of grey chalcedony. DDH 81-58 @ 34 metres depth. Dago Hill deposit. BQ drill core.

Plate 4.3C: Cross-cut through the main orebody of the Big Missouri mine shows ringed wallrock clasts representing classic cockade texture in the quartz-calcite gangue. 2816 Cross-cut.

Plates 4.3D: Dark grey, fine chalcedonic veinlets in moderately bleached and altered andesite lapilli tuff. Sample from DDH 81-58 at 37 metres depth. Dago Hill Deposit. BQ drill core.

Plate 4.3A

Plate 4.3B

Plate 4.3C

Plate 4.3D

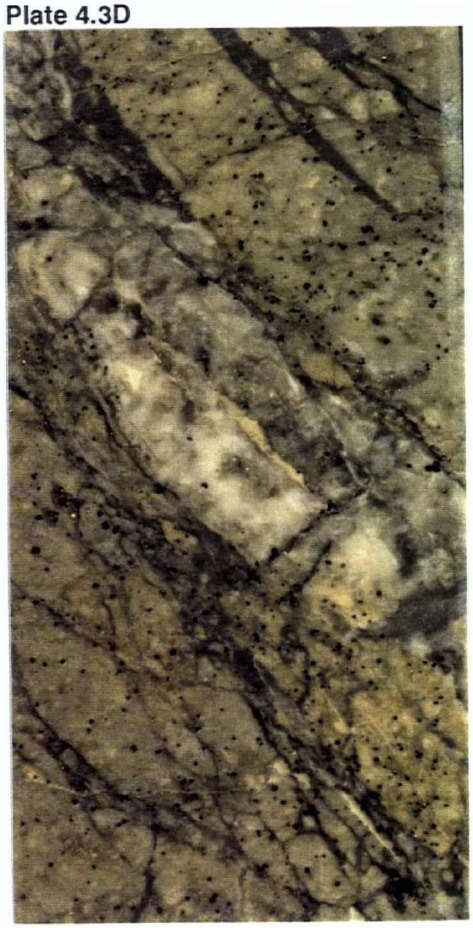

Quartz, carbonate and quartz-carbonate clasts vary from irregular, ragged chips in the Dago Hill veins to smoothly rounded "pebbles" in at least some locations in the Province deposit (Plate 4.3A). These clasts typically host only minor to trace amounts of sulphides and no carbon and may represent early (pre-sulphide) brecciation episodes. Internal textures are medium to coarse grained crystal aggregates although some clasts show coarse comb quartz and others show segments of cockade texture as alternating bands of quartz and carbonate (Plate 4.3A).

Blue-grey microcrystalline quartz clasts are interpreted to be fragments of chalcedony vein material. Blue-grey chalcedonic veins and veinlets are common in outcrop, trenches and drill core adjacent to deposits of the Big Missouri area (Plates 4.3B and D, and 4.6B). Clasts are small (<3 centimetres), sulphide free and subrounded. These same clasts noted by company geologists have been interpreted as "chert" (S. Dykes, personal communication, 1983) or termed "microcrystalline quartz" (Galley, 1981, p.65 and 125).

Sulphide clasts are rare, small angular chips of fine grained pyrite aggregate.

Vein material consists of variably textured quartz and chalcedonic quartz, calcite, sulphide minerals, graphite, sericite and chlorite. Gangue minerals are commonly distinctly laminated (Plates 4.3A and B), with bands of fine to medium to coarse grained crystalline quartz, crystalline calcite and, less commonly, blue-grey microcrystalline quartz, graphite and sulphides. Undulating to arcuately banded or crustified gangue alongside vein walls ("dish structures" of Galley, 1981, p.68-71) drape around original irregularities of the vein walls and/or clasts incorporated in earlier deposited layers. Quartz textures range from cryptocrystalline chalcedonic quartz, through fine to medium grained and locally coarse grained crystalline comb quartz rich in primary fluid inclusions. Quartz of differing textures may grow in adjacent layers. Cockade texture, consisting of distinctive rings of alternating, variably textured quartz-calcite-sulphide layers can completely envelope wallrock clasts (Plate 4.3C).

Documented features such as symmetric growth layers (Plate 4.3B), colloform growth (Plate 4.5A), cockade texture (Plate 4.3C), rebrecciated veins (Plate 4.3A), coarse elongate comb quartz (Plate 4.3B), fluid inclusion trains and drusy cavities are characteristic of vein growth and open space filling in the subvolcanic environment.

Carbon, as amorphous carbon (*see* Boyle, 1979), occurs in the veins as thin seams between adjacent quartz and quartz-carbonate layers. Carbon is fine grained, powdery and charcoal to jet black in colour. Granules range up to 2 millimetres in diameter with lustrous, conchoidally fractured surfaces. Carbon locally comprises up to 15 percent of the vein volume at Dago Hill where recent mining has exposed large blebs and pods up to 15 centimetres across. It also occurs in fine veinlets and small patches and commonly is associated with pyrite. Open cavities containing euhedral, drusy quartz and pyrite may be coated with a film of carbon (Galley, 1981, p.76). The most probable source for this material is the strongly carbonaceous turbidites of the upper siltstone member which stratigraphically underlie this area.

Fine to medium grained semi-massive sulphides are characteristic of the Silver Butte, Province West, Creek and Martha Ellen zones. Sulphides show crude book structure (interlayered sheets of gangue) at centimetre-scale. These zones generally have higher base metal values but lower precious metal values relative to sulphide-poor sections of veins. Pyrite is the most abundant sulphide; other sulphides noted in drill core and hand samples include sphalerite, galena and chalcopyrite.

Altered wallrocks are cut by multiple generations and orientations of variably textured veins and veinlets of chalcedony, crystalline quartz, quartz-calcite and calcite veins. Westmin geologists have documented up to five generations of cross-cutting veinlets at Dago Hill (S. Dykes, personal communication, 1984). All these wallrock veins contain trace to minor sulphides, but late calcite veins host the least sulphides. No obvious asymmetry was noted in the distribution of these complex overprinted vein networks in the structural hangingwall and footwall rocks.

Broad patterns of mineralogical zoning have been documented by Galley (1981) and Dykes *et al.* (1986, 1988). These include abundant galena and carbon at Dago Hill *versus* more abundant sphalerite, calcite and iron carbonate and a general absence of carbon at the Province deposit. Figure 4.6 shows that these deposits may have formed at significantly different paleo-depths and pressure-temperature conditions within the major fractures that transected the Upper Andesite Member.

SAMPLING

Two diamond-drill holes from the Big Missouri area were logged and sampled (Appendix IV). DDH 81-58 from Dago Hill deposit and DDH 82-42 from S-1 deposit both intersected three major subparallel veins and many minor veins and veinlets. Forty-one core intervals were sampled for petrographic and textural studies. Samples were divided at lithological boundaries, at alteration boundaries and at vein boundaries. Sections of whole core were 50 percent sampled, sections of previously split core were 67 percent sampled. From these large sample volumes, pieces displaying both typical and atypical features of the sample interval were selected for slabbing and for microscope study. An additional twelve selective grab samples were collected from trench exposures at several deposits for trace element analysis. Analytical results are listed in Appendix IV and summarized in Table 4.7 (in pocket).

MINERALOGY

Ore petrography in the Big Missouri area has been completed by Galley (1981) and Holbek (1983). Holbeks conclusion from his scanning electron microscope (SEM) study was that mineralogy of deposits in the Big Missouri area was simple and coarse grained enough to be resolved by optical methods alone. For this study ore, gangue and wallrock were examined in 15 polished thin sections, 18 polished sections, 65 thin sections and 98 polished rock slabs from six deposits.

In order of abundance opaque minerals include pyrite, sphalerite, minor to accessory chalcopyrite and galena, trace tennantite and pyrrhotite, and rare electrum (Plate 4.4A), covellite and delafossite (Plate 4.4B and C). Holbek (1983) identified trace amounts of electrum, acanthite, native silver, freibergite and chalcocite. Galley (1981) also reported rare pyrargyrite and polybasite. Mineral paragenesis deduced by Galley (1981) and Holbek (1983) both indicate an overall simple sequence of sulphide precipitation that suggests progressively lower temperatures with time.

Sulphide mineral textures range from disseminated euhedral crystals to irregular crystal aggregates of mixed sulphides. Grains range from micron size up to coarse euhedral pyrite crystals and large sphalerite blebs or aggregates up to 2 centimetres long. Many samples show cracked and shattered grains of pyrite, with remobilization of other sulphides among these fragments, suggesting post-ore deformation by local faulting or regional tectonism. In apparently undeformed samples most sulphide minerals are closely associated with each other suggesting contemporaneous deposition, although there is clearly an early pyrite phase. Galena and chalcopyrite are mostly included within sphalerite but also occur as fine blebs. Chalcopyrite also is distributed as sinuous grains along fractures (Plate 4.4A).

Pyrite forms as disseminations, veinlets and thin bands interlayered with gangue. It is the most abundant mineral in semi-massive sulphide zones and also occurs as veinlets and disseminations in surrounding wallrocks. Disseminated pyrite in wallrocks has strongly striated surfaces and may be of a different generation than vein-hosted pyrite. Most vein-hosted pyrite is earlier than other sulphides which enclose or partially replace it. Holbek (1983) reports minor post-ore pyrite, so that as many as three generations of pyrite may be present in these deposits.

Vein-hosted pyrite occurs as sharply euhedral crystals, sharply angular fragments and "crushed" ragged chips. Some pyrite grains show internal crystalline skeletons suggesting later overgrowths in crystallographic continuity. Local thin arcuate bands of pyrite grains and aggregates conform to thicker crustiform layers of enclosing gangue

Plate 4.4A: Close up of fracture through pyrite grain hosting chalcopyrite, galena and two grains of electrum. Length of photo 0.32 mm.

Plates 4.4B and C: Botryoidal growth, rose-brown colour, moderate pleochroism and strong anisotropy in shades of blue or greenish blue are characteristic of delafossite. Sample 82-42-9A. S-1 deposit. Length of photos 0.64 mm.

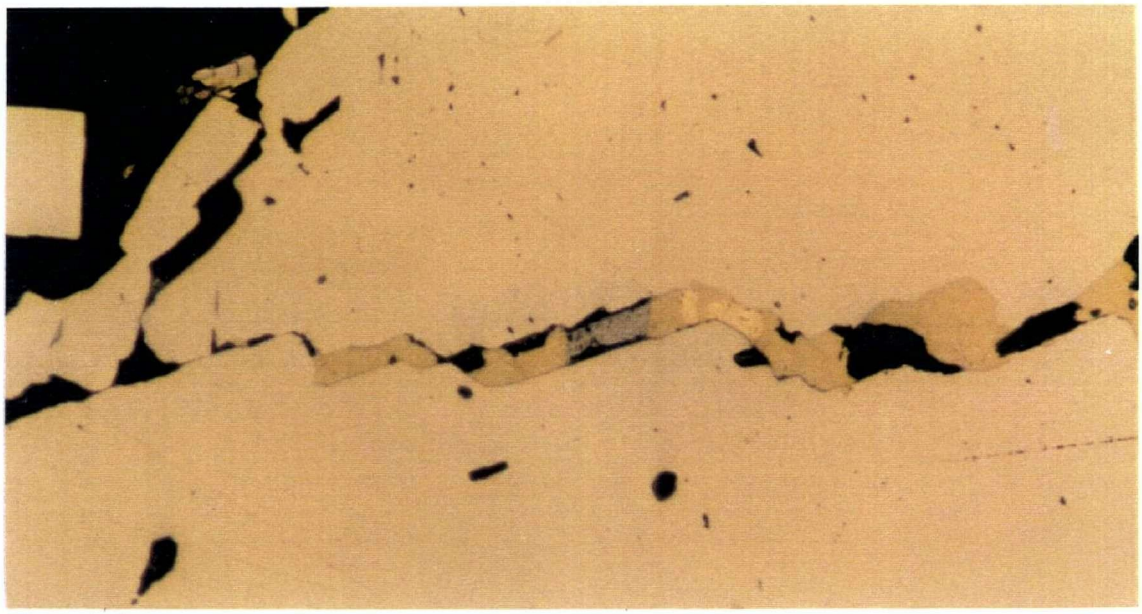

Plate 4.4A

Plate 4.4B

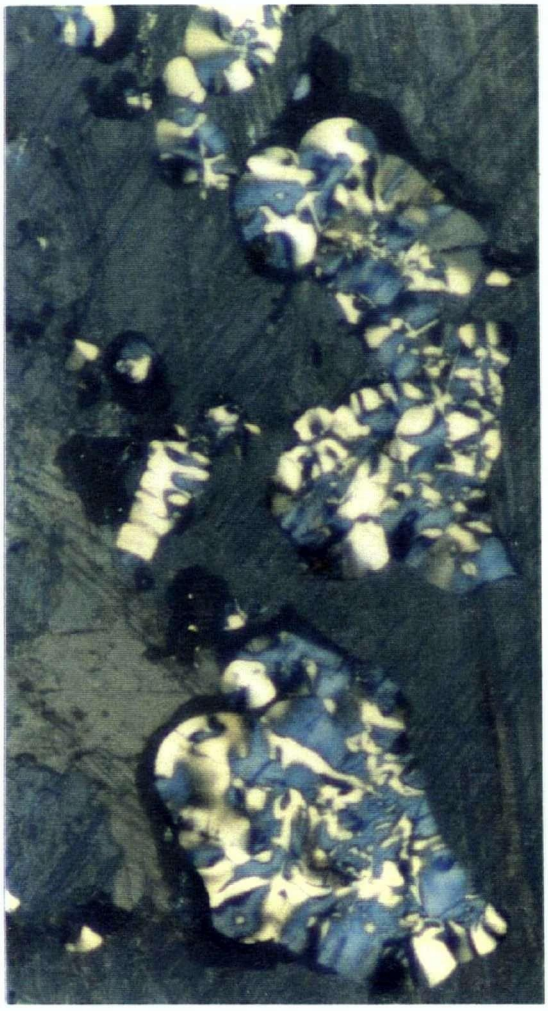

Plate 4.4C

Plate 4.5A: Colloform pyrite growth leaves gangue filled spaces. Sample 82-42-4. S-1 deposit. Length of photo 2.6 mm.

Plate 4.5B: Pyrite encrustations around coarser gangue crystal (quartz). Sample 82-42-2. S-1 deposit. Length of photo 2.6 mm.

Plate 4.5C: Carbon-rich matrix to breccia vein. Note strongly bleached and altered wallrock and fragments. Sample 81-58-10. 15 metres depth. Dago Hill deposit. BQ drill core.

Plate 4.5A

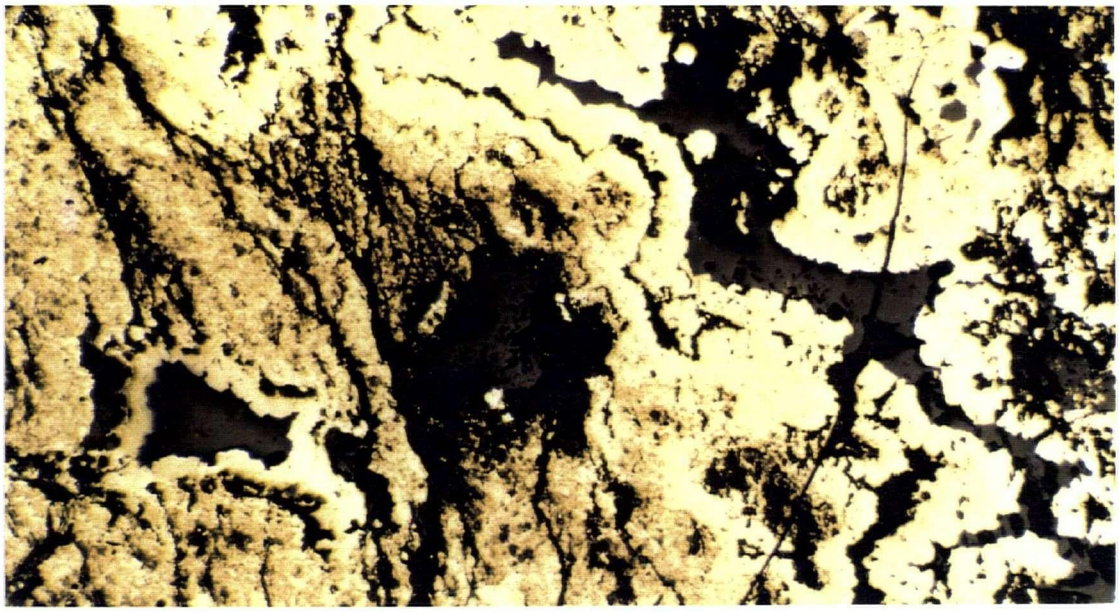

Plate 4.5B

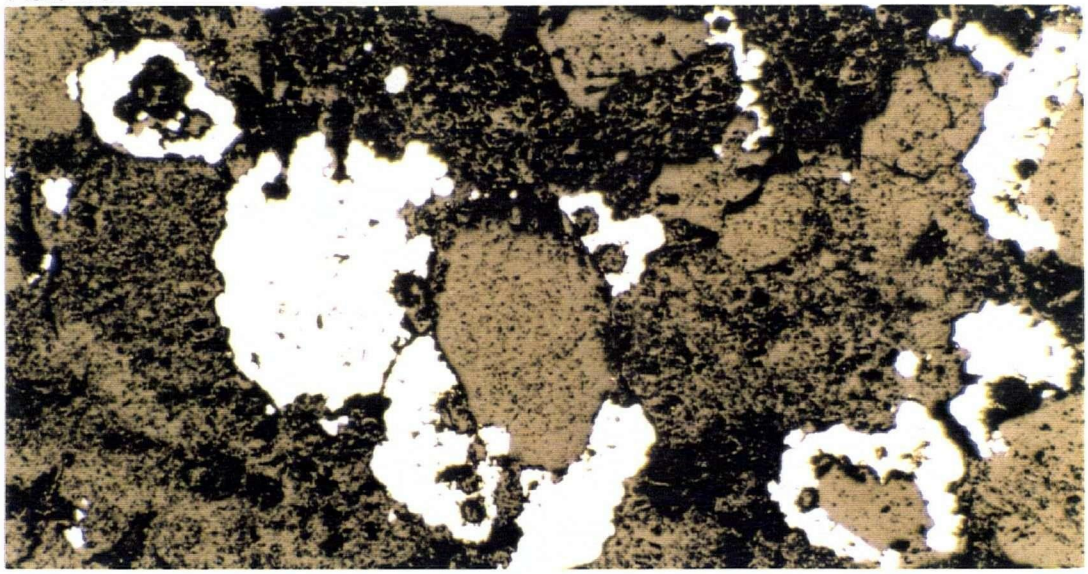

Plate 4.5C

minerals (Plate 4.5B). Some large pyrite grains show internal rings or diffuse bands of encapsulated gangue and sulphide grains suggesting pulses of more rapid growth (Fleet *et al.*, 1990, Barton *et al.*, 1977 and Barton and Bethke, 1987). Tiny internal blebs of pyrrhotite, tennantite and chalcopyrite were noted. Galley (1981) reported large pyrite grains with rounded inclusions of tetrahedrite and native gold up to 70 microns across. Pyrite is commonly cracked with the fractures filled by chalcopyrite, sphalerite and galena.

Sphalerite is present in both low-sulphide and in semi-massive sulphide zones. It is locally more abundant than pyrite; Holbek (1983) reports one grab sample consisting of 50 percent sphalerite. Colour ranges from red to red-brown to purple to black. Typical textures are medium to coarse grained subhedral to anhedral aggregates. Individual grains vary from anhedral to amoeboid shapes that suggest remobilization. Galley (1981) reports sphalerite at the Northstar-Lindeborg prospects that forms rims up to 1 centimetre thick around andesite fragments; these in turn are enveloped by thin crusts of galena suggesting cockade texture of alternating sulphides. The writer has identified atoll sphalerite at microscopic scale in samples from the underground workings that may represent skeletal growth or an early stage of cockade texture development.

Galena is most common as bands of grains within semi-massive sulphides but also occurs in minor amounts in low-sulphide vein sections. Intergrowths with chalcopyrite or sphalerite suggest co-precipitation. Blebs of tetrahedrite-tennantite are scattered through some galena crystals.

Chalcopyrite has been noted in all deposits of the area in minor to accessory amounts. The mineral occurs as intergrowths with other sulphides, as microscopic exsolution blebs in sphalerite and in late fine veinlets, presumably due to remobilization. Secondary copper minerals, chalcocite, covellite and delafossite, are intimately associated with, or entirely replace, chalcopyrite.

Rare pyrrhotite occurs as a few rounded blebs within a large pyrite grain. Holbek (1983) reported pyrrhotite as intergrowths with exsolution chalcopyrite within sphalerite.

Precious metal values are contained in electrum, acanthite, freibergite and native silver and extremely rare pyrargyrite and polybasite. In low-sulphide vein sections silver sulphides and native silver occur as free disseminations in gangue. In semi-massive sulphide vein sections silver sulphides generally form aggregates with galena and chalcopyrite and occur as inclusions in pyrite. Freibergite/tetrahedrite/tennantite occurs as minute blebs within sphalerite, galena and pyrite. Gold occurs only as electrum and has been reported only from the S-1 and Dago Hill zones. It may be useful as a depth-dependent mineral phase (Figure 4.7). Holbek (1983) determined an average gold:silver ratio of 1:1 for electrum grains. Electrum occurs as tiny rounded grains entirely contained within chalcopyrite, sphalerite or pyrite (Plate 4.4A), as coarser elliptical blebs along sulphide grain boundaries or fractures, and as free grains within gangue. Grain size varies from 2 to 70 microns.

Gangue is primarily quartz with lesser carbonate, sericite, oxides and carbon. Textures are characteristic of vein deposits in shallow subvolcanic environments; some represent open-space filling. Holbek (1983) has documented minor barite.

ALTERATION

Andesitic volcanic rocks become progressively more bleached toward each major vein (Plates 3.10A and 4.6A). There was no apparent asymmetry, either in thickness or mineralogy, noted in the alteration zones examined in core. These envelopes of bleached, foliated pyritic rocks initially were mapped as rhyolite during early exploration work. Light coloured rocks are still commonly referred to as "siliceous" or "silicified", but they are dominantly affected by sericite flooding with lesser patchy carbonate alteration. The bleached rock is generally quite soft; powdered material has a moderate to strong reaction to dilute HCl. Immediately adjacent to the quartz-carbonate veins wallrock is dominantly carbonate flooded or silicified.

Several metres from major veins, core samples show weak to moderate chlorite alteration (Plate 3.10A). This propylitic alteration can be overprinted by irregular zones of

Plate 4.6A: Progressive alteration front develops over this 10 cm length of BQ drill core. Alteration obscures the original andesitic lapilli tuff texture. Sample 81-58-19. Dago Hill deposit. Scale bar in centimetres.

Plate 4.6B: A truncated white quartz veinlet indicates that this chalcedony-pyrite veinlet was emplaced along a fracture that is probably a minor fault. Therefore this mineralization followed or was contemporaneous with brittle fracturing and offset. Sample 81-58-22. Dago Hill deposit. Scale bar in centimetres.

Plate 4.6C: The Silbak Premier minesite in September, 1989, with the upper benches of the open pit mine underway. Looking northeast.

Plate 4.6A

Plate 4.6B

Plate 4.6C

fine sericitic alteration. Closer to the main veins the zones of sericitic alteration coalesce and the rock is bleached and moderately to strongly sericitized with ragged patches of remnant chlorite alteration. Similar patches of later carbonate alteration overprint sericite. Closer still to the veins (<2 metres), fine calcite is the most abundant alteration mineral and areas of wholly calcite-flooded rock are common. Adjacent to the veins (<0.5 metre), alteration may be intense sericitization, calcite flooding or silicification, or mottled patchy combinations of all three alteration minerals. Fine to medium grained disseminated pyrite accompanies all alteration types, but is most abundant (up to 15 percent) in strong sericitic alteration.

(Discussion of Ore Genesis begins on page 256.)

4.3.1.3 SILBAK PREMIER MINE

The Silbak Premier mine is located 17 kilometres by road from Hyder and 20 kilometres by road from Stewart. The mine is situated below treeline on the western slope of the Bear River Ridge (Plate 4.6C). Brown (1987, p.8-13) provides a detailed history of ore production at the Silbak Premier mine.

GEOLOGIC SETTING

Four recent geological reports on the property provide references to previous studies dating back to 1919 (Phillips, 1989, Randall, 1988, McDonald, 1988c, and Brown, 1987). An extensive bibliography is also available in MINFILE (104B-054).

Like the Big Missouri area to the north, Silbak Premier mine and several nearby showings are all within the Upper Andesite Member of the Unuk River Formation (Figures 3.2a and 4.16b). The Upper Andesite Member is similar to the detailed descriptions of Section 3.1 except that the basal Black Tuff facies has not been identified in this area. The Main Sequence includes medium to dark green, moderately to strongly foliated andesitic ash tuffs, lapilli tuffs and crystal tuffs hosting abundant plagioclase ± hornblende crystals. Andesite is noticeably darker green and more strongly chloritized than

elsewhere in the region. Local beds of hematitic and chloritic conglomerate with well rounded volcanic cobbles crop out north and northwest of the mine workings between the Glory Hole and the Cooper Creek bridge. Conglomerates are purple, green, and mottled purple and green in colour.

No sedimentary bedding has been noted in the immediate mine area (200 metres radius). Ductile deformation has produced moderately westward-dipping (40 degrees) penetrative foliation and ductile shear zones characterized by spectacularly stretched clasts of angular lapilli and rounded cobbles that have all previously been recorded as evidence of west-dipping bedding in these strata (Langille, 1945). Many bedding measurements shown in the immediate mine area (Brown, 1987, plates 3 and 4) were taken from elongate cobbles that may have been deformed (Brown, personal communication, 1987).

To the west, the Upper Siltstone Member underlies the Upper Andesite Member. The sedimentary unit is offset in this area by major faults and thus provides a useful indication of relative direction and amount of offset that can be used to reconstruct fault-truncated ore zones and guide exploration. From north to south:

- The Upper Siltstone Member crops out west and downslope from the Indian mine workings where it dips moderately eastward (57 degrees) and shows tops to the east.
- Recent exploration work has located an exposure on the hilltop south of Indian Lake and west of the Woodbine prospect. Strata here are vertical; no tops indicators were noted (A. Randall, personal communication, 1988).
- Southeastward, the next area of outcrop is at the junction of Cascade Creek and Salmon River where a large well washed outcrop area of thin bedded siltstones is disrupted by the Boundary Dyke swarm. Dips range from 60 degrees west to vertical; no tops indicators were noted.
- Nearby, Brown (1987, plate 3) located siltstones in Logan Creek just upstream of the Granduc mine road. Beds here dip steeply westward, averaging 80 degrees, but show tops to the east, indicating that strata are overturned.

- Further south, geologists from Esso Minerals Canada documented dips averaging 80 degrees east with tops to the east from outcrops in Cabin, Boundary and Daly creeks.

Therefore the Upper Siltstone Member in the Silbak Premier area shows dips ranging from moderately westward to moderately eastward but dominantly sub-vertical; tops indicators are consistently to the east, so that westward-dipping exposures represent overturned strata.

Overlying the Upper Andesite Member to the east, the Premier Porphyry Member has its three facies exposed in the wooded slopes eastward and uphill from the Silbak Premier Glory Hole. Layering in the lowest massive to laminated tuff dips gently eastward in one outcrop (20 degrees, Plate 3.1A).

Further east and uphill, bedded wackes and siltstones of the Betty Creek Formation dip moderately eastward (30 to 50 degrees). Scour channels indicate tops to the east (Plate 3.3B). Along the crest of the Bear River Ridge, abundant bedding exposures indicate a broad synclinal trough with local minor folds developed in interbedded sediments and tuffs (Figure 3.2a).

In summary, the stratigraphic succession is a vertical to moderately eastward-dipping package lying on the western limb of a north-trending syncline (Figure 4.8). This structural setting fits observed sedimentary bed orientations and tops indicators, and is critically important for resolving the intrusive history of the dykes in the mine and the genesis of the mineral deposits.

Volcanic rocks at the mine are intruded by a variety of dykes and other irregular intrusive bodies. Dykes of Premier Porphyry, a K-feldspar megacrystic plagioclase-amphibole porphyry, are the most abundant intrusive rock and they are spatially associated with most, and possibly all, ore zones. Premier Porphyry dykes are described in Section 3.2.1.3 from their type exposures at the Silbak Premier mine. The dykes show a variety of forms (Figure 4.9) including:

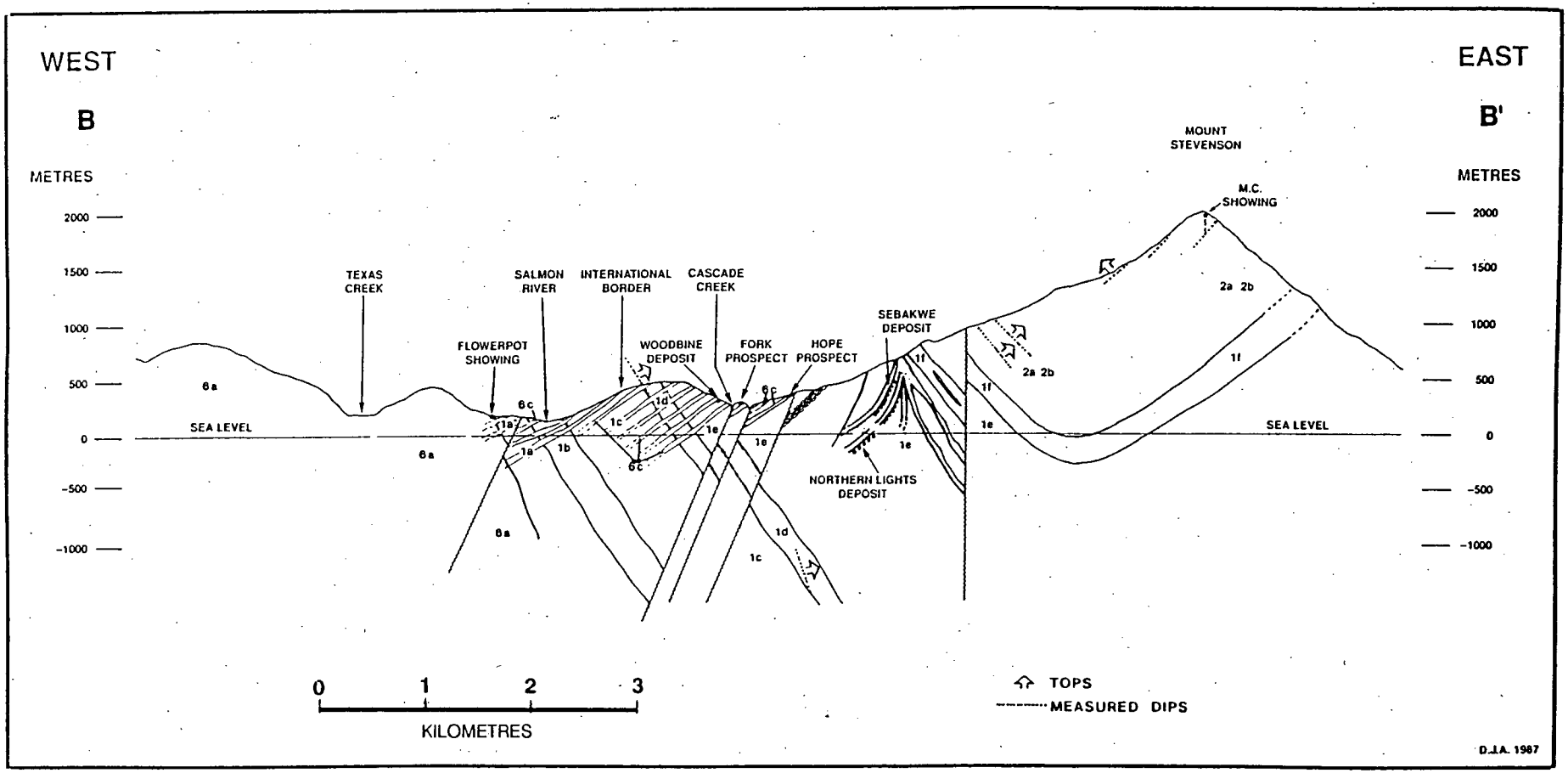

FIGURE 4.8: Geological cross section through the Silbak Premier mine area.
(See **Figure 3.2a** for cross-section location and for Legend)

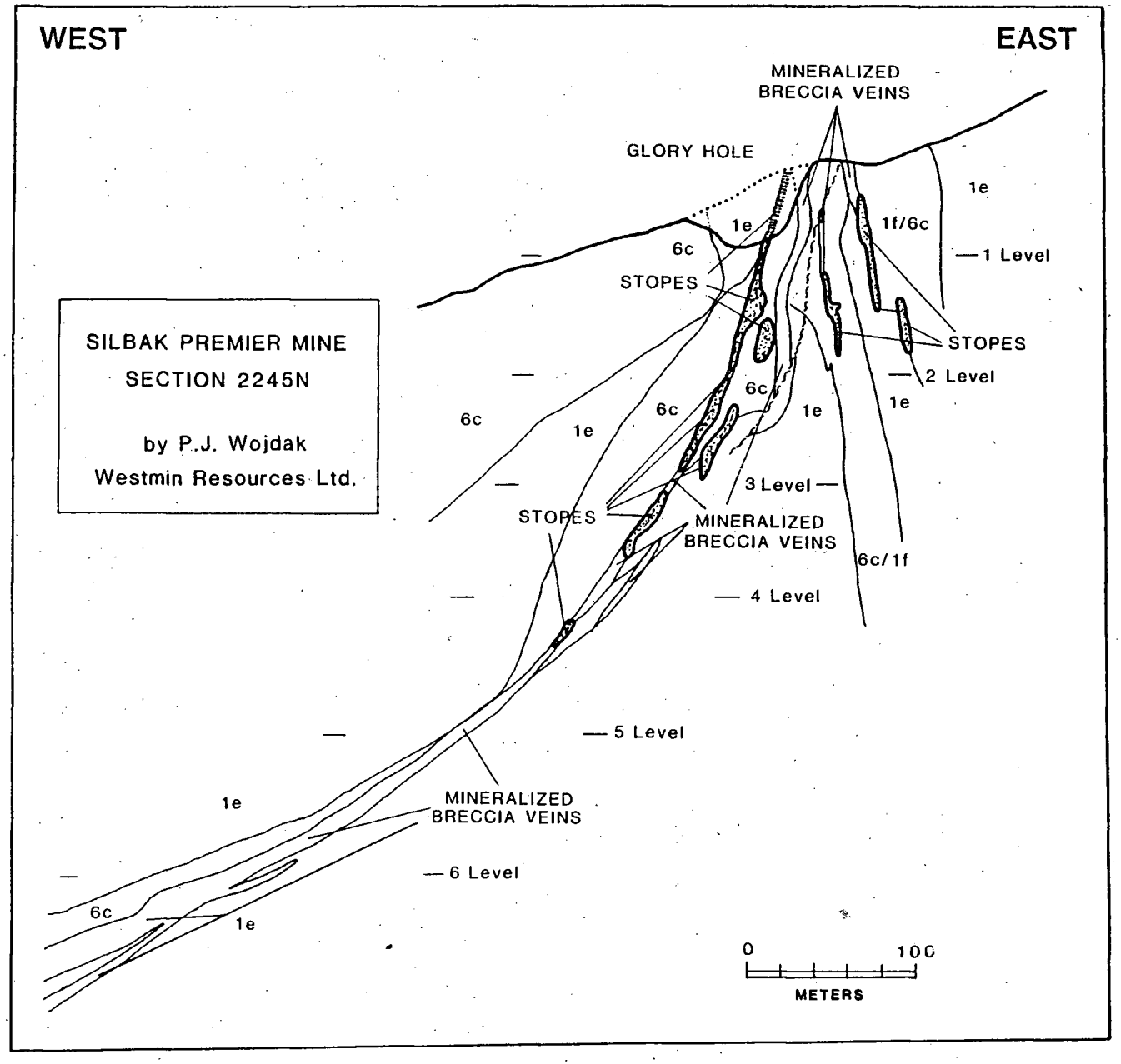

FIGURE 4.9: Geological cross section through the Main Zone, Silbak Premier mine (See **Figure 3.2a** for Legend)

- branching or anastomosing dykes which incorporate screens of country rock or brecciated mineral zones,
- fan-like radiating patterns of a few to several dykes, and
- large-scale curved dykes.

No process or model has accounted for the varying forms and the range of textures of these important intrusive rocks. They are generally regarded as folded and non-folded subvolcanic dykes, sills and possible extrusive flows, without explaining how folded and non-folded examples co-exist within a few hundred metres.

Other intrusive rocks in the mine area are dykes and a small stock of the Hyder Plutonic suite. One major granodiorite porphyry dyke, the 100-metre-wide Main Dyke, cuts through the centre of the Sebakwe underground workings.

Small-scale faulting has been a major problem in underground exploration in the mine area. Many ore shoots are offset, a few tens of metres or less, but relocating the continuing ore shoot can be a major delay and expense. Dykes, altered wallrock and mineralized zones are so abundant that it is difficult to be certain that the same ore shoot has been relocated.

Regional scale faults have important implications for exploration. The location of the Upper Siltstone Member west of the Woodbine prospect indicates that relative normal offset occured along the Slate Mountain fault and Cascade Creek lineament (Figure 4.8). Deposits such as Woodbine, Fork, Power and Hope in the hangingwall block may have been emplaced at a similar stratigraphic level as the West Zone in the footwall block and the mineralized dyke contact in each fault block could be the same structure (Figure 4.10).

The most enigmatic structure in the mine area is a ductile to brittle shear that trends subparallel to the West Zone and deforms ore at many sites including a spectacular exposure at the 2 Level portal. This ductile structure is well exposed in trenches on the south edge of the Glory Hole as bleached, ductily deformed Premier Porphyry (Plate 3.7CII). It is interpreted as a post-ore ductile shear, with later superimposed brittle

fracturing, that developed subparallel to the long linear dyke of Premier Porphyry rock because of the high resistance of the massive dyke rock and relative ductility or instability of the sulphide and breccia zones.

A hematitic, ductile shear zone crops out north of the mine workings and has been intersected in drilling at the Glory hole area (McDonald, 1990a, Figure 2-12-3). The zone shows pronounced stretching of both angular and rounded clasts that have been incorrectly mapped as "bedding" by early workers. Consequently it has been regarded as a stratigraphic marker for decades, *e.g.* Langille's (1945) "purple tuff" and it was a key piece of evidence for west-dipping strata in the mine area. This shear zone It is certainly an important planar marker, but it is not a stratigraphic unit.

MINERAL DEPOSITS

The geologic setting of the mine area was studied by Brown (1987). Company geologists have completely remapped the underground geology, compiled all old drill logs, and relogged all available core to resolve the detailed geometric and structural relationships between dykes, ore zones and alteration (McGuigan and Randall, 1987). Ore mineralogy is the focus of detailed studies by McDonald (1987a, 1987b, 1988a, 1988b, 1988c and 1990). The following description was prepared from the writer's studies and a review of Brown (1987) and McDonald's (1988c) comprehensive reports.

The historic Silbak Premier underground operation produced ore from eighteen separate shoots (Grove, 1971, figure 41), but when open pit mining begins many small, previously subeconomic ore shoots will be recovered. Past production and present published reserves for the Silbak Premier mine are listed on Table 4.10.

Production from two distinct breccia and vein stockwork trends, the Main and West Zones, came from ore shoots distributed along a combined strike length of 1600 metres (Figure 4.10a, in pocket), but roughly 80 percent of that production was recovered within 500 metres of the intersection of these two trends. The intersection area contained the widest ore shoots (up to 20 metres) and those with the highest gold and silver grades.

TABLE 4.10a: Past production in the Silbak Premier area

PROPERTY	MAP NO.	MINFILE NO.	DATE	PAST PRODUCTION (TONNES)	Au gm/T	Ag gm/T	Pb %	Zn %
INDIAN	N76	104B-031	1925,1952	12 870.	3.04	119.7	4.4	5.5
SILBAK PREMIER	N82,87, 88,89	104B-054	1919-1953, 1959-1968	4 292 247.	13.4	297.	2.14	2.84

TABLE 4.10b: Present reserves in the Silbak Premier area

PROPERTY	MAP NO.	MINFILE NO.	RESERVES (TONNES)	Au g/T	Ag g/T
GLORY HOLE	N82,87, 88,89	104B-054	6 500 000(m)	2.16	80.2
4G	"	"	181 760(g)	12.7	48.7
602	N87	104B-053	416 195(g)	6.4	28.5
609	N87	104B-053	321 230(g)	5.8	18.2
POWER	N86	104B-154	33 100(g)	11.2	107.4

[Reserve Categories: (m) = mineable; (g) = geological.]

The new open pit is located in the richest part of the old Premier underground workings where the Main and West Zones intersect (Figure 4.10a). This area also corresponds to a concentration of converging Premier Porphyry dykes (Figures 4.9 and 4.10a). The many small, sub-parallel ore shoots have an aggregate thickness of 20 to 50 metres.

The Main Zone trend of ore deposits strikes 050 degrees and extends 2000 metres northeast from the Glory Hole area. The trend includes the original Premier, B.C. Silver, and Sebakwe ore deposits and the Bush showings. The Main Zone dips about 60 degrees northwest at surface and progressively curves and flattens to a dip of about 30 degrees near 6-Level (Figures 4.9 and 4.10d).

Convergence of the Premier Porphyry dykes from depth toward surface means that continuous ore shoots are localized between Premier Porphyry dyke and andesite country rock at depth, but are emplaced between separate but similar Premier Porphyry dykes near surface (Figure 4.9). Ore shoots at the southwest end of the Main Zone trend were composed of two extensive sub-parallel sheets Langille (1945), but in the Sebakwe workings at the northeast end of the trend, ore zones consisted of many small *en echelon* shoots.

At its southern end the Main Zone is abruptly truncated at the West Zone which trends 290 degrees. The West Zone is vertical to steeply dipping throughout its extent. Mineralization and alteration are localized along the southern contact of a large sub-vertical Premier Porphyry dyke (Figure 4.10a). The West Zone is 350 metres long and occurs as a single 5 to 10 metre thick breccia zone open to depth. The northwestward extension of this trend includes the Hope, Power, Fork and Woodbine prospects over a total strike length of 1500 metres.

Northern Lights is a blind orebody that occurs in the structural hanging wall of the Main and West zones. It displays the same two distinct zone orientations (Figure 4.10a).

VEIN TYPES

Ores of the Silbak Premier mine are hosted in massive breccia veins and in peripheral vein networks or stockworks. Ore was deposited during one part of an extensive history of hydrothermal brecciation and veining that has been divided into three stages (McDonald, 1988c): pre-ore breccias and veins, ore-stage breccias and veins, and post-ore veins.

A. Pre-Ore Breccias and Veins

Pre-ore breccia is confined to andesitic volcanic rocks immediately adjacent to massive unbrecciated Premier Porphyry dykes. Breccia consists of rounded to angular fragments of country rock andesite ranging from 1 to 15 centimetres across. Fragment abundance ranges from 25 to 90 percent (McDonald, 1988c). Breccia matrix is medium to dark green and consists of pyrite, chlorite, sericite, quartz and carbonate. Pre-ore breccia may have been overprinted by later veining and brecciation; large clasts of pre-ore breccia are found within the ore breccias of the 602 ore zone. Quartz-carbonate and quartz-chlorite pre-ore veins cut pre-ore breccia, but are cut in turn by all later vein and breccia types.

B. Ore-Stage Breccias and Veins

Ore-stage veins and breccias contain most of the base metal sulphides and host all the precious metal ore of the mine area. The veins and breccias seem to record an extended, complex period of multiple, superimposed ore-bearing vein and breccia deposition. Veins and minerals show internal structures and textures indicating several pulses of mineral deposition and growth, and veins of later generation are superimposed on these. The ore types are best considered as four styles of mineralization that can be shown as an inter-related matrix (Table 4.11).

Brown (1987) puts the dividing line between low sulphide and high sulphide categories at 15 percent sulphide content; McDonald (1988c) defines low sulphide veins and breccias as those with less than 5 percent sulphides, high sulphide veins and breccias as

TABLE 4.11: Styles of mineralization at the Silbak Premier mine

	1 VEIN STOCKWORKS AND VEINS	2 BRECCIAS
3 LOW SULPHIDE (< 5% sulphide)	5 Precious metal veins Siliceous stockworks Low sulphide veins	6 Precious metal breccias Siliceous breccias Low sulphide breccias
4 HIGH SULPHIDE (> 20% sulphide)	7 Base metal veins Sulphide veins	8 Base metal breccias Sulphide breccias

(Numbers refer to sections in text)

those with 20 to 45 percent sulphides. Vein stockworks are areas of overprinted vein patterns that, together with zoned sulphide grains and layered sulphides, provide evidence for multiple pulses of mineralization. Breccias are areas of even greater dilation than the veins, so that these descriptive categories for veins, vein stockworks, and breccias are gradational. The distinction between low sulphide and high sulphide ore types is more sharply defined than the textural divisions. Even so, large low-sulphide breccia bodies may have local pods of high-sulphide breccia within them.

All styles of mineralization constitute precious metal ores. A vertical zoning pattern is indicated by the general distribution of these ore types (McDonald, 1988c); high-sulphide veins and breccias are more prominent in the lower levels of the deposit and in the West Zone, low-sulphide veins and breccias are more prominent near surface and in the Main Zone.

Breccias and veins are characterized by distinctive gangue textures indicating deposition in a subvolcanic environment, *e.g.* cockade structure, comb-textured quartz, chalcedonic quartz, crustiform banding, and open vugs lined with quartz, pyrite and sphalerite. Fluid inclusion studies indicate ore deposition occurred at an average depth of 600 metres (McDonald, 1990a). These important veins and breccia bodies are described and compared in the following sections, using the same numerical order indicated on the accompanying table (Table 4.11).

1. <u>Vein Stockworks and Veins</u>

Vein stockworks are irregular networks of banded to massive veinlets that vary from 0.5 to 4 centimetres in width (Plate 4.7A). Stockworks are generally peripheral to breccia zones and appear to be lateral, gradational extensions outward from the breccia bodies.

2. <u>Breccias</u>

Breccia bodies are extremely irregular, with subsidiary arms or splays off the main body. Breccia zones range up to 20 metres wide and have been located throughout the

Plate 4.7A: Shattered wallrock with vein network, 6 Level. 602 orebody, Silbak Premier mine. Hammer for scale.

Plate 4.7B: Photomicrograph of superimposed quartz-potassium feldspar veinlets of different ages. These cut altered wallrock tuff. Premier 2 Level trench area. Length of photo 3 mm.

Plate 4.7C: Sulphide cemented breccia of bleached, rounded wallrock clasts exposed in the floor of the Glory Hole, south wall, Silbak Premier mine. Hammer for scale.

Plate 4.7D: Low sulphide breccia shows late, coarsely intergrown calcite-quartz gangue. Clasts are locally ringed by early sequential layers of pyrite and mixed base metals (dark grey). Note single clast of blue-grey chalcedony. 2 Level trench, Silbak Premier mine. Length of photo 10 centimetres.

Plate 4.7A

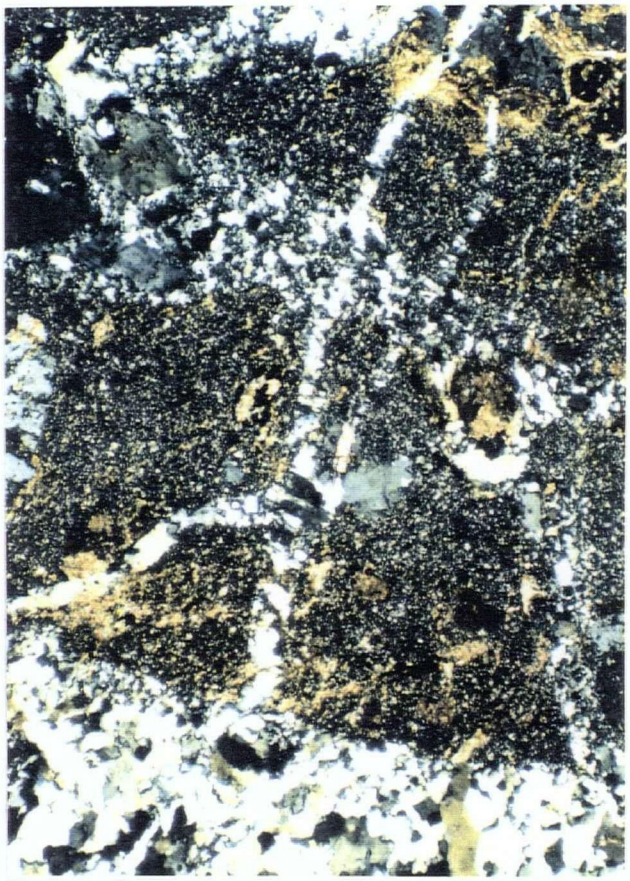

Plate 4.7B

Plate 4.7C

Plate 4.7D

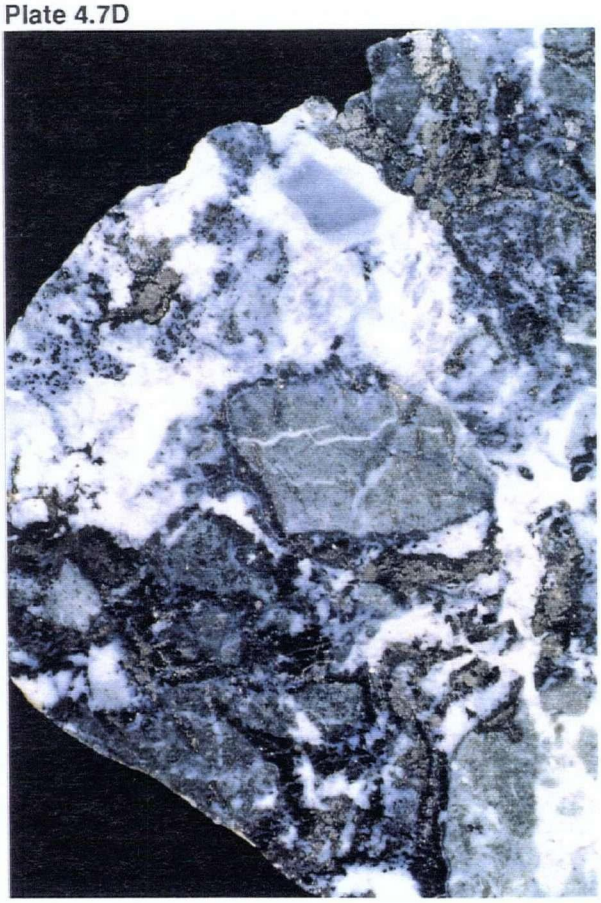

entire extent of Main and West Zones, from surface to the deepest mine workings. Most breccias pass gradually into vein stockwork zones, but some are bounded by faulted margins that display slickensides. Breccia matrix comprises up to 70 percent of the rock and hosts most of the precious metal minerals. Clasts include wallrock and ore fragments. Wallrock clasts are composed of either andesite or Premier Porphyry, but the original lithology of strongly altered clasts can be difficult to determine (Plate 4.7C).

3. Low-Sulphide Veins and Breccias

There is a progression from weakly altered host rock, to strongly altered host rock cut by minor quartz veins, to intensely altered host rock criss-crossed by low-sulphide vein stockworks, to low-sulphide breccias (siliceous breccias) (Figure 4.11).

4. High-Sulphide Veins and Breccias

High-sulphide veins, vein stockworks, and the matrix to breccia can host up to 45 percent pyrite, galena, sphalerite, chalcopyrite, pyrrhotite, tetrahedrite, native silver and electrum (McDonald, 1988c). Quartz, chalcedony, calcite, barite and albite gangue minerals are either randomly intergrown with the sulphides or locally form crude bands (McDonald, 1988c).

5. Low-Sulphide Veins

Low-sulphide veins and stockworks are localized preferentially within Premier Porphyry and along Porphyry-andesite contacts. These veins are more abundant closer to surface and in the Main Zone and generally constitute ore with the highest silver:gold ratios (Randall, 1988). Low-sulphide vein stockworks contain disseminations and patches of pyrite, sphalerite, chalcopyrite, pyrrhotite, tetrahedrite, native silver and electrum in quartz-rich gangue with associated calcite.

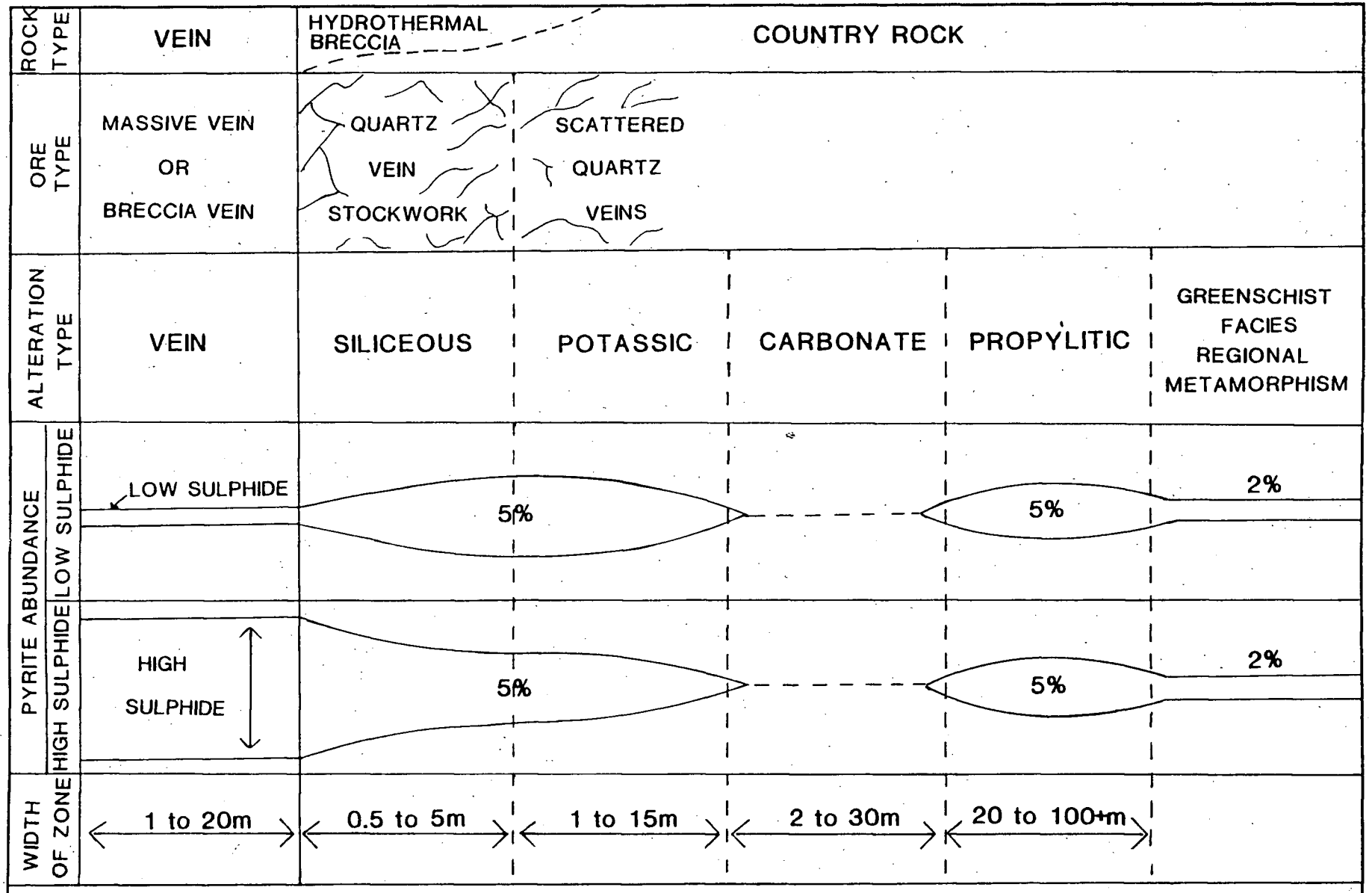

FIGURE 4.11: Distribution of ore structures and alteration zones in the Silbak Premier mine. Note change in scale.

6. Low-Sulphide Breccia

Low sulphide breccia is the most extensive of the four "end-member" ore types and also the highest grade ore. Alternate names are: precious metal breccia, siliceous breccia, bonanza ore, and breccia veins. Total sulphide content is less than 5 percent, composed mainly of pyrite with minor sphalerite and galena. Precious-metal-bearing minerals are polybasite, pyrargyrite, acanthite, tetrahedrite, freibergite, native silver, gold and electrum (Randall, 1988). Gold-silver values are not distributed uniformly within these zones. Higher grade "bonanza" sections consist of local concentrations of silver sulphosalts with electrum and native silver in later fractures (Brown, 1987).

Clasts are predominantly bleached, altered porphyry and andesite with rare chalcedonic clasts (Plate 4.7D). Near the margins of the breccia clasts are sharply angular and more distinct. Near the centre of the breccia, fragments are rounded and less distinct due to intense silicification. Breccia matrix is mainly chalcedonic quartz with patchy sulphide aggregates. Local high-sulphide zones have been discovered within these low-sulphide breccias.

7. High-Sulphide Veins

High sulphide veins and vein-stockworks are restricted to the immediate margins of high sulphide breccias, extending only 2 to 3 metres from the breccia contact. These veins are most common in the lower parts of the deposit and in the West Zone.

8. High-Sulphide Breccias

High-sulphide breccias are the most visually striking ore type (Plate 4.7C) although precious metal content is consistently lower than low-sulphide ores. Sulphides are dominantly pyrite with accessory sphalerite and galena and minor chalcopyrite and pyrrhotite. Base metal sulphides are massive textured, medium to coarse grained, and commonly vuggy. Breccia boundaries may be sharp fault contacts, a gradation into a high-sulphide vein stockwork, or gradational contacts into volcanic wallrock with scattered large

patches of sulphide aggregate grading outward into a disseminated pyritic halo. This ore type is characteristic of West Zone and deeper levels of Main Zone.

A different variety of high-sulphide breccia ore occurs at the 2 Level portal, the Ladder Trench and the Hope prospect. Striking surface exposures show semi-massive to massive polymetallic sulphides that are distinctly layered. Layering is regarded as post-ore, tectonically induced foliation within and adjacent to the major ductile shear that parallels the West Zone.

C. Post-Ore Veins

Post-ore veins are quartz-carbonate and quartz-chlorite *en echelon* sets. These resemble pre-ore veins, so cross-cutting relationships must be noted before classification is possible.

D. Post-Ore Deformation

Evidence for post-ore deformation includes: fractured and dislocated pyrite enveloped by more ductile chalcopyrite, galena and sphalerite; pressure shadows around pyrite in gangue (Plate 3.9A); porphyroblastic growth of coarse grained striated pyrite; and parallel foliation in sulphides and adjacent wall rock along the West Zone.

SAMPLING

Three chip sample sections, totalling 38 samples, were collected at the Silbak Premier mine from ore zones exposed in the 2 Level, 4 Level, and 6 Level (Appendix IV). All samples were from the West Zone due to hazardous access to the Main and Northern Lights Zones. Samples at 2 Level and 4 Level were collected in two-metre intervals to tie in with previous panel sampling by Westmin geologists. Samples from the 6 Level were collected in one-metre intervals. In addition, 21 selective grab samples were collected for trace element analysis from other sites in the mine and from nearby showings. Analytical results are listed in Appendix IV and summarized in Table 4.7 (in pocket).

MINERALOGY

There are significant variations in mineral textures, gangue and sulphide mineralogy, gangue and sulphide abundances, precious metal contents and precious metal ratios both within and among ore zones. Sulphide minerals include pyrite, sphalerite and galena with accessory to minor chalcopyrite and pyrrhotite and rare arsenopyrite. Silver- and gold-bearing minerals include tetrahedrite/freibergite, polybasite, pyrargyrite, acanthite, native silver and electrum (Brown, 1987, and McDonald, 1988c). McDonald (1988c) distinguishes between tetrahedite (0-20 percent contained silver) and freibergite (greater than 20 percent contained silver). Gold occurs mainly as electrum while silver occurs primarily within tetrahedrite, polybasite and freibergite.

Base metal sulphides, tetrahedrite, electrum and native silver occur in both low-sulphide and high-sulphide ores. Polybasite, pyrargyrite, freibergite and acanthite are specific to low-sulphide breccias and veins (McDonald, 1988c) where total metallic mineral content is less than 5 percent. High-sulphide breccias and veins host 20 to 45 percent pyrite, sphalerite, galena, chalcopyrite, pyrrhotite, arsenopyrite, tetrahedrite, native silver and electrum.

Pyrite is the most abundant sulphide mineral; grains range from microscopic dust up to 1 centimetre in diameter. Larger grains may host complex rings of inclusions of other sulphides (Plates 4.8A and B) suggesting a sequence of pulses of more rapid crystal growth (Fleet *et al.*, 1990, Barton *et al.*, 1977 and Barton and Bethke, 1987). Fractured grains are enveloped by more ductile sulphide minerals. Pyrite aggregate typically forms monomineralic layers in book structure or banded veins.

Sphalerite is the next most abundant sulphide mineral with irregular grains ranging up to 8 millimetres across. Microscopic study shows most sphalerite is inclusion-rich with chalcopyrite and rare galena and sulphosalts. Sphalerite is typically brown, but McDonald (1988c) also reports amber, deep red and black varieties. Galena is mostly a minor component but locally composes up to 10 percent of the vein material. Chalcopyrite occurs

Plates 4.8A and B: Concentrically zoned pyrite aggregates record pulses of rapid, inclusion-rich mineral growth interspersed with layers recording slower growth. 2 Level, underground sample 4417/18 from south wall, Silbak Premier mine. Length of photos 0.5 mm.

Plate 4.8C: Progressively bleached and silica/sericite/carbonate altered wallrock 'clasts' are sharply angular where coherent wallrock is cut by a succession of intersecting vein networks. They create a pattern that resembles mosaic breccia. This texture develops adjacent to the main breccia vein. 2 Level trench, Silbak Premier mine.

Plate 4.8D: Rebrecciated vein from Glory hole shows that chloritic wallrock clasts host early disseminated sulphide mineralization. They were then cut by thick, coarse grained quartz-calcite veins, subsequently cut by bright white quartz veinlets, and then rebrecciated and cemented by a base-metal-rich sulphide phase. Compare with Plate 4.18D. Glory Hole, Silbak Premier mine. Scale bar in centimetres.

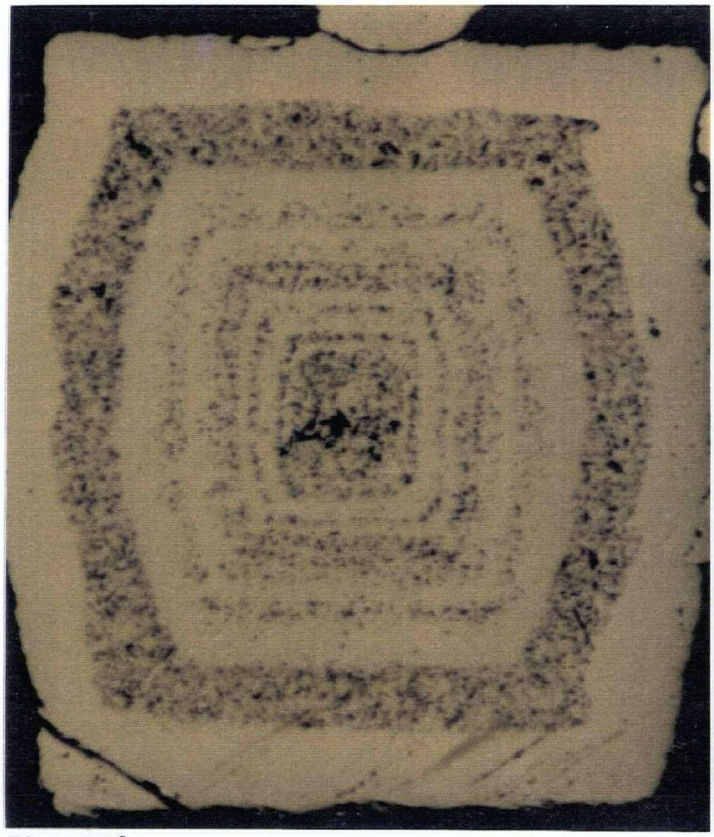

Plate 4.8A

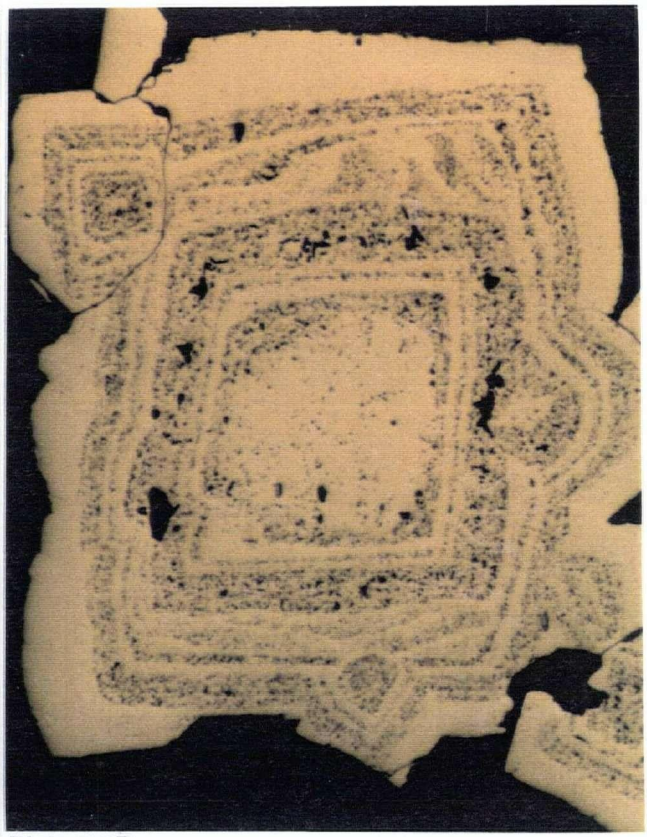

Plate 4.8B

Plate 4.8C

Plate 4.8D

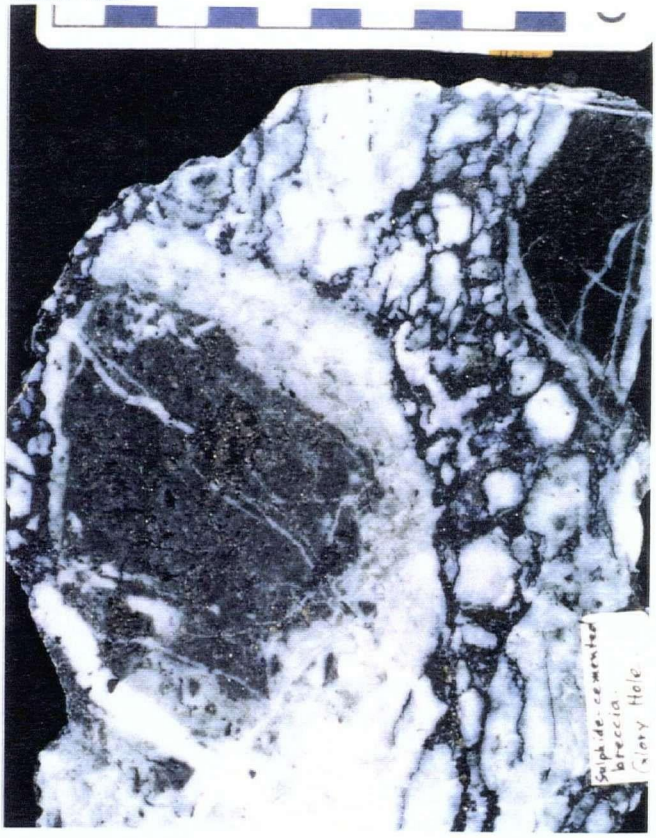

in trace to minor amounts, generally as minute inclusions within sphalerite. Some high-sulphide ore contains as much as 4 percent chalcopyrite McDonald (1988c).

Pyrrhotite can occur in minor amounts in most high-sulphide ores, spatially associated with the more abundant pyrite. High-sulphide breccias exposed in the 6 Level workings contain up to 8 percent pyrrhotite as large intergranular blebs. It may be significant that these zones are among the deepest exposures in the mine.

McDonald (1988c) has identified small (0.1 to 0.3 millimetre) rectangular to subhedral crystals of arsenopyrite in high-sulphide ores. Arsenopyrite has also been reported peripheral to the low-sulphide ore zones (Phillips, 1989).

Tetrahedrite and argentiferous tetrahedrite occur in low-sulphide and high-sulphide ores. The mineral forms irregular grains or occurs as inclusions within galena and sphalerite. Silver content of tetrahedrite increases with elevation and the mineral becomes freibergite above 2 Level McDonald (1988c).

Polybasite occurs only in low-sulphide ores where it is the most abundant silver mineral. It forms both irregular aggregates and minute inclusions in tetrahedrite. Pyrargyrite is a minor component in low-sulphide ores, forming irregular grains that are intergrown with polybasite (McDonald, 1988c). Acanthite occurs in trace amounts, always in contact with galena.

Native silver is present as minute inclusions in pyrite, galena, tetrahedrite and polybasite or as free grains in quartz. It also forms replacement rims around, and fine veins within, grains of polybasite, pyrargyrite and tetrahedite.

Electrum is present in both low-sulphide and high-sulphide ores as irregular blebs within pyrite and galena. The composition of electrum varies within individual grains and throughout the deposit; silver contents range between 44 to 65 weight percent and gold contents range between 35 to 56 weight percent (McDonald, 1988c). Grains are more silver-rich toward the rims.

Gangue minerals include chalcedony and quartz, plus carbonate, potassium feldspar, albite, barite and rare anhydrite.

McDonald (1988c) determined a primary paragenetic sequence for metallic minerals (Figure 4.12). Both low-sulphide and high-sulphide veins and breccias show a paragenetic sequence from sulphides to sulphosalts to native metals. In general, low-sulphide ores are earlier than high-sulphide ores; low-sulphide veins and breccias are cut by high-sulphide veins and breccias.

ALTERATION

A sequence of four distinctive alteration envelopes are developed around Silbak Premier ore zones and are important exploration guides at mine scale. Spatial distribution of these alteration zones is shown in Figure 4.11. Widths of the different alteration zones vary with depth (Brown, 1987). Widths of the silica, sericite and carbonate alteration all increase upwards from depth to surface. These zones may be locally discontinuous in the lower mine levels.

A. <u>SILICEOUS ALTERATION (SILICA)</u>

Wallrock immediately adjacent to breccia orebodies and within vein stockwork type ore zones is silicified (silica-flooded) and hosts accessory disseminated fine grained potassium feldspar, and disseminations and patchy aggregates of mixed sulphides. Feldspar and sulphides together do not exceed 10 to 15 percent of the rock volume. Sulphides may locally have enough precious metal content to constitute ore. Alteration is sufficiently intense that original rock features are obscured in hand sample; but polished slabs or thin sections reveal the volcanic or Premier Porphyry dyke textures. Silica flooding extends only a few metres outward from major silica breccia bodies and may fade out within a vein stockwork zone as the overall vein density decreases outwards (Figure 4.11). However, precious metal mineralization is everywhere bounded by at least a thin envelope of siliceous alteration.

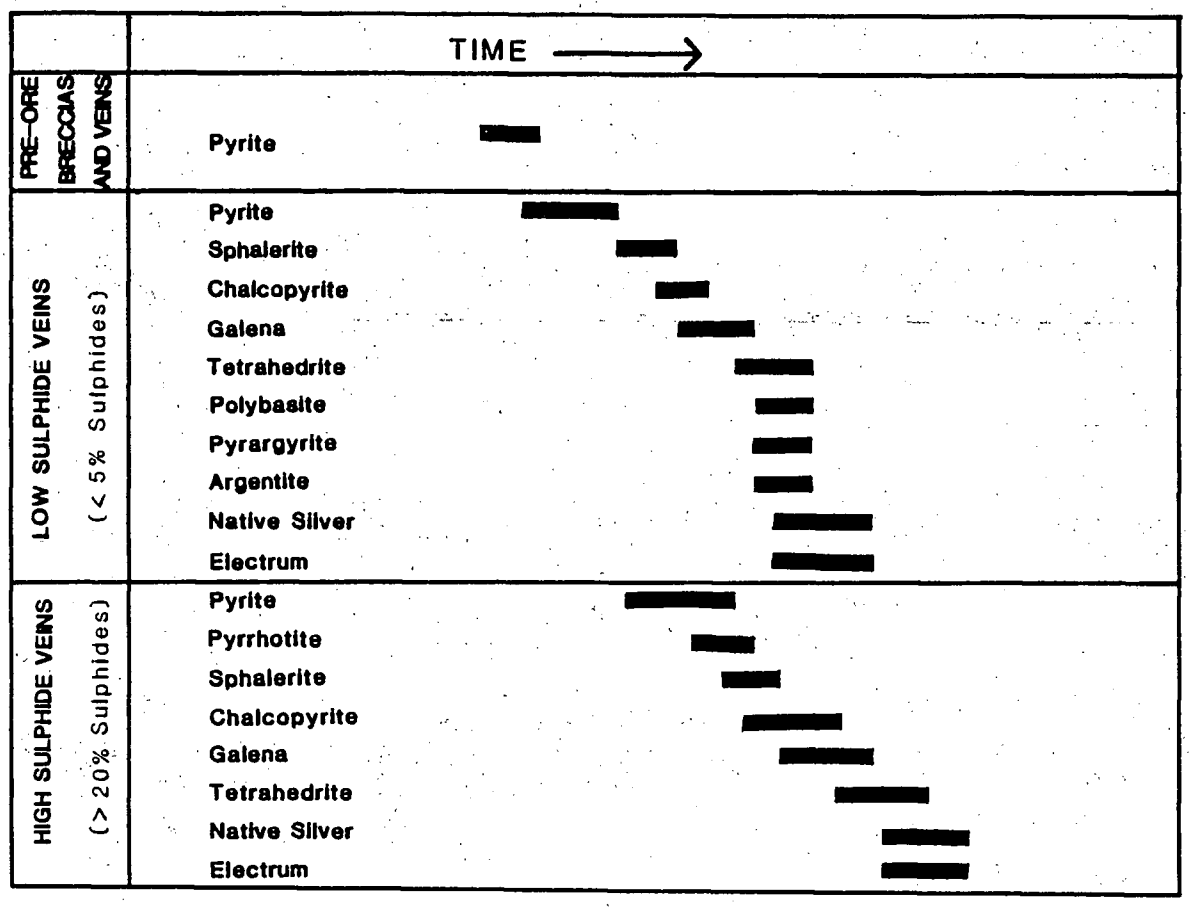

FIGURE 4.12: Paragenetic sequence of opaque minerals at the Silbak Premier mine (from McDonald, 1988a)

B. SERICITIC ALTERATION (POTASSIC)

Intense sericitic alteration with accessory pyrite, silica and minor potassium feldspar characterizes the next alteration envelope outward from the ore. This alteration may develop within the outer part of a vein stockwork ore zone (Figure 4.11). In these areas, margins of individual veins and veinlets may have a silicified wallrock envelope up to one centimetre thick (Plate 4.8C).

C. CARBONATE ALTERATION

Carbonate alteration bleaches still-recognizable country rock lithologies. Altered rock has an overall pale grey or bone colour but original textures, fragments and phenocrysts can still be observed. Pyrite occurs only in trace amounts or is absent in this zone, suggesting selective dissolution and replacement by calcite. This alteration type has been mapped as potassic or even as siliceous alteration in the past, but carbonate-flooded rocks are quite soft and powdered rock reacts strongly to dilute acid. Although the inner boundary seems gradational or patchy, the outer boundary of this alteration zone is marked by a relatively abrupt colour change over as little as a few centimetres or a more gradual change over a metre or less.

D. CHLORITE ALTERATION (PROPYLITIC)

Propylitic alteration consists of pervasive chloritization of wallrock, producing a distinctive deep green colour (Plate 4.8D). Associated with this alteration is up to 5 percent fine to coarse grained euhedral pyrite and minor to trace carbonate, sericite and epidote that are usually only noticeable in thin section. This alteration is distinct from the much less intense regional metamorphic greenschist facies alteration. Differences in alteration should be routinely documented during reconnaissance mapping in the region. Propylitic alteration should be regarded as a distal indicator of ore potential, defining an area worthy of follow-up prospecting or geochemical surveys.

E. DISCUSSION OF ALTERATION

McDonald (1988c) suggested the pyritic envelope or halo around both the low-sulphide and high-sulphide ore types may be independent of spatially associated silica and potassic alteration envelopes. In contrast, the writer has noted slightly varying pyrite textures that seem to be characteristic of each alteration zone (Figure 4.11). In either case, the pyritic envelope could be mapped as an independent alteration phenomenon and regarded as yet another proximal indicator of ore.

Silica alteration hosts very fine to fine grained anhedral to granular disseminated pyrite resembling dust or fine-ground-pepper. Potassic alteration is associated with generally coarser, more abundant (up to 8 to 10 percent), fine to medium grained euhedral disseminated pyrite that is more distinctive and produces a shotgun-pellet or coarse-ground-pepper size pattern. Pyrite is virtually absent from the carbonate altered zone and the propylitic alteration zone hosts fine to coarse grained euhedral disseminated pyrite with smooth faces. Pyrite in the propylitic alteration zone is distinctly coarser and more abundant (5 percent *versus* 2 percent) than pyrite in the regionally metamorphosed greenschist facies country rocks.

The overall alteration mineralogy suggests hydrothermal fluids were consistently rich in H_2O, CO_2, and S and were sequentially enriched in chlorine, carbonate, potassium and silica. The mineralogy, evolving fluid chemistry, and spatial and chronological sequence of these alteration envelopes is consistent with deposition in a subvolcanic, epithermal environment (Heald *et al.*, 1987, and Heims, 1989).

ZONING

As elevation increases, the decline in total amount of sulphide minerals (Brown, 1987) coincides with an increase in silver sulphosalt minerals (McDonald, 1988), an increase in the silver to gold ratio (Hanson, 1935 and Grove, 1971, 1986), and a decrease in fluid inclusion homogenization temperatures (McDonald, 1990a).

Low-sulphide veins and breccias are dominant in the upper levels of the deposit and in the northwest-trending Main Zone. High-sulphide veins and breccias are dominant in the lower part of the deposit and in the west-northwest trending West Zone.

Metallic minerals display strong vertical zonation within the mine. Mineral distribution shows changes from sulphosalt assemblages in the topographic top of the deposit to more base-metal-rich assemblages at the bottom. Below 3 level ore minerals are predominantly pyrite, galena, sphalerite and minor chalcopyrite. Silver-bearing minerals occur mainly between 3 Level and surface (polybasite, pyrargyrite, acanthite, native silver, electrum and tetrahedrite/freibergite). Tetrahedrite, native silver and electrum maintain relatively constant abundances. Tetrahedrite is found throughout the deposit but above 2 Level the content of silver exceeds 20 percent, indicating a change to freibergite. In addition, the greater abundance of silver sulphosalt minerals near the top of the deposit means silver grades and silver:gold ratios increase with elevation (Figure 4.10).

This mineralogical and metal zoning may provide a way-up indicator and correlates well with homogenization temperature isotherms of fluid inclusion which indicate that temperatures decreased upwards within the ore zones from 250°C to 205°C (McDonald, 1990a, figure 2-12-7).

Higher ore grades near surface suggest that secondary or supergene enrichment may have affected the upper levels of the Silbak Premier deposits. This has been considered by Burton (1926), White (1939), Grove (1971, 1986) and Barr (1980). Burton (1926) felt that some supergene enrichment of native silver and polybasite was probable, but White (1939) and all subsequent workers up to McDonald (1990a) concluded that the ores are primary based on their examinations of mineral textures and determination of paragenesis. A review of the geologic history of the deposit supports this latter conclusion. Silbak Premier ores were emplaced at a considerable depth; McDonald (1990a) suggests 600 metres based on fluid inclusion studies. The deposit was covered by many hundreds of metres of volcanic and sedimentary rocks, with no lithostratigraphic evidence of a downcutting Jurassic

erosional episode that could have exposed the uppermost ores to weathering or supergene enrichment. Burial was followed by regional metamorphism. Deformation textures post-date the entire paragenetic sequence of ore minerals, including the paragenetically late polybasite (Mcdonald, 1988). Therefore there was no time in the history of the deposit that it was unroofed--until its very recent exposure by Quaternary glaciation--and there was no period when supergene processes could have generated the paragenetically youngest minerals in these ores.

(Discussion of Ore Genesis begins on page 259.)

4.3.1.4 STRATABOUND PYRITIC DACITE

The stratabound pyritic dacite tuff facies exposed along the western edge of the Mount Dilworth Snowfield has been described in Section 3.1. This unit forms a striking gossan that has attracted attention for decades. No other sulphide minerals have been noted in this area and no significant precious or base metal values have been reported.

As part of this study, samples of the unit were collected for assay at 300 metre intervals between its southern termination and Summit Lake. It was hoped results might indicate an anomalous zone of base or precious metals that would warrant additional sampling and ultimately drill testing of the down dip extension. Base metal and precious metal values from 14 samples were uniformly low; 'peak' values are: <3 ppm Au, <10 ppm Ag, 0.006% Cu, 0.07% Pb and 0.016% Zn. Iron ranged up to 14% and vanadium, thallium, germanium, chromium, barium, beryllium and fluorine were relatively high when compared to other ores and altered rocks of the district (Table 4.7, in pocket).

At the northeast end of Long Lake, an additional exposure of a similar lithology in the same stratigraphic position has been described by Dupas (1985, p.313) and Plumb (1955, p.8). Because Plumb's report is unpublished the relevant section is reproduced here in full:

IRON CAP ZONE

> This name derives from the iron-stained erosion surface of a single gently-dipping basaltic volcanic flow exposed for 3,000 feet along the south side of Joan Creek. It forms the uppermost horizon of the Bear River volcanics and dips at about twenty degrees conformably under the lowest sedimentary beds of the Salmon River Formation. The upper four feet or so is heavily impregnated with fine grained iron pyrite that appears to fill vesicles in the dense, black, fine grained rock. In addition to pyrite this rock contains a little chalcopyrite, galena and sphalerite as well as minute blebs and veinlets of opaque, pale-blue chalcedony. While the gossan is widespread, no economic concentrations of the base or noble metals were found.
>
> Two open cuts had been blasted by the owners near the top and bottom of the zone, and they report low but consistent values in silver, lead and zinc. One sample, No. 326, was channeled by the writer across eight feet in the upper cut (elevation 4,420 feet) and assayed 0.20 ounces in silver with a trace of gold. No other areas worthy of sampling were observed and nothing further was done with this zone.

No base metal sulphides were noted during examination of this pyritic unit at Long Lake, but galena lead isotope data from this stratigraphically controlled "fixed point" with a known biostratigraphic age could be useful for comparison to the established Early Jurassic lead isotope data cluster.

(Discussion of Genesis begins on page 264.)

4.3.2 EOCENE DEPOSITS

Eocene deposits have lead isotope ratios suggesting a Tertiary age; other features of these deposits indicate a more specific Eocene age. Some of these deposits were regarded as Tertiary age prior to this study, others were regarded as Jurassic or Cretaceous deposits, most were not categorized. The Prosperity/Porter Idaho mine was examined in detail.

4.3.2.1. PROSPERITY/PORTER IDAHO MINE

High grade silver-lead-zinc veins of the Prosperity and Porter Idaho mines crop out on the upper slopes of Mount Rainey, 4.5 kilometres southeast of Stewart (Figure 4.1b). Workings are on the south face of the mountain at 1550 metres elevation (Figure 4.13). Reserves are 826,400 tonnes at 668.5 grams silver per tonne with 5 percent combined lead-zinc (Canadian Mines Handbook, 1989, p.355). The Silverado mine is exposed on the north face of the mountain, 2.5 kilometres northwest of the Prosperity/Porter Idaho workings.

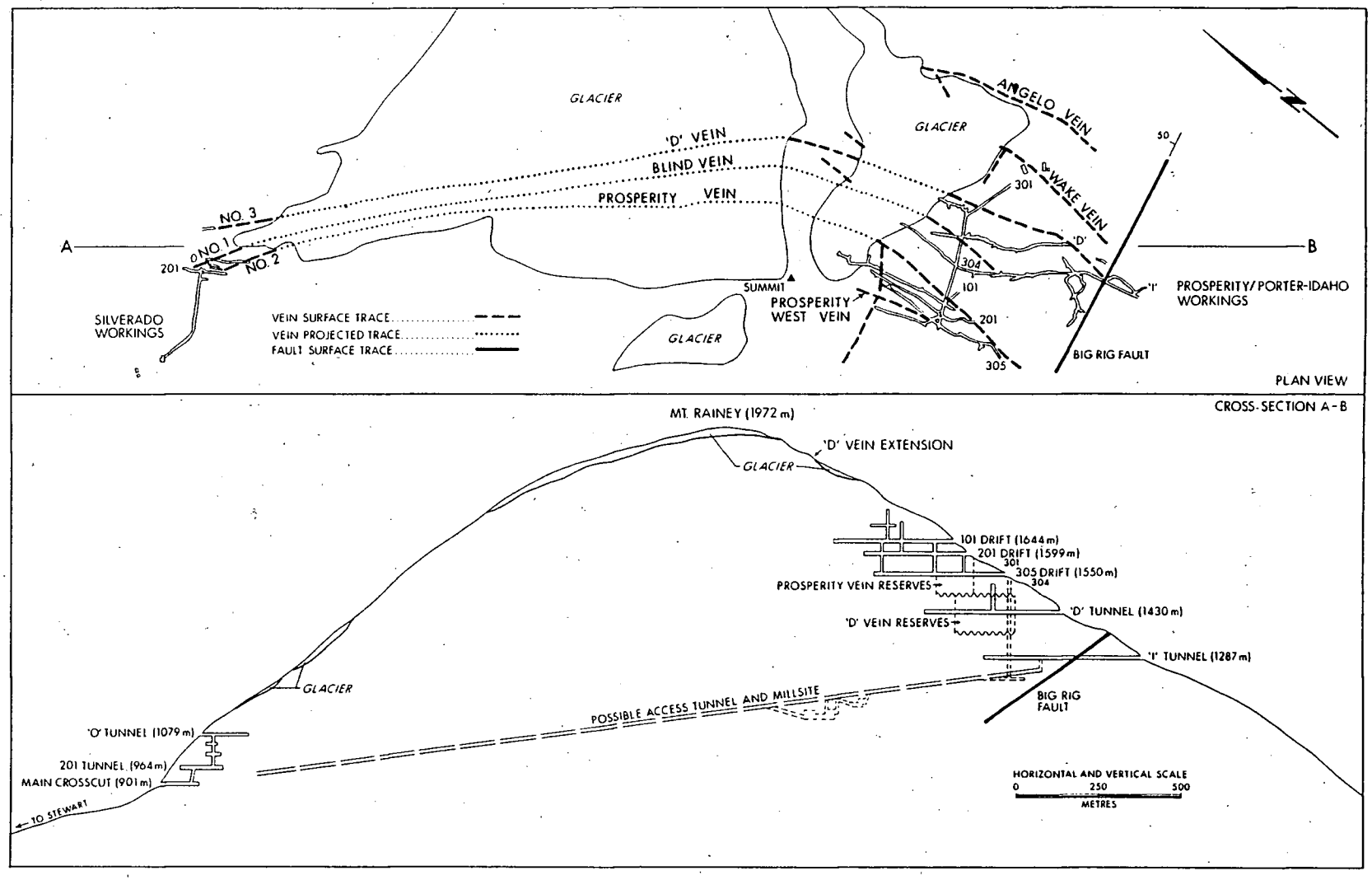

FIGURE 4.13: Distribution of veins at the Prosperity, Porter Idaho and Silverado mines near the summit of Mount Rainey. (From plans of Pacific Cassiar Limited)

[See Figure 3.2a for topographic and geologic setting and latitude/longitude.]

GEOLOGIC SETTING

The geology of these deposits has been described by McDougall (1950), Grove (1971), Kenyon (1983a) and Alldrick and Kenyon (1984); a comprehensive bibliography is available in MINFILE (103P-088). Silver deposits on Mount Rainey occur in an andesitic to dacitic volcanic sequence that is the stratigraphic extension of lithologies hosting precious metal deposits in the Salmon River valley to the north. Lithologies and stratigraphy are similar (Figures 3.1, 4.14 and 4.16).

The Hyder batholith intrudes volcanic rocks on the west and north sides of Mount Rainey (Figure 3.2b). The pluton is medium to coarse grained biotite granodiorite; the core is unaltered but the outer 100 metres of the batholith is cut by a network of widely spaced (50 to 100 centimetres apart) epidote veinlets. Volcanic rocks at the contact are sheared and cut by epidote and chlorite veinlets.

The intruded volcanic section comprises a thick sequence of green andesitic coarse ash tuffs interpreted as the top of the Unuk River Formation (Figure 3.2b). A one hundred-metre-thick section of massive purple epiclastic conglomerate crops out as a prominent knob on the ridge top, 700 metres east of the western intrusive contact and is interpreted as the base of the Betty Creek Formation. The overlying volcanic sequence further eastward (Figure 4.14) is a complex succession of andesitic crystal and lithic tuffs, including lapilli tuffs and medium to coarse tuff breccias, and interbedded dacitic crystal tuffs, lapilli tuffs, welded and thinly bedded tuffs, with local thin epiclastic conglomerate beds, black siltstones and argillaceous limestones. A thick section of massive felsic tuffs and interbedded coarse tuff breccias is exposed on the arête at the head of Barney Glacier to the northeast of the mine workings. The arête continues eastward to the peak of Mount Magee. Beyond the peak, siltstones of the Salmon River Formation have been identified, so the unmapped peak area is the expected location of the stratigraphic extension of the Mount Dilworth Formation and the basal fossiliferous limestone of the Salmon River Formation.

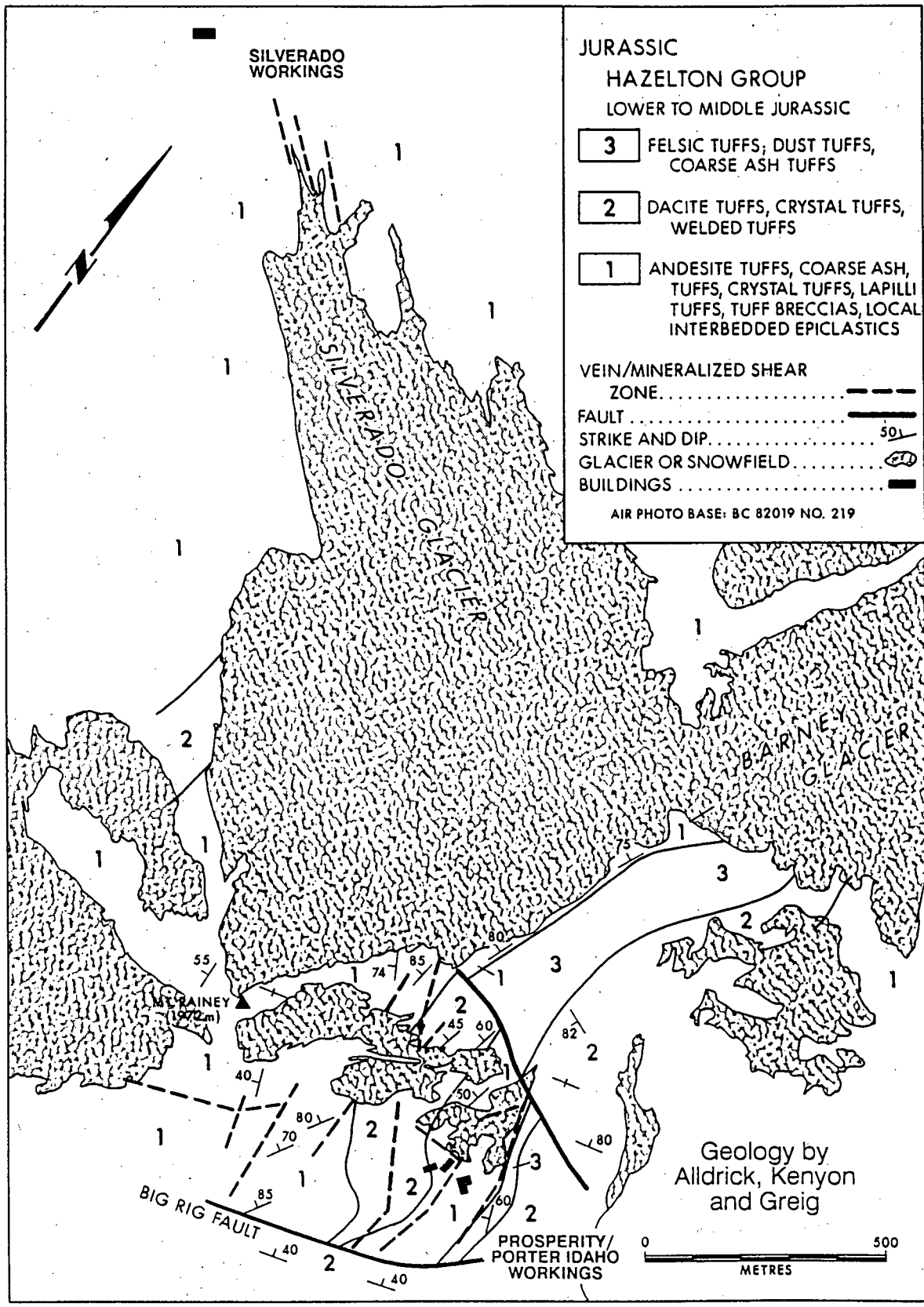

FIGURE 4.14: Geological map of the Mount Rainey summit around the Prosperity, Porter Idaho and Silverado mines.

[See Figure 3.2a for topographic and geologic setting and latitude/longitude.]

The overall strike of volcanic units in the mine area is north-south with dips moderately to steeply westward to vertical, but large variations in the strike have been noted. No tops indicators were found. In order to correlate this package with the stratigraphic sequence established to the north, the stratigraphic sequence in the mine area would have to be overturned to the east (Figure 3.2b).

Host rocks to mineral zones at Prosperity/Porter Idaho are predominantly dacitic volcanic rocks, varying from lapilli and crystal tuffs to welded tuffs with minor units of thinly bedded tuff. In contrast, host rocks at Silverado to the northwest are andesitic lapilli tuffs and coarse tuff breccias. Various felsic and lamprophyre dykes outcrop in and around the Silverado deposits but are less evident in the Prosperity/Porter Idaho workings.

Silver mineralization on Mount Rainey occurs as veins within a set of major sub-parallel brittle fault zones or "shears" (Figures 4.14, 4.15, and 4.16). Six of these shear structures, spaced roughly 175 metres apart, have been located at Prosperity/Porter Idaho while four fault structures are known at Silverado to the northwest. At Prosperity/Porter Idaho the main shear zones trend 165 degrees and dip 60 degrees westward. These zones do not splay and are cut but not offset by lamprophyre dykes in the underground workings. All shear zones continue northward until covered uphill by talus or ice. Southward, the shears terminate at, or are displaced by, a major north-dipping east-west fault zone called the Big Rig fault. At Silverado, the main mineralized shears trend 155 degrees and dip 65 degrees westward and the structures split along horse-tail-like splays.

Offset along shears has not been determined. Slickenside orientations range from horizontal to directly downdip. Since there are no marked lithological changes across the shears--and in one area no lithological change at all, even on a microscopic scale--total offset is thought to be minor, 200 metres or less.

ORE ZONES

The Porter Idaho shear zones are continuous structures up to 13 metres wide hosting discontinuous mineralized lenses or shoots. In unmineralized or weakly mineralized

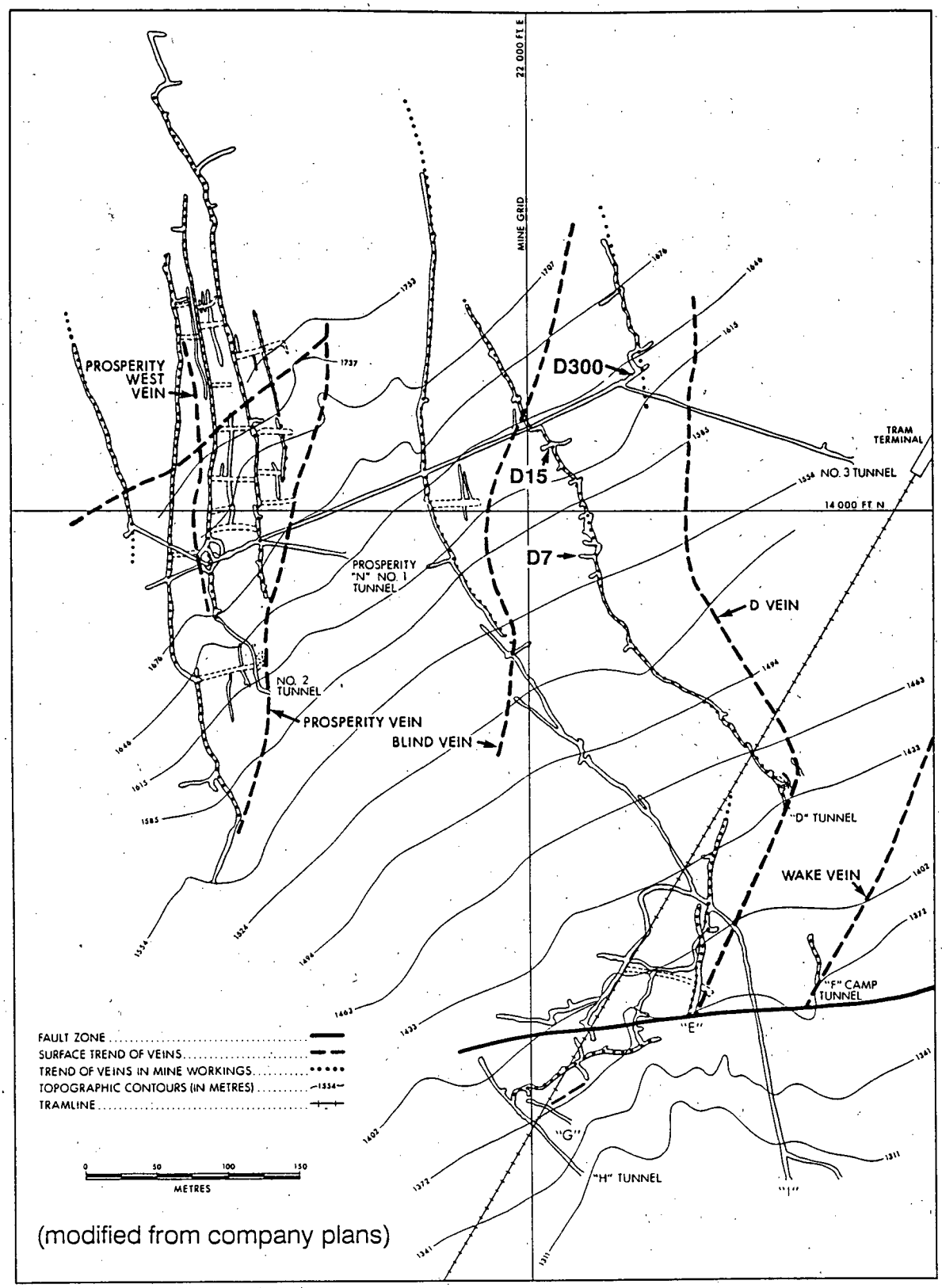

FIGURE 4.15a: Plan of the Prosperity/Porter Idaho mine workings. Plan shows the surface trace of veins, the underground mine workings, the location of the veins within the main mine levels, and the location of the three channel sample sections for this study.

[See Figure 3.2a for topographic and geologic setting and latitude/longitude.]

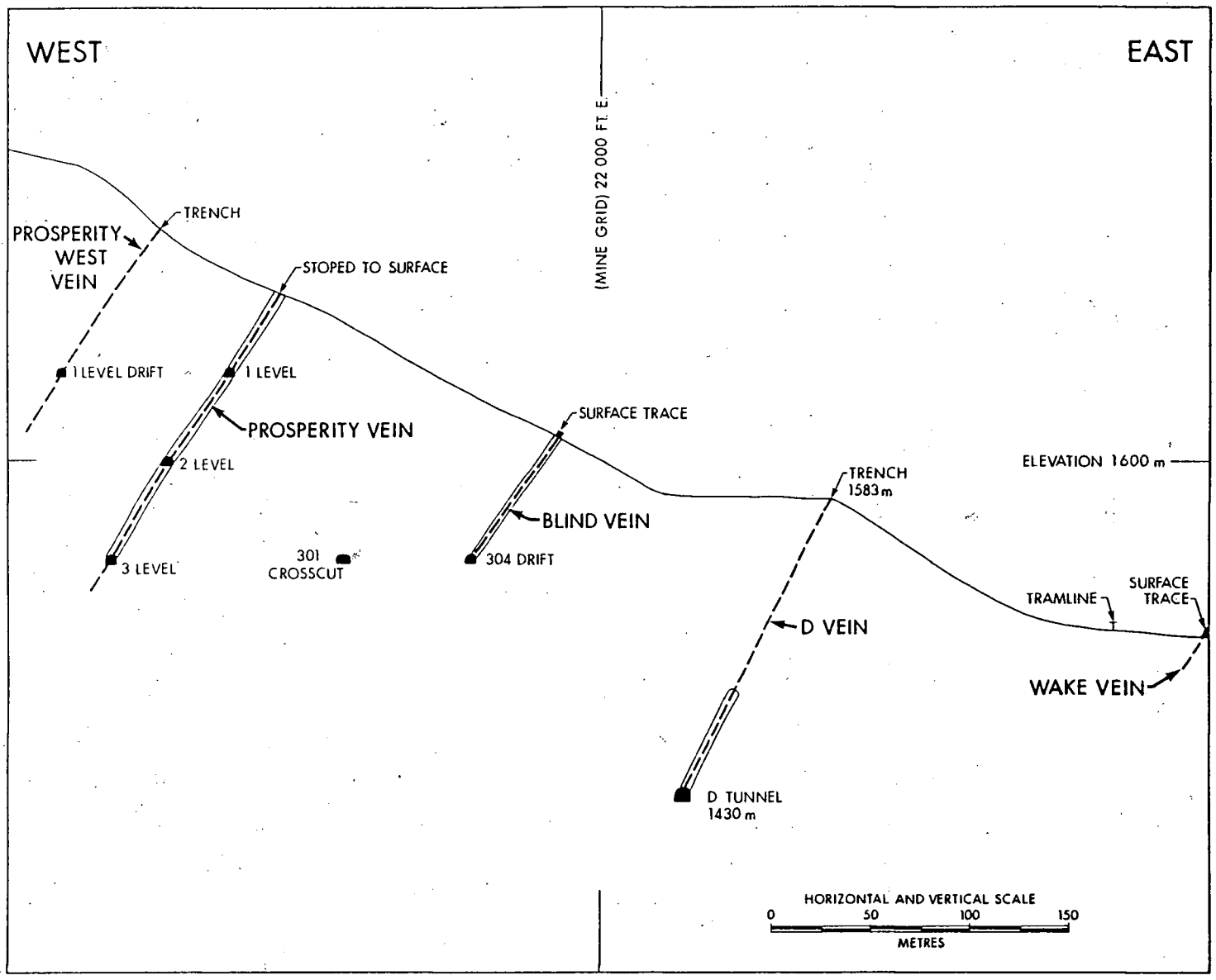

FIGURE 4.15b: Cross-section through the Prosperity/Porter Idaho mine workings, along map section 14,000 N. (See **Figure 4.15a**.)

Plate 4.9A: Prosperity Vein. Polished slab showing weakly mineralized, lithified fault breccia. Fragments are country rock dacite tuff and bull quartz chips. Scale bar in centimetres.

Plates 4.9B and C: Well mineralized breccia from the Blind Vein shows strongly bleached and fractured wallrock clasts. Black mineral is sphalerite; minor galena and pyrite and trace chalcopyrite are also present. Scale bar in centimetres.

Plate 4.9A

Plate 4.9B

Plate 4.9C

areas material within shear structures consists of varying amounts and sizes of intensely sheared wallrock fragments and blocks set in a gouge or clay matrix. Some shear zone sections display silicification, others are carbonate-cemented (Plate 4.9A), still others are soft unlithified gouge. Mineralized zones pinch and swell within shear zones resulting in well-mineralized shoots up to 13 metres wide and 250 metres long. High grade ore shoots extend from surface to a depth of 200 metres where old mine workings end, still in mineralization. There is no mineralization in the country rock between the parallel shears.

The distribution of sulphide mineralization is complex in the high grade sections. Ore lenses consist of one or typically two veins of massive sulphide, each about 60 centimetres wide. Veins are hosted in recemented fault gouge and in screens of sheared, altered, and mineralized country rock. Massive sulphide veins typically follow, or are near, the footwall and hanging wall of the main shear structure. They locally converge and swell to form a single vein up to 2 metres wide anywhere within the shear. These larger veins are composed of argentiferous galena, minor brown to black sphalerite and quartz. Adjacent to the massive sulphide veins, the shear zone is mineralized with disseminations, blebs, and veinlets of quartz, buff-weathering carbonate, black manganese oxide, and sulphides.

Snowfields and glaciers on Mount Rainey have retreated substantially in recent years, exposing extensions of known veins and reinforcing the concept that the shear structures are continuous through the mountain between Prosperity/Porter Idaho and Silverado (Figure 4.13). Discovery of new mineralized outcrops has increased the mineralized strike length to a horizontal distance of 750 metres with a vertical relief of 335 metres. Icefield retreat also exposed other areas on the mountain for prospecting.

On surface, shear zones are recessive weathering and exposures are sparse. A typical outcrop shows a well-sheared zone containing distinctive black and orange coarsely mottled rock. This colour is due to manganese and carbonate alteration. In some outcrops manganese alteration predominates, producing massive to sheared sooty black gossan; in other exposures alteration is predominantly buff-orange weathering carbonate. Sulphide

minerals are partially preserved in some shear zone outcrops, but are leached from others where limonitic boxwork remains. Shear zones exposed by recent glacial retreat show less oxidation of sulphides; galena and sphalerite are exposed at surface and traces of yellowish powdery greenockite have been noted.

SAMPLING

Three continuous chip sections were completed across the D Vein, totalling 23 samples (Appendix IV). Sampling was divided at geological boundaries: wall rock, mineralized and unmineralized fault gouge, and lithified slabs within the fault zone. In addition, four grab samples were collected for trace element analysis. Analytical results are listed in Appendix IV and summarized in Table 4.7 (in pocket).

MINERALOGY

In hand sample massive sulphide veins consist of an aggregate of coarse galena and black sphalerite (Plates 4.9A and B) with accessory pyrite and quartz; wire silver has been noted with the aid of a hand lens. Accessory amounts of tetrahedite/tennantite/freibergite are often suspected in hand sample examination, particularly in high silver samples, but if the trace amounts of these minerals noted in all microscopic studies is typical, then the grains noted in hand sample are more likely sheared or anhedral galena.

Early workers reported a mineral suite of galena, sphalerite, native silver, ruby silver, tetrahedrite, and minor amounts of pyrite, chalcopyrite and acanthite. A petrographic description of a grab sample of massive sulphide vein material adds polybasite, arsenopyrite, and trace electrum to the mineral suite (J. McLeod, written communication, 1982). For this study, ore and gangue mineralogy and textures were examined in 13 polished sections, 68 thin sections and 67 polished rock slabs. Petrography from this study identified galena, sphalerite, pyrite, chalcopyrite, tennantite, tetrahedrite and native silver, adding only ubiquitous trace tennantite to the established list of minerals (Plate 4.10C).

Plate 4.10A: Shatter zone in wallrock dacites is outlined by manganese, and shows the excellent ground preparation conditions that may have preceeded mineralization. Minor chloritic alteration along some fractures appears pale yellow in this photo. Sample D-302. Length of photo 3.0 mm.

Plate 4.10B: Lacy pyritic network along fractures, and small quartz knots in strongly sericitized groundmass. Sample from a block of country rock in the core of the fault zone. Sample D7-4(1). Crossed nicols, length of photo, 3.0 mm.

Plate 4.10C: Native silver cutting coarse galena crystal within sphalerite. Note olive tennantite bleb within the galena. Sample D7-UHS, length of photo 2.6 mm.

Plate 4.10D: Native silver within and adjacent to galena, enveloped by sphalerite with trains of chalcopyrite exsolution blebs. Sample D7-UHS, length of photo 2.6 mm.

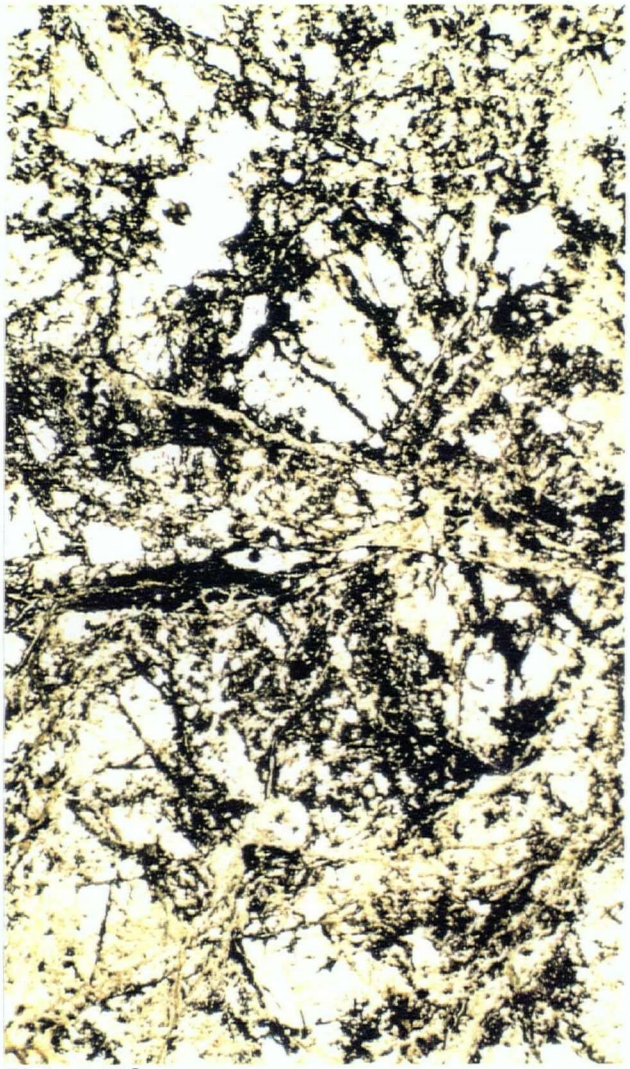

Plate 4.10A

Plate 4.10B

Plate 4.10C

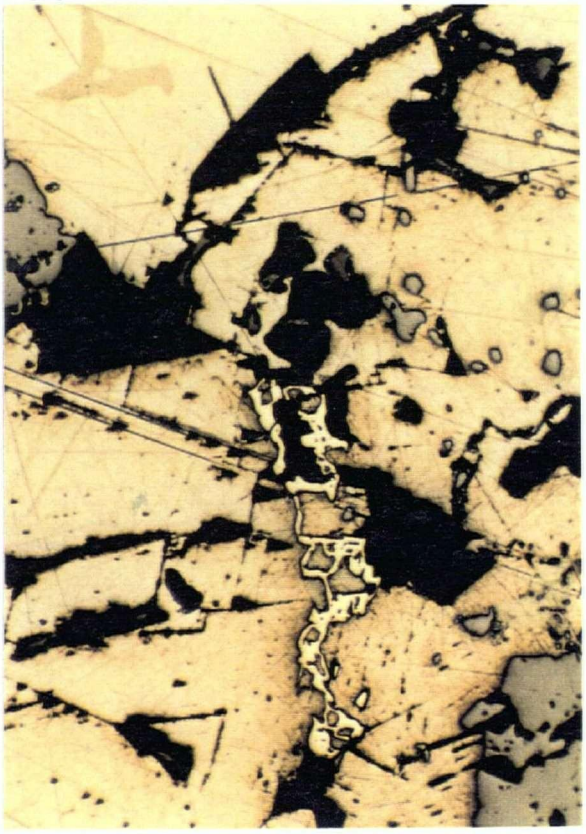

Plate 4.10D

Gangue minerals include early quartz veins, now preserved as angular chips; syn-mineralization sericite flooding with associated knots of fine prismatic quartz crystals and minor chlorite and carbonate; and a later phase of quartz-chlorite-calcite veining that might be resolved into different pulses with additional work. Superimposed on all of these, the final vein phase is an episode of ribbon veins of coarse grained calcite. Overprinted patches of fine carbonate, manganese oxide, and hematitic mud are attributed to recent surface weathering and redeposition from groundwater.

The sequence of ground preparation, veining, mineralization and alteration has been determined from underground mapping and microscopy. This is summarized on Table 4.12. There was only one main pulse of sulphide mineralization; but local areas of physical sulphide remobilization along narrow, reactivated shear planes may account for descriptions of late crosscutting sulphide veins.

ALTERATION

The sequence of alteration is schematically represented on Table 4.12. Shear zones have sharp borders against the country rock. Extensive zones of intense chloritization and local zones of silicification of volcanic host rocks can be seen in hand sample. Both alteration types are accompanied by minor disseminated fine to medium grained pyrite. Thin section study shows that all chloritized rocks are dacitic, although in places they are mapped as andesite. Some 'silicified' wallrock has up to 20 percent pervasive sericite; the rock is not so much silicified as bleached and sericitized.

Drill core shows abundant fine to medium grained disseminated epidote in dacitic wallrocks for a considerable distance away from the shears, but it is replaced or overprinted by chlorite or sericite/silica alteration immediately adjacent to the shears. Epidote weathers from surface exposures and had not been recognized as an alteration mineral at Prosperity/Porter Idaho, although it is conspicuous at Silverado (Plate 3.9C).

(Discussion of Ore Genesis begins on page 264.)

TABLE 4.12: Sequence of ore deposition at the Prosperity/Porter Idaho mine

STAGE	RELATIVE TIMESPAN AND [AGE]	GROUND PREPARATION	SULPHIDES	GANGUE	ALTERATION
V	Long	? Minor reactivation of shears		Surface Weathering: carbonate; manganese oxides; hematitic mud.	Minor carbonate
IV	Long [45-20 Ma]	Minor reactivation of shears; Late cross-faults; Late dykes		coarse banded calcite, coarse quartz, quartz + calcite, quartz + hematite + chlorite, qtz/chlor/qtz + chlor/ qtz + chlor + calcite	Patchy carbonate overprint
III	Short [~45 Ma]		Silver-bearing base metal sulphides	Sericite flooding, minor fine grained quartz knots, ser > > qtz > > chlor + carb	intense sericitic overprint of chlorite, local wall rock silicification
II	Short [~50 Ma]	Major brittle shear (cataclasis)			
I	Moderate [~55 Ma]	Extensional cracks	Disseminated euhedral pyrite	Quartz veins	Chloritized wall rocks

4.4. LOCAL EXPLORATION GUIDELINES

> Genetic concepts may exert an influence on the areas into which exploration is directed, but the geological facts observed are the true basis for directing such exploration.
>
> **J.D. Ridge, 1983**

The exploration applications of objective geological data, without the interpretive 'filter' of genetic models, have been argued by Routhier (1970), Ridge (1983) and Hodgson (1990). This approach is presented here, before continuing with genetic analyses in the following chapter.

Areas favourable for exploration for the four main deposit types are highlighted on Figures 4.16a and b. Local geological settings within these broad zones will be more highly prospective. These are discussed in the following sections which recommend exploration strategies for each deposit type and highlight specific occurrences.

GOLD-PYRRHOTITE DEPOSITS

The perimeter of the Early Jurassic plutons and the inner margin of the pluton should be the exploration focus for deposits similar to the Scottie Gold mine. A zone extending from 100 metres inside the pluton contact to 400 metres beyond the contact should be thoroughly prospected or covered by soil sampling grids. The outer exploration limit can be extended if dykes or alteration distributions suggest a hidden projection of the pluton into the country rock.

Gossans are strong but small. Areas where dozens of veins and veinlets are clustered, such as the Shasta prospect or the banks of the Salmon River downhill from the Lower Daly-Alaska workings, should be carefully mapped. Samples of high-sulphide rock may return erratic gold values, this should not discourage a thorough evaluation.

The four mineral deposits at Scottie Gold mine produce strong, sharp airborne electromagnetic (E.M.) anomalies; the L Zone vein subcrops under a glacier, but still produces a subdued but distinctive E.M. anomaly. Despite the massive pyrrhotite all zones

respond as magnetic lows, attributed to breakdown of magnetite in strong propylitic alteration envelopes proximal to ore zones (Sheldrake, 1983).

SILVER-GOLD-BASE METAL DEPOSITS

Although the entire thickness of the Upper Andesite Member of the Unuk River Formation is prospective for silver-gold-base metal deposits, the strata immediately underlying the Premier Porphyry Member should be specifically targetted. Large pyritic alteration haloes usually provide extensive gossans that are proximal indicators to mineralization. Thorough prospecting will be the single most productive tool, although soil geochemistry can be expected to work well. Geophysical surveys have not been particularly helpful. Low sulphide veins may yield consistently higher precious metal values than the visually more impressive high sulphide veins.

Specific prospects that deserve reassessment are: High Ore, several showings in the Stoner-Clegg-O'Rourke area, Showings on the Silver Coin and Dan claims, the 2 kilometre long belt of gossans between Dago Hill and Union Lake, the Oxedental-49-Yellowstone trend and the nearby Dumas, Lila and Harry showings, and Rainbow.

STRATABOUND PYRITIC DACITES

Although the pyritic dacites in the Mount Dilworth area were subaerially deposited, the Mount Dilworth Formation has both subaerial and submarine depositional settings on a regional scale. In their subaqueous setting, these rocks represent the classic stratigraphic and paleotopographic environment for formation of volcanogenic massive sulphide deposits. At the Eskay Creek property in the Unuk River valley, high-grade massive sulphide ore lenses are hosted in thin-bedded pyritic siltstones, immediately overlying stockwork style mineralization in pyritic dacites at the top of the Mount Dilworth Formation (Alldrick *et al.*, 1989; Britton *et al.*, 1990). Consequently, the Iron Cap zone deserves a thorough re-examination in view of reported minor base metals and anomalous silver values (Plumb, 1955).

LEGEND

PLUTONIC ROCKS

HYDER PLUTONIC SUITE

h - Hyder Batholith
mh - Mineral Hill Stock
b - Boundary Stock

TEXAS CREEK PLUTONIC SUITE

tc - Texas Creek Batholith
sl - Summit Lake Stock

STRATIFIED ROCKS

SALMON RIVER FORMATION

4b - Lower Siltstone Member
4a - Basal Limestone Member

MOUNT DILWORTH FORMATION

3f - Black Tuff Facies
3e - Pyritic Tuff Facies
3d - Upper Lapilli Tuff Member
3c - Middle Welded Tuff Member
3b - Lower Dust Tuff Member

BETTY CREEK FORMATION

2b - Sedimentary Members
2a - Volcanic Members

UNUK RIVER FORMATION

PP - Premier Porphyry Member
1e - Upper Andesite Member
1d - Upper Siltstone Member
1c - Middle Andesite Member
1b - Lower Siltstone Member
1a - Lower Andesite Member

POTENTIAL FOR STRATABOUND PYRITIC DACITE

POTENTIAL FOR SILVER-GOLD-BASE METAL VEINS

POTENTIAL FOR GOLD-PYRRHOTITE VEINS

TEXAS CREEK PLUTONIC SUITE

PREMIER PORPYRY DYKES

PREMIER PORPHYRY MEMBER

VEIN DEPOSIT

TEXAS CREEK SILLS

TEXAS CREEK PORPHYRY PHASE

MF - MILLSITE FAULT

CCF - CASCADE CREEK FAULT

SMF - SLATE MOUNTAIN FAULT

KEY TO MINERAL DEPOSITS

1 EAST GOLD MINE
2 BEND VEIN (PYRRHOTITE)
3 SCOTTIE NORTH PROSPECT (PYRRHOTITE-PYRITE)
4 SCOTTIE GOLD MINE (O, M, N, L ZONES)
5 HICKS' VEINS (PYRRHOTITE)
6 49 PROSPECT
7 MARTHA ELLEN ZONE
8 LION GROUP (SILVER HILL)
9 SILVER CREST
10 SILVER TIP MINE
11 H VEIN
12 VEINS 400 METRES NORTHEAST OF BIG MISSOURI POWERHOUSE
13 VEINS ON WEST SLOPE OF SLATE MOUNTAIN
14 DAGO HILL PROSPECT (SEVERAL VEINS)
15 UNICORN NO. 1 (INCLUDES GOOD HOPE)
16 A VEIN
17 PROVINCE ZONE
18 BIG MISSOURI MINE (S-1 ZONE)
19 CONSOLIDATED SILVER BUTTE PROSPECT
20 TERMINUS PROSPECT
21 MASSIVE PYRRHOTITE VEINS ALONG FLOOR OF SALMON RIVER
22 INDIAN MINE
23 HOPE PROSPECT (GRANDUC ROAD SHOWING)
24 PREMIER EXTENSION
25 WOODBINE
26 LAKESHORE WORKINGS, SOUTH OF MONITOR LAKE
27 BUSH WORKINGS
28 SEBAKWE WORKINGS
29 B.C. SILVER WORKINGS
30 PREMIER WORKINGS
31 PREMIER BORDER WORKINGS
(27–31: SILBAK PREMIER MINE)
32 PICTOU WORKINGS
33 UNNAMED PYRRHOTITE VEIN
34 UNNAMED PYRRHOTITE VEIN
35 SCHAFT CREEK COPPER VEIN (PYRRHOTITE)
36 RIVERSIDE MINE
37 TITAN PROSPECT
38 UNNAMED PYRRHOTITE VEIN
39 ROANAN COPPER VEIN (PYRRHOTITE)
40 VEINS IN SKOOKUM/MOUNTAINVIEW ADIT
41 UPPER BAYVIEW VEINS
42 LOWER BAYVIEW VEINS
43 MOLLY B AND RED REEF VEINS
44 ORAL M VEIN
45 SILVERADO MINE
46 PROSPERITY/PORTER IDAHO MINES

FIGURE 4.16a: Prospective areas for Early Jurassic ore deposit types within the Stewart mining camp

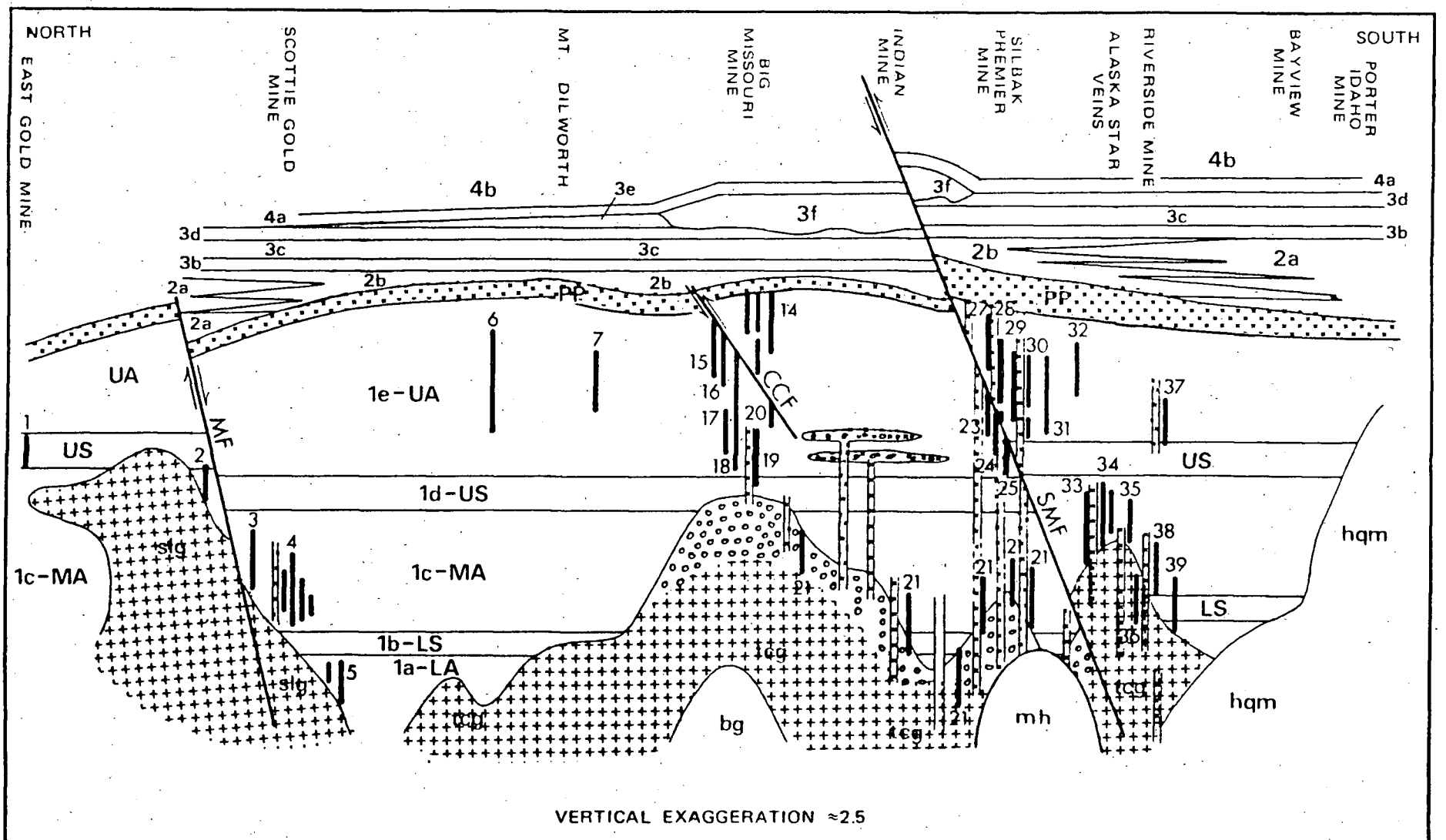

FIGURE 4.16a: Prospective areas for Early Jurassic ore deposit types within the Stewart mining camp

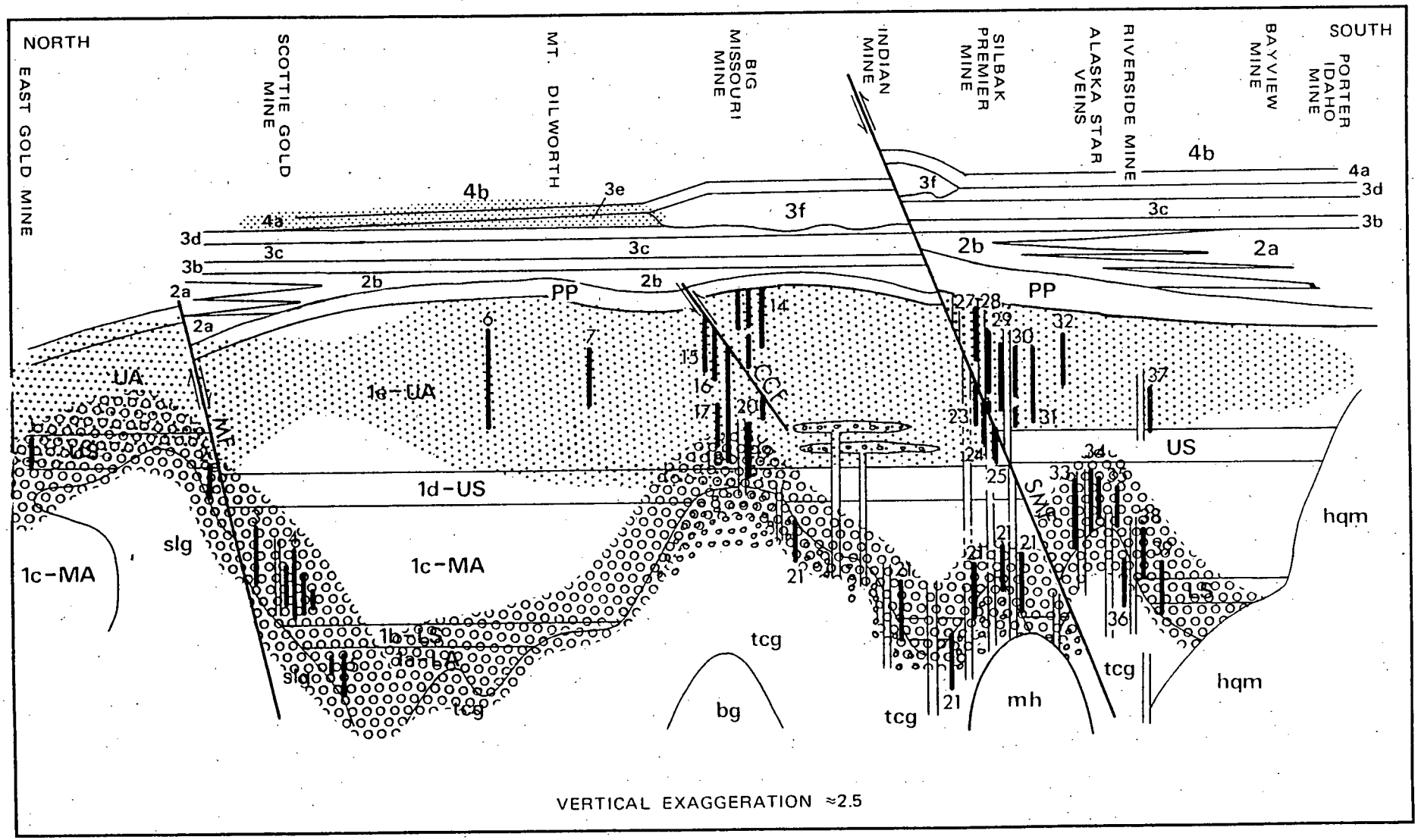

FIGURE 4.16a: Early Jurassic mineral potential overlay

LEGEND

PLUTONIC ROCKS

HYDER PLUTONIC SUITE

h - Hyder Batholith
mh - Mineral Hill Stock
b - Boundary Stock

TEXAS CREEK PLUTONIC SUITE

tc - Texas Creek Batholith
sl - Summit Lake Stock

STRATIFIED ROCKS

SALMON RIVER FORMATION

4b - Lower Siltstone Member
4a - Basal Limestone Member

MOUNT DILWORTH FORMATION

3f - Black Tuff Facies
3e - Pyritic Tuff Facies
3d - Upper Lapilli Tuff Member
3c - Middle Welded Tuff Member
3b - Lower Dust Tuff Member

BETTY CREEK FORMATION

2b - Sedimentary Members
2a - Volcanic Members

UNUK RIVER FORMATION

PP - Premier Porphyry Member
1e - Upper Andesite Member
1d - Upper Siltstone Member
1c - Middle Andesite Member
1b - Lower Siltstone Member
1a - Lower Andesite Member

POTENTIAL FOR SILVER-LEAD-ZINC VEINS

HIGH

HIGH

MODERATE

HYDER PLUTONIC SUITE

HYDER DYKES

VEIN DEPOSIT

TEXAS CREEK SILLS

TEXAS CREEK PORPHYRY PHASE

MF - MILLSITE FAULT

CCF - CASCADE CREEK FAULT

SMF - SLATE MOUNTAIN FAULT

KEY TO MINERAL DEPOSITS

1 EAST GOLD MINE
2 BEND VEIN (PYRRHOTITE)
3 SCOTTIE NORTH PROSPECT (PYRRHOTITE–PYRITE)
4 SCOTTIE GOLD MINE (O, M, N, L ZONES)
5 HICKS' VEINS (PYRRHOTITE)
6 49 PROSPECT
7 MARTHA ELLEN ZONE
8 LION GROUP (SILVER HILL)
9 SILVER CREST
10 SILVER TIP MINE
11 H VEIN
12 VEINS 400 METRES NORTHEAST OF BIG MISSOURI POWERHOUSE
13 VEINS ON WEST SLOPE OF SLATE MOUNTAIN
14 DAGO HILL PROSPECT (SEVERAL VEINS)
15 UNICORN NO. 1 (INCLUDES GOOD HOPE)
16 A VEIN
17 PROVINCE ZONE
18 BIG MISSOURI MINE (S-1 ZONE)
19 CONSOLIDATED SILVER BUTTE PROSPECT
20 TERMINUS PROSPECT
21 MASSIVE PYRRHOTITE VEINS ALONG FLOOR OF SALMON RIVER
22 INDIAN MINE
23 HOPE PROSPECT (GRANDUC ROAD SHOWING)
24 PREMIER EXTENSION
25 WOODBINE
26 LAKESHORE WORKINGS, SOUTH OF MONITOR LAKE
27 BUSH WORKINGS
28 SEBAKWE WORKINGS
29 B.C. SILVER WORKINGS
30 PREMIER WORKINGS
31 PREMIER BORDER WORKINGS
(27–31: SILBAK PREMIER MINE)
32 PICTOU WORKINGS
33 UNNAMED PYRRHOTITE VEIN
34 UNNAMED PYRRHOTITE VEIN
35 SCHAFT CREEK COPPER VEIN (PYRRHOTITE)
36 RIVERSIDE MINE
37 TITAN PROSPECT
38 UNNAMED PYRRHOTITE VEIN
39 ROANAN COPPER VEIN (PYRRHOTITE)
40 VEINS IN SKOOKUM/MOUNTAINVIEW ADIT
41 UPPER BAYVIEW VEINS
42 LOWER BAYVIEW VEINS
43 MOLLY B AND RED REEF VEINS
44 ORAL M VEIN
45 SILVERADO MINE
46 PROSPERITY/PORTER IDAHO MINES

FIGURE 4.16b: Prospective areas for Eocene ore deposit types within the Stewart mining camp

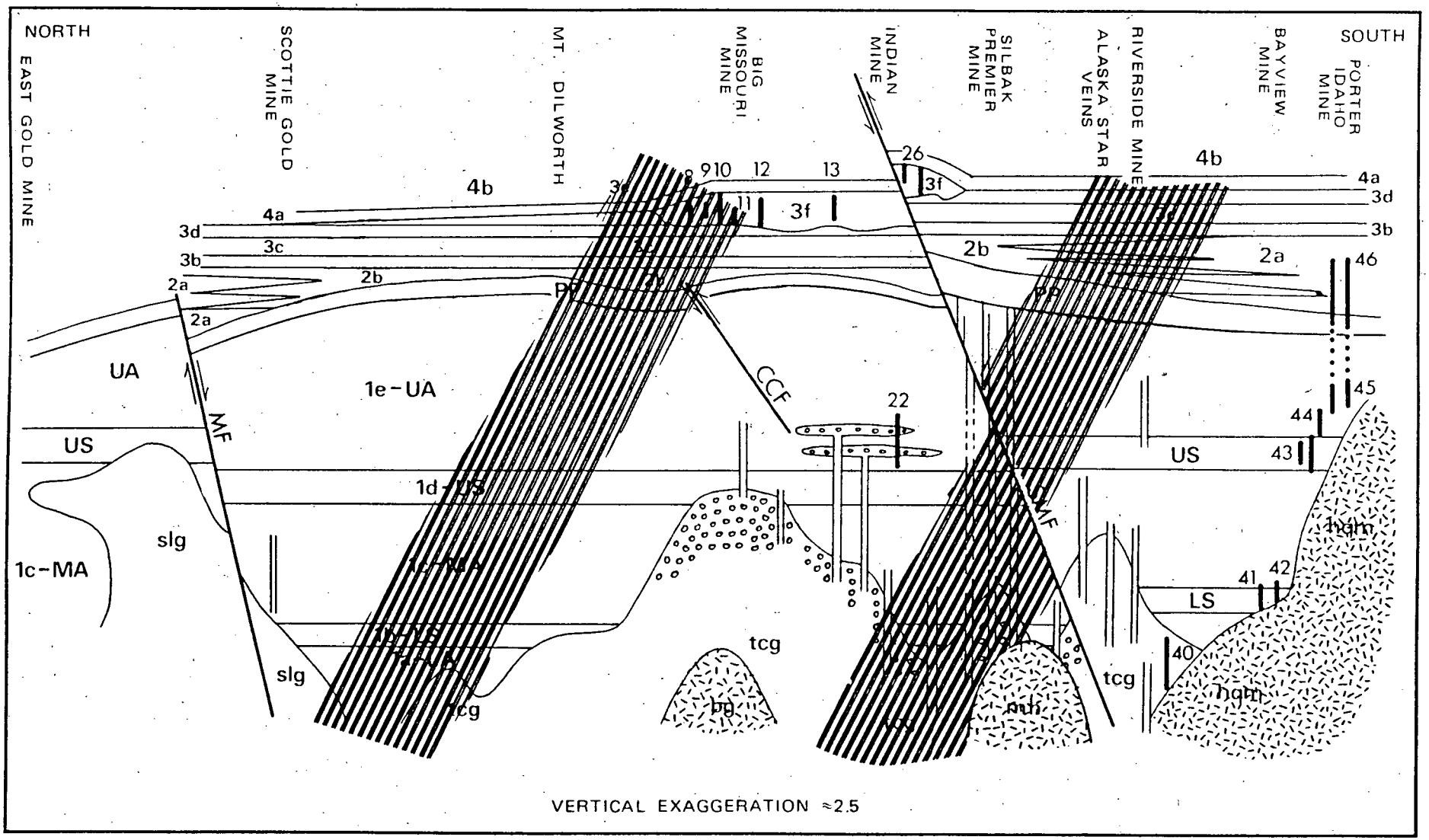

FIGURE 4.16b: Prospective areas for Eocene ore deposit types within the Stewart mining camp

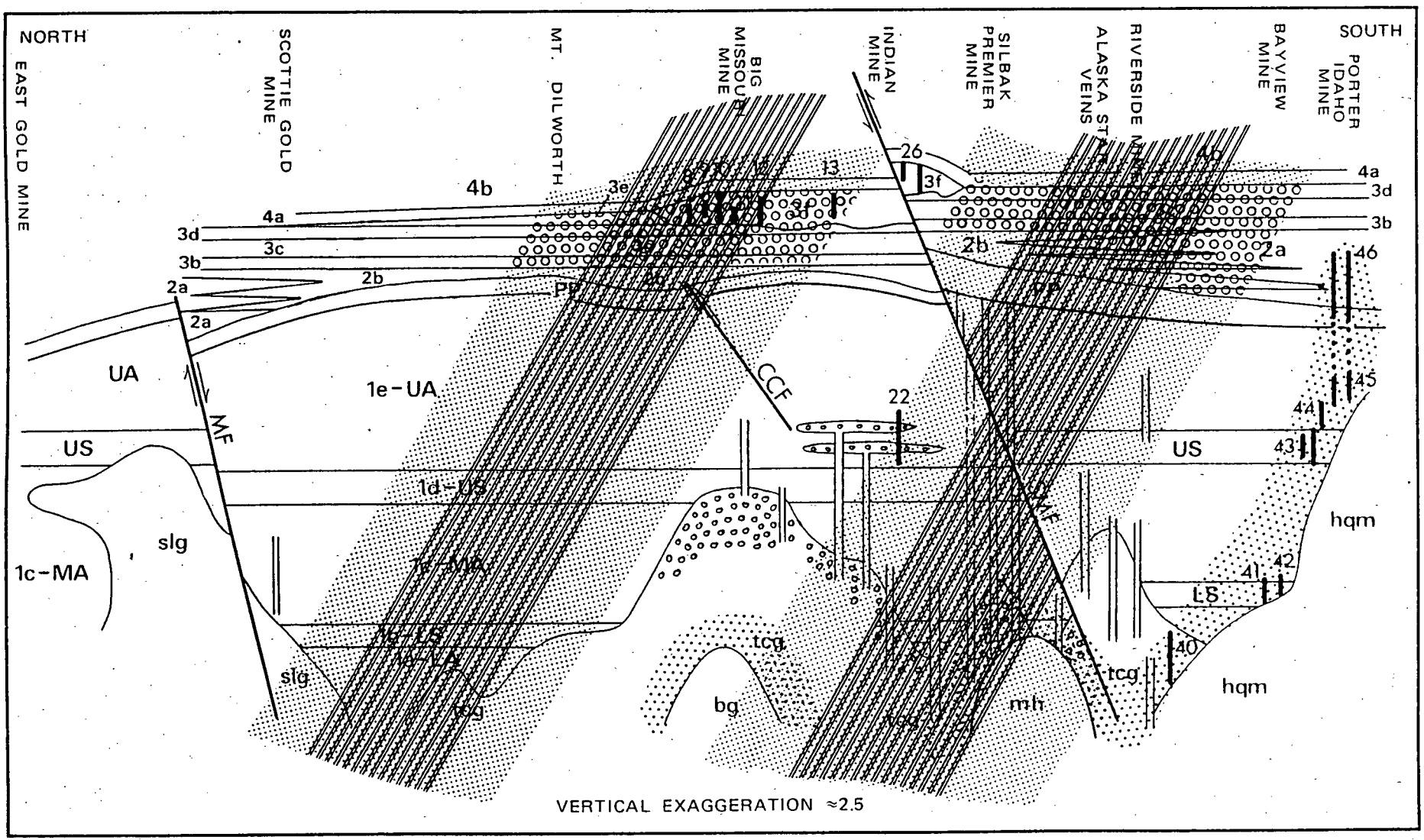

FIGURE 4.16b: Eocene mineral potential overlay

Extensive pyritic intervals recur in this unit regionally: at the toe of Frankmackie Glacier, at the head of D.C. Glacier, at the toe of Knipple Glacier, along the south wall of Knipple Glacier, along the north arm of Treaty Glacier, along the upper canyon of Storie Creek, on the Unuk River near the mouth of Coulter Creek and at the Eskay Creek property east of Tom MacKay Lake (Alldrick *et al.*, 1988; Alldrick *et al.*, 1989). These regionally distributed pyritic zones are favourable sites for subaerial hotspring-related deposits or for submarine volcanogenic massive sulphide deposits, both along the upper dacite contact and in the immediately overlying pyritic sedimentary rocks.

SILVER-LEAD-ZINC DEPOSITS

Prospective settings for these deposits are the perimeters of Eocene plutons and the interiors and perimeters of the Eocene dyke swarms. The greatest potential for these deposits lies along the perimeter of the Hyder batholith, especially where the pluton cuts brittle units (dacites, Texas Creek batholith). The exploration potential in the dyke swarms is also greatest where these dykes cut resistant units (dacites, Texas Creek batholith).

These deposits do not provide strong or large gossans. The mineralized shears are recessive weathering, making them difficult prospecting targets, and they do not generate geophysical anomalies. Peripheral epidote alteration in country rocks is a subtle but important proximal indicator. Late in each summer, a small outcrop area appears within the upper, flat portion of the Silverado Glacier near the summit of Mount Rainey. The rock is wholly epidotized and bright apple green in colour but contains no sulphides.

Once located, southeast-trending mineralized structures are persistant and may host up to four widely separated mineral zones over a distance of a few kilometres. The intersection of these southeast-trending mineralized structures with the few north-trending structures that are known to host mineralization should be specific prospecting targets. Considerable exploration potential lies along the intersection of the Portland Canal dyke swarm with the Mount Dilworth Formation, on the hillslope east and southeast of the Riverside mine, and on Mount Rainey.

CHAPTER 5
ORE GENESIS AND METALLOGENY

5.1. DEPOSIT-SCALE MODELS

5.1.1 EARLY JURASSIC DEPOSITS

Although Early Jurassic deposits are restricted to limited stratigraphic intervals, wide variations in sulphide content, mineralogy and textures, gangue content and textures, alteration mineralogy, ore grades, and metal ratios are displayed not only between deposits but within individual ore zones (Table 4.7, in pocket, and Section 4.3).

Early Jurassic deposits pre-date deformation and metamorphism. Determination of ore genesis is complex because effects of mid-Cretaceous metamorphism must be understood and 'removed' to illustrate conceptual genetic models.

5.1.1.1 GOLD-PYRRHOTITE DEPOSITS

SCOTTIE GOLD MINE

En echelon distribution of the Scottie Gold ore zones is evident in both plan and section (Figure 4.4). Ore veins at the mine are hosted in complex, subparallel shear or fracture zones. They have been called shear veins, cymoid veins and loops, sigmoidal veins, extension veins, tension gashes, and ladder veins. The zones have undergone post-ore ductile and brittle shearing that complicates structural studies.

Outcrop patterns and underground geometry of ore zones suggest the Sixties veins are a series of *en echelon* tension gash veins. However, the massive, planar "Main Veins" indicate a more complex process involving shearing (Figure 5.1). The reader is particularly referred to Hancock (1972) for a concise review of these contrasting structures and to Beach (1975, 1977, 1980), Durney and Ramsay (1973), Kerrich and Allison (1978), McClay (1987, p.98-111), Roering (1968), Naylor *et al.* (1986) and Hodgson (1989) for more detailed discussions on vein formation and vein geometries.

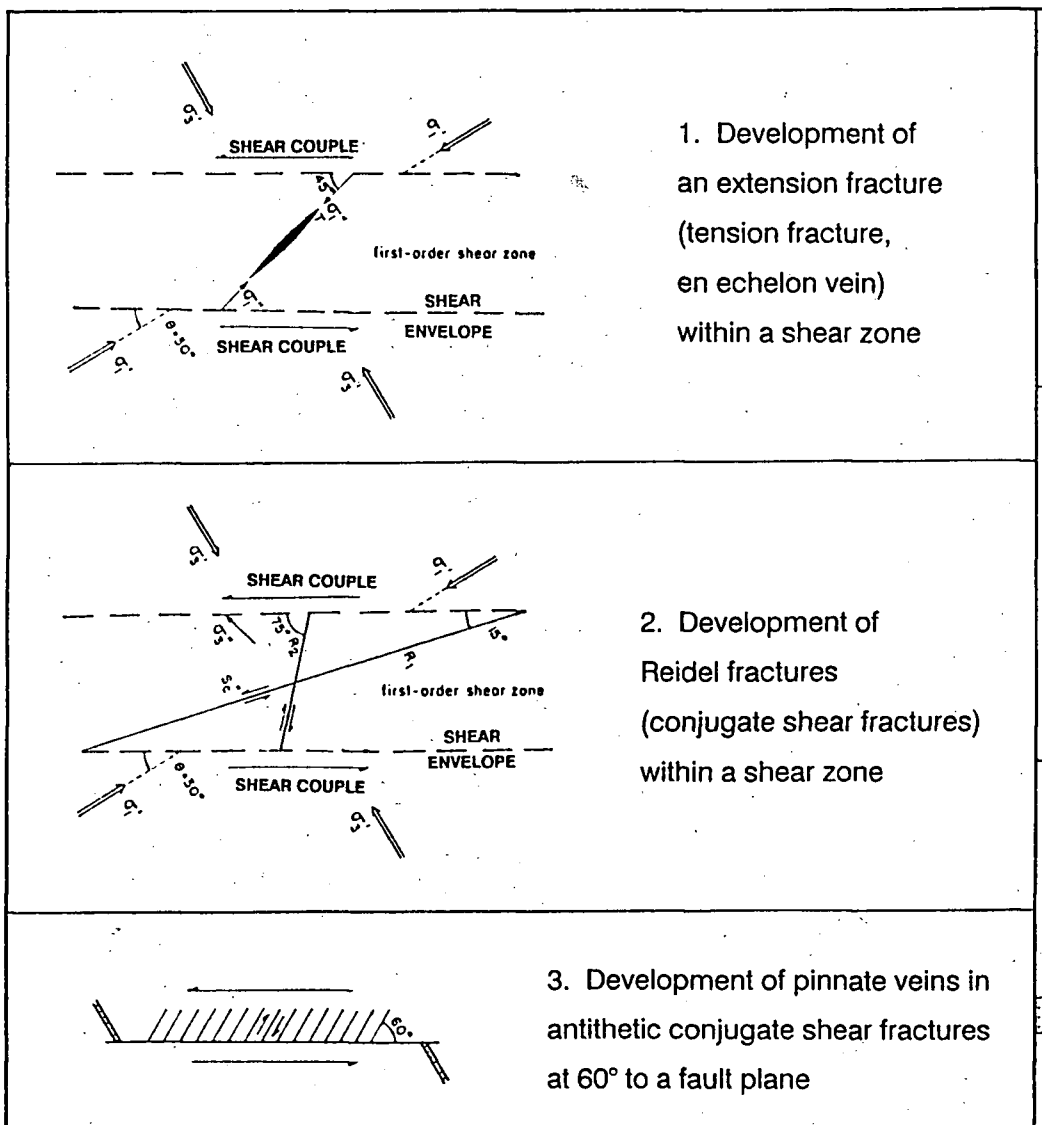

Figure 5.1a: Possible fracturing mechanisms (from Hancock, 1972; Hodgson, 1989)

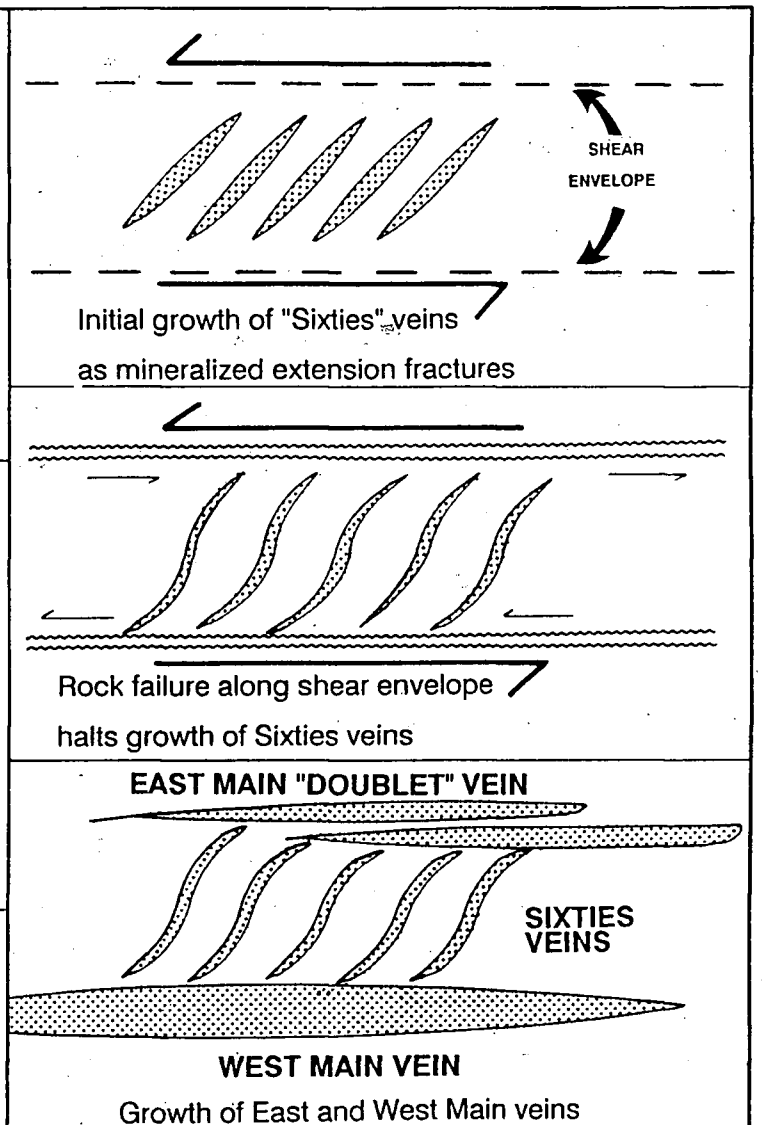

Figure 5.1b: Probable fracturing mechanism

Figure 5.1: Fracturing mechanisms at Scottie Gold mine

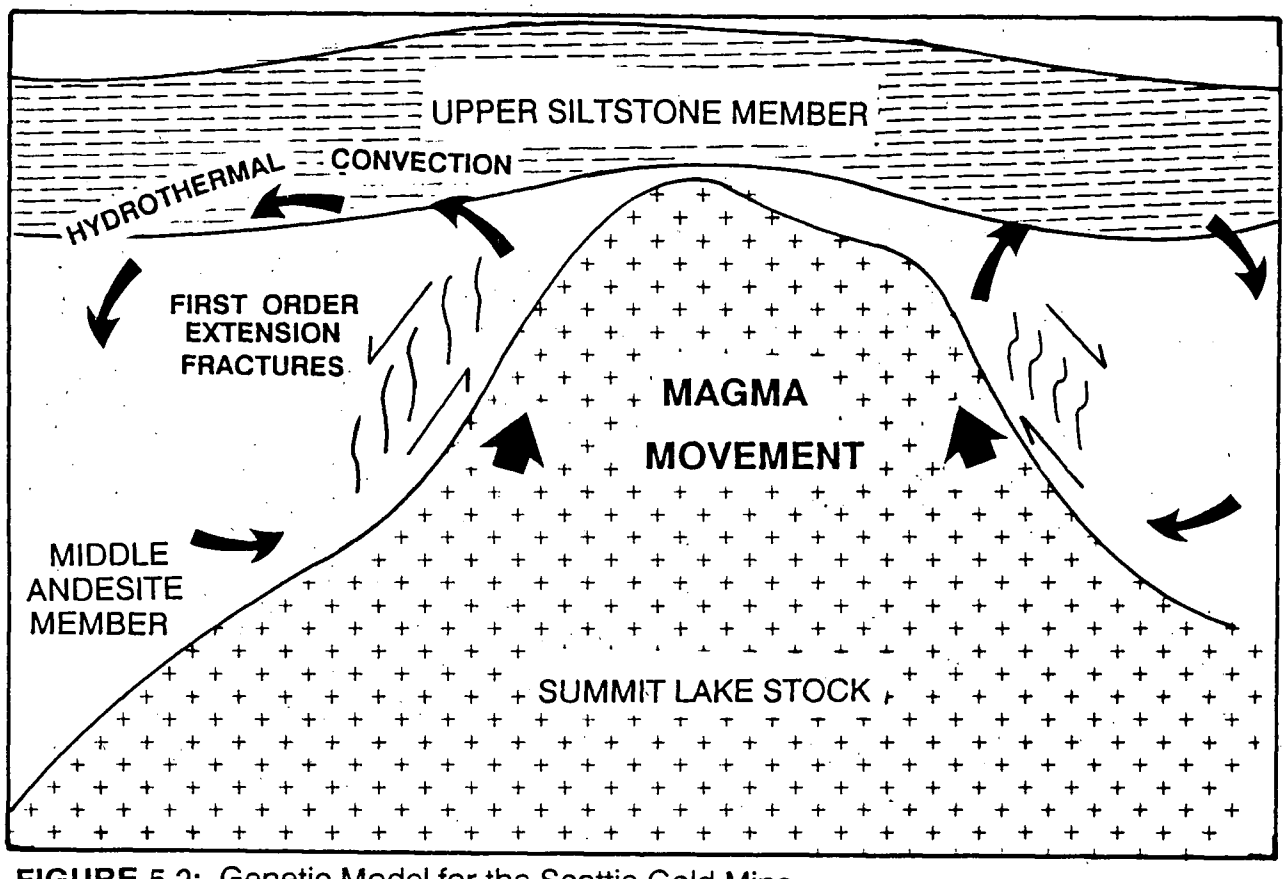

FIGURE 5.2: Genetic Model for the Scottie Gold Mine

The ore-hosting structures at Scottie Gold mine began as a series of *en echelon* tension veins that became a locus for subsequent shearing (Figure 5.1). The tensional structures developed in the country rock around the Summit Lake pluton during late magma movement (Figure 5.2).

5.1.1.2 SILVER-GOLD-BASE METAL DEPOSITS

BIG MISSOURI MINE

The subtle, but real, progressive steepening of dip in the Big Missouri ore zones (Figure 5.3) is an important clue to the pre-folding orientation of these deposits. Prior to mid-Cretaceous deformation, ore zones in the Big Missouri area formed as veins emplaced in a series of parallel, vertical, brittle faults (Figure 5.4). There was relatively minor offset across these faults, on the order of a few tens of metres at most; offset between blocks was more a matter of differential settling rather than major tectonic disturbance (Figure 5.8). Faults formed as part of a series of synvolcanic radial fractures around an active volcanic centre. 'Radial' fracture sets may appear to be truly radial on a regional scale, but in detail are commonly composed of several parallel sets, *e.g.* Spanish Peaks and Dyke Mountain, Colorado (Knopf, 1936 and Johnson, 1961).

Hydrothermal fluids were concentrated above a local dome in the underlying Texas Creek batholith, exposed near the mill portal of the Big Missouri mine and in underground workings at the Silver Butte deposit (Figure 4.16a). Dykes of Premier Porphyry that crop out along the Granduc mine road may have penetrated up into the mineralized region. Fluids precipitated epithermal breccia veins into several parallel fault zones. A series of fluid pulses deposited ore and gangue repeatedly along each fault. Possibly only one fault structure at a time served as a fluid conduit; other faults becoming conduits as the 'active' fault sealed due to precipitating ore and gangue minerals.

Metal and mineral distribution is less well documented at Big Missouri than at Silbak Premier, and post-ore faulting has disturbed the continuity of individual ore shoots (Figure 4.7). However, two Silbak Premier patterns--elevated precious metal grades in low

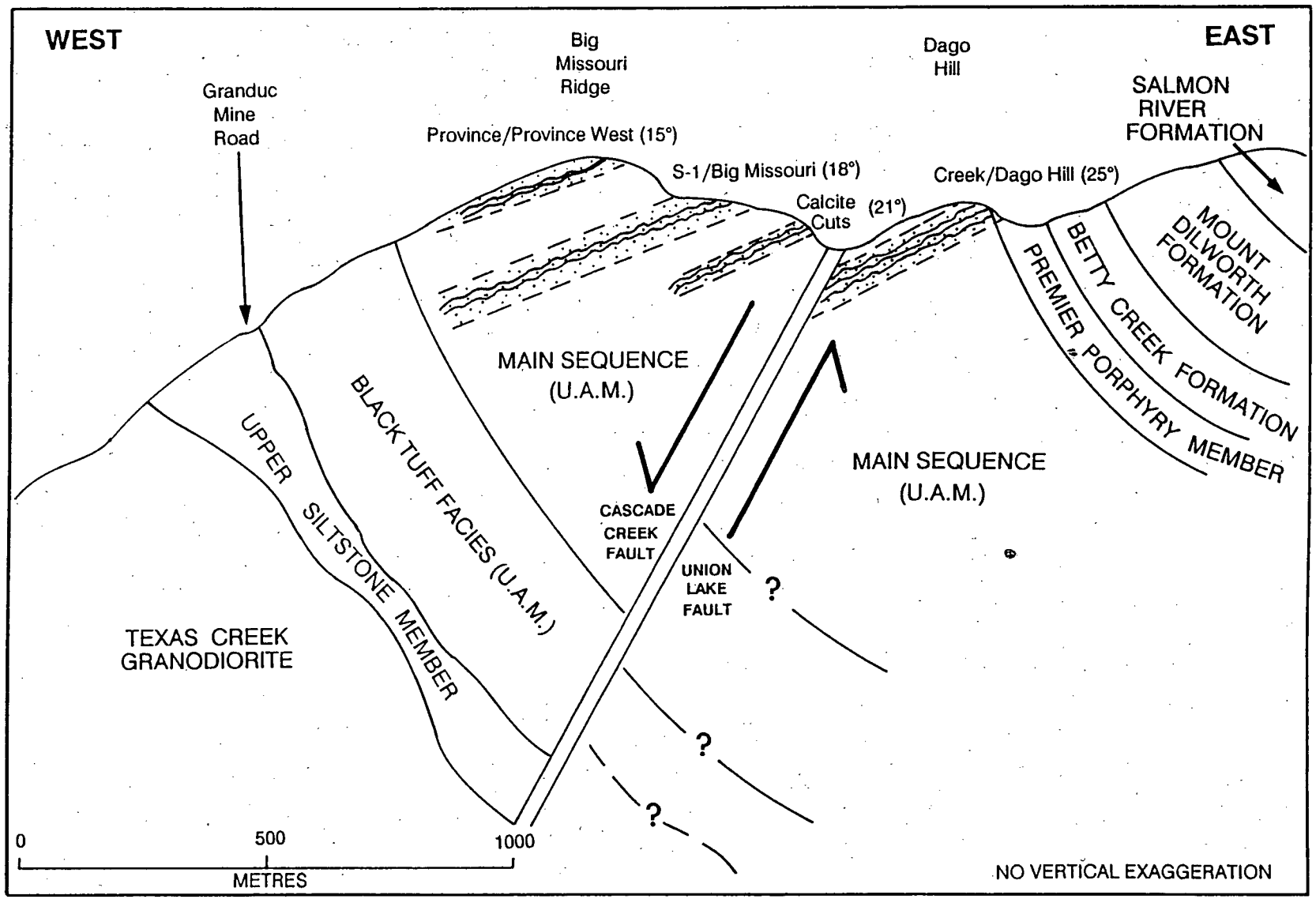

FIGURE 5.3: Interpretive cross-section through the Big Missouri mine area.
Compare to **Figures 4.6** and **4.7**. Dips of ore zones are shown in parentheses. Note that progressive steepening of ore zone dips coincides with the curvature of the folded host rocks, so that each ore zone maintains a perpendicular attitude with respect to the paleosurface. Stippled areas are alteration envelopes around the veins. Broad outcrop exposures of alteration represent areas where the topographic slope roughly parallels the dip of the ore zone. Interpreted relative fault offsets imply that additional ore zones could exist at depth.

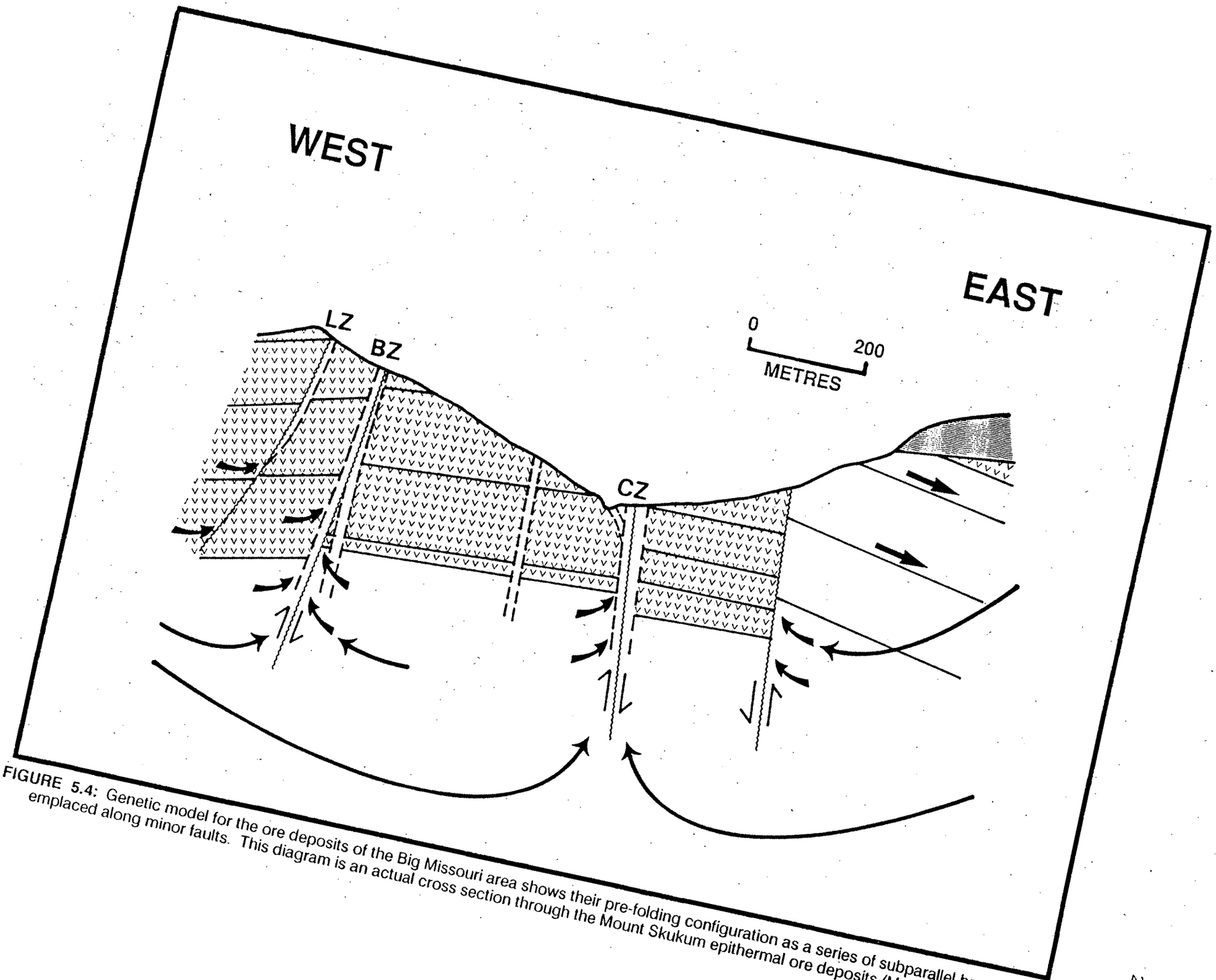

FIGURE 5.4: Genetic model for the ore deposits of the Big Missouri area shows their pre-folding configuration as a series of subparallel breccia veins emplaced along minor faults. This diagram is an actual cross section through the Mount Skukum epithermal ore deposits (MacDonald, 1987).

sulphide ores, and deposition of high sulphide ore shoots at depth *versus* stratigraphically shallower deposition of low sulphide ores--fit present Big Missouri data.

SILBAK PREMIER MINE

A simple intrusive sequence relates the different intrusive lithologies to stratigraphically stacked extrusive equivalent rocks. This intrusive 'model' accounts for all the types of intrusive rock and predicts that hydrothermal breccia veins will be concentrated in exactly the same position (relative to dykes and the paleosurface) as many of the Silbak Premier ore zones. The model resolves the problems of:

- 'folded' and 'non-folded' subvolcanic dykes and sills and extrusive flows
- the phenomenon of the "telescoped" epithermal deposits (Barr, 1980; Grove, 1986)
- apparent lateral mineralogical zoning (McDonald, 1988c, 1990a, 1990b).

In addition the model accounts for unusual features such as the hematitic rock-flour dykes first documented by Grove (1971).

Premier Porphyry dykes in the mine area record three subvolcanic intrusive events that each produced extrusive equivalent rocks now preserved as the three mappable units of the Premier Porphyry Member. The events occurred over a relatively short period of time since little or no sediment accumulated between extrusive units. The volcanic edifice was emergent and the mine area represented a local topographic high (Figure 5.8). The peculiar dike pattern at Silbak Premier can be projected into a pre-erosional cross-section (Figure 5.5) that emphasizes the difference in orientation between early sub-vertical plagioclase-hornblende porphyry dykes and later curving potassium feldspar megacrystic dykes of the Main Zone and West Zone (Figure 4.10).

The intrusive sequence and genetically related hydrothermal brecciation and veining are illustrated schematically in Figure 5.6. The initial subvolcanic magma (Figure 5.6a) was composed of plagioclase-hornblende porphyry-- texturally similar to the 'type' Premier Porphyry dykes but lacking the characteristic potassium feldspar megacrysts. The accompanying extrusive unit was deposited as a thinly laminated to thin bedded,

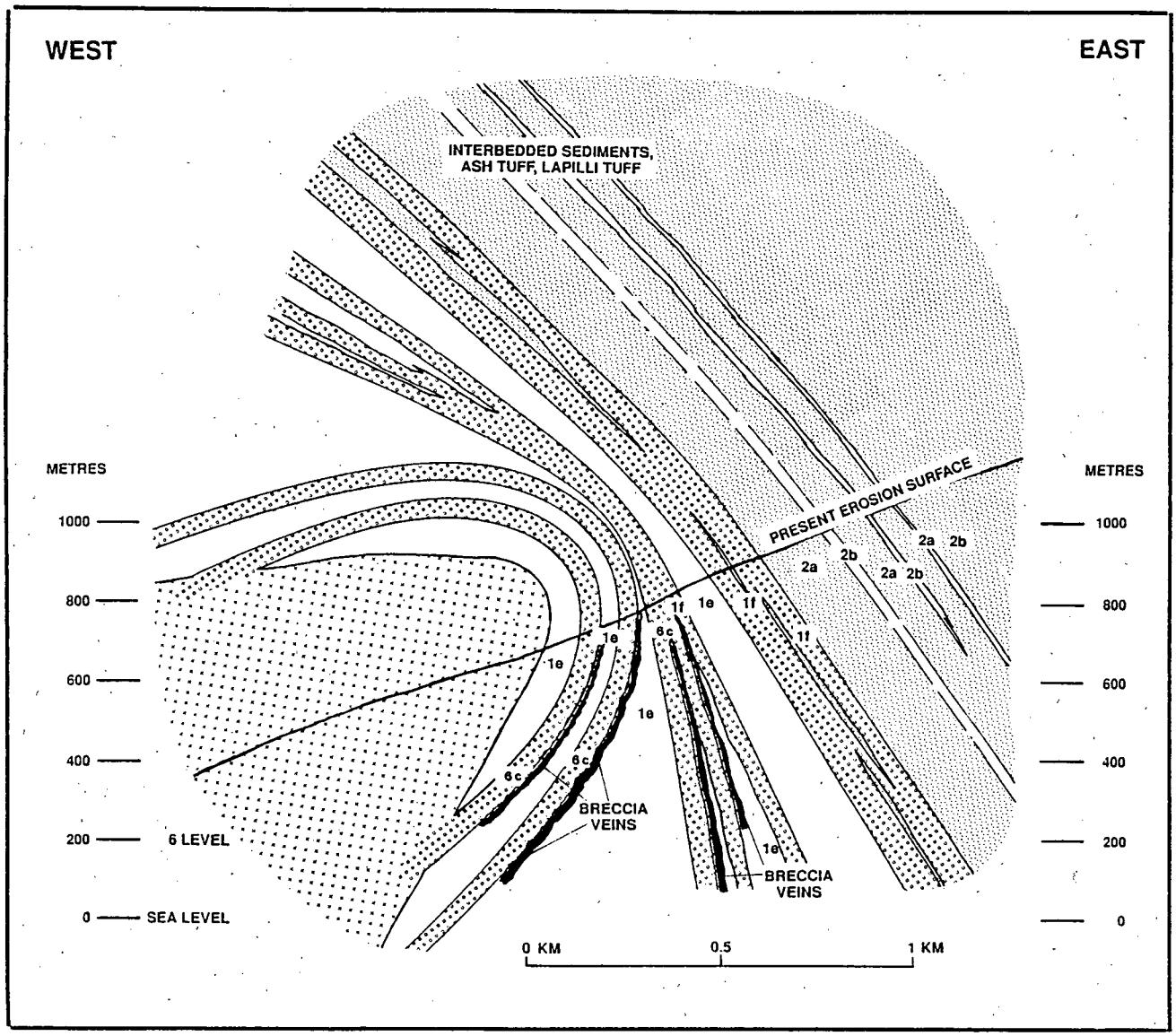

FIGURE 5.5: Pre-erosional geologic reconstruction in the Silbak Premier mine area. Compare with **Figures 4.9** and **4.10**.

1e = Upper Andesite Member; **1f** = Premier Porphyry Member (undivided); **2a** and **2b** = Betty Creek Formation sedimentary strata and tuffs respectively; **6c** = Premier Porphyry dykes.

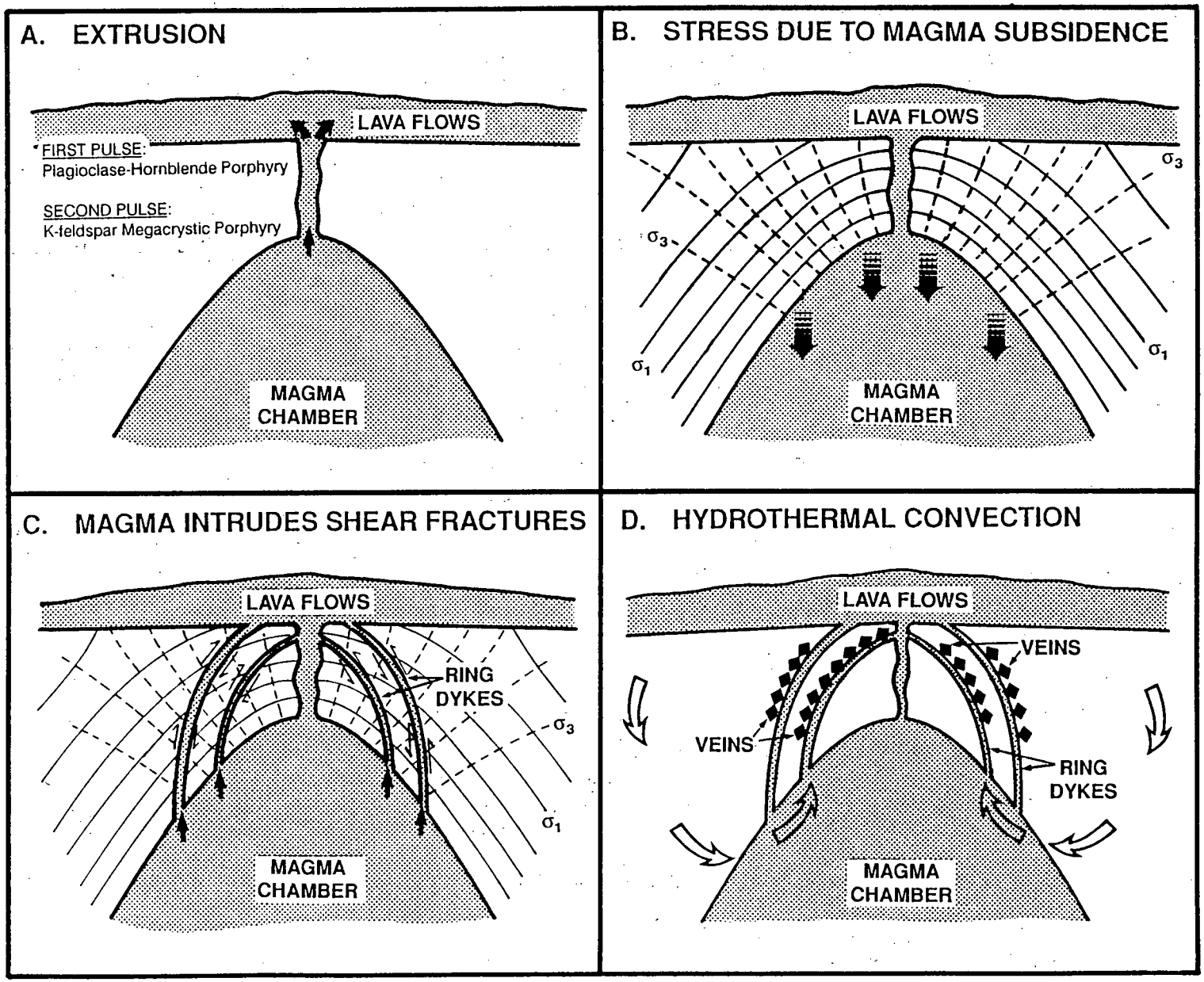

FIGURE 5.6: Genetic model for the Silbak Premier mine (modified from Anderson, 1937; Phillips, 1986)

rhythmically bedded, crystal-rich ash flow (laminated plagioclase porphyry, Plate 3.2A). The original conduit might have been a single elongate fissure. A large body of this plagioclase-hornblende porphyry lies structurally above the main ore zones at the Silbak Premier mine. It is an apparently homogeneous mass that hosts little brecciation, alteration or mineralization and has consequently been a disappointing exploration target despite its similarities to the thinner, curving potassium feldspar megacrystic dykes.

Pressure release was followed by adiabatic cooling within the subvolcanic magma chamber during a period of quiescence (Figure 5.6b) that initiated growth of potassium feldspar megacrysts and quartz crystals. Seismic activity or magma subsidence caused a new fracture to form near the existing volcanic neck, allowing injection and extrusion of the potassium feldspar megacrystic magma. Magma crystallized in the fracture as massive subvertical dykes, including the one that now forms the northern contact of the West Zone (Figure 4.10).

This second eruption produced the Premier Porphyry flow (green) and was the most voluminous of the three eruptions. It was followed by a second period of quiesence and magma subsidence. This created increasing stress in rocks overlying the magma chamber (Figure 5.6c). The hemispherical distribution of this stress field is governed by decreasing lithostatic pressures as the surface is approached. As stress increased, shear fractures propagated through the caprock along a parabolic trace due to the hemispherical shape of the tensile stress field (Figure 5.6c). This mechanism, originally proposed by Anderson (1937), has been presented with modifications by Phillips (1986). Magma, now rich in newly formed potassium feldspar and quartz, intruded the opening shear fractures to form ring dykes, and extruded at surface (Figure 5.6d). These ring dykes were thinner but more numerous than the earlier central feeders. The extrusive equivalent is maroon Premier Porphyry tuff, and perhaps the upper part of the Premier Porphyry flow, which represent the last phases of this eruptive event.

An integral part of the final intrusive/extrusive event is the formation of hydrothermal breccia zones on the hangingwall sides of the curved shear fractures (Phillips, 1986, p.B19-B20). Hydrothermal solutions derived from late magmatic volatiles and groundwater rise upward from the area of the top of the magma chamber. Pathways to surface were intermittently sealed due to mineral deposition and lithostatic load so that fluids accumulated in lower-pressure, dilational spaces above the magma chamber. These spaces existed along the hangingwall side of the ring dykes due to minor contraction during crystallization and cooling. In contrast, the footwall side of a ring dyke was a closed, high-pressure environment because the dyke itself provided a dome-shaped impervious cap.

Hydrothermal solutions gradually accumulated, producing a fluid sheet that progressively precipitated minerals. As fluid pressure increased and exceeded lithostatic load, major and minor fractures popped open abruptly. These fractures extended the existing fluid-filled fracture network both upward along the dyke contact and outward into the wallrock. Each new fracture opening caused a small, abrupt fluid pressure drop which resulted in mineral precipitation that reflected the chemistry of the solutions at that moment. Mineral layers in ore display textures reflecting periods of slow, static high-pressure mineral precipitation during cooling, alternating with periods of mineral 'dumping' during abrupt pressure drops.

Fractures occasionally propagated near to the surface and resulted in breaching, flash boiling and catastrophic pressure drop throughout the system with considerable mineral precipitation and accompanying chaotic wallrock spalling into the now unsupported fluid chambers. As the fluid chambers clapped shut rock fragments in the centre of the zone were crushed and ground in a natural autogenous mill. Consequently, older clasts in the core of the breccia veins are crudely rounded in contrast to sharply angular, younger clasts near the breccia vein margins. The shallow fractures that were open to surface sealed rapidly; then the more typical cycle of moderate to high pressure fluid accumulation and propagation of minor fractures resumed.

A rock cut along the old track between the B.C. Silver and Sebakwe portals sits stratigraphically above (eastward and uphill from) the 'blind' B.C. Silver ore shoots. The rock consists of green ash tuff shattered into a sharply angular mosaic breccia with a matrix of red, hematitic rock-flour (Grove, 1971, plate IXc). This feature was formed by a gas blast and is a monolithologic equivalent of a hydrothermal pebble dyke. Such structures characteristically cut the barren caprock that overlies the mineralized interval of an epithermal vein system (Sillitoe, 1986).

5.1.1.3 STRATABOUND PYRITIC DACITE

Pyritic dacites cap a blanket of dacitic pyroclastics. This facies represents penecontemporaneous or post-depositional impregnation of pyrite into a variety of lithologies although the predominant rock type is dacitic lapilli tuff. In some exposures the pyritized rock is a carbonate-mudstone-cemented debris flow with heterolithic volcanic and carbonate clasts. The pyritic facies is interpreted as local pyrite impregnation around fumaroles, hotsprings and calcareous-mud-filled brine pools that were scattered about on the cooling volcanic sheet (Figure 5.7).

5.1.2 EOCENE DEPOSITS

The geologic setting of Eocene deposits is remarkably consistent even though host rocks vary from the oldest rocks of the stratigraphic column through to the youngest and include Early Jurassic to Eocene plutonic rocks (Table 4.7). All occurrences are locallized in brittle faults or fractures and there is a dominant trend for most of these veins, southeastward with a subvertical dip. Economic concentrations of argentiferous sulphides appear to be restricted to the portion of the mineralized shear that transects more brittle, resistant rocks. Major deposits are hosted in dacitic volcanics of the Mount Dilworth Formation (Silver Tip, Lion, Start, Unicorn No. 3), or the Betty Creek Formation (Prosperity/Porter Idaho), or in massive granodiorite of the Texas Creek batholith (Riverside). There is a close spatial association between silver-lead-zinc deposits and Early

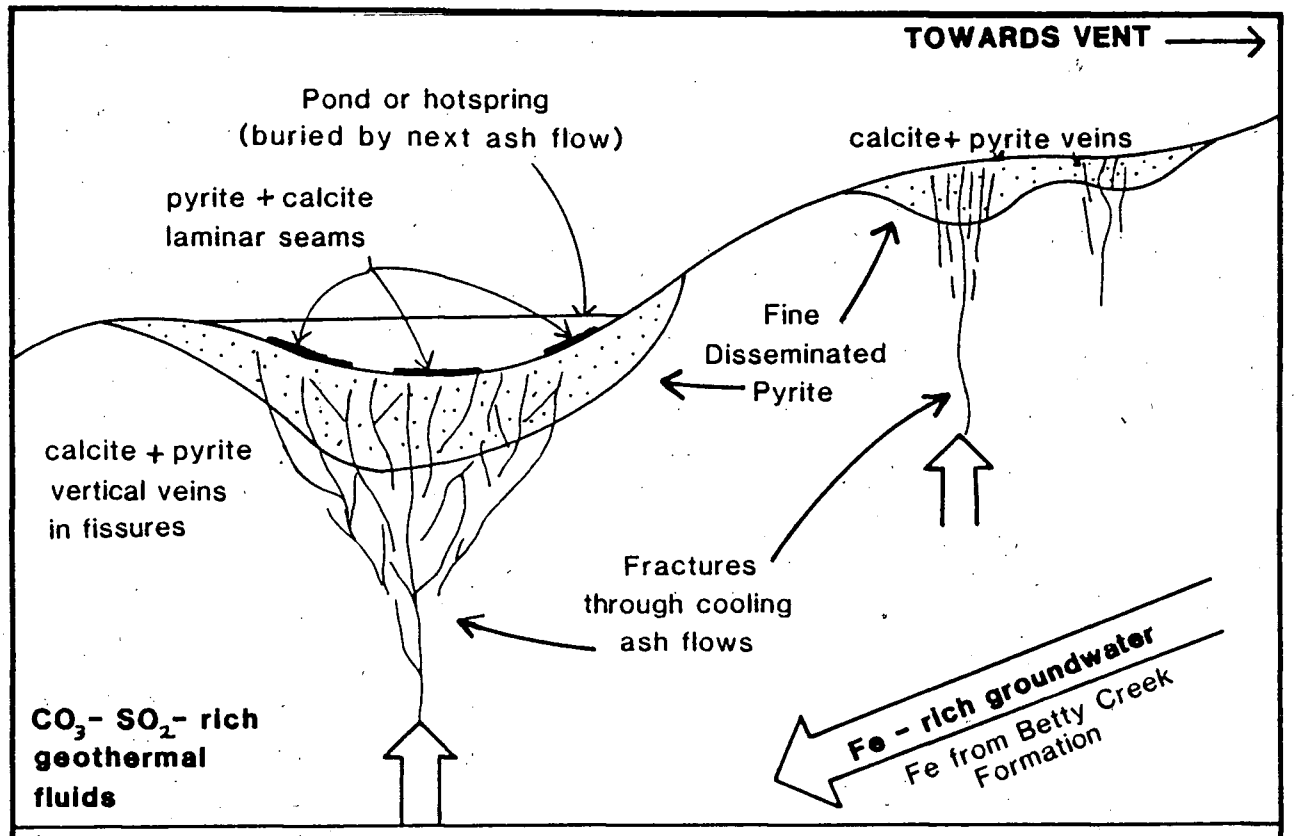

FIGURE 5.7: Genetic model for the stratabound pyritic dacite

to Middle Eocene igneous rocks, both earlier dykes (55 Ma) and later plutons (52-48 Ma). In the Stewart camp molybdenite is hosted only in dyke phases.

A less obvious correlation, but one that is critical for explaining the difference between Jurassic and Eocene metal suites, is a close spatial association between Tertiary deposits and turbidite sequences. Reduced, carbonaceous turbidite sequences characteristically have elevated contents of silver. Contents of 20-30 ppm silver represent a geochemical concentration factor of the order of 100-500 (Laznicka, 1985). The minor turbidite sequences within the Unuk River Formation near the Indian, Silver Basin, and Riverside prospects, and the thicker, infolded stratigraphic package of the Salmon River Formation near the Prosperity/Porter Idaho, Unicorn No.3, Lion, Silver Tip, and Start deposits are likely the main source beds for the metals of these Tertiary deposits.

The genetic model for Eocene ore deposits (Figures 5.11 and 5.12) emphasizes: the black turbidite source rocks, the hydrothermal heat source provided by the intrusive rocks, and structurally and stratigraphically controlled deposition in well-shattered dacitic rock units (Figure 4.16b).

5.2. REGIONAL MODELS

5.2.1 ORE DEPOSIT MODELS/GENETIC MODELS

Regional scale models are presented in Figures 4.16, 5.8, 5.9, 5.10, 5.11 and 5.12.

For Jurassic deposits, Figure 4.16a emphasizes the stratigraphic position of the mineral deposits, and indicates that all deposits except pyritic dacites cross-cut stratigraphy, *i.e.*, they are epigenetic. The interpreted paleotopographic setting for the main Early Jurassic deposit types is shown in Figure 5.8. Figure 5.9 emphasizes the variety of structural conduits and depositional sites that were available in and around the Early Jurassic volcano. **Transitional** deposits (Figure 5.9) are: deposits that are transitional in setting beween the settings for porphyry copper and epithermal deposits (Panteleyev, 1990; Schroeter *et al.*,1989); deposits that are transitional in depth of emplacement and in mineralogy and textures between mesothermal and epithermal deposits ("leptothermal" of

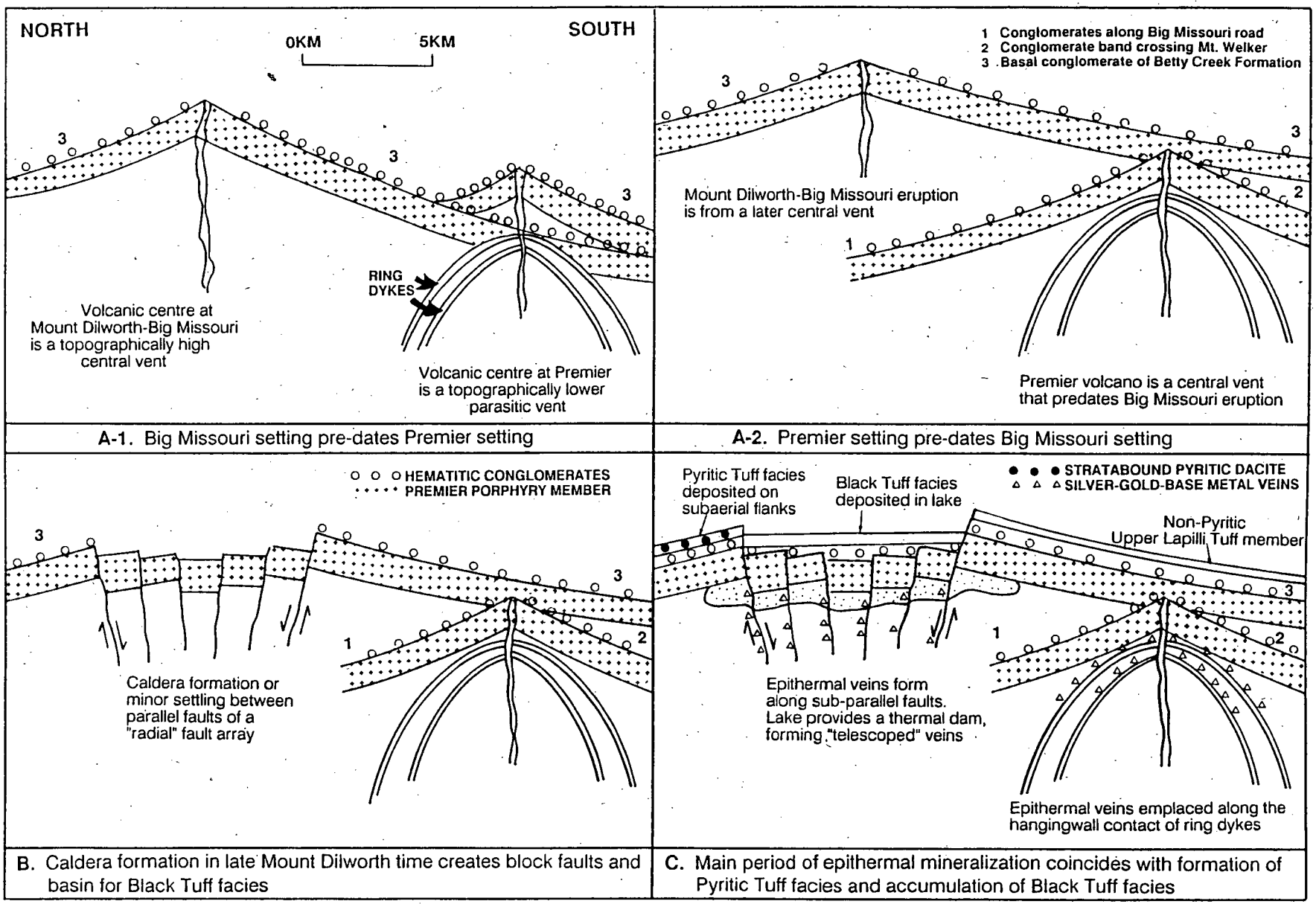

FIGURE 5.8: Sequence of development of epithermal settings

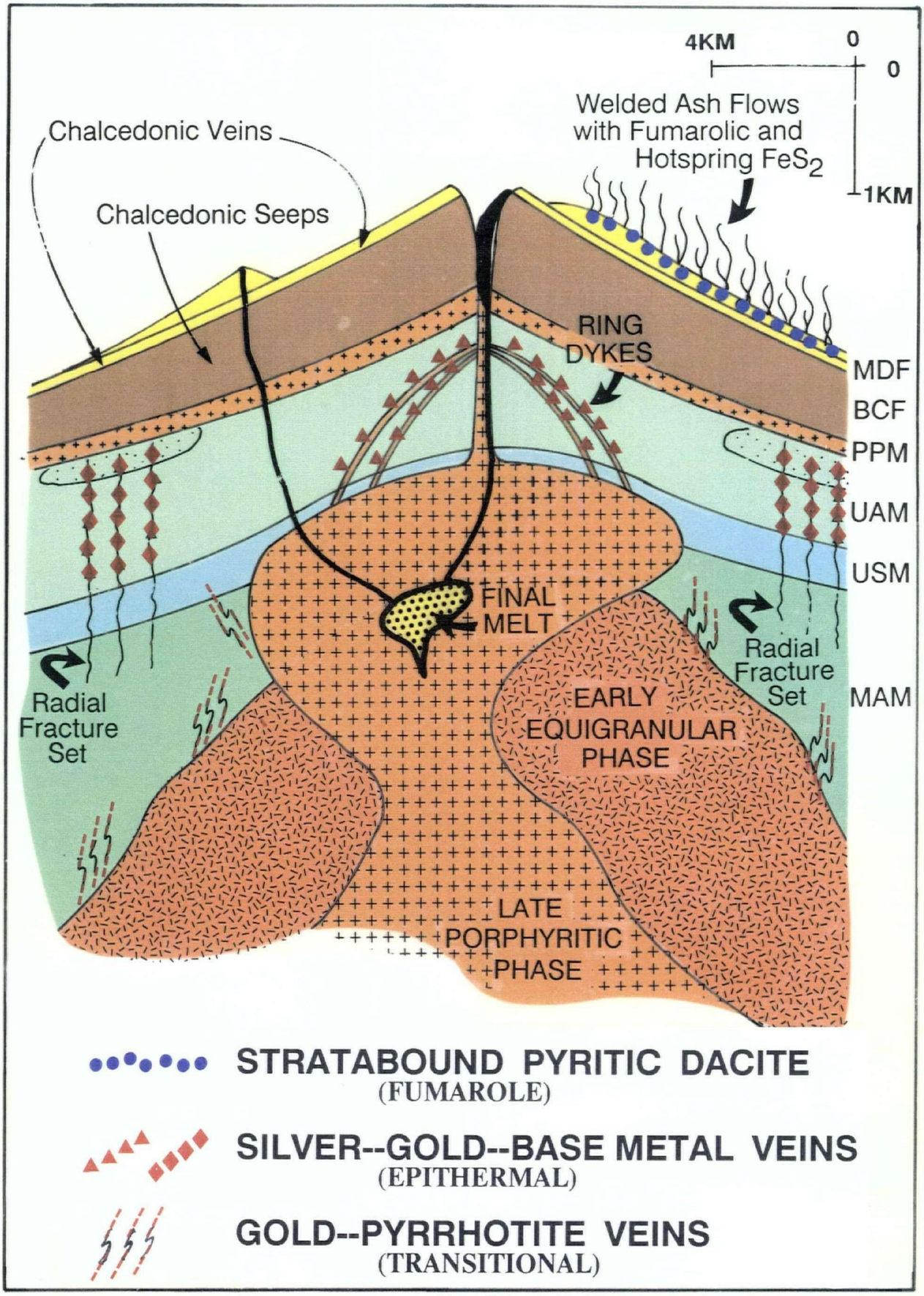

FIGURE 5.9: Genetic model for the Early Jurassic

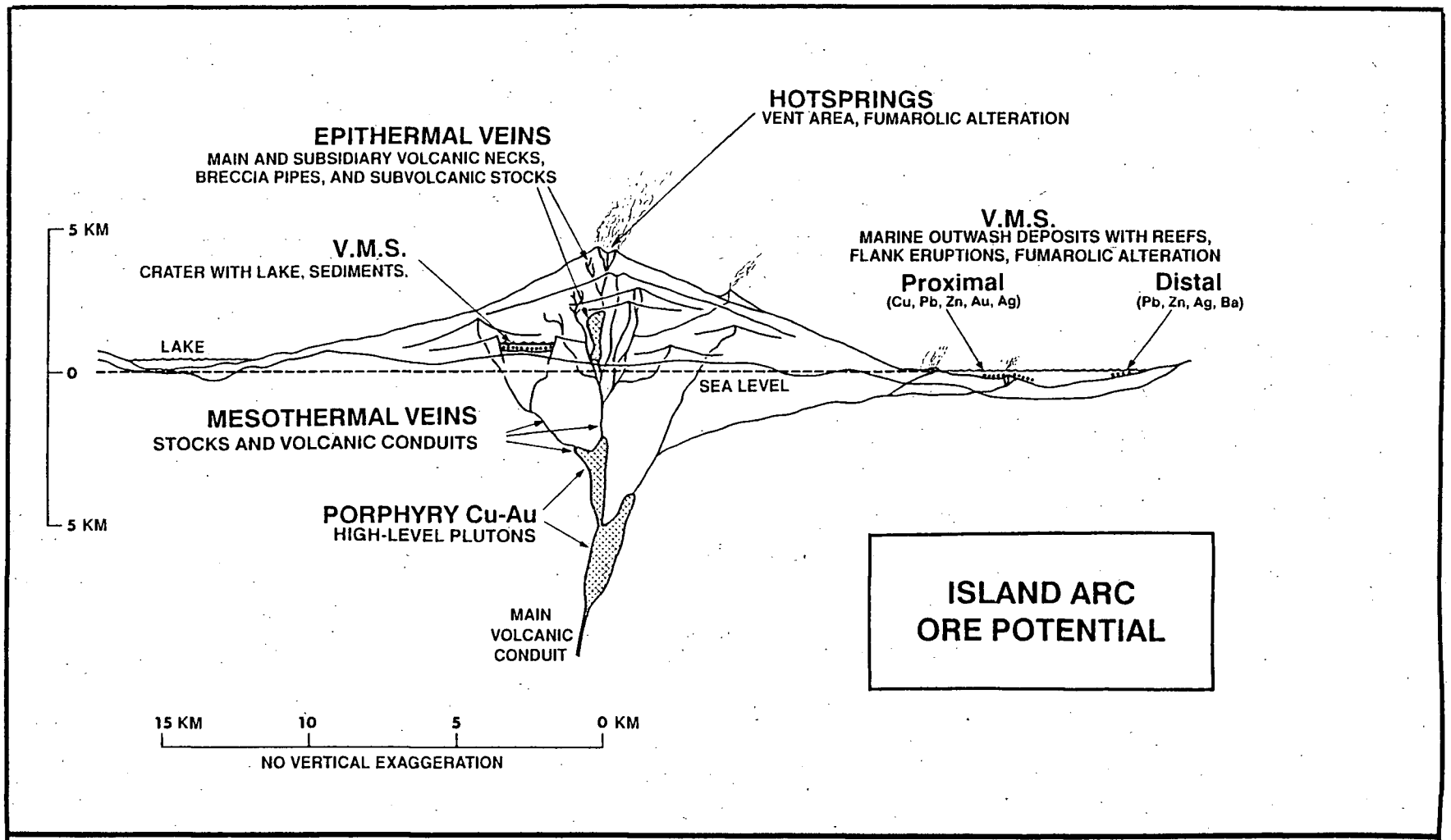

FIGURE 5.10: Ore potential in an andesitic stratavolcano (Branch, 1976).

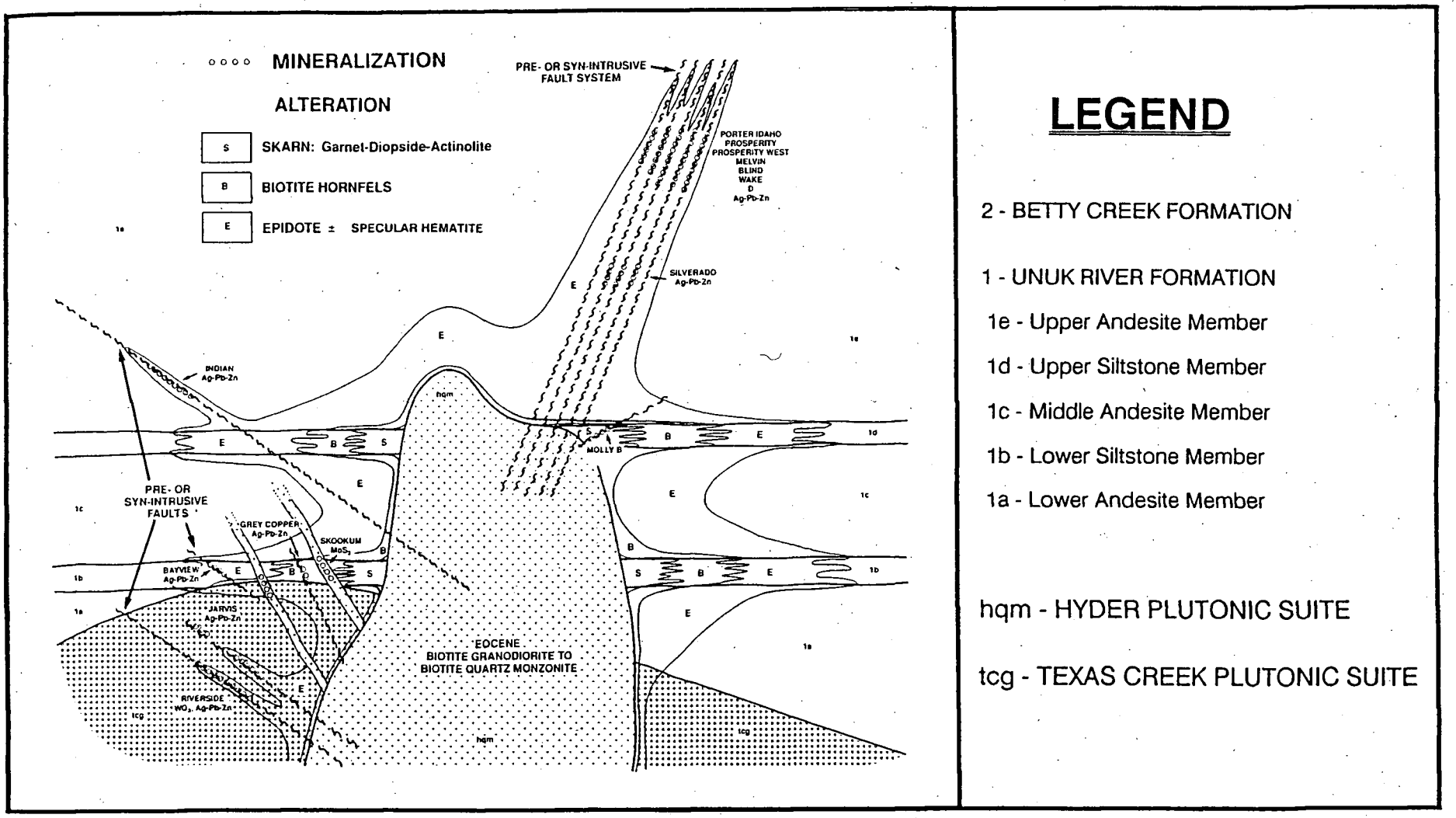

FIGURE 5.11: Ore deposit model for the Middle Eocene

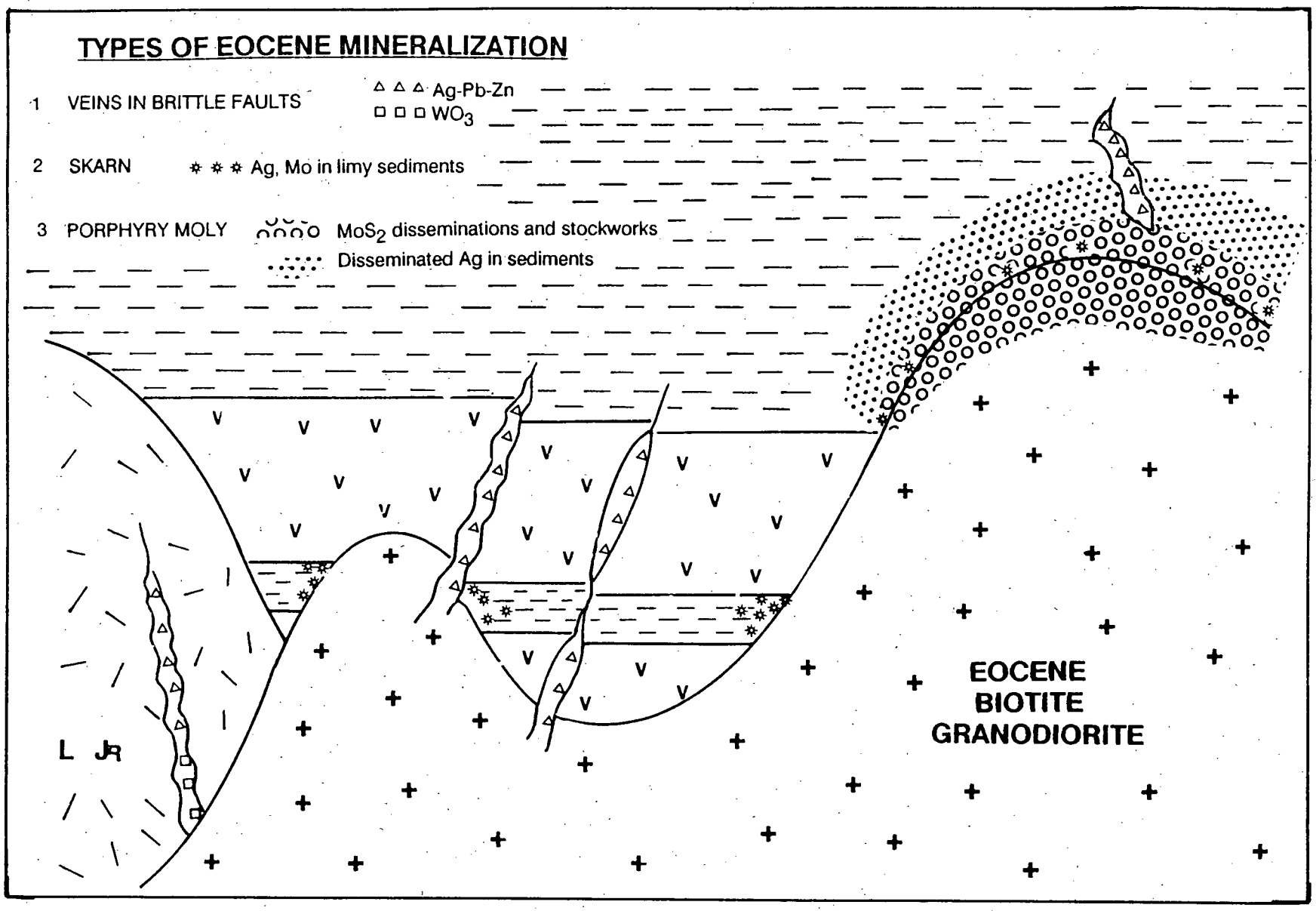

FIGURE 5.12: Genetic model for the Middle Eocene

Lindgren, 1933; "telescoped" of Buddington, 1935); and deposits emplaced along the thermal transition between the ductile and brittle shearing regiemes (Nesbitt, 1988).

Many features of the geologic setting and ore deposits of the Stewart district are depicted in Figure 5.10, which was originally developed for island arc porphyry and epithermal systems in the southwest Pacific (Branch, 1976).

For Middle Eocene deposits, Figures 4.16b, 5.11 and 5.12 show the spatial relationships between deposits and igneous rocks, the range of host rock types, and the most favourable host rocks. Figure 5.12 illustrates geologic settings that have concentrated economic quantities of mineralization.

5.2.2 METALLOGENIC MODELS

Metallogenic models for the Early Jurassic and Middle Eocene are presented in Figure 5.13. Tectonic settings are remarkably similar. Differences in pluton composition, in depth of ore emplacement, and in textures, mineralogy and metal content of deposits are attributed to differences in crustal thickness, crustal composition and effects of regional metamorphism.

This specific tectonic setting of 'stacked arcs' -- a young arc constructed on a foundation or crust consisting of a much older arc -- has been predicted as *the* metallogenic association with the greatest variety of accumulated metals and mineralization styles (Laznicka, 1985, p.397-403). Examples include the Cretaceous volcanic belt of Puerto Rico, The "Green Tuff" belt of Japan, and the Hazelton Group of British Columbia. Modern analogues exist in the New Ireland/Solomon Islands chain and the eastern Aleutians.

5.2.2.1 EARLY JURASSIC METALLOGENY

Eastward-plunging subduction generated arc volcanism on crust 25-30 kilometres thick (Gill, 1981, p.46-49), consisting of metamorphosed Paleozoic rocks of the Stikine assemblage (Figure 5.13a). Volcanism continued through 40 million years, evolving from basalt to dacite. Hydrothermal convection cells developed around the cooling subvolcanic

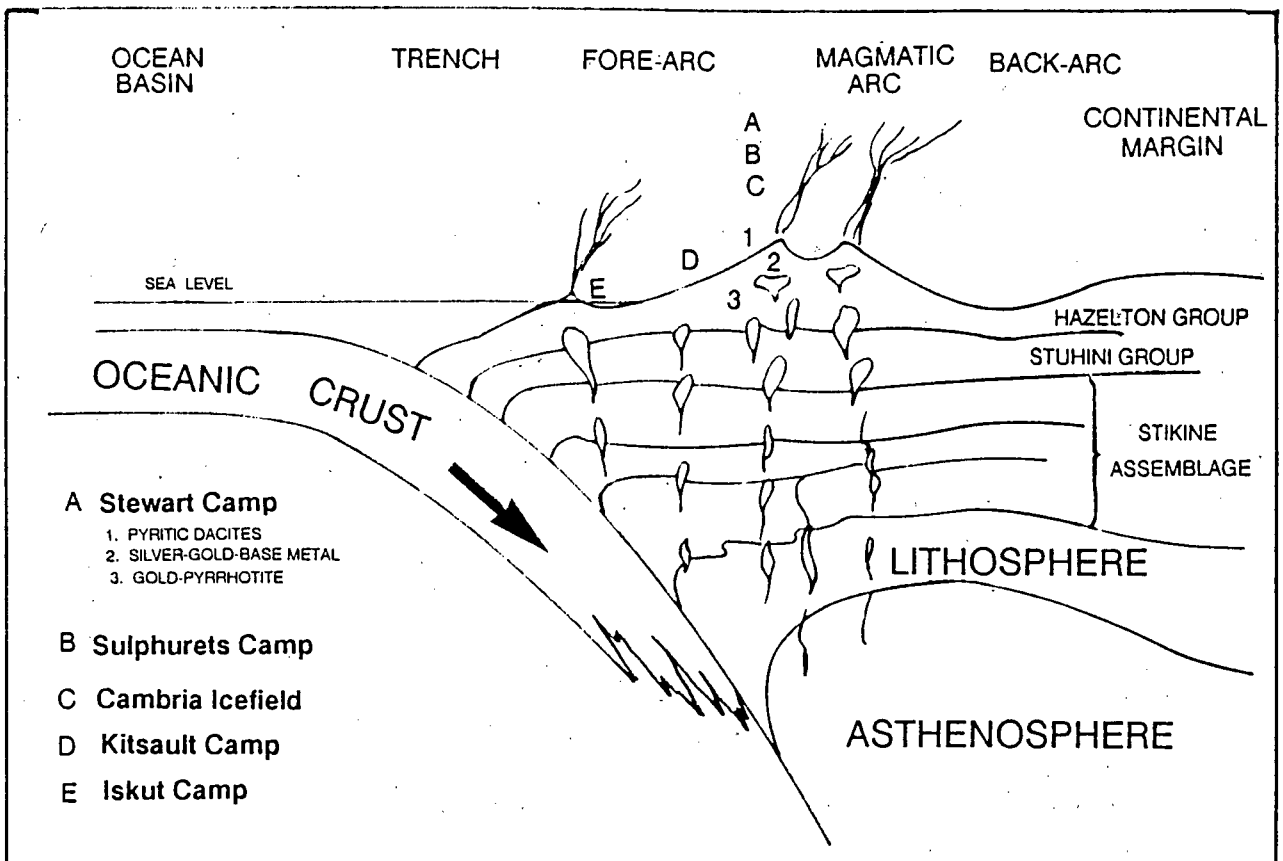

FIGURE 5.13a: Early Jurassic tectonic setting and ore deposits

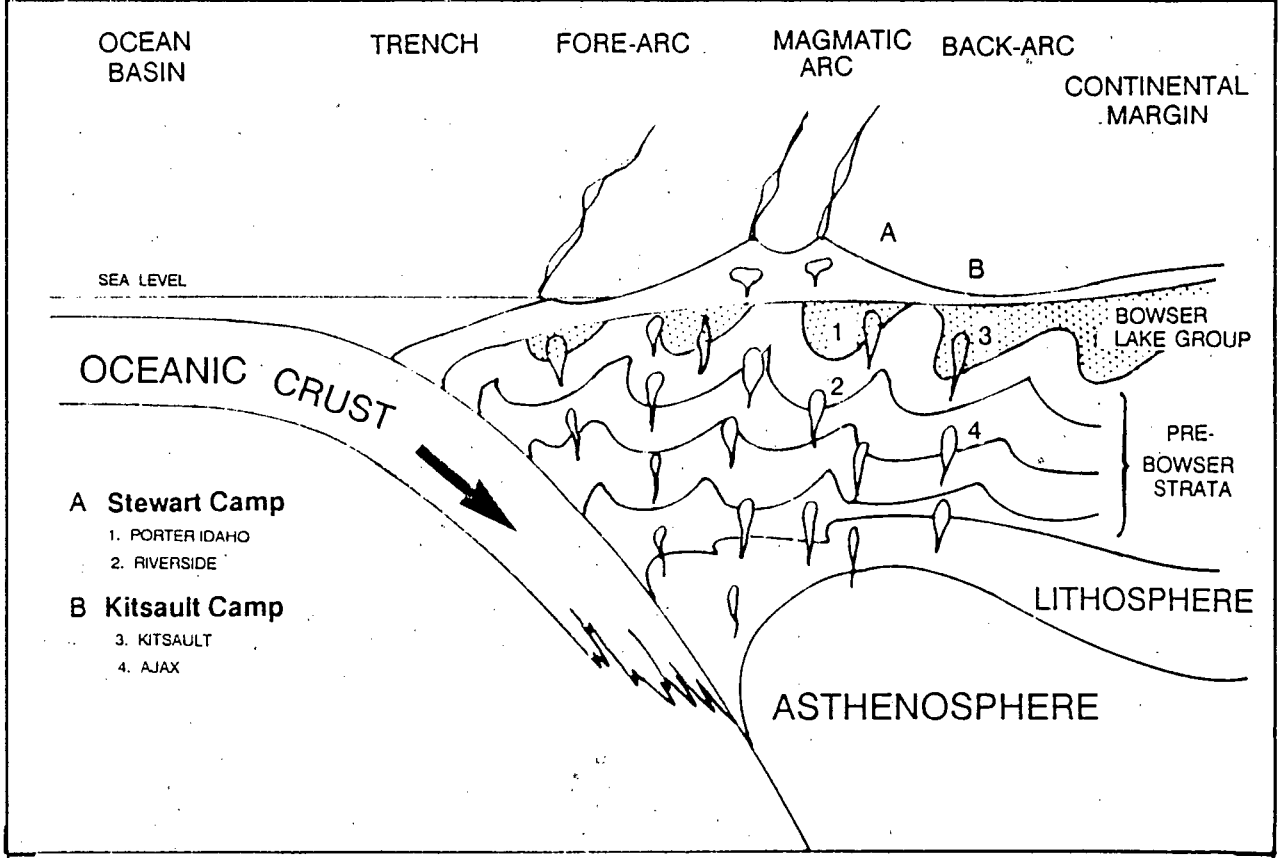

FIGURE 5.13b: Eocene tectonic setting and ore deposits

FIGURE 5.13: Early Jurassic and Eocene metallogeny in the Stewart mining camp. Width of diagram = 200 kilometres. Vertical exaggeration ~4:1

plutons. These hydrothermal systems which concentrated metals in solution and deposited ores at depths ranging from as much as 5 kilometres up to the paleosurface, should be regarded as separate and independant convection cells with separate chemical, thermal and pressure characteristics. There are broad horizontal bands with little or no record of mineral deposition or major hydrothermal alteration that separate the three horizontal zones of distinctly different mineral deposit types (Figure 4.16a).

Although fluids might may derived their characteristic suites of silver, gold, zinc, lead and copper from the metal-rich dominantly andesitic country rocks (Gill, 1981, p.137; Laznicka, 1985, p.54), Gill (1981, P.291) argues that most if not all of the metals in deposits hosted by andesitic volcanic rocks are of primary magmatic origin.There is a relatively high volatile content in magmas in volcanic arcs; in orogenic andesites this vapour lies in the H-C-O-S-Cl-F system (Gill, 1981, p.291). Although H_2O is the most abundant volatile constituent in an orogenic andesite magma, the magma is likely to become first saturated with CO_2 or a sulphur species than with H_2O. Once the vapour phase forms in Cl-rich systems, the vapour is an effective solvent for alkalis, metals and silica (Gill, 1981, p.291). Exsolution of vapour from the residual andesite liquid causes magma depletion in the elements which partition strongly into the vapour. Orogenic andesite magmas typically contain 200-2000 ppm sulphur, and could be sulphur-saturated, coexisting with a sulphide liquid or solid or an S-spesies vapour (Gill, 1981, p.122). Subaerially erupted andesite lose much of this excess SO_2 by exsolution during eruption. McDonald (1990b) concludes that mixing of cool, meteoric groundwater with hot sulphur and metal-bearing primary magmatic fluids is the most likely mechanism for base and precious metal deposition at the Silbak Premier mine, because there is no evidence of boiling.

Gold-pyrrhotite veins formed in *en echelon* tension gashes developed in the immediate country rock around the plutons during late magma movement. **Silver-gold-base metal veins and breccia veins** were deposited at critical pressure-temperature transitions in

shallower subvolcanic faults and shears and in hydrothermal breccia zones along dyke contacts. These deposits formed from many pulses of mineralizing fluid.

Residual trapped volatiles and magma erupted in a final series of violent dacitic pyroclastic blasts. Venting fumarolic fluids and hotspring pools scattered on this cooling volcanic sheet impregnated local areas with abundant fine disseminated pyrite, forming the **stratabound pyritic dacite** tuffs. The area subsided beneath sea level before subaerial erosion could dissect the composite volcano or remove any of the deposits.

5.2.2.2 MIDDLE EOCENE METALLOGENY

Eastward-plunging subduction generated the plutons of the Coast Plutonic Complex that were emplaced within a plate of continental crust 50-70 kilometres thick (Gill, 1981, p.46-49), consisting of Paleozoic and Mesozoic sedimentary and volcanic rocks (Figure 5.13b). Brittle dacitic units and Jurassic plutons, shattered by mid-Cretaceous tectonism, provided local sites of extensive fracturing favourable for mineral deposition in Eocene time.

The Eocene magmatic pulse began with dike swarms followed by intrusion of the main batholith and satellitic hypabyssal plutons. Hydrothermal convection cells developed around these cooling intrusions; the volume of country rock affected was proportional to the size of the igneous body. Associated mineral deposits vary in size according to the amount of circulating fluid and the cooling period for the pluton.

The thick turbidite package of the Salmon River Formation and minor turbidite members of the Unuk River Formation contributed silver, lead and zinc to the Eocene hydrothermal system. The metals precipitated out as coarse grained galena-sphalerite-pyrite veins adjacent to dykes or in fractures and shear zones some distance away from larger plutons. Minor molybdenite rosettes hosted within dykes are of magmatic origin.

The last plutons of this magmatic pulse are rare stocks emplaced in late Oligocene time within the main Coast Range batholith. These include the more highly evolved stock that generated the molybdenite-rich, silver-depleted Quartz Hill ore deposit (27-30 Ma,

Hudson *et al.*, 1979). In this geologic setting, in the heart of the Coast Range batholithic complex, no turbiditic sediments were available to supply silver, lead or zinc to the hydrothermal system.

5.3 REGIONAL EXPLORATION STRATEGIES

5.3.1 EARLY JURASSIC

Three of the major mineral camps of the district are all hosted in proximal volcanic facies (Figure 5.14), suggesting they are all locallized around Early Jurassic volcanic centres (Alldrick, 1989). These three camps have slightly different geologic settings (Alldrick, 1989 and Figure 5.14) and include similar and contrasting Early Jurassic mineral deposit types.

Kitsault Camp. Early Jurassic deposits of the Kitsault valley include high-grade stratabound and cross-cutting silver-lead-zinc-strontium-barite deposits (Dolly Varden, Northstar, Torbrit, Wolf, Kitsault Lake), bulk-tonnage, low-grade disseminated copper-gold deposits (Copperbelt, Kinskuch Lake, Homestake Ridge), and minor stratabound pyritic dacites at the top of the volcanic section (west side of the Kitsault Glacier).

Stewart Camp. Early Jurassic deposits of the Stewart camp include gold-pyrrhotite deposits (Scottie Gold, Shasta), silver-gold-base metal deposits (Silbak Premier, Big Missouri, Silver Butte), and stratabound pyritic dacites (Mount Dilworth, Iron Cap).

Sulphurets Camp. Early Jurassic deposits consist of deeper level bulk-tonnage, low-grade, disseminated copper-gold deposits (Kerr, Mitchell, Iron Cap Copper), shallower silver-gold-base metal deposits (Brucejack Lake, Sulphurets), and stratabound pyritic dacites (Knipple Lake, Knipple Glacier, Treaty Glacier, Storie Creek, DC Glacier).

Regional Exploration Strategies for Early Jurassic deposits:

- There is high potential for epithermal deposits up-section from porphyry-style deposits in a broad, mushroom-shaped rock volume. Conversely, Early Jurassic plutons underlying epithermal deposits should be targetted as a potential locus for porphyry copper-gold systems.

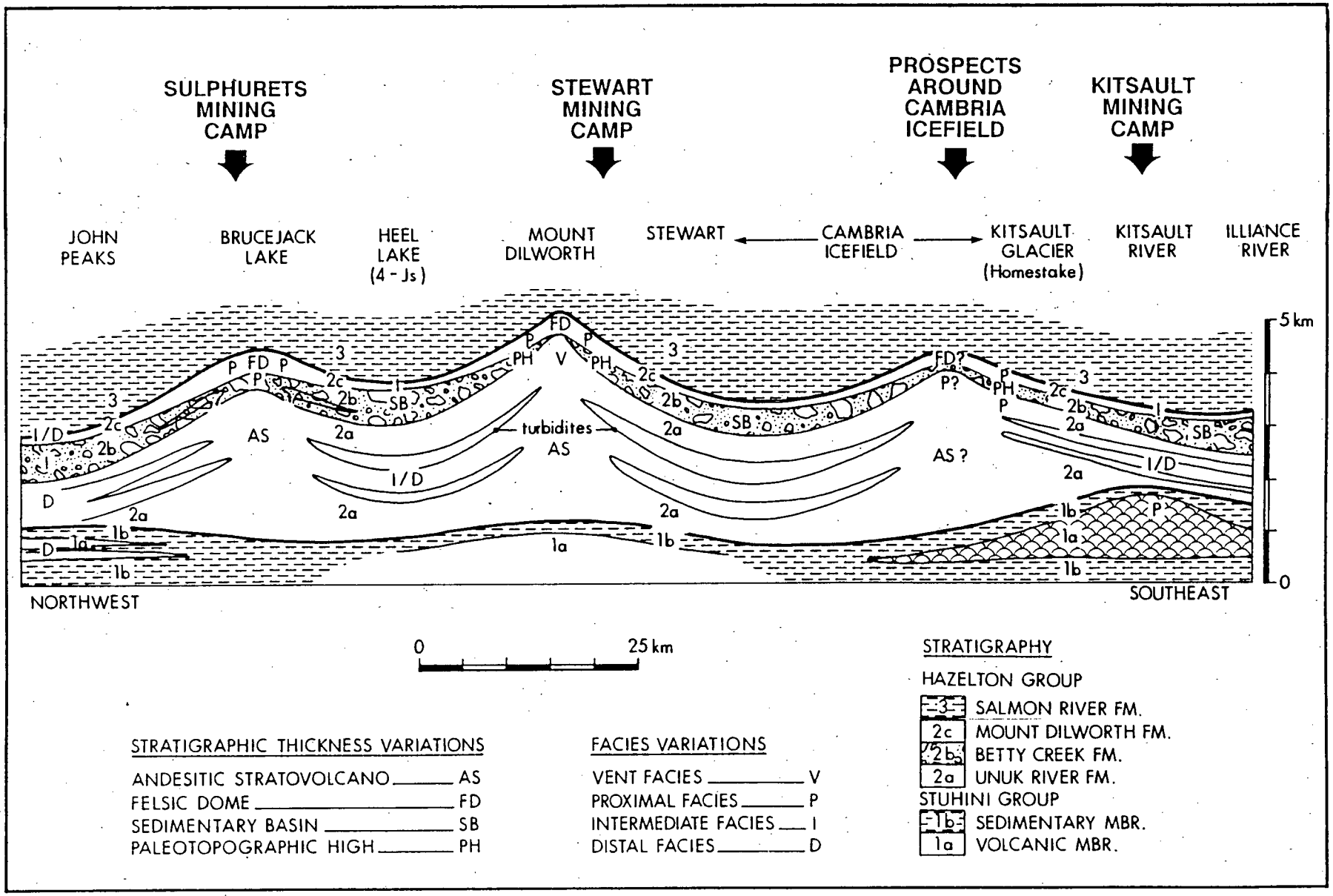

FIGURE 5.14: Schematic longitudinal section showing volcanic centres and mining camps within the Stewart Complex

- Clusters of showings, however minor, within broad alteration envelopes should be systematically investigated, *e.g.* Homestake Ridge west of the Kitsault Glacier, Illiance River valley east of Alice Arm, the Bitter Creek area east of Stewart, the Eskay Creek/Coulter Creek drainages east of Tom MacKay Lake, and the large area of showings along the south side of the Iskut River including Sericite Ridge, Pins Ridge and Pyramid Hill.
- Areas of extensive gossans without known mineral occurrences need thorough prospecting, *e.g.* Treaty Glacier area, the Copperbelt north of the Dolly Varden mine, the Red Bluff area west of the Ajax orebody, the spine of rock that splits the Frankmackie Icefield south-southwest of the Kerr property, gossans two kilometres southeast of Mount Robert Dunn, and the upper canyon of Storie Creek,
- Areas with proximal volcanic indicators deserve at least a first-pass prospecting program, *e.g.* ridges north-northwest of Homestake Ridge.
- Where even limited amounts of geological control are absent, a reconnaissance stream sediment survey with sample sites at one per square kilometre density could cover a broad swath (3 to 5 km wide) designed to follow the inferred position of the upper contact of the Unuk River Formation, more or less along the stratigraphic position of the Premier Porphyry Member. A wider swath (5 to 8 km wide) could cover all stratigraphy below the base of the Salmon River Formation.

5.3.2 EOCENE

Vast amounts of magma were generated from early Cretaceous through to mid-Tertiary time, producing a continental-scale composite batholith. Satellitic stocks and dyke swarms were emplaced in Mesozoic strata peripheral to the main batholith.

Silver. High-grade silver-lead-zinc veins (Prosperity/Porter Idaho, Start, Indian, Riverside) are hosted by brittle fractures, faults and ductile shears around the perimeters of the batholith, satellitic stocks and dykes. Where discrete fluid conduits are lacking, large lower-grade haloes of disseminated silver mineralization formed (Kitsault).

Molybdenum. The world's largest molybdenum deposit (Quartz Hill), is associated with one of the youngest stocks in the composite Coast range batholith. Economic deposits of molybdenum, with by-product silver, occur with Eocene satellitic stocks in the Alice Arm area (Kitsault, Ajax, Roundy Creek). A few dykes also host minor to trace molybdenite.

Regional Exploration Strategies for Eocene Deposits

It is difficult to propose a more appropriate exploration strategy within the Coast Plutonic Complex than a program launched along the northwest coast by U.S. Borax several years ago. A ship cruised island channels and mainland fjords setting out reconnaissance geochemical sampling crews on islands and the mainland by ship-based helicopter (B.D. Devlin, personal communication, 1985). A laboratory aboard ship generated a spectrum of single- and multi-element anomalies that can be followed up whenever specific metal prices justify the effort.

Location and evaluation of satellite stocks east of the Coast Plutonic Complex could be achieved by reconnaissance geochemical surveys or regional-scale mapping. However, the fastest, most cost-effective method to find stocks within turbidites of the Bowser Basin--where potential for silver-rich vein and porphyry molybdenum deposits is probably greatest--would be a high-density aeromagnetic survey (flight-lines no more than 500 metres apart) covering an 80- to 100-kilometre-wide belt along the eastern edge of the Coast Plutonic Complex.

CHAPTER 6
CONCLUSIONS

The Stewart mining camp is underlain by an Upper Triassic to Lower Jurassic island arc complex. The sub-aerial volcanic pile is constructed of differentiated calc-alkaline basalts, andesites and dacites with interbedded sedimentary rocks. Lateral facies variations indicate that the district was a regional paleotopographic high with volcanic vents centred at Mount Dilworth and at Long Lake. Following subsidence this succession was capped by Middle Jurassic marine basin turbidites.

Early Jurassic calc-alkaline hornblende granodiorite plutons of the Texas Creek plutonic suite represent coeval, epizonal subsidiary magma chambers that underlay the stratovolcano at depths of two to five kilometres. From these plutons, late stage two-feldspar-porphyritic dykes cut up through the volcanic sequence to feed surface flows.

Mid-Cretaceous tectonism was characterized by greenschist facies regional metamorphism, east-northeast compression, and deformation. It produced upright north-northwest-trending *en echelon* folds and later east-verging ductile reverse faults and related penetrative fabrics.

Mid-Tertiary calc-alkaline biotite granodiorite of the Coast Plutonic Complex intruded the deformed arc complex, emplacing the batholith, stocks and differentiated dykes of the Hyder plutonic suite.

The 200 mineral occurrences of the district formed during two mineralizing events that were characterized by different base and precious metal suites. One ore-forming episode occurred in Early Jurassic time and the other in Eocene time. Both metallogenic epochs were brief, regional-scale phenomena. Some deposits from the younger mineralizing episode were emplaced adjacent to older deposits.

All Early Jurassic deposits were emplaced in andesitic to dacitic host rocks at the close of volcanic activity, about 185 million years ago. These deposits show regional zoning patterns that are spatially related to plutons of the Texas Creek suite and to the

stratigraphic position within the volcanic-sedimentary sequence. The Early Jurassic hydrothermal system derived its characteristic suite of silver, gold, zinc, lead and copper from the dominantly andesitic country rock.

Early Jurassic deposits include contemporaneous gold-pyrrhotite veins, silver-gold-base metal veins, and stratabound pyritic dacites. Gold-pyrrhotite veins formed in a transitional-mesothermal environment adjacent to the sub-volcanic plutons during late magma movement. Epithermal silver-gold-base metal veins and breccia veins were deposited along shallower faults and shears, and in hydrothermal breccia zones along sub-volcanic dyke contacts. Stratabound pyritic dacites are barren fumarole- and hotspring-related deposits that formed on the paleosurface from shallow groundwater circulation within hot dacitic pyroclastic sheets.

Tertiary silver-rich galena-sphalerite veins are related to intrusion of Middle Eocene biotite granodiorite stocks of the Coast Plutonic Complex. All deposits are locallized in brittle faults or fractures; most have southeast trends and subvertical dips. Likely sources for the silver in these Tertiary deposits are turbidite sequences within the Unuk River Formation and thicker, infolded turbidites of the Salmon River Formation.

Within the Stewart camp, these four deposit types can be selectively explored for by using diagnostic features such as stratigraphic and plutonic associations, alteration assemblages, gangue mineralogy and textures, sulphide mineralogy and textures, and precious metal ratios and lead isotope signatures. The most prospective geologic settings for each of these deposit types has been defined as a direct aid to exploration.

Variations in crustal thickness, composition, rock permeability and magma composition between Jurassic and Tertiary time produced the significant differences between deposits formed during growth of the Jurassic and Eocene magmatic arcs.

Minor lithostratigraphic and plutonic variations between widespread Early Jurassic volcanic centres contributed to differences in style, mineralogy and metal content of the Stewart, Kitsault and Sulphurets mining camps.

BIBLIOGRAPHY

Alldrick, D.J. (1983): Salmon River Project, Stewart, British Columbia (104B/1), *B.C. Ministry of Energy, Mines and Petroleum Resources*, Geological Fieldwork, 1982, Paper 1983-1, pages 182-195.

_____ (1984): Geologic Setting of the Precious Metal Deposits in the Stewart Area (104B/1), *B.C. Ministry of Energy, Mines and Petroleum Resources*, Geological Fieldwork, 1983, Paper 1984-1, pages 149-164.

_____ (1985): Stratigraphy and Petrology of the Stewart Mining Camp (104B/1), *B.C. Ministry of Energy, Mines and Petroleum Resources*, Geological Fieldwork, 1984, Paper 1985-1, pages 316-341.

_____ (1986): Stratigraphy and Structure in the Anyox Area (103P/5), *B.C. Ministry of Energy, Mines and Petroleum Resources*, Geological Fieldwork, 1985, Paper 1986-1, pages 211-216.

_____ (1987): Geology and Mineral Deposits of the Salmon River Valley, Stewart Area (104A, B), 1:50 000, *B.C. Ministry of Energy, Mines and Petroleum Resources*, Open File Report 1987-22.

_____ (1988): Detailed Stratigraphy of the Stewart Mining Camp, *in* Precious Metal Deposits of the Stewart Mining Camp, *Geological Association of Canada*, Field Trip Guidebook C, 15 pages.

_____ Editor (1988): Precious Metal Deposits of the Stewart Mining Camp, *Geological Survey of Canada*, Cordilleran Section, Geology and Metallogeny of Northwestern British Columbia Workshop, Field Trip Guidebook C.

_____ (1989): Volcanic Centres in the Stewart Complex, *B.C. Ministry of Energy, Mines and Petroleum Resources*, Geological Fieldwork, 1988, Paper 1989-1, pages 233-240.

Alldrick, D.J. and Britton, J.M. (1988): Geology and Mineral Deposits of the Sulphurets Area (104A/5, 12; 104B/8, 9), *B.C. Ministry of Energy, Mines and Petroleum Resources*, Open File 1988-4.

Alldrick, D.J., Britton, J.M., Webster, I.C.L. and Russell, C.W.P. (1989): Geology and Mineral Deposits of the Unuk Area (104B/7E, 8W, 9W, 10E), *B.C. Ministry of Energy, Mines and Petroleum Resources*, Open File 1989-10.

Alldrick, D.J., Brown, D.A., Harakal, J.E., Mortensen, J.K. and Armstrong, R.L. (1987): Geochronology of the Stewart Mining Camp (104B/1), *B.C. Ministry of Energy, Mines and Petroleum Resources*, Geological Fieldwork, 1986, Paper 1987-1, pages 81-92.

Alldrick, D.J. and Dawson, G.L. (1986): Geology of the Kitsault River Area (103P), *B.C. Ministry of Energy, Mines and Petroleum Resources*, Open File Map 1986-2.

Alldrick, D.J., Drown, T.J., Grove, E.W., Kruchkowski, E.R. and Nichols, R.F. (1989): Iskut-Sulphurets Gold, *Northern Miner*, January 1989, pages 46-49.

Alldrick, D.J., Gabites, J.E. and Godwin, C.I. (1987): Lead Isotope Data from the Stewart Mining Camp (104B/1), *B.C. Ministry of Energy, Mines and Petroleum Resources*, Geological Fieldwork, 1986, Paper 1987-1, pages 93-102.

Alldrick, D.J., Godwin, C.I., Gabites, J.E., and Pickering, A.D.R. (1990): Turning lead into gold: galena lead isotope data from the Anyox, Kitsault, Stewart, Sulphurets and Iskut Mining Camps, Northwest B.C., Geological Association of Canada/Mineralogical Association of Canada Annual Meeting, Program with Abstracts, page A-2.

Alldrick, D.J. and Kenyon, J.M. (1984): The Prosperity/Porter Idaho Silver Deposits (103P/13), *B.C. Ministry of Energy, Mines and Petroleum Resources*, Geological Fieldwork, 1983, Paper 1984-1, pages 165-172.

Alldrick, D.J., Mortensen, J.K. and Armstrong, R.L. (1986): Uranium-lead Age Determinations in the Stewart Area (104B/1), *B.C. Ministry of Energy, Mines and Petroleum Resources*, Geological Fieldwork, 1985, Paper 1986-1, pages 217-218.

Allen, D.G. (1964): Geology and Mineralogy of the Riverside Mine, Alaska, Unpublished B.Sc. Thesis, *The University of British Columbia*, 25 pages.

Allen, D.G., Panteleyev, A. and Armstrong, A.T. (1976): Galore Creek, *in* Porphyry Deposits of the Canadian Cordillera, *Canadian Institute of Mining and Metallurgy*, Special Volume 15, pages 402-414.

Anderson, E.M. (1937): The Dynamics of Formation of Cone Sheets, Ring Dykes and Cauldron Subsidences, Proceedings of the Royal Society of Edinburgh, Volume 56, pages 128-157.

Anderson, R.G. (1978): Preliminary Report on the Hotailuh Batholith, its Distribution, Age and Contact Relationships in the Cry Lake, Spatsizi and Deese Lake Map Areas, North-central British Columbia, *in* Current Research, Part A, *Geological Survey of Canada*, Paper 78-1A, pages 29-31.

_____ (1979): Distribution and Emplacement History of Plutons within the Hotailuh Batholith in the Cry Lake and Spatsizi Map Areas, North-central British Columbia, *in* Current Research, Part A, *Geological Survey of Canada*, Paper 79-1A, pages 393-395.

_____ (1980): Satellitic Stocks, Volcanic and Sedimentary Stratigraphy and Storucture around the Northern and Western Margins of the Hotailuh Batholith, North-central British Columbia, *in* Current Research, Part A, *Geological Survey of Canada*, Paper 80-1A, pages 37-40.

_____ (1983): Geology of the Hotailuh Batholith and Surrounding Volcanic and Sedimentary Rocks, North-central British Columbia, Unpublished Ph.D. Thesis, *Carleton University*, 669 pages.

_____ (1984): Late Triassic and Jurassic Magmatism along the Stikine Arch and the Geology of the Stikine Batholith, North-central British Columbia, *in* Current Research, Part A, *Geological Survey of Canada*, Paper 84-1A, pages 67-73.

_____ (1989): A Stratigraphic, Plutonic and Structural Framework for the Iskut River Map Area (NTS 104B), Northwestern British Columbia, *in* Current Research, Part E, *Geological Survey of Canada*, Paper 89-1E.

Anderson, R.G., and Bevier, M.L. (1990): A note on Mesozoic and Tertiary K-Ar Geochronometry of Plutonic Suites, Iskut River map area, northwestern British Columbia, *in* Current Research, Part E, *Geological Survey of Canada*, Paper 90-1E, p.141-147.

Anderson, R.G., and Thorkelson, D. J. (1990): Mesozoic stratigraphy and setting for some mineral deposits in Iskut River map area, northwestern British Columbia, in Current Research, Part E, Geological Survey of Canada, Paper 90-IF, pages 131-139.

Andrew, A., Godwin, C.I. and Sinclair, A.J. (1984): Mixing Line Isochrons: A New Interpretation of Galena Lead Isotope Data from Southeastern British Columbia, *Economic Geology*, Volume 79, pages 919-932.

Armstrong, J.E. (1944a): Preliminary Map, Smithers, British Columbia, *Geological Survey of Canada*, Paper 44-23.

_____ (1944b): Preliminary Map, Hazelton, British Columbia, *Geological Survey of Canada*, Paper 44-24.

_____ (1949): Fort St. James Map Area, *Geological Survey of Canada*, Memoir 252.

Armstrong, R.L. (1966): K/Ar Dating of Plutonic and Volcanic Rocks in Orogenic Belts, *in* Potassium-Argon Dating, O.A. Schaeffer and J. Zahringer, Editors, *Springer-Verlag*, Berlin, pages 117-133.

_____ (1968): A Model for the Evolution of Strontium and Lead Isotopes in a Dynamic Earth, *Review of Geophysics*, Volume 6, pages 175-199.

_____ (1986): Rb-Sr Dating of the Bokan Mountain Granite Complex and Its Country Rocks: Reply, *Canadian Journal of Earth Sciences*, Volume 23, pages 744-745.

_____ (1988): Mesozoic and Early Cenozoic Magmatic Evolution of the Canadian Cordillera, *Geological Society of America*, Special Paper 218, pages 55-91.

Arth, J.G., Barker, F., Stern, T.W. and Zmuda, C. (1986): The Coast Batholith near Ketchikan, Southeast Alaska: Geochronology and Geochemistry, *Geological Society of America*, Program with Abstracts, page 529.

Barnes, H.L., Editor (1979): Geochemistry of Hydrothermal Ore Deposits, *John Wiley and Sons*, Second Edition, 798 pages.

Barr, D.A. (1980): Gold in the Canadian Cordillera, *Canadian Institute of Mining and Metallurgy*, Bulletin, Volume 73, Number 818, pages 59-76.

Barton, P.B., Jr. and Bethke, P.M. (1987): Chalcopyrite disease in sphalerite: Pathology and epidemiology: Am. Mineralogist, Volume 72, pages 451-467.

Barton, P.B., Jr., Bethke, P.M., and Roedder, E. (1977): Environment of ore deposition in the Creede mining district, San Juan Mountains, Colorado: Part III. Progress toward interpretation of the chemistry of the ore-forming fluid for the OH vein, *Economic Geology*, Volume 72, pages 1 -24.

Beach, A. (1975): The Geometry of En-echelon Veins, *Tectonophysics*, Volume 28, pages 245-263.

_____ (1977): Vein Arrays, Hydraulic Fractures and Pressure-solution Structures in a Deformed Flysch Sequence, Southwestern England, *Tectonophysics*, Volume 40, pages 201-225.

_____ (1980): Numerical Models of Hydraulic Fracturing and the Interpretation of Syntectonic Veins, *Journal of Structural Geology*, Volume 2, Number 4, pages 425-438.

Berg H.C., Jones, D.L. and Richter, D.H. (1972): Gravina-Nutzotin Belt; Tectonic Significance of an Upper Mesozoic Sedimentary and Volcanic Sequence in Southern and Southeastern Alaska and Adjacent Areas, U.S. Geological Survey Professional Paper 800D, pages 1-24.

Berg, H.C., Jones, D.L. and Coney, P.J. (1978): Map Showing Pre- Cenozoic Tectonostratigraphic Terranes of Southeastern Alaska and Adjacent Areas, *United States Geological Survey*, Open File Report 78-1085.

Berger, G.W. and York, D. (1981): Geothermometry from $^{40}Ar/^{39}Ar$ Dating Experiments, *Geochimica et Cosmochimica Acta*, Volume 45, pages 795-811.

Beswick, A.E. and Soucie, G. (1978): A Correction Procedure for Metasomatism in an Archean Greenstone Belt, *Precambrian Research*, Volume 6, pages 235-248.

Bevins, R.E. and Rowbottom, G. (1983): Low-grade Metamorphism within the Welsh Sector of the Paratectonic Caledonides, *Geological Journal*, Volume 18, pages 141-167.

Boyle, R.W. (1979): The Geochemistry of Gold and its Deposits, Geological Survey of Canada, Bulletin 280, 584 pages.

Brew, D.A. and Morrell, R.P. (1983): Intrusive Rocks and Plutonic Belts of Southeastern Alaska, U.S.A., *in* Circum-Pacific Plutonic Terranes, *Geological Society of America*, Memoir 159, pages 171-194.

Britten, R.M. and Alldrick, D.J. (1990): Gold deposits in the Iskut-Stikine, Northwestern B.C., Abstract in Geological Association of Canada/Mineralogical Association of Canada Annual meeting, Program with Abstract, page A-15.

Britton, J.M. and Alldrick, D.J. (1988): Sulphurets Map Area (104A/05W, 12W; 104B/08E, 09E), *B.C. Ministry of Energy, Mines and Petroleum Resources*, Geological Fieldwork 1987, Paper 1988-1, pages 199-210.

Britton, J.M., Blackwell, J.D. and Schroeter, T.G. (1990): #21 Zone Deposits, Eskay Creek, Northwestern British Columbia, *B.C. Ministry of Energy, Mines and Petroleum Resources*, Exploration in British Columbia 1989, pages 197-223.

Britton, J.M., Fletcher, B.F. and Alldrick, D.J. (1990): Snippaker Map Area (104B/6E, 7W, 10W, 11E), *B.C. Ministry of Energy, Mines and Petroleum Resources*, Geological Fieldwork, 1989, Paper 1990-1, pages 115-125.

Britton, J.M., Webster, I.C.L. and Alldrick, D.J. (1989): Unuk Map Area, *B.C. Ministry of Energy, Mines and Petroleum Resources*, Geological Fieldwork 1988, Paper 1989-1, pages 241-250.

Brookfield, A.J., Compiler, (in preparation): Terrane Map of British Columbia, Compiled from Tectonic Assemblage Map of the Canadian Cordillera, J.O. Wheeler.

Brown, D.A. (1987): Geological Setting of the Volcanic-hosted Silbak Premier Mine, Northwestern British Columbia, Unpublished M.Sc. Thesis, *The University of British Columbia*, 216 pages.

Brown, G.C. (1982): Calc-alkaline Intrusive Rocks: Their Diversity, Evolution, and Relation to Volcanic Rocks, *in* Andesites, R.S. Thorpe, Editor, *John Wiley and Sons*, pages 437-461.

Buddington, A.F. (1925): Mineral Investigation in Southeastern Alaska, *United States Geological Survey*, Bulletin 773, pages 71-140.

_____ (1929): Geology of Hyder and Vicinity, Southeastern Alaska, *United States Geological Survey*, Bulletin 807, 124 pages.

_____ (1935): High-Temperature Mineral Associations at Shallow to Moderate Depths, *Economic Geology*, Volume 30, P.205-222.

Burton, W.D. (1926): Ore Deposition at Premier Mine, British Columbia, *Economic Geology*, Volume 21, Number 6, pages 586- 604.

Byers, F.M. and Sainsbury, C.L. (1956): Tungsten Deposits of the Hyder District, Alaska, *United States Geological Survey*, Bulletin 1024-F, pages 123-140.

Cannon, R.S., Pierce, A.P. and Antweiler, J.C. (1971): Suggested Uses of Lead Isotopes in Exploration, *in Canadian Institute of Mining and Metallurgy*, Special Volume 11, R.W. Boyle, Editor, pages 457-463.

Carter, N.C. (1972): Toodoggone River Area, *B.C. Department of Mines and Petroleum Resources*, Geology Exploration and Mining in British Columbia, pages 63-70.

_____ (1981): Porphyry Copper and Molybdenum Deposits of West-central British Columbia, *B.C. Ministry of Energy, Mines and Petroleum Resources*, Bulletin 64, 150 pages.

Cas and Wright, (1987): Volcanic Successions - Modern and Ancient, Allen and Unwin, 528 pages.

Cho, M. and Liou, J.G. (1987): Prehnite-Pumpellyite to Greenchist Facies Transition in the Karmutsen Metabasites, Vancouver Island, B.C., Journal of Petrology, Volume 28, pages 417-443.

Church, B.N. (1970): Geology of the Owen Lake, Parrott Lakes, and Goosly Lake area, B.C. Ministry of Energy, Mines and Petroleum Resources, GEM, pages 119-125.

_____ (1975): Quantitative Classification and Chemical Comparison of Common Volcanic Rocks, *Geological Society of America*, Bulletin, Volume 86, pages 257-263.

_____ (1978): Shackanite and Related Analcite-bearing Lavas in British Columbia, *Canadian Journal of Earth Sciences*, Volume 15, pages 1669-1672.

Church, B.N. and Barakso, J.J. (1989): Geology, Lithogeochemistry and Mineralization in the Buck Creek Area, British Columbia, *B.C. Ministry of Energy, Mines and Petroleum Resources*, Bulletin 78, 96 pages.

Coney, P.J., Jones, D.L. and Monger, J.W.H. (1980): Cordilleran Suspect Terranes, *Nature*, Volume 288, pages 329-333.

Cookenboo, H.O. and Bustin, R.M. (1989): Jura-Cretaceous (Oxfordian to Cenomanian) Stratigraphy of the North-central Bowser Basin, Northern British Columbia, Canadian Journal of Earth Sciences, Volume 26, pages 1001-1012.

Cox, D.P. and Singer, D.A., Editors (1986): Mineral Deposit Models, *United States Geological Survey*, Bulletin 1693, 379 pages.

Cox, K.G., Bell, J.D. and Pankhurst, R.J. (1979): The Interpretation of Igneous Rocks, *Allen and Unwin*, London.

Craig, J.R. and Vaughan, D.J. (1981): Ore Microscopy and Ore Petrography, *John Wiley and Sons*, New York, 406 pages.

Cumming, G.L. and Richards, J.R. (1975): Ore Lead Isotope Ratios in a Continuously Changing Earth, *Earth and Planetary Science Letters*, Volume 28, pages 155-171.

Currie, L. (1984): The Provenance of Chert Clasts in the Ashman Conglomerate of the Northeastern Bowser Basin, B.Sc. Thesis, *Queen's University*, 55 pages.

Davis, G.H. (1984): Structural Geology of Rocks and Regions, *John Wiley and Sons*, New York, 492 pages.

Dawson, G.L. and Alldrick, D.J. (1986): Geology and Mineral Deposits of the Kitsault Valley (103P/11, 12), *B.C. Ministry of Energy, Mines and Petroleum Resources*, Geological Fieldwork, 1985, Paper 1986-1, pages 219-224.

Dawson, G.M. (1877): Report on Explorations in British Columbia, *Geological Survey of Canada*, Report on Progress, 1875-1876, pages ??-??.

Deer, W.A., Howie, R.A. and Zussman, J. (1963): Rock Forming Minerals, Volume 3, *Longman's*, London, 270 pages.

Deer, W.A., Howie, R.A. and Zussman, J. (1966): An Introduction to the Rock-forming Minerals, *Longmans*, London, 528 pages.

de Rosen-Spence, A.F. (1976): Stratigraphy, Development and Petrogenesis of the Central Noranda Volcanic Pile, Noranda, Quebec, Unpublished Ph.D. Thesis, *University of Toronto*.

_____ (1985): Shoshonites and Associated Rocks of Central British Columbia, *B.C. Ministry of Energy, Mines and Petroleum Resources*, Geological Fieldwork, 1984, Paper 1985-1, pages 426-442.

de Rosen-Spence, A.F. and Sinclair, A.J. (1987): Classification of the Cretaceous Volcanic Sequences of British Columbia and Yukon, *B.C. Ministry of Energy, Mines and Petroleum Resources*, Geological Fieldwork, 1986, Paper 1987-1, pages 419-427.

de Rosen-Spence, A.F. and Sinclair, A.J. (1988): Lower Jurassic Volcanism of the Stikine Super-terrane, *B.C. Ministry of Energy, Mines and Petroleum Resources*, Geological Fieldwork, 1987, Paper 1988-1, pages 211-216.

Devlin, B.D. and Godwin, C.I. (1986): Geology and Genesis of the Dolly Varden Silver Camp, Alice Arm Area, Northwestern British Columbia, *in* Geoexpo '86, Program with Abstracts, *Geological Association of Canada*, page 34.

Diakow, L.J. (1990): Volcanism of the Toodoggone Formation, B.C., unpublished Ph.D. thesis, The University of Western Ontario, 179 pages.

Diakow, L. and Koyanagi, V. (1988): Stratigraphy and Mineral Occurrences of Chickamin Mountain and Whitesail Reach Map Areas (93E/06, 10), *B.C. Ministry of Energy, Mines and Petroleum Resources*, Geological Fieldwork, 1987, Paper 1988-1, pages 155-168.

Dick, D.L. (1988): Summit Lake Mine, *B.C. Ministry of Energy, Mines and Petroleum Resources*, Assessment Report 16768, 16 pages.

Dodson, M.H. (1973): Closure Temperature in Cooling Geochronological and Petrological Systems, *Contributions, Mineralogy and Petrology*, Volume 40, pages 259-274.

Doe, B.R. and Zartman, R.E. (1979): Plumbotectonics, the Phanerozoic, *in* Geochemistry of Hydrothermal Ore Deposits, H.L. Barnes, Editor, *John Wiley and Sons*, New York, pages 22- 70.

Duffell, S. (1959): Whitesail Lake Map Area, British Columbia. Geological Survey of Canada, Memoir 299, 119 pages.

Duffell, S. and Souther, J.G. (1964): Geology of Terrace Map-area, British Columbia, *Geological Survey of Canada*, Memoir 329, 117 pages.

Dupas, J.P. (1985): Geology of the Spider Claim Group on Long Lake (104A/4), *B.C. Ministry of Energy, Mines and Petroleum Resources*, Geological Fieldwork, 1984, Paper 1985-1, pages 308-315.

Durney, D.W. and Ramsay, J.G. (1973): Incremental Strains Measured by Syntectonic Crystal Growths, *in* Gravity and Tectonics, K.A. DeJong and R. Scholten, Editors, *John Wiley and Sons*, New York, pages 67-96.

Dykes, S.M., Meade, H.D. and Galley, A.G. (1986): Big Missouri Precious-base Metal Deposit, Northwest British Columbia, *in* Mineral Deposits of the Northern Cordillera, *Canadian Institute of Mining and Metallurgy*, Special Volume 18, pages 202-215.

Dykes, S.M., Payne, J. and Sisson, W. (1988): Big Missouri Precious-base Metal Deposit, Northwest British Columbia, *in* Northern Cordilleran Precious Metal Deposits, *Society of Economic Geologists*, Field Trip Guidebook, 24 pages.

Eisbacher, G.H. (1973): Sedimentary History and Tectonic Evolution of the Sustut and Sifton Basins, North-central British Columbia, *Geological Survey of Canada*, Paper 73-31, 58 pages.

_____ (1974a): Sedimentary History and Tectonic Evolution of the Sustut and Sifton Basins, North-central British Columbia, *Geological Survey of Canada*, Paper 73-31, 57 pages.

_____ (1974b): Deltaic Sedimentation in the Northeastern Bowser Basin, British Columbia, *Geological Survey of Canada*, Paper 73-33, 13 pages.

_____ (1974c): Evolution of Successor Basins in the Canadian Cordillera, *in* Modern and Ancient Geosynclinal Sedimentation, *Society of Economic Paleontologists and Mineralologists*, Special Publication 19, pages 274-290.

_____ (1977): Mesozoic-Tertiary Basin Models for the Canadian Cordillera and their Geological Constraints, *Canadian Journal of Earth Sciences*, Volume 14, pages 2414-2531.

_____ (1981): Late Mesozoic-Paleogene Bowser Basin Molasse and Cordilleran Tectonics, Western Canada, *in* Sedimentation and Tectonics in Alluvial Basins, A.D. Miall, Editor, *Geological Association of Canada*, Special Paper 23, pages 125-151.

Erdman, L.R. (1985): Chemistry of Neogene Basalts of British Columbia and Adjacent Pacific Ocean Floor: A Test of Tectonic Discrimination Diagrams, Unpublished M.Sc. Thesis, *The University of British Columbia*, 294 pages.

Evenchick, C.A. (1986): Structural Style of the Northeast Margin of the Bowser Basin, Spatsizi Map Area, North-central British Columbia, *in* Current Research, Part B, *Geological Survey of Canada*, Paper 86-1B, pages 733-739.

_____ (1987): Stratigraphy and Structure of the Northeast Margin of the Bowser Basin, Spatsizi Map Area, North-central British Columbia, *in* Current Research, Part A, *Geological Survey of Canada*, Paper 87-1A, pages 719-726.

Ewanchuk, H.G. (1961): Geology and Ore-deposition of the Silbak Premier Mine Glory Hole, Unpublished B.Sc. Thesis, *The University of British Columbia*, 45 pages.

Ewart, A. (1979): A Review of the Mineralogy and Chemistry of Tertiary-Recent Dacitic, Latitic, Rhyolitic and Related Rocks, *in* Trondhjemites, Dacites and Related Rocks, F. Barker, Editor, *Elsevier Scientific Publishing Company*, New York, pages 13-121.

_____ (1982): The Mineralogy and Petrology of Tertiary-Recent Orogenic Volcanic Rocks: With Special Reference to the Andesitic-basaltic Compositional Range, *in* Andesites: Orogenic Andesites and Related Rocks, R.S. Thorpe, Editor, *John Wiley and Sons*, England, pages 25-95.

Ewing, T.E. (1981): Petrology and Geochemistry of the Kamloops Group Volcanics, British Columbia, *Canadian Journal of Earth Sciences*, Volume 18, pages 1478-1491.

Faure, G. (1977): Principles of Isotope Geology,, *John Wiley and Sons*, New York, 464 pages.

_____ (1986): Principles of Isotope Geology, *Second Edition, John Wiley and Sons*, New York, 589 pages.

Fisher, R.V. and Schminke, H.-U. (1984): Pyroclastic Rocks, Springer-Verlag, 472 pages.

Fleet, M.E., MacLean, P.J., and Barbier, J. (1989): Oscillatory-zoned As-bearing pyrite from strata-bound and stratiform gold deposits: an indicator of ore fluid formation, in Economic Geology Monograph 6, pages 356-362.

Forster, D.B. (1984): Geology, Petrology and Precious Metal Mineralization, Toodoggone River Area, North-central British Columbia, Unpublished M.Sc. Thesis, *The University of British Columbia*, 313 pages.

Gabites, J.E., Pickering, A.D.R., and Godwin, C.I. (1990): Lead isotope analysis, laboratory techniques and accumulated wisdom, unpublished Laboratory Manual, Geochronology Laboratory, Department of Geological Sciences, The University of British Columbia, 41 pages.

Gabrielse, H. (1979): Geology of Cry Lake Map Area, *Geological Survey of Canada*, Open File Map 610.

_____ (1985): Major Dextral Transcurrent Displacement along the Northern Rocky Mountain Trench and Related Lineaments in North-central British Columbia, *Geological Society of America*, Bulletin, Volume 96, pages 1-14.

Gabrielse, H., Monger, J.W.H., Tempelman-Kluit, D.J. and Woodsworth, D.J. (in preparation): Intermontane Belt, *in* Decade of North American Geology, Special Volume.

Gabrielse, H., Wanless, R.K., Armstrong, R.L. and Erdman, L.R. (1980): Isotopic Dating of Early Jurassic Volcanism and Plutonism in North-central British Columbia, *in* Current Research, Part A, *Geological Survey of Canada*, Paper 80-1A, pages 27-32.

Galley, A.G. (1981): Volcanic Stratigraphy and Gold-silver Occurrences on the Big Missouri Claim Group, Stewart, British Columbia, Unpublished M.Sc. Thesis, *University of Western Ontario*, 181 pages.

Gebauer, D. and Grunenfelder, M. (1979): U-Th-Pb Dating of Minerals, *in* Lectures in Isotope Geology, E. Jager and J.C. Hunziker, Editors, *Springer*, Berlin, pages 105-131.

Geological Survey of Canada (1957): Stikine River Area, Cassiar District, British Columbia, Operation Stikine, Map 9-1957.

Gill, J.B. (1981): Orogenic Andesites and Plate Tectonics, *Springer-Verlag*, New York, 390 pages.

Godwin, C.I. and Sinclair, A.J. (1982): Average Lead Isotope Growth Curves for Shale-Hosted Lead-Zinc Deposits, Canadian Cordillera, *Economic Geology*, Volume 77, pages 675-690.

Godwin, C.I., Gabites, J.E., and Andrew, A., (1988): Leadtable: a galena lead isotope database for the Canadian Cordillera, B.C. Ministry of Energy, Mines and Petroleum Resources, Paper 1988-4, 188 pages.

Griffiths, J.R. (1977): Mesozoic-Early Cenozoic Volcanism, Plutonism and Mineralization in Southern British Columbia: A Plate Tectonic Synthesis, *Canadian Journal of Earth Sciences*, Volume 14, pages 1611-1624.

Griffiths, J.R. and Godwin, C.I. (1983): Metallogeny and Tectonics of Porphyry Copper-molybdenum Deposits in British Columbia, *Canadian Journal of Earth Sciences*, Volume 20, pages 1000-1018.

Grove, E.W. (1971): Geology and Mineral Deposits of the Stewart area, British Columbia, *B.C. Ministry of Energy, Mines and Petroleum Resources*, Bulletin 58, 229 pages.

_____ (1973): Detailed Geological Studies in the Stewart Complex, Northwestern British Columbia, Unpublished Ph.D. Thesis, *McGill University*, 434 pages.

_____ (1986): Geology and Mineral Deposits of the Unuk River - Salmon River - Anyox Area, *B.C. Ministry of Energy, Mines and Petroleum Resources*, Bulletin 63, 152 pages.

Grove, T.L. and Kinzler, R.J. (1986): Petrogenesis of Andesites, *in* Annual Review, *Earth and Planetary Sciences*, Volume 14, pages 417-454.

Gulson, B.L. (1986): Lead Isotopes in Mineral Exploration, *Elsevier*, Amsterdam, 258 pages.

Hamilton, W. (1969): The Volcanic Central Andes - A Modern Model for the Cretaceous Batholiths and Tectonics of Western North America, Proceedings of the Andesite Conference, *Oregon Department of Geology and Mineral Industries*, Bulletin 65, pages 175-184.

Hancock, P.L. (1972): The Analysis of En-echelon Veins, *Geological Magazine*, Volume 109, Number 3, pages 269-276.

Hanson, G. (1929): Bear River and Stewart Map-areas, Cassiar District, British Columbia, *Geological Survey of Canada*, Memoir 159, 84 pages.

_____ (1935): Portland Canal Area, British Columbia, *Geological Survey of Canada*, Memoir 175, 179 pages.

Harper, C.T. (1964): Potassium-argon Ages of Slates and their Geological Significance, *Nature*, Volume 203, pages 468-470..

_____ Editor, (1973): Geochronology: Radiometric Dating of Rocks and Minerals, *Dowden, Hutchinson and Ross*, Stroudsberg, 469 pages.

Hayba, D.O., Bethke, P.M., Heald, P. and Foley, N.K. (1985): Geologic, Mineralogic and Epithermal Characteristics of Volcanic-hosted Epithermal Precious-metal Deposits, *in* Geology and Geochemistry of Epithermal Systems, B.R. Berger and P.M. Bethke, Editors, *Reviews in Economic Geology*, Volume 2.

Heald, P., Foley, N.K. and Hayba, D.O. (1987): Comparative Anatomy of Volcanic-hosted Epithermal Deposits: Acid-sulfate and Adularia-sericite Types, *Economic Geology*, Volume 82, Number 1, pages 1-26.

Henley, R.D. and Ellis, A.J. (1983): Geothermal Systems, Ancient and Modern; Earth Science Reviews, Volume 19, pages 1-50.

Hietanen, A. (1967): On the Facies Series in Various Types of Metamorphism, *Journal of Geology*, Volume 75, pages 187-214.

Hill, M.L. (1984): Geology of the Redcap Mountain Area, Coast Plutonic Complex, British Columbia, Unpublished Ph.D. Thesis, *Princeton University*, 216 pages.

Hodgson, C.J. (1990): Uses (and Abuses) of Ore Deposit Models in Mineral Exploration, Geoscience Canada, Volume 17, Number 2, pages 79-89.

Holbek, P.M. (1983): Ore Petrography of the Big Missouri Deposit, Northwestern British Columbia, Unpublished Directed Studies Report, *The University of British Columbia*, 35 pages.

_____ (1984): Ore Petrography and Sulphide Mineralogy of the Mount Walker-Mineral Basin Property, Hyder, Alaska, Unpublished Report, *Pulsar Energy and Resources*, 32 pages.

Holmes, A. (1946): An Estimate of the Age of the Earth, *Nature*, Volume 157, pages 681-684.

_____ (1947): A Revised Estimate of the Age of the Earth, *Nature*, Volume 159, page 127.

Holopainen, K. (1984): Mineralogy of Eight Sulphide Specimens from the Scottie Gold Mine, Unpublished Course Report, *The University of British Columbia*, 14 pages.

Houtermans, F.G. (1946): The Isotopic Abundances in Natural Lead and the Age of Uranium, *Naturwissenschaften*, Volume 33, pages 185-186.

Höy, T. and Andrew, K. (1989): The Rossland Group, Nelson Map Area, Southeastern British Columbia (82F/6), *B.C. Ministry of Energy, Mines and Petroleum Resources*, Geological Fieldwork, 1988, Paper 1989-1, pages 33-43.

Hudson, T., Smith, J.G., and Elliott, R.L. (1979): Petrology, composition and age of intrusive rocks associated with the Quartz Hill molybdenite deposit, southeastern Alaska. Canadian Journal of Earth Sciences, Volume 16, pages 1805-1822.

Irvine, T.N. and Baragar, W.R.A. (1971): A Guide to the Chemical Composition of the Common Volcanic Rocks, *Canadian Journal of Earth Sciences*, Volume 8, pages 523-548.

Jäger, E. (1965): Rb-Sr Age Determinations on Minerals and Rocks from the Alps, *in* Geochronologie Absolute, Centre.

Jenson, L.S. (1976): A New Cation Plot for Classifying Subalkalic Volcanic Rocks, *Ontario Department of Mines*, Miscellaneous Paper 66, 22 pages.

Johnson, R.B. (1961): Patterns and Origin of Radial Dyke Swarms Associated with West Spanish Peak and Dyke Mountain, South-Central Colorado: Geological Society of America Bulletin, Volume 72, pages 579-590.

Jones, D.L., Howell, D.G., Coney, P.J. and Monger, J.W.H. (1983): Recognition, Character, Analysis of Tectonostratigraphic Terranes in Western North America, *in* Accretion Tectonics in the Circum-Pacific Regions, M. Hashimoto and S. Uyeda, Editors, *Terra Scientific Publishing Company*, Tokyo, pages 21-35.

Jordan, T.E., Isacks, B.L., Allmendinger, R.W., Brewer, J.A., Ramos, V.A. and Ando, C.J. (1983): Andean Tectonics Related to Geometry of Subducted Nazca Plate, *Geological Society of America*, Bulletin, Volume 94, pages 341-361.

Kemp, C.J.T. (1988): The Jökulhlaup Phenomenon in the Stewart Area, British Columbia, Unpublished Work Term Report, *University of Victoria*, 29 pages.

Kenyon, J.M. (1983a): 1983 Summary Report on the Prosperity, Porter-Idaho Silver Property, Unpublished Company Report, 11 pages.

_____ (1983b): Probable, Possible and Geological Reserves of the Prosperity, Porter-Idaho Mine, Unpublished Company Report, 11 pages.

Kerr, F.A. (1948a): Lower Stikine and Iskut River Areas, British Columbia, *Geological Survey of Canada*, Memoir 246, 94 pages.

_____ (1948b): Taku River Map Area, *Geological Survey of Canada*, Memoir 248.

Kerr, P.F. (1959): Optical Mineralogy, *McGraw-Hill*, New York, 442 pages.

Kerrich, R. and Allison, I. (1978): Vein Geometry and Hydrostatics during Yellowknife Mineralization, *Canadian Journal of Earth Sciences*, Volume 15, pages 1653-1660.

Kindle, E.D. (1940): Mineral Resources, Hazelton and Smithers Areas, Cassiar and Coast Districts, British Columbia, *Geological Survey of Canada*, Memoir 223, 107 pages.

_____ (1954): Mineral Resources, Hazelton and Smithers Areas, Geological Survey of Canada Memoir 223 (revised).

Klepaki, D. (1980): Silver Bar Property Geology Map, in B.C. Ministry of Energy, Mines and Petroleum Resources Assessment Report No. 8909.

Knopf, A. (1936): Igneous Geology of the Spanish Peaks Region, Colorado, Geological Society of America Bulletin, Volume 47, pages 1727-1784.

Koppel, V. and Grunenfelder, M. (1979): Isotope Geochemistry of Lead, *in* Lectures in Isotope Geology, E. Jager and J.C. Hunziker, Editors, *Springer-Verlag*, Berlin, pages 134-153.

Kretschmar, U. and Kretschmar, D. (1980a): Geological Report - Munro Claim Group, *B.C. Ministry of Energy, Mines and Petroleum Resources*, Assessment Report 8540.

_____ (1980b): Geological Report - Snow Claim Group, *B.C. Ministry of Energy, Mines and Petroleum Resources*, Assessment Report 8602.

Krogh, T.E. (1973): A Low Contamination Method for Hydrothermal Decomposition of Zircon and Extraction of U and Pb for Isotopic Age Determinations, *Geochimica et Cosmochimica Acta*, Volume 37, pages 485-494.

_____ (1982a): Improved Accuracy of U-Pb Zircon Ages by the Creation of more Concordant Systems using an Air Abrasion Technique, *Geochimica et Cosmochimica Acta*, Volume 46, pages 637-649.

_____ (1982b): Improved Accuracy of U-Pb Zircon Dating by Selection of more Concordant Fractions using a High Gradient Magnetic Separation Technique, *Geochimica et Cosmochimica Acta*, Volume 46, pages 631-635.

Kuno, H. (1966): Lateral Variation of Basalt Magma Types across Continental Margins and Island Arcs, *Volcanology*, Bulletin, Volume 29, pages 195-222.

Lane, R.W. (1986): Silbak Premier Assessment Report, B.C. Ministry of Energy, Mines and Petroleum Resources Assessment Report No. 15762, 13 pages.

Langille, E.G. (1945): Some Controls of Ore Deposits at the Premier Mine, *Western Miner*, Volume 18, Number 6, pages 44- 50.

Laznicka, P. (1985): Empirical Metallogeny, Developments in Economic Geology, Volume 19, *Elsevier*, Amsterdam, 1758 pages.

Leach, W.W. (1909): The Bulkley Valley and Vicinity, *Geological Survey of Canada*, Summary Report, 1908.

_____ (1910): The Skeena River District, *Geological Survey of Canada*, Summary Report, 1909.

LeBas, M.J., LeMaitre, R.W., Steckeisen, A.L. and Zanettin, B. (1986): Chemical Classification of Volcanic Rocks based on the Total Alkali-silica Diagram, *Journal of Petrology*, Volume 27, pages 745-750.

LeMaitre, R.W. (1976): The Chemical Varibility of some Igneous Rocks, *Journal of Petrology*, Volume 17, pages 589-637.

Lindgren, W. (1933): Mineral Deposits, 4th edition, New York, *McGraw-Hill*, 930 pages.

Liou, J.G., Maruyama, S. and Cho, M. (1985): Phase Equilibria and Mineral Parageneses of Metabasites in Low-grade Metamorphism, *Mineralogical Magazine*, Volume 49, pages 321-333..

Lord, C.S. (1948): McConnell Creek Map Area, Cassiar District, British Columbia, *Geological Survey of Canada*, Memoir 251, 72 pages.

Lowell, J.D. and Guilbert, J.M. (1970): Lateral and Vertical Alteration-mineralization Zoning in Porphyry Ore Deposits, *Economic Geology*, Volume 65, Number 4, pages 373-408.

Ludwig, K.R. (1980): Calculation of Uncertainities of U-Pb Isotopic Data, *Earth and Planetary Science Letters*, Volume 46, pages 212-220.

McClay, K.R. (1987): The Mapping of Geological Structures, *Open University Press*, Mitton Keynes, England, 161 pages.

McConnell, R.G. (1910): Portland Canal District, *Geological Survey of Canada*, Summary Report, 1909, pages 59-90.

_____ (1911a): Salmon River District, British Columbia, *Geological Survey of Canada*, Summary Report, 1910, pages 50- 56.

_____ (1911b): Portland Canal District, British Columbia, *Geological Survey of Canada*, Summary Report, 1910, pages 56- 71.

_____ (1913): Portions of Portland Canal and Skeena Mining Divisions, Skeena District, British Columbia, *Geological Survey of Canada*, Memoir 32, 101 pages.

MacDonald, B.W.R. (1987): Geology and Genesis of the Mount Skukum Tertiary Epithermal Gold-Silver Vein Deposit, Southwestern Yukon Territory (105D/SW), unpublished M.Sc. thesis, The University of British Columbia.

McDonald, D.W. (1987a): Proposal for B.C. Geoscience Research Grant, B.C. Ministry of Energy, Mines and Petroleum Resources, 10 pages.

_____ (1987b): Progress Report for B.C. Geoscience Research Grant, B.C. Ministry of Energy, Mines and Petroleum Resources, 5 pages.

_____ (1988a): Metallic Minerals in the Silbak Premier Silver-Gold Deposit, Stewart (104B/1), Geological Fieldwork, 1987, Paper 1988-1, pages 349-352.

_____ (1988b): Timing of Mineralization and Alteration at the Silbak Premier Silver-Gold Deposit, British Columbia, Abstract in Proceedings of BICENTENNIAL GOLD '88, Melbourne, Australia, May, 1988.

_____ (1988c): Progress Report for Westmin Resources Limited, May, 1988, 72 pages.

_____ (1988d): Geologic Setting, Structural Control and Wall Rock Alteration of the Epithermal Silver-Gold Silbak Premier Deposit, Stewart, B.C., Abstract In G.A.C. Proceedings, May 1988, page A3.

_____ (1990a): Temperature and Composition of Fluids in the Base Metal Rich Silbak Premier Ag-Au Deposit, Stewart, B.C., Geological Fieldwork, 1989, Paper 1990-1, pages 323-335.

_____ (1990b): The Silbak Premier Silver-Gold Deposit: A Structurally controlled, Base Metal Rich Cordilleran Epithermal Deposit, Stewart, B.C., unpublished Ph.D. thesis, The University of Western Ontario, London, Canada, 411 pages.

McDougall, B.W.W. (1950): The Big Four Silver Mine, Marmot River Area, Unpublished Company Report, 22 pages.

McGuigan, P.J. (1985): Summary Report of 1985 Exploration Program on the Indian Property, *B.C. Ministry of Energy, Mines and Petroleum Resources*, Assessment Report 14111.

MacIntyre, D.G. (1985): Geology and Mineral Deposits of the Tahtsa Lake District, West-central British Columbia, *B.C. Ministry of Energy, Mines and Petroleum Resources*, Bulletin 75, 82 pages.

McKenzie, K.J. (1985): Sedimentology and Stratigraphy of the Southern Sustut Basin, North-central British Columbia, M.Sc. Thesis, *The University of British Columbia*, 120 pages.

MacKenzie, W.S., Donaldson, C.H. and Guilford, C. (1982): Atlas of Igneous Rocks and their Textures, London, *Longman*, 148 pages.

Marsden, H. and Thorkelson, D.J. (in press): Geology of the Hazelton Volcanic Belt in British Columbia; Implications for the Early to Middle Jurassic Evolution of Stikinia, Tectonics.

Massey, N.M. (1988): Trace Element Discrimination Diagrams: Some Notes, Observations, Cautions and a Modus Operandi, unpublished course notes, 19 pages.

Mattinson, J.M. (1978): Age, Origin and Thermal Histories of some Plutonic Rocks from the Salinian Block of California, *Contributions to Mineralogy and Petrology*, Volume 67, pages 233-245.

Meade, H.D. (1977): Petrology and Metal Occurrences of the Takla Group and Hogem and Germansen Batholiths, North Central British Columbia, Unpublished Ph.D. Thesis, *The University of Western Ontario*.

Mihalynuk, M.G. (1987): Evolution of the Telkwa Formation near Terrace, British Columbia, Unpublished M.Sc. Thesis, *The University of Calgary*, 130 pages.

Miyashiro, A. (1973): Metamorphism and Metamorphic Belts, George Allen & Unwin, 481 pages.

_____ (1974): Volcanic Rock Series in Island Arcs and Active Continental Margins, *American Journal of Science*, Volume 274, pages 321-355.

_____ (1975): Volcanic Rock Series and Tectonic Setting, *in* Annual Review, *Earth and Planetary Sciences*, Volume 3, pages 251-269.

Miyashiro, A. and Shido, F. (1975): Tholeiitic and Calc-alkalic Series in Relation to the Behaviors of Titanium, Vanadium, Chromium and Nickel, *American Journal of Science*, Volume 275, pages 265-277.

Monger, J.W.H. (1977a): Upper Paleozoic Rocks of the Western Cordillera and their Bearing on Cordilleran Evolution, *Canadian Journal of Earth Sciences*, Volume 14, pages 1832- 1859.

_____ (1977b): The Triassic Takla Group in McConnell Creek Map-area, North-central British Columbia, *Geological Survey of Canada*, Paper 76-29, 45 pages.

_____ (1984): Cordilleran Tectonics: A Canadian Perspective, *Societe Geologique de France*, Bulletin, Volume XXVI, Number 2, pages 255-278.

Monger, J.W.H. and Church, B.N. (1977): Revised Stratigraphy of the Takla Group, North-central British Columbia, *Canadian Journal of Earth Sciences*, Volume 14, pages 318-326.

Monger, J.W.H. and Price, R.A. (1979): Geodynamic Evolution of the Canadian Cordillera - Progress and Problems, *Canadian Journal of Earth Sciences*, Volume 16, pages 770-791.

Monger, J.W.H., Price, R.A. and Tempelman-Kluit, D.J. (1982): Tectonic Accretion and the Origin of the Two Major Metamorphic and Plutonic Welts in the Canadian Cordillera, *Geology*, Volume 10, pages 70-75.

Monger, J.W.H., Richards, T.A. and Paterson, I.A. (1978): The Hinterland Belt of the Canadian Cordillera: New Data from Northern and Central British Columbia, *Canadian Journal of Earth Sciences*, Volume 15, pages 823-830.

Monger, J.W.H., Souther, J.G. and Gabrielse, H. (1972): Evolution of the Canadian Cordillera: A Plate Tectonic Model, *American Journal of Science*, Volume 272, pages 577-602.

Monger, J.W.H. and Thorstad, L.E. (1978): Lower Mesozoic Stratigraphy, Cry Lake and Spatsizi Map Areas, British Columbia, *in* Current Research, Part A, *Geological Survey of Canada*, Paper 78-1A, pages 21-24.

Moorbath, S. (1985): The Age of the Earth and the Oldest Rocks, *Geology Today*, Volume 1, pages 75-79.

Morton, R.L. (1976): Alkalic Volcanism and Cu Deposits of the Horsefly Area, Central British Columbia, Unpublished Ph.D. Thesis, *Carleton University*.

Mullen, E.D. (1983): $MnO/TiO_2/P_2O_5$: A Minor Element Discriminant for Basalt Rocks of Oceanic Environments and its Implications for Petrogenesis, *Earth and Planetary Science Letters*, Volume 62, pages 53-62.

Nesbitt, B.E. (1988): Gold Deposit Continuum: A Genetic Model for Lode Au Mineralization in the Continental Crust, Geology, Volume 16, pages 1044-1048.

Nicolini, P. (1970): Gitologie des Concentrations Minerales Stratiformes, *Gauthier-Villars*, Paris, 792 pages.

North American Commission on Stratigraphic Nomenclature (1983): North American Stratigraphic Code, *American Association of Petroleum Geologists*, Bulletin, Volume 67, Number 5, pages 841-875.

Northern Miner Press (1989): Canadian Mines Handbook 1988-1989, Northern Miner Press, Toronto, Canada.

O'Neill, J.J. (1919): Salmon River District, Portland Canal Mining Division, British Columbia, *Geological Survey of Canada*, Summary Report, 1909, Part B, pages 7-11.

Ozand, J.M. and Russell, R.D. (1970): Discrimination in Solid Source Lead Isotope Abundance Measurement, *Earth and Planetary Science Letters*, Volume 8, pages 331-336.

Palmer, A.R. (1983): The Decade of North American Geology, 1983 Geological Time Scale, *Geology*, Volume 11, Number 9, pages 503-504.

Panteleyev, A. (1986): Ore Deposits Number 10, A Canadian Cordilleran Model for Epithermal Gold-silver Deposits, *Geoscience Canada*, Volume 13, Number 2, pages 101-111.

_____ (1990): Gold in the Canadian Cordillera -- A focus on mesothermal and epithermal environments; in: Ore deposits, tectonics and metallogeny in the Canadian Cordillera, GAC/MAC Short Course Notes, May, 1990. 44 pages.

Parrish, R. and Roddick, J.C. (1984): Geochronology and Isotope Geology for the Geologist and Explorationist, *Geological Association of Canada*, Cordilleran Section, Short Course Number 4, 71 pages.

Paterson I.A. and Harakal, J.E. (1974): Potassium-argon Dating of Blueschists from Pinchi Lake, Central British Columbia; Canadian Journal of Earth Sciences, Volume 11, pages 1007-1011.

Pearce, J.A. (1982): Trace Element Characteristics of Lavas from Destructive Plate Boundaries, *in* Andesites: Orogenic Andesites and Related Rocks, R.S. Thorpe, Editor, *John Wiley and Sons*, England, pages 25-95.

_____ (1983): Role of the Sub-continental Lithosphere in Magma Genesis at Active Continental Margins, *in* Continental Basalts and Mantle Xenoliths, C.J. Hawkesworth and M.J. Norry, Editors, *Shiva Publishing Limited*, pages 230-249.

Pearce, T.H., Gorman, B.E. and Birkett, T.C. (1975): The TiO_2-K_2O-P_2O_5 Diagram: A Method of Discriminating between Oceanic and Non-oceanic Basalts, *Earth and Planetary Science Letters*, Volume 24, pages 419-426.

Pearce, T.H., Gorman, B.E. and Birkett, T.C. (1977): The Relationship between Major Element Chemistry and Tectonic Environment of Basic and Intermediate Volcanic Rocks, *Earth and Planetary Science Letters*, Volume 36, pages 121-132.

Petro, W.L., Vogel, T.A. and Wilband, J.T. (1979): Major-element Chemistry of Plutonic Rock Suites from Compressional and Extensional Plate Boundaries, *Chemical Geology*, Volume 26, pages 217-235.

Phillips, P. (1989): Silbak Premier, The Northern Miner Magazine, May, 1989, pages 15-16.

Phillips, W.J. (1986): Hydraulic Fracturing Effects in the Formation of Mineral Deposits, Transactions, *Institute of Mining and Metallurgy*, Section B, Applied Earth Science, Volume 95, pages B17-B24.

Phillips, W.R. and Griffen, D.T. (1981): Optical Mineralogy, *W.H. Freeman and Company*, San Francisco, 677 pages.

Picot, P. and Johan, Z. (1977): Atlas des Mineraux Metalliques, *Bureau de Recerches Geologiques et Minieres*, Memoir 90, 403 pages.

Plumb, W.N. (1956): Report on the M.J. Mineral Deposits, Unpublished Company Report, 10 pages.

_____ (1957): Preliminary Geological Report on the Silver Tip Mine, Unpublished Company Report, 13 pages.

Price, R.A., Monger, J.W.H. and Muller, J.E. (1981): Cordilleran Cross-section - Calgary to Victoria, *in* Field Guides to Geology and Mineral Deposits, *Geological Association of Canada*, 1981 Annual Meeting.

Ramdohr, P. (1980): The Ore Minerals and their Intergrowths, *Pergamon Press*, Oxford, 1205 pages.

Randall, A.W. (1988): Premier Gold Project: Geological Setting and Mineralization of the Silbak Premier and Big Missouri Deposits, *in* Precious Metal Deposits of the Stewart Mining Camp, *Geological Association of Canada*, Geology and Metallogeny of Northwestern British Columbia Workshop, Field Trip Guidebook C, 13 pages.

Ray, G.E. and Spence, A. (1986): The Potassium-rich Volcanic Rocks at Tillicum Mountain - Their Geochemistry, Origin and Regional Significance, *B.C. Ministry of Energy, Mines and Petroleum Resources*, Geological Fieldwork, 1985, Paper 1986-1, pages 45-49.

Read, P.B. (1979): Preliminary Geological Mapping of the Big Missouri Property near Stewart, Northern British Columbia, *Geotex Consultants Limited*, Unpublished Report, 17 pages.

Richards, J.R., Fletcher, I.R. and Blockley, J.G. (1981): Pilbara Galenas - Precise Isotopic Assay of the Oldest Australian Leads, *Mineralium Deposita*, Volume 16, pages 7-30.

Ridge, J.D. (1983): Genetic Cencepts Versus Observational Data in Governing Ore Exploration, *Canadian Institute of Mining and Metallurgy*, Bulletin, Volume 76, Number 852, pages 47-54.

Roberts, R.G., and Sheahan, P.A. (1988): Ore Deposit Models. Geological Association of Canada, Geoscience Canada Reprint Series, 200 pages.

Rock, N.M.S. (1977): The Nature and Origin of Lamprophyres: Some Definitions, Distinctions, and Derivations; Earth-Science Reviews, Volume 13, pages 123-169.

Rock, N.M.S. and Groves, D.I. (1988): Can Lamprophyres Resolve the Genetic Controversy over Mesothermal Gold Deposits? *Geology*, Volume 16, June 1988, pages 538-541.

Roddick, J.A. (1983): Geophysical Review and Composition of the Coast Plutonic Complex, South of Latitude 55°N, *in* Circum Pacific Plutonic Terranes, J.A. Roddick, Editor, *Geological Society of America*, Memoir 159, pages 195-212.

Roering, C. (1968): The Geometrical Significance of Natural En-echelon Crack-arrays, *Tectonophysics*, Volume 5, pages 107-123.

Russell, R.D. and Farquhar, R.M. (1960): Lead Isotopes in Geology, *Interscience*, New York, 243 pages.

Sabine, P.A., Harrison, R.K. and Lawson, R.I. (1985): Classification of Volcanic Rocks of the British Isles on the Total Alkali Oxide-silica Diagram, and the Significance of Alteration, British Geological Survey Report, Volume 17, Number 4, 9 pages.

Schofield, S.J. and Hanson, G. (1922): Geology and Ore Deposits of the Salmon River District, British Columbia, *Geological Survey of Canada*, Memoir 132, 81 pages.

Schroeter, T.G., Lund, C. and Carter, G. (1989): Gold Production and Reserves in British Columbia, *B.C. Ministry of Energy, Mines and Petroleum Resources*, Open File 1989-22, 55 pages.

Seraphim, R.H. (1947): The Scotty Group, Unpublished B.Sc. Thesis, *The University of British Columbia*, 31 pages.

_____ (1979): Report on Silbak Premier Property near Stewart, British Columbia, Unpublished Report, 46 pages.

Sheldrake, R.F. (1983): Report on a Multifrequency Electromagnetic and Magnetic Survey in the Summit Lake Area, *B.C. Ministry of Energy, Mines and Petroleum Resources*, Assessment Report 12342, 15 pages.

Siems, P.L. (1984): Hydrothermal Alteration for Mineral Exploration Workshop Lecture Manual; University of Idaho, 580 pages.

Silberman, M.L. and Berger, B.R. (1985): Relationship of Trace-element Patterns to Alteration and Morphology in Epithermal Precious-metal Deposits; Reviews in Economic Geology, Volume 2, pages 203-232.

Sillitoe, R.H. (1973): The Tops and Bottoms of Porphyry Copper Deposits, *Economic Geology*, Volume 68, pages 799-815.

Sillitoe, R.H. (1985): Ore-related Breccias in Volcano-plutonic Arcs; Economic Geology, Volume 80, pages 1467-1514.

Smith, D.G., Editor (1981): The Cambridge Encyclopedia of Earth Sciences, *Prentice-Hall*, Scarborough, 496 pages.

Smith, J.G. (1973): A Tertiary Lamprophyre Dike Province in Southeastern Alaska, *Canadian Journal of Earth Sciences*, Volume 10, pages 408-420.

_____ (1977): Geology of the Ketchikan D-1 and Bradfield Canal A-1 Quadrangles, Southeastern Alaska, *United States Geological Survey*, Bulletin 1425, 49 pages.

Smith, J.G., Elliot, R.L., Berg, H.C. and Wiggins, B.D. (1977): Map Showing Geology and Location of Chemically and Radiometrically Analysed Samples in Parts of the Ketchikan, Bradfield Canal and Prince Rupert Quadrangles, Southeastern Alaska, *United States Geological Survey*, United States D.I., Miscellaneous Field Studies, Map MF-825.

Smith, J.G., Stern, T.W. and Arth, J.G. (1979): Isotopic Ages Indicate Multiple Episodes of Plutonism and Metamorphism in the Coast Mountains near Ketchikan, Alaska, *Geological Society of America*, Program with Abstracts, Volume 11, page 519.

Smith, R.L., Thomson, R.C. and Tipper, H.W. (1984): Lower and Middle Jurassic Sediments and Volcanics of the Spatsizi Map Area, British Columbia, *in* Current Research, Part A, *Geological Survey of Canada*, Paper 84-1A, pages 117-120.

Soregaroli, A. and Meade, H. (1983): Promise of the Stewart Area, British Columbia, *Western Miner*, Volume 56, Number 5, pages 27-29.

Souther, J.G. (1967): Acid Volcanism and its Relationship to the Tectonic History of the Cordillera of British Columbia, Canada, *Volcanogique*, Bulletin, Volume 30, pages 161-176.

_____ (1970): Volcanism and its Relationship to Recent Crustal Movements in the Canadian Cordillera, *Canadian Journal of Earth Sciences*, Volume 7, Number 2, pages 553-568.

_____ (1971): Geology and Mineral Deposits of Tulsequah Map-area, British Columbia, *Geological Survey of Canada*, Memoir 362, 84 pages.

_____ (1972): Telegraph Creek Map-area, British Columbia, *Geological Survey of Canada*, Paper 71-44, 38 pages.

_____ (1977): Volcanism and Tectonic Environments in the Canadian Cordillera, *Geological Association of Canada*, Special Paper 16, pages 3-24.

_____ (1988): Mount Edziza Volcanic Complex, British Columbia, Geological Survey of Canada, Map 1623A, 2 sheets.

_____ (in press): Post Accretionary Volcanism, *in* Decade of North American Geology, Special Volume (part of the Volcanism Chapter).

Souther, J.G., Brew, D.A. and Okulitch, A.V., Compilers (1979): Iskut River, British Columbia - Alaska Sheet, 104, 114, *Geological Survey of Canada*, 1:1 000 000 Scale, Map 1418A.

Spence, A.F. (1985): Shoshonites and Associated Rocks of Central British Columbia, *B.C. Ministry of Energy, Mines and Petroleum Resources*, Geological Fieldwork, 1984, Paper 1985-1, pages 426-442.

Stacey, J.S. and Kramers, J.D. (1975): Approximation of Terrestrial Lead Isotope Evolution by a Two-stage Model, *Earth and Planetary Science Letters*, Volume 26, pages 207- 221.

Stanton, R.L. and Russell, R.D. (1959): Anomalous Leads and the Emplacement of Lead Sulphide Ores, *Economic Geology*, Volume 54, pages 588-607.

Steiger, R.H. and Jager, E. (1977): Subcommission on Geochronology - Convention on the Use of Decay Constants in Geo- and Cosmochronology, *Earth and Planetary Science Letters*, Volume 36, pages 359-362.

Steininger, R.C. (1985): Geology of the Kitsault Molybdenum Deposit, British Columbia, *Economic Geology*, Volume 80, pages 57-71.

Streckeisen, A. (1975): To Each Plutonic Rock Its Proper Name, *Earth-Science Reviews*, Volume 12, pages 1-33.

Sutherland Brown, A. (1960): Geology of the Rocher Deboule Range, *B.C. Ministry of Energy, Mines and Petroleum Resources*, Bulletin 43, 78 pages.

_____ Editor (1976): Porphyry Deposits of the Canadian Cordillera, *The Canadian Institute of Mining and Metallurgy*, Special Volume 15, 510 pages.

Sylvester, A.G., Miller, C.F. and Nelson, C.A. (1978): Monzonites of the White-Inyo Range, California, and their Relation to the Calc-Alkalic Sierra Nevada Batholith, Geological Society of America Bulletin, Volume 89, pages 1677-1687.

Tatsumoto, M., Knight, T.J. and Allegre, C.J. (1973): Time Differences in the Formation of Meteorites as Determined from the Ratio of Lead-207 to Lead-206, *Science*, Volume 180, pages 1279-1283.

Thompson, R.N., Morrison, M.A., Dickin, A.P. and Hendry, G.L. (1983): Continental Flood Basalts - Arachnids Rule OK?, *in* Continental Basalts and Mantle Xenoliths, C.J. Hawkesworth and M.J. Norry, Editors, *Shiva Publishing Limited*, pages 158- 185.

Thomson, R.C. (1985): Lower to Middle Jurassic (Pleinsbachian to Bajocian) Stratigraphy and Pliensbachian Ammonite Fauna of the Northern Spatsizi Area, North-central British Columbia, M.Sc. Thesis, *The University of British Columbia*, 211 pages.

Thomson, R.C., Smith, P.L. and Tipper, H.W. (1986): Lower to Middle Jurassic (Pliensbachian to Bajocian) Stratigraphy of the Northern Spatsizi Area, North-central British Columbia, *Canadian Journal of Earth Sciences*, Volume 23, pages 1963- 1973.

Thorkelson, D.J. (1988): Jurassic and Triassic Volcanic and Sedimentary Rocks in Spatsizi Map Ara, North-central British Columbia, *in* Current Research, Part E, *Geological Survey of Canada*, Paper 88-1E, pages 43-48.

Thorstad, L.E. (1983): The Upper Triassic "Kutcho Formation", Cassiar Mountains, North-central British Columbia, M.Sc. Thesis, *The University of British Columbia*, 271 pages.

Thorstad, L.E. and Gabrielse, H. (1986): The Upper Traissic Kutcho Formation, Cassiar Mountains, North-central British Columbia, *Geological Survey of Canada*, Paper 86-16, 53 pages.

Tipper, H.W. (1959): Revision of the Hazelton and Takla Groups of Central British Columbia, *Geological Survey of Canada*, Bulletin 47, 51 pages.

_____ (1963): Nechako River Map-area, British Columbia, *Geological Survey of Canada*, Memoir 324, 59 pages.

_____ (1976): Biostratigraphic Study of Mesozoic Rocks in the Intermontane and Insular Belts of the Canadian Cordillera, in Current Research, Geological Survey of Canada Paper 76-1A, pages 57-61.

_____ (1978): Jurassic Stratigraphy, Cry Lake Map Area, British Columbia, *in* Current Research, Part A, *Geological Survey of Canada*, Paper 78-1A, pages 25-27.

_____ (1984a): The Allochthonous Jurassic-Lower Cretaceous Terranes of the Canadian Cordillera and their Relation to Correlative Strata of the North America Craton, *Geological Association of Canada*, Special Paper 27, pages 113-120.

_____ (1984b): The Age of the Jurassic Rossland Group of Southeastern British Columbia, Geological Survey of Canada Paper 84-1A, pages 631-632.

Tipper, H.W. and Richards, T.A. (1976): Jurassic Stratigraphy and History of North-central British Columbia, *Geological Survey of Canada*, Bulletin 270, 73 pages.

Tipper, H.W., Woodsworth, G.J. and Gabrielse, H., Coordinators (1981): Tectonic Assemblage Map of the Canadian Cordillera and Adjacent Parts of the United States of America, *Geological Survey of Canada*, Map 1505A.

Uytenbogaardt, W. and Burke, E.A.J. (1971): Tables for the Microscopic Identification of Ore Minerals, *Elsevier*, Amsterdam, 430 pages.

Van der Heyden, P. (1989): U-Pb and K-Ar geochronometry of the Coast Plutonic Complex, 53°N to 54°N, British Columbia, and implications for the Insular-Intermontane Superterrane boundary, unpublished Ph.D. Thesis, The University of British Columbia, 392 p.

Vernon, R.H. (1986): K-feldspar Megacrysts in Granites - Phenocrysts, not Porphyroblasts, *Earth-Science Reviews*, Volume 23, pages 1-63.

Walker, R.G. (1979): Turbidites and Associated Coarse Clastic Deposits, *in* Facies Models, *Geoscience Canada*, Reprint Series 1, pages 91-103.

Wanless, R.K., Stevens, R.D., Lachance, G.R. and DeLabio, R.N. (1979): Age Determinations and Geological Studies, K-Ar Isotopic Ages, Report 14, *Geological Survey of Canada*, Paper 79-2, page 23.

Wares, R. and Gewargis, W. (1982): Scottie Gold Mines Surface Geology Map Series, *B.C. Ministry of Energy, Mines and Petroleum Resources*, Assessment Report 10738.

Wernicke, B. and Klepacki, D.W. (1988): Escape Hypothesis for the Stikine Block, *Geology*, Volume 16, pages 461-464.

Westgate, L.G. (1921): Ore Deposits of the Salmon River District, Portland Canal Region, Alaska, *United States Geological Survey*, Bulletin 722C, pages 117-140.

Wheeler, J.O. and McFeely, P. (1987): Tectonic Assemblage Map of the Canadian Cordillera and Adjacent Parts of the United States of America, *Geological Survey of Canada*, Open File 1565.

Wheeler, J.O., Brookfield, A.J., Gabrielse, H., Monger, J.W.H., Tipper, H.W., and Woodsworth, G.J. (1988): Terrane map of the Canadian Cordillera, Geological Survey of Canada, Open File Map No. 1894.

White, W.H. (1939): Geology and Ore-deposition of Silbak Premier Mine Limited, Unpublished M.A.Sc. Thesis, *The University of British Columbia*, 78 pages.

_____ (1946): Big Four Silver Mines, Ltd., *Minister of Mines, B.C.*, Annual Report, 1946, pages A74-A78.

White, W.H., Sinclair, A.J., Harakal, J.E. and Dawson, K.M. (1970): Potassium-argon Ages of Topley Intrusions near Endako, British Columbia, *Canadian Journal of Earth Sciences*, Volume 7, pages 1172-1178.

Wilkinson, J.F.G. (1986): Classification and Average Chemical Compositions of Common Basalts and Andesites, *Journal of Petrology*, Volume 27, Part 1, pages 31-62.

Wilson, F.H., Dadisman, S.V. and Herzon, P.L. (1979): Map Showing Radiometric Ages of Rocks in Southeastern Alaska, *United States Geological Survey*, Open File Report 79-594, 33 pages.

Winkler, H.G.F. (1979): Petrogenesis of Metamorphic Rocks, Springer-Verlag, 345 pages.

Wojdak, P.J. and Brown, D.A. (1985): Silbak Premier, Stewart, British Columbia, 1984 Summary Exploration Report, *Westmin Resources Limited*, Company Report, 55 pages.

Wojdak, P.J., Dykes, S.M. and LeBlanc, E.R. (1984): Exploration at Silbak Premier, Stewart, British Columbia, 1983 Report, *Westmin Resources Limited*, Company Report, 72 pages.

Woodcock, J.R. and Hollister, V.F. (1978): Porphyry Molybdenite Deposits of the North American Cordillera, *Minerals Science Engineering*, Volume 10, pages 3-18.

Woodsworth, G.J. (1979): Geology of the Whitesail Lake Map-area, British Columbia, *in* Current Research, Part A, *Geological Survey of Canada*, Paper 79-1A, pages 25-29.

_____ (1980): Geology of Whitesail Lake (93E) Map Area, British Columbia, *Geological Survey of Canada*, Open File Map 708.

Woodsworth, G.J., Anderson, R.G., Struik, L.C. and Armstrong, R.L. (in press): Plutonic Regimes, Chapter 15, *in* Decade of North American Geology, Special Volume.

Woodsworth, G.J., Loveridge, W.D., Parrish, R.R. and Sullivan, R.W. (1983): Uranium-lead Dates from the Central Gneiss Complex and Ecstall Pluton, Prince Rupert Map Area, British Columbia, *Canadian Journal of Earth Sciences*, Volume 20, pages 1475-1483.

York, D. (1967): The Best Isochron, *Earth and Planetary Science Letters*, Volume 2, pages 479-482.

_____ (1969): Least Squares Fitting of a Straight Line with Correlated Errors, *Earth and Planetary Science Letters*, Volume 5, pages 320-324.

_____ (1984): Cooling Histories from $^{40}Ar/^{39}Ar$ Age Spectra, Annual Review, *Earth and Planetary Sciences Letters*, Volume 12, pages 383-409.

Zen, E. and Thompson, A.B. (1974): Low-grade Regional Metamorphism: Mineral and Equilibrium Relations, *Annual Reviews of Earth and Planetary Sciences*, Volume 2, pages 179-212.

APPENDIX 1

PETROCHEMICAL DATA

All petrochemical data from studies by Brown (1987) and Alldrick (1985), are listed in Table I-1 and grouped by stratigraphic division. Petrochemical data from intrusive rocks from Carter (1981), Brown (1987) and this study are listed in Table I-2 and grouped by lithodeme. Details about sample descriptions, sample locations and analytical procedures can be obtained from the original references.

No data from Galley (1981) are included in these tables. Galley's analytical values are included in Figure 3.8 to emphasize the extent and intensity of alteration, but they cannot be used in discriminant plots due to sample identity problems. Galley's appendices include references to: 28 sample pulps (p. 165); 27 whole rock analyses (p.166-168); and 26 accompanying footnotes (p.166-168). Concern about sample misidentification is confirmed by G-7 and G-14, which the footnotes describe as the same sample--but corresponding analyses are clearly not from the same rock.

TABLE I-1: Major element analyses from stratified rocks in the Stewart mining camp

SALMON RIVER FORMATION (Basal Limestone Member)

LBNO	SIO2	TIO2	AL2O3	FE2O3	FEO	MNO	MGO	CAO	NA2O	K2O	P2O5	LOI
629A	38.50	0.35	5.63	1.52	0.57	0.119	0.52	28.46	1.47	1.010	0.19	22.30

MOUNT DILWORTH FORMATION

LBNO	SIO2	TIO2	AL2O3	FE2O3	FEO	MNO	MGO	CAO	NA2O	K2O	P2O5	LOI
626	65.87	1.11	12.27	0.00	17.49	0.060	3.18	1.03	0.52	0.920	0.00	5.00
627	61.43	0.97	13.82	0.00	16.48	0.101	1.61	3.70	4.16	0.480	0.20	5.00
628	59.17	1.19	14.13	0.00	8.96	0.049	0.72	2.06	3.69	2.100	0.28	6.70
633	66.12	1.26	13.51	0.00	8.11	0.003	7.68	0.02	0.03	4.450	0.00	6.00
B-394	67.50	0.65	13.60	1.00	7.00	0.180	4.30	0.50	1.02	1.400	0.05	4.20
632	53.31	1.16	14.02	0.00	4.54	0.152	0.59	9.68	4.59	1.520	0.25	9.30

BETTY CREEK FORMATION (Sedimentary Units)

LBNO	SIO2	TIO2	AL2O3	FE2O3	FEO	MNO	MGO	CAO	NA2O	K2O	P2O5	LOI
622A	49.24	1.24	24.83	12.47	2.64	0.106	1.84	0.13	1.82	4.330	0.00	3.70
625A	65.34	0.48	16.22	5.28	1.24	0.099	1.80	4.37	3.45	2.050	0.15	2.10

BETTY CREEK FORMATION (Volcanic Units)

LBNO	SIO2	TIO2	AL2O3	FE2O3	FEO	MNO	MGO	CAO	NA2O	K2O	P2O5	LOI
623A	61.31	0.77	18.23	7.24	5.18	0.107	2.46	2.14	2.13	3.120	0.13	3.00

UNUK RIVER FORMATION (Premier Porphyry Member--Premier Porphyry Tuff [maroon])

LBNO	SIO2	TIO2	AL2O3	FE2O3	FEO	MNO	MGO	CAO	NA2O	K2O	P2O5	LOI
B255	55.90	0.82	18.40	7.70	0.40	0.180	2.59	3.22	7.53	1.070	0.26	2.10
B454	59.40	0.76	17.00	7.50	0.70	0.160	1.82	4.06	4.35	2.030	0.39	3.04

UNUK RIVER FORMATION (Premier Porphyry dykes. See also Table I-2.)

LBNO	SIO2	TIO2	AL2O3	FE2O3	FEO	MNO	MGO	CAO	NA2O	K2O	P2O5	LOI
405X	59.38	0.49	14.98	4.60	0.00	0.360	1.47	3.74	0.00	8.100	0.20	0.00
624A	57.54	0.52	14.47	4.86	2.08	0.270	1.65	7.34	0.24	4.740	0.10	3.10
DB70	59.60	0.50	14.80	0.70	3.60	0.280	1.55	4.46	0.39	4.960	0.19	4.86
B15	62.50	0.51	15.00	0.90	3.40	0.150	1.20	4.96	2.47	2.830	0.22	6.30
B360	78.10	0.31	10.00	3.00	0.00	0.050	0.15	0.51	2.70	4.150	0.01	1.43
B366	61.60	0.49	15.10	0.80	3.40	0.300	1.49	3.83	0.17	7.890	0.22	5.72
B524	62.80	0.55	16.00	0.60	3.90	0.140	1.82	3.49	3.31	3.990	0.26	2.80
B546	60.10	0.52	14.50	0.60	4.00	0.260	1.60	7.20	0.16	3.890	0.19	8.93

UNUK RIVER FORMATION (Upper Andesite Member -- Main Sequence)

	SIO2	TIO2	AL2O3	FE2O3	FEO	MNO	MGO	CAO	NA2O	K2O	P2O5	H2OT	CO2	S	TOTAL
DB-40	57.4	0.83	22.6	1.6	5.1	0.09	1.02	0.30	0.26	5.93	0.09	4.3	0.1	0.00	99.62
DB-105	63.3	0.48	14.3	1.8	2.5	0.11	0.99	4.86	2.39	2.64	0.23	2.4	3.6	0.00	99.60
B-22	76.7	0.07	12.7	0.4	0.4	0.05	0.15	0.51	2.70	4.15	0.01	1.0	0.4	0.03	99.27
B-96	56.2	0.81	19.4	7.4	1.4	0.14	0.98	1.20	0.61	5.45	0.12	3.5	1.0	0.00	98.21
B-251	53.7	1.09	22.0	1.6	8.0	0.12	1.83	0.09	1.02	3.57	0.02	5.0	0.0	0.00	98.04
B-294	57.1	0.61	16.7	0.4	4.3	0.11	1.62	5.36	1.89	3.23	0.25	3.3	3.9	0.33	99.10
B-332	47.9	0.78	18.0	1.7	6.2	0.29	2.18	7.53	0.20	4.55	0.30	4.1	5.8	0.04	99.57
B-340	56.4	0.73	15.4	6.3		0.48	2.08	5.65	0.95	3.47	0.30		4.3	1.45	97.52
B-357	56.7	0.96	21.1	8.1	1.5	0.08	1.02	0.20	0.45	5.85	0.12	3.6	0.0	0.02	99.70
B-359	57.0	0.71	17.8	2.5	9.8	0.35	3.60	0.22	0.22	2.79	0.16	5.1	0.2	0.03	100.48
B-379	68.9	0.64	14.2	1.9	4.7	0.14	2.62	0.90	0.67	2.63	0.18		0.6	0.61	98.69
B-381	64.2	0.59	14.9	0.9	3.7	0.13	1.84	4.86	2.23	2.17	0.23	3.0	3.0	0.03	101.78
B-382	62.1	0.64	17.4	4.0	2.0	0.16	1.87	4.29	5.25	1.46	0.24	2.0	0.5	0.00	101.91
B-455	58.6	0.56	15.1	5.6		0.17	1.08	6.01	2.37	3.33	0.28		4.2	3.38	100.68
B-458	59.4	1.03	20.5	8.0		0.11	1.84	0.57	0.19	5.29	0.17		0.2	1.01	98.00
B-535	50.1	1.10	18.0	2.1	7.8	0.31	4.11	5.09	0.14	4.03	0.48		3.5	0.57	97.33
B-543	57.7	0.68	14.2	3.9	2.6	0.26	1.09	7.02	0.71	3.55	0.30	2.3	7.2	0.01	101.52

UNUK RIVER FORMATION (Upper Andesite Member -- Black Tuff Facies)

LBNO	SIO2	TIO2	AL2O3	FE2O3	FEO	FETOT	MNO	MGO	CAO	NA2O	K2O	P2O5	LOI
630A	53.09	0.64	14.19	0.00	14.49		0.119	5.94	4.98	2.45	2.930	0.15	6.90
634A	60.01	0.63	16.10	0.00	11.72		0.062	3.34	0.38	0.81	3.770	0.31	5.50

UNUK RIVER FORMATION (Middle Andesite Member)

LBNO	SIO2	TIO2	AL2O3	FE2O3	FEO	MNO	MGO	CAO	NA2O	K2O	P2O5	LOI
631A	57.49	1.39	15.31	0.00	9.29		0.130	2.80	4.34	3.43	3.190	0.25
344X	45.55	0.96	16.24	0.00	13.47		0.210	4.06	7.38	3.02	1.240	0.34

TABLE I-2: Major element analyses from intrusive rocks in the Stewart district

SOURCE	LBNO	SIO2	TIO2	AL2O3	FE2O3	FEO	MNO	MGO	CAO	NA2O	K2O	P2O5	LOI	ROCK UNIT
	TEXAS CREEK SUITE (EARLY JURASSIC)													
Alldrick	327X	58.52	0.54	15.79	6.57	0.00	0.140	2.32	4.82	2.36	3.550	0.23	0.00	Texas Creek batholith (porphyry phase)
Alldrick	325X	60.59	0.53	15.83	6.24	0.00	0.120	1.83	4.26	2.80	2.970	0.18	0.00	Summit Lake stock
Alldrick	624A	57.54	0.52	14.47	4.86	2.08	0.270	1.65	7.34	0.24	4.740	0.10	3.10	Premier Porphyry dyke
* Alldrick	405X	59.38	0.49	14.98	4.60	0.00	0.360	1.47	3.74	0.00	8.100	0.20	0.00	Premier Porphyry dyke
* Brown	B366	61.60	0.49	15.10	0.80	3.40	0.300	1.49	3.83	0.17	7.890	0.22	5.72	Premier Porphyry dyke
Brown	DB70	59.60	0.50	14.80	0.70	3.60	0.280	1.55	4.46	0.39	4.960	0.19	4.86	Premier Porphyry dyke
Brown	B15	62.50	0.51	15.00	0.90	3.40	0.150	1.20	4.96	2.47	2.830	0.22	6.30	Premier Porphyry dyke
Brown	B524	62.80	0.55	16.00	0.60	3.90	0.140	1.82	3.49	3.31	3.990	0.26	2.80	Premier Porphyry dyke
Brown	B546	60.10	0.52	14.50	0.60	4.00	0.260	1.60	7.20	0.16	3.890	0.19	8.93	Premier Porphyry dyke
Brown	B360	78.10	0.31	10.00	3.00	0.00	0.050	0.15	0.51	2.70	4.150	0.01	1.43	Premier Porphyry dyke
Alldrick	326X	58.20	0.51	14.66	7.63	0.00	0.120	1.86	3.58	2.96	3.240	0.19	0.00	Salmon River dyke
	HYDER SUITE (MIDDLE EOCENE)													
Carter	NC38	71.38	0.33	12.01	0.99	0.62	0.030	0.78	1.90	1.07	6.720	0.19	1.50	B.C. Moly stock (Alice Arm)
Carter	NC30	66.98	0.54	14.64	0.69	2.02	0.040	1.00	3.08	3.76	4.650	0.20	1.18	Bell Moly stock (Alice Arm)
Carter	NC33	65.78	0.52	13.56	1.29	2.22	0.030	1.32	3.53	3.97	4.250	0.38	1.27	Ajax stock (Alice Arm)
Carter	NC35	71.16	0.31	14.23	0.36	1.86	0.040	0.29	1.40	3.22	4.580	0.15	1.39	Roundy Creek stock (Alice Arm)
Carter	NC26	68.92	0.57	15.20	1.02	0.87	0.010	0.64	2.23	3.32	4.430	0.38	0.23	Valley stock (Alice Arm)

* samples 405 and B 366 were collected independently from the same trench exposure

APPENDIX II

URANIUM-LEAD ANALYTICAL TECHNIQUES

Rock samples (40-60 kg) were reduced to coarse sand size (20 mesh) in a jaw crusher and a disc mill. Pulverized rock was passed over a Wilfley table twice to obtain a heavy mineral concentrate. Further concentration was accomplished by heavy liquid (bromoform, methyl iodide) and magnetic separations (Franz isodynamic separator). Standard nitric acid/aqua regia washes were avoided for all but the first sample processed. Mineral concentrates were sized using nylon mesh screens. Uniform, clean, inclusion-free, euhedral zircon crystals were hand-picked. No crystal abrasion was necessary. Zircon extraction, dissolution, U and Pb isolation, analytical runs and data reduction and plotting were completed by J. K. Mortensen following procedures outlined by Krough (1973) and the U.B.C Geochronology Laboratory Manual (Mortensen and Parkinson, 1985). Concordia diagrams are shown in Figures II-1, II-2, II-3 and II-4.

Isotopic ratios were measured on a Vacuum Generators Isomass 54R solid source mass spectrometer linked to a Hewlett Packard HP-85 computer. Solutions were loaded onto single rhenium filaments coated with H_3PO_4-silica gel. Precisions for $^{207}Pb/^{206}Pb$ and $^{208}Pb/^{206}Pb$ were better than 0.1 percent. Precisions for $^{206}Pb/^{204}Pb$ were better than 0.5 percent. Total Pb blanks were 0.12 ± 0.05 ng and total U blanks were 0.05 ± 0.02 ng, based on repeated procedural blank runs. U-Pb and Pb-Pb errors for individual zircon fractions were obtained by individually propagating all calibration and analytical uncertainties through the entire data calculation program and summing the individual contributions to the total variance. Errors on individual dates and on calculated intercept ages are quoted at the 2 sigma level.

LEAD LOSS AND ZIRCON INHERITANCE

Uranium-lead analyses from zircon are susceptible to errors caused by lead loss or zircon inheritance. Although the <u>concordia ages</u> listed in Table II-1 and shown on Figures II-1 to II-4 are not significantly affected, examination of all the <u>model ages</u> presented in the table suggests that both phemomena may be present in the zircon populations to a small

degree. Two fractions from sample A84-1 show some evidence of minor lead loss. Specific fractions from A84-5 and A84-1 may show subtle effects arising from zircon inheritance.

Lead Loss

Lead loss from zircon is caused by a thermal episode (metamorphism) or by continuous diffusion (Faure, 1977, P.206). If significant lead loss has occurred, all the uranium-lead model ages will be discordant, and none will represent a specific geological event. In such a case, the effect of lead loss can be minimized by using the model age based on the $^{207}Pb/^{206}Pb$ ratio, which is relatively insensitive to lead loss.

In the present data set, lead loss is minimal for all samples and **negligible** for the specific zircon fractions that provided the concordia ages. This can be demonstrated by two sets of relationships:

- There is very little difference between the U/Pb model ages from the most concordant and most discordant fractions from each sample. The greatest difference is between 188.2 and 192.8 Ma, for sample A84-1. This indicates only a minor amount of lead loss in a single fraction (*cf* Faure, 1977, p.211). The cause of the lead loss might be leaching during sample preparation (at time O Ma), or a thermal event such as the regional metamorphism (about 110 Ma) or emplacement of Tertiary intrusions (at time 50 Ma).

Leaching during sample preparation is an unlikely explanation for lead loss since the hot nitric acid bath step of the preparation procedure was deliberately avoided for all samples *except for the first sample prepared,* A84-1. There was no Tertiary pluton near the sample site, but microdiorite dykes from the Berendon swarm do crop out less than 50 metres from the sample site. Since lead loss for all samples is not systematic, as would be expected if lead loss were due to regional metamorphism, the lead loss in sample A84-1 is attributed to leaching of lead from the zircon crystal rims during the hot nitric acid bath, or to the thermal effects of the Late Eocene (?) microdiorite dykes. The writer suspects the acid bath is the more likely cause.

▪ For the most concordant fractions, the U/Pb and Pb/Pb model ages are essentially identical, except for a small difference between the $^{206}Pb/^{238}U$ and $^{207}Pb/^{206}Pb$ model ages for sample A84-5. Since the U/Pb model age for this fraction is concordant, the difference between the U/Pb and Pb/Pb model ages for this sample is more likely due to zircon inheritance (see below).

Inherited Zircon

Sample A84-1 shows a small amount of inherited lead in the $^{207}Pb/^{206}Pb$ analyses from the fine, magnetic zircon population but none in the analyses from the coarse non-magnetic zircon fraction. This supports the arguement that only the $^{207}Pb/^{206}Pb$ model ages from the most concordant zircon fraction should be used for a measure of the "maximum age" of the rock, since the more discordant U/Pb fractions are likely to have less accurate Pb/Pb model ages as well. In this case the Pb/Pb age is within the 2o error limit of the U-Pb concordia age, and confirms the accuracy of the U-Pb age.

One can speculate on the source of the inherited zircon. The age difference is small so we should look for rocks that only slighlty predate the 189-195 Ma plutonic phase. Regionally distributed Upper Triassic plutons range from 213-226 Ma (Anderson and Bevier, 1990), but none are known in the immediate area. Potassium-argon dates from the older, equigranular 'core' phase of the Texas Creek batholith range from 202-211 Ma (Table 3.8) and this is a more proximal and more plausible source for slightly older zircons that might have been incorporated in a younger magma and overgrown by younger zircon during crystallization of the later porphyry phase of the Texas Creek batholith.

TABLE II-1: Uranium-lead zircon dates from the Stewart mining camp

Sample No.	Location [UTM]	Sample Properties	Weight (mg)	Concentration (ppm) U	Concentration (ppm) Pb	Observed $^{206}Pb/^{204}Pb$	Atomic Ratios[3,4] $^{206}Pb/^{238}U$	Atomic Ratios[3,4] $^{207}Pb/^{235}U$	Atomic Ratios[3,4] $^{207}Pb/^{206}Pb$	Model Ages (Ma)[4] $^{206}Pb/^{238}U$	Model Ages (Ma)[4] $^{207}Pb/^{235}U$	Model Ages (Ma)[4] $^{207}Pb/^{206}Pb$	Concordia Age (Ma)[4]
A84-1	(130°05'55"W 56°14'00"N)	nm, 150-215μm	16.3	459	13.6	8841	0.03035±16	0.2092±11	0.04998± 07	192.8±1.0	192.9±0.9	194.2± 3.3	192.8±2.0
	[09-432250E 6232320N]	m, <45μm	1.3	1908	55.6	8473	0.02952±16	0.2041±11	0.05014± 09	187.5±1.0	188.6±0.9	201.4± 4.0	
		m, <45μm	1.5	887	26.2	6499	0.02962±16	0.2048±11	0.05015± 13	188.2±1.0	189.2±0.9	202.0± 5.8	
A84-2	(130°03'13"W 56°05'28"N)	nm, >150μm	14.2	349	10.2	8110	0.02979±17	0.2049±11	0.04990± 06	189.2±1.1	189.3±0.9	190.3± 2.8	189.2±2.2
	[09-434400E 6216475N]	m, <75μm	0.3	898	27.8	1278	0.03056±17	0.2101±73	0.04987±162	194.1±1.1	193.7±6.1	189.1±76.	
A84-3	(130°03'13"W 56°05'28"N)	nm, >150μm	10.5	596	18.6	1839	0.03062±17	0.2113±15	0.05006± 25	194.4±1.0	194.7±1.3	197.7±11.7	195.0±2.0
	[09-434400E 6216475N]	nm, >150μm, abd	4.3	510	15.6	6189	0.03072±16	0.2117±11	0.04999± 09	195.0±1.0	195.0±0.9	194.4± 4.1	
		m, <45μ	1.3	1272	38.3	6639	0.03004±16	0.2078±11	0.05016± 09	190.8±1.0	191.7±0.9	202.6± 4.1	
A84-5	(130°00'50"W 56°03'06"N)	nm, >150μm	5.3	343	10.84	1081	0.03020±16	0.2090±12	0.05018± 17	191.8±1.0	192.7±1.0	203.5± 7.6	194.8±2.0
	[09-436760E 6212240N]	nm, >150μm, abd	2.9	378	11.7	1864	0.03067±16	0.2120±13	0.05013± 19	194.8±1.0	195.2±1.1	201.2± 8.9	
AT-34-3[2]	(130°01'22"W 56°03'02"N)	nm, >150μm	5.0	362.2	4.14	629	0.01064±06	0.0702±05	0.04789± 02	68.2±0.4	68.9±0.5	93.7±10.1	54.8±1.3
	[09-436300E 6212130N]	m, <75μm	1.0	431.2	4.34	226	0.00853±12	0.0554±14	0.04713± 93	54.8±0.8	54.8±1.3	55.6±46.	

[1] All analyses by J.K. Mortensen, Geological Survey of Canada, Ottawa.
[2] Data provided by R.G. Anderson, Geological Survey of Canada, Vancouver.
[3] The errors apply to the last digits of the atomic ratios.
[4] All errors shown are 1σ errors, except for 2σ errors in final column.
Isotopic composition of blank: 6/4:17.75, 7/4:15.5, 8/4:37.3
Isotopic composition of common lead is based on the Stacey and Kramer (1975) model: 6/4 = 11.152, 7/4 = 12.998, 8/4 = 31.23 at 3.7 Ga with $^{238}U/^{204}Pb = 9.74$, $^{232}Th/^{204}Pb = 37.19$.
Decay constants: 6/4 = 0.155125, 7/4 = 0.98485, 8/4 = 137.88.

NOTE: $^{206}Pb/^{238}U$ analyses on the coarse, non-magnetic zircon fractions of samples A84-1-,2,-3 and -5 are concordant*, and thus represent very precise ages for these rocks. Nevertheless, uranium-lead analyses from zircon are always susceptible to errors caused by lead loss or zircon inheritance. Although the concordia ages listed in this table are not significantly affected, examination of the total data set of model ages suggests that both phemomena may be present in the zircon populations to a small degree. The effects of these phenomena and their geological significance are discussed in Appendix II.

* A concordant U-Pb analysis can be defined as any data point having a 2σ error ellipse that significantly overlaps concordia (J.K. Mortensen, personal communication, 1991).

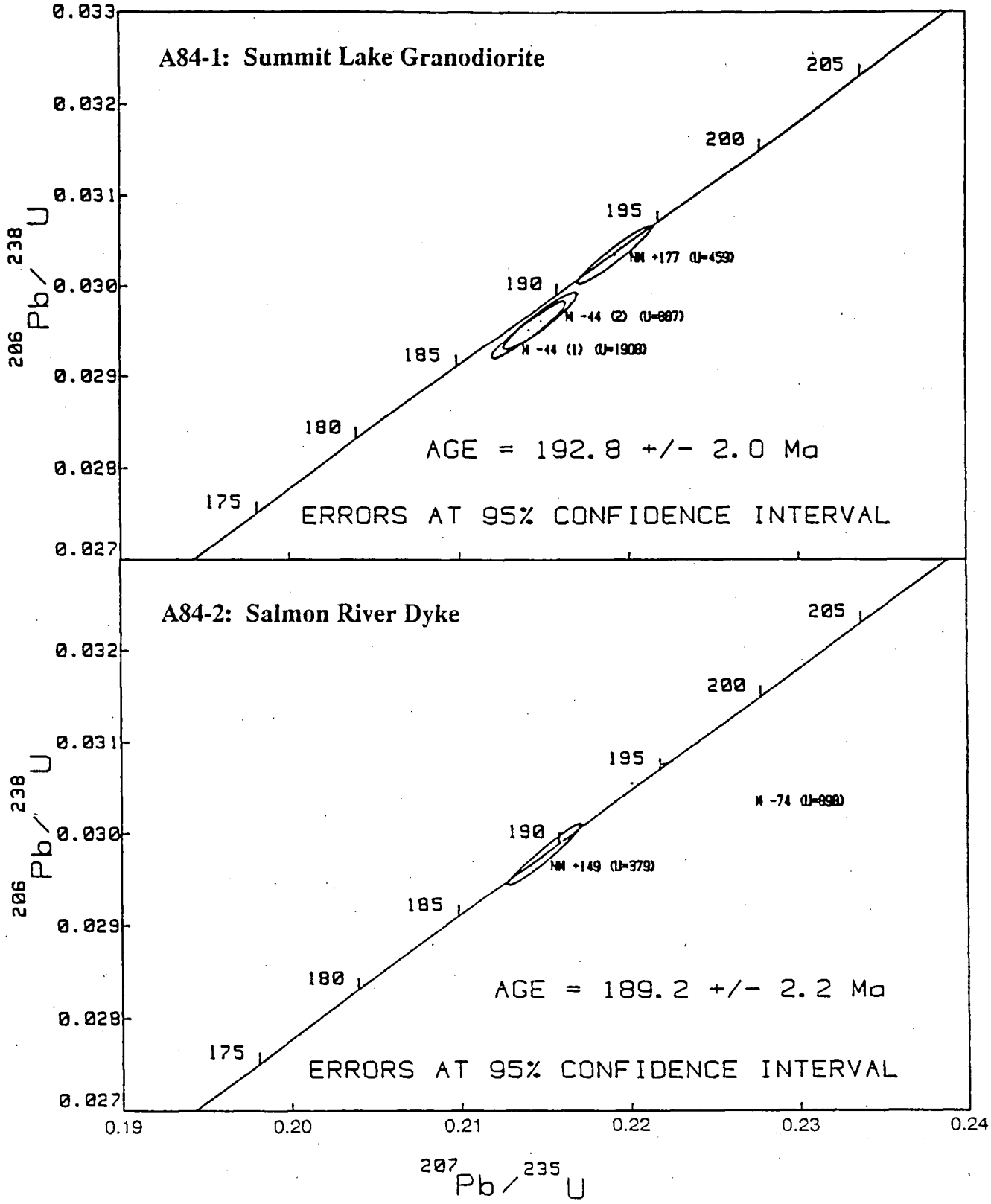

FIGURES II-1 AND II-2: Concordia plots for U-Pb samples A84-1 and A84-2.
(Plots by J.K. Mortensen, G.S.C., Ottawa)

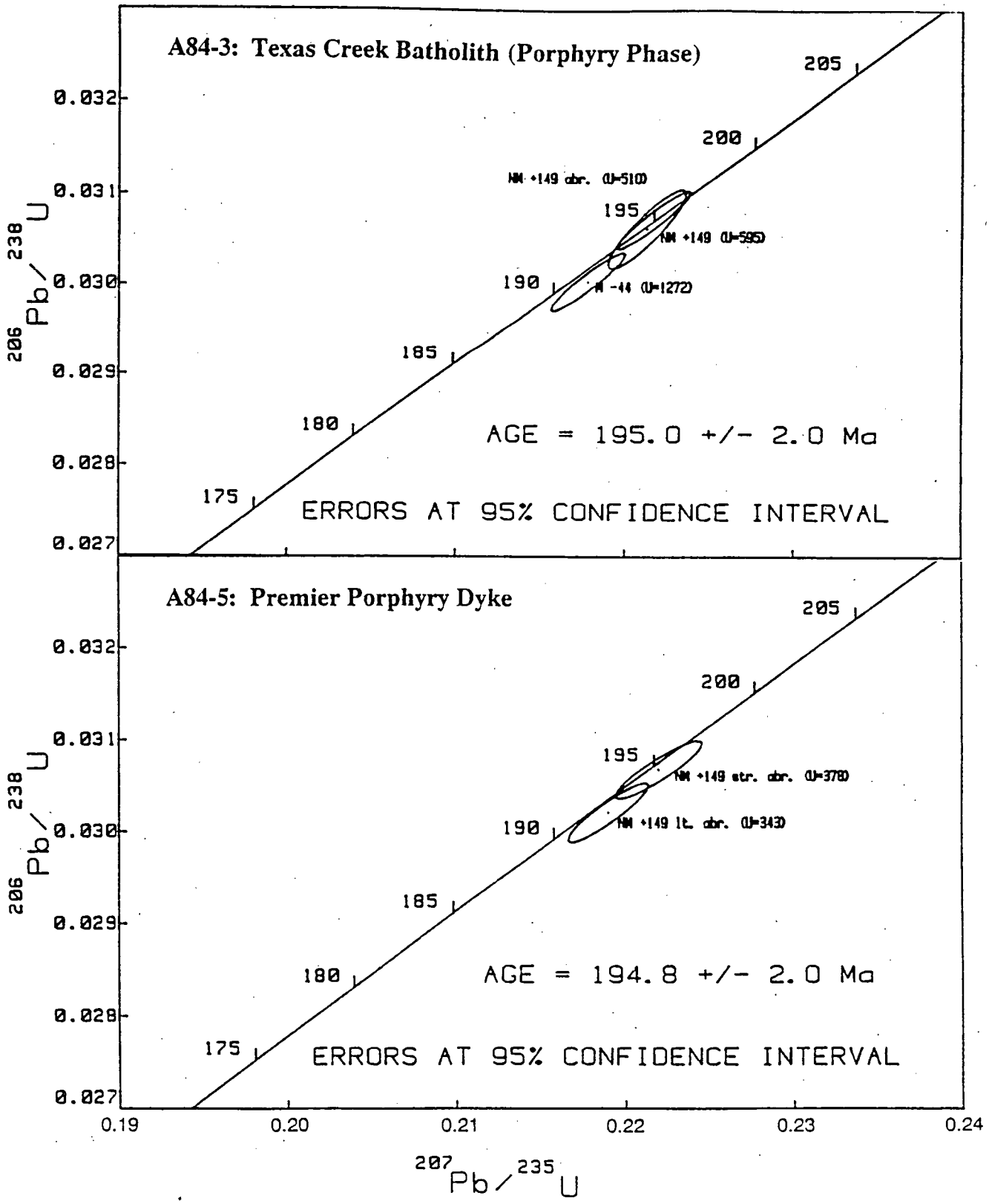

FIGURES II-3 AND II-4: Concordia plots for U-Pb samples A84-3 and A84-5.
(Plots by J.K. Mortensen, G.S.C., Ottawa)

APPENDIX III

Lead Isotope Data and Analytical Procedures

Sample information is listed in Table III-1 and all analyses are listed in Table III-2. Plots of the full and partial dataset are presented in Figures III-1, III-2, III-3 and III-4.

Sample preparation and lead isotope analyses were completed by J.E. Gabites in the Geochronology Laboratory, Department of Geological Sciences, The University of British Columbia. Lead isotope ratios were measured on a Vacuum Generators Isomass 54R solid source mass spectrometer linked to a Hewlett-Packard HP-85 computer. Samples were loaded using phosphoric acid and silica gel. Details of the analytical procedure are outlined in Gabites *et al.* (1990), Godwin *et al.* (1988), and Gulson (1986).

Run instability, or within-run error, reflects the inherent electronic instability within the mass spectrometer (machine error), plus the variability of ion emission during the analysis. Repeated measurement of the Broken Hill standard (BHS-UBC1) and systematic analyses of duplicates were used to monitor analytical precision of runs. Isotopic fractionation is the main source of analytical variations in single-filament spectrometer sources; even under optimum analytical conditions errors arise from fractionation processes which cause relative depletion of one or more lead isotopes with respect to the others. Another analytical error is associated with measurement of the low intensity ^{204}Pb spectrometer peak due to low abundance of this isotope. The ^{204}Pb error can be avoided by using plots that do not involve ^{204}Pb such as the $^{208}Pb/^{206}Pb$ *versus* $^{207}Pb/^{206}Pb$ plot (Figure III-4). Slopes of the fractionation error and the ^{204}Pb error are shown on all figures.

TABLE III-1: Lead isotope sample location data

SAMPLE NUMBER	DEPOSIT NAME	SAMPLE SOURCE	DATE ACQUIRED	NTS LOCATION	LATITUDE	LONGITUDE
30415-001	BIG MISSOURI (CREEK)	S DYKES: LOWER HORIZON: OLIVER 1982	00/00/80	104/B/01/E:SE-092	58.12	130.01
30415-002	BIG MISSOURI (CALCITE CUTS)	S DYKES: MIDDLE HORIZON: OLIVER 1982	00/00/80	104/B/01/E:SE-046	58.11	130.03
30415-003	BIG MISSOURI (TERMINUS F/WALL)	S DYKES: MIDDLE HORIZON: OLIVER 1982	00/00/80	104/B/01/E:SE-082	58.11	130.03
30415-004	BIG MISSOURI (PROVINCE)	S DYKES: UPPER HORIZON: OLIVER 1982	00/00/80	104/B/01/E:SE-046	58.11	130.03
30415-005	BIG MISSOURI (PROVINCE W)	S DYKES: UPPER HORIZON: OLIVER 1982	00/00/80	104/B/01/E:SE-046	58.11	130.03
30415-006	BIG MISSOURI (CREEK)	D ALLDRICK: SE-114: ALLDRICK ET AL., 1987	08/15/82	104/B/01/E:SE-092	58.12	130.01
30415-007	BIG MISSOURI (TERMINUS)	D ALLDRICK: SE-169: ALLDRICK ET AL., 1987	08/15/82	104/B/01/E:SE-002	58.11	130.02
30415-008	BIG MISSOURI (MARTHA ELLEN)	D ALLDRICK: HEZ-1: ALLDRICK ET AL., 1987	08/15/82	104/B/01/E:SE-092	58.13	130.03
30415-008R	BIG MISSOURI (MARTHA ELLEN)	D ALLDRICK: HEZ-1: ALLDRICK ET AL., 1987	08/15/82	104/B/01/E:SE-092	58.13	130.03
30415-008A	BIG MISSOURI (MARTHA ELLEN,N=2	D ALLDRICK: HEZ-1: ALLDRICK ET AL., 1987	08/15/82	104/B/01/E:SE-092	58.13	130.03
30415-009	BIG MISSOURI (PROVINCE)	D ALLDRICK: SE-70	08/15/82	104/B/01/E:SE-046	58.13	130.03
30415-009D	BIG MISSOURI (PROVINCE)	D ALLDRICK: SE-70	08/15/82	104/B/01/E:SE-046	58.13	130.03
30415-009A	BIG MISSOURI (PROVINCE, N=2)	D ALLDRICK: SE-70	08/15/82	104/B/01/E:SE-046	58.13	130.03
30415-010!	BIG MISSOURI	C GODWIN: G78BM-001, UBC X COL: OLIVER 1982	00/00/78	104/B/01/E:SE-046	58.11	130.03
30415-011	BIG MISSOURI (MARTHA ELLEN)	D ALLDRICK: HE-16-1	00/00/86	104/B/01/E:SE-092	58.13	130.03
30415-012	BIG MISSOURI (MARTHA ELLEN)	D ALLDRICK: HE-16-2	00/00/86	104/B/01/E:SE-092	58.13	130.03
30415-013	BIG MISSOURI (HERCULES, DUHAS)	C GODWIN: G79HR-001, T GROVE	00/00/79	104/B/01/E:SE-092	58.13	130.05
30415-013	BIG MISSOURI (HERCULES, DUHAS)	C GODWIN: G79HR-001, T GROVE: OLIVER 1982	00/00/79	104/B/01/E:SE-092	58.13	130.05
30415-AV1	BIG MISSOURI (MARTHA ELLEN,N=3	D ALLDRICK: HEZ-1, HE-16-1, HE-16-2	00/00/82	104/B/01/E:SE-092	58.13	130.03
30415-AVG	BIG MISSOURI (N=6)	D ALLDRICK: SE-70, -114, -169, HEZ-1, HE-16-1, HE-16-2	00/00/82	104/B/01/E:SE-	58.13	130.03
30415-AVG	BIG MISSOURI (N=5)	S DYKES, C GODWIN, UBC X COL		104/B/01/E:SE-046	58.11	130.03
30492-001	PROSPERITY-PORTER IDAHO	D ALLDRICK: D-VEIN, PI-7: ALLDRICK ET AL., 1987	00/00/82	103/P/13/W:NW-089	55.91	129.94
30492-002	PROSPERITY-PORTER IDAHO	D ALLDRICK: PI-10: ALLDRICK ET AL., 1987	00/00/82	103/P/13/W:NW-089	55.91	129.94
30492-003	PROSPERITY-PORTER IDAHO	D ALLDRICK: D-VEIN, PI-11: ALLDRICK ET AL., 1987	00/00/82	103/P/13/W:NW-089	59.91	129.94
30492-003R	PROSPERITY-PORTER IDAHO	D ALLDRICK: D-VEIN, PI-11: ALLDRICK ET AL., 1987	00/00/82	103/P/13/W:NW-089	59.91	129.94
30492-003A	PROSPERITY-PORTER IDAHO (N=2)	D ALLDRICK: D-VEIN, PI-11: ALLDRICK ET AL., 1987	00/00/82	103/P/13/W:NW-089	55.91	129.94
30492-AVG	PROSPERITY-PORTER IDAHO (N=3)	D ALLDRICK: PI-7, -10, -11: ALLDRICK ET AL., 1987	00/00/82	103/P/13/W:NW-089	55.91	129.94
30493-001	SCOTTIE GOLD	D ALLDRICK: SG-8: ALLDRICK ET AL., 1987	00/00/82	104/B/01/E:SE-074	58.22	130.09
30494-001	SILBAK PREMIER (WEST)	C GODWIN: G78SP-001, UBC X COLLECTION #108: OLIVER 1982	00/00/78	104/B/01/E:SE-054	56.05	130.02
30494-002	SILBAK PREMIER (IQ)	C GODWIN: G78SP-002, UBC X COLLECTION #108: OLIVER 1982	00/00/78	104/B/01/E:SE-054	56.05	130.02
30494-003	SILBAK PREMIER (WEST)	C GODWIN: G78SP-003, UBC X COLLECTION #108: OLIVER 1982	00/00/78	104/B/01/E:SE-054	56.05	130.02
30494-004	SILBAK PREMIER	T GROVE, C GODWIN: G79PR-001	00/00/79	104/B/10/E:SE-054	56.05	130.02
30494-004!	SILBAK PREMIER	T GROVE, C GODWIN: G79PR-001: OLIVER 1982	00/00/79	104/B/10/E:SE-054	56.05	130.02
30494-005	SILBAK PREMIER (LESLEY CK BR)	D ALLDRICK	08/30/84	104/B/01/E:SE-054	56.05	130.01
30494-005D	SILBAK PREMIER (LESLEY CK BR)	D ALLDRICK	08/30/84	104/B/01/E:SE-054	56.05	130.01
30494-005A	SILBAK PREMIER (LESLEY CK,N=2)	D ALLDRICK	08/30/84	104/B/01/E:SE-054	56.05	130.01
30494-006	SILBAK PREMIER (GLORY HOLE)	D ALLDRICK: GH-1	00/00/86	104/B/01/E:SE-054	56.05	130.02
30494-007	SILBAK PREMIER	D ALLDRICK: SE-45: ALLDRICK ET AL., 1987	10/00/82	104/B/01/E:SE-054	56.05	130.01
30494-010	SILBAK PREMIER (NORTH LIGHTS)	D ALLDRICK: PH-6L 6/7	00/00/86	104/B/01/E:SE-054	56.05	130.02
30494-011	SILBAK PREMIER (NORTH LIGHTS)	D ALLDRICK: PH-6L 7/8	00/00/86	104/B/01/E:SE-054	56.05	130.02
30494-012	SILBAK PREMIER (2 LEVEL)	D ALLDRICK: 2L-1	00/00/86	104/B/10/E:SE-054	56.05	130.02
30494-013	SILBAK PREMIER (2 LEVEL)	D ALLDRICK: 2L-2	08/30/86	104/B/01/E:SE-054	56.05	130.01
30494-AV1	SILBAK PREMIER (N LIGHTS, N=2)	D ALLDRICK: PH-6L 6/7, 7/8	00/00/86	104/B/01/E:SE-054	56.05	130.02
30494-AV2	SILBAK PREMIER (2 LEVEL, N=2)	D ALLDRICK: 2L-1, -2	00/00/86	104/B/10/E:SE-054	56.05	130.02
30494-AVG	SILBAK PREMIER (N=7)	D ALLDRICK: G79PR-001, SE-45, PH-6L, 2L, GH-1	00/00/86	104/B/10/E:SE-054	56.05	130.02
30494-AVG	SILBAK PREMIER (N=3)	C GODWIN: G78SP-001, 002 & 003: OLIVER 1982	00/00/78	104/B/01/E:SE-054	56.05	130.02
30495-001	CONSOLIDATED SILVER BUTTE	D ALLDRICK: SE-168: ALLDRICK ET AL., 1987	00/00/82	104/B/01/E:SE-095	56.11	130.03
30495-001D	CONSOLIDATED SILVER BUTTE	D ALLDRICK: SE-168: ALLDRICK ET AL., 1987	00/00/82	104/B/01/E:SE-095	56.11	130.03
30495-001A	CONSOLIDATED SILVER BUTTE(N=2)	D ALLDRICK: SE-168: ALLDRICK ET AL., 1987	00/00/82	104/B/01/E:SE-095	56.11	130.03
30616-001	SPIDER ADITS	D ALLDRICK	08/20/84	104/A/04/W:SW-010	56.13	129.99
30720-001	PACKER FRACTION	C. GODWIN: G79SR-001, T. GROVE	79	104/B/01/E:SE-	56.11	130.02
30720-001	PACKER FRACTION	C. GODWIN: G79SR-001, T. GROVE	79	104/B/01/E:SE-	56.11	130.02
30765-001	BAYVIEW	C GODWIN: G78BY-001: OLIVER 1982	00/00/78	103/P/13/W:NW-051	55.96	129.98
30765-002	BAYVIEW	D ALLDRICK: PIT 3/1: ALLDRICK ET AL., 1987	08/30/84	103/P/13/W:NW-051	55.96	129.98
30765-003	BAYVIEW	D ALLDRICK: PIT 3/2: ALLDRICK ET AL., 1987	08/30/84	103/P/13/W:NW-051	55.96	129.98
30765-004	BAYVIEW	D ALLDRICK: PIT 3/3: ALLDRICK ET AL., 1987	08/30/84	103/P/13/W:NW-051	55.96	129.98
30765-AVG	BAYVIEW (N=3)	D ALLDRICK: PIT 3/1,2,3: ALLDRICK ET AL., 1987	00/00/78	103/P/13/W:NW-051	55.96	129.98
30766-001	SILVERADO	D ALLDRICK: ZERO LEVEL	08/16/84	103/P/13/W:NW-088	55.92	129.96
30766-001R	SILVERADO	D ALLDRICK: ZERO LEVEL	08/16/84	103/P/13/W:NW-088	55.92	129.96
30766-001A	SILVERADO (N=2)	D ALLDRICK: ZERO LEVEL	08/16/84	103/P/13/W:NW-088	55.92	129.96
30766-002	SILVERADO	D ALLDRICK: A84-25-6 #4 ADIT	08/16/84	103/P/13/W:NW-088	55.92	129.96
30766-002R	SILVERADO	D ALLDRICK: A84-25-6 #4 ADIT	08/16/84	103/P/13/W:NW-088	55.92	129.96
30766-002A	SILVERADO (N=2)	D ALLDRICK: A84-25-6 #4 ADIT	08/16/84	103/P/13/W:NW-088	55.92	129.96
30766-AVG	SILVERADO (N=2)	D ALLDRICK: ZERO LEVEL, A84-25-6	08/16/84	103/P/13/W:NW-088	55.92	129.96
30923-001	START	D ALLDRICK: START 1	08/25/84	104/B/01/E:SW-051	56.10	130.00
30923-001R	START	D ALLDRICK: START 1	08/25/84	104/B/01/E:SW-051	56.10	130.00
30923-001A	START (N=2)	D ALLDRICK: START 1	08/25/84	104/B/01/E:SW-051	56.10	130.00
30923-002	START	D ALLDRICK: START 2	08/25/84	104/B/01/E:SW-051	56.10	130.00
30923-002R	START	D ALLDRICK: START 2	08/25/84	104/B/01/E:SW-051	56.10	130.00
30923-002A	START (N=2)	D ALLDRICK: START 2	08/25/84	104/B/01/E:SW-051	56.10	130.00
30923-003	START	D ALLDRICK: START 3	08/25/84	104/B/01/E:SW-051	56.10	130.00
30923-003R	START	D ALLDRICK: START 3	08/25/84	104/B/01/E:SW-051	56.10	130.00
30923-003A	START (N=2)	D ALLDRICK: START 3	08/25/84	104/B/01/E:SW-051	56.10	130.00
30923-AVG	START (N=3)	D ALLDRICK: START 1,2,3	08/25/84	104/B/01/E:SW-051	56.10	130.00
30939-001	INDIAN	D ALLDRICK: IN-1: ALLDRICK ET AL., 1987	00/00/82	104/B/01/E:SE-031	56.08	130.03
30939-002	INDIAN	D ALLDRICK: IN-1A: ALLDRICK ET AL., 1987	00/00/82	104/B/01/E:SE-031	56.08	130.03
30939-AVG	INDIAN (N=2)	D ALLDRICK: IN-1, IN-1A: ALLDRICK ET AL., 1987	00/00/82	104/B/01/E:SE-031	56.08	130.03
50055-001	JARVIS	D ALLDRICK: JA-1 N PIT: ALLDRICK ET AL., 1987	06/20/84	103/O/16/E:NE-	55.99	130.07
50055-001D	JARVIS	D ALLDRICK: JA-1 N PIT: ALLDRICK ET AL., 1987	06/20/84	103/O/16/E:NE-	55.99	130.07
50055-001A	JARVIS (N=2)	D ALLDRICK: JA-1 N PIT: ALLDRICK ET AL., 1987	06/20/84	103/O/16/E:NE-	55.99	130.07
50055-002	JARVIS	D ALLDRICK: JA-7: ALLDRICK ET AL., 1987	06/20/84	103/O/16/E:NE-	55.99	130.07
50055-002R	JARVIS	D ALLDRICK: JA-7	06/20/84	103/O/16/E:NE-	55.99	130.07
50055-002A	JARVIS (N=2)	D ALLDRICK: JA-7	06/20/84	103/O/16/E:NE-	55.99	130.07
50055-003	JARVIS	D ALLDRICK: JA-11: ALLDRICK ET AL., 1987	06/20/84	103/O/16/E:NE-	55.99	130.07
50055-AVG	JARVIS (N=3)	D ALLDRICK: JA-1,7,11: ALLDRICK ET AL., 1987	06/20/84	103/O/16/E:NE-	55.99	130.07
50058-001	RIVERSIDE	D ALLDRICK: A84-4-6	06/25/83	104/B/01/E:SE-073	56.00	130.07
50058-001R	RIVERSIDE	D ALLDRICK: A84-4-6	06/25/83	104/B/01/E:SE-073	56.00	130.07
50058-001A	RIVERSIDE (N=2)	D ALLDRICK: A84-4-6	06/25/83	104/B/01/E:SE-073	56.00	130.07

TABLE III-2: Lead isotope analytical data

SAMPLE NUMBER	DEPOSIT NAME	ANALYST	DATE OF ANALYSIS	RUN QUALITY	$^{206}Pb/^{204}Pb$	% ERROR	$^{207}Pb/^{204}Pb$	% ERROR	$^{208}Pb/^{204}Pb$	% ERROR	$^{207}Pb/^{206}Pb$	$^{208}Pb/^{206}Pb$
30415-001	BIG MISSOURI (CREEK)	B RYAN	01/22/81:	FAIR:	18.858	0.03	15.604	0.08	38.683	0.11	0.82745	2.04067
30415-002	BIG MISSOURI (CALCITE CUTS)	B RYAN	01/22/81:	FAIR:	18.858	0.10	15.646	0.16	38.468	0.15	0.82967	2.03988
30415-003	BIG MISSOURI (TERMINUS F/WALL)	B RYAN	01/26/81:	FAIR:	18.817	0.07	15.625	0.13	38.529	0.19	0.83037	2.04756
30415-004	BIG MISSOURI (PROVINCE)	B RYAN	01/28/81:	FAIR:	18.804	0.09	15.656	0.17	38.506	0.17	0.83259	2.04776
30415-005	BIG MISSOURI (PROVINCE W)	B RYAN	01/26/81:	FAIR:	18.781	0.05	15.643	0.09	38.524	0.10	0.83292	2.05122
30415-006	BIG MISSOURI (CREEK)	J GABITES	10/18/84:06/26/85	GOOD: 1100:07	18.820	0.02	15.615	0.02	38.456	0.02	0.82970	2.04332
30415-007	BIG MISSOURI (TERMINUS)	J GABITES	10/18/84:06/26/85	GOOD: 1120:07	18.823	0.02	15.609	0.02	38.435	0.03	0.82927	2.04195
30415-008	BIG MISSOURI (MARTHA ILLEN)	J GABITES	10/18/84:06/26/85	GOOD: 1080:07	18.824	0.03	15.610	0.02	38.458	0.03	0.82928	2.04304
30415-008R	BIG MISSOURI (MARTHA ILLEN)	J GABITES	11/22/84:06/26/85	GOOD: 1150:08	18.822	0.01	15.611	0.01	38.453	0.02	0.82939	2.04300
30415-008A	BIG MISSOURI (MARTHA ILLEN,N=2	J GABITES		GOOD:	18.823	0.02	15.611	0.02	38.456	0.03	0.82933	2.04302
30415-009	BIG MISSOURI (PROVINCE)	J GABITES	10/10/86:06/26/85	GOOD: 1150:07	18.812	0.00	15.592	0.02	38.373	0.00	0.82882	2.03986
30415-009D	BIG MISSOURI (PROVINCE)	J GABITES	06/11/87:06/36/85	GOOD: 1200:07	18.835	0.00	15.615	0.00	38.450	0.00	0.82904	2.04139
30415-009A	BIG MISSOURI (PROVINCE, N=2)	J GABITES		GOOD:	18.824	0.00	15.604	0.00	38.412	0.00	0.82893	2.04042
30415-010!	BIG MISSOURI	B RYAN		POOR:	18.176	0.06	15.522	0.12	37.628	0.15	0.85398	2.07020
30415-011	BIG MISSOURI (MARTHA ILLEN)	J GABITES	01/30/87:06/26/85	good: 1150:18	18.827	0.00	15.616	0.00	38.464	0.00	0.82945	2.04301
30415-012	BIG MISSOURI (MARTHA ILLEN)	J GABITES	02/05/87:06/26/85	good: 1150:09	18.828	0.00	15.617	0.01	38.474	0.00	0.82949	2.04346
30415-013	BIG MISSOURI (HERCULES, DUMAS)	J GABITES	01/09/87:06/26/85	good: 1200:11	18.734	0.00	15.612	0.02	38.990	0.00	0.83333	2.08127
30415-013	BIG MISSOURI (HERCULES, DUMAS)	B RYAN		FAIR:	18.754	0.07	15.635	0.13	39.050	0.17	0.83369	2.08222
30415-AV1	BIG MISSOURI (MARTHA ILLEN,N=3	J GABITES		GOOD:	18.826	0.02	15.615	0.02	38.465	0.03	0.82942	2.04316
30415-AVG	BIG MISSOURI (N=6)	J GABITES		GOOD:	18.824	0.02	15.612	0.02	38.450	0.03	0.82936	2.04253
30415-AVG	BIG MISSOURI (N=5)	B RYAN		FAIR:	18.824	0.07	15.635	0.13	38.502	0.15	0.83059	2.04537
30492-001	PROSPERITY-PORTER IDAHO	J GABITES	10/11/84:06/26/85	GOOD: 1150:07	19.130	0.03	15.627	0.02	38.644	0.03	0.81687	2.02009
30492-002	PROSPERITY-PORTER IDAHO	J GABITES	10/11/84:06/26/85	GOOD: 1150:06	19.116	0.02	15.624	0.01	38.616	0.02	0.81732	2.02012
30492-003	PROSPERITY-PORTER IDAHO	J GABITES	10/11/84:06/26/85	GOOD: 1150:06	19.114	0.02	15.610	0.01	38.589	0.03	0.81667	2.01891
30492-003R	PROSPERITY-PORTER IDAHO	J GABITES	11/22/84:06/26/85	GOOD: 1150:08	19.122	0.02	15.619	0.01	38.614	0.02	0.81677	2.01933
30492-003A	PROSPERITY-PORTER IDAHO (N=2)	J GABITES		GOOD:	19.118	0.02	15.615	0.01	38.597	0.02	0.81686	2.01912
30492-AVG	PROSPERITY-PORTER IDAHO (N=3)	J GABITES		GOOD:	19.121	0.02	15.622	0.01	38.620	0.02	0.81697	2.01978
30493-001	SCOTTIE GOLD	J GABITES	10/18/84:06/26/85	GOOD: 1100:07	18.804	0.02	15.608	0.01	38.426	0.02	0.83007	2.04352
30494-001	SILBAK PREMIER (WEST)	B RYAN		FAIR:	18.826	0.06	15.578	0.12	38.351	0.13	0.82747	2.03713
30494-002	SILBAK PREMIER (IQ)	B RYAN		FAIR:	18.850	0.06	15.640	0.10	38.545	0.16	0.82971	2.04483
30494-003	SILBAK PREMIER (WEST)	B RYAN		FAIR:	18.840	0.05	15.633	0.11	38.469	0.12	0.82978	2.04188
30494-004	SILBAK PREMIER	J GABITES	06/11/87:06/25/85	FAIR: 1200:10	18.833	0.00	15.611	0.02	38.450	0.01	0.82891	2.04167
30494-004!	SILBAK PREMIER	B RYAN		POOR:	18.768	0.06	15.595	0.19	38.488	0.08	0.83094	2.05072
30494-005	SILBAK PREMIER (LESLEY CK BR)	J GABITES	10/10/86:06/26/85	FAIR: 1170:08	19.229	0.01	15.758	0.04	38.251	0.01	0.81947	2.04122
30494-005D	SILBAK PREMIER (LESLEY CK BR)	J GABITES	05/28/87:06/26/85	good: 1170:05	19.210	0.00	15.738	0.01	39.201	0.00	0.81923	2.04063
30494-005A	SILBAK PREMIER (LESLEY CK,N=2)	J GABITES		good:	19.220	0.00	15.748	0.05	39.320	0.00	0.81935	2.04580
30494-006	SILBAK PREMIER (GLORY HOLE)	J GABITES	02/05/87:06/26/85	good: 1150:18	18.836	0.00	15.617	0.02	38.464	0.00	0.82907	2.04202
30494-007	SILBAK PREMIER	J GABITES	10/29/84:06/26/85	GOOD: 1150:09	18.825	0.01	15.611	0.01	38.421	0.02	0.82926	2.04096
30494-010	SILBAK PREMIER (NORTH LIGHTS)	J GABITES	02/05/87:06/26/85	good: 1150:06	18.817	0.00	15.602	0.01	38.382	0.00	0.82915	2.03973
30494-011	SILBAK PREMIER (NORTH LIGHTS)	J GABITES	04/02/87:06/26/85	fair: 1150:11	18.838	0.00	15.612	0.02	38.421	0.00	0.82871	2.03952
30494-012	SILBAK PREMIER (2 LEVEL)	J GABITES	04/13/87:06/26/85	good: 1170:07	18.841	0.00	15.619	0.01	38.465	0.00	0.82901	2.04160
30494-013	SILBAK PREMIER (2 LEVEL)	J GABITES	04/13/87:06/26/85	good: 1200:07	18.833	0.00	15.618	0.01	38.450	0.00	0.82930	2.04160
30494-AV1	SILBAK PREMIER (N LIGHTS, N=2)	J GABITES		FAIR/ GOOD	18.828	0.00	15.607	0.02	38.402	0.00	0.82893	2.03962
30494-AV2	SILBAK PREMIER (2 LEVEL, N=2)	J GABITES		GOOD	18.837	0.00	15.619	0.01	38.468	0.00	0.82916	2.04160
30494-AVG	SILBAK PREMIER (N=7)	J GABITES		GOOD	18.832	0.00	15.613	0.01	38.441	0.00	0.82907	2.04117
30494-AVG	SILBAK PREMIER (N=3)	B RYAN		FAIR:	18.839	0.60	15.617	0.11	38.455	0.14	0.82897	2.04124
30495-001	CONSOLIDATED SILVER BUTTE	J GABITES	10/29/84:06/26/85	GOOD: 1250:09	18.828	0.02	15.619	0.02	38.474	0.02	0.82954	2.04348
30495-001D	CONSOLIDATED SILVER BUTTE	J GABITES	06/07/85:06/26/85	FAIR: 1150:07	18.812	0.04	15.605	0.04	38.432	0.04	0.82957	2.04301
30495-001X	CONSOLIDATED SILVER BUTTE(N=2)	J GABITES		GOOD:	18.820	0.03	15.612	0.03	38.453	0.03	0.82955	2.04325
30616-001	SPIDER ADITS	J GABITES	10/03/86:06/26/85	GOOD: 1150:11	19.085	0.05	15.609	0.05	38.590	0.01	0.81788	2.02202
30720-001	PACKER FRACTION	J GABITES	05/28/87:06/26/85	GOOD: 1200:18	19.177	0.00	15.629	0.00	38.661	0.00	0.81509	2.01600
30720-001	PACKER FRACTION	B RYAN		FAIR:	19.155	0.08	15.585	0.13	39.602	0.14	0.81363	2.06745
30765-001	BATTIEN	B RYAN		FAIR:	18.502	0.14	15.593	0.22	38.207	0.22	0.84277	2.06502
30765-002	BATTIEN	J GABITES	09/22/86:06/26/85	GOOD: 1150:19	19.153	0.00	15.616	0.01	38.608	0.00	0.81532	2.01578
30765-003	BATTIEN	J GABITES	09/30/86:06/26/85	GOOD: 1150:08	19.151	0.00	15.623	0.01	38.633	0.00	0.81582	2.01732
30765-004	BATTIEN	J GABITES	09/22/86:06/26/85	GOOD: 1150:07	19.152	0.01	15.622	0.00	38.633	0.01	0.81570	2.01714
30765-AVG	BATTIEN (N=3)	J GABITES		GOOD:	19.152	0.01	15.620	0.01	38.625	0.01	0.81561	2.01675
30766-001	SILVERADO	J GABITES	09/24/86:06/26/85	GOOD: 1180:18	19.162	0.00	15.650	0.02	38.731	0.00	0.81669	2.02119
30766-001R	SILVERADO	J GABITES	12/01/86:06/26/85	GOOD: 1150:12	19.148	0.00	15.631	0.02	38.656	0.00	0.81634	2.01883
30766-001A	SILVERADO (N=2)	J GABITES		GOOD:	19.155	0.00	15.641	0.02	38.694	0.00	0.81651	2.02001
30766-002	SILVERADO	J GABITES	09/24/86:06/26/85	GOOD: 1150:18	19.167	0.00	15.645	0.01	38.713	0.00	0.81623	2.01974
30766-002R	SILVERADO	J GABITES	12/02/86:06/26/85	GOOD: 1170:07	19.156	0.00	15.630	0.01	38.672	0.00	0.81595	2.01877
30766-002A	SILVERADO (N=2)	J GABITES		GOOD:	19.162	0.00	15.638	0.01	38.693	0.00	0.81609	2.01926
30766-AVG	SILVERADO (N=2)	J GABITES		GOOD:	19.159	0.00	15.640	0.02	38.694	0.00	0.81617	2.01963
30923-001	START	J GABITES	09/30/86:06/26/85	GOOD: 1150:18	19.150	0.00	15.654	0.02	38.749	0.00	0.81747	2.02347
30923-001R	START	J GABITES	12/11/86:06/26/85	GOOD: 1150:08	19.132	0.00	15.629	0.01	38.642	0.00	0.81689	2.01981
30923-001A	START (N=2)	J GABITES		GOOD:	19.141	0.00	15.642	0.02	38.696	0.00	0.81718	2.02164
30923-002	START	J GABITES	10/01/86:06/26/85	FAIR: 1250:10	19.159	0.01	15.663	0.23	38.719	0.04	0.81755	2.02099
30923-002R	START	J GABITES	12/11/86:06/26/85	GOOD: 1150:12	19.134	0.00	15.641	0.01	38.683	0.00	0.81746	2.02176
30923-002A	START (N=2)	J GABITES		GOOD:	19.142	0.00	15.648	0.02	38.716	0.00	0.81746	2.02261
30923-003	START	J GABITES	01/10/86:06/26/85	GOOD: 1150:10	19.114	0.00	15.621	0.01	38.629	0.00	0.81729	2.02101
30923-003R	START	J GABITES	12/02/86:06/26/85	GOOD: 1150:09	19.121	0.00	15.628	0.00	38.643	0.00	0.81733	2.02098
30923-003A	START (N=2)	J GABITES		GOOD:	19.118	0.00	15.635	0.00	38.636	0.00	0.81731	2.02099
30923-AVG	START (N=3)	J GABITES		GOOD:	19.134	0.00	15.638	0.00	38.683	0.00	0.81731	2.02175
30939-001	INDIAN	J GABITES	10/18/84:06/26/85	GOOD: 1080:08	19.150	0.02	15.625	0.01	38.665	0.03	0.81595	2.01909
30939-002	INDIAN	J GABITES	10/26/84:06/26/85	GOOD: 1150:09	19.159	0.02	15.621	0.02	38.650	0.02	0.81537	2.01736
30939-AVG	INDIAN (N=2)	J GABITES		GOOD:	19.155	0.02	15.623	0.02	38.658	0.03	0.81566	2.01823
50055-001	JARVIS	J GABITES	09/22/86:06/26/85	GOOD: 1150:10	19.164	0.00	15.607	0.02	38.579	0.01	0.81439	2.01307
50055-001D	JARVIS	J GABITES	06/12/87:06/26/85	GOOD: 1200:18	19.114	0.00	15.642	0.02	38.555	0.01	0.81835	2.01708
50055-001A	JARVIS (N=2)	J GABITES		GOOD:	19.137	0.00	15.625	0.02	38.567	0.01	0.81637	2.01507
50055-002	JARVIS	J GABITES	10/03/86:06/26/85	GOOD: 1150:07	19.158	0.00	15.625	0.01	38.616	0.00	0.81556	2.01560
50055-002R	JARVIS	J GABITES	12/02/86:06/26/85	FAIR: 1170:13	19.180	0.00	15.643	0.01	38.695	0.00	0.81561	2.01750
50055-002A	JARVIS (N=2)	J GABITES		GOOD/FAIR	19.167	0.00	15.634	0.01	38.657	0.00	0.81558	2.01654
50055-003	JARVIS	J GABITES	09/30/86:06/26/85	GOOD: 1150:07	19.174	0.00	15.635	0.01	38.656	0.00	0.81545	2.01608
50055-AVG	JARVIS (N=3)	J GABITES		GOOD:	19.168	0.00	15.625	0.02	38.631	0.01	0.81514	2.01523
50058-001	RIVERSIDE	J GABITES	09/29/86:06/26/85	GOOD: 1180:10	19.191	0.00	15.656	0.02	38.726	0.01	0.81578	2.01786
50058-001R	RIVERSIDE	J GABITES	12/01/87:06/26/85	GOOD: 1150:19	19.160	0.01	15.621	0.02	38.594	0.01	0.81529	2.01433
50058-001A	RIVERSIDE (N=2)	J GABITES		GOOD:	19.176	0.00	15.639	0.02	38.610	0.02	0.81553	2.01605

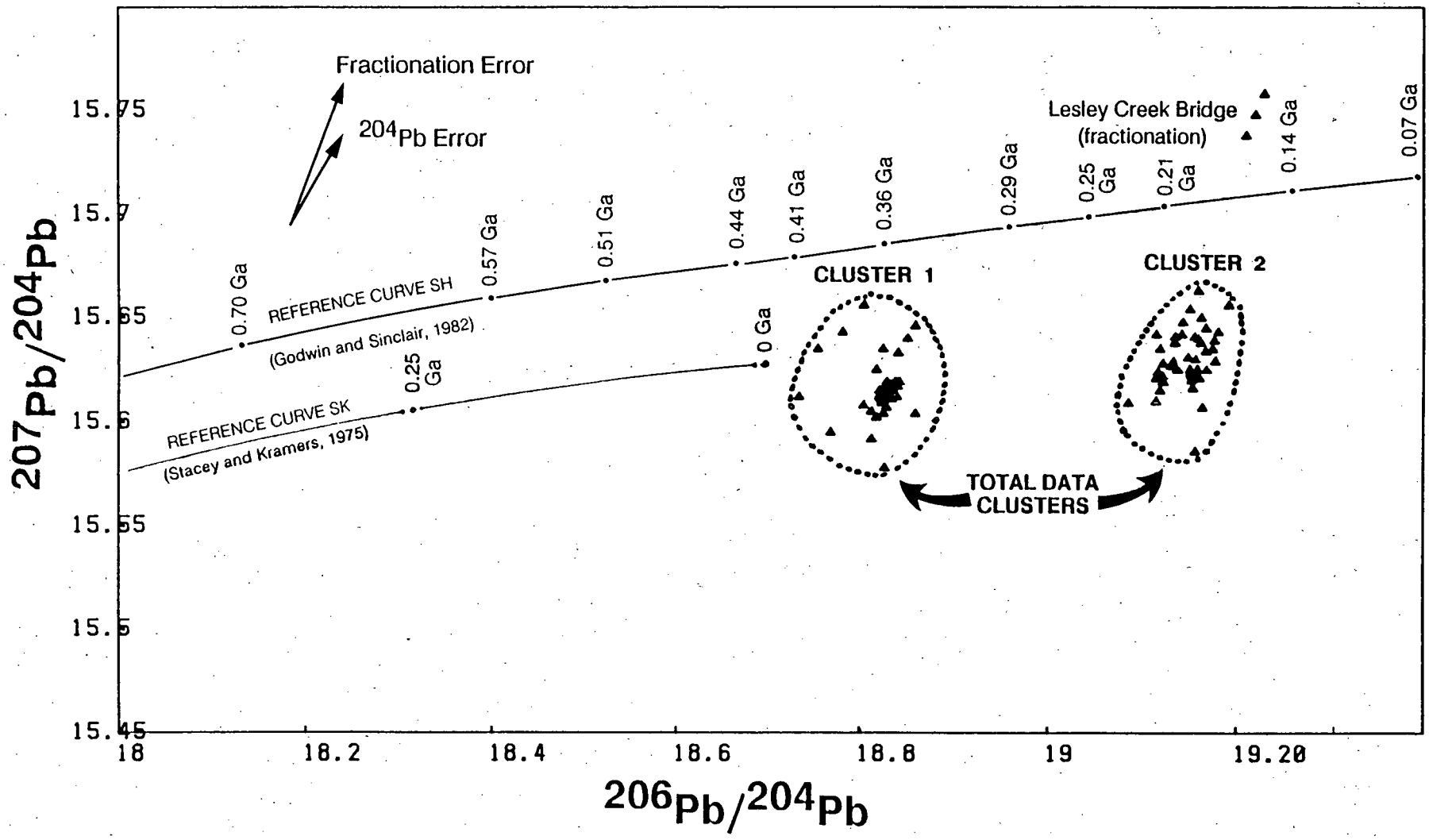

Figure III-1: Plot of Stewart lead isotope data set showing two reference curves.

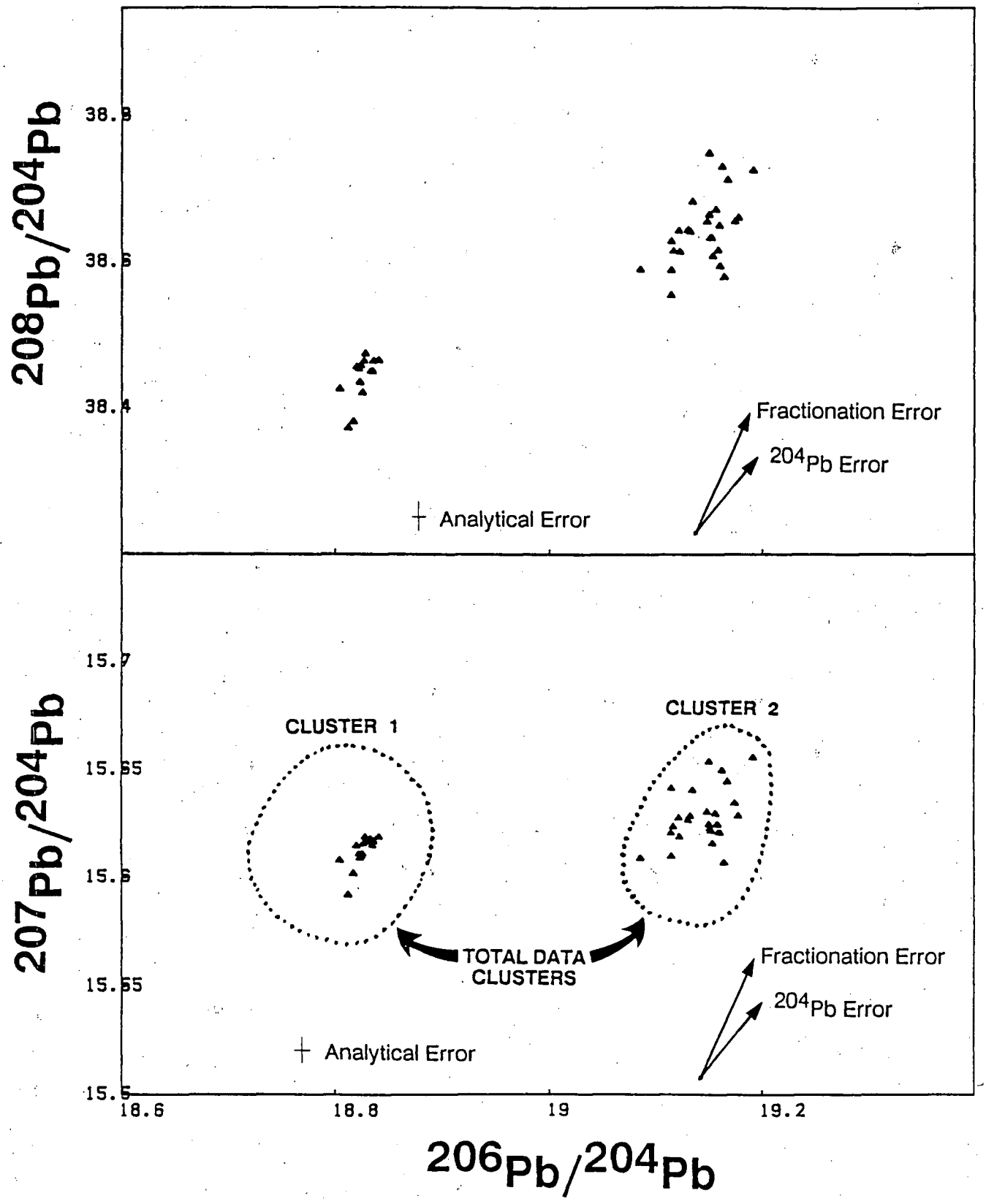

FIGURE III-2: Conventional lead isotope plots
show outlines of the "total data" clusters from Figure III-1. However, only 'good' analytical data from Table III-2 have been plotted (41 values). This shows significant improvement in the overall precision of the dataset, but no change in accuracy. Analytical error is 2σ.

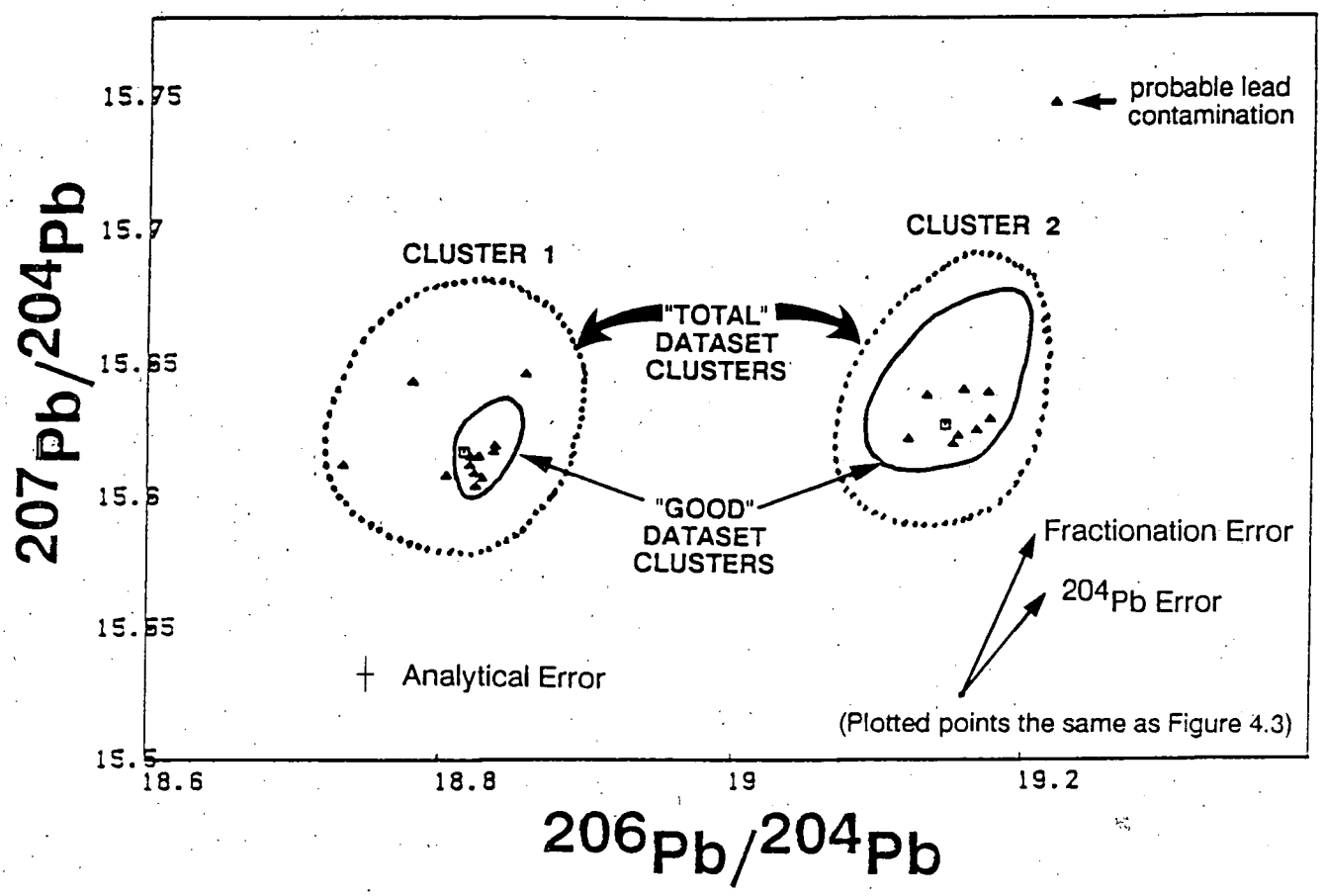

FIGURE III-3: Lead isotope data from 21 mineral occurrences are replotted here (see also Figure 4.3) together with the outlines of the data plots from Figures III-1 and III-2. In order to include data from as many deposits as possible in this study, some "FAIR" quality data were included in the dataset for Figure 4.3 (e.g. Province West and Calcite Cuts). This figure shows that these included values do not compromise the accuracy of the data plots or the resulting interpretations. Analytical error is 2σ.

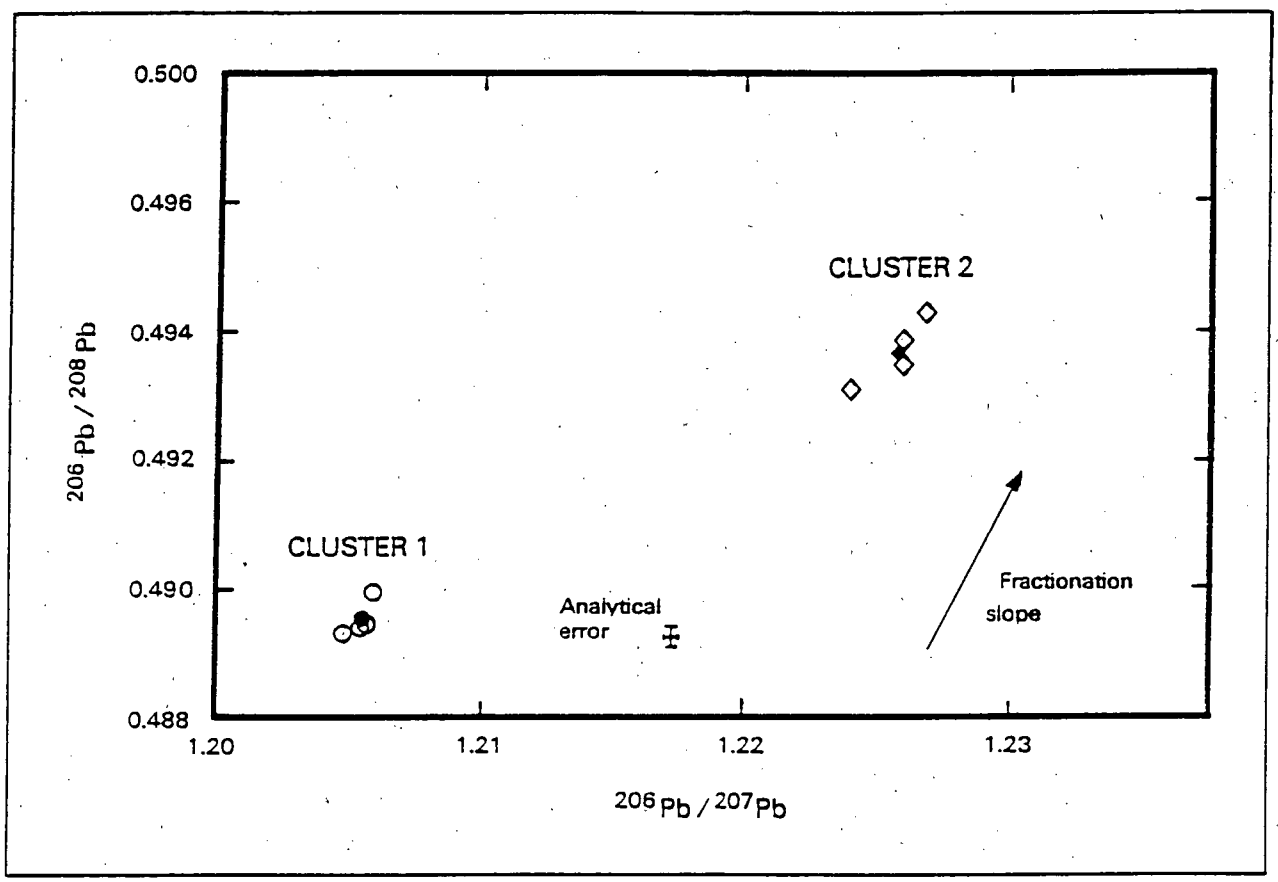

FIGURE III-4: This plot eliminates any ^{204}Pb analytical errors from the dataset.

In comparison to previous figures, the data distribution suggests that ^{204}Pb errors must be small and that there is somewhat more fractionation error present in the "Cluster 2" data. Solid symbols represent group means; open circles indicate deposits with Jurassic lead signatures; open diamonds indicate deposits with Tertiary lead signatures **(from Alldrick et al., 1987; figure 2-12-4C).**
Analytical error is 2σ.

APPENDIX IV

DEPOSIT SAMPLING AND ANALYTICAL RESULTS

IV.1 Sampling at Scottie Gold mine

Three chip sample sections totalling 25 samples were collected at Scottie Gold mine (Figures IV-1, IV-2 and IV-3). Each sample exceeded 10 kilograms. Two were collected from the West Main Vein of the M Zone on the 3200 and 3600 Levels (32-93 and 36-95 stopes), and one was collected across a Sixties vein of the N Zone (32-92 stope). M Zone samples were collected across current stope faces, N Zone samples were collected along the walls and roof of a drift. Sampling was divided at vein boundaries; at N Zone wallrock sampling was divided where alteration styles showed gradational changes. In addition, four selective grab samples were collected for trace element analysis (Table IV-1) which are summarized in Table 4-7.

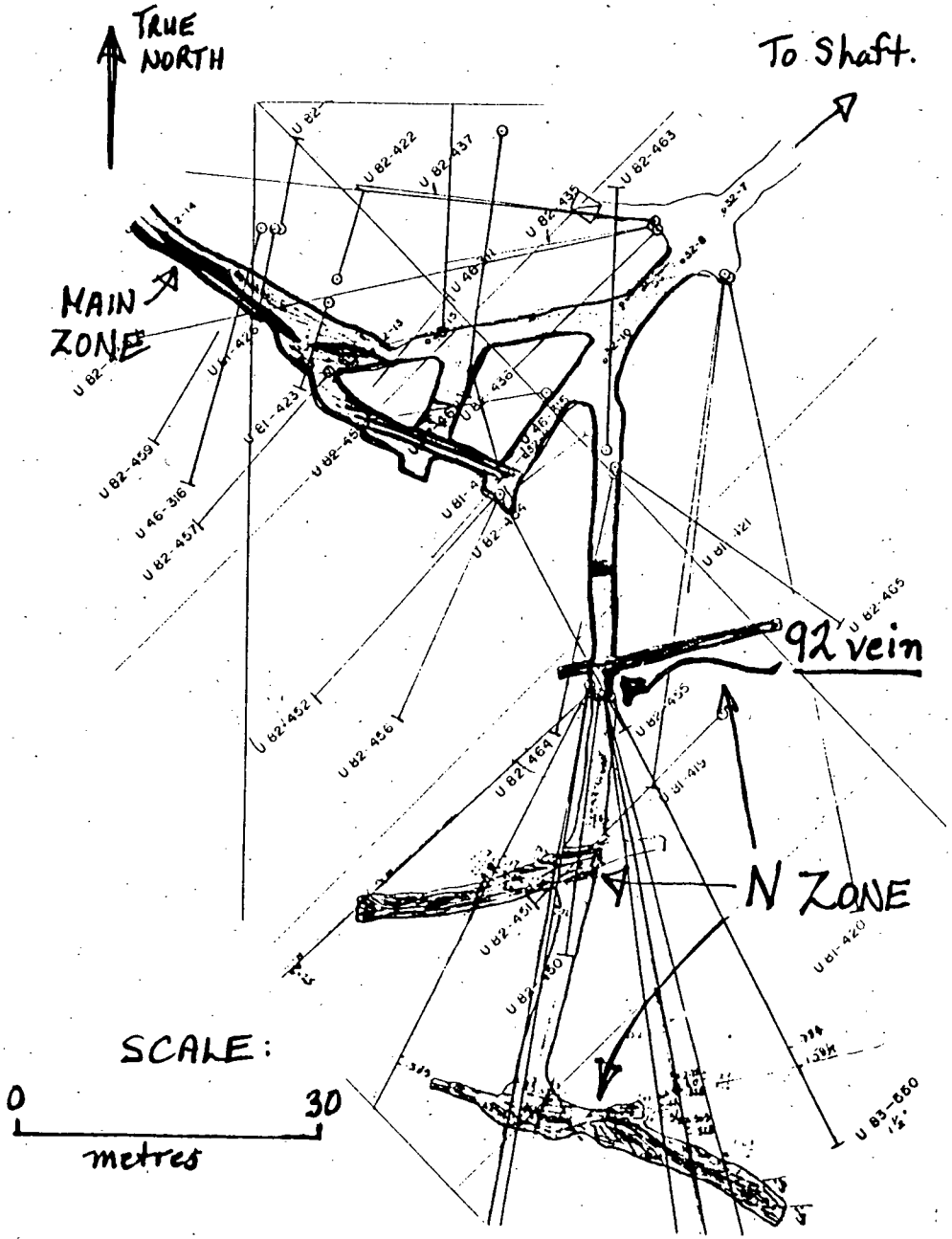

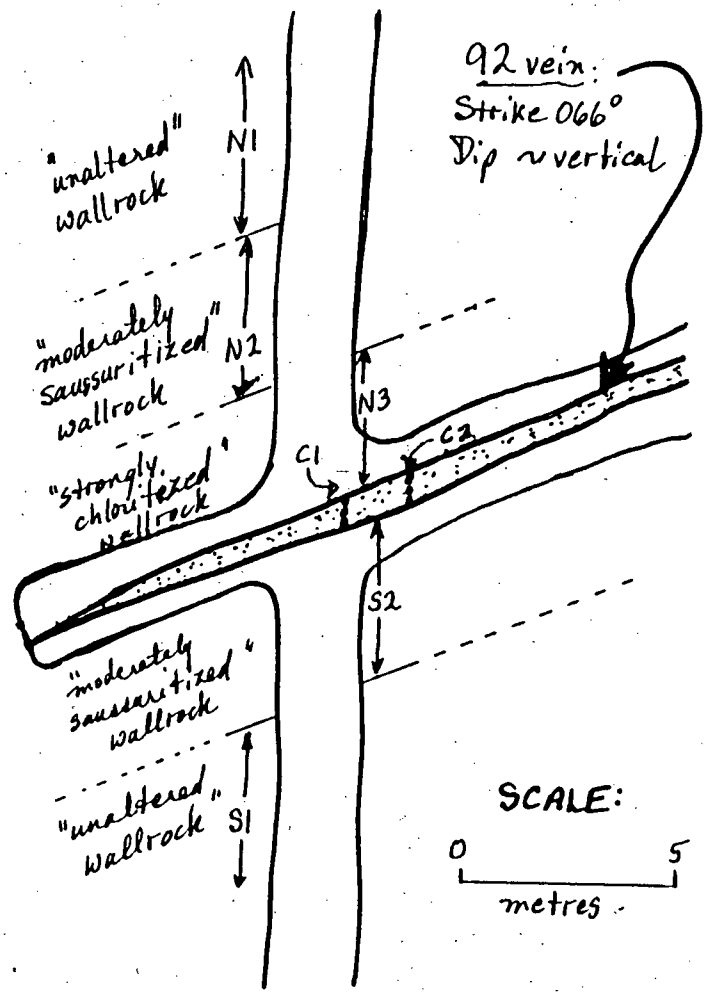

FIGURE IV-1: Scottie Gold mine:
N-Zone sampling site 32-92.
3200 level, South cross-cut, 92 vein drift.
August 14, 1984

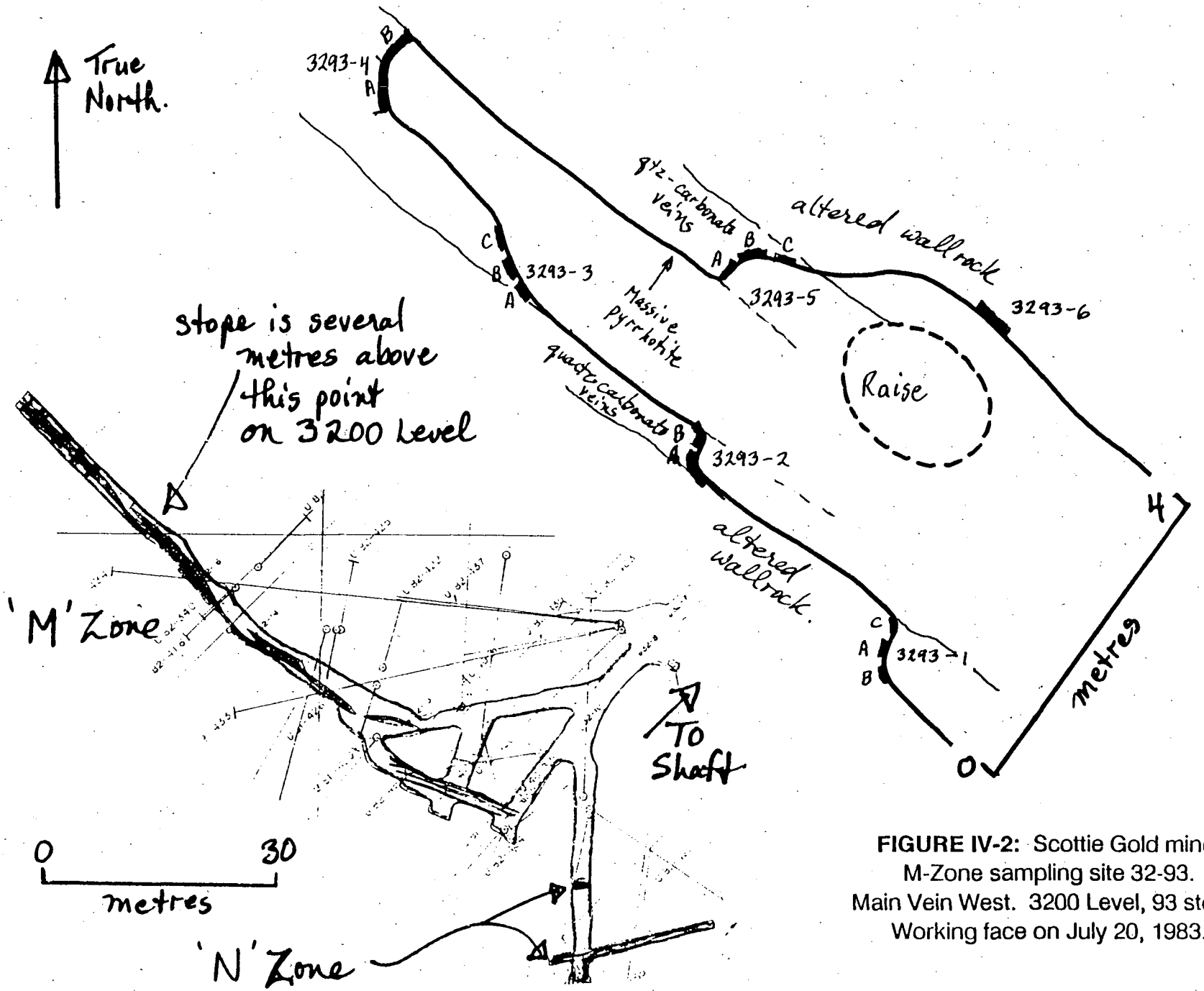

FIGURE IV-2: Scottie Gold mine: M-Zone sampling site 32-93. Main Vein West. 3200 Level, 93 stope. Working face on July 20, 1983.

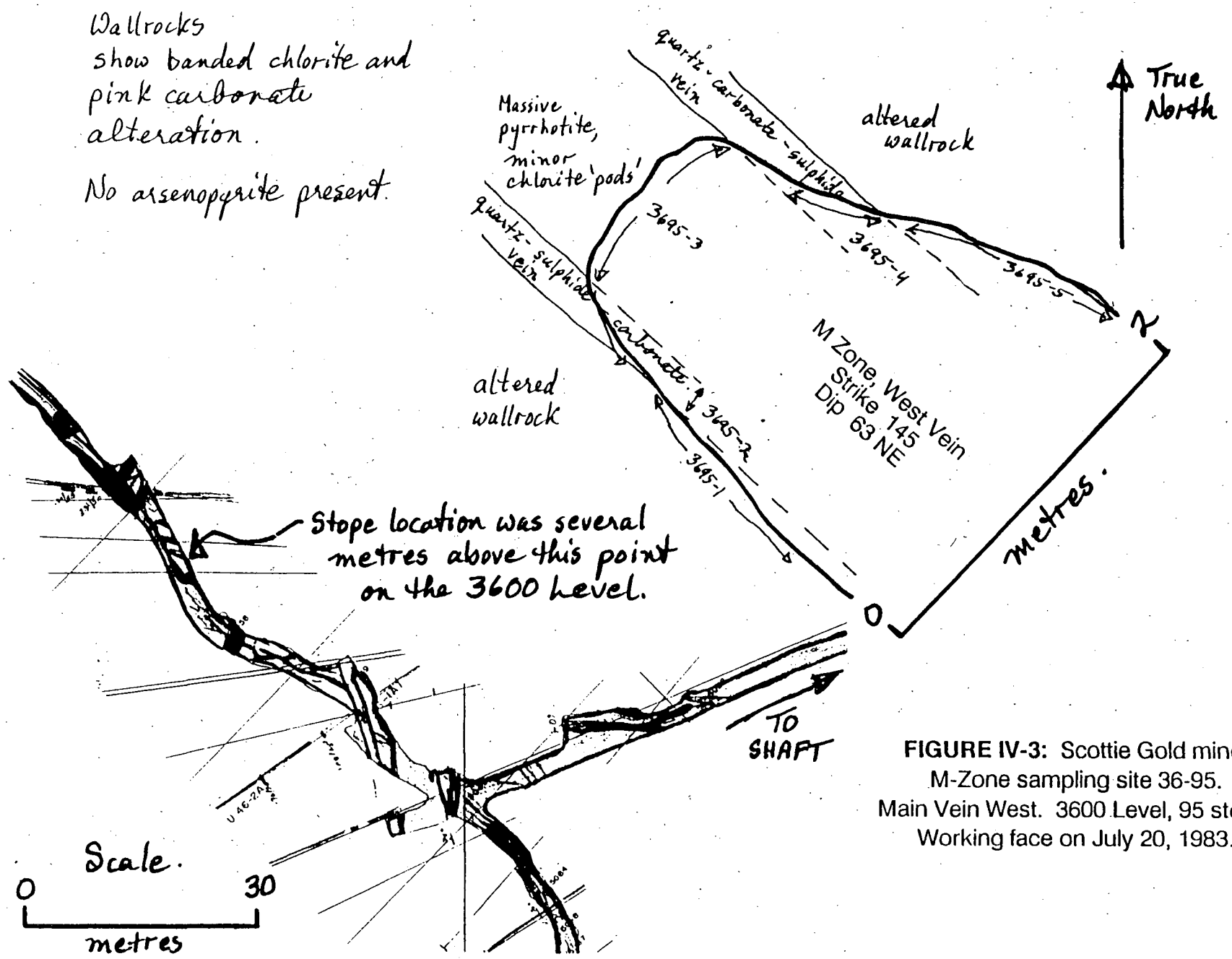

FIGURE IV-3: Scottie Gold mine: M-Zone sampling site 36-95. Main Vein West. 3600 Level, 95 stope. Working face on July 20, 1983.

TABLE IV-1: ASSAYS AND MINOR ELEMENT ANALYSES FROM SCOTTIE GOLD MINE
(all values in ppm except where indicated as %)

	SAMPLE NUMBER			
ELEMENT	SG-1	SG-2	SG-3	SG-4
Au	212	42.5	4.1	460
Ag	67	365	115	73
As	630	107	2.45%	432
Ba	<50	<50	<50	<50
Be	<3	<3	<3	<3
Bi	24	51	81	30
Cd	<10	4 629	916	<10
Cr	<20	<20	20	34
Cu	0.12%	2.32%	0.59%	0.10%
F	225	<60	<60	<60
Fe	43.22%	9.78%	18.37%	19.24%
Ge	0.8	<0.5	0.6	1.9
Hg	1.2	<0.5	6.5	<0.5
Mn	1 160	3 397	1 565	2 166
Mo	25	<2	3	434
Pb	0.02%	7.73%	3.86%	0.04%
Sb	21	223	141	6
Se	<10	10	<10	<10
Sn	4.0	4.0	7.0	7.7
Tl	0.6	<0.5	0.5	0.6
V	265	<5	20	500
W	<3	<3	12	7
Zn	0.03%	31.32%	5.21%	0.05%
LOI	9.02%	15.53%	17.07%	12.04%

SAMPLE DESCRIPTION

SG-1: 3300 Level; Main West Vein. Massive pyrrhotite sample collected 10 centimetres from a cross-cutting lamprophyre dyke.

SG-2: 3300 Level; Main West Vein; 33-1 stope. Sample collected from 'typical' massive pyrrhotite ore. Rock is 80% sulphide. Working face is 5 metres wide and averages 1.5 oz Au/ton.

SG-3: 3300 Level; Main West Vein; 33-2 stope. Sample of 'lower grade' quartz-carbonate-sulphide vein margin. Rock is 60% sulphide.

SG-4: 3100 Level; Sixties Vein; 'Rats Nest' stopes. Sample of bronze-coloured massive pyrrhotite vein. This vein is narrow, averaging less than 0.5 metres wide, but consistently grades better than 1.5 oz. Au/ton.

IV.2 Sampling at the Big Missouri deposits

Two diamond-drill holes from the Big Missouri area were logged and sampled (Figures IV-4 and IV-5). These holes were selected by S. Dykes of Westmin Resources Ltd. as representative of typical textures and grades of the main ore deposits on the property. DDH 81-58 from Dago Hill deposit and DDH 82-42 from S-1 deposit both intersected three major subparallel veins and many minor veins and veinlets. Forty-one core intervals were sampled for petrographic and textural studies. Samples were divided at lithological boundaries, at alteration boundaries and at vein boundaries. Sections of whole core were 50 percent sampled, sections of previously split core were 67 percent sampled. From these large sample volumes, pieces displaying both typical and atypical features of the sample interval were selected for slabbing and for microscope study. An additional twelve selective grab samples were collected from trench exposures at several deposits for trace element analysis. Analytical results are listed in Table IV-2 and summarized in Table 4-7.

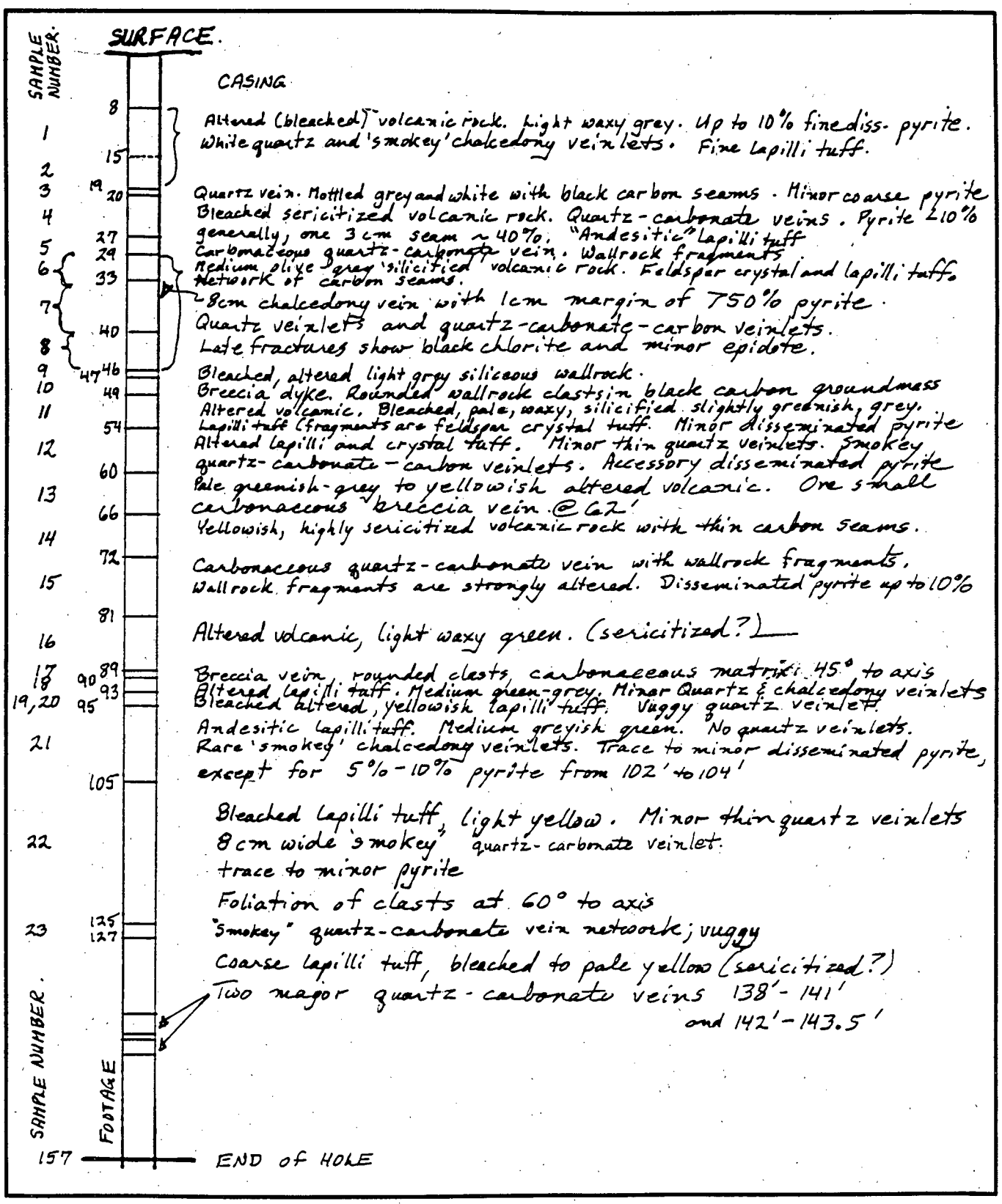

FIGURE IV-4: Big Missouri area, Dago Hill deposit.
DDH 81-58. Logged on August 25,1984.

SAMPLE NUMBER	FOOTAGE	
	SURFACE	
		CASING
	11	
1		fine hornblende crystal tuff. Andesite. Thin quartz veinlets throughout (68° to axis) Minor chalcedonic veinlets (40° to axis). Grades downward into bleached rock.
	14	(Rare fine galena in qtz veinlet at 15' within)
2		Altered fine hornblende crystal tuff. Andesite. Massive pyritic veinlets up to 8cm thick. 5-10% disseminated pyrite. Hornblende content decreases.
4	21	
	22	Weakly altered Andesite ash tuff.
5		Weakly altered hornblende crystal tuff. Many phases of quartz and chalcedony veinlets. Grades downward into altered rock.
	26	
6		Vein density and thickness increasing in moderately altered hornblende crystal tuff. Sharp lower contact
7	33	
	34	Quartz breccia vein hosts angular andesite clasts and minor sph., gal. pyrite.
No.	35	Moderately altered hornblende crystal tuff (may be a fragment).
8	37	Quartz breccia vein with abundant mixed sulphides.
9		Quartz vein hosts carbon and sulphides, shows local colloform textures. Calcite has faint pink to coral colours
10	39	Rebrecciated vein with darker (more carbon) grey colour. Late quartz cement is white.
	41	
11		Light to medium grey, bleached, silicified andesite. Cut by a network of quartz veinlets. Up to 40% disseminated pyrite; trace disseminated galena and sphalerite. After 42 feet sulphides are >50% of rock and are layered at 50° to axis. Texture is still as disseminated grains. Host rock is siliceous. Gradational lower contact.
	50	
12		Chloritized hornblende crystal tuff (Andesite). Heavily pyritized, abundant quartz veinlets. Rock grades downward into crystal-free ash tuff. Below 57' zones or bands of coarse disseminated pyrite overprint quartz veinlets and altered, sericitized greenish andesite. Quartz veinlets area network or stockwork.
	63	
13		Dark green, chloritized andesite ash tuff. Cut by minor white quartz veinlets. Minor disseminated pyrite & sph.
	67	
14		Zone of massive (>50%) but disseminated coarse pyrite in andesite ash tuff.
	71	
15		Light grey, silicified andesite ash tuff. Quartz and quartz-chlorite veinlets; one hosts coarse galena, 74'-76' hosts 30% disseminated pyrite. 76'-81' zone of massive, white crosscutting quartz veins host coarse chlorite and have coarse disseminated pyrite on margins.
	80	
16		Massive (>50%) disseminated pyrite, cut by chalcedony veinlet.

END of accessible core at 82 feet.
Not end of hole.

FIGURE IV-5: Big Missouri area, S-1 deposit.
DDH 82-42. Logged on August 25, 1984.

TABLE IV-2: ASSAYS AND MINOR ELEMENT ANALYSES FROM THE BIG MISSOURI AREA
(all values in ppm except where indicated as %)

ELEMENT	SR-6	SR-7	SR-114A	SR-114B	SR-164A	SR-164B	SR-166	SR-168A	SR-168B	SR-169	SR-170	SR-174	ELEMENT
Au	0.3	<0.3	2.4	18.8	22	30.5	<0.3	0.7	12	22.6	1.4	6.8	Au
Ag	38	64	288	595	62	95	85	88	519	269	50	217	Ag
As	101	0.11%	85	114	158	363	114	88	122	245	392	260	As
Ba	336	1 202	354	85	1 223	295	384	225	<50	345	305	1 152	Ba
Be	<3	<3	<3	<3	<3	<3	<3	<3	<3	<3	<3	<3	Be
Bi	<10	17	73	198	53	43	39	29	28	27	14	14	Bi
Cd	<10	<10	284	2 651	188	254	1609	802	536	499	580	1 202	Cd
Cr	33	21	26	<20	<20	<20	51	23	<20	<20	23	21	Cr
Cu	0.01%	<0.01%	2.40%	4.53%	0.31%	0.44%	1.16%	0.61%	2.87%	2.0%	0.36%	1.18%	Cu
F	<60	<60	<60	<60	190	<60	125	<60	<60	<60	<60	<60	F
Fe	2.30%	8.95%	11.51%	15.04%	15.89%	22.64%	9.47%	2.92%	11.48%	20.00%	7.77%	7.46%	Fe
Ge	<0.5	1.4	<0.5	<0.5	<0.5	0.8	<0.5	1.2	<0.5	<0.5	0.9	0.8	Ge
Hg	<0.5	60	10.0	<0.5	<0.5	13.3	60.3	15.9	<0.5	9.5	20.0	22.2	Hg
Mn	146	161	808	2 189	1 724	1 048	1 934	2 805	597	106	1 258	1 528	Mn
Mo	3	5	<2	<2	24	12	3	<2	<2	7	<2	4	Mo
Pb	0.08%	0.03%	12.92%	10.16%	0.39%	0.09%	4.76%	2.09%	12.58%	11.79%	2.06%	0.11%	Pb
Sb	<5	187	136	495	9	59	24	61	473	278	466	355	Sb
Se	10	16	42	192	<10	<10	<10	<10	90	<10	<10	10	Se
Sn	<3	4.2	5.2	4.9	4.4	<3	3.5	3.4	3.3	3.9	<3	3.7	Sn
Tl	0.65	14.5	<0.5	<0.5	0.8	0.8	0.55	<0.5	<0.5	<0.5	<0.5	0.55	Tl
V	19	45	55	<5	60	30	23	15	<5	34	10	35	V
W	<3	<3	5	3	5	<3	9	<3	4	3	3	9	W
Zn	0.07%	0.07%	3.42%	22.38%	2.15%	2.86%	16.19%	7.29%	5.03%	5.06%	5.61%	13.23%	Zn
LOI	1.26%	10.81%	10.22%	17.58%	11.85%	17.89%	12.99%	11.71%	11.39%	17.11%	7.93%	8.54%	LOI

SAMPLE DESCRIPTION

SR-6: Grab sample from the adit on the east side of Dago Hill.

SR-7: Grab Sample from surface trench (Trench 13?) on the east side of Dago Hill, near the hilltop.

SR-114A: Grab sample from the Creek Zone adit on the lower west side of Dago Hill. Banded polymetallic semi-massive sulphides.

SR-114B: Grab sample from the Creek Zone adit on the lower west side of Dago Hill. Banded polymetallic semi-massive sulphides.

SR-164A: Grab Sample from Trench 2, high on the rockslide. Consolidated Silver Butte deposit. Polymetallic massive sulphide rock.

SR-164B: Grab Sample from Trench 2, high on the rockslide. Consolidated Silver Butte deposit. Polymetallic massive sulphide rock.

SAMPLE DESCRIPTION

SR-166: Grab sample from Trench 16, high on the rockslide. Consolidated Silver Butte deposit. Polymetallic laminated massive sulphide rock.

SR-168A: Grab sample from Trench 3, high on the rockslide. Consolidated Silver Butte deposit. Coarse-grained polymetallic massive sulphide rock.

SR-168B: Grab sample from Trench 3, high on the rockslide. Consolidated Silver Butte deposit. Coarse-grained polymetallic massive sulphide rock.

SR-169: Grab sample from the adit portal at the Terminus Zone, southwest of Hog Lake. Quartz-carbonate-sulphide rock.

SR-170: Grab Sample from long trench, Province Zone. Coarse-grained quartz-carbonate-sulphide rock.

SR-174: Grab sample from trench at Martha Ellen zone. Andesite fragments in polymetallic massive sulphide matrix.

IV.3 Sampling at the Silbak Premier mine

Two chip sample sections, totalling 30 samples, were collected at the Silbak Premier mine from ore zones exposed in the 2 Level and 4 Level (Figures IV-6, and IV-7). Suitable ore zones were selected with the assistance of P. Wojdak, Westmin Resources Ltd. All samples were from the West Zone due to hazardous access to the Main and Northern Lights Zones. Samples were collected in two-metre intervals to tie in with previous panel sampling by Westmin geologists. In addition, 19 selective grab samples were collected for trace element analysis from other sites in the mine and from nearby showings. Analytical results are listed in Table IV-3 and summarized in Table 4-7.

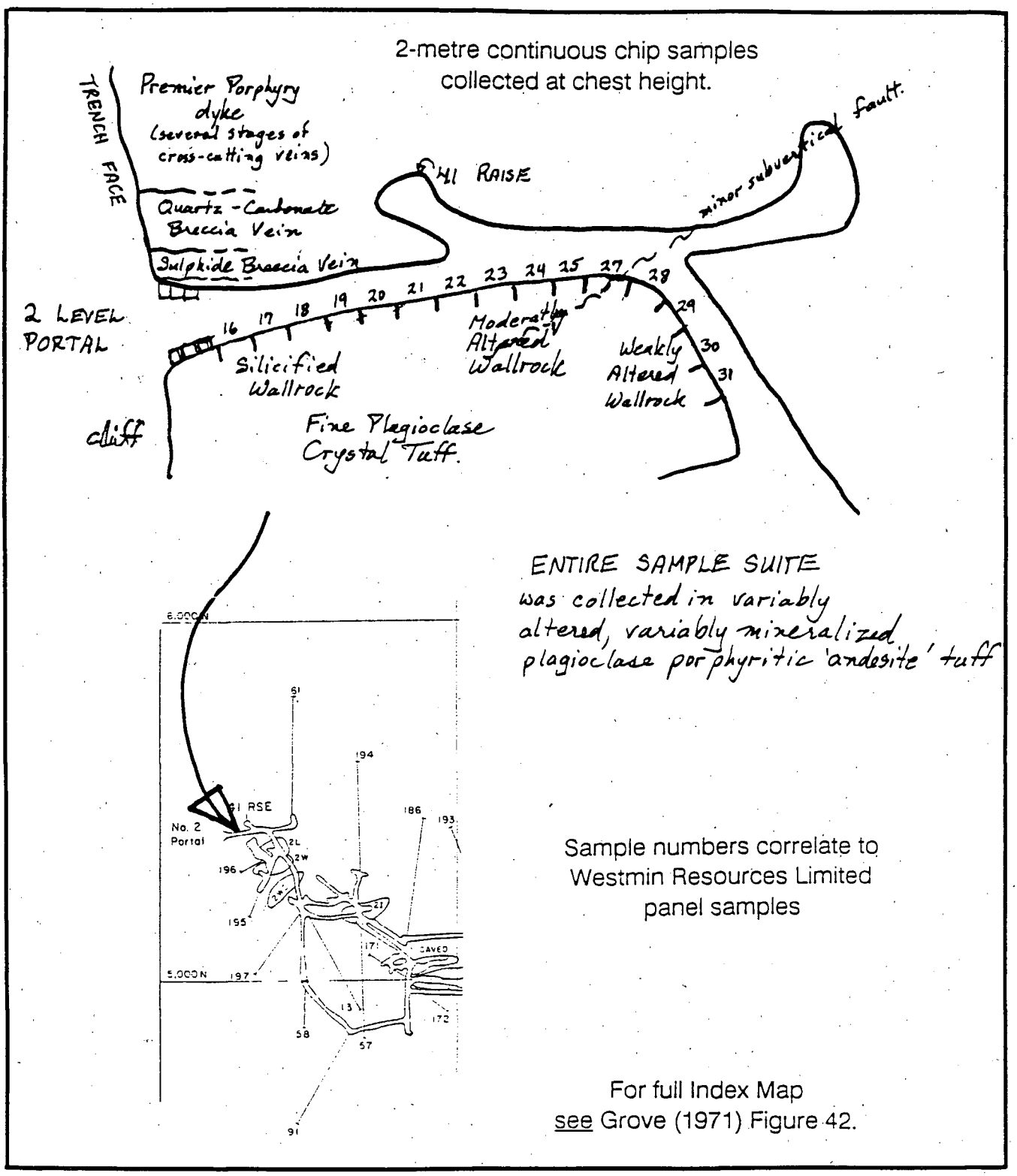

FIGURE IV-6: Silbak Premier mine: 2 Level sampling site. 2 Level Portal. June 13, 1984.

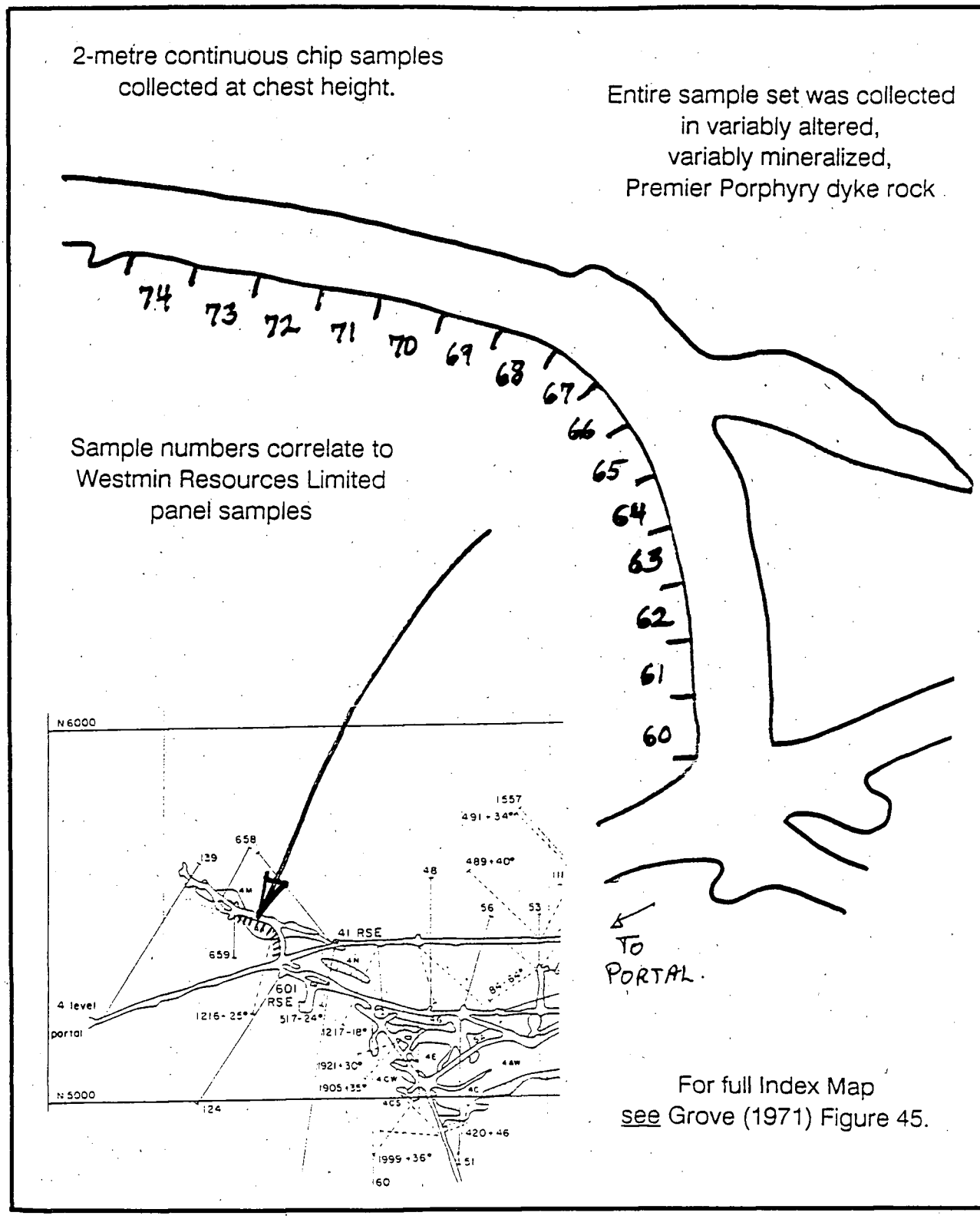

FIGURE IV-7: Silbak Premier mine: 4 Level sampling site. 4-I stope area. June 13, 1984.

TABLE IV-3: ASSAYS AND MINOR ELEMENT ANALYSES FROM THE SILBAK PREMIER MINE
(all values in ppm except where indicated as %)

ELEMENT	PM-2	PM-3	PM-4	PM-5	SR-20	SR-30A	SR-30B	SR-36	SR-37	SR-38
Au	62	29	11	18.5	3.4	1.3	2.4	18	7	<0.3
Ag	158	12 600	1 600	1 240	526	<10	53	323	1 212	<10
As	242	630	207	153	0.40%	122	140	167	295	88
Ba	680	846	7 443	2 714	810	1 545	977	63	1 579	1 071
Be	<3	<3	<3	<3	<3	<3	<3	<3	<3	<3
Bi	23	12	20	20	10	28	12	92	42	45
Cd	844	1 200	496	43	<10	<10	100	3 129	136	<10
Cr	<20	<20	<20	<20	<20	<20	<20	<20	<20	<20
Cu	0.24%	0.99%	0.16%	0.02%	<0.01%	<0.01%	<0.01%	2.23%	0.08%	<0.01%
F	<60	<60	<60	<60	200	325	125	<60	160	240
Fe	21.29%	8.22%	16.05%	13.77%	5.52%	5.49%	4.49%	14.46	16.37	2.53
Ge	<0.5	<0.5	<0.5	<0.5	0.6	0.7	0.6	<0.5	1.0	<0.5
Hg	5.6	56.1	3.6	<0.5	0.8	<0.5	2.1	<0.5	<0.5	<0.5
Mn	110	80	110	120	1 130	5 909	3 442	2 286	2 826	16 554
Mo	4	15	3	5	11	6	3	<2	7	<2
Pb	11.14%	6.0%	2.83%	0.47%	0.05%	0.11%	0.05%	6.92%	0.08%	<0.01%
Sb	160	1.09%	250	111	86	<5	11	66	9	12
Se	<10	10	<10	<10	<10	<10	10	20	<10	<10
Sn	5.1	3.7	6.4	7.4	5.1	4.0	3.9	<3	6.7	3.7
Tl	<0.5	<0.5	0.6	0.9	1.25	0.75	1.0	<0.5	0.8	0.5
V	<5	<5	18	22	79	117	33	<5	55	58
W	3	5	3	3	<3	<3	<3	<3	<3	<3
Zn	9.00%	13.59%	5.24%	0.65%	0.05%	0.03%	1.09%	24.46%	1.37%	0.03%
LOI	17.29%	9.09%	12.03%	9.32%	4.35%	11.03%	3.14%	17.37%	12.15%	19.36%

ELEMENT	SR-65	SR-69	SR-95A	SR-95B	SR-96	SR-97	SR-99	SR-172	SR-173
Au	<0.3	62.7	8.6	1.7	3	1	1	2.7	17
Ag	15	75	12	24	15	<10	26	20	157
As	75	744	265	531	348	141	357	143	144
Ba	2 219	923	4 688	2 851	1 083	3 598	943	<50	<50
Be	6.0	<3	<3	<3	<3	<3	<3	<3	<3
Bi	15	42	26	41	39	<10	20	30	56
Cd	<10	27	72	16	<10	22	205	68	3 740
Cr	<20	<20	<20	<20	<20	<20	21	20	<20
Cu	<0.01%	<0.01%	<0.01	0.02	0.01%	0.01%	0.01%	0.03%	2.60%
F	550	<60	160	<60	<60	<60	<60	<60	<60
Fe	4.96	26.94	14.67	26.42	14.89%	5.55%	12.11	1.63	13.15
Ge	1.0	<0.5	1.8	<0.5	<0.5	1.3	0.9	<0.5	<0.5
Hg	<0.5	<0.5	0.6	<0.5	<0.5	<0.5	<0.5	2.9	0.6
Mn	960	1 078	144	64	79	90	198	16 186	2 760
Mo	2	<2	6	<2	<2	3	<2	<2	2
Pb	<0.01%	0.14%	0.13%	0.04%	0.05%	0.15%	1.49%	0.18%	1.88%
Sb	<5	13	<5	11	<5	120	19	24	86
Se	<10	<10	<10	<10	<10	<10	<10	<10	15
Sn	4.5	3.3	4.5	<3	4.0	5.4	<3	5.3	<3
Tl	0.8	0.7	1.5	0.7	0.8	1.75	0.7	<0.5	<0.5
V	95	40	37	12	10	15	10	<5	<5
W	<3	<3	5	5	<3	<3	<3	<3	5
Zn	0.02%	0.30%	0.63%	0.23%	0.04%	0.25%	2.48%	0.68%	30.95%
LOI	5.68%	19.49%	10.54%	18.61%	10.04%	4.71%	8.99%	29.90%	13.71%

SAMPLE DESCRIPTION

PM-2: Sample from main Gloryhole, Silbak Premier mine. Laminated massive sulphide rock with bleached silicified wallrock clasts. Rock is 70% sulphide, including 30% fine pyrite. Massive seams of fine-grained silvery mineral is probably tetrahedrite/freibergite.

PM-3: Sample from main Gloryhole, Silbak Premier mine. Massive sulphide rock , not banded. Rock is 60% sulphides with bleached wallrock clasts.

PM-4: Sample from main Gloryhole, Silbak Premier mine. Breccia, grey matrix with bleached porphyritic fragments: overprinted by 30% sulphides. Mainly pyrite with traces of a fine silver grey mineral (tetrahedrite/freibergite?).

PM-5: Sample from main Gloryhole, Silbak Premier mine. Bleached, silicified wallrock with 25% fine to medium-grained disseminated pyrite. Trace dark silver-grey mineral.

SR-20: ?sample from old adit

SR-30A: Pictou showing. Grab sample from portal of old adit. Coarse-grained quartz-carbonate-galena-sphalerite-pyrite rock.

SR-30B: Pictou showing. Grab sample from portal of old adit. Coarse-grained quartz-carbonate-galena-sphalerite-pyrite rock.

SR-36: Hope Prospect (Granduc Road showing). Crudely laminated polymetallic massive sulphide rock.

SAMPLE DESCRIPTION

SR-37: Hope Prospect (Granduc Road Showing). Silicified and chloritized andesite wallrock on south side of the sulphide zone.

SR-38: Hope prospect (Granduc Road showing). Carbonate-altered, bleached andesite tuff on south side of sulphide zone.

SR-65: Medium green andesite tuff with disseminated pyrite. Strong propylitic alteration of country rock.

SR-69: Disseminated galena and sphalerite in calcite.

SR-95A: Laminated massive pyrite from the rim of the small glory hole. >70% pyrite in a grey silica matrix.

SR-95B: Laminated massive pyrite from the rim of the small glory hole. >70% pyrite in a grey silica matrix.

SR-96: Massive pyritic lens.

SR-97: Pyrite blebs in pumiceous rock>

SR-99: Pyrite + galena + sphalerite vein.

SR-172: Hope Prospect (Granduc Road showing). Quartz-carbonate breccia rock with <2% coarse red-brown sphalerite localized along fractures.

SR-173: Hope Prospect (Granduc Road showing). Large boulder of crudely laminated massive sulphide (> 95% sulphide). 30% coarse pyrite, 65% fine brown sphalerite, 1 % galena, trace chalcopyrite and 4% quartz + calcite.

IV.4 Sampling from the Stratabound Pyritic Dacite

Four selective grab samples from the pyritic dacites on Mount Dilworth were collected for trace element analyses. Analytical results are listed in Table IV-4 and summarized in Table 4-7.

TABLE IV-4: ASSAYS AND MINOR ELEMENT ANALYSES FROM THE PYRITIC DACITE FACIES OF THE MOUNT DILWORTH FORMATION
(all values in ppm except where indicated as %)

	SAMPLE NUMBER			
ELEMENT	SR-127	SR-142	SR-151	SR-153
Au	<0.3	<0.3	<0.3	<0.3
Ag	<10	<10	<10	<10
As	<10	101	75	59
Ba	1 023	1 871	2 913	1 123
Be	4.5	3.0	<3	3.0
Bi	18	19	17	<10
Cd	<10	<10	<10	<10
Cr	21	24	42	36
Cu	<0.01%	<0.01%	<0.01%	<0.01%
F	260	360	350	450
Fe	11.37%	13.85%	13.74%	5.31%
Ge	2.2	1.8	4.0	5.0
Hg	<0.5	<0.5	<0.5	<0.5
Mn	96	150	60	48
Mo	2	6	<2	8
Pb	0.07%	<0.01%	<0.01%	0.01%
Sb	<5	<5	15	6
Se	<10	10	<10	<10
Sn	6.0	6.0	5.4	3.7
Tl	0.8	0.7	11.3	1.0
V	108	115	95	100
W	<3	<3	3	<3
Zn	0.06%	0.03%	0.01%	0.06%
LOI	8.61%	10.23%	11.01%	5.26%

Sample Description

SR-127: Grab sample of pyritic dacite lapilli tuff. South edge of Mount Dilworth snowfield.

SR-142: Grab sample of a semi-massive pyritic seam or nodule in pyritic dacitic lapilli tuff. 200 metres north of the north end of 49 Ridge.

SR-151: Grab sample of black carbonaceous dacitic tuff.

SR-153: Grab sample of silicified carbonaceous tuff with pumice.

IV.5 Sampling at the Prosperity/Porter Idaho

Three continuous chip sections, totalling 23 samples, were completed across the D Vein (Figures IV-8 and IV-9). Suitable vein exposures were selected with the assistance of M. Kenyon and J. Greig, Pacific Cassiar, Ltd. Sampling was divided at geological boundaries: wall rock; mineralized and unmineralized fault gouge; and lithified slabs within the fault zone. In addition, four grab samples were collected for trace element analysis. Analytical results are listed in Table IV-5 and summarized in Table 4-7.

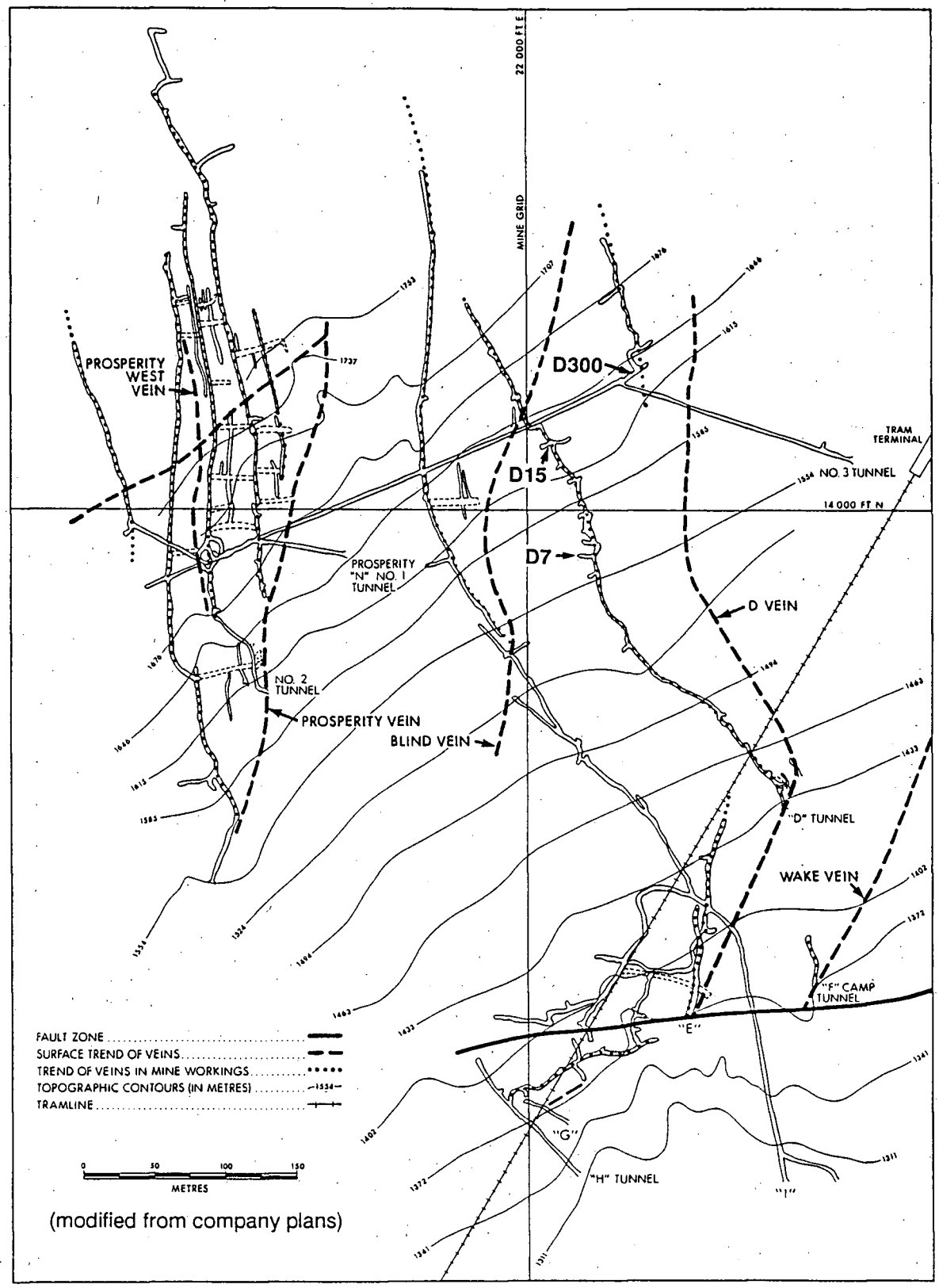

FIGURE IV-8: Plan of the Prosperity/Porter Idaho mine workings. Plan shows the surface trace of veins, the underground mine workings, the location of the veins within the main mine levels, and the location of the three channel sample sections for this study.

[See Figure 3.2a for topographic and geologic setting and latitude/longitude.]

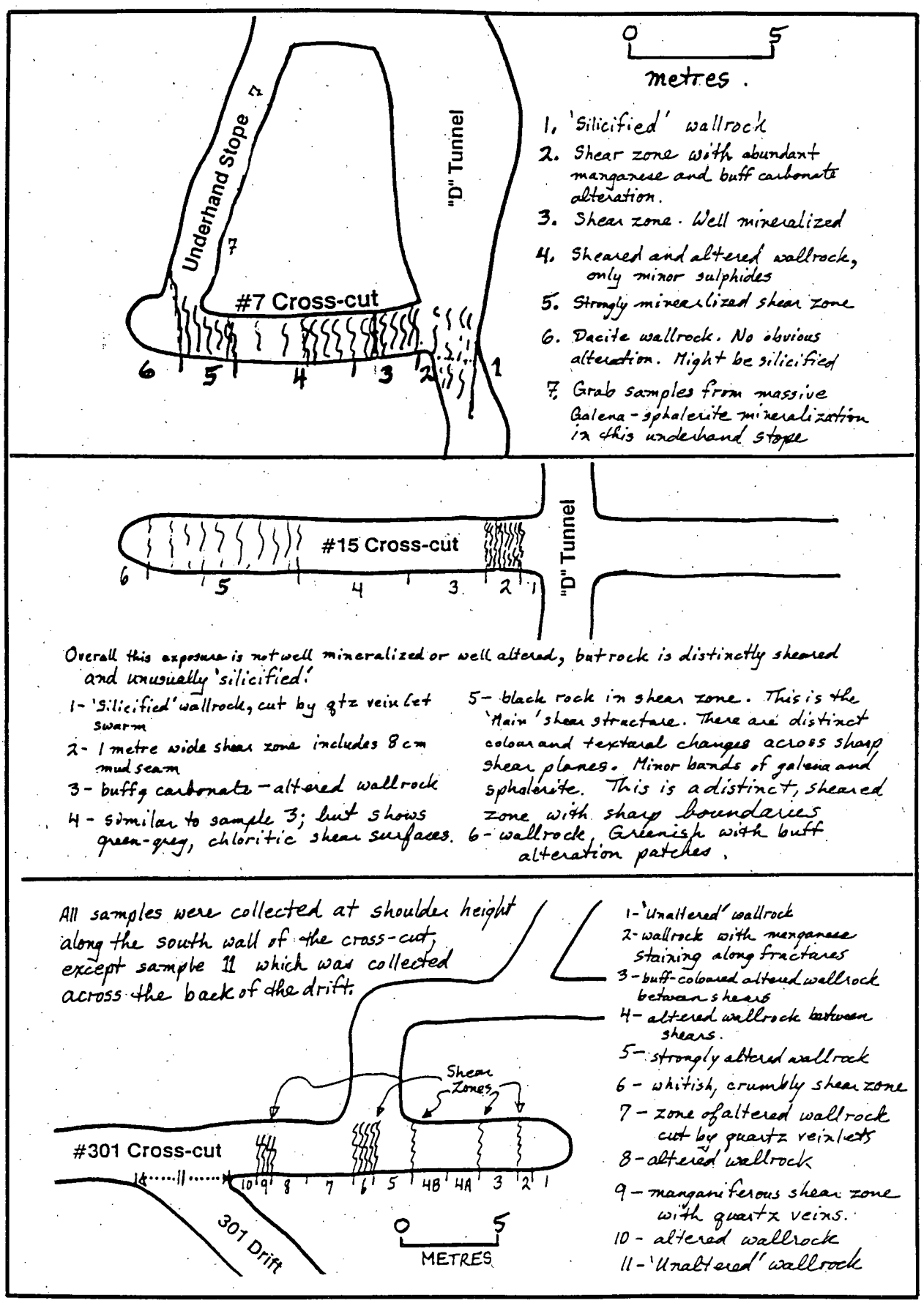

FIGURE IV-9: Prosperity/Porter Idaho mine: Sampling sites. D7, D15 and D301 Cross-cuts on D Vein. August 16, 1983.

TABLE IV-5: ASSAYS AND MINOR ELEMENT ANALYSES FROM THE PROSPERITY/PORTER IDAHO MINE
(all values in ppm except where indicated as %)

	SAMPLE NUMBER			
ELEMENT	PI-1	PI-3	PI-6	PI-7
Au	1	<0.3	2.4	2.7
Ag	5 215	20	14 165	12 545
As	577	26	292	0.45%
Ba	158	609	99	75
Be	<3	3.5	<3	<3
Bi	17	<10	<10	17
Cd	1 004	28	387	2 150
Cr	<20	<20	<20	<20
Cu	0.45%	0.01%	0.69%	0.63%
F	<60	275	<60	<60
Fe	6.19%	2.96%	2.73%	5.52%
Ge	<0.5	2.3	<0.5	<0.5
Hg	12.2	<0.5	7.4	9.2
Mn	170	7 920	559	4 965
Mo	<2	<2	<2	2
Pb	11.92%	1.09%	12.89%	11.53%
Sb	0.53%	12	0.52%	0.59%
Se	<10	10	<10	<10
Sn	6.2	7.4	3.8	5.1
Tl	<0.5	1.0	<0.5	<0.5
V	12	50	20	15
W	7	3	3	6
Zn	9.07%	0.27%	2.57%	19.05%
LOI	8.63%	3.02%	9.63%	9.44%

Sample
Description

PI-1: D Vein Extension. Main ore zone.

PI-3: D Vein, 300 Level, Underhand stope in #7 cross-cut. Sample from hangingwall (west side of drift). Intense manganese alteration.

PI-6: Blind Vein at 301 cross-cut. Massive galena-sphalerite rock.

PI-7: D Vein. 300 Level, underhand stope in #7 cross-cut. Massive sulphide rock.

APPENDIX V

HISTORIC GENETIC MODELS

Genetic processes and models have been proposed for many deposits in the Stewart mining camp over the past sixty years (Table V-1). Two patterns seem evident:

- some early theories seem closest to current ideas, and
- there is a tendency to apply fashionable (current) and 'salable' ore genesis concepts despite the objective features of the deposits.

One wonders if the same two generalizations will also be appropriate in twenty years time.

TABLE V-1: Evolution of Theories of Ore Genesis

REPORT	SILBAK PREMIER MINE	BIG MISSOURI MINE	SCOTTIE GOLD MINE	PROSPERITY/ PORTER IDAHO MINE
McConnell 1919	Fissure veins and replacement deposits			
Westgate 1922	Mesothermal			
Schofield & Hanson 1922	Mesothermal	Mesothermal		
Buddington 1923	Epithermal veins, disseminations and replacements			
Burton 1926	Epithermal veins in shears			
Jewell 1927	Hypothermal to mesothermal (~3000m)			
Buddington 1928	Mesothermal to hypothermal (600-3000m)			
Langille 1945	Veins in shears			
Seraphim 1947			Mesothermal to Hypothermal	
Black & White 1947	Veins and replacements			
McDougall 1950				Veins in shears
Plumb 1957	Veins in tension fractures			
Grove 1971	Sulphide-rich shoots in siliceous replacement ores	Quartz veins and silicification in cataclasites		Quartz fissure veins in shear (schist) zones
Grove 1973 & 1986	Replacement veins in metasomatized cataclasite; shallow, subvolcanic			
Smitheringale 1977		Volcanogenic massive sulphides		
Seraphim 1979	Volcanogenic massive sulphides		Volcanogenic massive sulphides	
Read 1979		? (unlikely to be V.M.S.)		
Barr 1980	Telescoped epithermal			

TABLE V-1: Evolution of Theories of Ore Genesis (continued)

REPORT	SILBAK PREMIER MINE	BIG MISSOURI MINE	SCOTTIE GOLD MINE	PROSPERITY/ PORTER IDAHO MINE
Galley 1981		Volcanogenic massive sulphides		
Williams (pers.comm.) 1982			Veins in shears	
Alldrick 1983	(?)	Stratabound, genesis uncertain	Veins in shears	Veins in shears
Alldrick 1984	Epithermal vein networks	Cross-cutting, quartz-carbonate breccias	Mesothermal veins in shears	
Alldrick 1985	Subvolcanic quartz-carbonate breccia veins	Subvolcanic quartz-carbonate breccia veins	Mesothermal veins	Mesothermal veins in shears
Panteleyev & Schroeter 1985	Epithermal	Epithermal	Mesothermal	Epithermal
Dykes et al. 1987		Volcanogenic massive sulphides		
Brown 1987	Porphyry-related epithermal-mesothermal transition			
Dykes et al. 1988		Volcanogenic massive sulphides		
Randall 1988	Syngenetic, stratabound and stockwork ores	Stratabound ores		
MacDonald 1988c	Epithermal; adularia-sericite type			
Brown & Wojdak 1989	Epithermal			
Schroeter et al. 1989	Epithermal vein	Mesothermal vein	Mesothermal vein	Mesothermal vein stockwork
MacDonald 1990	Epithermal; 600 metres depth; ~stratabound			
This Study	Epithermal, moderate depth, cross-cutting; Early Jurassic	Epithermal, moderate to shallow depths cross-cutting; Early Jurassic	Mesothermal veins; Early Jurassic	Mesothermal veins in brittle shears; Eocene